# The formation of lithium-rich melts during early crustal evolution — a case study from the Archean Zimbabwe Craton


Lot Koopmans

University College

University of Oxford

A thesis submitted for the degree of

*Doctor of Philosophy*

Trinity 2025

# Acknowledgements

This project was completed because of the immense support I received during my time at Oxford, and because of that I have many acknowledgements to give! I am very grateful for support I received from NERC and the Oxford–Radcliffe scholarship for funding this research. The project also greatly benefited from support, either by funding or in-kind, by the Geological Society of London, the Society of Economic Geologists, Premier African Minerals and Prospect Mineral Resources, to which I am very grateful. I would also like to thank the Research Council of Zimbabwe for enabling this research, and Midlands State University for supporting me during my fieldwork in Zimbabwe.

I would also like to sincerely thank Richard Palin, Nick Gardiner, and Laurence Robb for being fantastic supervisors as we all jumped into the pegmatite world together. Thank you for giving me the freedom to explore my interests and supporting the direction the project went.

A huge thank you to Tania Martins and Bob Linnen for being open to discussing every crazy question I had about pegmatites, and for making me feel part of your community since we met in Maine. A special thanks also goes to Catriona Breasley for the fantastic discussions we have had about all things pegmatite.

I am indebted to Brian Mapingire, Antony Mamuse, Tony Martin, Brayden St. Pierre, and Liberty Ndlovu for their support in the field during my field seasons. I am also very grateful for the support and assistance Bruce Cumming, George Roach, Jabulani Chirasha, Tinashe Muzondo, Tendai Gumi, Rutendo Musinga, Dereck Muchingami, and the rest of the team at Premier African Minerals have given me during my stays on-site and beyond. A very big thank you also goes to James Winch, Adam Moodley, and especially Roger Tyler for their help around Arcadia and sample logistics.

I want to extend my sincerest gratitude to Jane Barling for diligently teaching me everything there is to know about digestions in the clean lab. The geochemistry could not have been done without you. Owen Green, Matthew Beverly-Smith, and Emily Donald, thank you for teaching me all things rock prep, and keeping me sane during dark days in the basement. Sebastian (Batzi) Fischer and Martin Mangler

are sincerely thanked for their time (and patience) whilst teaching me how to use the laser during my analytical runs at the StAGE lab in St Andrews. I am also very grateful to Cyril Chelle-Michou for inviting me to ETH in Zurich to do additional geochronology, and Lorenzo Tavazzani for assisting me during my time there. My thanks also to Brendan Dyck and Kyle Larson for being fantastic and running my Rb–Sr geochronology in the Fipke lab at UBC Okanagan.

To my officemates – Hannah, Ally, Lewis, Harri, and Kate – thank you for making the past four years as fun (and chaotic) as they were, and thanks for being such fantastic support. My appreciation also goes out to Nikki, Bei Bei, Ian, Toby, Rebecca, Vicky, and everyone else in the department who have made my time in Oxford so special. Thanks also to the Assynt team every year, this trip was a highlight of my time here. Claire Nichols is especially thanked for being a sounding board during the car rides in and around Assynt, Marc St Onge for his infinite geological wisdom, and the undergraduates for keeping the trips fun and a pleasure to teach. To my family, thank you for supporting me through thick and thin, and always being there for me. Thank you also for entertaining my interesting passion for rocks, which I (understandably) still think hasn't rubbed off on any of you!

And most importantly, thank you to Charlotte for being the best. Your endless support and affection have constantly encouraged me to push myself beyond what I imagined possible, and I am eternally grateful for you always being there for me.

Thank you all!

# Statement of Authorship

I confirm the work submitted here is my own and has not been submitted in whole or in part for consideration for any other degree or qualification in this, or any other university.

Whilst this thesis is my own work, as with any science, parts were completed in collaboration with others as outlined below.

The work in **Chapter 3** has been published in the journal *Geology* under the following title: *"The formation of lithium-rich pegmatites through multi-stage melting"*. **Koopmans, L.**, Martins, T., Linnen, R., Gardiner, N.J., Breasley, C.M., Palin, R.M., Groat, L.A., Silva, D. Robb, L.J. **doi:10.1130/G51633.1**

- *Conceptualisation and project design*: L. Koopmans, T. Martins, R. Linnen. *Modelling*: L. Koopmans. *Data analysis*: L. Koopmans. *Manuscript drafting*: L. Koopmans. *Editing*: R.M. Palin, N.J. Gardiner, C.M. Breasley, L.A. Groat, D. Silva.

The work in **Chapter 4** has been published in the journal *Mineralium Deposita* under the following title: *" Structural controls on lithium mineralization in shear-zone hosted granitic pegmatites of the Zulu pegmatite field, Zimbabwe – implications for exploration"*. **Koopmans, L.**, Gardiner, N.J., St. Pierre, B., Palin, R.M., Musinga, R., Robb, L.J. **doi:10.1007/s00126-025-01371-x**

- *Conceptualisation and project design*: L. Koopmans. *Sampling and data collection*: L. Koopmans, R. Musinga, B. St. Pierre. *Data analysis*: L. Koopmans. *Manuscript drafting*: L. Koopmans. *Editing*: L. Koopmans, N.J. Gardiner, R.M. Palin, B. St. Pierre.

The work in **Chapters 5.2.1, 5.2.2, and 5** has been invited for submission in *Earth Science Reviews*, with the following author list: **Koopmans, L.**, Palin, R.M., Mapingire, B., Gardiner, N.J., Mamuse, A., Robb, L.J., Martin, A.R.

- *Conceptualisation and project design*: L. Koopmans, N.J. Gardiner, R.M. Palin. *Sampling and fieldwork*: L. Koopmans, B. Mapingire, A. Mamuse, A.R. Martin. *Analytical campaign*: L. Koopmans, N.J. Gardiner. *Data analysis*: L. Koopmans. *Project advisor*: R.M. Palin, N.J. Gardiner, L.J. Robb.

# Abstract

The exponential increase in demand for electric vehicles as part of the renewable energy transition is driving a surge in production of the critical metal lithium. Several forecasts have predicted a deficit in supply owing to declining rates of new economic discoveries at a time where over 50 new mines are needed to come online by 2030 to meet demand. The primary source of lithium is hard rock (pegmatite) deposits, which account for 70% of current reserves. Given their critical importance in securing sufficient lithium supply, a better understanding of how these deposits form is of vital importance to aid new discoveries. This thesis aims to contribute towards a mineral system model for lithium-rich pegmatites, by integrating new petrological modelling to detailed field-based, geochemical, and geochronological studies of the Zimbabwe craton – a relatively understudied Archean craton which supplied 9% of global lithium production in 2024. In this thesis, I propose that the Zimbabwe craton grew through episodic felsic magmatism between 3.8 and 2.5 Ga, and that major siliciclastic supracrustal successions formed through erosion as a result of continental emergence which was driven by a major orogenic episode c. 2.68 Ga. Through petrologic modelling, I show that whilst conventional pegmatite formation models are feasible, they do not sufficiently account for the necessary enrichment required to generate economic hard rock lithium deposits. Importantly, the absence of potential metasedimentary sources in source regions for lithium-rich pegmatites in Zimbabwe suggests an alternative process may have occurred. I show that the formation of intermediate, K-rich, granitoids through melt-driven crustal recycling can sufficiently enrich the source region to form the geochemical signatures found in lithium-rich pegmatites. Finally, transcurrent shear zones are proposed as fundamental components of the lithium mineral system, and future exploration should focus on delineating these structures to identify new targets.

# Contents


**1 Introduction** **1**

1.1 Lithium as a critical metal . . . . . 1
1.2 Hard rock lithium deposits . . . . . 4
1.2.1 What is a pegmatite? . . . . . 4
1.2.2 Pegmatite classification schemes . . . . . 5
1.2.3 Formation models . . . . . 6
1.3 The Archean paradox for lithium enrichment . . . . . 8
1.4 Towards a mineral system model for lithium . . . . . 9
1.5 Research motivation . . . . . 10
1.6 The Zimbabwe craton . . . . . 11
1.6.1 Adopted stratigraphic nomenclature . . . . . 14
1.7 Thesis structure . . . . . 14

**2 Methods** **17**

2.1 Dataset compilation . . . . . 17
2.2 Sample collection and preparation . . . . . 17
2.3 Geochemistry . . . . . 18
2.3.1 X-ray fluorescence . . . . . 18
2.3.2 ICP-MS . . . . . 18
2.4 Geochronology . . . . . 20
2.4.1 BSE Imaging . . . . . 20
2.4.2 Zircon geochronology . . . . . 20
2.4.3 Titanite geochronology . . . . . 21
2.4.4 Apatite geochronology . . . . . 22
2.4.5 Mica geochronology . . . . . 23
2.5 Modelling . . . . . 24
2.5.1 Petrologic modelling . . . . . 24
2.5.2 Trace element modelling . . . . . 25

2.5.3 Fractional crystallisation modelling . . . . . 26

**3 The formation of lithium-rich pegmatites through multi-stage melting 27**

3.1 Introduction . . . . . 28
3.2 Modeling Li enrichment during crustal anatexis . . . . . 29
3.2.1 Lithium in sedimentary rocks . . . . . 29
3.2.2 Lithium in the melting environment . . . . . 31
3.3 Results . . . . . 33
3.4 Multi-step distillation model for Li pegmatites . . . . . 37

**4 Structural controls on lithium mineralization in shear-zone hosted granitic pegmatites of the Zulu pegmatite field, Zimbabwe – implications for exploration 39**

4.1 Introduction . . . . . 40
4.2 Geological setting . . . . . 43
4.2.1 Geological history . . . . . 43
4.2.2 Structural history . . . . . 44
4.3 The Zulu pegmatite field . . . . . 44
4.3.1 The Zulu pegmatite field . . . . . 44
4.3.1.1 Type 1 pegmatites . . . . . 47
4.3.1.2 Type 2 pegmatites . . . . . 49
4.3.2 Lithostructural observations on the Zulu pegmatite field . . . 51
4.4 Discussion . . . . . 54
4.4.1 Relative timing and structural setting of pegmatite emplacement at Zulu . . . . . 54
4.4.2 Comparison with other pegmatite fields . . . . . 57
4.4.3 The influence of shear zones on pegmatite migration and emplacement . . . . . 61
4.4.3.1 Mechanisms of pegmatite melt extraction . . . . . 62
4.4.3.2 Pegmatite melt migration . . . . . 62
4.4.4 Implication for exploration strategies . . . . . 65
4.5 Conclusions . . . . . 66

**5 Archean tectonic evolution of the Zimbabwe Craton and the mechanisms of lithium enrichment 67**
5.1 Introduction . . . 67
5.1.1 Chapter outline . . . 67
5.1.2 Sources of TTG melts . . . 67
5.2 Results . . . 71
5.2.1 New geochronological data from the Zimbabwe craton . . . 71
5.2.1.1 U-Pb zircon standards . . . 73
5.2.1.2 Tokwe segment . . . 76
5.2.1.3 Shabani gneiss . . . 78
5.2.1.4 Gwenoro dam and surroundings . . . 80
5.2.1.5 Shangani batholith . . . 83
5.2.1.6 Granitoids around the Odzi greenstone belt . . . 85
5.2.1.7 Chillimanzi/Razi suite granites . . . 89
5.2.1.8 Northern Marginal Zone . . . 97
5.2.1.9 Apatite geochronology . . . 99
5.2.1.10 Titanite geochronology in the Irisvale-Lancaster shear zone . . . 99
5.2.1.11 Rb-Sr mica geochronology around the Zulu pegmatite field . . . 102
5.2.2 Geochemistry of the Zimbabwe craton . . . 104
5.2.3 Intrusive rocks . . . 104
5.2.3.1 Tokwe suite . . . 108
5.2.3.2 Chingezi suite . . . 108
5.2.3.3 Sesombi and Wedza suite . . . 108
5.2.3.4 Chillimanzi and Razi suites . . . 109
5.2.3.5 Northern Marginal Zone . . . 110
5.2.4 Extrusive rocks . . . 112
5.2.4.1 Belingwean group . . . 112
5.2.4.2 Lower Bulawayan . . . 112
5.2.4.3 Upper Bulawayan . . . 112
5.2.4.4 Shamvaian . . . 114
5.3 Discussion . . . 115
5.3.1 Early cratonic nuclei in the Zimbabwe Craton (3.8–3.2 Ga . . . 115
5.3.2 Quiescence, followed by renewed Mesoarchean magmatism (3.0–2.85 Ga) . . . 116

5.3.3 Plume-related growth of the craton (2.8–2.7 Ga) . . . . . 120
5.3.4 Accretion of the Western Successions and Shamvaian deposition (2.71–2.60 Ga) . . . . . 123
5.3.5 Emplacement of potassic granites (2.68–2.51 Ga) . . . . . 125
5.3.6 Emplacement of the Great Dyke (2.575 Ga) . . . . . 126
5.3.7 Lithium fertility during crustal evolution . . . . . 129
5.3.8 Conclusions . . . . . 131

**6 Conclusions** **135**
6.1 Thesis conclusions . . . . . 135
6.1.1 Modelling of pegmatite sources . . . . . 135
6.1.2 Structural controls on economic deposits . . . . . 136
6.1.3 Tectonic evolution of the Zimbabwe craton . . . . . 137
6.1.4 Implications for lithium enrichment . . . . . 138
6.1.5 Implications for exploration . . . . . 139
6.1.6 Summary . . . . . 139
6.2 Future Work . . . . . 140
6.2.1 Archean evolution of Zimbabwe . . . . . 140
6.2.2 Testing source models . . . . . 140
6.2.3 Refining structural model . . . . . 141
6.3 The lithium mineral system model . . . . . 141

**A List of sample locations** **143**
A.1 Surface samples . . . . . 144
A.2 Drill core samples . . . . . 146

**B Field photgraphs of sample locations** **147**

**C Geochronological data** **175**
C.1 Zircon U-Pb data . . . . . 176
C.2 Apatite U-Pb data . . . . . 197
C.3 Titanite U-Pb data . . . . . 200
C.4 Dioctahedral (White) mica Rb–Sr data . . . . . 206
C.5 Trioctahedral (Brown) mica Rb–Sr data . . . . . 210

**D Geochemical data** **215**

**References** **224**

# List of Figures


1.1 Lithium production (all sources) through time. . . . . 2
1.2 An overview of reported lithium resources and reserves. . . . . 3
1.3 Schematic diagrams for typical zoned and unzoned pegmatites. . . . . 3
1.4 Schematic diagram of main pegmatite formation models. . . . . 6
1.5 Time–space plot for felsic intrusive and siliciclastic supracrustal events in various cratons. . . . . 8
1.6 Simplified diagram of the mineral system model. . . . . 9
1.7 Simplified geological map of the Zimbabwe craton. . . . . 11

3.1 Violin plots of Li concentrations binned by lithological class. . . . . 30
3.2 Representative results of petrologic modeling of a metasedimentary rock and granite undergoing isobaric heating. . . . . 33
3.3 The behavior of lithium (Li) in the extracted melt during Rayleigh fractionation. . . . . 34
3.4 Evolution of Li concentrations during melting and fractionation of melt components generated during crustal anatexis. . . . . 35
3.5 Schematic petrogenetic model for generating lithium (Li)-rich pegmatites in the via crustal anatexis. . . . . 36

4.1 Geological maps of the Zimbabwe Craton and region around the study area. . . . . 42
4.2 Geological map of the main Zulu pegmatite field. . . . . 47
4.3 Representative photographs of pegmatites in the Zulu Pegmatite Field. 49
4.4 Photomicrographs from pegmatites in the Zulu pegmatite field. . . . 50
4.5 Typical deformation microstructures within Type 1 pegmatites. . . . 52
4.6 Hand sample images of Type 1 pegmatites. . . . . 53
4.7 Outcrop images of host rocks within the Zulu Pegmatite Field. . . . . 54
4.8 Thin section images of host rocks in the Zulu Pegmatite Field. . . . . 55
4.9 Image and sketch of Type 1 pegmatite in excavated pit. . . . . 56

4.10 Simplified geological map discriminating between group one and two pegmatites. . . . . 58
4.11 Schematic diagram highlighting the different styles of emplacement relative to the regional structure for pegmatites emplaced at different times during shear-dominated deformation. . . . . 60
4.12 Simplified geological maps of case study areas. . . . . 63
4.13 Schematic sketches of melt flow orientations relative to three major structural types. . . . . 65

5.1 Simplified geological map of the Zimbabwe craton, highlighting key locations discussed in this chapter. . . . . 68
5.2 Summary diagram of newly collected geochronological data. . . . . 72
5.3 Wetherill concordia plots with analyses of natural zircon 91500. . . . 73
5.4 Wetherill concordia plots with analyses of Plešovice. . . . . 74
5.5 Weighted mean plots with analyses of Maniitsoq. . . . . 75
5.6 Weighted mean plots with analyses of OG1. . . . . 76
5.7 Wetherill concordia plot with analyses of TR02. . . . . 77
5.8 Wetherill concordia plots with analyses of TR06. . . . . 77
5.9 Wetherill concordia and weighted mean plots for analyses of TR07. . 78
5.10 Wetherill concordia and weighted mean plots for analyses of TR08. . 79
5.11 Wetherill concordia plots with analyses of SG01. . . . . 79
5.12 Wetherill concordia plots with analyses of SG02. . . . . 80
5.13 Wetherill concordia plot with analyses of GW02. . . . . 81
5.14 Wetherill concordia plot with analyses of GW03. . . . . 81
5.15 Wetherill concordia plots with analyses of GW04. . . . . 82
5.16 Wetherill concordia plot with analyses of NM02. . . . . 83
5.17 Wetherill concordia plots with analyses of SC03. . . . . 84
5.18 Wetherill concordia plots with analyses of ZB01. . . . . 84
5.19 Wetherill concordia plot with analyses of ZB02. . . . . 85
5.20 Wetherill concordia plots with analyses of ZB03. . . . . 86
5.21 Wetherill concordia plots with analyses of ZB06. . . . . 86
5.22 Wetherill concordia plots with analyses of SR01. . . . . 87
5.23 Wetherill concordia plot with analyses of SR02. . . . . 88
5.24 Wetherill concordia plots with analyses of WG02. . . . . 88
5.25 Wetherill concordia plots with analyses of WG03. . . . . 89
5.26 Wetherill concordia plots with analyses of GH02. . . . . 90

5.27 Wetherill concordia plots with analyses of CH01. . . . . 90
5.28 Wetherill concordia plot with analyses of BL05. . . . . 91
5.29 Wetherill concordia plots with analyses of PG01. . . . . 92
5.30 Wetherill concordia plot with analyses of ZB05. . . . . 92
5.31 Wetherill concordia plots with analyses of ZB07. . . . . 93
5.32 Wetherill concordia plots with analyses of DP01. . . . . 94
5.33 Wetherill concordia plots with analyses of NY01. . . . . 94
5.34 Wetherill concordia plots with analyses of NY02. . . . . 95
5.35 Wetherill concordia plot with analyses of NY03. . . . . 96
5.36 Wetherill concordia plot with analyses of LP02. . . . . 96
5.37 Wetherill concordia plot with analyses of LP03. . . . . 97
5.38 Wetherill concordia plot with analyses of LP04. . . . . 98
5.39 Wetherill concordia plot with analyses of LP10. . . . . 98
5.40 Wetherill concordia plot with analyses of LP11. . . . . 99
5.41 Tera-Wasserberg plot of apatite analyses from sample GW06. . . . . 100
5.42 Tera-Wasserberg plot of apatite analyses from sample NG01. . . . . 100
5.43 Tera-Wasserburg plots of titanite analyses from ZLC32. . . . . 101
5.44 Tera-Wasserburg plots of titanite analyses from samples ZL181 and ZL182. . . . . 101
5.45 Rb–Sr isochron plots for muscovite analyses. . . . . 103
5.46 Rb-Sr isochrons of biotite analyses. . . . . 103
5.47 Normative Ab–An–Or diagram with intrusive samples from the Zimbabwe Craton and Northern Marginal Zone. . . . . 104
5.48 Harker diagrams with intrusive samples from the Zimbabwe Craton and Northern Marginal Zone. . . . . 105
5.49 Geochemical discrimination diagrams for granitoids. . . . . 106
5.50 $La/Yb_N$ vs $Yb_N$ and $Sr/Y_N$ vs $Y_N$ discrimination diagrams. . . . . 107
5.51 Trace element geochemistry of the Tokwe suite. . . . . 108
5.52 Trace element geochemistry of the Chingezi suite. . . . . 109
5.53 Trace element geochemistry of the Sesombi suite. . . . . 109
5.54 Trace element geochemistry of the Chillimanzi and Razi suites. . . . . 110
5.55 Trace element geochemistry of samples from the Northern Marginal Zone. . . . . 110
5.56 Trace element geochemistry of the Belingwean group. . . . . 111
5.57 Trace element geochemistry of the Bulawayan group. . . . . 113
5.58 Trace element geochemistry of the Shamvaian group. . . . . 114

5.59 Summary of events in the Zimbabwe craton. . . . . 115
5.60 Trace element plots comparing modelling to TTG chemistry in the Zimbabwe craton. . . . . 117
5.61 La/Yb vs Yb and Sr/Y vs. Y plots comparing modelling to TTG chemistry in the Zimbabwe craton. . . . . 118
5.62 Schematic diagram summarizing the major stages of Zimbabwe craton evolution. . . . . 119
5.63 Trace element plots comparing modelling to mafic volcanic chemistry in the Zimbabwe craton. . . . . 120
5.64 Trace element plots comparing modelling to late K-rich granite chemistry in the Zimbabwe craton. . . . . 127
5.65 A/NK vs. A/CNK and Mg # vs. $K_2O$ diagrams comparing modelling to late K-rich granite chemistry in the Zimbabwe craton. . . . . 128
5.66 Lithium compositions in melts modelled to form by melting EAT. . . 128
5.67 Lithium compositions in melts modelled to form by melting TR02. . . 130
5.68 Lithium compositions in melts modelled to form by melting ZB02. . . 130
5.69 K/Rb vs. Rb plot comparing modelling to late K-rich granite chemistry in the Zimbabwe craton. . . . . 131

B.1 Locality BL17 . . . . . 148
B.2 Locality CH01 . . . . . 148
B.3 Locality DP01 . . . . . 149
B.4 Locality GH02 . . . . . 149
B.5 Locality GH03 . . . . . 150
B.6 Gwenoro Dam . . . . . 150
B.7 Locality LP02 . . . . . 151
B.8 Locality LP03 . . . . . 151
B.9 Locality LP04 . . . . . 152
B.10 Locality LP10 . . . . . 152
B.11 Locality LP11 . . . . . 153
B.12 Locality MO01-5 . . . . . 153
B.13 Locality MU01 . . . . . 154
B.14 Locality MU03 . . . . . 154
B.15 Locality NG01 . . . . . 155
B.16 Locality NG02 . . . . . 155
B.17 Locality NM . . . . . 156

B.18 Locality NY01 . . . . . 156
B.19 Locality NY02 . . . . . 157
B.20 Locality NY03 . . . . . 157
B.21 Locality PG01 . . . . . 158
B.22 Locality SC03 . . . . . 159
B.23 Locality SC04 . . . . . 160
B.24 Locality SG . . . . . 160
B.25 Locality SR01 . . . . . 161
B.26 Locality SR02 . . . . . 161
B.27 Locality TR02 . . . . . 162
B.28 Locality TR04 . . . . . 162
B.29 Locality TR06 . . . . . 163
B.30 Locality TR07 . . . . . 163
B.31 Locality TR08 . . . . . 164
B.32 Locality WG01 . . . . . 164
B.33 Locality WG02 . . . . . 165
B.34 Locality WG03 . . . . . 165
B.35 Locality ZB01 . . . . . 166
B.36 Locality ZB02 . . . . . 166
B.37 Locality ZB03 . . . . . 167
B.38 Locality ZB04 . . . . . 168
B.39 Locality ZB05 . . . . . 169
B.40 Locality ZB06 . . . . . 170
B.41 Locality ZB07 . . . . . 171
B.42 Locality ZL01 . . . . . 172
B.43 Locality ZL09 . . . . . 172
B.44 Locality ZL11 . . . . . 173
B.45 Locality ZL15 . . . . . 173
B.46 Locality ZL16 . . . . . 174
B.47 Locality ZL20 . . . . . 174

# Chapter 1

# Introduction

## 1.1 Lithium as a critical metal

Lithium (Li) is the lightest metal and lowest density solid element in the periodic table (Rumble, 2025). It forms the basis of various pharmaceuticals (Kesler and Simon, 2015), is used as a treatment for psychiatric disorders (Rybakowski, 2020), doped in specialty ceramics to improve their thermal properties (Kesler and Simon, 2015), and is mixed into lubricating greases to improve the useable temperature range and water resistance (Delgado et al., 2006). Most importantly, lithium's very high electrochemical potential (-3.04 V vs. standard hydrogen electrode, Xie and Lu, 2020), and charge:weight ratio, make it prized in high energy density batteries. This has driven a surge in demand because of two main use-cases: firstly, efforts to increase the proportion of renewable energy in national grids are coupled with the need to balance the poorly aligned peak supply from renewable sources (e.g., wind, solar) to the consumer demand. Whilst this is currently largely done by combined cycle gas generators (CCGT) in the UK, batteries are well positioned to replace CCGTs in national grids to help achieve net-zero goals (Chowdhury et al., 2020). Secondly, the electrification of the global vehicle fleet requires a significant increase in the production of large but lightweight batteries (Benson et al., 2025). The exponential increase in electric vehicle (EV) production over the past five years has therefore caused an explosion in demand for lithium, with production attempting to follow suit (Figure 1.1). Supply is currently c. 1 Mt lithium carbonate equivalent(LCE, Figure 1.1), and demand is forecast to double in the next four years, before reaching 3 Mt by 2032 (Benchmark Mineral Intelligence, 2025). In order to meet this demand, Benchmark Mineral Intelligence (2025) predict 52 additional mines (assuming new mines are equivalent to the current average mine size) need to come online by 2030.

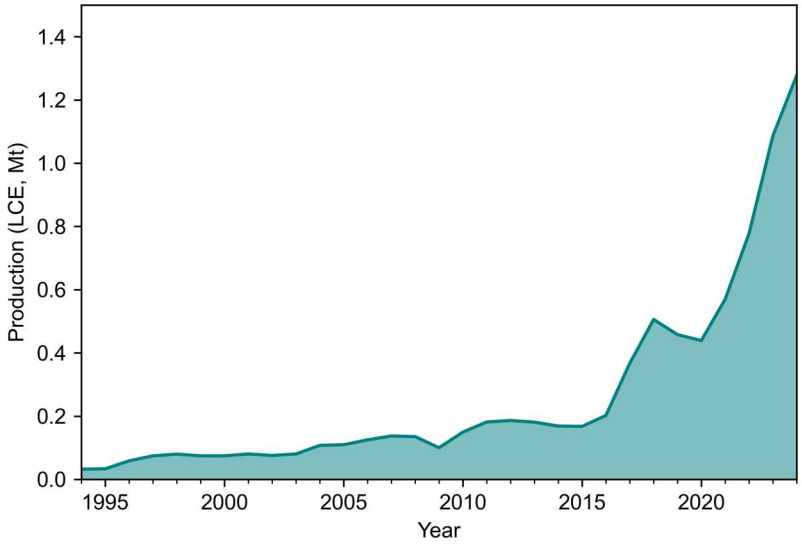


Figure 1.1: Lithium production (all sources) through time. Data reported by the United States Geological Survey (2025).

Because no metal has better physicochemical properties, lithium is unlikely to be substituted and will remain a key component of battery technology (Benson et al., 2025). Lithium is therefore one of the most critical metals in national and organisational critical minerals reports (Gardiner et al., 2024a; McNulty and Jowitt, 2021; European Commission, 2020; Nassar and Fortier, 2021), and significant research has been stimulated to better understand the ore deposit geology (Benson et al., 2025).

Lithium is sourced primarily from hard rock (pegmatite) deposits (Černý and Ercit, 2005; Müller et al., 2025; Benson et al., 2025) and closed-basin brine ("salar") deposits (Munk et al., 2016), however unconventional deposit types are also being explored (e.g., oilfield brines, clay, Putzolu et al., 2025, Benson et al., 2025). Hard rock deposits account for 40% of the currently known lithium resources, and 70% of current reserves (Figure 1.2). Given hard rock deposits are uniquely positioned to rapidly come online (Yao, 2022), a better understanding of how these bodies form, in order to find new deposits, is critical (Gardiner et al., 2024a).

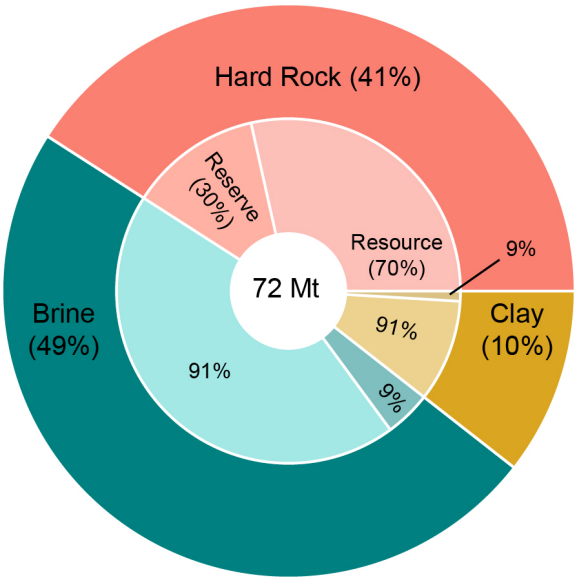


Figure 1.2: An overview of reported lithium resources and reserves (as of September 2024), classified by deposit type. Darker and lighter portions of the inner circle are reserves and resources, respectively.

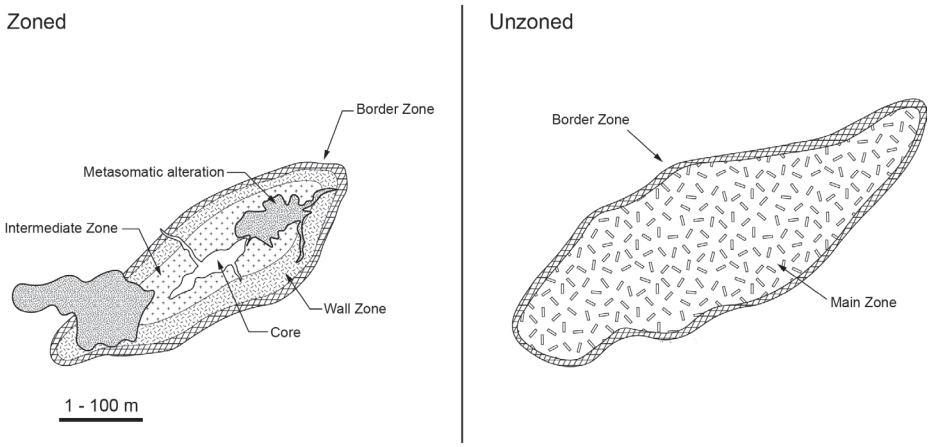


Figure 1.3: Schematic diagrams for typical zoned (left) and unzoned (right) pegmatites, outlining the standard zonation scheme. Adapted from Černý (1991a).

## 1.2 Hard rock lithium deposits

### 1.2.1 What is a pegmatite?

Granitic pegmatites (hereafter pegmatites) are small-scale, highly evolved igneous rocks which exhibit textures indicative of significant disequilibrium during crystallisation (London, 2008, 2014; Simmons and Webber, 2008). Disequilibrium results in the many distinctive features of pegmatites; large variability in crystal sizes, graphic intergrowths, and abrupt changes in mineralogy across pegmatite intrusions (London, 2014).

Experimental work has demonstrated that the pressure–temperature (P–T) conditions during crystallisation have a significant influence on which, and in what order, minerals crystallise (e.g., London, 1984; Sirbescu et al., 2017). Estimates for crystallisation conditions using pre-existing mineral geothermobarometers, however, did not always match regional P–T estimates, which led to the recognition that pegmatites can begin crystallising below the haplogranite solidus (e.g., London, 2005; Simmons and Webber, 2008). This "undercooling" is driven by the significant proportions of fluxing components, such as $H_2O$, Li, B, F, and P in the melt, which inhibit polymerisation of the silicate melt and greatly diminish the number of nucleation sites available in the system (London, 2014; Linnen, 1998; Sirbescu et al., 2017; Nabelek et al., 2010). The resultant melt is highly sensitive to perturbations, and changes in melt conditions and/or degassing of fluxing components drives rapid crystallisation and various textures observed in pegmatites (Simmons and Webber, 2008; Nabelek et al., 2010; Sirbescu et al., 2017; London, 2014).

A common feature of pegmatites is a strong mineralogical zonation (although unzoned varieties also exist, Figure 1.3). The zoning scheme of a simple pegmatite typically includes; a border zone (considered to be a chilled margin, cf. London 2014), a mineralogically equivalent but coarser wall zone, an intermediate zone (defined by the appearance of exotic, incompatible element-rich phases), and a core zone that is predominantly composed of late-stage quartz (± accessory phases). This magmatic zonation is thought to be the result of a process called *constitutional zone refinement*, where rapid crystallisation from the margin of a pegmatite body expels incompatible elements into a boundary layer between the crystallising front and the residual melt, which can become periodically saturated in exotic phases (e.g., tourmaline, phosphates, etc.) thereby generating a mineralogic zoning (London, 2014, 2018). A pegmatite is considered to be complexly zoned when metasomatic processes such as albitisation (e.g., Ballouard et al., 2020; Kaeter et al., 2018; Černý, 1991a), and

greisenisation (e.g., Černý, 1989; Fuchsloch et al., 2018; Goodenough et al., 2025) lead to a patchy and irregular replacement of earlier (magmatic) phases (Černý, 1991a, , Figure 1.3). Although zoned pegmatites can be economic (e.g., Tanco, Canada; Stilling et al., 2006), the majority of economic deposits of lithium are poorly- or un-zoned (and referred to as simple albite-spodumene pegmatites, Černý, 1991b).

### 1.2.2 Pegmatite classification schemes

Pegmatites come in many shapes and sizes, and are commonly found in swarms of 10s to 100s of individual bodies (Černý, 1991b). Several attempts have been made to group pegmatites into meaningful classes. This has been attempted on the basis of formation depth (e.g., Ginsburg and Rodionov, 1960; Ginsburg, 1984; Ye. Zagorsky et al., 2003), mineralogy (e.g., Wise, 1999; Wise et al., 2013), and geochemistry (e.g., Niggli, 1920; Landes, 1933). Those that have caught most traction incorporate all components (Černý and Ercit, 2005; Wise et al., 2022b). Pegmatites are therefore typically divided into two major groups based on geochemical affinity and mineralogy (thought to result from variations in source and depth, Muller et al., 2025).

- The LCT (Černý and Ercit, 2005) or Group 1 (Wise et al., 2022b) pegmatites are commonly enriched in lithium, caesium, and tantalum, however can also have economic quantities of rubidium, beryllium, and tin (McCaffrey and Jowitt, 2023). Group 1/LCT pegmatites are classically thought to crystallise from melts sourced (either indirectly, and staged through a parental granite, or directly) by partial melting of a metasedimentary source, and therefore have S-type (peraluminous) geochemical affinities (Chappell and White, 1992; Černý et al., 2012).

- The NYF (Černý and Ercit, 2005) or Group 2 (Wise et al., 2022b) pegmatites are commonly enriched in niobium, yttrium, and fluorine, and may additionally contain economic quantities of REEs (McCaffrey and Jowitt, 2023). Group2/NYF pegmatites are considered to have a metaigneous (i.e. amphibolite) source and occur in either anorogenic (A-type) or orogenic (I-type) settings (Černý et al., 2012).

An uncommon third group (Group 3) is distinguished by Wise et al. (2022a), which is moderately enriched in aluminium, beryllium, and boron. Other classification schemes (e.g., Černý and Ercit, 2005) often include an “Abyssal” or “Barren” group defined by an absence in exotic minerals that may enable a classification into a

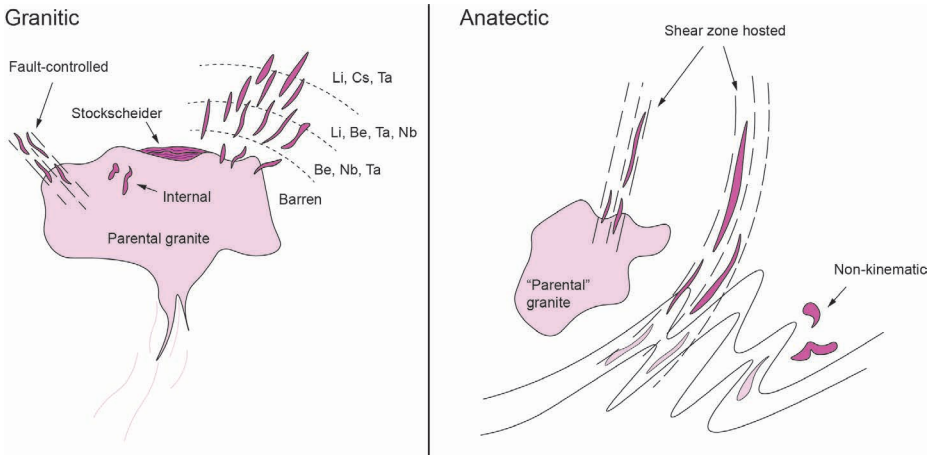


Figure 1.4: Schematic diagram outlining the two main models proposed for pegmatite formation. In the granitic model (left), fault controlled, internal, stockscheider, and regionally zoned (after Černý, 1991b) varieties are shown. In the anatectic model (right), both meta-igneous and metasedimentary sources are shown. Not to scale.

different group, however the distinction as to when a pegmatite becomes sufficiently enriched so as to become an LCT or NYF is then unclear. Wise et al. (2022b) suggests that all pegmatites can be classified based on the mineralogy of their border zone (Figure 1.3), and should therefore always be classed by their mineralogical and geochemical affinity.

Hard rock lithium deposits (including albite-spodumene pegmatites) fall under the LCT/Group 1 pegmatite class. These pegmatites typically contain quartz, alkali-feldspar, plagioclase (albite), and muscovite. Economic lithium deposits will also contain the lithium ore minerals spodumene ($LiAlSi_2O_6$, with an ideal $Li_2O$ content of 8.0 wt. %), and/or petalite ($LiAlSi_4O_{10}$, with an ideal $Li_2O$ content of 4.5 wt. %) (Bowell et al., 2020). Whether spodumene or petalite is the dominant lithium aluminosilicate is thought to be dependent on the P–T conditions of crystallisation (London, 1984). In either case, the melt must become saturated in spodumene or petalite, which occurs at c. 5000–10000 ppm Li (Maneta et al., 2015). Whether an economic lithium pegmatite is zoned or unzoned (Figure 1.3) is therefore dependent on the initial Li concentration of the melt which controls the amount of crystallisation required to achieve saturation.

### 1.2.3 Formation models

Two main formation models exist for LCT pegmatites; a granite fractionation model (cf. London, 2005; Černý et al., 2012; Cameron et al., 1949; Černý, 1991b; Černý and

Ercit, 2005; Jahns, 1953; London, 2018), and an anatectic model (cf. Stewart, 1978; Shaw et al., 2016; Müller et al., 2017; Simmons et al., 1995).

Under the granite fractionation model (Figure 1.4), pegmatites are considered to be the result of extensive (>90%) fractionation of a parental granitic melt, resulting in a volatile- (flux) and incompatible-rich residual melt (London, 2005). The residual melt may rise to the top of the granitic magma chamber, forming enriched cupolas and stockscheider intrusions (e.g., Müller et al., 2025; Roda-Robles et al., 2018, Figure 1.4). Under a suitable stress regime, low viscosity pegmatitic melts (London, 2014) can be ejected from the parental granite and generate a regional zonation pattern around a parental granite (Brisbin, 1986; Černý, 1991b). Similarly, shear zones may focus melt away from the source granite in a spatially restricted direction (Müller et al., 2025). In exceptional scenarios, fractionation can thus be traced from the primitive cumulate at the base of large granitic intrusions through to genetically related pegmatites using geochemical tracers in accessory phases (e.g., Liu et al., 2023).

By contrast, the anatectic model proposes that pegmatites can form directly from low-degree partial melting of a fertile (in the case of LCT, metasedimentary) source, forming a similarly volatile- and incompatible-rich melt (Simmons et al., 1995; Shaw et al., 2016; Müller et al., 2017, Figure 1.4). The low degree of melt promotes high degrees of enrichment, and the composition of the melt is controlled by restitic assemblage (e.g., Kunz et al., 2022; Knoll et al., 2023). The melt can then either migrate passively, or be concentrated along a shear zone prior to emplacement (Bhatt et al., 2019; Müller et al., 2025; Demartis et al., 2011). This model is mostly invoked in areas with no apparent parental granite (Shaw et al., 2016; Müller et al., 2017), or in areas where crystallisation ages of pegmatites are younger (10–50 Myr) than neighbouring granites (Brou et al., 2022; Goodenough et al., 2014; Zhang et al., 2016; Liu et al., 2025).

Although strong cases have been made for both models for pegmatites in general, the application of these models to economically extractable pegmatite deposits is uncertain, as the degree of enrichment either model can invoke is not well constrained. Given the extreme levels of enrichment required to generate spodumene (5000–10000 ppm Li, Maneta et al., 2015) from incipient crystallisation (in the case of albite-spodumene pegmatites), a petrogenetic model which can suitably explain the formation of economic hard rock lithium deposits must be able to account for this (Gardiner et al., 2024b).

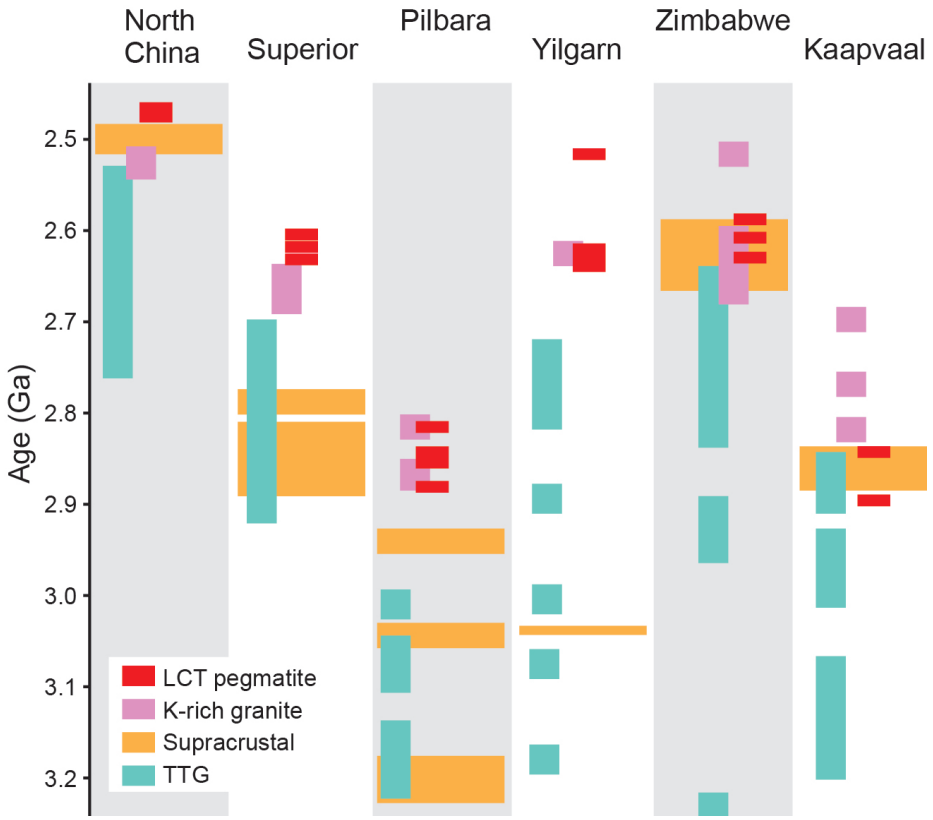


Figure 1.5: Time–space plot for felsic intrusive and siliciclastic supracrustal events in the North China, Superior, Pilbara, Yilgarn, Zimbabwe, and Kaapvaal cratons. Modified from Gardiner et al. (2024b). TTG: tonalite–trondhjemite–granodiorite.

## 1.3 The Archean paradox for lithium enrichment

Archean terranes are the current largest single source of battery grade lithium, and are therefore arguably the most prospective lithium provinces (Bowell et al., 2020). Understanding Archean crustal formation and evolution is therefore a necessary pre-requisite to understanding how and why these terranes are so well endowed in lithium.

Archean cratons fundamentally develop through a protracted (or multiple discrete) period(s) of juvenile continental crust (termed tonalite–trondhjemite–granodiorite, or TTG) formation during their early history to form cratonic nuclei (Cawood et al., 2022; Brown et al., 2020, Figure 1.5). These cratonic nuclei subsequently assembled, thickened, and stabilised during the late Archean to form stable cratonic blocks, which is commonly linked to horizontal plate motions, a defining feature of plate tectonics (Palin et al., 2020; Cawood et al., 2018). This cratonic assembly coincides with the first appearance of potassium-rich granites in the late Meso- to Neoarchean, which is possibly driven by a shift in geodynamics (Gardiner et al., 2024b; Nebel et al., 2018,

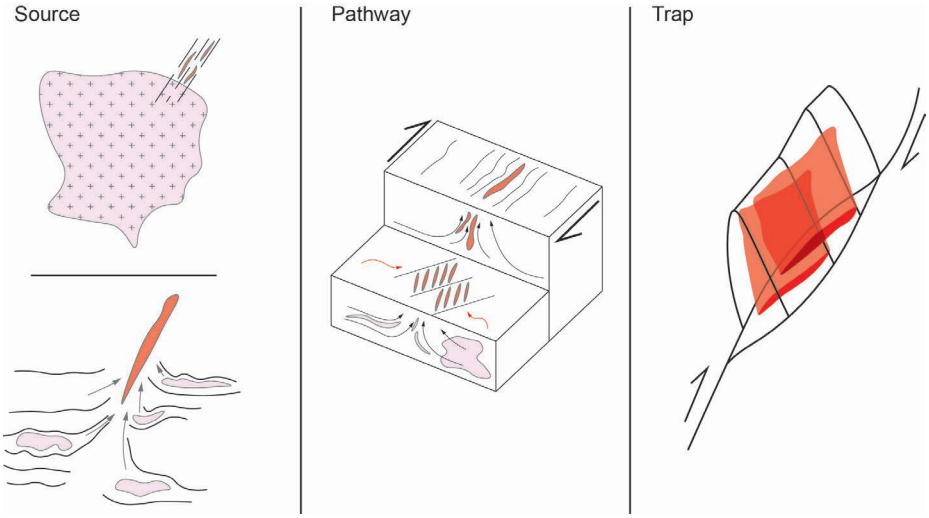


Figure 1.6: A simplified diagram denoting the three main stages (source, pathway, and trap) of the mineral system model (in sequential order from left to right) studied in this thesis.

Figure 1.5). In many cases, this is also when LCT/Group 1 pegmatites first occur (Figure 1.5). Assuming LCT/Group 1 pegmatites must incorporate metasedimentary material into their source, they may therefore signify that crustal recycling has matured in the cratonic block (Kendall-Langley et al., 2020; Gardiner et al., 2024b; Laurent et al., 2014; Dittrich et al., 2019).

However, in some cratons, such as the Zimbabwe or Kaapvaal, pegmatites form contemporaneously with (or precede) the formation of major sedimentary cover successions (Figure 1.5). This raises questions as to how sedimentary material could have been incorporated into the melt source.

This is the Archean lithium paradox — do LCT/Group 1 pegmatites record recycling of continental crust through a cycle of erosion and deposition, followed by burial and melting, or are there other mechanisms to generate LCT/Group 1 signatures?

## 1.4 Towards a mineral system model for lithium

To better explore for lithium-rich pegmatites, a mineral system model (Wyborn et al., 1994; Hagemann et al., 2016) must be developed which accounts for the paradox described above (Figure 1.6). The mineral system model approach for use in exploration for other commodities arose due to the observation that many mineral deposits have distinct signatures on various geologic scales, and are commonly clustered into provinces that are particularly enriched in select elements (e.g., Carlson, 1991). In

its simplest sense, a mineral system model for lithium must appropriately delineate a source which can sufficiently enrich a melt in lithium to form albite–spodumene pegmatites; a pathway that enables extraction and migration of the melt from the source region to final emplacement; and a trap that controls the spatial distribution and orientation of individual pegmatite intrusions (Figure 1.6). Subsequent mineralisation and preservation of the ore-forming minerals of interest during later processes are pivotal for the ore deposit to persist through time.

## 1.5 Research motivation

In this thesis, I use the Zimbabwe craton as a case study to test our understanding of lithium pegmatite petrogenesis, and thus contribute towards a robust mineral system model for economic hard rock lithium deposits. Given Zimbabwe is particularly well endowed in lithium (supplying 9% of global production in 2024; US Geological Survey, 2025), and it contains a craton in which siliciclastic-dominant supracrustal belts are unlikely to have been a source component in the melting environment (Figure 1.5), the Zimbabwe craton is an excellent natural laboratory to challenge our current petrogenetic models for lithium-rich pegmatites.

In order to do this, a more holistic understanding of the broader Archean crustal evolution in Zimbabwe is required, which better integrates the intrusive (TTG) history to the tectonic models developed primarily from studies on the supracrustal successions (e.g., Wilson et al., 1995; Jelsma et al., 2021). New tools have recently been developed that allow us to do this more efficiently, and in this thesis I will integrate detailed geochronological and geochemical analyses and state-of-the-art thermodynamic models (e.g., MAGEMin, Riel et al., 2022), with traditional field-based structural studies to develop an understanding of the relative timing of lithium-rich pegmatite formation in the broader cratonic evolutionary context.

More broadly, this research will therefore provide insight into whether sedimentary material is a necessary component in the source of LCT/Group 1 pegmatites, and demonstrate how a more robust understanding of the regional geologic (and structural) history can enable more efficient exploration targeting for deposits with small surface footprints.

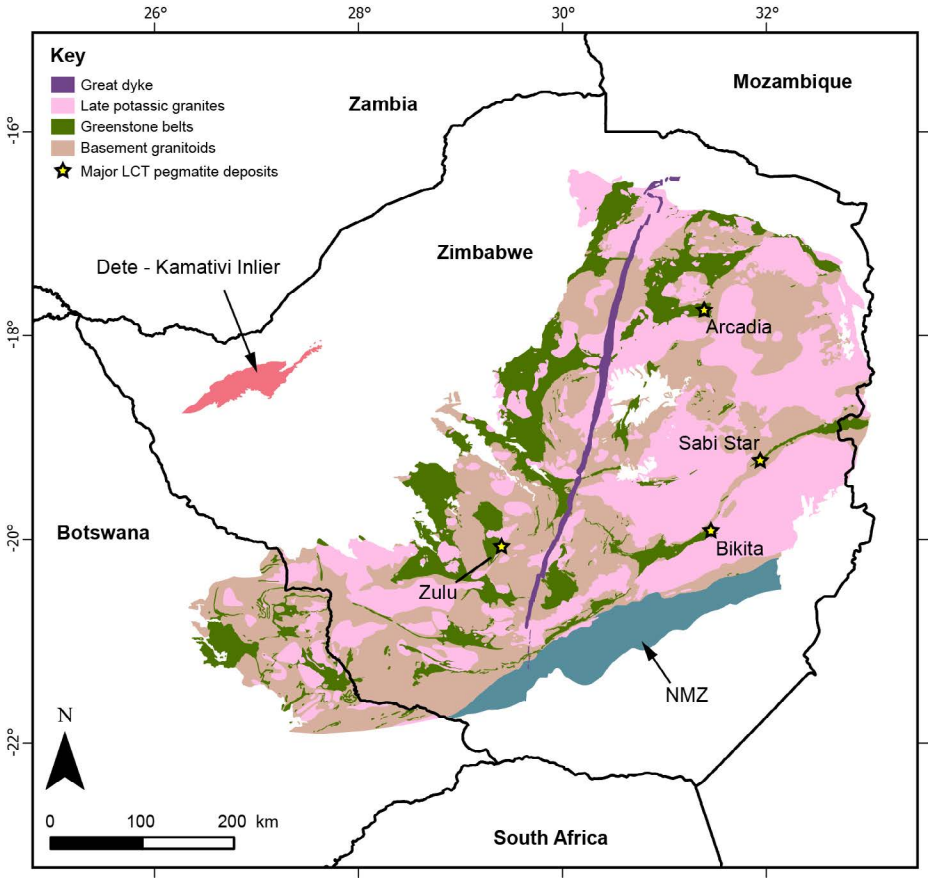


Figure 1.7: Simplified geological map of the Zimbabwe craton (modified from Ncube, 1994). Both the central craton, northern marginal zone (NMZ) and the Dete–Kamativi inlier are highlighted. Cover sequences and bounding orogens are white.

## 1.6 The Zimbabwe craton

The Zimbabwe craton is an Archean cratonic block with a present-day surface area of c. 300 000 km$^2$ (Figure 1.7, Jelsma et al., 2021; Ncube, 1994). Extending from north-east Botswana, through Zimbabwe, into western Mozambique, the craton is composed of Eo- to Neoarchean TTGs, Neoarchean potassic granites, and a series of greenstone belts that are scattered across the craton (Hofmann et al., 2022; Macgregor, 1951; Moorbath et al., 1976; Taylor et al., 1991; Wilson et al., 1995; Blenkinsop et al., 1997). The Zimbabwe craton is notably one of the most fertile terranes in Africa for hard rock lithium deposits (Goodenough et al., 2025).

The craton is bound by five orogenic belts; the Limpopo belt (c. 2000 Ma) to the south (Kamber et al., 2015), the Magondi belt (c. 1800-2000 Ma) to the west (Master et al., 2010), the Pfunzi (2600 Ma, Vinyu et al. 2001) and Zambezi belts (c. 500-850

Ma) to the north (Hanson et al., 1994; Goscombe et al., 2020; Kuribara et al., 2019), and the Mozambique belt to the east (Chaúque et al., 2017). Three major periods of TTG magmatism have been identified during cratonic growth; a 3.6-3.2 Ga magmatic episode (Horstwood et al., 1999; Dodson et al., 2001; Taylor et al., 1991; Wilson et al., 1995; Hofmann et al., 2022), a 3.0–2.85 Ga episode (Wilson et al., 1995; Jelsma et al., 2021), and major craton expansion at 2.7–2.6 Ga (Wilson et al., 1995; Chagondah et al., 2023; Jelsma et al., 1996; Blenkinsop et al., 1997). Cratonisation culminated in the emplacement of voluminous potassic granites (2.68–2.54 Ga, Jelsma et al. 2021), and finally the emplacement of the Great Dyke (2.575 Ga, Oberthür et al., 2002).

Each intrusive event has a corresponding extrusive (predominantly mafic volcanic) succession preserved in the greenstone belts throughout the craton. These were initially subdivided into the Magnesian (Sebakwian), Lower Series (Bulawayan), and Upper Series (Shamvaian) supergroups (in younging order, Macgregor, 1947, Stagman, 1978), Later revision by Wilson (1979) further subdivided the Bulawayan supergroup into the Lower and Upper Greenstones, proposing a regional unconformity between the two. Further work, most notably in the Belingwe greenstone belt (Bickle et al., 1993; Martin et al., 1993) introduced a Belingwean succession, which encompassed the majority of the Lower Greenstone succession of Wilson (1979) (Wilson et al., 1995). More recent work has proposed a two final stratigraphic divisions; in the upper Bulawayan, a distinction was introduced between the Western and Eastern succession, largely driven by difficulties in correlating the stratigraphy between greenstone belts along the western margin and central parts of the craton (e.g., Wilson et al., 1995; Jelsma et al., 2021), and a separation of the Shamvaian (the major supracrustal siliciclastic cover sequence, Figure 1.5) into an upper and lower Shamvian (Wilson et al., 1995). Given inconsistent use of the stratigraphic nomenclature of Zimbabwe, an outline of the stratigraphy as used in this study is outlined in Section 1.6.1.

Over the past half century, the tectonic evolution of the Zimbabwe craton has been the focus of considerable debate, with two contrasting models having been proposed. A vertical accretion and growth model is favoured, in which the stratigraphy of the greenstone belts can be correlated across the craton (e.g., Bickle et al., 1993; Blenkinsop et al., 1993; Hunter, 1998; Macgregor, 1951; Wilson et al., 1995), whereas an allochtonous, horizontal accretion model was spearheaded by Kusky and Kidd (1992, and supported by other authors (e.g., Dirks et al., 2002; Hofmann et al., 2001; Jelsma and Dirks, 2002; Kusky, 1998; Hofmann and Kusky, 2004).

Further uncertainty in the Archean evolution of the craton is the nature of the Northern Marginal Zone (NMZ), which is exposed along the south-eastern margin of the craton and has classically been considered part of the Limpopo belt (Fedo et al., 1995; Kamber and Biino, 1995; Rollinson and Blenkinsop, 1995). However, reinterpretation of earlier work (Frei et al., 1999; Berger et al., 1995; Blenkinsop, 2004; Rollinson and Whitehouse, 2011) by Rollinson (2022) proposed that the NMZ is a deep-crustal equivalent of the Zimbabwe craton. Similarly, recent geochronology has revealed that the Dete-Kamativi inlier (Figure 1.7), previously considered to have exclusively Magondi-age protoliths (Master et al., 2010) also contains Archean protoliths, potentially expanding the footprint of the craton (Glynn et al., 2020).

Whilst recent reviews of geology of the Zimbabwe craton have primarily focused on reconciling the supracrustal stratigraphy (e.g., Jelsma et al., 2021), attempts at fully integrating the intrusive history of the craton remain limited, largely due to the limited number of coupled geochronological and geochemical analyses on the intrusive suites. Given the ongoing debates concerning the genesis of TTG magmas during the Archean, which form major components of all cratons worldwide, alongside their implications for the geodynamic characteristics of the early Earth (cf. Palin et al., 2020), improving our understanding of TTG formation in the Zimbabwe craton may shed light on evolution and stabilisation of the Zimbabwe craton as a whole (e.g., Bédard, 2018; Moyen and Martin, 2012; Wyman, 2013).

Central to the debate around the stabilisation of Archean cratons is whether potassic granites, are preceded by continental emergence and sedimentation, or else form due to crustal thickening, which promotes sedimentation and the formation of supracrustal cover sequences (Chowdhury et al., 2021; Reimink and Smye, 2024; Roberts, 2024). In the Zimbabwe craton potassic granites cover c. 50% of the presently exposed area (Blenkinsop and Treloar, 2001); thus, investigation of the genesis of these evolved melts will shed light on the nature of tectonics in and around the craton, and has implications for lithium enrichment. Given lithium-rich pegmatites are thought to require metasedimentary rocks in their source region (in both granite-fractionation and anatectic models) to generate their peraluminous signatures (Černý, 1991a; Černý et al., 2012; Martin and De Vito, 2005), the absence of voluminous sedimentary successions that represent potential source material (Jelsma et al., 2021, Figure 1.5) provides an interesting conundrum that needs to be resolved (Section 1.3).

### 1.6.1 Adopted stratigraphic nomenclature

This study adopts the following lithostratigraphic classifications (adapted from Blenkinsop et al., 1997 and Jelsma et al., 2021):

- Sebakwian group: The oldest greenstone belt group, comprised of tightly infolded remnants within the Tokwe and Rhodesdale terranes.
- Belingwean group: Named after the Belingwe greenstone belt which contains the type section, this group encompasses stratigraphy deposited or erupted between c. 3.1–2.8 Ga. Here, this group is expanded to include the Buhwa stratigraphy, which otherwise is excluded from traditional stratigraphic models.
- Bulawayan group: Largely consistent with that defined by Wilson et al. (1995) to comprise of the Koodoovale–Manjeri–Reliance–Zeederberg–Cheshire succession (as seen in the Belingwe greenstone belt, Martin et al., 1993), and equivalent formations in other greenstone belts that were deposited c. 2.75–2.70 Ga (Hofmann et al., 2024; Prendergast and Wingate, 2013).
- Western Succession: Broadly consistent with that defined by Wilson et al. (1995) and Jelsma et al. (2021), and comprises of the successions along the western margin of the Sebakwe protocraton which do not directly correlate to the Bulawayan group (discussed in detail below).
- Shamvaian group: The final supracrustal succession in the stratigraphy of the Zimbabwe craton, largely comprised of siliciclastic sediments deposited unconformably above earlier groups within syntectonic basins (discussed in detail in Chapter 5).

## 1.7 Thesis structure

This thesis will develop the building blocks for a mineral system model by working towards unraveling the mechanisms which can sufficiently enrich lithium in the source, and how these melts can subsequently migrate and be emplaced into sufficiently large deposits to form economic bodies. This will be done by using the Zimbabwe craton as a case study.

I will first outline the methods that were used to do this work (Chapter 2), followed by a modelling-based approach to testing various source models for lithium-rich pegmatites (Chapter 3). In Chapter 4, I will present a focused case study on the Zulu

pegmatite field (Figure 1.7), constraining the timing of and controls of emplacement relative to regional deformation events. In Chapter 5, I will present the results of the geochronological and geochemical campaigns completed on samples from the Zimbabwe craton. The complete work is synthesised into a revised tectonic model for the Zimbabwe craton, integrating the new data collected with previous work. Finally, the main findings of the thesis are summarised in Chapter 6.

# Chapter 2

# Methods

## 2.1 Dataset compilation

A dataset of published geochemical and geochronological data was compiled on relevant samples collected from the Zimbabwe craton. Samples were grouped into basement (i.e., granitoids) and greenstone (i.e., volcanic and sedimentary cover successions), and where available all possible context (including ages) for the sample retained. Geochemical data were compiled into a standardized reporting style. In some instances, the same samples were measured multiple times in different studies – in these cases, the most precise analyses were incorporated into the compilation. I also expanded the geochronological compilation presented in Jelsma et al. (2021), with analyses published since 2021, and included this into the new compilation

In total, the present compilation (including samples analysed in this study) comprises of 851 greenstone samples, and 300 basement samples. A total of 382 ages have been compiled, including 141 U–Pb magmatic crystallization ages.

## 2.2 Sample collection and preparation

Samples of basement units were collected during field campaigns to Zimbabwe in 2022, 2023, and 2024 (Appendix A). Sample collection focused on regions with limited published U-Pb geochronology and/or geochemistry and aimed to capture the full suite of magmatic events within the craton based on literature and observed field relations. Individual samples were 2–3 kg, and sampled localities logged using a Garmin GPSMap 62s and photographed using a Nikon D7200 DSLR camera.

Initial sample preparation was conducted at the Department of Earth Sciences, University of Oxford, UK. Samples were catalogued and imaged before being split using a hydraulic press. An off cut of each sample was crushed using a steel jaw

crusher to produce fragments <5 mm in diameter. Thirty grams of material was separated using a riffle splitter and placed into agate mortars with 10-mm agate balls for pulverisation. Samples were milled to <200 $\mu$m using a planetary ball mill, running for 20 minutes at 200 rpm and switching rotation direction every five minutes.

For *ex situ* geochronology, 500 g aliquots of crushed (not pulverised) material were dry-sieved to +100/-212 and +212/-500 $\mu$m and washed to remove fine residue. The sieved material was then panned under ethanol, and the heavy fraction picked under a binocular microscope. The mineral separates were then placed neatly on double sided electrical tape and mounted in Metprep EPO-FLO resin to produce standard 25 mm mineral mounts. Once cured, the mineral mounts were ground down to expose the cores of the mineral separates using grit paper, and polished in stages using 9 $\mu$m, 6 $\mu$m, 3 $\mu$m, and finally 1 $\mu$m polycrystalline diamond suspension paste on cloth lapping plates.

## 2.3 Geochemistry

### 2.3.1 X-ray fluorescence

X-ray fluorescence (XRF) was performed at Franklin and Marshall College, USA. One gram of each sample was dehydrated at 950 °C in a muffle furnace to calculate initial loss on ignition. A 400 mg aliquot was subsequently hand-mixed with 3600 mg of lithium tetraborate flux. The mixtures are then transferred to a Spex Mixer Mill for 10 minutes to homogenise. The mixtures were heated over a Meeker burner in a ∼95% Pt – 5% Au capped crucible with the addition of a 2% solution of lithium iodide (to reduce viscosity) until fully liquefied. The samples were then quenched on the crucible lid to form the flux beads for subsequent analyses. X-ray fluorescence was performed on a Malvern PANalytical Zetium XRF to calculate the major oxide composition of each sample – i.e. $SiO_2$, $Al_2O_3$, $Fe_2O_3$(T), MnO, $K_2O$, $Na_2O$, $TiO_2$, $P_2O_5$, CaO, MgO.

### 2.3.2 ICP-MS

Trace element concentrations of samples were obtained via inductively-coupled-plasma mass spectrometry (ICP-MS) at the Department of Earth Sciences, University of Oxford, UK. Fifty milligram powdered aliquots of each sample underwent a HF:$HNO_3$ Parr Bomb digestion method (adapted from Okina et al., 2016). Aliquots were measured on a Sartorius five-digit mass balance (precision ± 0.1 mg) three times, and

average masses were taken forward. Twelve sample aliquots, three blanks, and three standards (USGS standards GSP-2 or G-2) at a time were subsequently placed into 3mL octagonal Teflon vials (hex nuts) and 400 $\mu$L 29M HF + 600 $\mu$L 16M $HNO_3$ added to each vial prior to capping. Three hex nuts were then placed into each PTFE liner, to which 5 mL 8M $HNO_3$ was added to equalize pressure within the hex nuts during digestion. The PTFE liners were capped and placed into the steel jacket of Parr digestion vessels, screwed tight, and heated to 196 °C for 18 hours.

Once cooled, hex nuts were extracted from the digestion vessels, uncapped and heated on a hot plate to dryness. 500 $\mu$L 16M $HNO_3$ was then added to the dried residue and heated to dryness three times to dissolve any fluorides produced during the initial digestion phase. Dry downs were performed in ISO Class 5 laminar flow hoods within ISO Class 7 clean laboratories to minimize contamination to the samples. Following the drying steps, the residue was dissolved by adding 1 mL 8M $HNO_3$ to the hex nuts and capped, placed back into PTFE liners (to which 5 mL 8M $HNO_3$ was added), and sealed into Parr digestion vessels. The digestion vessels were left in an oven for 12 hours at 180 °C. Upon extraction from the digestion vessels, the sample solutions were visually assessed for clarity. If solutions were not clear, the digestion was re-run. Otherwise, the solution was dried down and re-diluted in 2% (w/w) $HNO_3$ for ICP-MS analyses.

An ESI PrepFAST autosampler and autodiluter was used to manage throughput, additional dilution, and the addition of internal analytical standards (rhenium and rhodium) to correct for instrumental drift. Samples, standards, and blanks were analysed for a suite of 43 trace and rare earth elements using a PerkinElmer NeXION 350D quadrupole ICP-MS. Precision across the run was calculated using the relative standard deviation (RSD), which was consistently <5% for most elements, and all below 10%. USGS standards GSP-2 and G-2 were used to verify complete digestion of refractory phases (e.g., zircons), as these minerals typically control the whole-rock budget of key trace elements (e.g., REEs, Zr, Hf). The detection limit was determined as ten times the standard deviation of ten back-to-back blank measurements and is typically <0.1 ppm. Analytical accuracy was assessed using the river reference standard SLRS-6, with external analytical uncertainties of <5%.

## 2.4 Geochronology

### 2.4.1 BSE Imaging

For *ex situ* analyses, samples were imaged to aid spot-selection using an FEI Quanta 650 FEG scanning electron microscope (SEM) equipped with a lens-mounted concentric backscatter detector (CBS) and a single energy dispersive (ED) Oxford Instruments X-Max50 spectrometer. The detectors are controlled by Oxford Instruments AZtec software, and spectral resolution is calibrated periodically to the position and intensity of a Mn K$\alpha$ peak (5.895 keV) achieving <124 eV at 20 kcps (kilo-counts per second). A specimen working distance of 10 – 12 mm was used. Mosaic-stitched backscatter electron (BSE) images were collected at an accelerating voltage of 20 kV, spot 4.0 with the final lens aperture of 30 $\mu$m, yielding a spot size of ca. 6 $\mu$m and X-ray output rates up to 35 kcps. BSE images were stitched using the AZtec software which controls the instrument.

### 2.4.2 Zircon geochronology

Zircons from basement units in the Zimbabwe Craton were analysed across seven analytical sessions *ex situ* from resin mounts by laser ablation inductively-coupled-plasma mass spectrometry (LA-ICP-MS). Analyses were carried out at the St Andrews Geochronology (StAGE) Laboratory using a New Wave UP-213 Nd:YAG 213 nm ablation system. The ablated material was sent to an Agilent 8800 'triple quadrupole' QQQ-ICPMS for simultaneous U–Pb isotopic and trace element analysis. The aerosol produced during ablation was carried to the mass spectrometer via an Ar-He (880 ml $min^{-1}$ Ar, 775 ml $min^{-1}$ He) mixture with $N_2$ gas (10 ml $min^{-1}$) added to the aerosol stream to enhance sensitivity. Individual zircons were ablated using a 30 or 40 $\mu$m static circular spot, with the laser repetition rate set to 10 Hz, 45% power, yielding an approximate fluence of 3.5–4.5 J $cm^{-2}$ measured at the sample.

Natural zircon reference materials were measured approximately every 10 unknowns during each analytical run and the drift between reference material brackets was corrected using a step–forwards function.

Dwell times for U, Th, and Pb isotopes on the Agilent were 10 ms for $^{202}$Hg and $^{232}$Th, 30 ms for $^{204}$Pb, 40 ms for $^{206}$Pb, 70 ms for $^{207}$Pb, and 20 ms for $^{208}$Pb and $^{238}$U. Measurements were collected using 2 s of background measurement, 30 s of ablation time, with a 30 s washout between samples. Isotopic data were reduced with the Iolite 4 software package (Paton et al., 2011) using the U-Pb data reduction scheme (DRS; Paton et al., 2010) with a smooth cubic spline to model down-hole fractionation.

Natural zircon 91500 (Horstwood et al., 2016; Wiedenbeck et al., 1995) was used as a primary standard to calibrate downhole fractionation of U and Pb. Reference zircons Maniitsoq (Marsh et al., 2019), OG1 (Stern et al., 2009) and Plešovice (Sláma et al., 2008) were used as secondary standards to validate U-Pb data. Final U–Pb ages were calculated using IsoplotR (Vermeesch, 2018), and analyses were considered if these defined a statistical uniform population. The ages for unknowns are reported with 2 SE propagated uncertainties calculated by iolite and are uncorrected for common Pb.

Dwell times for trace elements were 10 ms for $^{85}$Rb, $^{153}$Eu, and $^{157}$Gd, 20ms for $^{7}$Li, $^{118}$Sn, $^{139}$La, $^{140}$Ce, $^{141}$Pr, $^{146}$Nd, and $^{147}$Sm, and 50 ms for $^{31}$P, $^{43}$Ca, $^{47}$Ti, $^{49}$Ti, $^{89}$Y, $^{91}$Zr, $^{93}$Nb, $^{159}$Tb, $^{163}$Dy, $^{165}$Ho, $^{166}$Er, $^{169}$Tm, $^{172}$Yb, $^{175}$Lu, $^{178}$Hf and $^{181}$Ta. Measurements were collected using 2s of background measurement, 30s of ablation time, with a 30s washout between samples. Isotopic data were reduced with the Iolite 4 software package (Paton et al., 2011) using their trace element DRS, normalized to natural zircon 91500.

### 2.4.3 Titanite geochronology

In-situ analyses on syn-kinematic titanite crystals were conducted on 30 $\mu$m polished thin sections of samples from within the Irisvale–Lancaster shear zone. Titanite crystals were analysed for simultaneous U–Pb geochronology and trace element geochemistry by LA-ICP-MS at the Institute for Geochemistry and Petrology, ETH Zurich, Switzerland, using an ASI RESOlution S-155 193-nm ArF excimer laser ablation system connected to a Thermo Element XR sector-field ICP-MS. The titanites were ablated using a 29 $\mu$m static circular spot, with laser fluence of $\sim$2.5 J cm$^{-2}$, at a repetition rate of 4 Hz. Individual analyses began with 28 s of gas blank followed by 30 s of ablation. The ablated material was mixed in the S-155 Laurin Technic ablation cell with a carrier gas composed of helium (ca. 0.5 L min$^{-1}$) and a make-up gas composed of argon (ca. 0.9–0.99 L min$^{-1}$) and nitrogen (2 mL min$^{-1}$), homogenized, and introduced to the plasma torch.

The following masses were measured: $^{25}$Mg, $^{27}$Al, $^{29}$Si, $^{31}$P, $^{43}$Ca, $^{45}$Sc, $^{49}$Ti, $^{51}$V, $^{55}$Mn, $^{57}$Fe, $^{65}$Cu, $^{66}$Zn, $^{88}$Sr, $^{89}$Y, $^{90}$Zr, $^{93}$Nb, $^{115}$In, $^{118}$Sn, $^{138}$Ba, $^{139}$La, $^{140}$Ce, $^{141}$Pr, $^{146}$Nd, $^{147}$Sm, $^{153}$Eu, $^{157}$Gd, $^{159}$Tb, $^{163}$Dy, $^{165}$Ho, $^{166}$Er, $^{169}$Tm, $^{172}$Yb, $^{175}$Lu, $^{178}$Hf, $^{181}$Ta, $^{182}$W, $^{202}$Hg, $^{204}$Pb, $^{206}$Pb, $^{207}$Pb, $^{208}$Pb, $^{232}$Th, $^{235}$U, and $^{238}$U. Dwell times for $^{206}$Pb and $^{207}$Pb was 50 ms, 20 ms for $^{238}$U, and for all other masses was 11 ms.

The U- and Pb-isotopic ratios were derived using MKED-1 (1517.32 $\pm$ 0.1 Ma; Spandler et al., 2016) as primary reference material and the UcomPbine data reduction scheme available in Iolite 4 (Chew et al., 2014; Paton et al., 2011; Petrus

and Kamber, 2012). Final titanite U–Pb ages were determined using unanchored regressions in IsoplotR (Vermeesch, 2018) via linear regression on Tera-Wasserburg concordia plots, with the lower intercepts interpreted as crystallization ages. Analytical accuracy for U–Pb was assessed by measuring BLS (1049 ± 1.3 Ma; Aleinikoff et al., 2007), 94-35 (51.5 ± 0.7 Ma; Dana et al., 2023), Otter West (147.9 ± 1.2 Ma; Butler et al., 2002), Ecstall West (91.5 ± 1.0 Ma; Butler et al., 2002), Khan River (516.3 ± 1.3 Ma; Mazoz et al., 2022), and Bear Lake (1067.8 ± 0.7 Ma; Mazoz et al., 2022) as secondary standards. Trace elements were calibrated against NIST SRM610 (Jochum et al., 2011) as primary reference material, and validated by measuring GSD-1G (Guillong et al., 2005) as the secondary reference material.

### 2.4.4 Apatite geochronology

Apatite grains from samples GW06 and NG01 were analysed from mineral mounts as the samples had no identifiable and/or measurable zircon crystals. Apatite crystals were analysed for U–Pb geochronology and trace element geochemistry by LA-ICP-MS using the same analytical equipment described in section 2.4.3. Apatite cyrstals were ablated using a 43 $\mu$m static circular spot, with a laser fluence of $\sim$3 J cm$^{-2}$ and a repetition rate of 4 Hz. Analyses followed the same protocol (28 s of gas blank, 30 s of ablation) as titanite, with a make-up gas composed of argon (ca. 0.25 L min$^{-1}$) and nitrogen (2 mL min$^{-1}$).

The following masses were measured: $^{24}$Mg, $^{27}$Al, $^{29}$Si, $^{31}$P, $^{43}$Ca, $^{49}$Ti, $^{51}$V, $^{53}$Cr, $^{55}$Mn, $^{57}$Fe, $^{85}$Rb, $^{88}$Sr, $^{89}$Y, $^{90}$Zr, $^{93}$Nb, $^{137}$Ba, $^{139}$La, $^{140}$Ce, $^{141}$Pr, $^{146}$Nd, $^{147}$Sm, $^{151}$Eu, $^{157}$Gd, $^{159}$Tb, $^{163}$Dy, $^{165}$Ho, $^{166}$Er, $^{169}$Tm, $^{172}$Yb, $^{175}$Lu, $^{178}$Hf, $^{181}$Ta, $^{202}$Hg, $^{204}$Pb, $^{206}$Pb, $^{207}$Pb, $^{208}$Pb, $^{232}$Th, $^{235}$U, and $^{238}$U. Dwell times for $^{206}$Pb and $^{207}$Pb was 50 ms, 20 ms for $^{238}$U, and for all other masses was 11 ms.

The U- and Pb-isotopic ratios were calibrated using the Durango apatite (31.44 ± 0.18 Ma; McDowell et al., 2005) as primary reference material using the UcomPbine data reduction scheme in Iolite 4 (Chew et al., 2014; Paton et al., 2011; Petrus and Kamber, 2012). Final ages were determined using unanchored regressions in IsoplotR (Vermeesch, 2018), interpreting the lower intercept of a linear regression in Terra-Wasserburg space as the crystallization age. Analytical accuracy for U–Pb was assessed using Kovdor (377.5 ± 3.5 Ma; Chew et al., 2011), MAD (473.46 Ma ± 0.0 Ma; (Thomson et al., 2012), and Ap42 (CITE) as secondary standards. Trace elements were calibrated against G-NIST610 (Jochum et al., 2011) as primary reference material, and validated against GSD-1G (Guillong et al., 2005).

### 2.4.5 Mica geochronology

Lithium-rich muscovite from within the Zulu pegmatite field (Chapter 4), and biotite from the surrounding host rocks were analysed in-situ on 30 $\mu$m polished thin sections. Mica crystals were simultaneously analysed for Rb–Sr geochronology and trace elements by LA-ICP-MS at the Fipke Laboratory for Trace Element Research (FiLTER) at the University of British Columbia Okanagan, Canada following the methodology described in Larson et al. (2023, 2024). Analyses were conducted using an ESL Excimer 193 nm ArF laser equipped with a TwoVol3 sample chamber connected to an Agilent 8900 triple quadrupole ICP-MS. Individual crystals were ablated using a 50 $\mu$m diameter circular static spot, a laser fluence of 3.5 J cm$^{-2}$, and a repetition rate of 8 Hz. The ablated material was carried by a helium carrier gas (0.3 L min$^{-1}$), and mixed with a make-up gas composed of argon (0.9 L min$^{-1}$) and nitrogen (25 mL min$^{-1}$). Analyses consisted of 25 s of ablation, followed by 15 s of washout by a gas blank.

The following masses were measured: $^{7}$Li, $^{24}$Mg, $^{47}$Ti, $^{49}$Ti, $^{56}$Fe, $^{57}$Fe, $^{85}$Rb, $^{133}$Cs, $^{139}$La, and $^{172}$Yb, as well as mass shifted $^{86}$Sr, $^{87}$Sr, $^{88}$Sr (86-102, 87-103, and 88-104) post-reaction with $^{16}$O (see Hogmalm et al. 2017). The dwell time was 120 ms for $^{86}$Sr, and $^{87}$Sr, 50 ms for $^{85}$Rb, $^{87}$Rb, and $^{88}$Sr, 10 ms for $^{7}$Li, $^{47}$Ti, $^{49}$Ti, $^{56}$Fe, $^{57}$Fe, $^{133}$Cs, $^{139}$La, and $^{172}$Yb, and 5 ms for $^{24}$Mg.

Primary Rb-Sr isotope normalization was carried out using Mica Mg nanopowder (Hogmalm et al., 2017), with $^{87}$Sr/$^{86}$Sr homogeneity verified against the NIST610 glass reference material (Woodhead and Hergt, 2001). Data reduction was done in Iolite 4 (Paton et al., 2011), using an in-house developed data reduction scheme (Larson, 2024) based in part by that described in Redaa et al. (2021). The method was verified through analyses of multiple unknowns for both brown mica and white mica runs, which yielded results within uncertainty of expected ages.

For trioctahedral mica analyses, Mica Fe nanopowder yielded isochron ages of 307 ± 5 Ma (ZU01, MSWD = 1.8, n = 12/14) and 306 ± 6 Ma (ZU05, MSWD = 1.3, n = 10/10) in agreement with the expected age (ca.305 Ma; Rösel and Zack, 2022). The sample measured in the same run as the standard is indicated in parentheses). Mica 1B yielded isochron ages of 996 ± 17 (ZU01, MSWD = 0.7, n = 14/14) and 989 ± 20 Ma (ZU05, MSWD = 0.29, n = 10/10), within error of the reported age (990 ± 5 Ma, Camacho et al., 2020). Mica 1O yielded isochron ages of 1003 ± 15 Ma (ZU01, MSWD = 1.9, n = 13/14) and 984 ± 15 Ma (ZU05, MSWD = 0.98, n = 10/10), within error of the reported age (986 ± 5 Ma; Camacho et al., 2020). QT yielded an isochron age of 1716 ± 20 Ma (ZU01, MSWD = 0.38, n = 14/14), which

overlaps with the corresponding 1720 Ma Ar/Ar age (internal unpublished reference material), and TQ yielded an isochron age of 1737 ± 23 Ma (ZU01, MSWD = 1.4, n = 12/14), which overlaps with the 1720 Ma Ar/Ar age (internal unpublished reference material).

For dioctahedral mica analyses, Mica Fe nanopowder yielded an isochron age of 306 ± 2 Ma (MSWD = 1.9, n = 25/25), in agreement with the expected age. MA1 yielded an isochron age of 349 ± 2 Ma (MSWD = 1, n = 25/25), in agreement with internally accepted ages (340 – 360 Ma). Tanco high-Li white mica yielded isochron ages of 2690 ± 55 Ma (MSWD = 0.35, n = 25/25), within error of the accepted age (2620 ± 20 Ma; Camacho et al. 2012).

Final ages were determined using isochrons in IsoplotR (Vermeesch, 2018).

## 2.5 Modelling

### 2.5.1 Petrologic modelling

For Chapter 3, petrological calculations were performed using the modelling program Theriak-Domino (De Capitani and Petrakakis, 2010) in the compositional system MnO — $Na_2O$ — CaO — $K_2O$ — FeO — MgO — $Al_2O_3$ — $SiO_2$ — $H_2O$ — $TiO_2$ — $O_2$ (MnNCKFMASHTO), which is most suitable for calculating phase equilibria in metasedimentary rock types. MnO and $TiO_2$ were excluded from modelling of the second stage of melting due to the absence of MnO and $TiO_2$ as components in the haplogranite melt model (Holland and Powell, 2011; White et al., 2014a). For metasediments, modelling considered the internally consistent thermodynamic dataset ds62 of Holland and Powell (2011), considering the activity-composition (a-x) relations for feldspars (Holland et al., 2022), sapphirine (Wheller and Powell, 2014), magnetite-spinel, ilmenite-hematite (White et al., 2000), garnet, epidote, margarite, muscovite-paragonite, biotite, orthopyroxene, cordierite, staurolite, chlorite, chloritoid, and melt (Holland and Powell, 2011; White et al., 2014c,a). Pure phases considered were kyanite, andalusite, sillimanite, quartz, rutile, titanite, and aqueous fluid ($H_2O$).

In chapter 3, the modelled melts considered the internally consistent thermodynamic dataset ds633 of Holland et al. (Holland et al., 2018), with the a-x relations for feldspars (Holland et al., 2022), cordierite (White et al., 2014b; Holland et al., 2018), ilmenite-hematite (White et al., 2000), epidote (Holland and Powell, 2011), muscovite-paragonite, biotite (White et al., 2014b), clinoamphibole (Green et al., 2016), garnet, olivine, orthopyroxene, clinopyroxene, spinel, and melt considered (Holland et al.,

2018). Pure phases considered were kyanite, andalusite, sillimanite, quartz, rutile, titanite, and aqueous fluid ($H_2O$).

In chapter 5, petrological calculations were performed using a Gibbs free energy minimisation approach in the modelling program MAGEMin (Riel et al., 2022) in the $Na_2O$ – CaO – $K_2O$ – FeO – MgO – $Al_2O_3$ – $SiO_2$ – $H_2O$ – $TiO_2$ – $O_2$ – ($Cr_2O_3$) (NCKFMASHTO(Cr)) compositional system. Chromium oxide ($Cr_2O_3$) was only included when modelling (ultra)-mafic rock types to accurately predict the stability of spinel phases. Modelling considered the internally consistent thermodynamic dataset ds636 of Green et al. (2025). Activity-composition (a-x) relations for epidote (Holland and Powell, 2011), clinoamphibole (Green et al., 2016), muscovite (White et al., 2014a), ilmenite/hematite, orthopyroxene, clinopyroxene, garnet (Weller et al., 2024), ternary feldspars (Holland et al., 2022), olivine (Holland et al., 2018), spinel-group minerals (Tomlinson and Holland, 2021) and biotite, cordierite, aqueous fluid, and silicate melt (Green et al., 2025). Kyanite, andalusite, sillimanite, nepheline, quartz, cristobalite, tridymite, coesite, rutile, sphene, and $H_2O$ were treated as pure phases.

For modelling partial melting of hydrated basalts and granitoids, the water content was fixed using the $H_2O$-saturation tool in MAGEMin in order to minimally saturate the system at the point of incipient melting (cf. Palin et al., 2016a). Modelling phase equilibria in primitive mantle was conducted under anhydrous conditions.

### 2.5.2 Trace element modelling

Trace element modelling was performed by using phase proportions calculated using the model setups described above. The trace element concentration of the melt during partial melting was calculated using a batch melt model:

$$C_{liq} = \frac{C_{bulk}}{D_{bulk} + F(1 - D_{bulk})} \tag{2.1}$$

where $C_{liq}$ is the concentration of the trace element in the melt, $C_{bulk}$ is the bulk concentration of the trace element, $D_{bulk}$ is the bulk partition coefficient of the residuum assemblage, and F is the melt weight fraction in equilibrium with the residuum. The bulk partition coefficient was calculated through the following equation:

$$D_{\text{bulk}} = \sum_{k=0}^{n} K_n X_n \tag{2.2}$$

where $K_n$ is the mineral/melt partition coefficient of the element of interest for the given phase, and $X_n$ is the weight fraction of the given phase in the system. For modelling of lithium in the melting environment, we used partition coefficients compiled by Simons et al. (2017) and Chakraborty and Upadhyay (2020) (Table 2.1).

### 2.5.3 Fractional crystallisation modelling

Fractional crystallization was modelled using the Raleigh fractionation equation (Shaw, 1970):

$$C_{liq} = C_0 F^{D_{bulk}-1} \tag{2.3}$$

where $C_{liq}$ is the concentration of the trace element in the residual melt, $C_0$ is the initial concentration of the trace element in the melt, $F$ is the melt fraction remaining, and $D_{bulk}$ is the bulk partition coefficient of the crystallizing phases. The bulk partition coefficient was calculated using Equation 2.2, using the corresponding stable assemblage near the solidus modelled in Theriak.

| **Mineral-melt pairing** | **Partition coefficient** | **Reference** |
|---|---|---|
| plagioclase/melt | 0.02 | Jolliff et al., 1992 |
| alkali feldspar/melt | 0.01 | Jolliff et al., 1992 |
| cordierite/melt | 0.44 | Evensen and London, 2003 |
| biotite/melt | 1.67 | Icenhower and London, 1995 |
| muscovite/melt | 0.82 | Icenhower and London, 1995 |

Table 2.1: Mineral–melt partition coefficients for Li used in modelling

Trace element partitioning between melt and residuum for all other elements (Rb, Ba, Th, U, Nb, Ta, La, Ce, Pb, Pr, Sr, Nd, Zr, Hf, Sm, Eu, Gd, Tb, Dy, Y, Ho, Er, Tm, Yb, Lu, V, Sc) was modelled using the trace element modelling tool in MAGEMin. The trace element calculations in this tool are performed using the same calculations desribed above, with the addition of predicting the stability of zircon using the zircon saturation model of Crisp and Berry (2022). Partition coefficients for other elements were taken from Laurent (2012).

# Chapter 3

# The formation of lithium-rich pegmatites through multi-stage melting

## Foreword

This chapter has been published in the journal *Geology* under the following title: *"The formation of lithium-rich pegmatites through multi-stage melting"*. **Koopmans, L.**, Martins, T., Linnen, R., Gardiner, N.J., Breasley, C.M., Palin, R.M., Groat, L.A., Silva, D. Robb, L.J. **doi:10.1130/G51633.1**. Author contributions are described in the statement of authorship.

# Abstract

Lithium-cesium-tantalum type pegmatites – the primary source of lithium – crystallize from highly evolved, volatile- felsic melts that incorporated crustal material in their source. Pegmatites are classically thought to form either from extreme fractionation of a parental granite body or via low-degree partial melting of a metamorphic rock (anatectic-origin). However, the processes that lead to the formation of economic lithium pegmatite deposits remain enigmatic, since precipitation of lithium ore minerals requires melt lithium concentrations in excess of 5000 ppm – approximately 500 times upper crustal abundances. Here, we use petrological modeling to quantify lithium enrichment in an anatectic-origin scenario and show that it is primarily driven by the relative stability of residual biotite and muscovite at medium to high pressures ($\sim$ 8 kbar), and biotite and cordierite at low pressures ($\sim$ 3 kbar). We show anatexis of an average lithium-enriched metasedimentary source cannot sufficiently elevate the lithium content of the ensuing melt to form economic deposits; however, if this first-generation melt – now crystallized as granitic crust – is re-melted, the second-generation melt will be sufficiently concentrated in lithium to crystallize lithium ore minerals. We propose a petrogenetic model for anatectic-origin lithium pegmatites, in which a region experiences at least two stages of partial melting, ultimately generating lithium-rich melts without invoking extensive fractional crystallization. This mechanism can account for both the occurrence of unzoned lithium pegmatites and explains why economic pegmatites in many terranes are younger than their inferred source granites.


## 3.1 Introduction

Lithium–cesium–tantalum (LCT) pegmatites are formed from highly fractionated melt (Černý, 1991b) and dominate global lithium (Li) production (U.S. Geological Survey, 2023). LCT pegmatites first appeared in the Neoarchean (c. 2.8 Ga), are dominantly hosted in greenschist- to amphibolite-grade supracrustal rocks (Dittrich et al., 2019), and retain geochemical signatures which imply their genesis involved reworking of existing (typically metasedimentary) crust (Černý, 1991b). However, fundamental questions remain regarding how these evolved rocks become highly concentrated in Li, since the primary extractable Li ore minerals – the Li-aluminosilicates spodumene and petalite – only crystallize when melt Li contents exceed 5000 ppm (London, 1984; Maneta et al., 2015), representing an enrichment of ca. 500 times

above ordinary crustal abundances (Taylor and McLennan, 2003). Furthermore, to be economically viable, an economic Li-pegmatite deposit must contain a sufficiently large mineralized zone (Bradley and Mccauley, 2017), the extent of which is controlled by the initial Li concentration in the emplaced pegmatitic melt (London, 2014).

In general, concentrating incompatible elements such as Li within a small-volume melt fraction occurs through either (i) high-degree crystal fractionation of a larger body of magma, or (ii) siphoning low-degree (e.g., 7–10%) partial melts away from a source rock undergoing anatexis. These contrasting processes underpin two proposed LCT pegmatite petrogenetic models: (1) extreme fractionation of a granitic magma that carries a typical (crustal) Li concentration, generating a minor volatile- and metal-rich melt fraction which migrates from the source region and ultimately crystallizes as a pegmatite (Cameron et al., 1949; Jahns, 1953; Černý, 1991b; Černý and Ercit, 2005), or (2) low-degree partial melting of Li-rich host rocks during prograde metamorphism ('anatectic origin'), generating a volatile-rich melt that does not require significant additional fractionation (Stewart, 1978; Simmons et al., 1995; Shaw et al., 2016; Müller et al., 2017). Recent research has focused on the anatectic model as a viable mechanism to form economic pegmatite deposits (Müller et al., 2017; Kunz et al., 2022; Knoll et al., 2023). Here, we use petrological modelling to quantify the extent of Li enrichment during crustal melting of metasedimentary protoliths, and then assess how subsequent melting of their crystallized magmatic products might serve to further concentrate Li in newly formed melt fractions. Our results imply that multi-step anatexis in long-lived orogenic systems can act as a highly efficient mechanism to produce economic grade LCT pegmatites.

## 3.2 Modeling Li enrichment during crustal anatexis

### 3.2.1 Lithium in sedimentary rocks

The concentration of Li in a given melt fraction is principally controlled by the original Li concentration in the protolith undergoing partial melting. Reported geochemical estimations of an 'average' metapelite proposed a Li concentration of ∼55 ppm (Shaw, 1956); however, the upper limits of Li concentrations in different sedimentary lithologies are unconstrained. To address this knowledge gap, we filtered the Sedimentary Geochemistry and Paleoenvironments Project (SGP) database (Farrell et al., 2021) to

produce a compilation (n = 11,634) of the measured Li contents of global sediments, attached in Supplementary file 2.

The filtered dataset shows an average Li concentration of 50.06 ppm in siliciclastic sediments, 18.83 ppm in carbonate sediments, and 18.04 ppm in chemical sediments (e.g. cherts). Nonetheless, all sediment types recorded outliers, with Li concentrations exceeding 1500 ppm in some cases (Figure 3.1). These data likely represent geological anomalies; for example, Li may become enriched in metasedimentary aureoles surrounding LCT pegmatites, Li is highly mobile under hydrothermal conditions and therefore diffuses rapidly through host rocks (Morgan and London, 1987; Linnen et al., 2012; Roza Llera et al., 2019), or else Li may be enriched in evaporitic sediments, such that these anomalously high values represent primary concentrations (Roda Robles et al., 1999).

There is reason to suggest that Li can be enriched in sedimentary rocks. Surface weathering processes preferentially enrich Li in the washed sediment, inferring surface interaction in enriched metasedimentary lithologies (Teng et al., 2010). Given the potential for enrichment above a baseline value, we take the statistical upper bound of outliers as our theoretical maximum for Li concentration (125.5 ppm for siliciclastic rocks) in metasediments that have not been affected by extraneous metasomatic or hydrothermal processes.

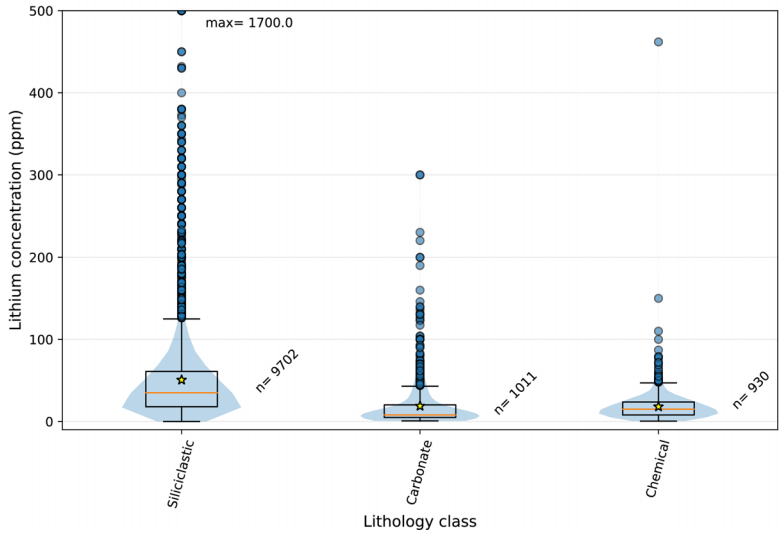


Figure 3.1: Violin plots of Li concentrations in the filtered SGP dataset binned by lithological class. Number of data points in each class is given as n.

### 3.2.2 Lithium in the melting environment

Lithium in metasedimentary rocks is primarily hosted in biotite, muscovite, cordierite, and staurolite (Simons et al., 2017; Kunz et al., 2022; Knoll et al., 2023). During anatexis, the Li content of a melt is controlled both by the breakdown of these minerals, and by the partitioning of Li between restitic minerals and melt as they re-equilibrate. We examined Li mineral–melt partitioning during crustal anatexis via a batch melting geochemical model, which assumes that generated melt remains in equilibrium with the source rock until extraction (Rosenberg and Handy, 2005); an assumption validated in experimental studies (e.g., Acosta-Vigil et al., 2012). The onset of melting, as well as the stability and thus presence of restitic minerals in equilibrium with the melt, depends on the source composition and thermobarometric conditions of melting. As such, we performed Gibbs free energy minimization calculations using the petrological modeling program Theriak-Domino (De Capitani and Petrakakis, 2010) to determine the stable mineral–silicate melt assemblages at different pressure (P, i.e. depth) and temperature (T) conditions within the continental crust for two putative metasedimentary source rocks: the average metapelite of Ague (1991) and a greywacke (Composition I of Pettijohn (1963)). Although Li contents vary between metasedimentary rocks, for ease of comparison we assume both compositions have a starting Li composition of 125.5 ppm, the maximum (excluding outliers) of 11,634 siliciclastic sedimentary rocks worldwide (Figure 3.1).

We calculated P–T phase diagrams for both metasedimentary protoliths and examined the crystallized products of extracted melts. Initial anatexis was examined along isobaric heating paths at 3 kbar (∼9 km depth, i.e., intrusion-related heating) and 8 kbar (∼24 km, i.e., a standard orogenic geotherm intersecting the solidus) under both dehydration melting (minimal saturation) and flux melting scenarios to quantify how Li behaves during partial melting. Our approach allowed the calculation of changes in melt Li content during crustal anatexis and then the behavior of that melt fraction after extraction (set at 7 vol. % melt, the threshold at which melt can escape its source, after Rosenberg and Handy, 2005).

Melt Li concentration was then modeled for two end-member scenarios: (1) the melt extracted undergoes fractional crystallization in a closed system; and (2) the resulting extracted melt crystallizes to form a granitic body which then undergoes a second (later) stage of anatexis. Bulk Li partition coefficients for fractional crystallization were calculated using stable assemblages present at the solidus and published mineral/melt partition coefficients (Table 2.1). All models were run through TDMelts (Koopmans et al., 2023).

For non-flux melting models, the water content in the bulk composition for each protolith was fixed in order to provide minimal free (aqueous) fluid at the point of first melting, defined here as having less than 1 mol. % $H_2O$ at the solidus (cf. Palin et al., 2016b). We note that the absolute amount of $H_2O$ in the bulk composition to allow minimal saturation was determined independently for runs at 3 kbar and 8 kbar, given the different parageneses in the subsolidus domain. The modelled bulk compositions, given in terms of atomic proportions, were as follows:

| Protolith | Pressure (kbar) | Bulk composition |
|---|---|---|
| Greywacke | 3 | SI(73.45)AL(18.28)CA(2.34)MG(3.09)FE(2.71)K(3.64)NA(8.02)TI(0.2)H(4.00)O(190.77) |
| Granite | 3 | SI(71.34)AL(14.85)CA(0.23)MG(0.47)FE(0.92)K(7.15)NA(6.19)TI(0)H(1)O(173.815) |
| Greywacke | 8 | SI(73.45)AL(18.28)CA(2.34)MG(3.09)FE(2.71)K(3.64)NA(8.02)TI(0.2)H(5.14)O(191.34) |
| Granite | 8 | SI(63.69)AL(15.51)CA(0.42)MG(0.49)FE(0.86)K(5.98)NA(7.5)TI(0)H(2)O(160.23) |
| Pelite | 3 | SI(59.92)AL(19.85)CA(1.54)MG(3.98)FE(5.51)K(4.61)NA(2.98)TI(0.57)MN(0.08)H(5.06)O(168.81) |
| Granite | 3 | SI(72.13)AL(14.44)CA(0.22)MG(0.45)FE(0.9)K(6.96)NA(6.02)TI(0)H(1.00)O(174.55) |
| Pelite | 8 | SI(59.92)AL(19.85)CA(1.54)MG(3.98)FE(5.51)K(4.61)NA(2.98)TI(0.57)MN(0.08)H(9.20)O(170.88) |
| Granite | 8 | SI(59.16)AL(14.59)CA(0.49)MG(0.07)FE(0.15)K(6.3)NA(5.83)TI(0)H(2)O(147.985) |

Table 3.1: Theriak-Domino inputs for all model runs (compositions in atomic proportions).

Modebox plots were produced by running an isobaric pressure–temperature (P–T) path in Theriak. The outputs keep track of both the melt composition and modal abundances of the residuum phases to use as inputs for the trace element modelling. Flux melting was modelled by introducing excess $H_2O$ into the system until 7 mol. % partial melt was generated at the P–T point of interest on the solidus. Then, the composition of melt predicted at that point was 'extracted' from the model, used as a starting bulk composition in a new calculation with minimal fluid saturation, and allowed to cool isobarically until fully crystallized.

The starting lithium concentration for each model is shown in Table 3.2.

| **Protolith** | **Pressure (kbar)** | **Lithium concentration (ppm)** |
|---|---|---|
| Metasedimentary rocks | 3, 8 | 125.5 |
| Granite – Greywacke source | 3 | 538 |
| Granite – Greywacke source | 8 | 528 |
| Granite – Pelite source | 3 | 411 |
| Granite – Pelite source | 8 | 255 |

Table 3.2: Lithium concentration in different protoliths under varying pressures.

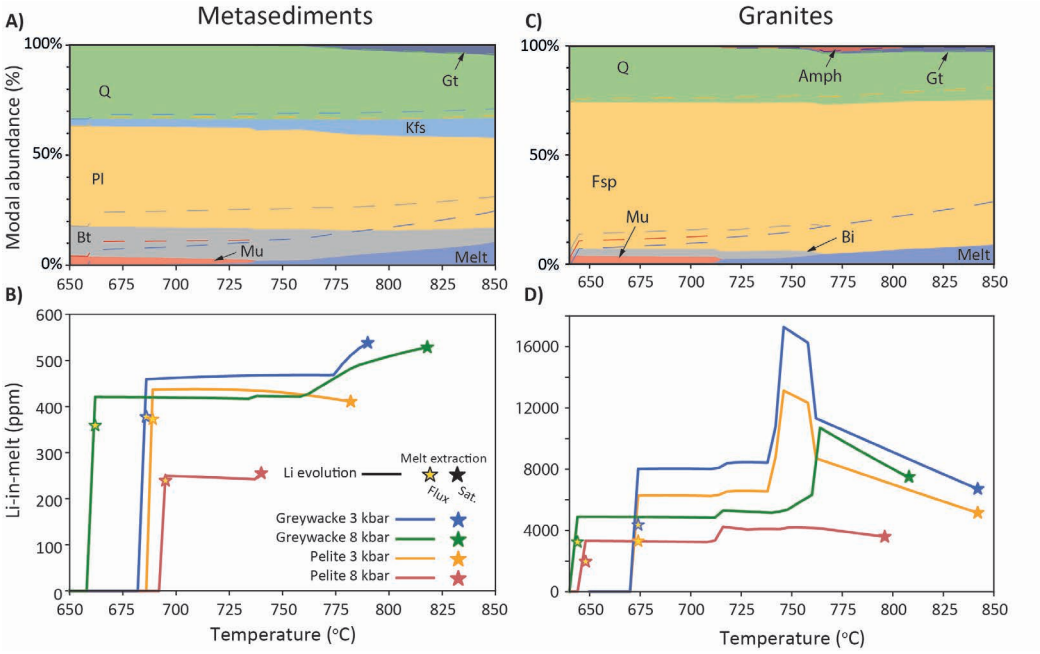


Figure 3.2: Representative results of petrologic modeling of a metasedimentary rock (a, b, here the greywacke at 8 kbar) and granite (c, d, sourced from greywacke at 8 kbar) composition undergoing isobaric heating. Modebox diagrams (a, c) show the equilibrium assemblages across the modelled temperature range. The dashed lines highlight the stable assemblage under flux melting conditions. The graph in (b) traces the concentration of lithium in the melt component of the modelled metasedimentary scenarios. (d) as (b), though of the melt components of the corresponding metasedimentary rocks of (b). Stars denote melt extraction points for each condition, where Flux corresponds to flux melting and Sat. corresponds to dehydration melting. Mineral abbreviations: Amph: amphibole; Bt: biotite; Cd: cordierite; Fsp: feldspar; Gt: garnet; Kfs: Alkali feldspar; Mu: muscovite; Pl: plagioclase; Opx: orthopyroxene; Q: quartz.

## 3.3 Results

During melting, both metasedimentary compositions (Figure 3.2) stabilize cordierite and biotite at low pressures, whereas muscovite and biotite are stable at higher pressures. Figure 3.2 (b) shows the predicted partitioning of Li between metasediment-derived melt and residuum for both starting compositions. At fluid-present conditions, the solidus occurs between 660 and 690 °C and the release of Li into the melt is largely controlled by the initial breakdown of muscovite and later breakdown of biotite.

Metapelites are typically enriched in Al compared to greywackes and stabilize higher proportions of cordierite and mica at equivalent P–T conditions. At equivalent

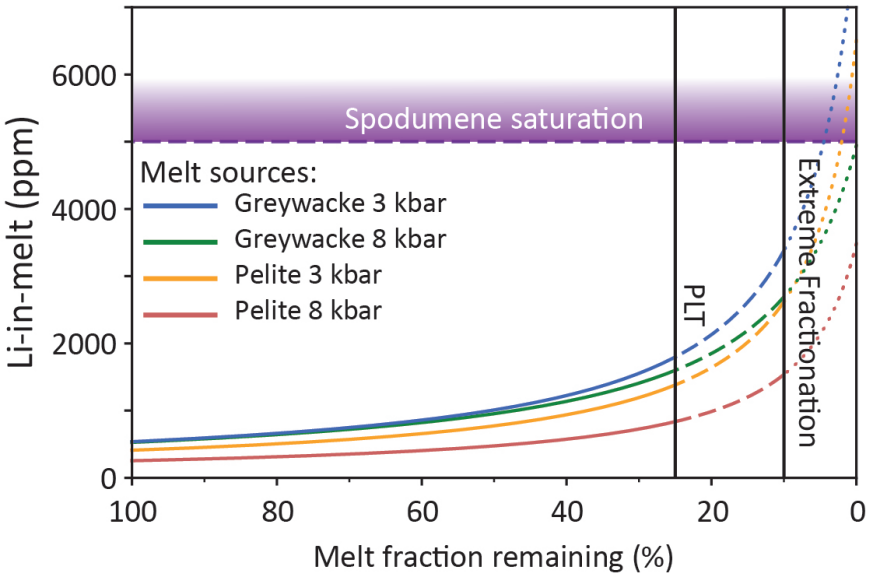


Figure 3.3: The behavior of lithium (Li) in the extracted melt during Rayleigh fractionation. The initial Li content of each melt corresponds to the concentration of Li at extraction in each of the modelled scenarios. The partition coefficients are taken from the model near the solidus of each individual melt. The particle-locking threshold (PLT) of Vigneresse et al. (1996) and the extreme fractionation boundary of Zhao et al. (2022) are highlighted, as well as the minimum threshold for spodumene saturation (Maneta and Baker, 2014).

pressures, greywacke-derived melts contain higher Li contents (by a factor of 1.3–2.1) than metapelite-derived melts (Figure 3.2b); this difference is amplified at higher pressure due to the extended stability of mica compared to cordierite.

Micas are the main hosts of Li in the subsolidus, and our models confirm that Li enrichment during partial melting of metasedimentary rocks is primarily controlled by biotite and muscovite stability, with cordierite having a minor influence, and feldspar playing an insignificant role (Figure 3.2), agreeing with previous work (Kunz et al., 2022; Knoll et al., 2023). Li is released into the melt upon mica breakdown, but importantly, the persistence of micas during melting sequesters Li and serves to inhibit melt Li enrichment.

At a melt proportion of ∼7 vol.%, we calculate maximum Li concentrations of 411 ppm at 788 °C and 538 ppm at 785 °C for metapelites and metagreywackes, respectively. These values represent a potential maximum Li enrichment factor of ∼4.3 at extraction compared to the source. Additionally, flux melting (i.e., ingress of external $H_2O$) also serves to depress melt Li enrichment under all conditions, largely due to the higher proportion of micas present at melt extraction conditions that have

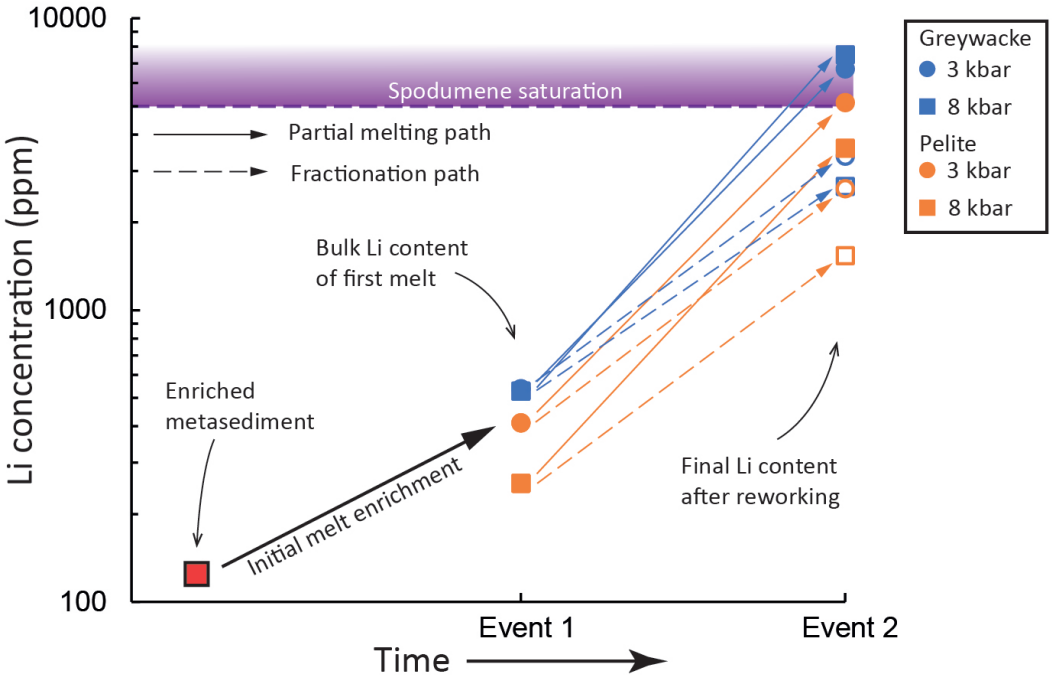


Figure 3.4: Evolution of Li concentrations during melting and fractionation of melt components generated during crustal anatexis – with the spodumene saturation boundary highlighted (Maneta et al., 2015). After initial melt extraction, the granite either: 1) undergoes fractional crystallization (hollow symbols, the compositions of fractional crystallization was taken as the composition at % crystallization); or (2) is assumed to crystallize and then remelted and extracted at the 7 vol. % melt (filled shapes).

not broken down during melting reactions, although we note melts are extractable at a significantly lower temperature (Figure 3.2b).

Fractional crystallization (our scenario 1) during cooling may further enrich the melt phase in incompatible elements including Li. Modeled Rayleigh fractionation trends for melts extracted at the 7 vol. % threshold are shown in Figure 3.3. In all cases, the concentration of Li reaches 800–1800 ppm at 75% fractionation and 1500–3400 ppm at extreme fractionation conditions (Zhao et al., 2022), still below the minimum saturation point for spodumene. Spodumene saturation is only achieved at low pressure (3 kbar) during the final stages of crystallization (Figure 3.3), when the melt fraction is reduced below 5 vol. %, at which point the melt is not physically extractable (Vigneresse et al., 1996).

Alternatively (scenario 2), the melt produced during anatexis of a metasedimentary protolith may crystallize as a granitic body in the crust and experience a separate, later stage of melting. We modeled the remelting of the granitic compositions pro-

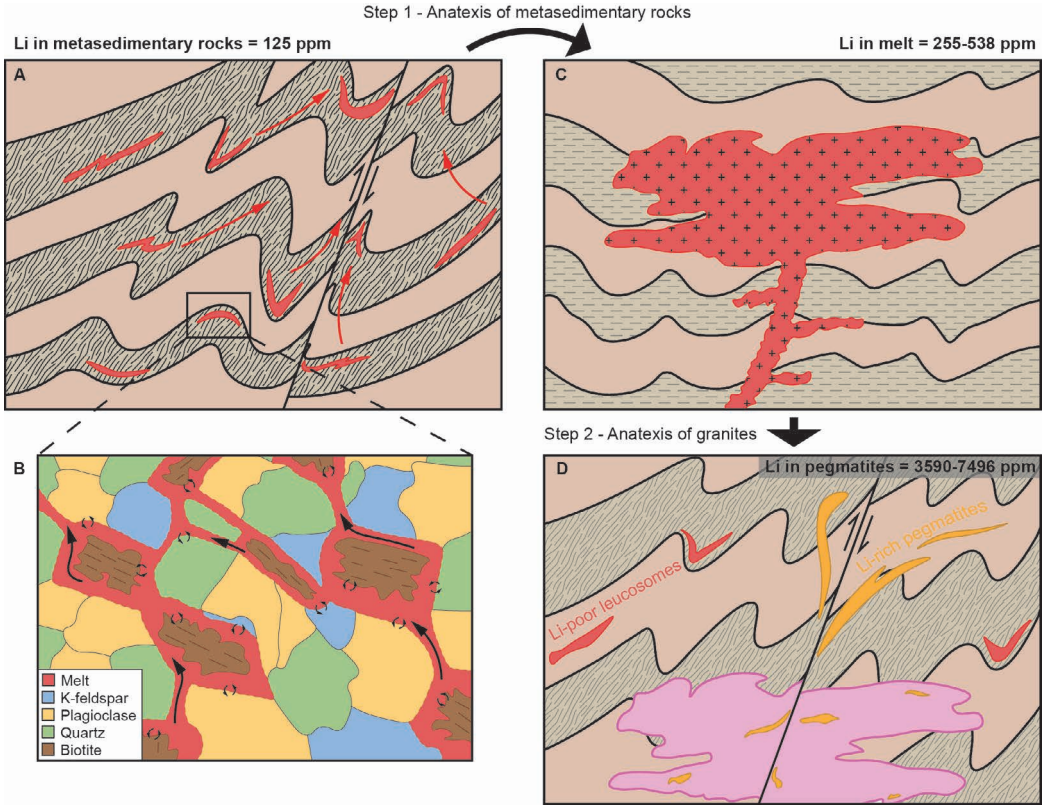


Figure 3.5: Schematic petrogenetic model for generating lithium (Li)-rich pegmatites in the via crustal anatexis. (A) Partial melting of a metasedimentary rock generates melt lenses, which periodically lose melt. (B) grain-scale diagram visualizing melt films connecting and driving melt out of the system in (A). The breakdown of hydrous phases and mineral-melt diffusion controls the Li budget of the resultant melt. (C) The melt accumulates and crystallizes as a granite structurally above the anatectic zone. (D) A subsequent melting event, either associated with the primary metamorphic event, or during a later orogenic cycle melts the granite, generating Li-rich pegmatites (orange) in their vicinity.

duced through primary anatexis (Figure 3.2c, d) to calculate potential second stage melt Li concentrations. In this scenario, melt first appears between 640 °C and 675 °C, and coexists with a smaller proportion of micas (<8 wt. %) relative to metasedimentary rocks, and no stable cordierite in any of the modeled scenarios (Figure 3.2c). Accordingly, the secondary melting stage generates significantly higher melt Li concentrations of 3590–7496 ppm at a 7 vol. % extraction point (Figure 3.2d), equal to a potential Li enrichment factor of ∼14.2 (Figure 3.2d, 3.4). These results importantly indicate that a second stage of melting substantially enriches Li; in two stages driving Li concentration from 125.5 to 7496 ppm, with the resultant secondary melts having economic potential without invoking fractional crystallization.

## 3.4 Multi-step distillation model for Li pegmatites

Our results show that partial melting of typical metasedimentary sources followed by closed-system fractional crystallization of those melt fractions cannot concentrate Li to the saturation limit required (>5000 ppm) to generate a large zone of Li-aluminosilicates within a pegmatite. Thus, production of a melt capable of saturating Li ore minerals in economic quantities within a single stage melt scenario would require a rare, extremely enriched protolith (e.g., 1160 ppm in the metasedimentary rock). While such concentrations have been documented in reworked Li-rich volcanic sediments (e.g., Kadir et al., 2023), they are typically not documented near Li-rich pegmatite provinces (e.g., Roda Robles et al., 1999) and therefore their role in Li pegmatite formation is equivocal. By contrast, additional processing (i.e., remelting) of a package of continental crust can increase the Li concentration in a second-generation in order to allow spodumene/petalite saturation very early in the fractionation history, obviating the need for extensive fractional crystallization.

We therefore propose the following petrogenetic model for anatectic-origin Li pegmatites with economic potential (Figure 3.5):

(1) Partial melting of a metasedimentary succession during prograde metamorphism, which produces a granitic melt that is modestly enriched in Li;

(2) This melt crystallizes as a granitic intrusion structurally above the migmatite zone;

(3) A subsequent melting event, either an extension of the initial metamorphic event or later during an unrelated orogenic cycle, reheats and remelts the granite forming a highly enriched melt that ultimately crystallizes as a Li-rich pegmatite.

Our two-stage anatectic model indicates that the size of the pegmatite generated is approximately 200 times smaller than the metasedimentary protolith; for example, a deposit the size of Tanco (0.021 $km^3$, Stilling et al., 2006) likely formed from an initial metasedimentary package of c. 4.5 $km^3$.

This mechanism also accounts for two particular features of pegmatites. Firstly, pegmatites can be unzoned with economic minerals homogenously distributed throughout, requiring Li-bearing minerals to crystallize from the margin inwards (e.g., Kings Mt pegmatites, Swanson (2012); Mt Cattlin pegmatites, Sweetapple et al., 2019). This suggests the emplaced melt has sufficiently high Li concentrations prior to crystallization.

Secondly, where pegmatite fields have a spatial relationship with granites, they are often significantly younger (e.g., Stilling et al., 2006), which is at odds with arguments for the rapid crystallization of pegmatites from the granitic melt when standard magmatic fractionation is invoked (Simmons and Webber, 2008). Alternatively, many orogenic events are long-lived and experience multiple cycles of melting (e.g., Mulcahy et al., 2014). Together, this suggests the possibility of granites remelting as a mechanism for pegmatite genesis (e.g., Issia Zone, Brou et al., 2022).

A multi-step anatectic model for the formation of Li pegmatites therefore satisfies these geochemical and geochronological constraints, providing an efficient mechanism to elevate Li concentrations and generate economic Li deposits.

# Chapter 4

# Structural controls on lithium mineralization in shear-zone hosted granitic pegmatites of the Zulu pegmatite field, Zimbabwe – implications for exploration

## Foreword

This chapter has been published in the journal *Mineralium Deposita* under the following title: *" Structural controls on lithium mineralization in shear-zone hosted granitic pegmatites of the Zulu pegmatite field, Zimbabwe – implications for exploration"*. **Koopmans, L.**, Gardiner, N.J., St. Pierre, B., Palin, R.M., Musinga, R., Robb, L.J. **doi:10.1007/s00126-025-01371-x**. Author contributions are described in the statement of authorship.

# Abstract

Granitic pegmatites are a significant source of critical metals including tin, tantalum, and most notably lithium. To meet future demand, a comprehensive exploration model is required to assist in the discovery of new hard rock deposits. Whereas recent work has largely focused on understanding the source and mineralization processes of pegmatites, the structural controls on the distribution and size of individual deposits remains poorly understood and understudied. In this contribution, we present a structural study on the Zulu pegmatite field in Zimbabwe, which provides a good example of the influence of shear zones, host rock rheology, and lithological competency contrasts on the orientation, size, and distribution of pegmatite bodies within a pegmatite field. At Zulu, we observe both structural and petrographic evidence for two types of pegmatite emplacement within an active shear zone during $D_2$ strike-slip dominated deformation. An early generation (Type 1) was emplaced syn-kinematic to $D_2$ within dilational jogs subparallel to the shear fabric, and continued ductile shearing also drove significant recrystallization which affected the primary magmatic phases and therefore influenced the preserved mineralogy. A later generation (Type 2) was emplaced syn-to-late-kinematic to $D_2$ along tension gashes and subordinate fracture sets oblique to the shear fabric, which served to truncate the cooling history and preserve a primarily magmatic mineralogy within this pegmatite group. By comparing Zulu to other large pegmatite deposits, we conclude that geologic structures are critical to source-to-sink connectivity in lithium pegmatite systems, and affect the mineralization potential of individual deposits by driving recrystallization.

Assessing the structural history and relative timing of emplacement within a pegmatite field, in conjunction with detailed (micro)textural observations from within pegmatite bodies, is essential to understanding pegmatite emplacement geometries. A more systematic approach in constraining these relationships will therefore aid in generating new exploration targets in both greenfield and brownfield settings.


## 4.1 Introduction

Granitic pegmatites are the primary source of several key metals critical to green technologies including tin, tantalum, and niobium, but, most importantly, lithium (Bowell et al., 2020; McCaffrey and Jowitt, 2023). To meet projected lithium demand, pegmatite deposits are forecast to account for more than 80% of future supply (Yao, 2022). Granitic pegmatites result from small-volume granitic melts through either

extreme fractionation (Jahns and Wayne Burnham, 1969; Černý, 1991b; London, 2005) or low-degree partial melting of a fertile source (anatectic pegmatites) in the mid-crust (Simmons et al., 1995; Müller et al., 2017, , Chapter 3). These melts migrate upwards to be emplaced at shallower depths in the upper crust (Plunder et al., 2022), typically as bodies up to 1 km in length and in swarms of 10–100 individual intrusions (Černý, 1991b).

A comprehensive exploration model for economic-grade lithium pegmatites must encompass a mineral system approach (Wyborn et al., 1994; Hagemann et al., 2016), which at its simplest defines a source, a migration pathway and a trap, as well as the preservation mechanisms that enable a deposit to persist. Much recent work has focused on the source of pegmatites (Černý, 1991b; Simmons et al., 1995; Shaw et al., 2016; Müller et al., 2017; London, 2018, , Chapter 3) and preservation of their magmatic mineralogy, including the primary lithium ore minerals spodumene and petalite (Maneta et al., 2015; Ballouard et al., 2020; Wilde et al., 2021; Shaw et al., 2022; Pfister et al., 2023). However, the control that pathways such as faults and folds play on the distribution and size of economic pegmatites is relatively poorly understood (Hall and Kisters, 2012; Silva et al., 2023; Gardiner et al., 2024b).

Globally, pegmatites have a clear spatial relationship with regional structures such as faults and shear zones on scales up to 10s of km (Kontak et al., 2005; Dill et al., 2012; Deveaud et al., 2013). Most importantly for exploration, the majority of large lithium pegmatite deposits are spatially associated with significant shear zones (Partington et al., 1995; Sweetapple, 2000; Selway, 2005; Morissette et al., 2022). Further, detailed studies of pegmatite districts have shown how such structures may affect the distribution and remobilization of mineralized pegmatites within an individual district (Keyser et al., 2023; Silva et al., 2023), highlighting how regional stresses, and the resultant structures, affect the orientation, shape, and (re)crystallization of pegmatites. A key question relates to whether structures such as brittle faults and ductile shear zones play a role in pegmatitic melt migration and emplacement by providing a fundamental tapping mechanism, or do pegmatitic melts simply migrate passively through pre-existing crustal weaknesses (cf. Vanderhaeghe, 1999; Brown et al., 2011; Hall and Kisters, 2012)?

Here, we address this question through a comprehensive structural study of the Archean Zulu Pegmatite Field (Main pegmatite: 24.75 Mt at 0.43% $Li_2O$, Premier African Minerals Limited, 2024), situated within the Fort Rixon–Shangani greenstone belt in the south of the Zimbabwe Craton. The Zulu Pegmatite Field offers an excellent demonstration of how a combination of the structural history, host rocks,

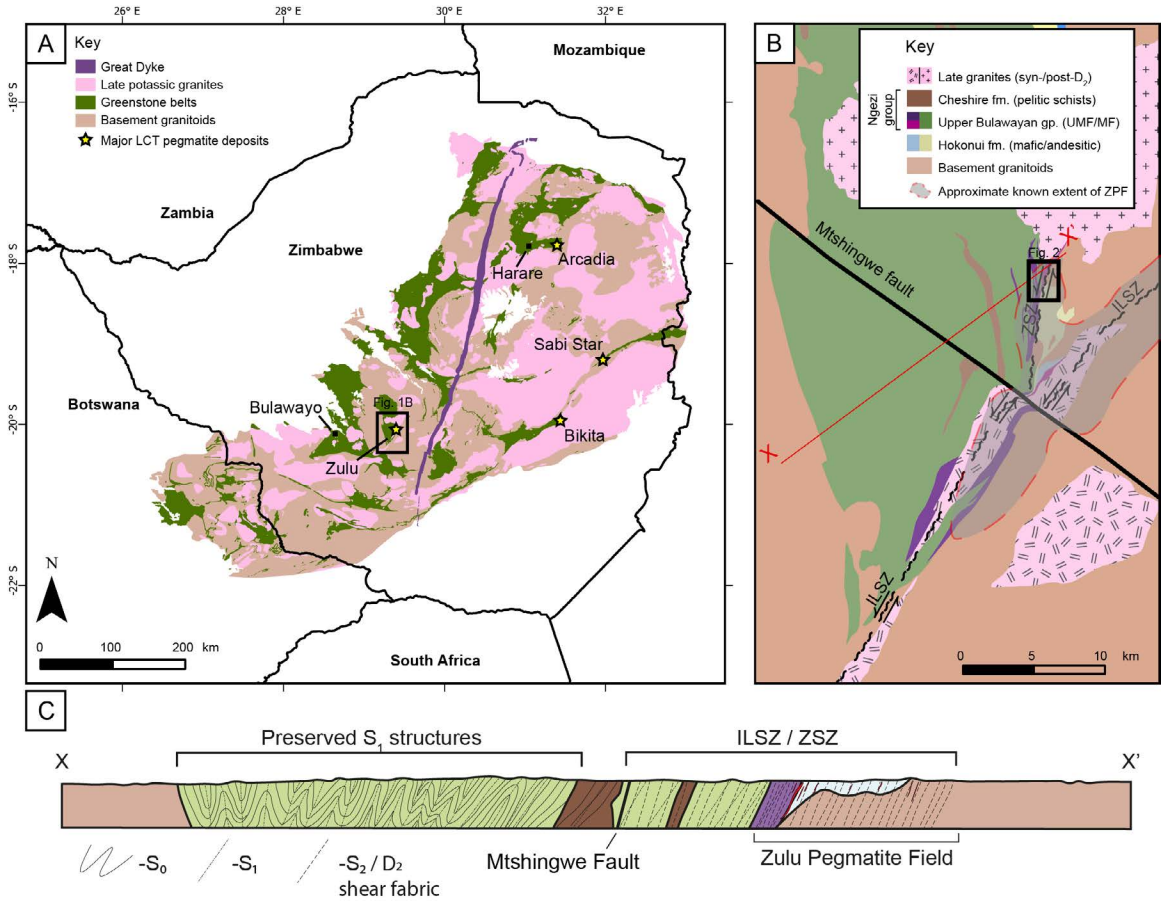


Figure 4.1: A) Simplified geological map of the Zimbabwe Craton, adapted from Ncube (1994). Major lithium deposits of Archean age are shown with yellow stars. Location of Figure 1B noted by black square. B) Regional geological map around the core of the currently known Zulu pegmatite field, adapted from Harrison (1969). Location of Figure 2 noted by black square. C) Schematic cross section X-X' through the Fort Rixon – Shangani greenstone belt, highlighting structural fabrics preserved in the belt. ILSZ: Irisvale – Lancaster Shear Zone, ZSZ: Zulu Shear Zone, ZPF: Zulu Pegmatite Field.

the spatial association with regional granitic bodies, major lithological variations, and crustal-scale fault systems affect the formation and distribution of mineralized lithium-bearing pegmatites. Using geological and structural mapping, field observations, and thin section microscopy, we demonstrate how the stress regime, major lithological competency contrasts, and structural history together influenced the localization and kinematics of shear zones and controlled the geometry, texture, mineralogy and degree of recrystallization of pegmatites during emplacement.

## 4.2 Geological setting

### 4.2.1 Geological history

The Zulu Pegmatite Field is situated in the centre of the Zimbabwe Craton, a large cratonic block predominantly exposed in Zimbabwe (Figure 4.1). The Zimbabwe Craton experienced two major magmatic-metamorphic events during the Archaean (Wilson et al., 1995), resulting in a series of folded granite-greenstone belts within a deformed granitoid gneiss terrane (Figure 4.1). Early felsic crust formation occurred at c. 3600–3200 Ma, with magmatic activity preserved in the central Tokwe and Rhodesdale segments (Horstwood et al., 1999; Hofmann et al., 2022), located between the Zulu and Bikita pegmatite fields (Figure 4.1). These segments formed the cratonic nuclei around which the rest of the craton accreted (Jelsma et al., 2021), with the majority of craton growth occurring during c. 3000–2500 Ma. Magmatism culminated during the Neoarchean with the emplacement of abundant potassic granites (the Chillimanzi and Razi suites; Wilson et al., 1995; Rollinson, 2022; Chagondah et al., 2023). The formation of several lithium-bearing pegmatite fields (Zulu, Bikita and Arcadia) was contemporaneous with this late felsic magmatism, and a tentative genetic link has been placed between the pegmatite fields and neighbouring granites by some authors based on spatial relationships and geochronological overlap (e.g., Chagondah et al., 2024). Emplacement of the Great Dyke signifies final craton stabilization at c. 2575 Ma (Armstrong and Wilson, 2000; Jelsma et al., 2021).

The c. 3000–2700 Ma Fort Rixon–Shangani greenstone belt (FRSGB) is situated 60 km north-east of Bulawayo (Figure 4.1). It is exposed as a major syncline with a N-S axis and is dominantly comprised of mafic/ultramafic extrusive volcanic units (Harrison, 1969). Large pegmatites of the Zulu Pegmatite Field were emplaced along the eastern margin of the Fort Rixon section of the greenstone belt, where a basal mafic/andesitic tuff succession is unconformably overlain by a mafic/ultramafic extrusive volcanic succession with minor sedimentary input (Figures 4.1 and 4.2). These units can be respectively correlated to the Hokonui and Ngezi Formations (with associated intrusive rocks) of the Belingwe Greenstone Belt (Bickle et al., 1993) to the south-east (Prendergast, 2004a). Following deposition and emplacement, the greenstone belt underwent regional metamorphism to upper greenschist-facies conditions, which overprinted and recrystallized most of the primary magmatic fabrics (Harrison, 1969). The age of this regional metamorphic episode is currently unknown.

A series of potassic granites intruded into and around the greenstone belt; three smaller synkinematic porphyritic intrusions granites (dated to 2653 ± 15 Ma and

2616 ± 21 Ma, Chapter 5), a sheared porphyritic granite along the core of the Irisvale–Lancaster shear zone (2679 ± 18 Ma, Chapter 5), and the postkinematic Nalatale granite (2513 ± 36 Ma, Chapter 5), which almost completely transects the belt north of the Mtshingwe fault, (Figure 4.2, Harrison, 1969; Campbell and Pitfield, 1994). These granites have been correlated with the Chilimanzi suite granites (Chapter 5). There is no clear genetic relationship between the Zulu Pegmatite Field and any of the spatially associated granites.

### 4.2.2 Structural history

The FRSGB experienced three phases of regional deformation (Table 4.1). The oldest phase ($D_1$) consisted of folding by WNW-ESE directed shortening, which resulted in a major isoclinal $F_1$ syncline, and a weak axial-planar $S_1$ foliation (Campbell and Pitfield 1994).The second phase of deformation ($D_2$) marked a change in shortening direction from WNW-ESE to NNW-SSE resulting in the formation of large, open, S-shaped warps and tight Z-shaped $F_2$ kink folds, as well as the formation of a regional-scale transpressive sinistral wrench fault system concentrated along the major NE-SW Irisvale–Lancaster shear zone (ILSZ) and along major lithological boundaries such as the NNE-SSW trending Zulu Shear Zone (ZSZ) (Stowe 1980). This $D_2$ event locally produced a penetrative shear fabric ($S_2$) which locally transposed $S_1$ fabrics into a parallel orientation. Both sinistral and later dextral reactivation shearing has been identified along the ILSZ (Campbell and Pitfield, 1994).

The third phase of deformation ($D_3$) consisted of NNW-SSE directed shorting, which formed the major NW-SE trending Mtshingwe Fault (Figure 4.2, Harrison, 1969). This fault system drags the earlier $S_0/S_1$ and $D_2$ shear zones from striking NNE-SSW to NE-SW. The drag folds and the en-echelon dolerite dyke emplacement filling the fault-system suggest a dextral sense of movement with significant lateral displacement (Campbell and Pitfield, 1994). The Mtshingwe Fault crosscuts the Great Dyke (c. 2575 Ma) further to the south-east.

## 4.3 The Zulu pegmatite field

### 4.3.1 The Zulu pegmatite field

The Zulu Pegmatite Field contains >100 individual intrusions that lie along a generally NNE–SSW trend (Figures 4.1, 4.2). Pegmatites of the Zulu Pegmatite Field are LCT-type (after Černý and Ercit, 2005), or Group 1 pegmatites (after Wise

| **Phase of deformation** | **Description** | **Associated structures** | **Mean attitude of fabrics*** |
|---|---|---|---|
| $D_1$ | • WNW–ESE directed shortening<br>• Bedding parallel to $F_1$ isoclinal folding<br>• Weak axial planar $S_1$ development | $F_1$<br>$S_1$ | 190/70<br>190/70 |
| $D_2$ | • NNW–SSE directed shortening<br>• S-shaped and Z-shaped $F_2$ kink folds<br>• Ductile and sinistral shearing along ILSZ and associated $2^{nd}$ order structures<br>• Shear fabric ($S_2$) | $F_2$<br>$S_2$ | 68/167**<br>208/72 |
| $D_3$ | • NW–SE directed shortening?<br>• Brittle dextral faulting along WNW–ESE Mtshingwe fault system | Fault planes<br>Dolerite-filled tension gashes | WNW–ESE<br>NNE–SSW |

*Attitude is presented as strike/dip using right-hand-rule conventions.
**Plunge and trend of fold axis

Table 4.1: Summary of structural events in the Fort Rixon – Shangani greenstone belt

et al., 2022b), and are significantly enriched in lithium (Harrison, 1969; Goodenough et al., 2025). The largest bodies occur along the intrusive boundary between the Sonop serpentinite and the metamorphosed mafic/andesitic tuffs, although smaller intrusions occur up to 30 km towards the NE within the basement granitoids (Stowe, 1968). The primary mineralogy of bodies in the Zulu Pegmatite Field typically consists of petalite (5–25%), quartz (25–30%), K-feldspar (10–30%), albite (5–30%), and muscovite (5–10%). Abundant spodumene (up to 30%) has also been described in the larger pegmatites, and also occurs within some of the smaller pegmatites hosted within the basement granitoids (Premier African Minerals Limited, 2023).

Individual pegmatite bodies vary in width from 0.5 m to ∼50 m, and some strike for up to 2 km. Contacts are sharp with the host rock. Two distinct pegmatite types can be distinguished based on mineralogy and texture (summarized in Table 4.2).

| Event | Pegmatites affected | Description and primary mineralogy | Crystal size | Li-aluminosilicate textures |
|---|---|---|---|---|
| 1–Magmatic | Type 1+2 | • Spodumene (Spd1, Type 1 only), Petalite (Type 2 only), K-feldspar, Quartz, Muscovite, Albite | 5–15 cm | Classic SQUI (Type 1), Petalite (Type 2) |
| 2–Dynamic recrystallisation | Type 1 | • Albite, quartz, spodumene, muscovite (purple), ± spessartine<br>• Strong fabric development, strong alignment of albite + muscovite, pre-/syn-kinemaitc spessartine growth | 1–5 mm | Equant spodumene, fine grained |
| 3–Albitisation | Type 1+2 | • Albite, quartz, muscovite (green), ± spessartine<br>• Weak/absent alignment of albite | 1–5 mm | N/A |
| 4–Late-spodumene | Type 1+2 | • Spodumene, quartz ± muscovite (green)<br>• Along fractures and cleavage planes within petalite (Type 2) | $<$ 1–5 mm | Equant spodumene (Type 1), SQS (Type 2) |
| 5–Low-T hydrothermal | Type 1+2 | • Fine grained clay assemblages | $<$ 1 mm | N/A |

SQUI: spodumene–quartz intergrowths
SQS: spodumene–quartz symplectites (after Breasley et al., 2025)

Table 4.2: Summary of (re)crystallistion events in the Zulu pegmatite field

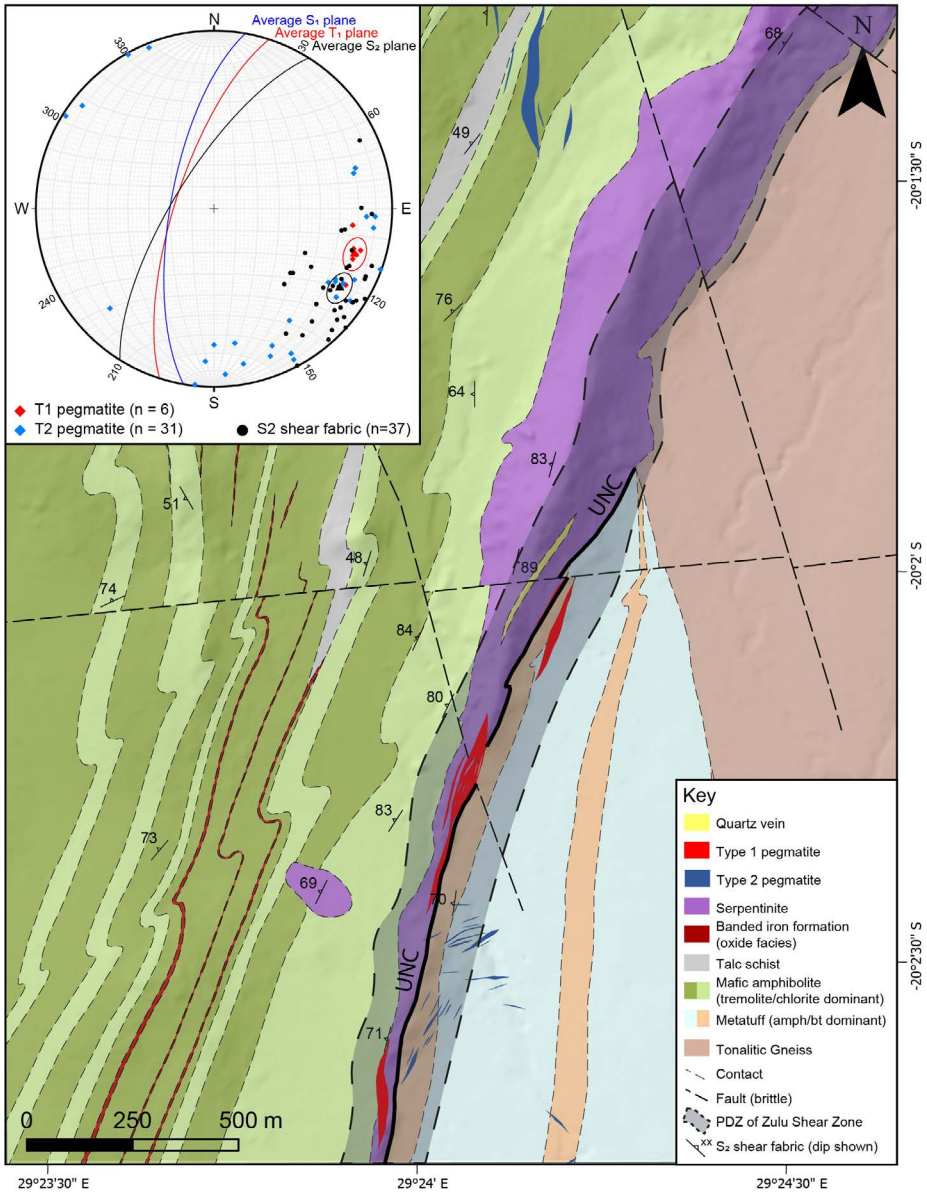


Figure 4.2: Inset: stereonet denoting main structural fabrics within the Zulu pegmatite field. A simplified description of each fabric can be found in Table 1. Main map: geological map of the region surrounding the major pegmatites of the Zulu pegmatite field. PDZ: principal deformation zone, UNC: major lithostratigraphic unconformity between the lower Hokonui and Ngezi formations.

#### 4.3.1.1 Type 1 pegmatites

Type 1 pegmatites attain widths up to 50 m and are therefore the volumetrically dominant pegmatite type in the field. Individual intrusions have asymmetric lenticular shapes with long axes subparallel to the principal deformation zone of their host shear

zone (Figure 4.2). The primary magmatic mineralogy is comprised of spodumene, K-feldspar, albite, quartz, and muscovite. Individual crystals are up to 15 cm long (Figure 4.3C, 4.3D). An early generation of spodumene (Event 1, Table 4.2) in Type 1 pegmatites predominantly consists of crystals (0.1–1 cm) with a strong crystallographic orientation within oikocrystic quartz (Classic SQUI of Breasley et al., 2025, Figure 4.3C, 4.4A).

Primary textures are otherwise poorly preserved. Where magmatic mineralogy is preserved, quartz crystals commonly exhibit chessboard and undulose extinction patterns, whereas plastic deformation of lamellar twins in coarser albite is common (Figure 4.5A, 4.5C). Microcline has well-developed tartan twinning and flame perthite is prevalent (Figure 4.5D). Primary muscovite, where preserved, also exhibits kinked cleavage planes (Figure 4.5B).

An early deformation-driven recrystallization event (Event 2, Table 4.2) is pervasive and largely replaced the primary mineralogy with a fine-grained (1–5 mm) albite + quartz + spodumene + muscovite ± spessartine assemblage (e.g., Figure 4.3C). Relict magmatic crystals are entrained as porphyroclasts (retaining deformation microstructures described above), and the muscovite has a deep purple colour in outcrop (Figures 4.3C, 4.3D, 4.6A). Individual crystals of spodumene within the replacement mineralogy are equant, although albite and muscovite within these aggregates are commonly strongly aligned to define a fabric within the pegmatites (described in more detail below). Locally, this unit developed a strong schistosity (possibly owing to a horizon of less competent magmatic mineralogy within the pegmatite), and euhedral spessartine is interpreted to be pre- to syn-kinematic with respect to the fabric (Figures 4.4C, 4.6B).

Later albitization (Event 3, Table 4.2) is most common along the hanging wall of the pegmatites, producing zones between 5 cm and 2 m wide of albite + quartz + muscovite and rare spessartine with a weak fabric (Figure 4.4A). Sporadic pockets of albitization also occur internal to the pegmatites. The muscovite in the albitized zones is typically light-green/grey in color. A later, spodumene-rich, replacement unit (Event 4, Table 4.2) is comprised of fine grained (<1 mm) spodumene + quartz + albite + muscovite with no defined orientation. This unit is only locally present and can be seen to overprint all previous crystallization events in the pegmatite (Figure 4.4A). Subsequent low temperature hydrothermal alteration products (Event 5, Table 4.2) are uncommon, though locally spodumene and feldspars are replaced by fine grained clay minerals.

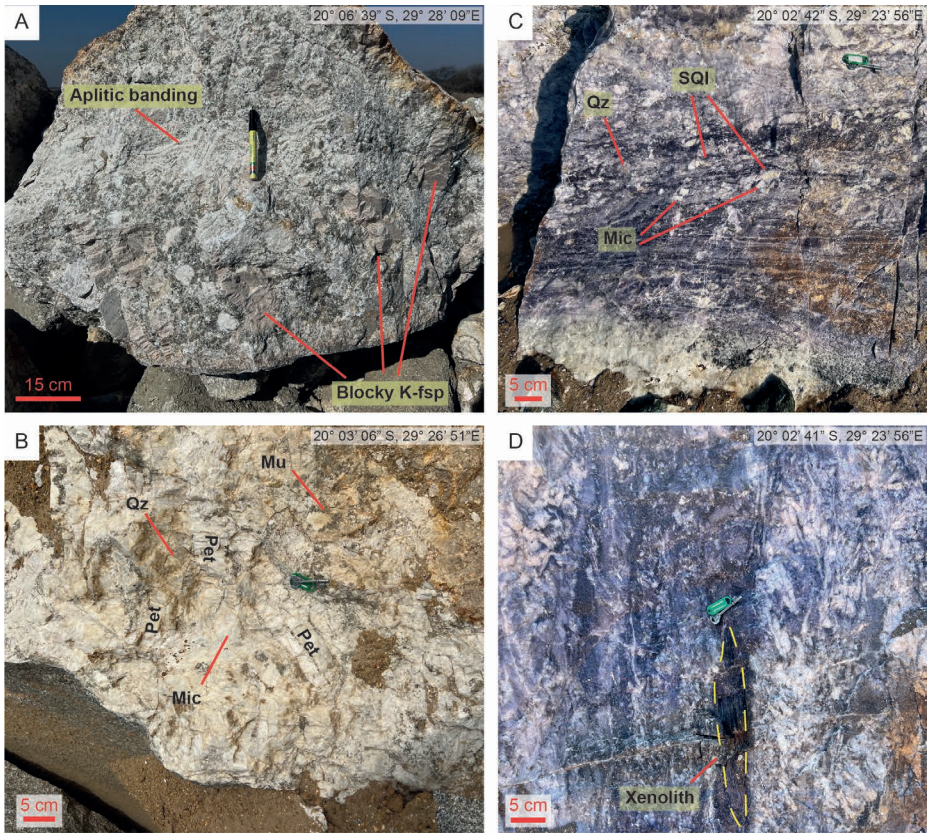


Figure 4.3: Representative photographs of pegmatites in the Zulu Pegmatite Field, with locations of images in top-right corner. A) Typical exposure of barren Type 2 pegmatite near the contact. Note the aplitic banding and unidirectional solidification texture expressed by the K-feldspar megacrysts. B) Mineralized Type 2 pegmatite with large petalite crystals randomly orientated in the intermediate zone. C) Typical exposure of the Type 1 pegmatites, with a strong fabric aligned left-right in the image. D) Rounded xenolith within Type 1 pegmatites within a localized high-strain domain. K-fsp: K-feldspar, Qz: quartz, SQI: spodumene-quartz intergrowths, Mic: microcline, Pet: petalite, Mu: muscovite.

#### 4.3.1.2 Type 2 pegmatites

These are characterized by their relatively simple magmatic mineralogy and textures. Individual intrusions are often limited in width, being no greater than 5 m. A simple pegmatite zonation is common, with a fine-grained border zone (10–30 cm) followed by a zone of irregular aplitic banding (5–30 cm) defined by alternating muscovite-rich and muscovite-poor bands subparallel to the contact (Figure 4.3A). A coarse-grained intermediate zone and a poorly developed quartz core occur towards the centre of the pegmatite bodies (Event 1, Table 4.2). The intermediate zone consists of crystals up to 15 cm in size and can be further subdivided into a mineralized (Figure 4.3B)

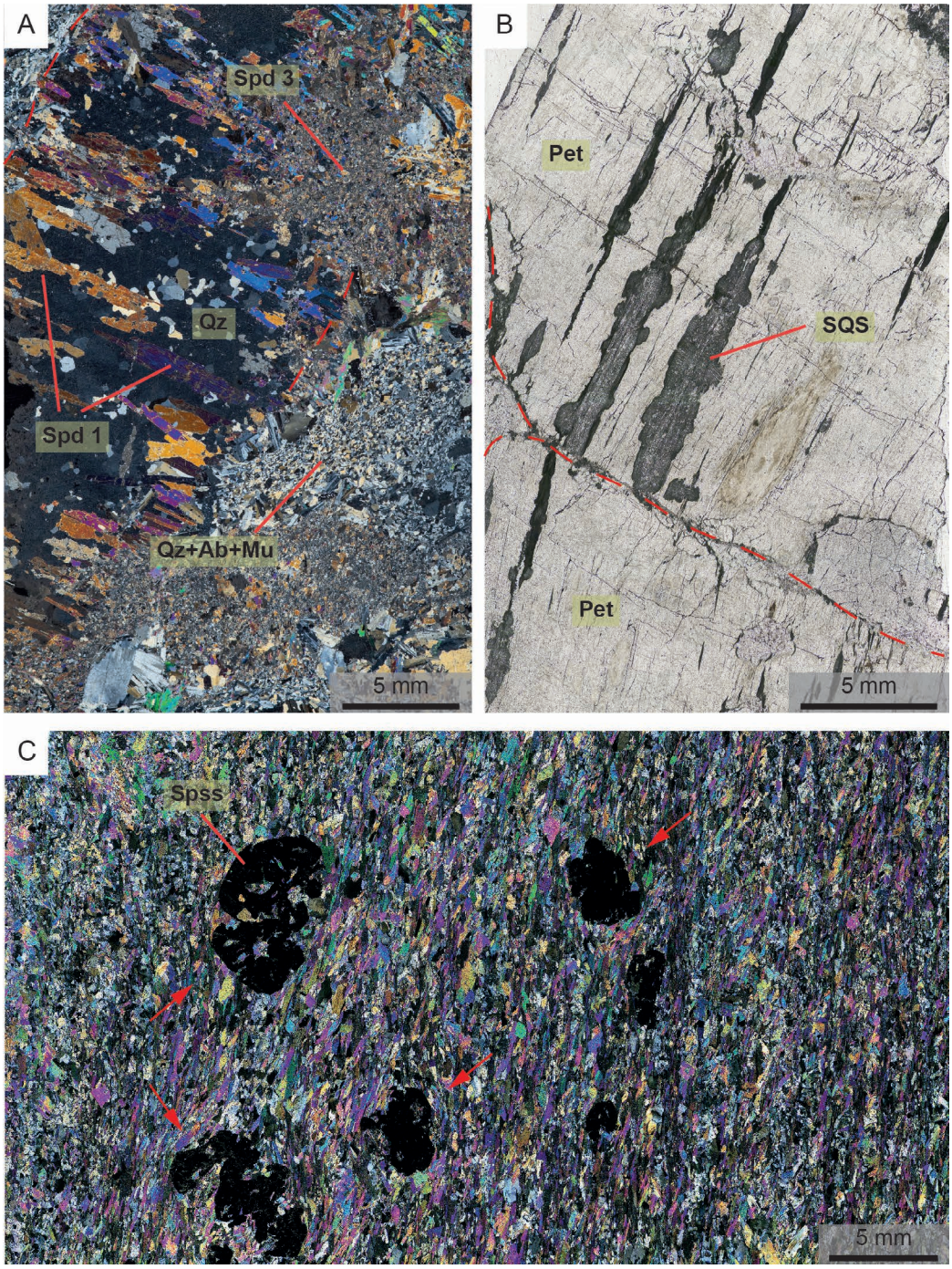


Figure 4.4: Photomicrographs from pegmatites in the Zulu pegmatite field. A) An example of Classic SQUI (Spd 1) within Type 1 pegmatites. Note the overprinting albitization (Event 3, Table 2) and subsequent late spodumene (Spd 3; Event 4, Table 2) events. B) Large petalite crystals in Type 2 pegmatites, with spodumene-quartz symplectites (SQS, Event 4, Table 2) occurring along petalite cleavage planes. C) A strongly foliated zone of a Type 1 pegmatite. Evidence of fabric-wrapping textures around spessartine (opaque mineral) highlighted in red arrows. Qz: quartz, Spd: spodumene, Ab: albite, Mu: muscovite, Pet: petalite, Spss: spessartine.

and barren (Figure 4.3A) subgroup. Petalite (in the mineralized subtype), blocky K-feldspar (in the barren subtype), quartz, albite, and muscovite constitute the major minerals in the intermediate zone. Crystals are commonly euhedral to subhedral. Fabric-forming recrystallization (Event 2, Table 4.2) is not observed within the Type 2 pegmatites.

Locally Type 2 pegmatites have been albitized (Event 3, Table 4.2), leading to replacement of the primary mineralogy by a fine-grained albite + quartz + muscovite assemblage. A muscovite + quartz greisen, predominantly along the margins of blocky K-feldspar and petalite, is sporadically developed. Some petalite in Type 2 pegmatites is partially replaced (Event 4, Table 4.2) by a complex symplectic intergrowth of spodumene + quartz along cleavage planes and fracture faces (Figure 4.4B). Evidence for further low-temperature alteration (Event 5, Table 4.2) is sparse, although feldspars and petalite are patchily replaced with clay-type minerals.

### 4.3.2 Lithostructural observations on the Zulu pegmatite field

Competency contrasts between lithologies generated distinct high-strain and low-strain domains during $D_2$ deformation. Across the study area the predominant foliation dips steeply towards the WNW (averaging 212° strike / 72° dip) across a region >5 km wide.

Within the basement granitoids the $S_2$ fabric is defined by the alignment of biotite and feldspar (Figures 4.7C, D). Strain appears to be heterogeneously distributed through the granitoids, with weakly foliated granitoids gradually obtaining strongly deformed and banded fabrics on the scale of 10s of m (Figure 4.7C). Local megacrystic granitoids within higher strain domains preserve sigma-type clasts indicating a sinistral, SSW oriented, sense of shear (Figure 4.7D).

The basal mafic/andesitic tuff succession on the eastern margin of the FRSGB is locally protomylonitic with the $S_2$ fabric defined by the alignment of relict amphibole and biotite crystals (Figure 4.8A). Similar mylonitic fabrics are preserved in the Sonop serpentinite, where S/C fabrics and relict phenocrysts also indicate sinistral shearing (Figure 4.8D). Low-strain domains are rarely observed within the Sonop serpentinite. $S_2$ high strain domains within the overlying mafic/ultramafic succession are defined by the alignment of tremolite/actinolite and chlorite-rich shear bands (Figure 4.8C). Low-strain domains occasionally preserve a $S_1$ fabric that is locally overprinted by thin, chlorite-rich shear bands (Figure 4.8C). S-shaped kink folds are common within the mafic/ultramafic succession and suggest sinistral NNE-SSW orientated shearing (Figures 4.7A,B).

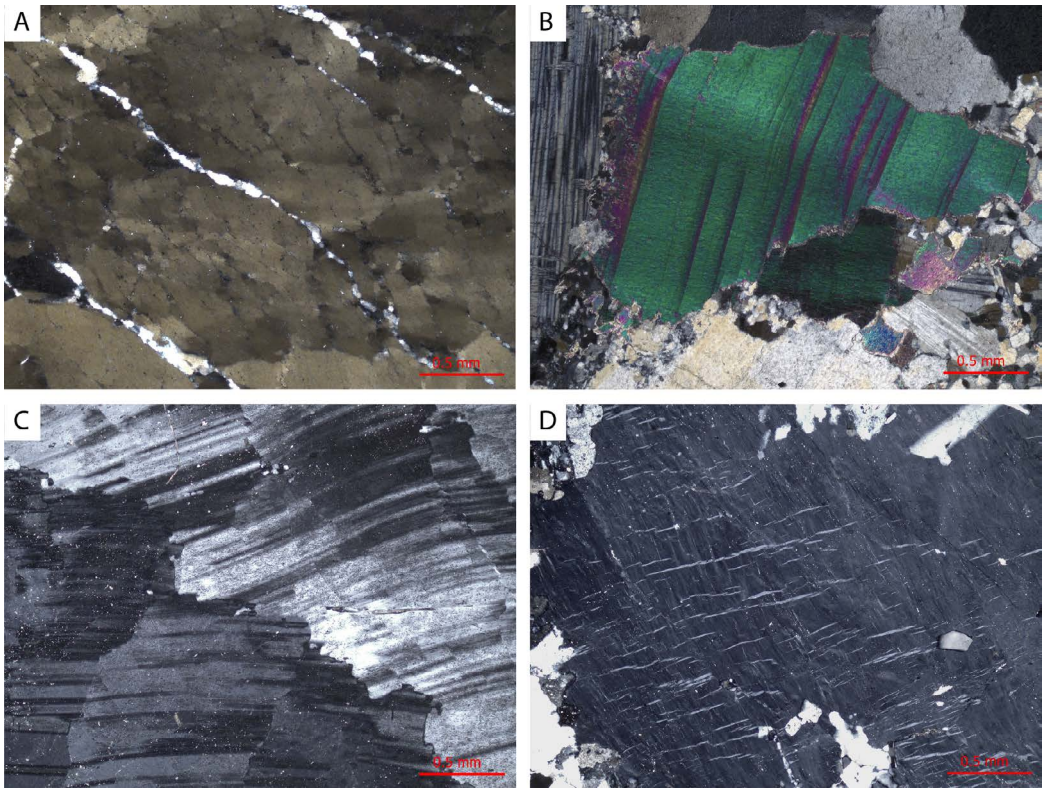


Figure 4.5: Typical deformation microstructures within Type 1 pegmatites. A) Chessboard extinction in relict magmatic quartz. B) Kinked cleavages within a relict muscovite crystal. C) Plastic deformation of early albite twins. D) Orientated flame perthite within early microcline.

Type 1 pegmatites are primarily emplaced within high-strain domains along the contact between the Sonop serpentinite and underlying mafic/andesitic tuff successions. Host rocks to Type 1 pegmatites have been affected by exomorphic wall rock alteration adjacent to the pegmatites which largely destroyed their pre-intrusion mineralogy. A biotite + quartz alteration zone, up to 20 cm thick, is typically observed along the serpentinite hanging wall with a pervasive foliation subparallel to $S_2$ (Figure 4.9). Asymmetric crenulations are common within the biotite-rich domains. Along the footwall of the pegmatites, a chlorite + biotite ± holmquistite alteration halo within the mafic/andesitic tuff succession is commonly observed, with the acicular amphibole and platy mica showing a preferred alignment subparallel to $S_2$ (Figure 4.8B). Fabrics defined by the alignment of albite and mica in the early dynamically recrystallized zones, together with the schistosity preserved in high-strain domains, are all subparallel to the long axis of the pegmatites and $S_2$ (Figure 4.9).

Type 2 pegmatites are mostly emplaced within the basement granitoids and low-strain domains within the basal mafic/andesitic tuff successions, and often obliquely

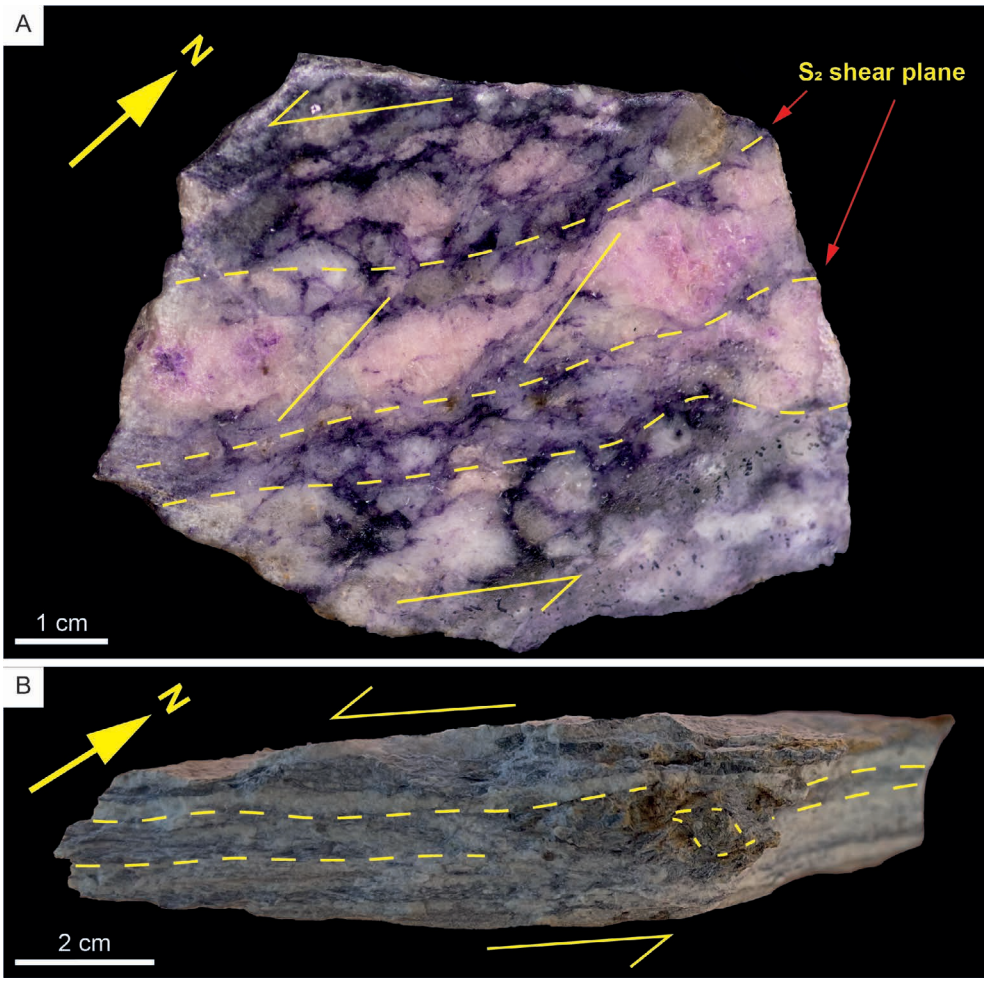


Figure 4.6: Hand samples of Type 1 pegmatites. A) Sheared pegmatite with fabric defined by aligned mica sheets, and antithetic rotation within relict SQI grains. B) Protomylonitic pegmatite with bands defined by albite and lithian muscovite. Spessartine porphyroclasts indicate the sense and direction of shear.

(30–90°) crosscut the primary fabric (Figure 4.10). There are no apparent deformation fabrics within Type 2 pegmatites, and only minor alteration can be observed within the wall rock.

Deformation features related to motion along the Mtshingwe fault ($D_3$) are absent in regions containing Type 1 pegmatites. Type 2 pegmatites adjacent to $D_3$ structures are only observed within the granitoid basement and are oriented oblique to the en-echelon dolerite dyke swarm within the Mtshingwe fault zone. In these examples, the primary magmatic mineralogy is pervasively altered to clays.

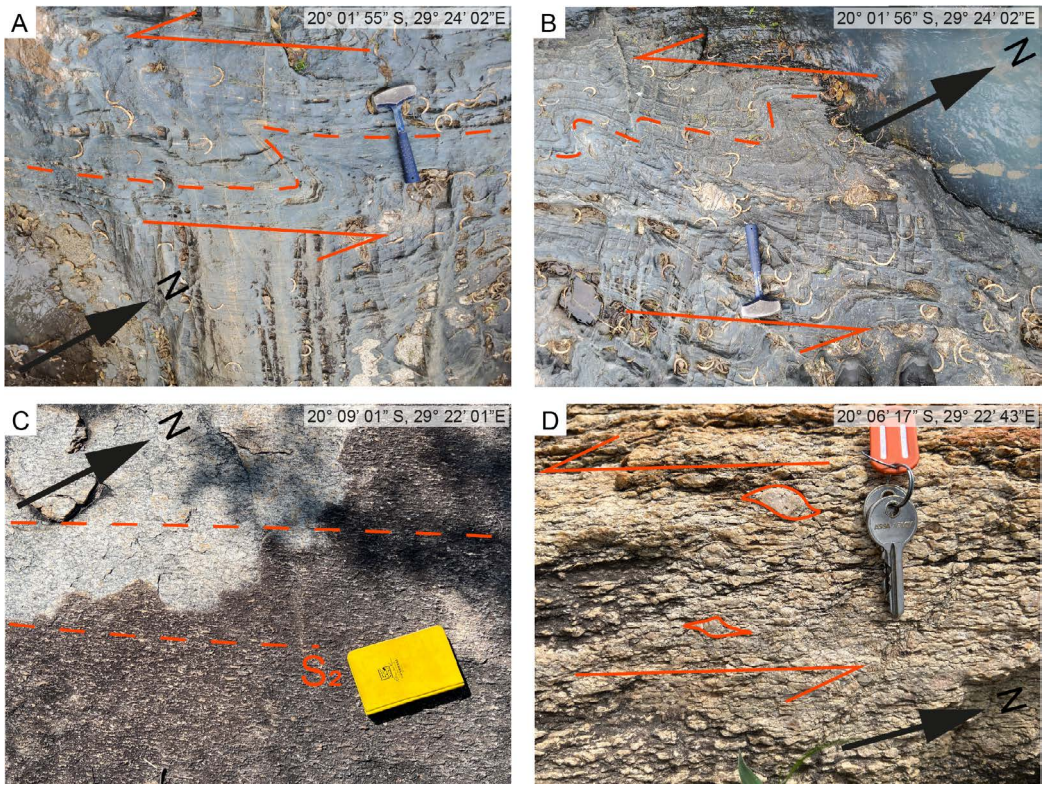


Figure 4.7: Top-down outcrop images of host rocks within the Zulu Pegmatite Field. Location of images in top right. A, B) S-shaped kink folds indicating sinistral sense of shear within mafic/ultramafic extrusives. C) $S_2$ fabric preserved in moderately deformed basement granitoids highlighted by the alignment of feldspar crystals. D) sigma-type clasts within highly deformed basement granitoids.

## 4.4 Discussion

### 4.4.1 Relative timing and structural setting of pegmatite emplacement at Zulu

Transcurrent sinistral shearing along the ISLZ and ZSZ is defined by asymmetric dragging of the pre-existing $S_1$ foliation along the $S_2$ shear fabric, asymmetrical sigma clasts, and s-shaped kink folds developed along the margins of the high-strain zones (Figure 4.7).

Type 1 pegmatites are interpreted to have been emplaced during $D_2$ shearing. Deformation within the pegmatites was accompanied by extensive recrystallization and remobilization of lithium, leading to the formation of lithian muscovite and the replacement of pre-existing lithium silicates with a later fine-grained generation of spodumene (Table 4.2). Critically, the syn-kinematic emplacement during sinistral shearing of the pegmatites is supported by three main lines of evidence: 1) the lentic-

ular

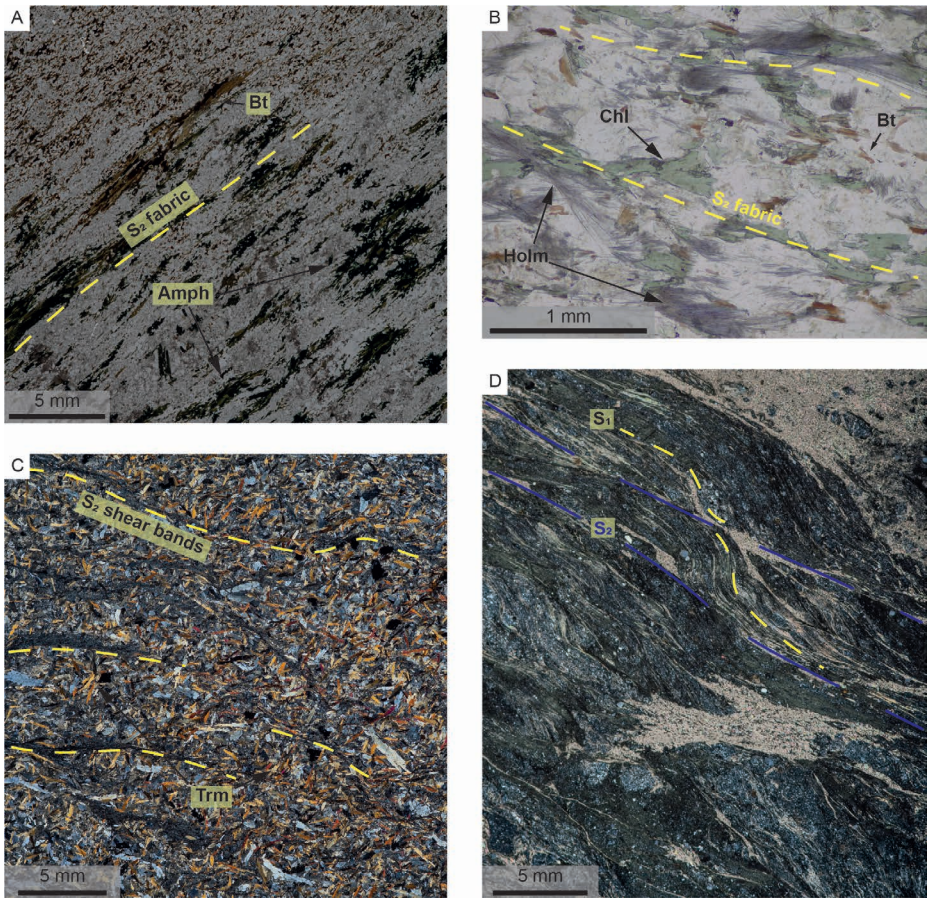


Figure 4.8: Thin section images of host rocks in the Zulu Pegmatite Field. A) Protomylonitic andesitic tuff with the fabric defined by highly attenuated biotite and amphibole crystals. B) Strongly altered andesitic tuff adjacent to a Type 1 pegmatite. Alteration phases are all strongly aligned to $S_2$. C) $S_2$ chlorite shear bands within a mafic/ultramafic extrusive in a low strain domain. D) Highly sheared serpentinite highlighting the relationship between the earlier $S_1$ fabric (yellow dashed lines) with the well-developed shear fabric ($S_2$, blue lines) forming S/C fabrics within the principal deformation zone of the Zulu shear zone. Bt: biotite, Amph: amphibole, Chl: chlorite, Holm: holmquistite, Trm: tremolite.

shape of some Type 1 pegmatites in agreement with emplacement into dilational jogs (in some cases, Type 1 pegmatites present a more contorted shape which may suggest deformation by subsequent shearing), because of which the orientation of the pegmatite-wallrock contacts locally cross-cuts the $S_2$ fabric (Figures 4.2, 4.10), 2) the internal fabric subparallel to $S_2$ within pegmatites (Figures 4.3, 4.5, 4.8), and 3) the synkinematic growth of minerals within the exomorphic haloes surrounding Type 1 pegmatites, which indicates that country rock metasomatism must have occurred

during active deformation (Figures 4.8B, 4.11). The significant rheological contrast between the weaker, more ductile Sonop serpentinite and the more competent underlying metamorphosed tuffs (Figure 4.2) likely acted as a concentrating mechanism, localizing melt flow during ascent (Papeschi et al., 2022).

In contrast to Type 1, the Type 2 pegmatites preserve a largely magmatic mineralogy, and have no internal fabric. Cross-cutting relationships with their host foliated granites indicate that these pegmatites were emplaced after the regional fabric was de-

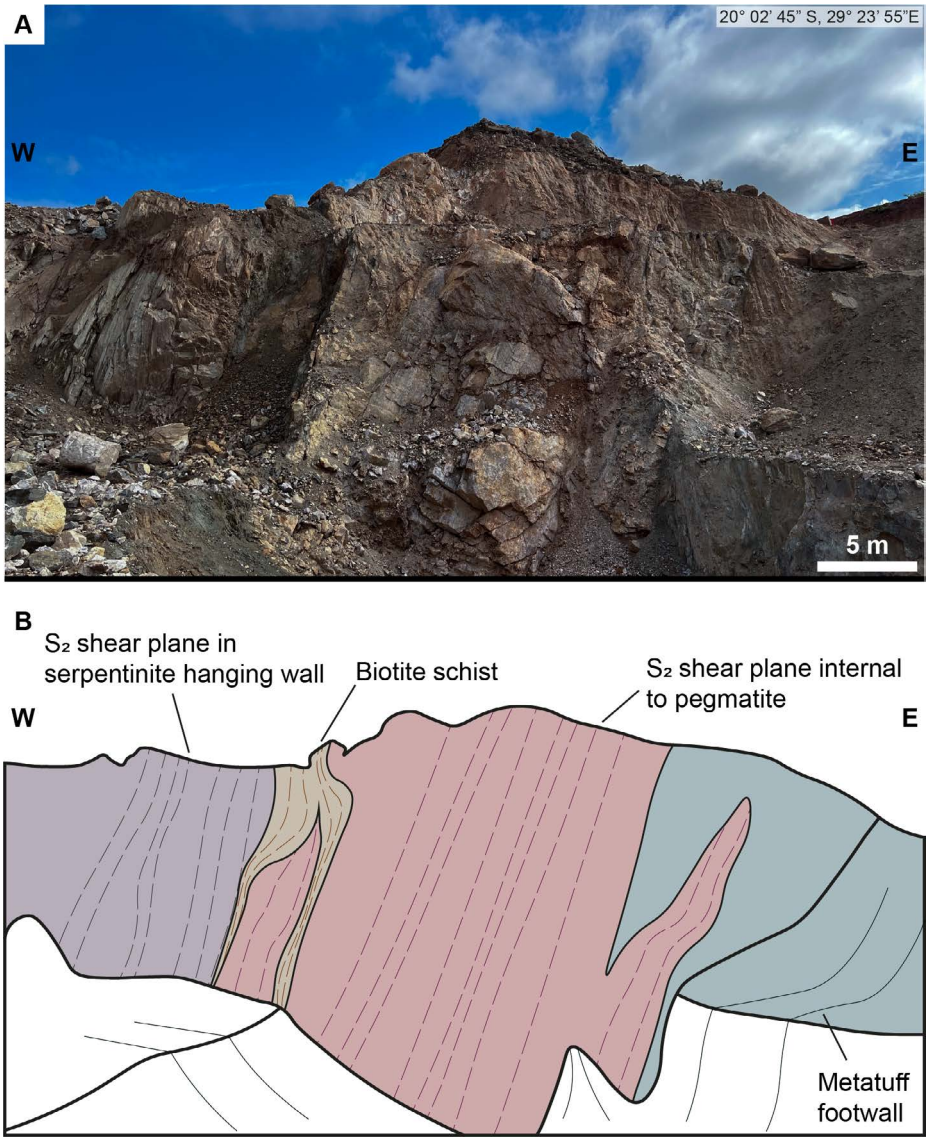


Figure 4.9: A) Outcrop image of a Type 1 pegmatite in an excavated pit. Image traced in B. B) Relationship of the $S_2$ fabric within the host rocks and the fabric internal to the pegmatite highlighted, with the common biotite schist along the hanging wall of the pegmatite. Location of image in top right.

veloped. Given the systematic orientation of individual bodies, we suggest that Type 2 pegmatites were syn-to-late-kinematic to $D_2$ and emplaced along typical sinistral strike-slip subordinate fracture sets and/or tension gashes (Figures 4.10 and 4.11). This timing, and emplacement into zones of lower strain, served to truncate the cooling history of Type 2, inhibiting extensive recrystallization and preserving primary magmatic mineralogy and textures.

As well as controlling the emplacement trajectory, host rock lithology also influenced the size of individual pegmatite bodies. As the Zulu pegmatite field extends away from the Fort – Rixon Shangani Greenstone belt into the basement granitoids, individual pegmatites become narrower in width. We interpret this to be driven by the absence of significant rheological contrast within the more competent granitoid host rocks. Whereas the relatively incompetent lithologies and lithological boundaries within the greenstone belt accommodated strain by ductile deformation and concentrated fluid flow along lithological boundaries, the more competent granitoid basement likely accommodated strain through localized brittle fracturing. Narrow mode-1 fractures formed as a result, facilitating pegmatite emplacement within the basement granitoids (Figure 4.11). This behavior would have limited dilation, promoting the formation of several thin, strike-parallel intrusions, instead of thick bodies.

### 4.4.2 Comparison with other pegmatite fields

Systematic structural analyses of economic pegmatite fields are rare in the literature. However, similar relationships to those observed in the Zulu pegmatite field have been described in other economic pegmatite districts and highlight the importance of regional-scale controlling structures on the size, orientation, and distributions of pegmatites themselves. Four well-studied examples are briefly mentioned here.

The Archaean Greenbushes pegmatite field, Western Australia, is one of the largest hard-rock Li deposits in the world (Bowell et al., 2020, , Figure 4.12A). The Greenbushes pegmatite is emplaced into the 150 km long and 15–20 km wide Donnybrook–Bridgetown shear zone, which preserves a major sinistral component of movement (Partington et al., 1986; Partington, 1988). Detailed fieldwork has shown that mineralized pegmatites of the Greenbushes pegmatite contain relict igneous structures and pegmatitic microstructures indicating syn-kinematic emplacement into structures related to the Donnybrook–Bridgetown shear zone. Individual pegmatite bodies strike subparallel to their controlling structures, as with the Type 1 pegmatites in the Zulu pegmatite field.

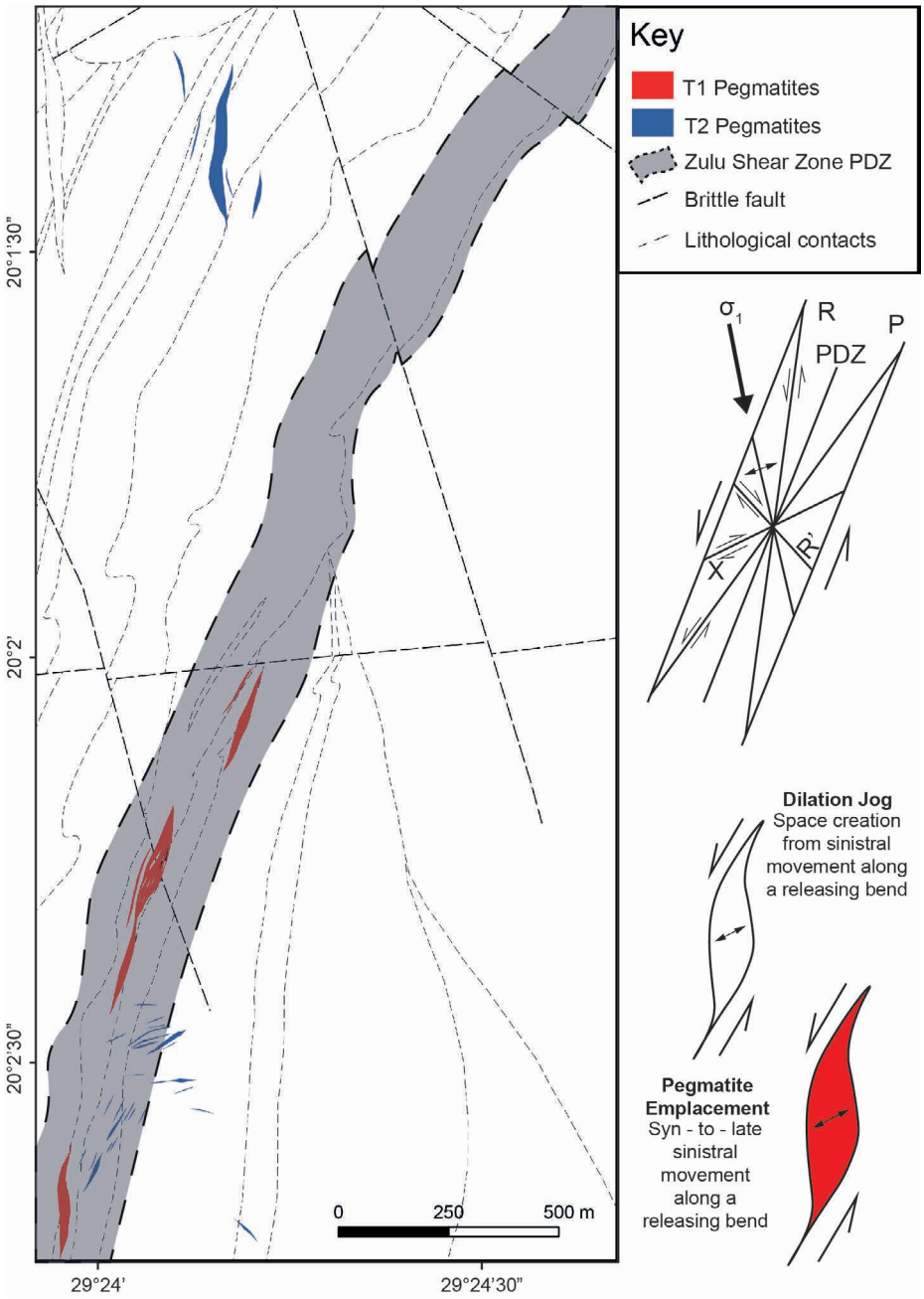


Figure 4.10: Simplified geological map discriminating between group one and two pegmatites. A schematic emplacement model of the Zulu Pegmatite Field with a parallel Riedel schematic is drawn to the right of the map. T1: Type 1, T2: Type 2, PDZ: principal deformation zone.

Pegmatites of the north-eastern Archaean Pilbara craton in Australia are also associated with major regional structures (Figure 4.12B). Several N–S to NNE–SSW trending sinistral shear zones transect the craton. Most large Li-rich pegmatites (e.g., Wodgina, Tabba Tabba) in the Pilbara are hosted within subparallel dilational

sites where greenstone belts are cross-cut by these shear zones (Sweetapple, 2000; Sweetapple and Collins, 2002). The Zulu pegmatite field is similarly located at the transect between a major regional structure and a greenstone belt.

The Brazil Lake pegmatite field was emplaced into the Meguma terrane (540 – 420 Ma) metasedimentary and metavolcanic successions (Figure 4.12D, Culshaw and Reynolds, 1997; Kontak, 2006). Shear zones are common in the area and were repeatedly reactivated during both deformational events. Pegmatites within the Brazil Lake pegmatite field were emplaced at 395 Ma along major lithological boundaries into dilational sites that have orientations sub-parallel to dextral strike-slip movement (Kontak, 2006). Similarly to the Type 1 pegmatites of the Zulu pegmatite field, deformation along the pegmatite–wall rock contact and deformation within primary magmatic phases at Brazil Lake indicate that pegmatite emplacement was syn-kinematic, with shearing having continued post-crystallization.

The Winnipeg River pegmatite district is largely hosted within the Archaean Bird River greenstone belt and hosts several pegmatite fields, including the world-class Tanco deposit (Figure 12C, Černý, 1982; Gilbert et al., 2008). Three major deformation events have been recognized in the region and are summarized by Duguet et al. (2009). Most pegmatites within the Winnipeg River pegmatite district are spatially and temporally associated with reactivated $D_3$ shear zones, such as the North Bernic Lake shear zone (Baadsgard and Černý, 1993; Kremer, 2010). Both ductile and brittle fabrics formed in response to $D_3$, and pegmatites were emplaced into both ductile and brittle dilational sites which in some cases result in pegmatite orientations oblique to the main shear zone (Brisbin and Trueman, 1982). As opposed to the Zulu pegmatite field, where the largest pegmatites formed syn-kinematic to ductile deformation, the largest pegmatites in the Winnipeg River pegmatite district (e.g., the Tanco pegmatite) appear to have occurred late-kinematic during colder, brittle deformation (akin to Type 2 pegmatites at in the Zulu Pegmatite Field, Kremer, 2010). In this way the timing of peak melt flux may be an important factor in determining which structural setting within shear zones are most amenable to large pegmatite deposits.

These examples, together with our observations at Zulu, highlight that major pegmatite fields hosting economic deposits formed by syn-kinematic pegmatite emplacement along major ductile shear zones.

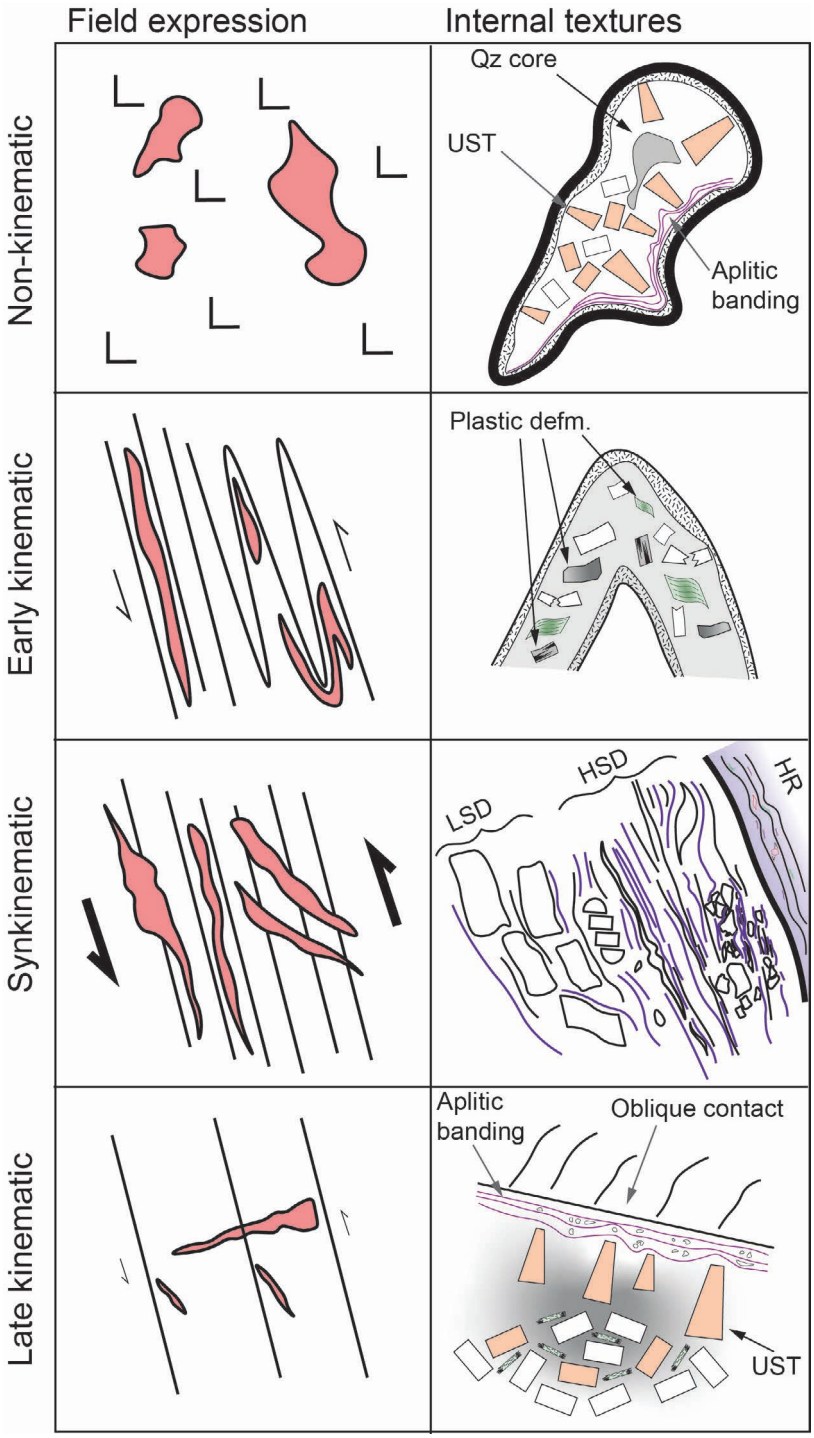


Figure 4.11: Caption on next page.

**Figure 4.11 (continued):** Schematic diagram highlighting the different styles of emplacement relative to the regional structure for pegmatites emplaced at different times during shear-dominated deformation. Both field expressions (left) and internal textures (right) are drawn. Non-kinematic pegmatites have no relationship to any fabric, nor preserve any dynamic recrystallization textures related to syn-emplacement deformation. Early kinematic pegmatites are likely to become tightly infolded with the shear fabric, and any magmatic phases preserved will exhibit extensive crystal-plastic deformation. In the syn-kinematic case, the fabric internal to the pegmatite is parallel, whilst the orientation of the intrusion locally crosscuts, deformation fabrics in the host rock. Syn-kinematic growth of exomorphic alteration phases provides additional evidence to support syn-kinematic emplacement, as is observed in Type 1 pegmatites in the Zulu pegmatite field. Late kinematic pegmatites will be emplaced into tension gashes and/or mode-1 fractures in the shear zone, and preserve a largely primary mineralogy, as is observed in Type 2 pegmatites in the Zulu pegmatite field. UST: unidirectional solidification textures, HSD: high-strain domain, LSD: low-strain domain, HR: host rock.

### 4.4.3 The influence of shear zones on pegmatite migration and emplacement

In the mineral systems framework, understanding the formation, migration, and crystallization of pegmatitic melt from source to trap is critical to constrain the expected distribution of such ore bodies in a particular district at the current level of exposure (Wyborn et al., 1994; Hagemann et al., 2016; Gardiner et al., 2024b). Whilst our observations of the Zulu pegmatite field are primarily focused on the trap (given the source is not exposed), the close association between the ILSZ and the Zulu Pegmatite Field inevitably leads to speculation on how such shear zones might be drivers and/or enablers of the localization and migration of pegmatitic melt, leading to the crystallization of economic pegmatites. This is irrespective of the source model (granite fractionation vs. anatectic) invoked, since regardless of melting mechanism, to form a large deposit significant volumes of pegmatitic melt must be extracted and physically accumulated within the mid-upper crust. Although pegmatitic melt migration into pre-existing structures may generate a spatial correlation without having to call upon a genetic association (Deveaud et al., 2013; Lee et al., 2020), here we briefly highlight how active shear zones may serve to promote the accumulation and crystallization of economic (i.e., large) pegmatites.

#### 4.4.3.1 Mechanisms of pegmatite melt extraction

The model of anatectic pegmatite formation requires low degrees of partial melting in a fertile protolith to generate melts that are enriched in incompatible elements (Simmons et al., 1995; Shaw et al., 2016; Müller et al., 2017). The threshold for physical interconnectivity of low-volume silicate melts, is often taken to be 7–10 vol. %, as determined experimentally (Rosenberg and Handy, 2005). However, Etheridge et al. (2021) showed that connectivity may be achieved at lower degrees of melt in actively deforming environments where dehydration melting processes dominate, given the volume increase caused by such reactions may drive sudden brittle failure and allow channelization of melt at proportions as small as 2 vol. %. Given that reducing the melt volume required for extraction enhances the degree of enrichment an anatectic source is able to achieve, active deformation may play an important role in realizing this model.

Similarly, the model of pegmatite melt extraction from highly fractionated granite systems (either as individual plutons or long-lived mid-crustal magma chambers) is also constrained by melt connectivity, in this case limiting the extent of fractionation that can be invoked prior to system lock-up (Vigneresse and Tikoff, 1999, Chapter 3). Although localized overpressure of melt can drive the ejection of melt from granitic source regions through dykes (Rubin, 1995; Baker, 1998), and pegmatitic intrusions formed in this way are frequently seen (e.g., Roda-Robles et al., 2023), these intrusions will be limited in size due to an absence of significant strain anisotropies in the surrounding host rocks (Brisbin, 1986). Alternatively, the presence of tectonic stresses within a melt-present environment facilitates efficient extraction of melt (Brown and Solar, 1998; Sawyer et al., 2011; Brown et al., 2011), and enable large volumes of highly fractionated melts to migrate out of their granite source region (Černý and Ercit, 2005).

It is thus worth noting that irrespective of the source mechanism invoked, the extraction of large amounts of melt is best facilitated in environments of active deformation. This promotes the formation of fewer, large, intrusions (as observed at Zulu), as opposed to several smaller pegmatitic bodies (e.g., pegmatitic pockets internal to –, or radial pegmatite haloes around the source granite).

#### 4.4.3.2 Pegmatite melt migration

Upon extraction of the final pegmatitic melt from the source region, the style and character of pegmatitic melt migration upwards through the crust before reaching a

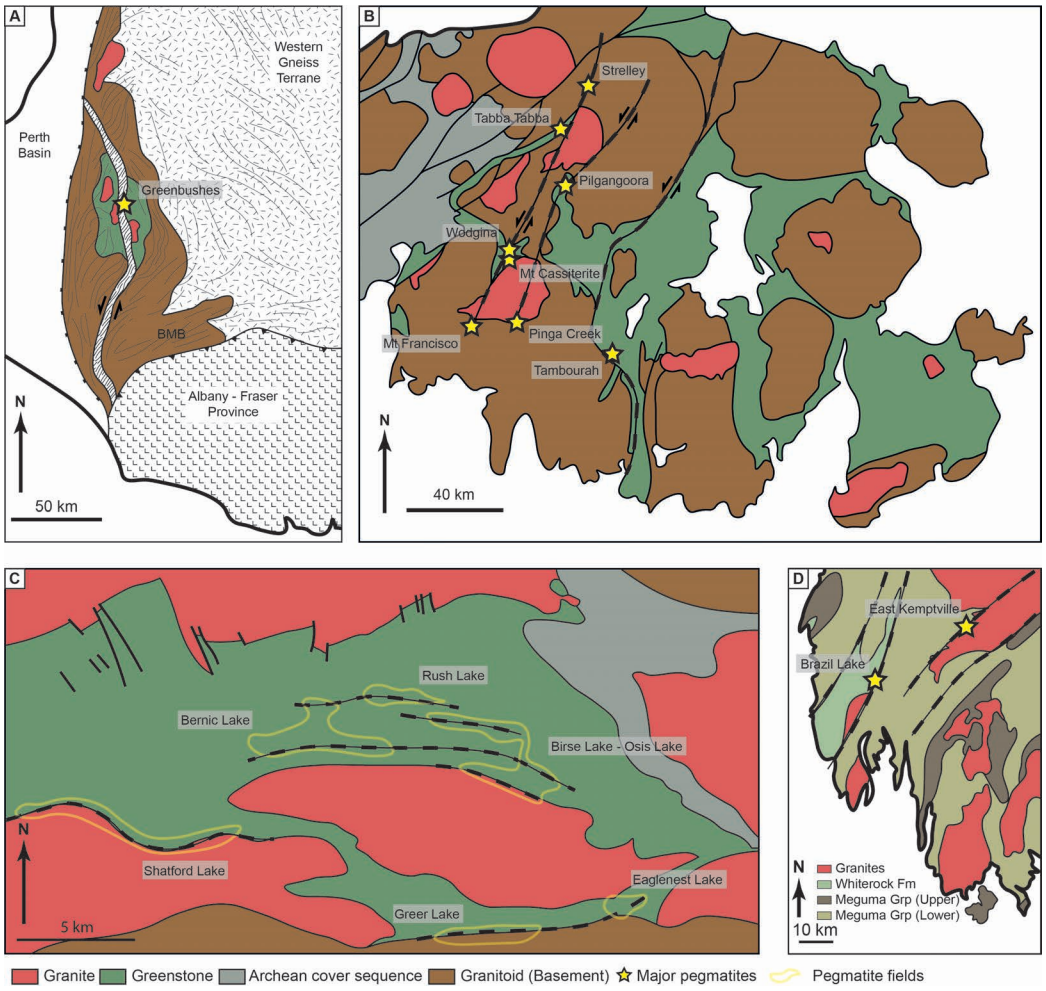


Figure 4.12: Example case studies from the A) Yilgarn Craton (after Partington et al., 1995), B) North-east Pilbara craton (after Sweetapple and Collins, 2002), C) Winniper River pegmatite district (after Kremer, 2010), and D) southwestern Nova Scotia (after Kontak, 2006).

trap depends on host rock rheology, temperature, and strength anisotropies within the crust (Brisbin, 1986). To promote the necessary undercooling to generate characteristic pegmatitic textures (Černý et al., 2005; London, 2005; Simmons and Webber, 2008; McCaffrey and Jowitt, 2023), pegmatitic melts need to be rapidly extracted from their source region and emplaced into cooler host rocks, or chemically quenched during ascent. If melt is present during ductile shearing, then these shear zones can generate regions of increased porosity and dilation, providing a siphon force for melt migration (Sibson et al., 1975; Etheridge et al., 2021), which is an effective way of forcing large volumes of melt to migrate through the crust (Brown, 2013).

The type of shear-zone system (transcurrent, normal, reverse, or oblique) also

has an effect on the vector of melt flow (Figure 4.13, Brisbin, 1986; Brown, 2013; Etheridge et al., 2021). Channelized flow along vertical dilatant conduits preferentially occurs in both transcurrent and reverse shear zones, and are therefore favourable targets for melt migration (Figure 4.13, Lindroos et al., 1996; Brown and Solar, 1998). Furthermore, transcurrent shear zones (such as the ILSZ) will promote a horizontal percolation of flow during shearing, enabling the concentration of melt from a large melt region towards sites of lower pressure prior to vertical extraction, enabling tapping of a large fertile source region (Figure 13, Sibson et al., 1975; Brown and Solar, 1998; Cavalcante et al., 2016). In this way, transcurrent releasing bends are highly favorable sites of pegmatitic melt migration and subsequent emplacement, given a fertile source is intersected, such as at Zulu or the examples presented above.

Importantly, during the waning stages of shearing, pre-existing anisotropies caused by lithological boundaries, fractures, or tensile cracks, will preferentially allow residual melt migration through the system as stress is relieved. This will result in a change of preferred orientation of late-kinematic pegmatites to oblique to the controlling structure, as is seen with Type 2 pegmatites in the Zulu pegmatite field (Brisbin, 1986; Araújo et al., 2001; Demartis et al., 2011; Bhatt et al., 2019). Given sufficiently high melt pressure and vertical flow, late pegmatitic melts may generate large intrusions (e.g., the Tanco deposit) into higher-order late brittle fractures or tension gashes (Brisbin, 1986; Duguet et al., 2009; Kremer, 2010; Bhatt et al., 2019). In this scenario, pegmatites of economic size may not be orientated parallel to the trend of the major shear zone, as subordinate structures can form oblique to the major shear zone strike (Figures 4.10 and 4.11).

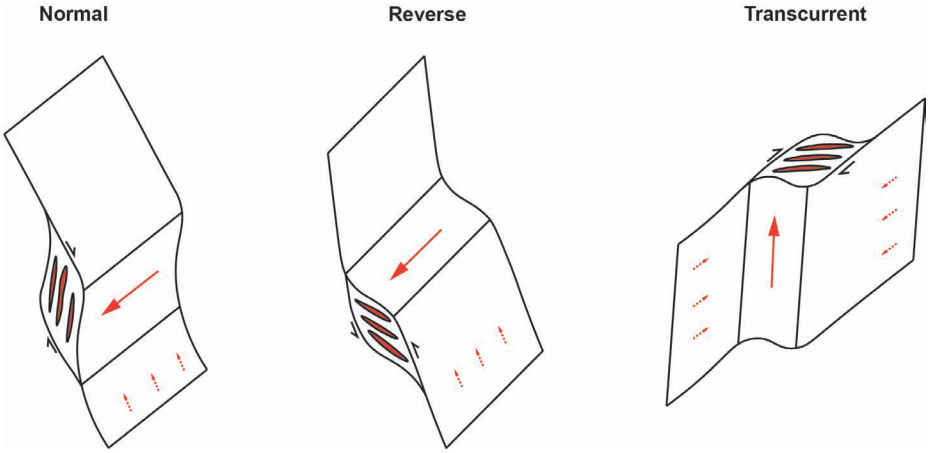


Figure 4.13: Schematic sketches of melt flow orientations relative to three major structural types (modified from Etheridge et al., 2021). Dashed lines represent preferred direction during percolative flow, and solid lines represent preferentially direction of channelized flow. The geometry of dilational jogs is shown for each fault type. Both normal and reverse faults generate subhorizontal zones of dilation, whereas transcurrent systems generate vertical conduits.

### 4.4.4 Implication for exploration strategies

Irrespective of the source of pegmatites, we suggest that crustal shear zones can play a fundamental role in allowing pegmatitic melt to migrate away from its source region. The localization of melt within shear zones enables the formation of large bodies of evolved melt, in contrast to smaller individual bodies formed around a parental granite in the absence of tectonic stresses (Černý, 1991b). Thus, when present, shear zones act as a first-order control on the spatial distribution of large pegmatite fields, as is seen at several major deposits such as Greenbushes, Tanco, and Zulu.

We propose that desktop studies should focus on delineating potential structural corridors through which pegmatitic melts may have migrated, with a preference for transcurrent shear zones. The presence of granites with fertile characteristics (reduced K/Rb, elevated concentrations of incompatible elements such as Li, Rb, F, Cs, Selway, 2005) along the shear zone may further indicate that the shear zone has intersected a fertile source region, though does not imply that the fertile granites are the source of pegmatites. Such a systematic approach can help delineate the new prospective regions for discovering economic pegmatite bodies.

## 4.5 Conclusions

The Zulu pegmatite field is an excellent case study with which to highlight the importance of ductile shear-related deformation on both the emplacement mechanisms of pegmatites – where they control the orientation, distribution, and width of individual bodies – alongside controlling the degree of subsolidus recrystallization a pegmatite experiences during deformation. At Zulu, major competency contrasts between lithologies localized high-strain domains during sinistral strike-slip shearing. Pegmatites were emplaced into subparallel dilational jogs syn-kinematic to shearing and subsequently extensively recrystallized during continued deformation, driving the (re)precipitation of fine-grained spodumene and muscovite. By contrast, late-kinematic pegmatites at Zulu are emplaced along late-kinematic subordinate fracture sets and tension gashes oblique to the principal shearing direction and preserve their magmatic mineralogy owing to limited subsolidus deformation.

Shear zones are known to be regions that allow efficient migration of silicate melt through the continental crust. In the presence of a fertile source, specifically transcurrent shear zones enable efficient migration of significant pegmatitic melt from a hot source region to a shallower level, cooler host rock, driving undercooling and enabling the rapid crystallization textures distinctive of pegmatites. Future greenfield exploration should therefore focus on constraining transcurrent shear zones where significant strength anisotropies are present, with indicators of fertility at the melt source (e.g., enriched granites along the shear zone). Constraining the structural history and relative timing of pegmatite emplacement through detailed fieldwork and petrographic analyses can subsequently shed light on the distribution and orientation of individual pegmatite bodies within a pegmatite field. Importantly, a focus on constraining the source (granite vs. anatectic) of a pegmatite district may therefore be of lesser importance, as regional structures have a more important control on the distribution of individual bodies within a district.

# Chapter 5

# Archean tectonic evolution of the Zimbabwe Craton and the mechanisms of lithium enrichment

## 5.1 Introduction

### 5.1.1 Chapter outline

In this study on the Zimbabwe craton, new coupled geochronology and geochemistry is integrated into a compilation of pre-existing data to develop a holistic understanding of cratonic evolution. Using this dataset, and testing it against the results of petrologic modelling, a complete model of craton development is proposed, which includes periods of both vertical and horizontal accretion. Early juvenile continental growth was submarine; later potassic (evolved) magmatism is suggested to have supported continental emergence and the formation of late supracrustal cover sequences. A new model for lithium pegmatite sources is therefore required, which based on the present data is proposed to revolve around repeated recycling of felsic continental crust through melting, rather than erosion, which sufficiently drove lithium enrichment to obviate the need for sedimentary sources in the melting environment.

### 5.1.2 Sources of TTG melts

Tonalite–trondhjemite–granodiorite (TTG) suite rocks are typically metaluminous, sodic granitoids that constitute >80% of preserved Archean crustal fragments (Bleeker, 2003; Polat, 2012). These juvenile intrusive rocks are characterised by high $Na_2O/CaO$, low $K_2O/Na_2O$ (TTG *sensu stricto*), and a relatively simple mineralogy of predominantly plagioclase feldspar and quartz, with biotite or amphibole ± epidote (Martin, 1994; Bédard, 2003; Moyen et al., 2006; Moyen and Martin, 2012). The TTG suite

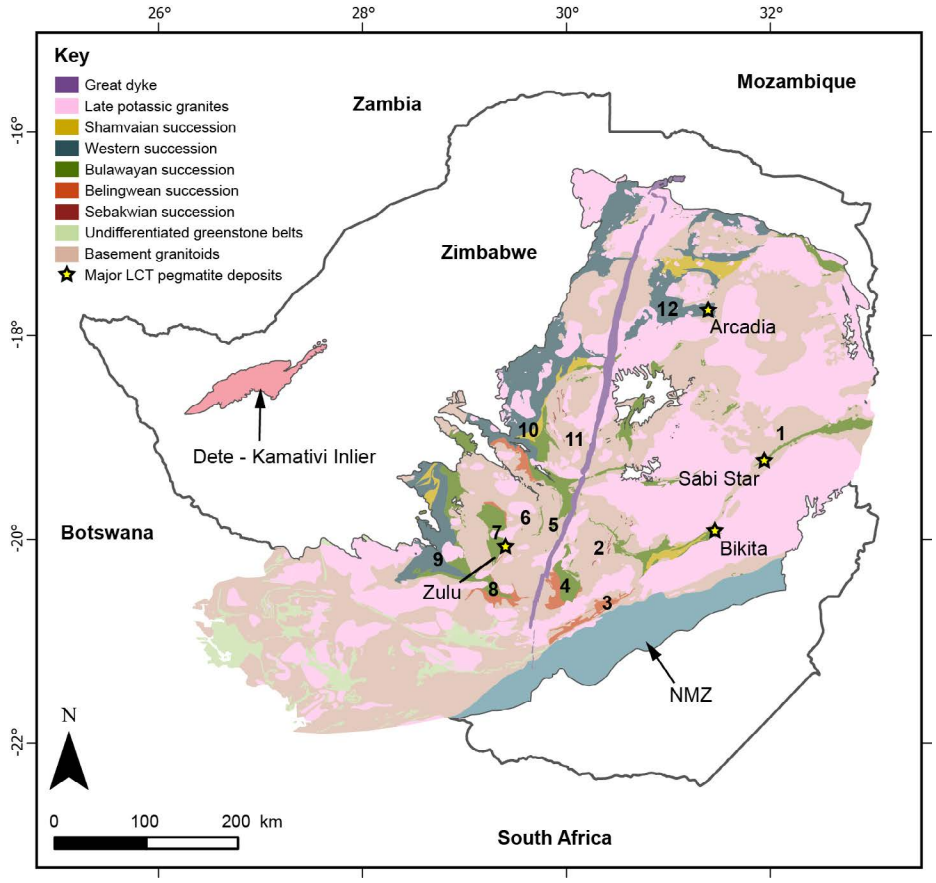


Figure 5.1: Simplified geological map of the Zimbabwe craton, highlighting key locations discussed in this chapter. 1: Murewa–Odzi greenstone belt, 2: Tokwe terrane, 3: Buhwa greenstone belt, 4: Belingwe greenstone belt, 5: Gwenoro dam, 6: Shangani batholith, 7: Fort Rixon–Shangani greenstone belt, 8: Filabusi greenstone belt, 9: Bulawayo greenstone belt, 10: Midlands greenstone belt, 11: Rhodesdale terrane, 12: Harare–Shamva greenstone belt. NMZ: Northern marginal zone.

is often divided into three geochemical groups, which historically have been inferred to represent the depth of melting of their source; 1) a 'high-pressure' group characterised by high $Al_2O_3$, $Na_2O$, Sr, and La/Yb, with low Y and Nb/Ta, 2) a 'low-pressure' group characterised by low $Al_2O_3$, $Na_2O$, Sr, and La/Yb, as well as high Y and Nb/Ta, and 3) a 'medium-pressure' group which displays transitional characteristics between high- and low-pressure groups (Martin and Moyen, 2002; Moyen, 2011; Moyen and Martin, 2012; Laurie et al., 2013). These geochemical characteristics are thought to arise through variations in the restitic mineralogy; high Sr contents in the melt likely indicate a plagioclase-poor residuum, low Nb/Ta corresponds to the presence of rutile, and high La/Yb arises from the presence of garnet in the residuum (Martin and Moyen, 2002; Foley et al., 2002; Rapp et al., 2003). However, varia-

tions in source chemistry, melt mixing, and fractional crystallisation can all impose additional variability in TTG chemistry (Moyen et al., 2006; Getsinger et al., 2009; Hoffmann et al., 2014).

It is generally accepted that TTGs are sourced by melting of a hydrous metabasalt (Drummond and Defant, 1990; Arculus and Ruff, 1990; Rapp et al., 1991; Wolf and Wyllie, 1994; Foley et al., 2002; Moyen and Martin, 2012), though some have argued that fluid absent conditions are preferable (Rapp et al., 2003; Moyen and Stevens, 2006). Experimental studies have shown that Archean TTGs likely formed at temperatures of 750–950 °C (Xiong et al., 2009; Qian and Hermann, 2013), which is supported by phase equilibria modelling (Palin et al., 2016a; Johnson et al., 2017; Kendrick and Yakymchuk, 2020). Generating voluminous melts in this temperature range requires water saturation (e.g., Palin et al., 2016a; Pourteau et al., 2020), therefore supporting a hydrous source. Many modelling studies consider the enriched Archean tholeiite (EAT) of Condie (1981) as a representative metabasaltic protolith, as melts derived from EAT provide a close match to natural Archean TTG compositions from both a major element and trace element perspective (Bédard, 2006; Martin et al., 2014; Palin et al., 2016a).

A key question related to Archean TTG formation is the geological setting in which the melts formed, which provides constraints on the geodynamic character of the early Earth. Given 50–60% of Earth's continental crust had formed by the Archean (e.g., Taylor and McLennan, 1995; Hawkesworth and Kemp, 2006; Dhuime et al., 2012), the geological processes responsible for generating Archean TTGs must have been highly efficient. Modern day continental crust is primarily formed in continental and island arcs (e.g., Rudnick, 1995; Taylor and McLennan, 1995; Jagoutz and Kelemen, 2015), where dehydration reactions in the subducting slab release water into the overlying mantle wedge, driving fluid-mediated melting of the mantle and the generation of basaltic melts. These basaltic melts either form the basis of arc magmatism (through assimilation and fractional crystallisation), or underplate the lower crust and heat the lower crust to promote fluid-present melting of the lower crust and generating andesitic-dacitic magmas.

A similar tectonic environment has been suggested for the formation of TTGs (e.g., Martin and Moyen, 2002; Rapp et al., 2003), largely based on geochemical similarities between TTGs and modern day adakites (Martin, 1999), the latter of which are derived by directly melting the subducting slab (Castillo, 2012). Experimental studies (see Moyen and Stevens, 2006) show that garnet first appears in metamorphosed EAT-like mafic rocks at pressures $> 10$ kbar, and so melting at these condi-

tions can generate characteristic 'high-pressure' La/Yb signatures. Proponents of this model where Archean TTGs formed in arc-like environments either invoke modern-day steep subduction zones and thick mantle wedges, or flat-slab subduction with little to no interaction with the asthenospheric mantle, with changes in Ni, Cr, and MgO content of TTGs used to discriminate between these processes (Martin et al., 2005). Given TTGs represent a significant portion of preserved Archean terranes, substantial amounts of hydrated mafic source material needs to be transported to garnet-stability conditions, and subduction zones are an efficient pathway for doing so on the modern Earth.

Whether modern day subduction could have operated on the early Earth is a matter of intense current debate (Stern, 2005), with many researchers concluding that this is an unlikely scenario given the paucity of key geological indicators of convergent plate margin processes in Archean terranes (c.f. paired metamorphic belts, Miyashiro, 1973; blueschists, though see Palin and White, 2016). The Archean mantle was also significantly hotter than today (Korenaga, 2006) and was associated with a thicker and more buoyant primary mafic oceanic crust (Herzberg et al., 2010), which would have reduced the efficiency of subduction (van Hunen and Moyen, 2012; Korenaga, 2013). Further, felsic crustal growth in several Archean terranes appears to have been episodic, which is in contrast to the continuous nature of formation in subduction terranes (Stein and Hofmann, 1994; Rino et al., 2004; Dhuime et al., 2012; Hawkesworth et al., 2016). Archean terranes also show large-scale dome-and-keel structures that are unlike linear fold and thrust belts of younger mountain belts (Macgregor, 1951; Goodwin, 1981; Hamilton, 1998), which has been argued as evidence in favour of a non-uniformitarian style of tectonics. However, others have suggested that these are in fact more typical of mid-crustal structures around diapirs in modern arc terranes (e.g., Kusky et al., 2021).

Opponents to the subduction model have proposed that TTG magma generation may have occurred at the base of thickened mafic crust, such as oceanic plateaux (e.g., Smithies, 2000; Bédard, 2006; Van Kranendonk, 2010). Studies on Archean sediment geochemistry suggest that oceanic plateaux were abundant (Kamber, 2010), and would have attained thicknesses between 40–45 km (Vlaar et al., 1994; Korenaga, 2006). Such thicknesses would have stabilised garnet at the base (corresponding to 12–14 kbar), thereby enabling plateaux-derived sources to impart 'high-pressure' TTG signatures on melts. Furthermore, LILE-enriched basaltic sources (such as EAT, Condie, 1981) were most likely generated by melting of undepleted mantle peridotite, such as those transported from the lower mantle to the surface via plumes

(Guitreau et al., 2012; Martin et al., 2014). Opponents to the plateaux model argue that it is unlikely that the bases of oceanic plateaux are sufficiently hydrated to generate voluminous TTG terranes (Arndt, 2013). However, syn-eruptive hydration during sub-aqueous eruption, followed by repeated burial of lava flows during vertical accretion likely acts as a mechanism to transport hydrated basalts to depths sufficient for partial melting (Kamber, 2015). Alternatively, komatiites may have played an important role in transporting fluid to the lower crust (Hartnady et al., 2022; Tamblyn et al., 2023). This is because the high $X_{Mg}$ in komatiites makes them more susceptible to hydration in low-temperature conditions, generating high-Mg chlorite which then acts as a water carrier during burial until dehydration at 680–800 °C. Given komatiites are a key component of several Archean terranes (e.g., Bickle et al., 1975), they provide a mechanism for water to be brought to suprasolidus conditions (Tamblyn et al., 2023). In either case, a surface water source for TTG melts is supported by recent Si-isotope studies (Murphy et al., 2024).

In reality, it is likely that a combination of these processes were active in the Archean (Bédard et al., 2013), supported by quantitative geodynamic models which support that both models may have been feasible under Archean conditions (e.g., Piccolo et al., 2019). It is therefore pertinent that each individual craton is scrutinised appropriately in order to fully understand its evolution.

In light of this and the newly collected data described below, I outline a model for the evolution of, and crustal formation in, the Zimbabwe craton by integrating the data collected described below (using methods described in Chapter 2) with previously published work.

## 5.2 Results

### 5.2.1 New geochronological data from the Zimbabwe craton

Geochronological data collected in this study comprises of zircon, apatite, and titanite U-Pb geochronology, and Rb-Sr geochronology of biotite and white mica samples, and is compiled in Appendix C. Sample locations and field context is provided in appendices A and B. A summary of new data is presented in Figure 5.2 and described in detail below.

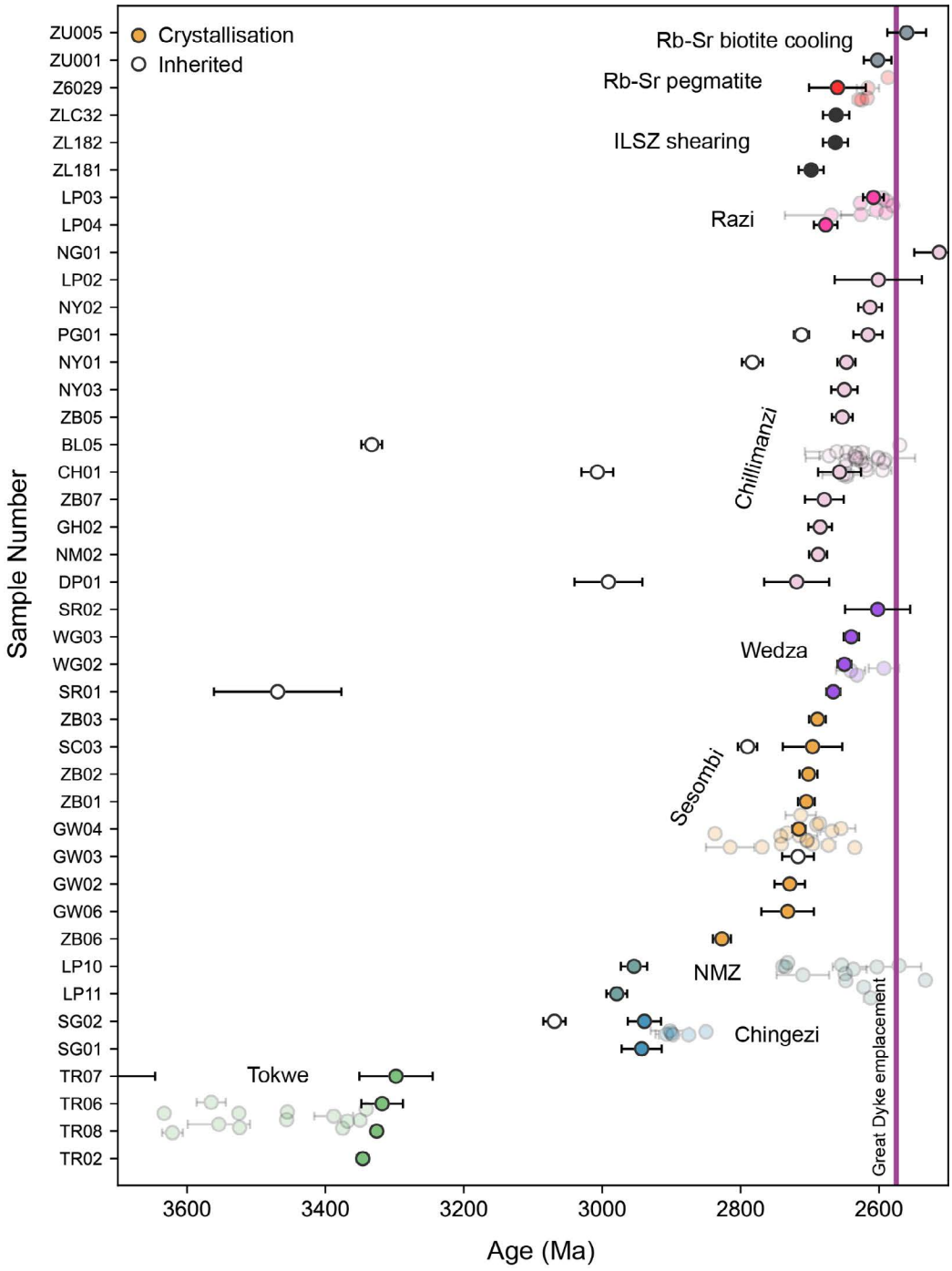


Figure 5.2: Summary diagram of newly collected geochronological data. Data from other studies (Appendix A) is shown as transparent markers, and clustered by the corresponding suites described here. Both crystallisation (full circles), and inherited (open circles) ages are shown.

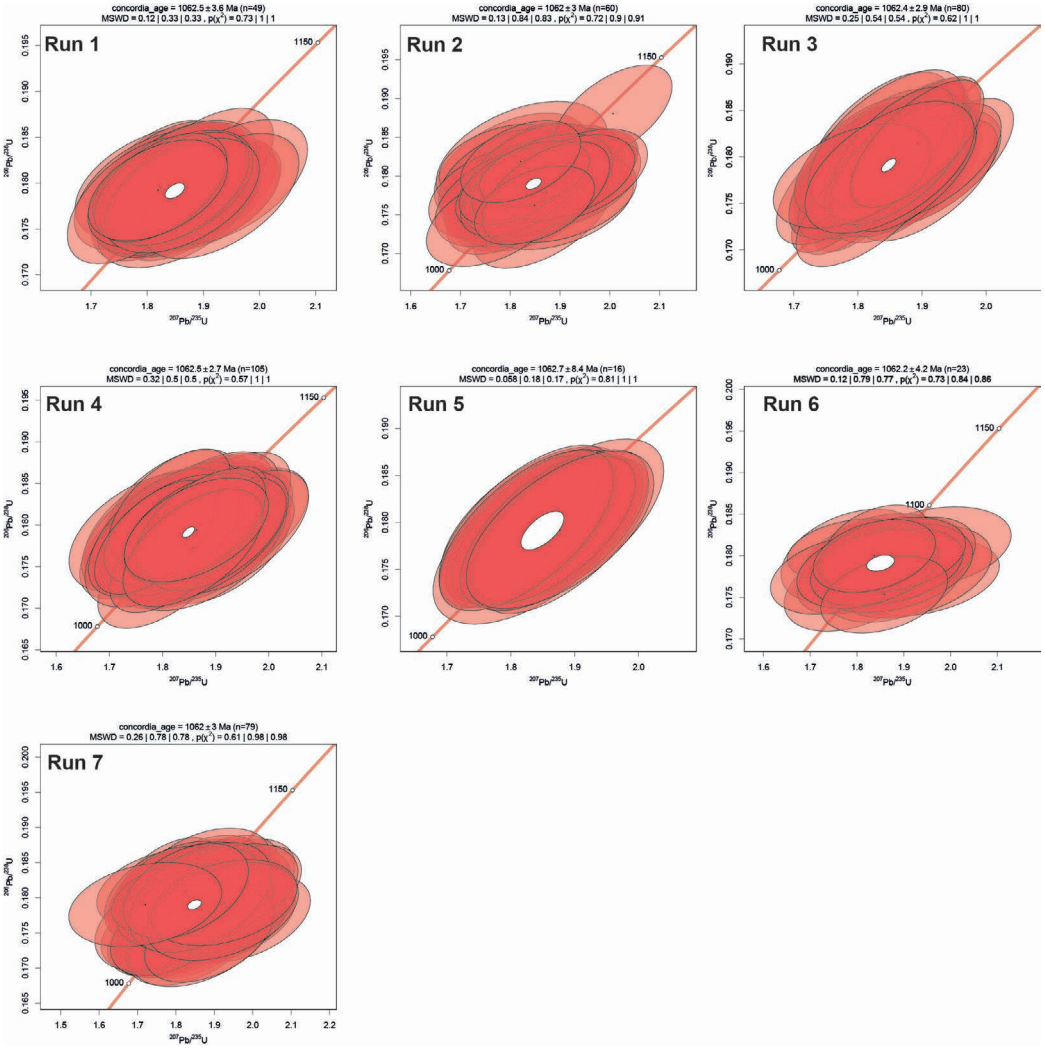


Figure 5.3: Wetherill concordia plots for primary reference standard 91500 grouped by analytical run.

#### 5.2.1.1 U-Pb zircon standards

Primary standard 91500 yielded consistent results across each analytical session (Figure 5.3). All ablated spots were concordant and tightly clustered, with mean square weighted deviates (MSWD) of concordance + equivalence between 0.17 and 0.83. All runs were within error of the accepted age (1063.78 ± 0.65 Ma; (Horstwood et al., 2016; Wiedenbeck et al., 1995).

Secondary standard Plešovice yielded more variable results, with a range in ages from 325.4–340.1 Ma (Figure 5.4). Runs 2–5 yielded several analyses that were discordant, which may be due to natural variability in the reference standard or ablation through inclusions/cracks in the grains. Excluding discordant analyses, MSWD

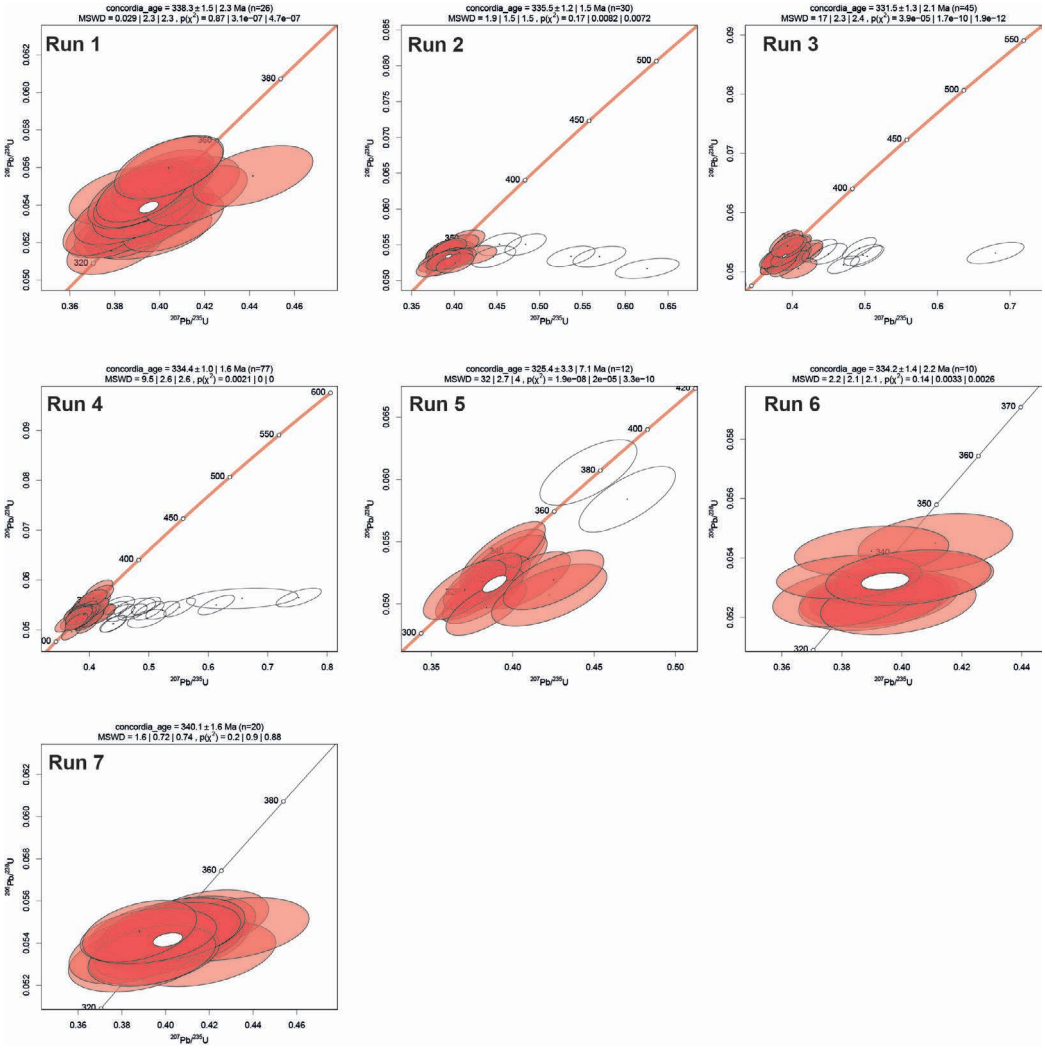


Figure 5.4: Wetherill concordia plots for secondary standard Plešovice grouped by analytical run

ranges from 0.74–4. The results are generally within error of the accepted age (337.13 ± 0.37 Ma; Sláma et al., 2008).

Analyses of Maniitsoq yielded internally consistent results (MSWD = 0.28–1.2) between each run, with reported ages $^{207}Pb/^{206}Pb$ ages ranging between 2990.5 ± 3.7 Ma to 3013 ± 18 Ma (Figure 5.5). Reported ages are all within error of the accepted age (3005 ± 2.6 Ma; Marsh et al., 2019) with the exception of runs 2 and 4 which returned marginally lower ages (2990.5 ± 3.7 Ma and 2992.4 ± 6.3 Ma, respectively).

Secondary standard OG1 was analysed during runs 1–3, and 6–7, and yielded consistent results (Figure 5.6). All $^{207}Pb/^{206}Pb$ ages are considered homogeneous ($p(\chi^2) > 0.05$), and are within error of the accepted age (3465.4 ± 0.6 Ma; Stern et al., 2009).

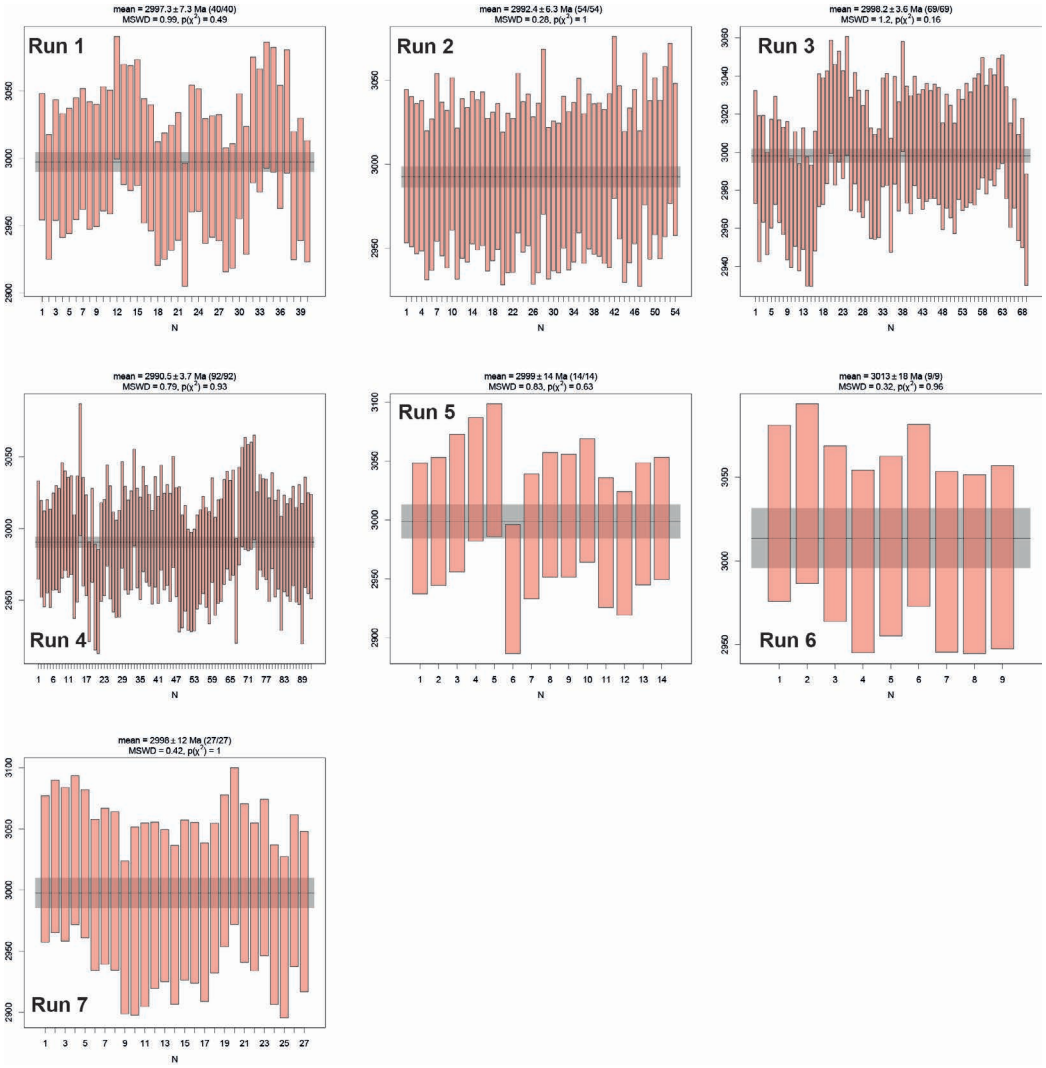


Figure 5.5: $^{207}Pb/^{206}Pb$ weighted mean plots for secondary reference material Manitsoq across analytical runs.

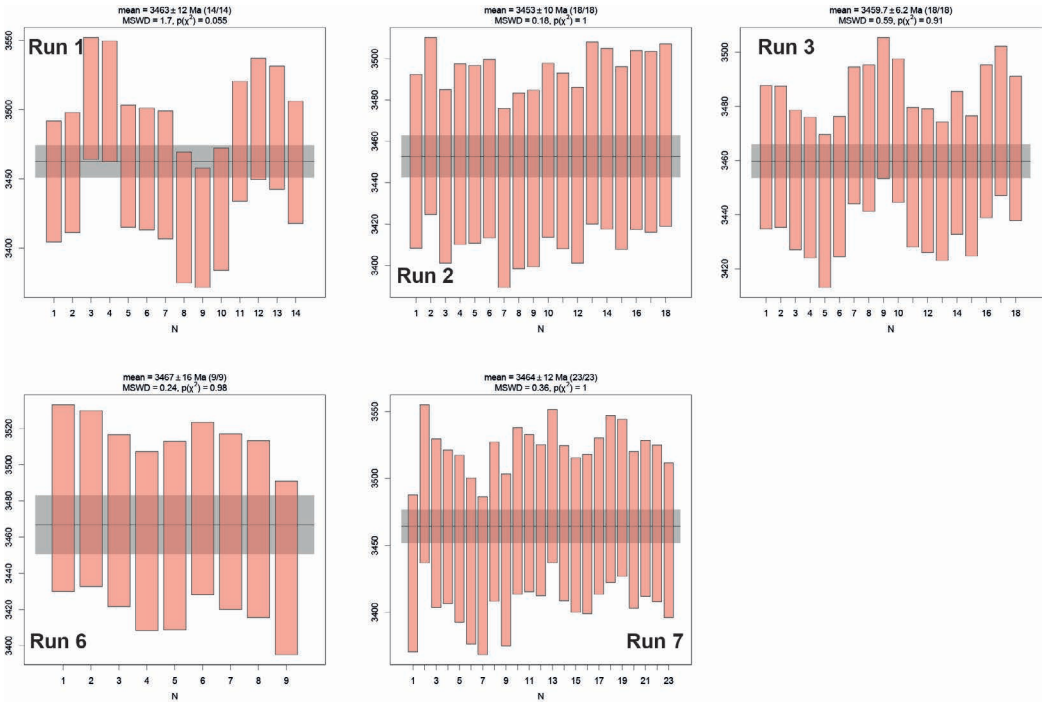


Figure 5.6: $^{207}Pb/^{206}Pb$ weighted mean plots for secondary standard OG1, grouped by analytical run.

#### 5.2.1.2 Tokwe segment

*TR02* is a complexly folded hornblende-rich tonalitic banded gneiss from the Tokwe river 3 km west of Bwanya. Melanosomes have a well-defined foliation defined by the alignment of hornblende laths, whilst leucosomes present only a weak foliation. Later folding, which post-dates leucosome formation, has caused reoriented some hornblende crystals into an axial-planar alignment. Thirty individual spots from 25 zircons yielded 11 concordant analyses for a concordia age of 3346.0 ± 8.6 Ma (MSWD = 1.2), which is interpreted as a crystallization age of the leucocratic material (Figure 5.7).

*TR06* is a strongly banded tonalitic gneiss from the Tokwe river 3 km west of Bwanya. Banding is on the mm–cm scale, with darker bands consisting more abundant well-foliated biotite and chlorite. Thirty individual spots from 21 zircons yielded 18 analyses which define a discordia model age of 3302 ± 40 Ma (MSWD = 4.8) (Figure 5.8). One concordant zircon produced a concordia age of 3318 ± 30 Ma (MSWD = 0.32), which is collectively interpreted with the discordia model age as the age of crystallization.

*TR07* is a garnet-bearing trondhjemitic sill which is intrusive to the banded tonalitic gneiss of *TR06*. Contact between the two units is fabric-parallel. The fab-

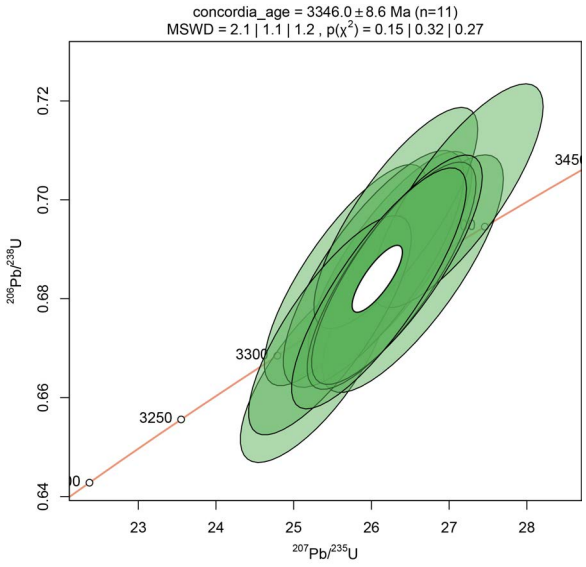


Figure 5.7: Wetherill plot of concordant analyses from sample TR02.

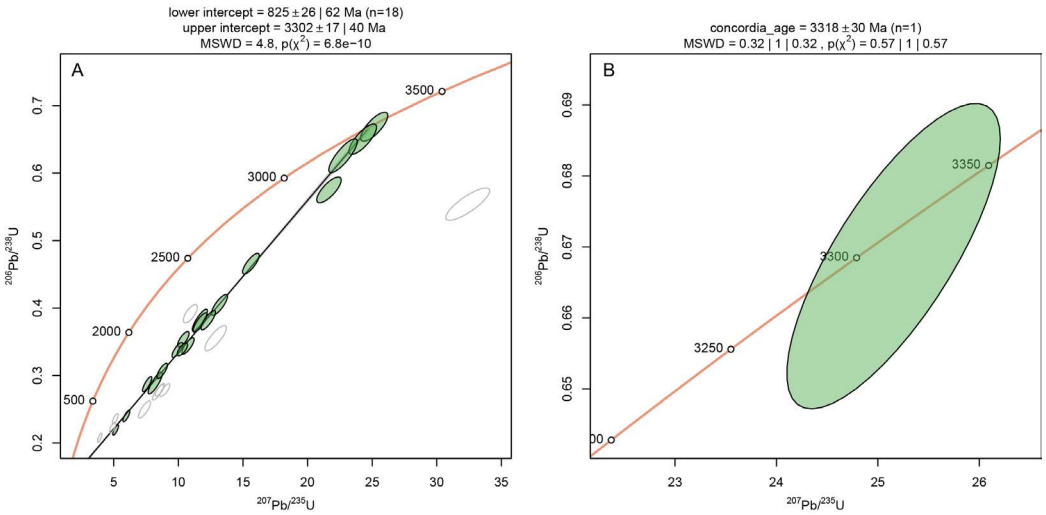


Figure 5.8: Wetherill concordia plots of sample TR06. A) Discordia model, B) zoom in of concordant analysis.

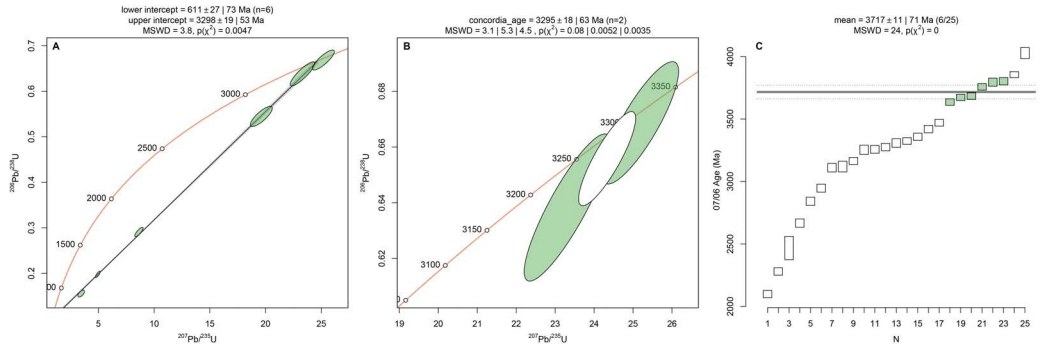


Figure 5.9: Wetherill concordia (A+B) and $^{207}Pb/^{206}Pb$ weighted mean (C) plots of sample TR07. A) Discordia model, B) zoom in on concordant analyses, C) inherited analyses cluster.

ric within *TR07* is defined by a strong alignment of muscovite, and garnet appears syn-kinematic to fabric formation. Forty individual spots from 33 zircons yielded 6 zircons which define a discordia age of 3298 ± 53 Ma (MSWD = 3.8, Figure 5.9). Two concordant zircon analyses return a concordia age of 3295 ± 63 Ma (MSWD = 4.5) which in conjunction with the discordia age is interpreted as the age of crystallization. Six analyses of zircon cores yield a $^{207}Pb/^{206}Pb$ weighted mean age of 3717 ± 71 Ma (MSWD = 24), which is interpreted as an inherited age.

*TR08* is a mafic tonalite collected near *TR02*. Leucosomes within the sample have amalgamated into cm–dm scale fabric-parallel bands along sub-parallel (to the dominant fabric) leucocratic veins. The foliation is defined by strongly aligned hornblende crystals within the melanocratic layers. Thirty analyses of 24 zircon grains returned 16 concordant spots which define a concordia age of 3325.9 ± 6.3 Ma (MSWD = 1.3) and a $^{207}Pb/^{206}Pb$ weighted mean age of 3319.9 ± 6.8 Ma (MSWD = 0.42) (Figure 5.10). Collectively, these ages are interpreted as the age of crystallization of the leucocratic material.

#### 5.2.1.3 Shabani gneiss

*SG01* is a migmatitic gneiss collected from the Runde river 15 km NE of Zvishavane. A fabric is defined by biotite in the restitic assemblage, that occasionally wraps sericitised feldspar phenocrysts. Radiation haloes are commonly seen within biotite. Thirteen individual analyses from 26 zircon crystals define a discordia with an upper intercept age of 2954 ± 34 Ma (MSWD = 2.2) (Figure 5.11). One concordant analysis yielded a concordia age of 2943 ± 29 Ma (MSWD = 0.32). These ages are collectively interpreted as the age of crystallization of the migmatite. One concordant analysis of an interpreted xenocryst returned a concordia age of 3160 ± 34 Ma (MSWD = 1.3).

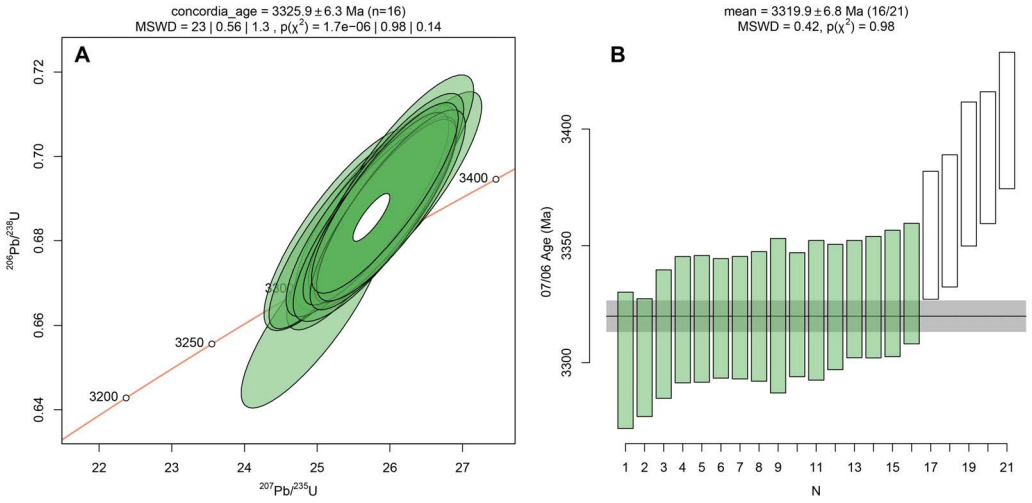


Figure 5.10: A) Wetherill plot of concordant analyses, B) $^{207}Pb/^{206}Pb$ weighted mean plot of sample TR08. Statistical outliers excluded in (B).

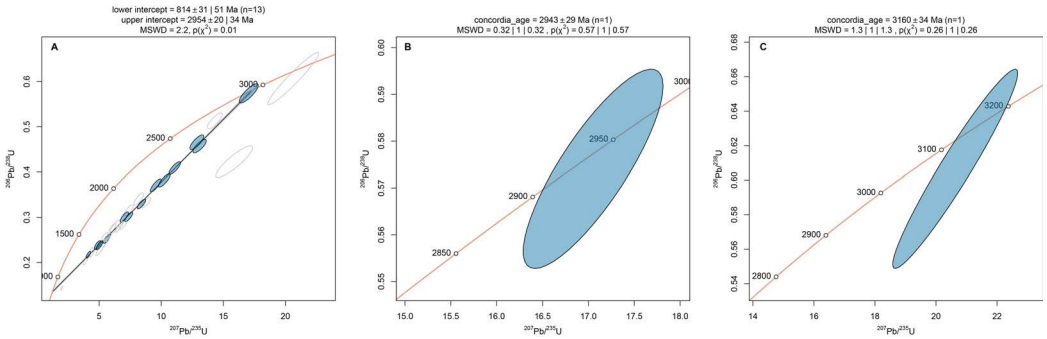


Figure 5.11: Wetherill plots of analyses from SG01. A) Discordia model with spots considered shaded, B) zoom in on concordant analysis of an interpreted crystallisation-age zircon, and C) concordant analysis of inherited grain.

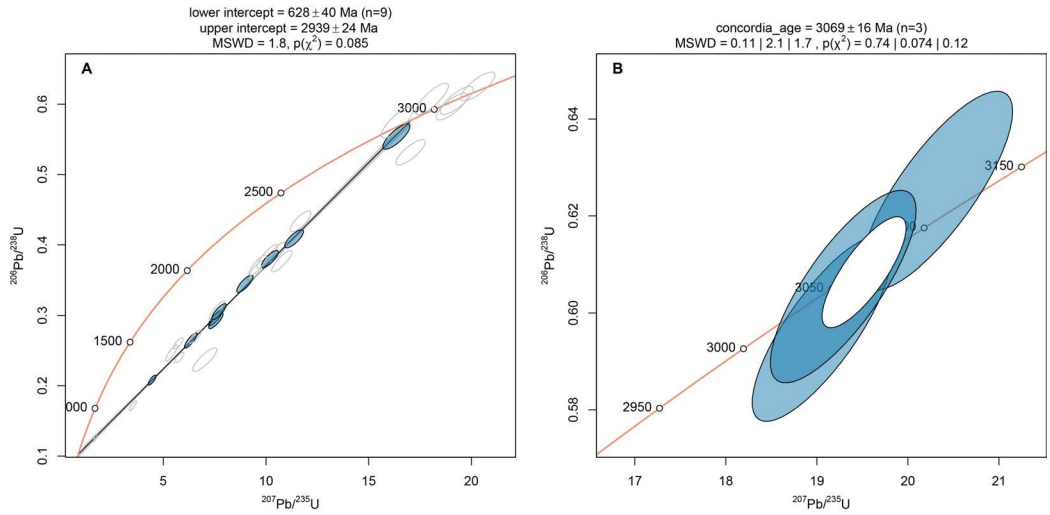


Figure 5.12: Wetherill plots of analyses from SG02. A) Discordia model with considered spots shaded, B) zoom in on concordant analyses of xenocrystic zircon analyses.

*SG02* is a foliated tonalitic dyke intrusive to *SG01*. An internal fabric is defined by the alignment of biotite (± muscovite) and is parallel to the external fabric in the host gneiss. Contacts between the units are sharp and subparallel to the deformation fabric. Nine individual analyses from 28 zircons returned comparable U/Th ratios (1.5–3.0) and yield an upper intercept age on a discordia model of 2939 ± 24 Ma (MSWD = 1.8), and is interpreted as the crystallization age (Figure 5.12). Three separate analyses returned a concordia age of 3069 ± 16 Ma (MSWD = 1.7), which is interpreted as xenocrystic material inherited from the melting protolith.

#### 5.2.1.4 Gwenoro dam and surroundings

*GW02* is a sample of a migmatitic raft hosted within a foliated gneiss on the western edge of the Gwenoro dam spillway. A foliation is defined by the alignment of amphibole and biotite in the melanocratic horizons, which appear in equilibrium. Banding is on the cm scale. Ten analyses from six zircons returned three concordant analyses with a concordia age of 2729 ± 22 Ma (MSWD = 0.73), which is considered to be the crystallization age of the migmatite (Figure 5.13).

*GW03* is a sample of a trondhjemitic vein that cross-cuts basement rocks of the Gwenoro dam spillway. The vein is primarily composed of quartz and plagioclase, with minor amounts of chlorite. Ten analyses of three zircons return four analyses that define a discordia model with an upper intercept age of 2717 ± 23 Ma (MSWD = 0.87) (Figure Y.8). All zircons are interpreted to be xenocrysts, and therefore the age is considered an inherited age.

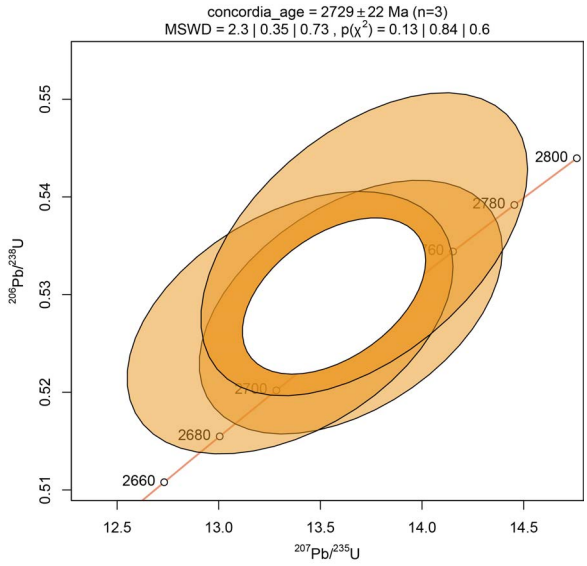


Figure 5.13: Wetherill concordia plot with concordant analyses of GW02 shown.

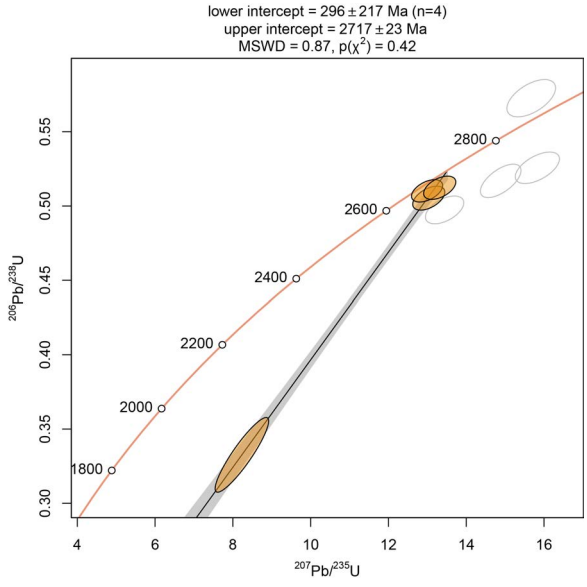


Figure 5.14: Wetherill concordia plot with analyses of GW03 shown. Analyses considered in the discordia model are coloured.

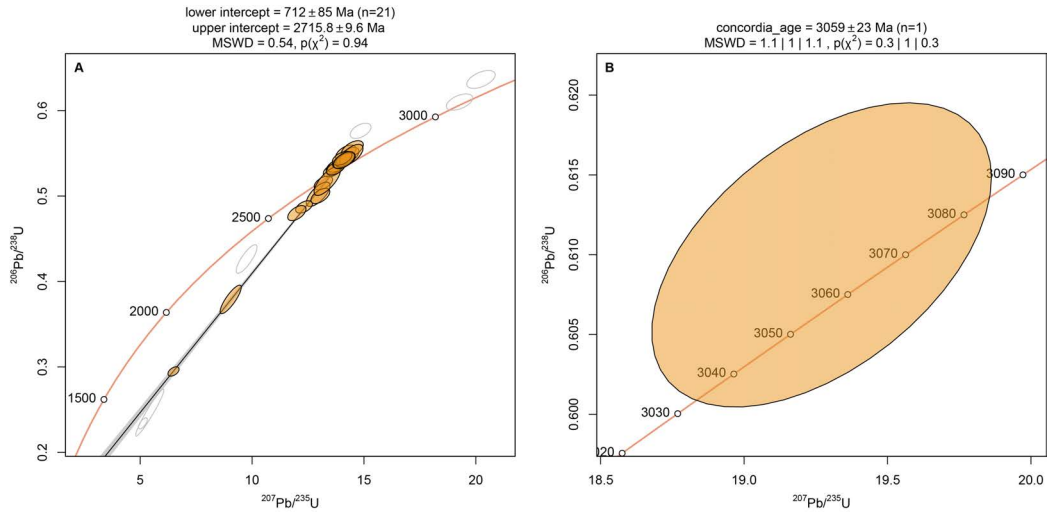


Figure 5.15: Wetherill concordia plots of analyses from GW04. A) Discordia model, with considered analyses shaded, B) zoom in on concordant analyses interpreted to represent the age of the protolith.

*GW04* is a sample of a leucosome rich migmatitic xenolith in the Gwenoro dam spillway. A fabric is primarily defined by biotite, with subordinate amphibole and titanite. Thirty analyses of 18 zircons returned 21 analyses that define a discordia model with an upper intercept age of 2715.8 ± 9.6 Ma (MSWD = 0.54), which is interpreted as the crystallisation age of the migmatite (Figure 5.15). One analysis provides a concordant age of 3059 ± 23 Ma (MSWD = 1.1), which is interpreted to represent a xenocryst from the melt source.

*NM02* is a granodiorite originally mapped as part of the basement gneisses by Stowe (1968). A weak fabric is defined by the alignment of biotite crystals. The rock has phenocrysts of stubby alkali feldspars, which in many cases preserve strong oscillatory growth zoning. Twenty analyses of 11 zircons yield 16 analyses that define a discordia model with an upper intercept age of 2688 ± 13 Ma (MSWD = 1.3), which is interpreted as the crystallization age of the unit (Figure 5.16).

*SC03* is a sample of intensely deformed migmatitic gneiss collected from the Mapongokwe river c. 8 km west of where the river transects the Great Dyke. The fabric is defined by the strong alignment of amphibole in the melanosomes parallel to cm-scale banding. Forty analyses of 35 zircons yield eight analyses that pass an Aitchison (1982) log-ratio discordance filter (Vermeesch, 2021) define a discordia model with an upper intercept age of 2696 ± 43 Ma (MSWD = 0.85), which is interpreted as the crystallization age of the migmatite (Figure 5.17). Three separate concordant analyses define a concordia age of 2790 ± 14 Ma (MSWD = 1.4), which

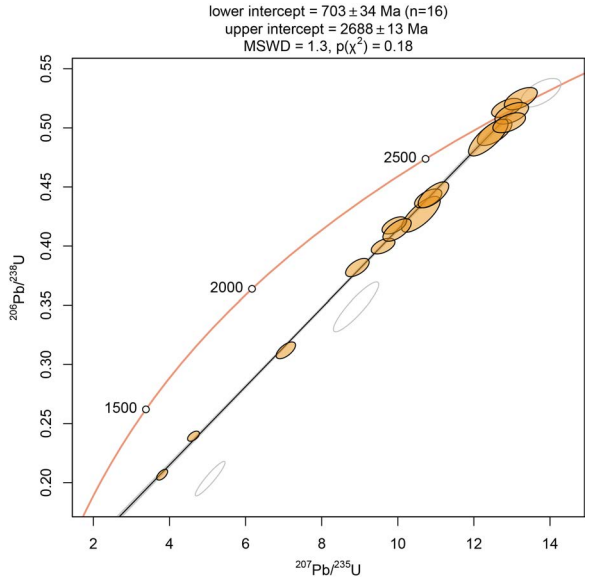


Figure 5.16: Wetherill concordia plot of analyses from NM02. Analyses considered for discordia model are shaded.

is interpreted as an inheritance age from xenocrysts entrained from the melt source.

#### 5.2.1.5 Shangani batholith

*ZB01* is a sample from a very weakly foliated tonalite c. 5 km from the eastern margin of the Fort Rixon–Shangani greenstone belt. A weak alignment of biotite laths defines the fabric. Thirty analyses from 22 zircons returned 19 analyses that define a discordia model with an upper intercept age of 2681 ± 11 Ma (MSWD = 1.1), and four concordant analyses which define a concordia age of 2705 ± 12 Ma (MSWD = 1.2, Figure 5.18). Collectively, these ages are interpreted to represent the crystallisation age of the tonalite.

*ZB02* is sample of a moderately foliated tonalite collected c. 3 km from the eastern margin of the Fort Rixon–Shangani greenstone belt and along the outer flanks of the Irisvale–Lancaster shear zone (ILSZ). Thirty analyses from 25 zircons returned 13 analyses that define a statistically significant discordia model with an upper intercept age of 2702 ± 13 Ma (MSWD = 1.2), which is interpreted as the crystallisation age of the tonalite (Figure 5.19.

*ZB03* is a migmatitic gneiss near the eastern margin of the Fort Rixon – Shangani greenstone belt, about five kilometres east of the Zinjanja monument along the Mtshingwe river. A fabric is defined by the alignment of hornblende laths in the restitic assemblage, and melt selvedges that have been deformed and chloritized by later shearing along the ILSZ. Sixteen of 30 analyses from 18 zircons yielded a discordant

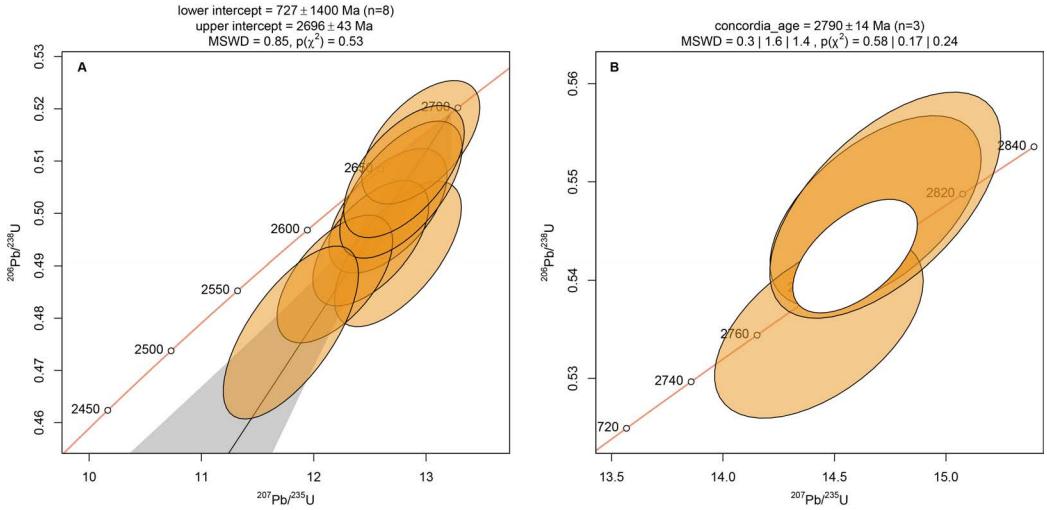


Figure 5.17: Wetherill concordia plots with analyses of SC03. A) Discordia model of analyses interpreted to represent the age of migmatite crystallisation, B) zoom in on concordant analyses of concordant xenocryst analyses.

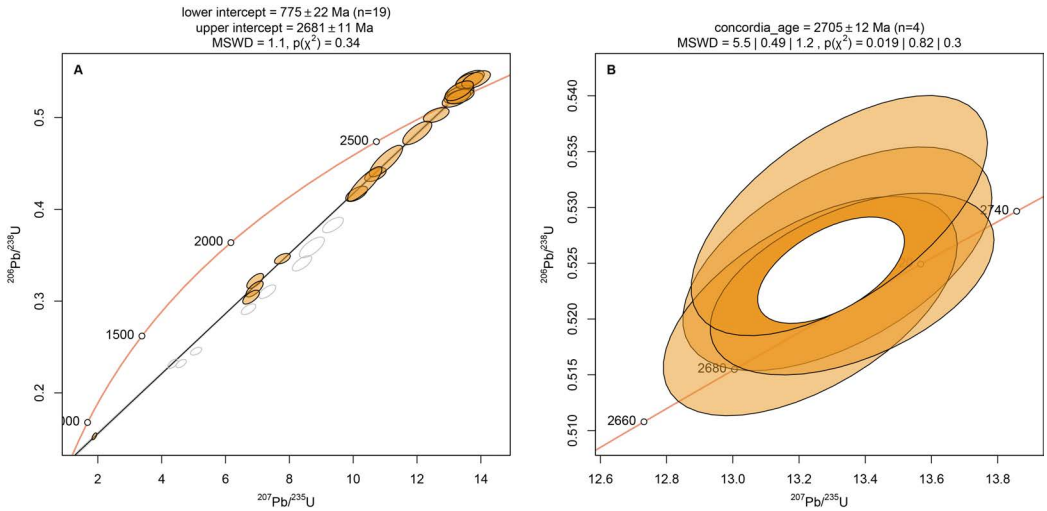


Figure 5.18: Wetherill concordia plots of analyses from sample ZB01. A) Discordia model, with considered analyses coloured, B) zoom in on concordant analyses.

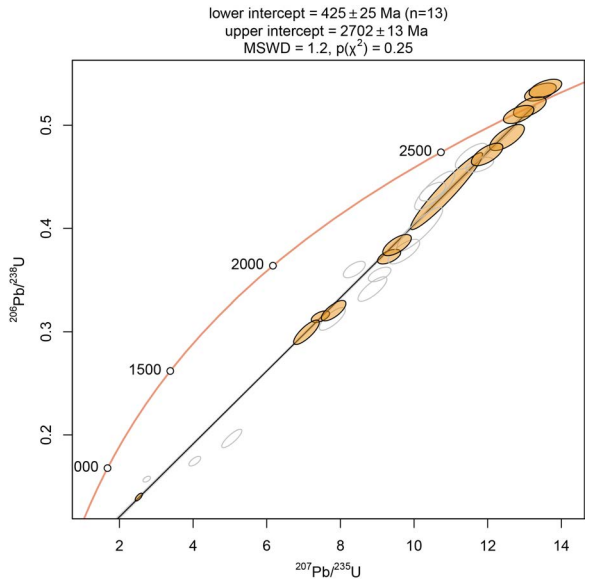


Figure 5.19: Wetherill concordia plot with the discordia model through analyses of ZB02. Analyses considered in the discordia model shaded.

model upper intercept age of 2689 ± 12 Ma (MSWD = 1.5) (Figure 5.20), and three concordant analyses produced a concordia age of 2683 ± 16 Ma (MSWD = 1.4). Both ages are interpreted as the age of crystallization.

*ZB06* is a strongly sheared tonalitic gneiss situated 200 m from the eastern margin of the Fort Rixon–Shangani greenstone belt, approximately five kilometres south of the Zinjanja monument. The fabric is defined by a strong alignment of biotite sheets, locally preserving S/C fabrics considered to have formed during shearing along the ILSZ. Twenty-eight analyses from 23 zircons yield a discordia model with an upper intercept age of 2835 ± 14 Ma (MSWD = 1.3) (Figure 5.21). Eight analyses were concordant and return a concordia age of 2827 ± 13 Ma (MSWD = 1.3). The two results are collectively interpreted as the age of crystallization of the original tonalite intrusion.

#### 5.2.1.6 Granitoids around the Odzi greenstone belt

*SR01* is a foliated tonalite (part of the Nyashanu Gneissic Belt of Lauerdale, 1988) exposed along the Save river, and sampled c. 1 km NW of the contact between the Odzi greenstone belt and the granitoids. The tonalite has a foliation defined by the alignment of biotite and amphibole laths, and biotite is overgrown over earlier amphibole. Fifteen of 30 analyses from 19 analysed zircons generate a discordia model with an upper intercept age of 2666 ± 10 Ma (MSWD = 1.7) (Figure 5.22). Five

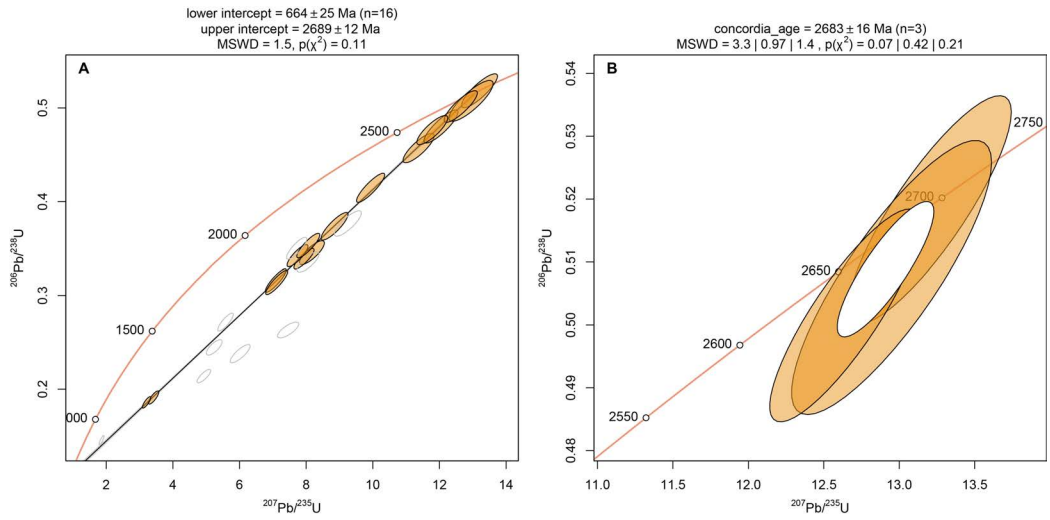


Figure 5.20: Wetherill plots of analyses from ZB03. A) Discordia model with considered analyses shaded, B) zoom in on concordant analyses.

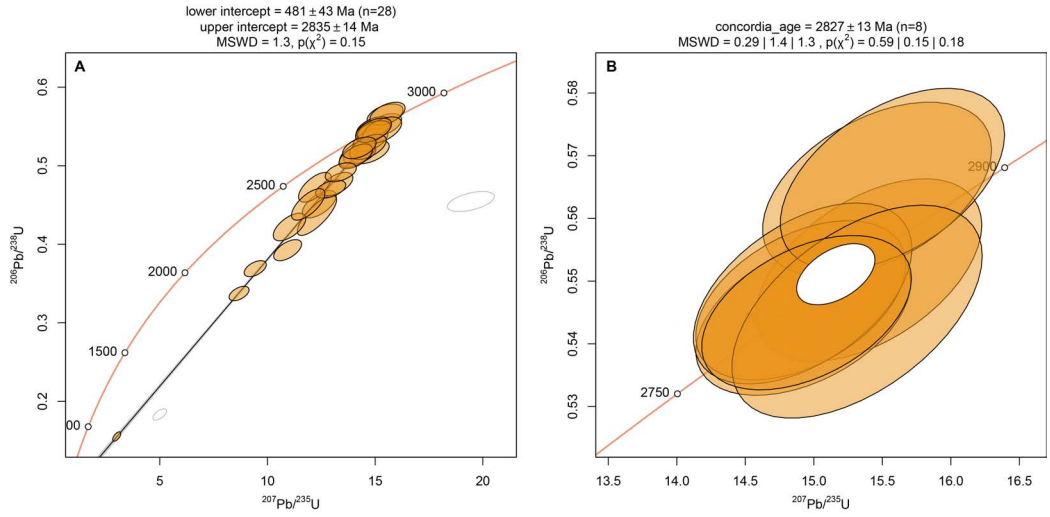


Figure 5.21: Wetherill plots of analyses from ZB06. A) Discordia model with considered analyses shaded, B) zoom in on concordant analyses.

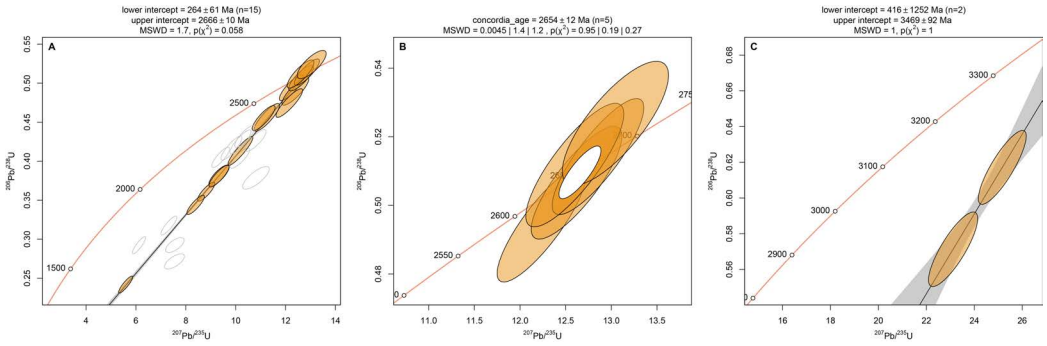


Figure 5.22: Wetherill concordia plots of analyses from SR01. A) Discordia model with considered analyses included, B) zoom in of concordant analyses assumed to represent crystallization, and C) discordia model of two analyses interpreted to represent an inheritance age.

analyses were concordant, and yield a concordia age of 2654 ± 12 Ma (MSWD = 1.2). These ages are collectively interpreted as the crystallization age. Two analyses returned an upper-intercept discordia age of 3469 ± 92 Ma (MSWD = 1), which is interpreted as an inherited age.

*SR02* is a strongly foliated tonalite (part of the Nyashanu Gneissic Belt) exposed along the Save river, c. 100 m NW of the contact between the Odzi greenstone belt and the granitoids. The foliation is defined by the alignment of biotite (± titanite), which occasionally wraps around feldspar phenocrysts. Three of 30 analyses from 21 zircons were semi-concordant and produce a concordia age of 2602 ± 47 Ma (MSWD = 4.3), which is interpreted as the age of crystallization (Figure 5.23).

*WG02* is a weakly foliated tonalite (part of the Romsley Gneiss suite of Lauerdale, 1988) exposed in the Murove river ∼3 km NW of Nyashanu. A weak fabric is defined by the alignment of stubby amphibole and biotite crystals. Seventeen of 30 analyses from 20 zircons return a discordia model with an upper intercept age of 2650 ± 10 Ma (MSWD = 0.99) (Figure 5.24). Six analyses returned concordant results, defining a concordia age of 2664 ± 17 Ma (MSWD = 1.9). The two dates are collectively interpreted as the crystallisation age.

*WG03* is a tonalite that belonging to the Romsley Gneiss suite. The unit has no clear fabric, and is composed of quartz, plagioclase, (retrogressed) biotite, chlorite, epidote ± calcite, and is considered a retrogressed equivalent of WG02. Twenty of 30 analyses from 22 zircons generated a discordia model with an upper intercept at 2640 ± 11 Ma (MSWD = 1.3) (Figure 5.25). Three analyses were concordant, and return a concordia age of 2648 ± 17 Ma (MSWD = 0.47). The two dates are collectively interpreted as the age of crystallisation.

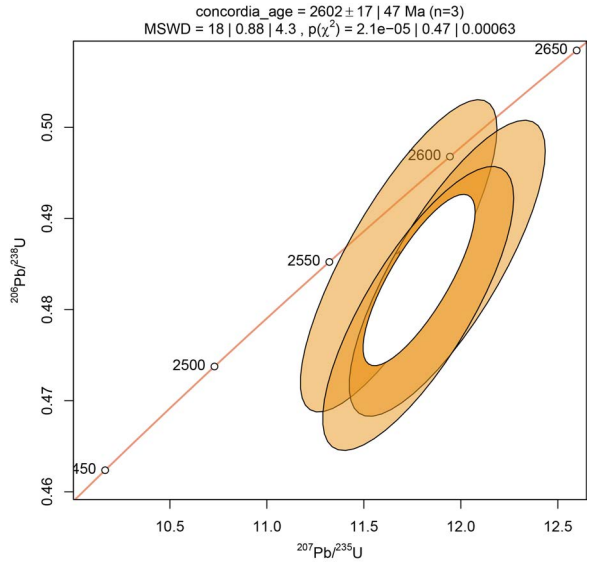


Figure 5.23: Discordia model of analyses from SR02 viewed on a wetherill concordia plot.

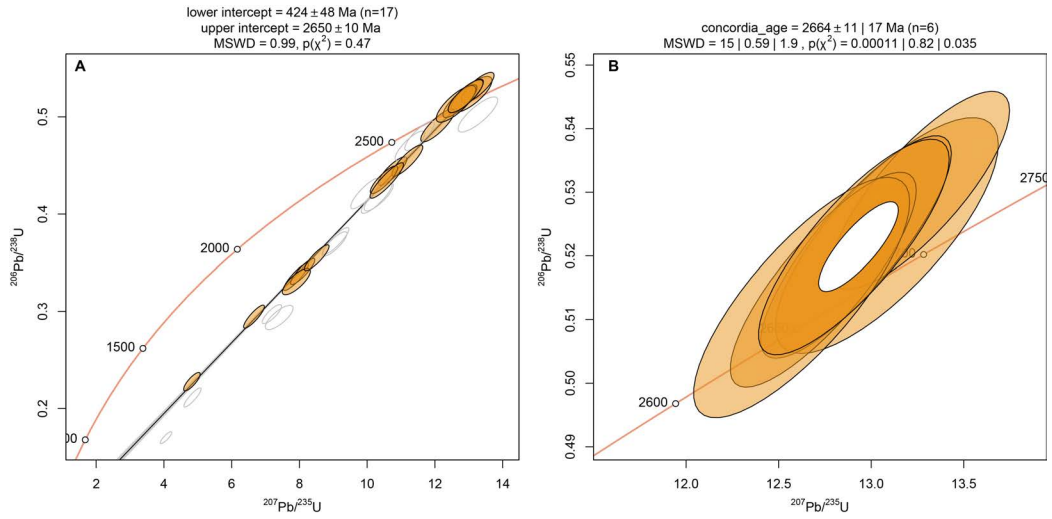


Figure 5.24: Wetherill concordia plots of analyses from WG02. A) Discordia model, with considered analyses shaded, B) Zoom in on concordant analyses.

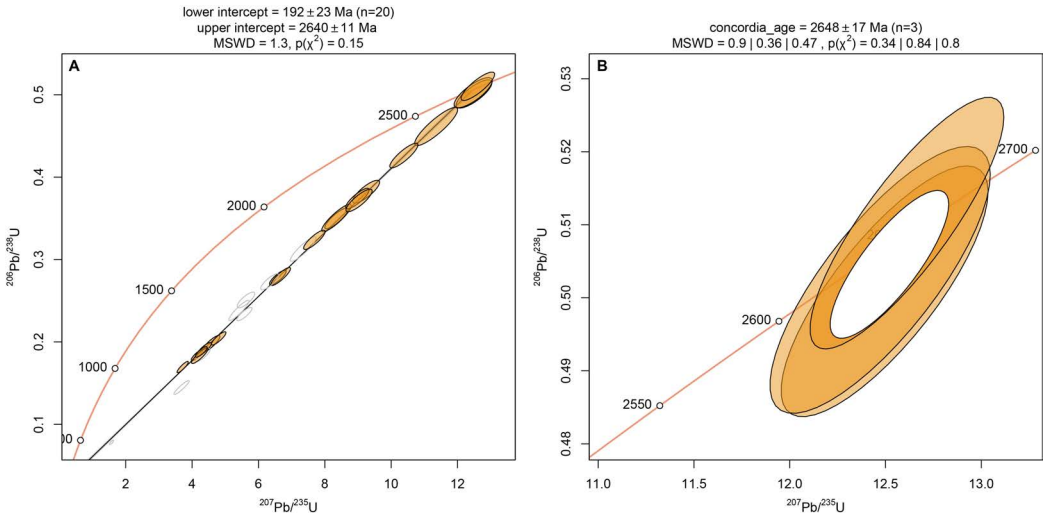


Figure 5.25: Wetherill concordia plots of analyses from sample WG03. A) Discordia model, with considered analyses shaded, and B) zoom in of concordant analyses.

#### 5.2.1.7 Chillimanzi/Razi suite granites

*GH02* was collected from a weakly foliated granodiorite that is part of the syntectonic suite of Stowe et al. (1968), collected c. 5 km west of Shurugwi. A weak fabric is defined by the alignment of biotite ± muscovite, and the sample contains more plagioclase than alkali feldspar. Three of 10 analyses from two zircons return a concordia age of 2688 ± 20 Ma (MSWD = 1.3) (Figure 5.26). Five analyses yield a $^{207}Pb/^{206}Pb$ weighted mean age of 2685 ± 17 Ma (MSWD = 0.99), and are collectively interpreted as the crystallisation age.

*CH01* is a two-mica granite named the Chinoia Stock granite (Phaup, 1973). The sample was collected 7 km north of the Mandamabwe road junction. Thirty analyses from 29 zircons yielded scattered results (Figure 5.27). One concordant analysis returned a concordia age of 2657 ± 31 Ma (MSWD = 2), which is interpreted as the age of crystallisation. Seven analyses define a discordia model with an upper intercept of 3007 ± 23 Ma (MSWD = 0.52), which is interpreted as an inherited age.

*BL05* is a two-mica granite sample collected 2 km north of the Mount Vugwe peak along the eastern boundary of the Belingwe greenstone belt. Thirty analyses from 22 zircons yielded 11 points which define a statistically significant discordia model with an upper intercept of 3333 ± 15 Ma (MSWD = 0.83), which is considered to be an inherited age (Figure 5.28).

*PG01* is a porphyritic two-mica granite named the Wabai porphyritic granite (Phaup, 1973), and intrudes into the Shangani batholith c. 12 km east of the Fort

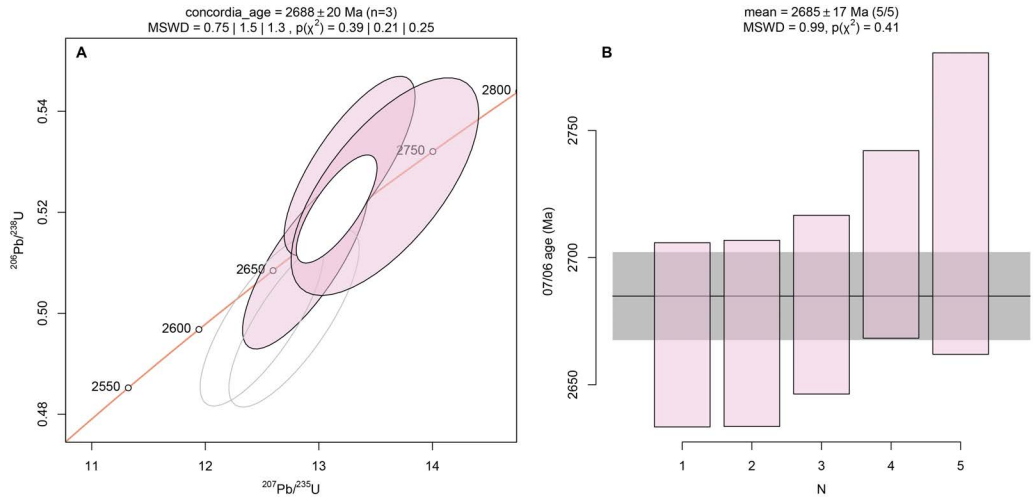


Figure 5.26: A) Wetherill concordia plot of sample GH02. Considered analyses are shaded. B) $^{207}Pb/^{206}Pb$ weighted mean plot of sample GH02.

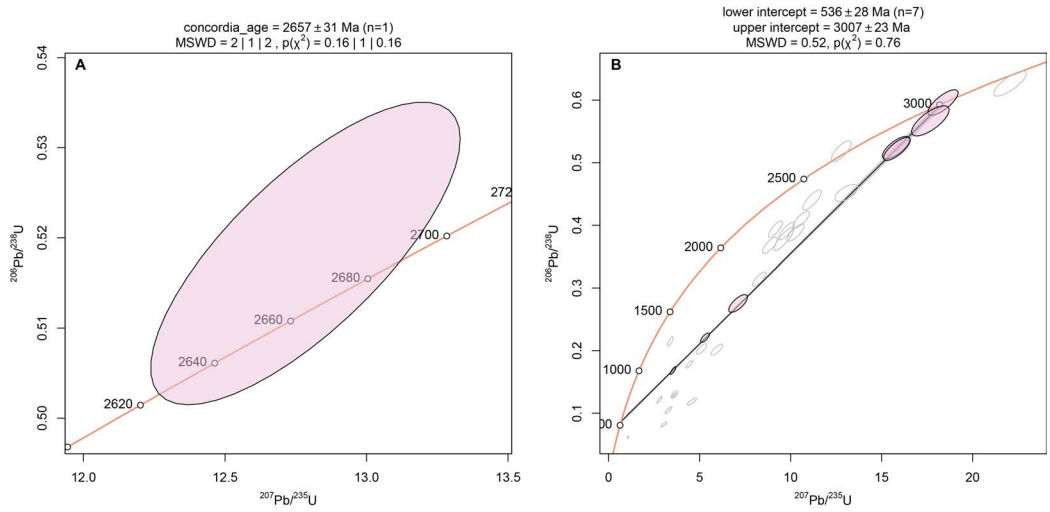


Figure 5.27: Wetherill concordia plots of CH01. A) Zoom in on concordant analysis interpreted to represent crystallisation. B) Discordia model of resolvable inherited population.

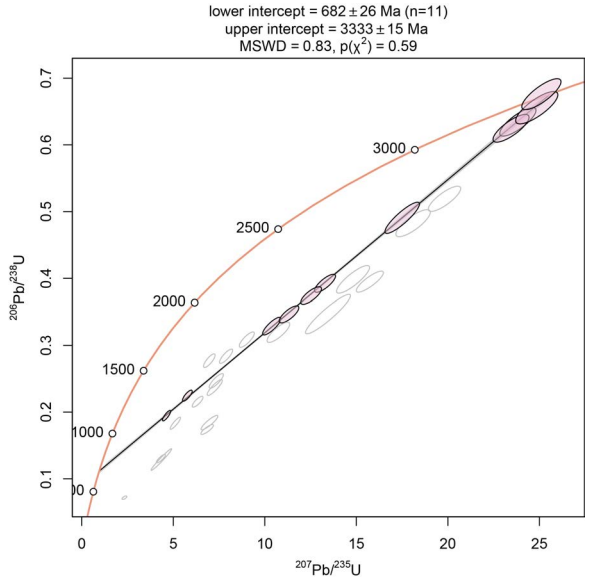


Figure 5.28: Wetherill concordia plot with a discordia model through analyses from BL05. Analyses considered in the model are shaded.

Rixon–Shangani greenstone belt. Forty-five analyses of 22 zircons yielded five analyses forming a statistically significant discordia model with an upper estimate of 2616 ± 21 Ma (MSWD = 0.96) (Figure 5.29). One concordant analysis with a concordia age of 2623 ± 24 Ma (MSWD = 0.48) is part of this cluster, and these ages are collectively interpreted as the crystallisation age of the granite. Seven concordant analyses yielded a concordia age of 2712 ± 11 Ma (MSWD = 7.1), which is interpreted as an inherited age.

*ZB05* is a porphyrytic two-mica granite named the Three Fingers porphyrtic granite (Phaup, 1973), and is intrusive to the Shangani batholith c. 5 km east of the Fort Rixon–Shangani greenstone belt. Thirty analyses of 17 zircons yield 26 analyses that generate a statistically significant discordia model with an upper intercept age of 2653 ± 15 Ma (MSWD = 1.3), interpreted to be the age of crystallization of the granite (Figure 5.30).

*ZB07* is a sheared porphyritic two-mica granite that intrudes into and along the eastern margin of the Fort Rixon–Shangani greenstone belt. The sample was collected 2 km south of the Zinjanja monument. Twenty analyses of 11 zircons yield 13 analyses with anomalously low U/Th (<0.02) which were discarded. Six analyses return a discordia model with a lower intercept age in Tera-Wasserburg space of 2693 ± 36 Ma (MSWD = 2.3), which is considered the crystallisation age of the intrusion (Figure 5.31). One concordant analysis returned a concordia age of 3947 ± 52 Ma (MSWD = 1.5) and is considered an inherited age.

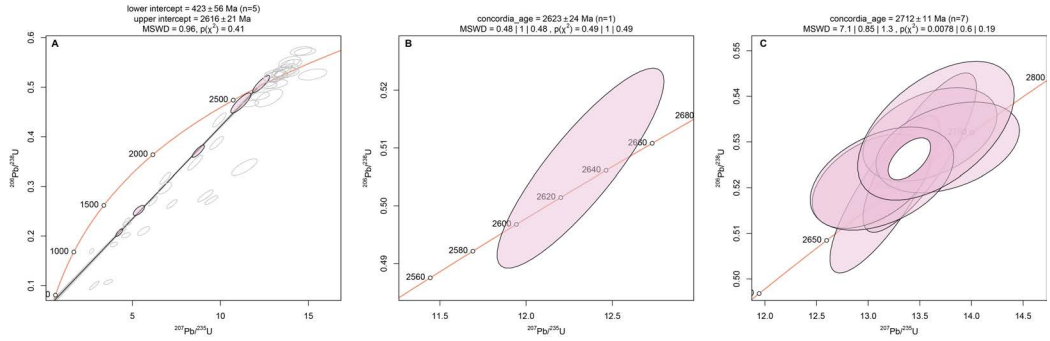


Figure 5.29: Wetherill concordia plots with data from sample PG01. A) Discordia model of interpreted crystallisation; B) zoom in on concordant analysis interpreted to be recording crystallisation; and C) zoom in on concordant analyses interpreted to represent an inheritance age.

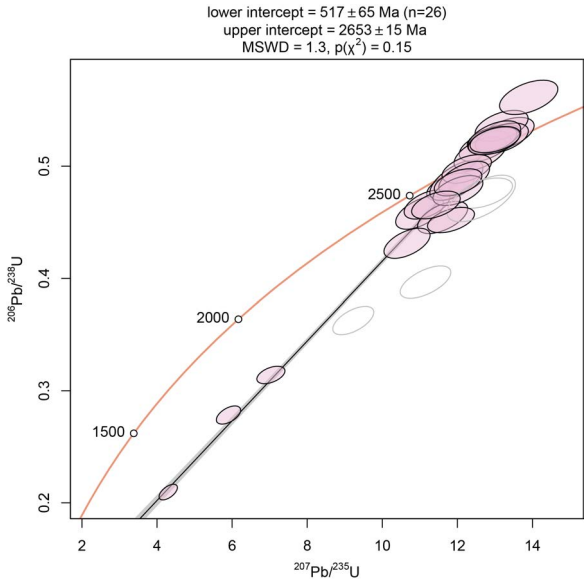


Figure 5.30: Wetherill concordia plot with discordia model through analyses of ZB05.

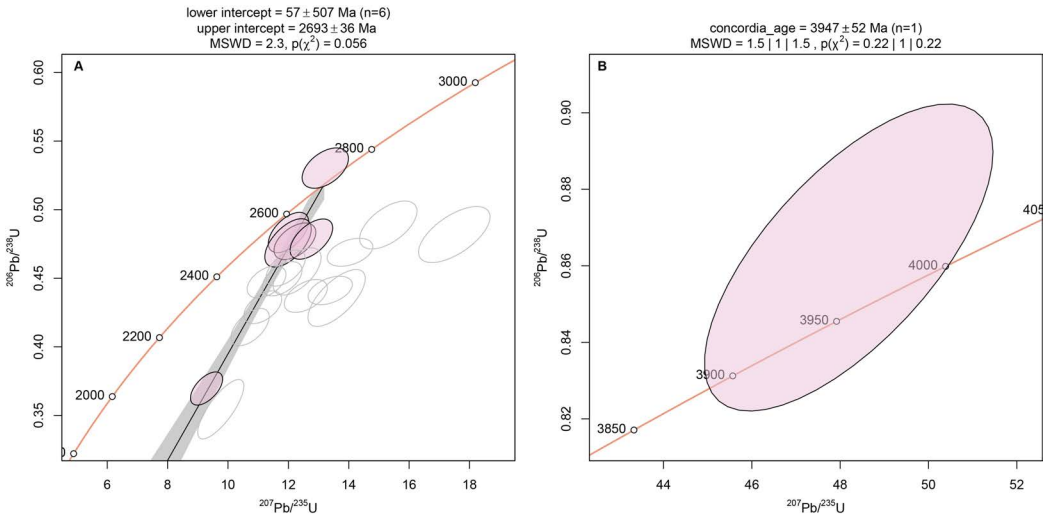


Figure 5.31: A) Wetherill concordia plot with discordia model for analyses of ZB07. Considered analyses shaded. B) Zoom in on an interpreted inheritance concordant analysis.

*DP01* is sampled from the same intrusion as ZB07 and collected 5 km NE of the Zinjanja monument. Thirty analyses of 21 zircons yield 5 analyses that return a discordia model with an upper intercept age of 2719 ± 47 Ma (MSWD = 0.89), within error of the age for ZB07 (Figure 5.32). This population is interpreted to record crystallisation. Ten analyses yield a discordia model with an upper intercept age of 2991 ± 49 Ma (MWSD = 1.1), which is interpreted to represent an inherited age.

*NY01* is a sample from a granite directly abutting the SW edge of the Odzi greenstone belt, collected c. 2 km NW of Nyashanu village. Thirty analyses of 23 zircons yielded four concordant analyses with a 2647 ± 13 Ma (MSWD = 1.9) concordia age, interpreted as the age of crystallisation of the granite body (Figure 5.33). Eight discordant analyses generate a discordia model with an upper intercept at 2783 ± 15 Ma (MSWD = 1.3), which is interpreted as an inherited age.

*NY02* is a sample from a granite on the southern margin of the Odzi greenstone belt, collected c. 3 km south of Nyashanu village. Crystal sizes are smaller than the granite of NY01, and alkali feldspars are sericitized, whilst biotite is commonly chloritized. Thirty analyses from 25 zircons returned 10 analyses that define a discordia model with an upper intercept age of 2613 ± 17 Ma (MSWD = 1.6) (Figure 5.34). Five analyses were concordant, returning a concordia age of 2640 ± 30 Ma (MSWD = 3.3). Collectively, these ages are interpreted to represent the crystallisation age of the granite body.

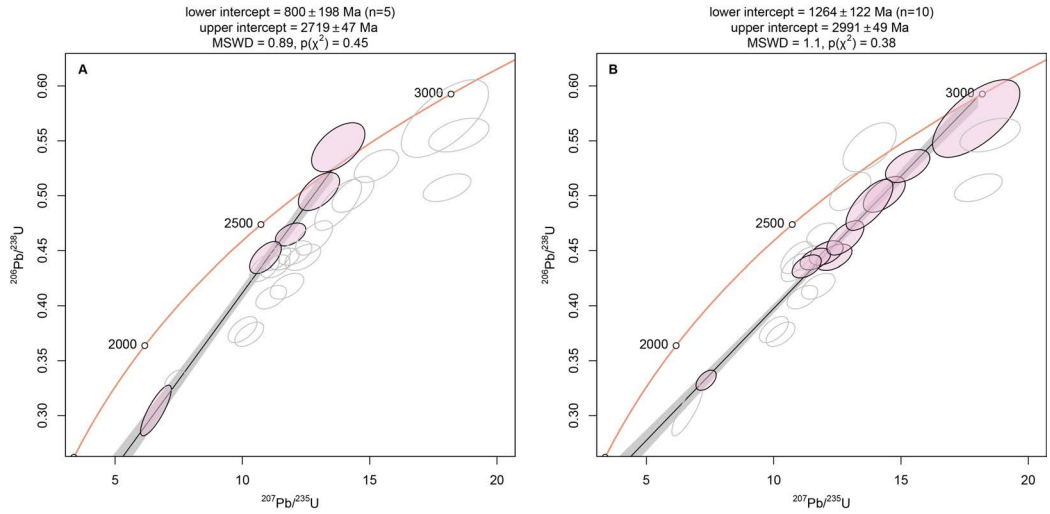


Figure 5.32: Wetherill concordia plots for analyses from DP01. A) Discordia model for analyses considered to represent crystallisation; B) discordia model for analyses considered to represent an inherited population.

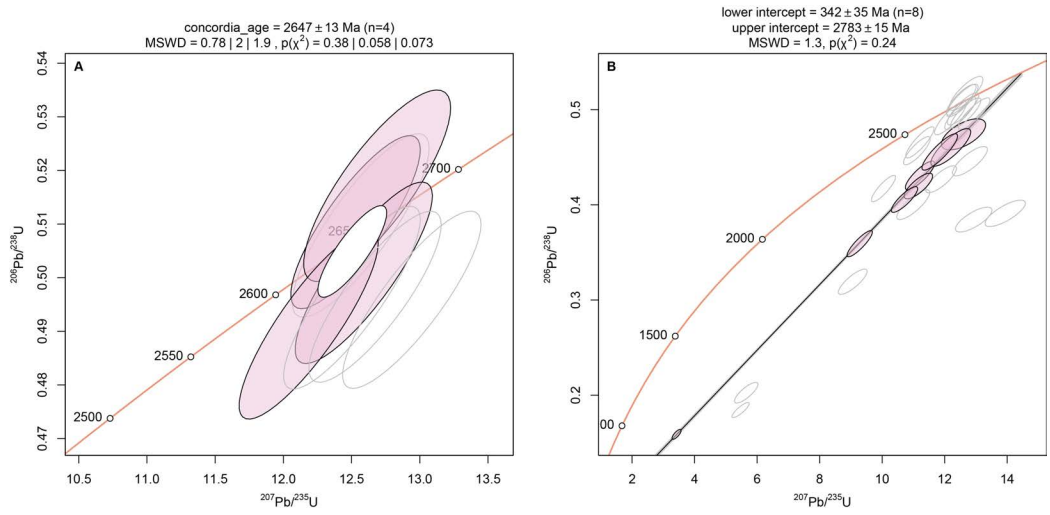


Figure 5.33: Wetherill concordia plots of analyses from sample NY01. A) Concordant analyses of interpreted crystallisation age; B) discordia model of an interpreted inherited population.

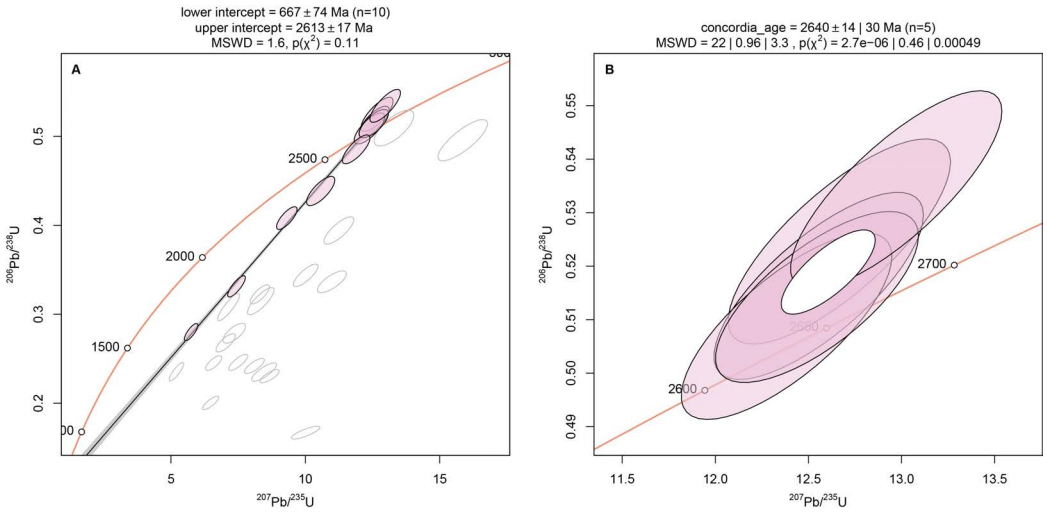


Figure 5.34: Wetherill concordia plots of analyses from sample NY02. A) Discordia model, considered analyses shaded; B) zoom in of concordant analyses.

*NY03* is a sample from a granite body c. 10 km north of the Odzi greenstone belt. The body has a foliation defined by the alignment of biotite (± muscovite), and alkali feldspar commonly displays growth zoning, tartan twinning, and flame perthitic textures. Thirty analyses from 20 zircons returned seven analyses that define a statistically significant discordia model with an upper intercept age of 2650 ± 19 Ma (MSWD = 1.1), which is interpreted as the crystallization age of the granite body (Figure 5.35).

*LP02* is a sample of equigranular granite that is part of the Great Zimbabwe pluton between the Masvingo greenstone belt and the Northern Limpopo thrust. The sample was collected c. 20 km south of Great Zimbabwe, and contains abundant alkali feldspar and biotite. Thirty analyses of 19 zircons yield a cluster of six analyses with comparable U/Th ratios (3.5–5.2) that define a discordia model with an upper intercept age of 2601 ± 63 Ma (MSWD = 2.6), which is interpreted as the age of crystallisation of the intrusion (Figure 5.36).

*LP03* is a sample of porphyritic granite along the southern margin of the Great Zimbabwe pluton, 10 km north of the major Northern Limpopo thrust zone (NLTZ). A strong fabric is present in the sample, defined by the alignment of biotite, amphibole, and titanite crystals. Thirty analyses of 25 zircons returned 19 analyses that define a discordia model with an upper intercept age of 2608 ± 15 Ma (MSWD = 1.5) (Figure 5.37. Three analyses were concordant, with a concordia age of 2610 ± 17 Ma (MSWD = 1.3) (Figure 5.37B). Collectively, these are interpreted to represent the crystallisation age of the granite body.

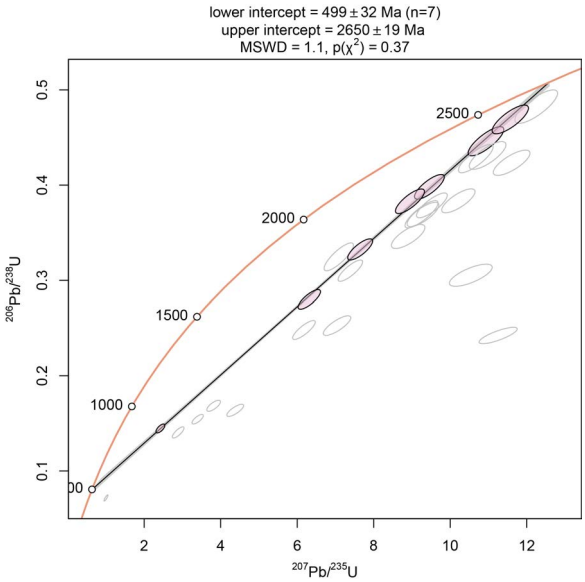


Figure 5.35: Wetherill concordia plot with the discordia model through analyses of NY03. Considered analyses are shaded.

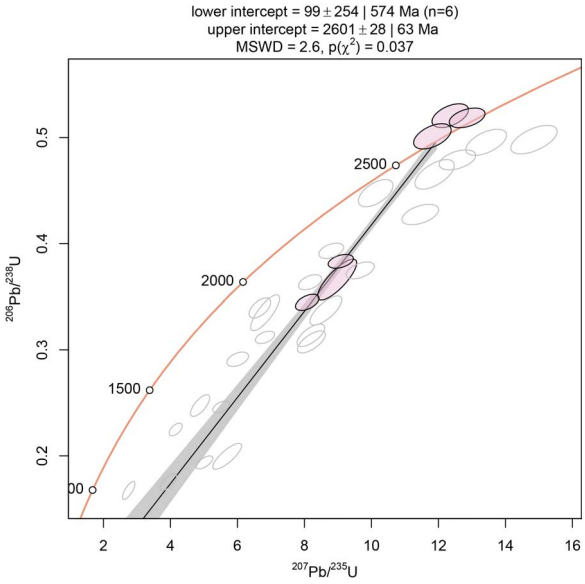


Figure 5.36: Wetherill concordia plot with the discordia model through analyses of LP02. Considered analyses are shaded.

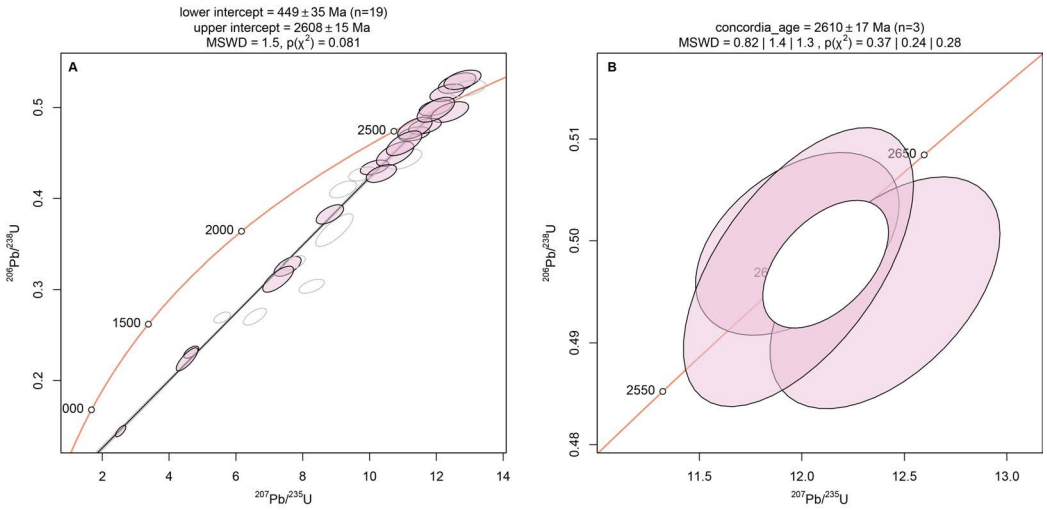


Figure 5.37: Wetherill concordia plots of analyses from LP03. A) Discordia model, considered analyses are shaded; B) zoom in on concordant analyses.

*LP04* is an amphibole-bearing granite collected 200 m south of LP03, where the granitic intrusion contains abundant amphibolite xenoliths. The fabric within the xenolith is parallel to that of the host granite. Twenty analyses of 12 zircons returned a statistically significant discordia age through nine analyses, with an upper intercept age of 2677 ± 17 Ma (MSWD = 1.6), which is considered to be the crystallisation age of the intrusion (Figure 5.38).

#### 5.2.1.8 Northern Marginal Zone

*LP10* is a sample of tonalitic gneiss from the basement of the Northern Marginal Zone (NMZ) and appears to indrude through *LP11* (described below). *LP10* was collected 1 km north of where the Nyamawanga river joins the Mtilikwe river, c. 2 km east of Renco. The gneiss consists of garnet, biotite, quartz, plagioclase, and trace alkali feldspar, and the fabric is parallel to the NLTZ. Thirty analyses of 26 zircons returned 22 analyses that define a discordia model with an upper intercept age of 2954 ± 19 Ma (MSWD = 1.5), which is considered to be the crystallisation age of the tonalitic body (Figure 5.39).

*LP11* is a sample of the felsic basement that LP10 intrudes through. It is strongly deformed, with a fabric defined by biotite (wrapping around synkinematic garnet) parallel to the NLTZ. Thirty analyses of 20 zircons enabled a discordia model through 19 analyses that yields an upper intercept age of 2979 ± 15 Ma (MSWD = 1.5), which is considered the age of crystallisation of the intrusive protolith (Figure 5.40).

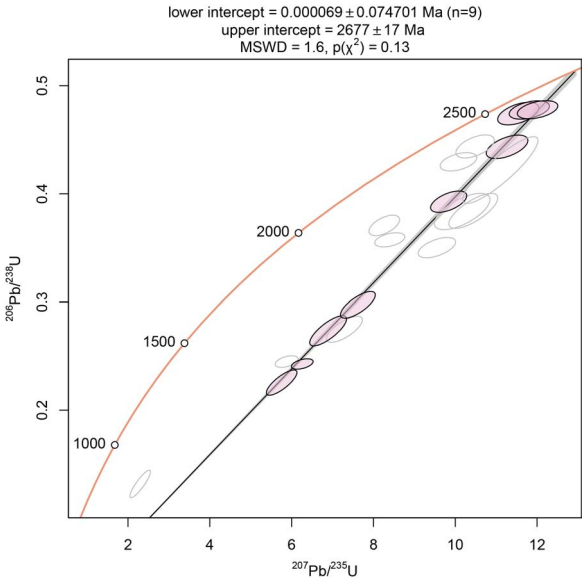


Figure 5.38: Wetherill concordia plot with the discordia model through considered analyses (shaded) of sample LP04.

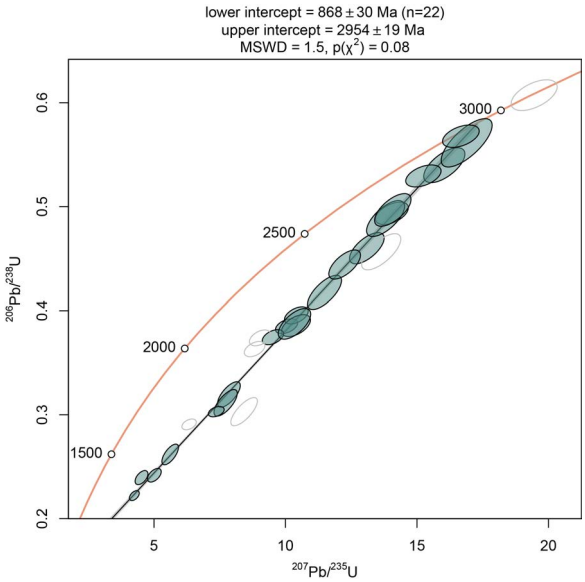


Figure 5.39: Wetherill concordia plot with analyses of LP10 shown. Considered analyses for plotted discordia model coloured.

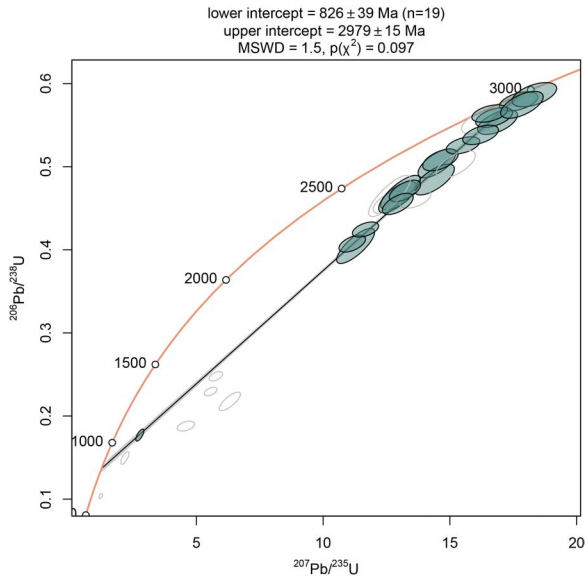


Figure 5.40: Wetherill concordia plot with analyses of LP11 shown. A discordia model is plotted, with considered analyses coloured.

#### 5.2.1.9 Apatite geochronology

*GW06* is a foliated tonalite from the Gwenoro dam spillway, which includes rafts of *GW02* and *GW04*. The fabric in *GW06* is defined by the alignment of biotite. Forty-six analyses of apatites yield a lower intercept age of 2732 ± 38 Ma (MSWD = 0.09), which is interpreted to represent the crystallisation age of the tonalite (Figure 5.41).

*NG01* is a sample of the Nalatale granite (Phaup, 1973) which almost completely bisects the Fort Rixon–Shangani greenstone belt. The granite contains both biotite and muscovite, and also accessory topaz. Sixty-two analyses of apatites yield a lower intercept age of 2512 ± 36 Ma (MSWD = 0.98), which is interpreted as the age of crystallisation of the granite (Figure 5.42).

#### 5.2.1.10 Titanite geochronology in the Irisvale-Lancaster shear zone

Titanite was analysed for U-Pb geochronology from three samples within the ILSZ. Sample *ZLC32* is a metamorphosed komatiitic basalt of the Reliance/Zeederbergs formation in the Fort Rixon–Shangani greenstone belt. The unit has a strong fabric parallel to the major trend of the ILSZ (Chapter 4). Titanite crystals form two textural populations: 1) mm-scale porphyroblasts within quartz knots, and 2) grains complexly intergrown with syn-kinematic tremolite. Seventy-two analyses of titanite grains returned a lower intercept age of 2662 ± 19 Ma (MSWD = 1.4) (Figure 5.43).

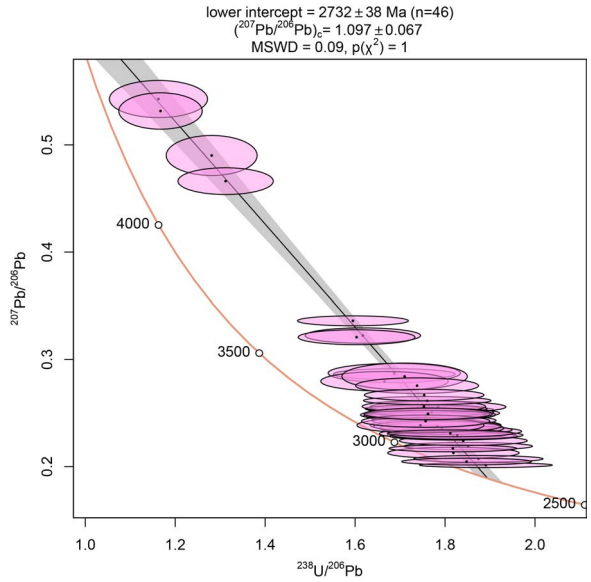


Figure 5.41: Tera-Wasserberg plot of apatite analyses from sample GW06.

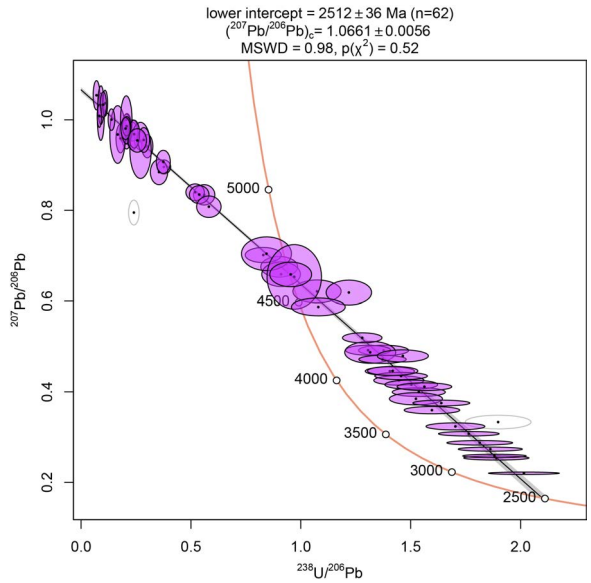


Figure 5.42: Tera-Wasserberg plot of apatite analyses from sample NG01.

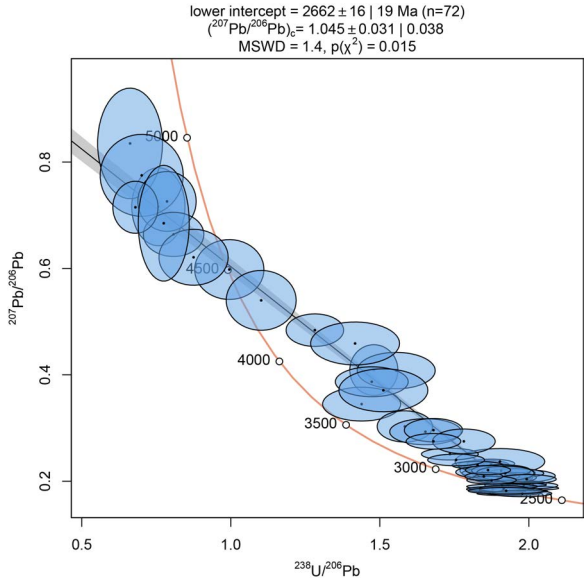


Figure 5.43: Tera-Wasserburg plot with analyses from titanite in sample ZLC32.

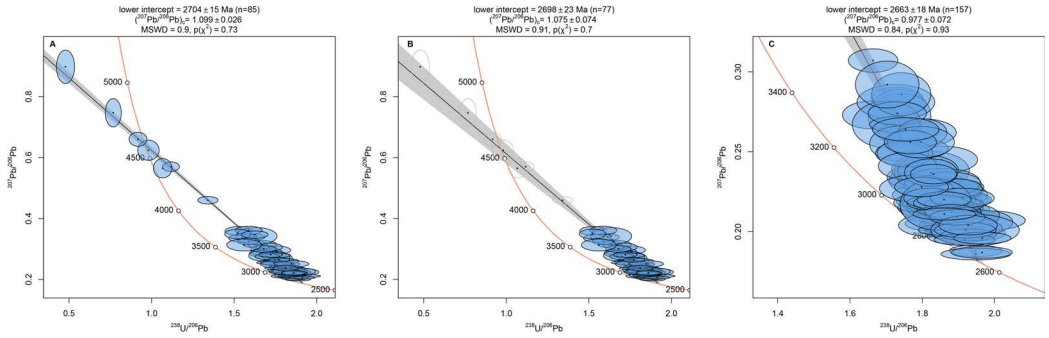


Figure 5.44: Tera-Wasserburg plots of titanite analyses from A) ZL181, B) ZL181, with the removal of extreme analyses, C) ZL182.

Samples *ZL181* and *ZL182* are Belingwean group metamorphosed tuffs that occur at the base of the Fort Rixon–Shangani greenstone belt. Titanites in both samples form porphyroblasts up to 1 cm wide within pressure shadows of ILSZ-related shearing. Within *ZL182*, titanite is also present as fine crystals parallel to the fabric defined by amphibole crystals. Considering all 85 analyses of titanites in *ZL181* (Figure 5.44A), produces a lower intercept age of 2704 ± 15 Ma (MSWD = 0.9). Removing the outliers, the lower intercept age becomes 2698 ± 23 Ma (MSWD = 0.91). Sample *ZL182* returns a lower intercept age of 2663 ± 18 Ma (MSWD = 0.84) (Figure 5.44C). Collectively, these ages are interpreted to bracket the age of deformation along the ILSZ.

#### 5.2.1.11 Rb-Sr mica geochronology around the Zulu pegmatite field

White micas were analysed from four samples from within the Zulu pegmatite field, which is described in Chapter 4, and all samples are from Type 1 pegmatites. Sample *Z6007* contains micas from both magmatic and albitisation events (Table 4.2), and returns an isochron age of 2763 ± 27 Ma (Figure 5.45A). Sample *Z6029* contains micas exlusively derived from dynamic recrystallisation (Table 4.2, and returns an isochron age of 2660 ± 41 Ma (Figure 5.45B). Sample *Z6035* contains micas crystallised in the magmatic stage (Table 4.2), and returns an isochron age of 2580 ± 19 Ma (Figure 5.45C). Sample *ZU008* contains micas derived in both magmatic and dynamic recrystallisation events (Table 4.2), and returns an isochron age of 2738 ± 22 Ma (Figure 5.45D).

Samples *Z6007* and *ZU008* are considered to reflect mixing "pseudo-chrons" (Siebel, 1994; Nebel, 2014) between distinct magmatic and metasomatic isotopic reservoirs. Sample *Z6029* is interpreted to reflect the crystallisation age of the pegmatite during deformation (see Chapter 4). Sample *Z6035* is interpreted to reflect an isotopic resetting event overlapping with the age of the Great Dyke (2575.4 ± 0.7 Ma, Oberthür et al., 2002).

Biotite was analysed in samples *ZU001* and *ZU005* from the ILSZ, which are Belingwean group metamorphosed tuffs located at the eastern margin of the Fort Rixon–Shangani greenstone belt (south of the Nalatale granite). Biotite is interpreted to have formed through metasomatic alteration driven by fluids expelled from the pegmatite bodies (Chapter 4). Sample *ZU001* returns an isochron age of 2602 ± 20 Ma (Figure 5.46A), and *ZU005* returns an isochron age of 2560 ± 28 Ma (Figure 5.46B), which are interpreted to represent cooling ages post-metasomatism.

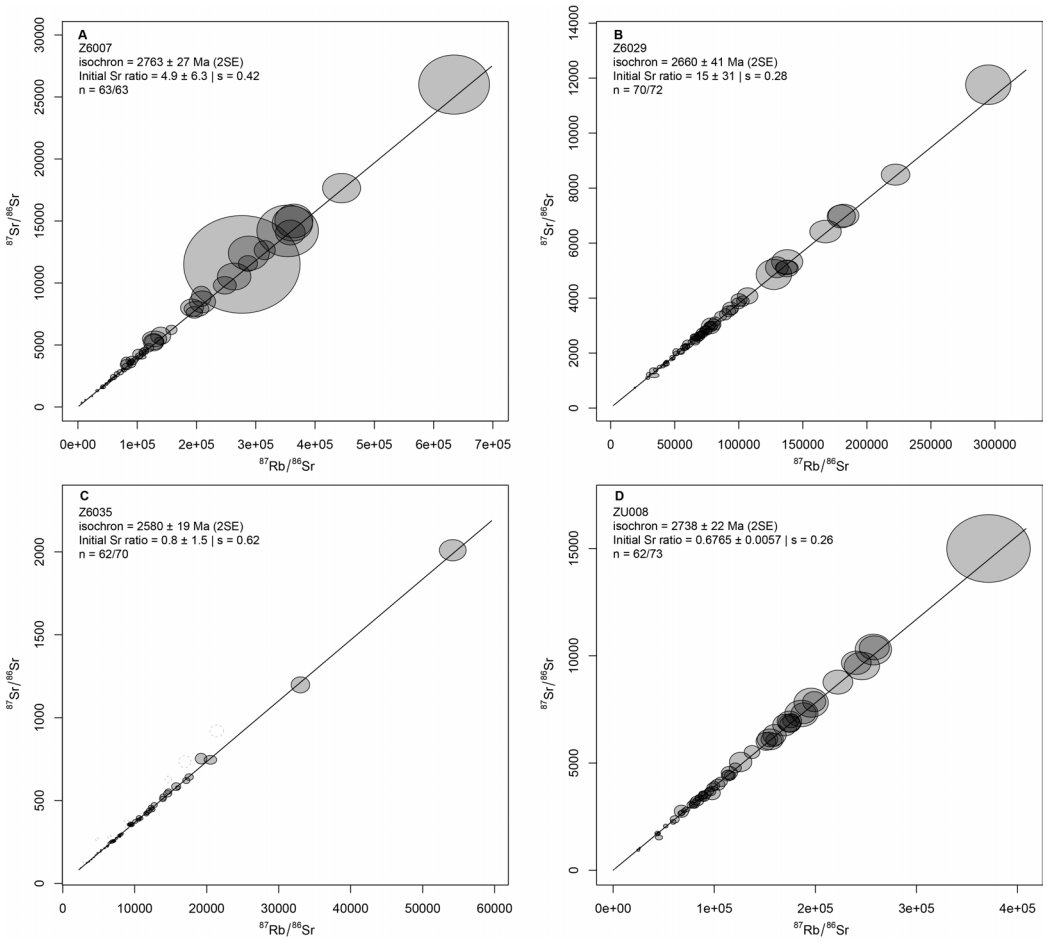


Figure 5.45: Rb–Sr isochron plots for A) Z6007, B) Z6029, C) Z6035, D) ZU008

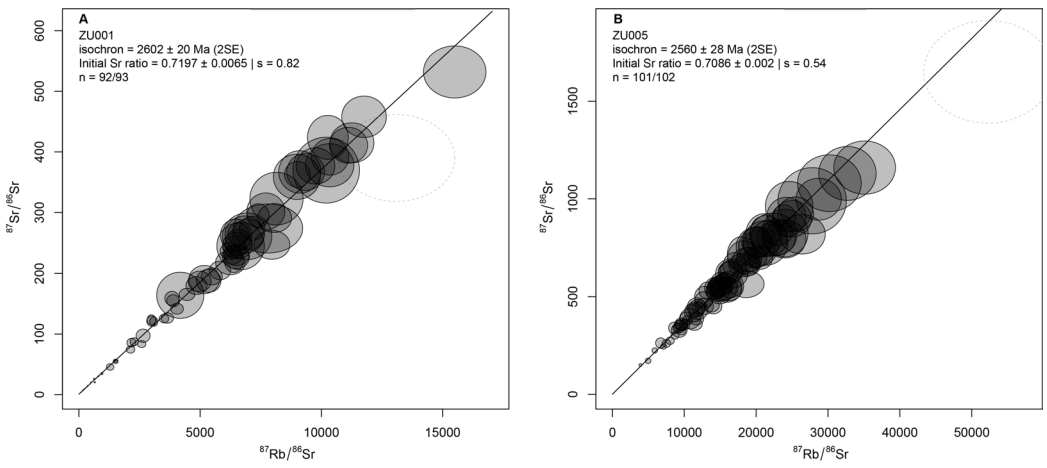


Figure 5.46: Rb-Sr isochrons of A) ZU001, and B) ZU005.

### 5.2.2 Geochemistry of the Zimbabwe craton

This study reports 76 new geochemical analyses of rocks (described in appendices A and B) from the Zimbabwe craton and the Northern Marginal Zone (Appendix D). Most analyses are of intrusive rocks and have been incorporated into the geochemical database described in section 2.1. In the following sections, granitoids are separated by major temporal suites determined by geochronology. The TTG suites are named in order of younging as follows; the Tokwe suite (3.7–3.2 Ga), the Chingezi suite (3.0–2.8 Ga), The Sesombi suite (2.8–2.7 Ga), the Wedza suite (2.7–2.6 Ga). All rocks of the NMZ are clustered, as the geochemical data are available in the literature lacks sufficient detail to segregate the basement gneisses from later intrusive charnockitic/enderbitic suites. The Late Archean granites are grouped into Chillimanzi and Razi suites, depending on whether they intrude into the ZC (Chillimanzi) or the NMZ and along the NLTZ (Razi).

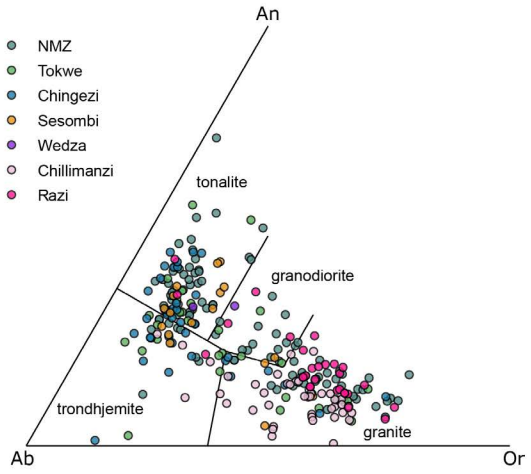


Figure 5.47: Normative Ab–An–Or diagram with granitoid discrimination lines of Barker et al (1979).

### 5.2.3 Intrusive rocks

Granitoids from the Zimbabwe Craton (ZC) and Northern Marginal Zone (NMZ) largely overlap in normative Ab-An-Or space, spanning all fields (Figure 5.47). Trondhjemitic rocks are rare in the NMZ, whereas granodioritic rocks are absent in the

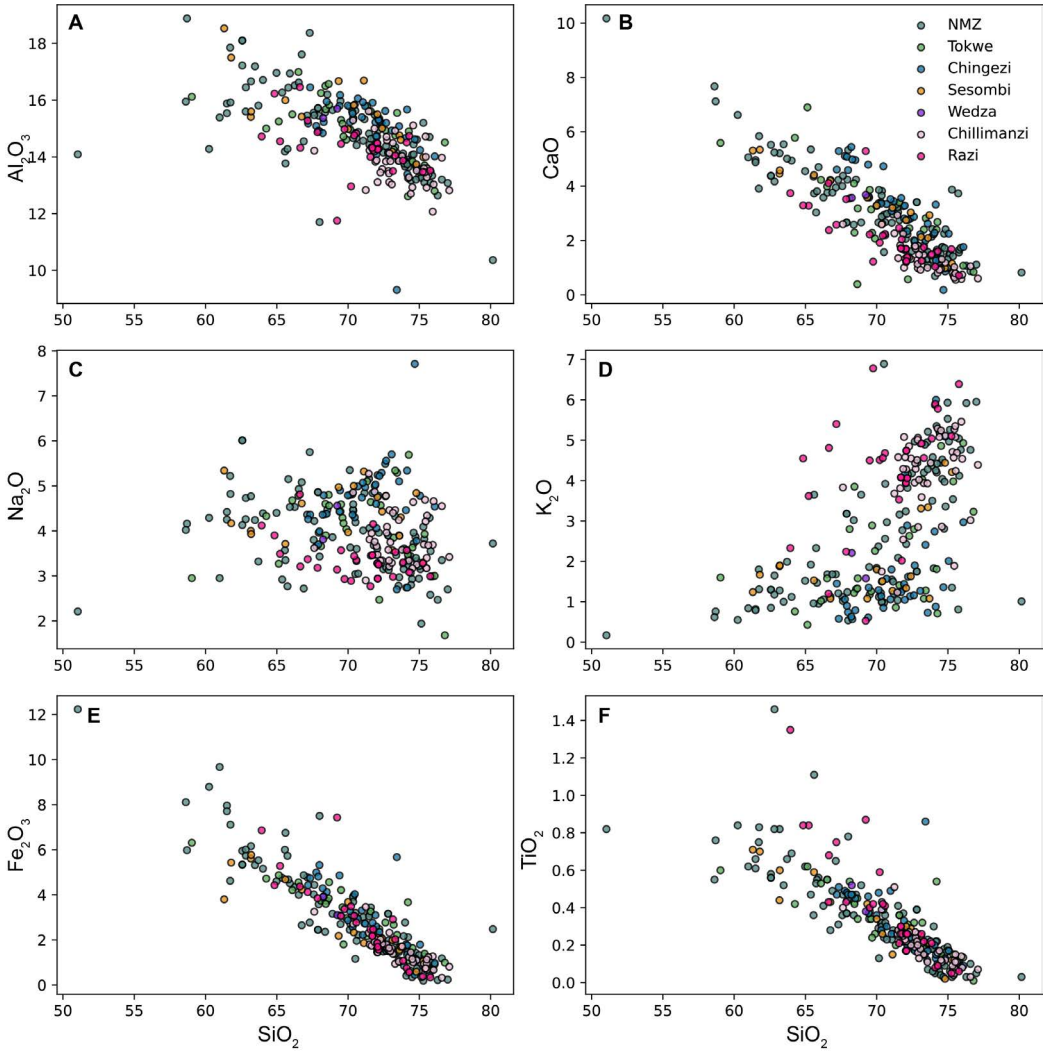


Figure 5.48: Harker diagrams for TTG and granite samples from the Zimbabwe Craton and the Northern Marginal Zone.

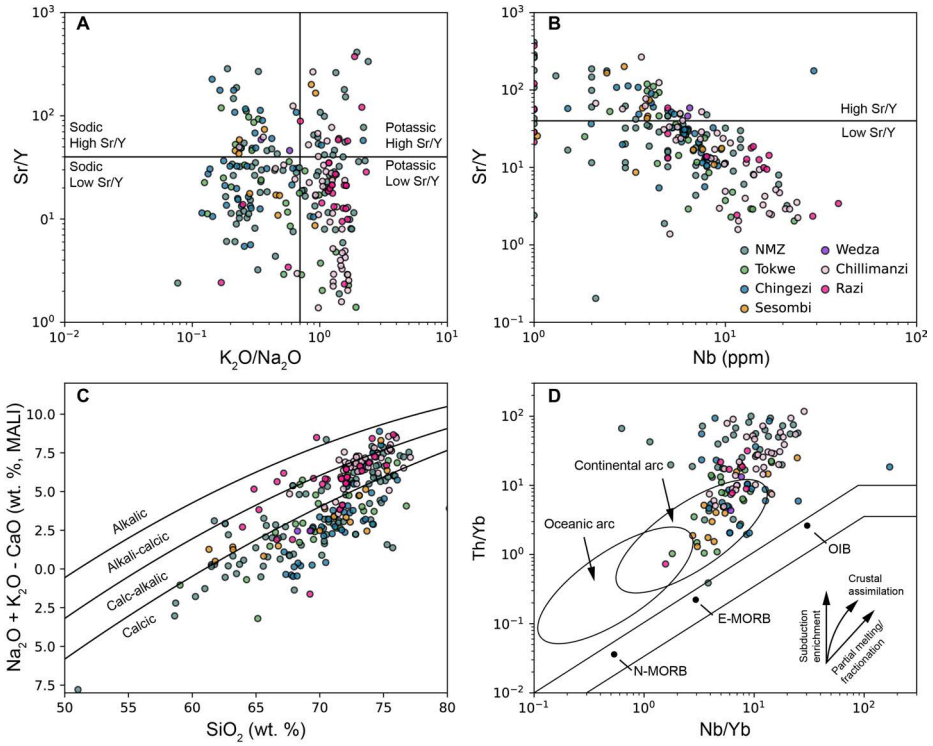


Figure 5.49: Geochemical discrimination diagrams for granitoids. A) Sr/Y vs. $K_2O$ / $Na_2O$ diagram with discriminating principles from Moyen and Martin (2012) and Smithies et al. (2018); B) Sr/Y vs. Nb for discrimination of adakites and TTGs against typical arc rocks after Drummond and Defant (1990) and Nymoen et al. (2025); C) Modified alkali-lime index (MALI) plot after Frost (2001); and D) Th/Yb vs Nb/Yb after Pearce (2008, with vectors for subduction enrichment, crustal assimilation, and partial melting/fractional crystallisation after Szilas et al. (2016).

Chingezi suite. Broadly, Razi suite granites exhibit more calcic (An-rich) affinities relative to the Chillimanzi suite.

Harker diagrams are plotted in Figure 5.48. Granitoids from the NMZ exhibit a wider range of $SiO_2$ content (c. 51–80 wt. %) relative to the ZC (c. 58–77 wt. %). All TTG and granite suites exhibit clear and parallel fractionation trends in $Al_2O_3$, $Fe_2O_3$, CaO, and $TiO_2$ (Figure 5.48A,B,E,F). Razi suite granites cover a wider potassic compositional space (c. 0.3–6.8 wt. %), whereas Chillimanzi suite granite are generally more constrained ($K_2O$ between c. 1.8–5.5 wt. %), and are both predominantly within the potassic field (Figure 5.49A). An inflection point in $K_2O$ at c. 70 wt. % $SiO_2$ is observed in both NMZ and ZC granitoids (Figure 5.48D), though not all samples follow this trend. Similarly, $Na_2O$ exhibits a weak negative correlation to $SiO_2$, and Razi suite granites are consistently less sodic than Chillimanzi suite granites. All TTG suites in the NMZ and ZC show sodic and potassic affinities, and both high and low Sr/Y values are observed (Figure 5.49A). A negative trend is evident in log-log space for Sr/Y vs. Nb in all suites of the NMZ and ZC (Figure 5.49B). The majority of less silicic TTG analyses fall within the calcic trend of Frost (2001), and trend towards being calc-alkaline with increasing $SiO_2$ (Figure 5.49C). Chillimanzi and Razi suite granites primarily straddle the calc-alkalic trend (Figure 5.49C). In Th/Yb vs. Nb/Yb space, all suites follow partial melting/fractionation and/or crustal assimilation trends away from continental arc compositions (Figure 5.49D).

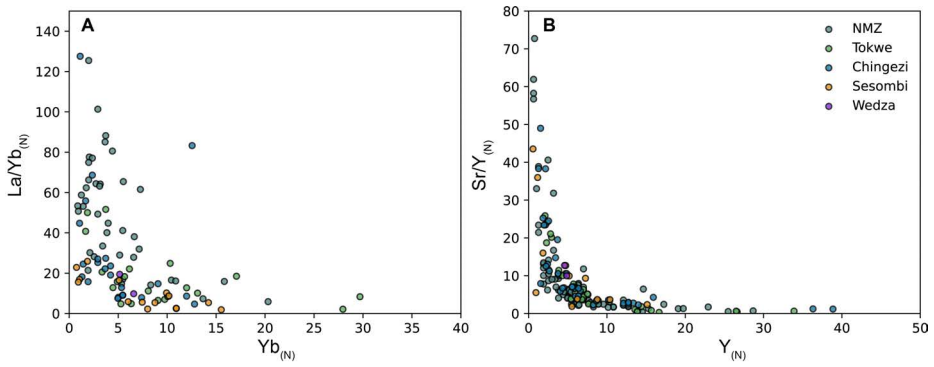


Figure 5.50: A) $La/Yb_N$ vs $Yb_N$; and B) $Sr/Y_N$ vs $Y_N$ for all TTG suites in the Zimbabwe craton and northern marginal zone.

Each suite has distinct REE and compatibility trends, described individually below.

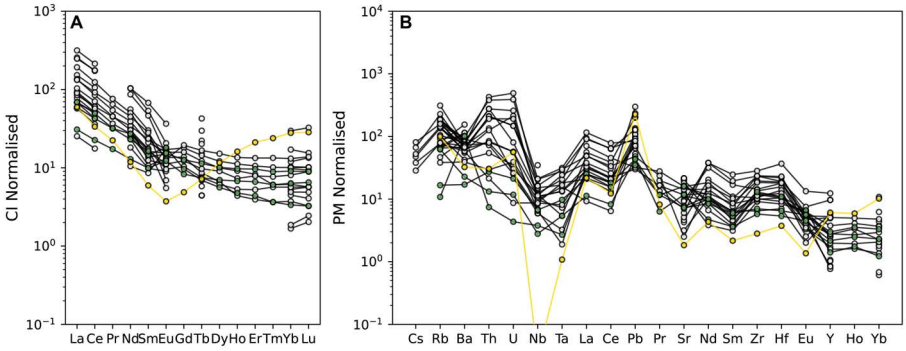


Figure 5.51: Chondrite-normalised REE plot (A), and primitive mantle-normalised spidergram (B) of samples from the Tokwe suite. Data collected during this study coloured in. Yellow line represents the early intrusive sample TR07. Elements are ordered in order of compatibility within a mantle-derived melt. Normalisation values from McDonough and Sun (1995).

#### 5.2.3.1 Tokwe suite

Samples from the Tokwe suite exhibit comparable REE and trace element profiles (with the exception of *TR07*, Figure 5.51). All REE profiles are negative towards the HREEs, with a minimal or absent Eu anomaly (Figure 5.51A). The slope of the profiles shallows at Eu in all samples. Incompatible elements are significantly enriched relative to primitive mantle (2–800 × PM), with notable positive Pb, and negative Nb-Ta anomalies (Figure 5.51B). Sample *TR07* exhibits a negative trend towards Eu, coupled with a strongly positive HREE trend (Figure 5.51A). Sample *TR07* additionally has a strongly negative Nb anomaly.

#### 5.2.3.2 Chingezi suite

Samples from the Chingezi suite display three distinct REE trends (Figure 5.52A); a very strong negative REE trend coupled with a moderate Eu anomaly, a moderately negative REE trend with no strong Eu anomaly, and a moderately negative REE trend with a minor positive Eu anomaly. The three groups have overlapping spidergrams, with a prominent positive Pb anomaly, and a more developed negative Nb-Ta anomaly when compared to the Tokwe suite (Figure 5.52B).

#### 5.2.3.3 Sesombi and Wedza suite

Samples from the Sesombi and Wedza suite overlap in both REE and spidergram patterns (Figure 5.53). La/YbN values are consistently $< 30$ and $\mathrm{Sr/Y}_N < 45$ (Figure 5.50). All samples display a negative REE slope, and Eu anomalies are weak (Figure

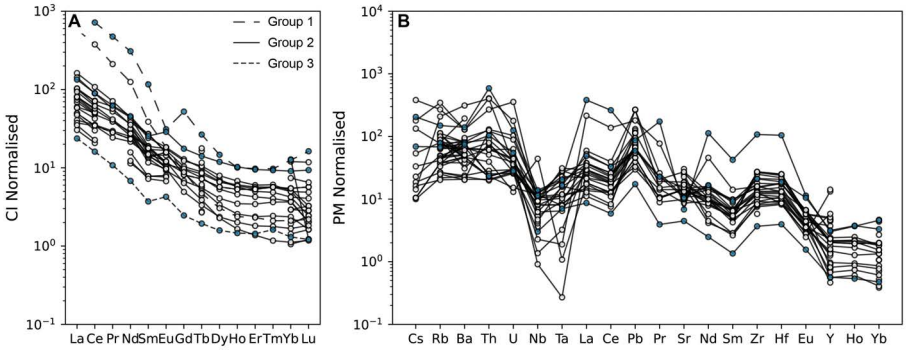


Figure 5.52: Chondrite-normalised REE plot (A), and primitive mantle-normalised spidergram (B) of samples from the Chingezi suite. Data collected during this study coloured in. Elements are ordered in order of compatibility within a mantle-derived melt. Normalisation values from McDonough and Sun (1995).

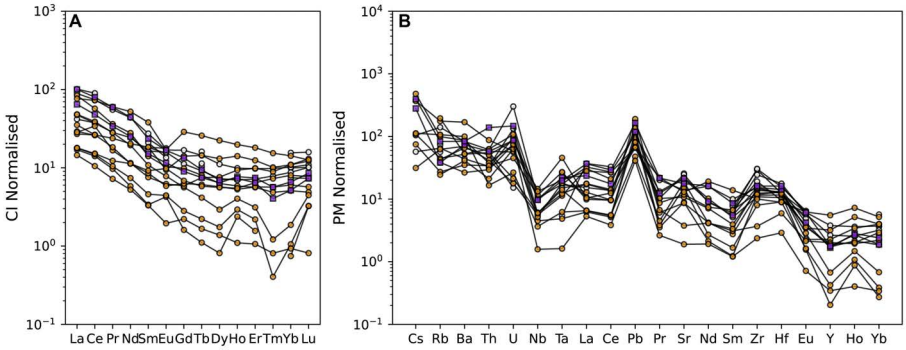


Figure 5.53: Chondrite-normalised REE plot (A), and primitive mantle-normalised spidergram (B) of samples from the Sesombi (orange circles) and Wedza (purple squares) suites. Data collected during this study coloured in. Elements are ordered in order of compatibility within a mantle-derived melt. Normalisation values from McDonough and Sun (1995).

5.53). Four samples have a positive trend from Tm to Lu. All samples exhibit a positive Pb anomaly, and Nb-Ta anomalies are absent. The four least evolved samples display sub-PM Y-Ho-Yb concentrations (Figure 5.53).

#### 5.2.3.4 Chillimanzi and Razi suites

Samples from both the Chillimanzi and Razi suites display overlapping trends in REE and spidergram patterns (Figure 5.54). All samples display a negative Eu anomaly and HREE are more depleted than LREE (Figure 5.54). Razi suite samples are systematically more enriched (20–800 × CI), than Chillimanzi suite samples (1.5–400 × CI). All samples display a positive Pb anomaly, strongly elevated Th-U values, and

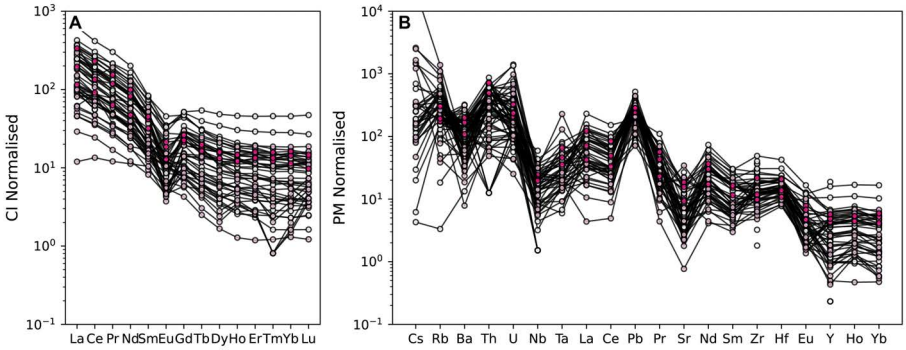


Figure 5.54: Chondrite-normalised REE plot (A), and primitive mantle-normalised spidergram (B) of samples from the Chillimanzi (light pink) and Razi (dark pink) suites. Data collected during this study coloured in. Elements are ordered in order of compatibility within a mantle-derived melt. Normalisation values from McDonough and Sun (1995).

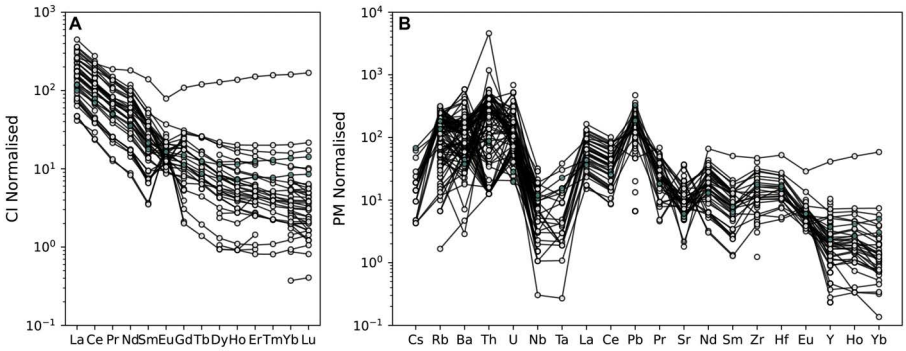


Figure 5.55: Chondrite-normalised REE plot (A), and primitive mantle-normalised spidergram (B) of samples from the Northern Marginal Zone. Data collected during this study coloured in. Elements are ordered in order of compatibility within a mantle-derived melt. Normalisation values from McDonough and Sun (1995).

negative Sr anomalies (Figure 5.54). Several samples display significantly elevated Cs and Rb (Figure Z.8B).

#### 5.2.3.5 Northern Marginal Zone

With one exception, all samples from the Northern Marginal Zone (NMZ) exhibit strongly depleted HREE patterns, and both positive and negative Eu anomalies (Figure 5.55). Samples display limited Rb-Cs enrichment, a negative Nb-Ta anomaly, and a positive Pb anomaly (Figure 5.55). Thorium and U values are commonly significantly elevated (10–1000 × PM, with one outlier at 5000 × PM).

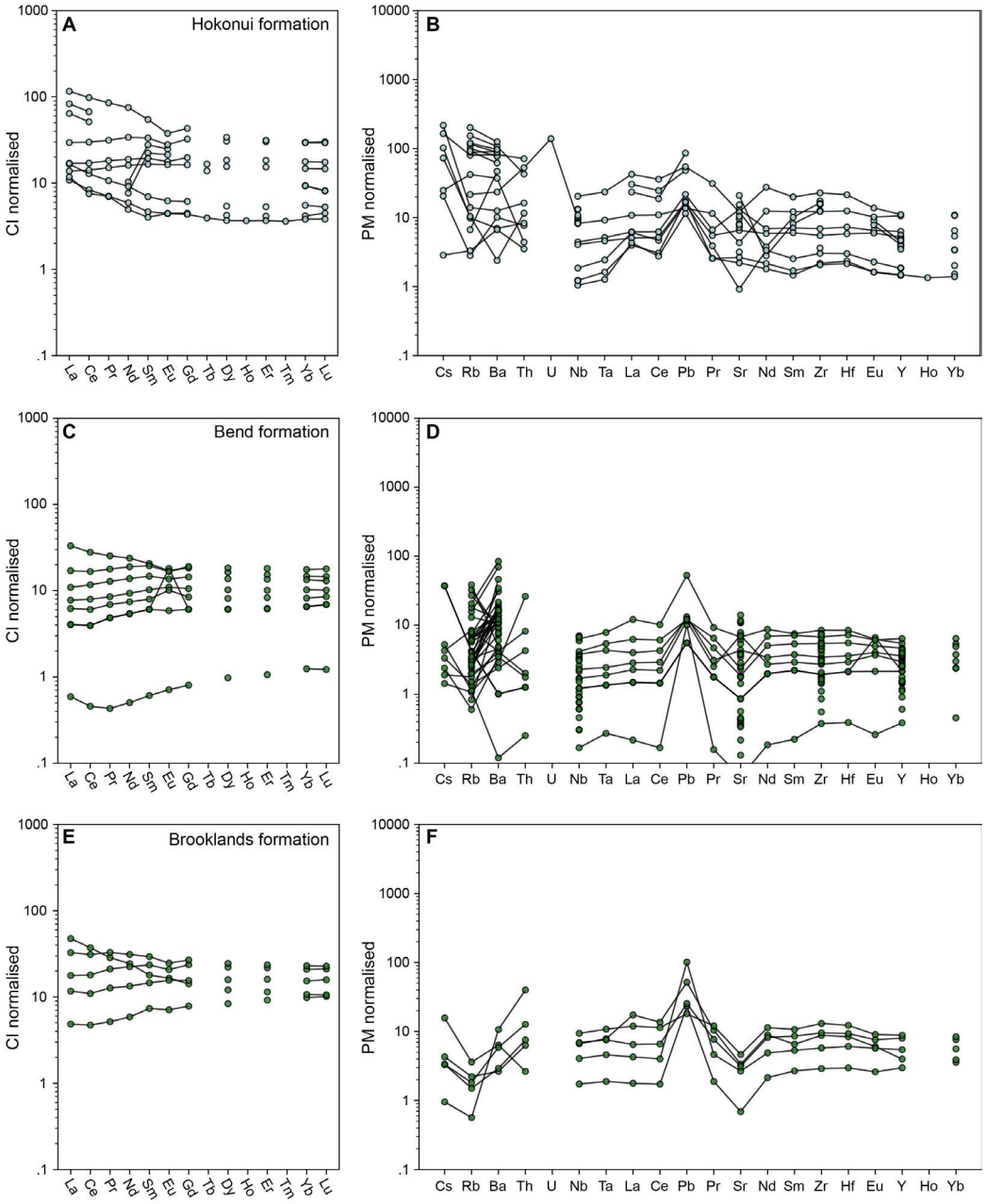


Figure 5.56: Chondrite-normalised REE diagrams (A,C,E), and primitive mantle-normalized spidergrams (B,D,F) for the andesitic Hokonui (A,B), (ultra)mafic Bend (C,D), and mafic Brooklands (E,F) formations.

### 5.2.4 Extrusive rocks

#### 5.2.4.1 Belingwean group

The Belingwean group comprises the Bvute, Hokonui, Bend, and Brooklands formation at the type locality in the Belingwe greenstone belt. No samples with trace element geochemistry from the Bvute formation are recorded in the literature. The Hokonui formation samples exhibit two trends – mafic lithologies display flat REE patterns, whilst andesitic successions have weakly depleted HREE patterns (Figure 5.56). A Pb anomaly is present in all samples, and trace elements are moderately to strongly enriched (1–200 × PM).

Samples from the Bend formation all display a relatively flat REE profile at 5–20 × CI. Trace elements are moderately enriched to sub-PM concentrations (0.1–100 × PM), with a flat spidergram profile with the exception of a positive Pb anomaly (Figure 5.56).

Samples from the Brooklands formation exhibit flat REE and spidergram profiles (Figure 5.56). Trace elements are weakly–moderately enriched (0.7–100 × PM), and a positive Pb anomaly is present in all samples.

#### 5.2.4.2 Lower Bulawayan

The lower Bulawayan Koodoovale formation has limited geochemical data. One sample with REE data exhibits strongly depleted HREE and negative spidergram profiles (Figure 5.57).

#### 5.2.4.3 Upper Bulawayan

The upper Bulawayan volcanics in the eastern greenstone belts (Murewa–Odzi, Masvingo, Belingwe, Gweru, Fort Rixon–Shangani, Gwanda, and the eastern portions of the Filabusi and Bulawayo belts) are predominantly komatiite–komatiitic basalt–basaltic successions of the Reliance and Zeederberg formations.

Samples of the Reliance formation have weakly depleted HREE to flat REE profiles (Figure 5.57). Samples are moderately to poorly enriched in trace elements relative to Primitive Mantle (0.2–200 × PM), with minor Pb anomalies. Normalised trace element profiles are flat (Figure 5.57).

Samples of the Zeederbergs formation similarly display a weakly HREE depleted to flat REE profiles (Figure 5.57). Trace element profiles are flat, and enrichment is weak–moderate (0.1–300 × PM). On average, samples are more enriched than the Reliance formation volcanics.

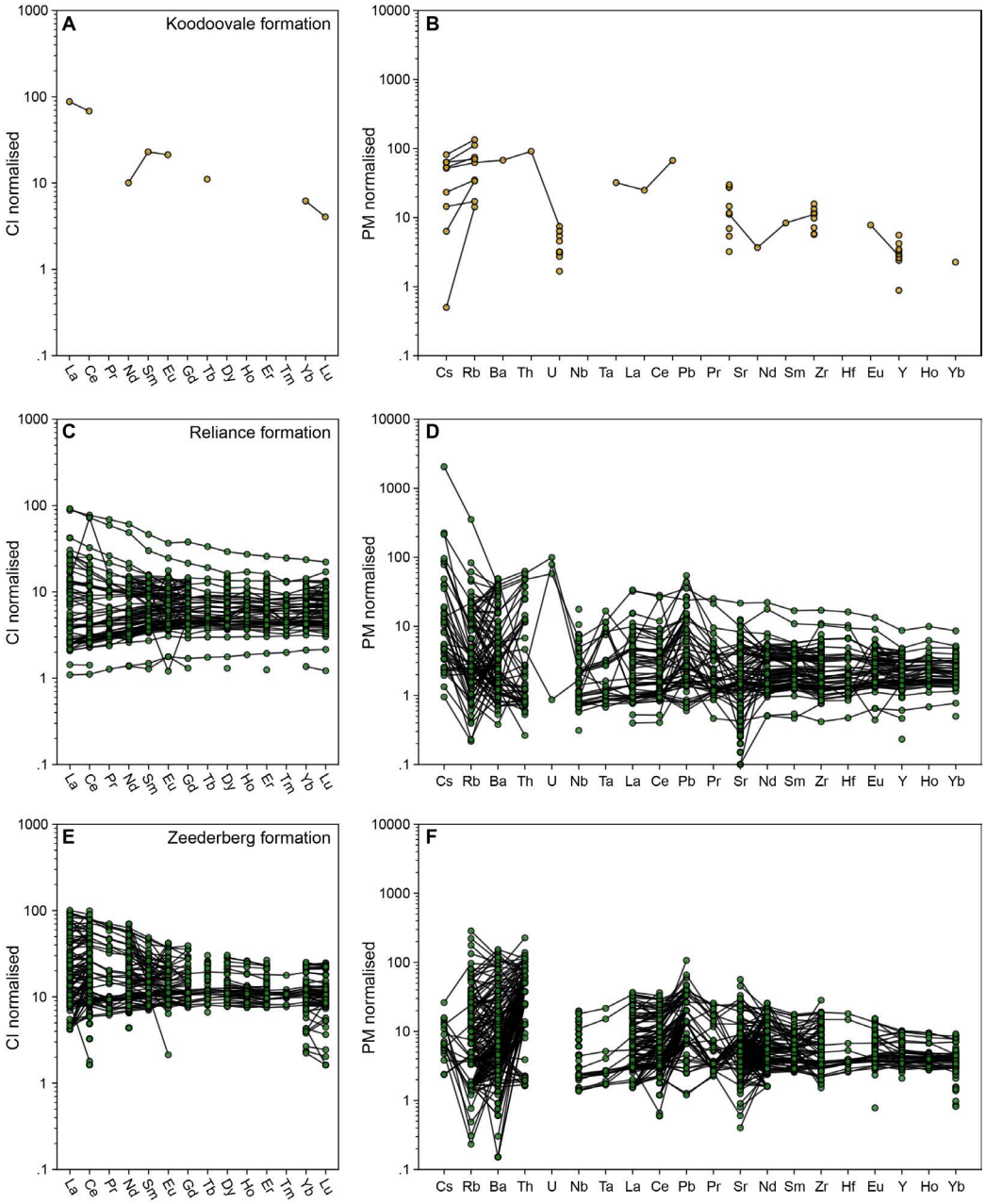


Figure 5.57: Chondrite-normalised REE diagrams (A,C,E), and primitive mantle-normalized spidergrams (B,D,F) for the Koodoovale (A,B), Reliance (C,D), and Zeederberg (E,F) formations.

#### 5.2.4.4 Shamvaian

Limited geochemistry on Shamvaian volcanics exhibit depleted HREE profiles (Figure 5.58). Trace element profiles also show a negative trend, with notably low U contents, and a general enrichment of 4–300 × PM.

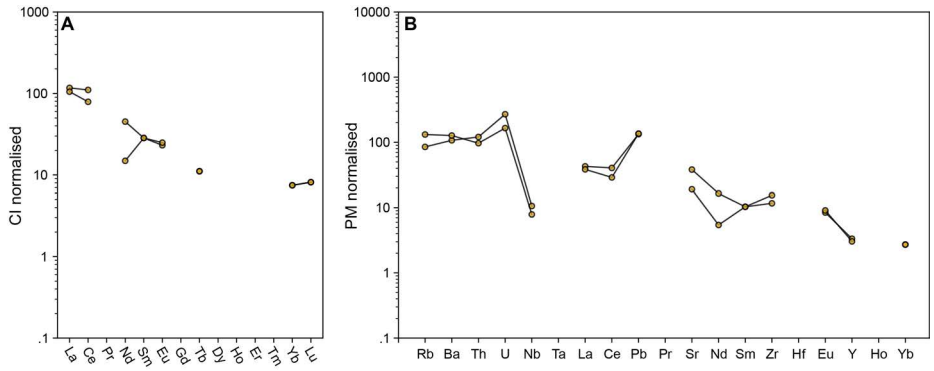


Figure 5.58: Chondrite-normalised REE plot (A), and primitive mantle-normalised spidergram (B) of samples from the Shamvaian group.

## 5.3 Discussion

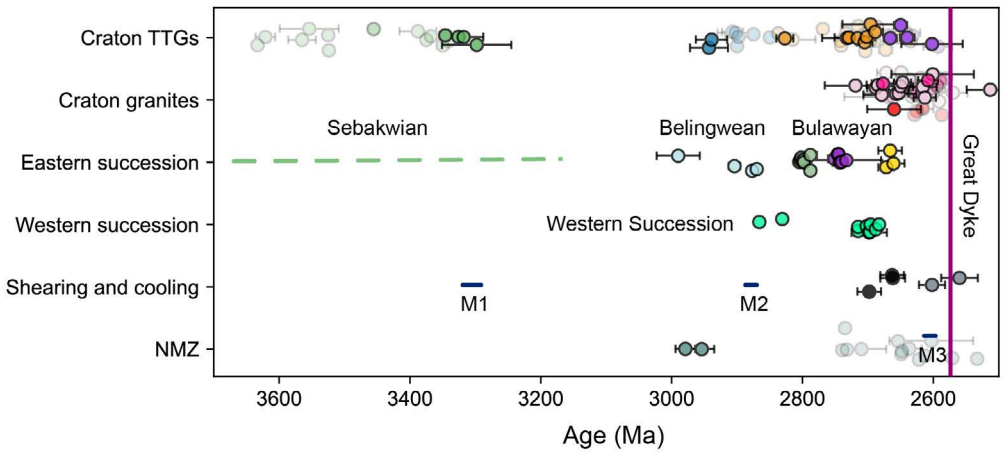


Figure 5.59: Summary of events in the Zimbabwe craton. Colours correspond to those used for suites for figures 5.47, with the addition of red circles (pegmatite crystallisation), and dark blue (metamorphic events).

### 5.3.1 Early cratonic nuclei in the Zimbabwe Craton (3.8–3.2 Ga

The earliest *in-situ* remnants of felsic magmatism in the Zimbabwe craton are preserved in two cratonic nuclei named the Tokwe and Rhodesdale terranes (Figure 5.1), with oldest ages of 3633 ± 3 Ma (Hofmann et al., 2022) and 3565 ± 21 Ma (Horstwood et al., 1999), respectively (Stowe, 1979; Wilson et al., 1995, ; Figure 5.59). The presence of earlier felsic magmatism is suggested by detrital (Bolhar et al., 2017; Dodson et al., 1988) and inherited zircons (e.g., Hoffman et al., 2022 and this study), though these have not yet been identified. It is unclear whether the Rhodesdale and Tokwe terranes were adjacent to each other during the Paleoarchean, however this early magmatic episode appears to have generated TTGs sporadically from at least 3633–3340 Ma with remarkably similar geochemistry (Figures 5.60 and 5.61). Tokwe suite TTGs are characterised by high $Na_2O/K_2O$, low La/Yb, Sr/Y, and shallow negative REE patterns, which suggests an absence of rutile and garnet in the source (Martin and Moyen, 2002; Foley et al., 2002; Rapp et al., 2003). The Tokwe suite was therefore likely sourced by melting of relatively shallow (< 30 km) melting of a mafic hydrated crust, arguing against formation in oceanic plateaux or subduction zone environments during this period (Figure 5.62). Both Re-Os and Lu-Hf isotope systematics suggest that the mafic proto-crust precursor to the Tokwe suite likely separated from the

primitive mantle by 3.8 Ga (Bolhar et al., 2017; Hofmann et al., 2022; Nägler et al., 1997).

Early crustal recycling related to an amphibolite facies metamorphic episode generated potassic/granodioritic melts – the Mushandike and Mont D'Or granites – at c. 3300–3375 Ma (Dodson et al., 2001; Hickman, 1974; Horstwood et al., 1999; Moorbath et al., 1976). These early 'potassic' granitoids have Sm-Nd isotopic ages of 3540–3670 Ma, suggesting the incorporation of older felsic crustal material (Taylor et al., 1991).

Sample *TR07* from this study is intruded into c. 3.4 Ga crust that has a remarkably distinct geochemical signature (yellow dataset in Figure 5.60A). Positive HREE, negative Eu, and << Nb/Ta anomalies suggest the presence of rutile/amphibole and plagioclase in the melt source, with magmatic garnet retaining the HREE. The presence of Eoarchean inherited zircons within error of the earliest detrital zircon data (Figure 5.59, Bolhar et al., 2017) suggest that similar recycling was required to form these early leucogranitic sills.

Remnants of early extrusive volcanism and surface sedimentation are limited to tightly infolded keels within the Paleoarchean gneisses. Little is known about their origin, although ultra-mafic talc-tremolite schist and serpentinites, and metamorphosed cherts and ironstones suggest that mafic magmatism was coupled with submarine chemical sedimentation during this time period.

### 5.3.2 Quiescence, followed by renewed Mesoarchean magmatism (3.0–2.85 Ga)

Following Paleoarchean magmatism, the Zimbabwe craton experienced a period of relative quiescence and stability. Along the southern margin of the Tokwe terrane a stable passive margin developed now preserved in the Buhwa greenstone belt (Figure 5.1), suggesting a period of (limited) crustal emergence must have occurred to provide Tokwe-age detritus that was largely deposited under submarine conditions (Brengman et al., 2021; Fedo et al., 1995; Fedo and Eriksson, 1996; Fedo et al., 1996).

Following a period of magmatic quiescence, activity resumed with the generation of the Chingezi TTG suite between 2.95–2.85 Ga (Figure 5.59). The type area of the Chingezi suite lies on the western and southern edges of the Belingwe greenstone belt (Martin et al., 1993; Wilson et al., 1995, Figure 5.1). Extensions of the Chingezi suite have been found in the Mashaba tonalite, which transects the Tokwe terrane along a N-S axis (Wilson et al., 1995), the Chipinda batholith around the Buhwa greenstone belt, which was emplaced along major ductile oblique-slip dextral shear zones (Fedo et al., 1995), and along the eastern edge of the Mutare-Odzi greenstone

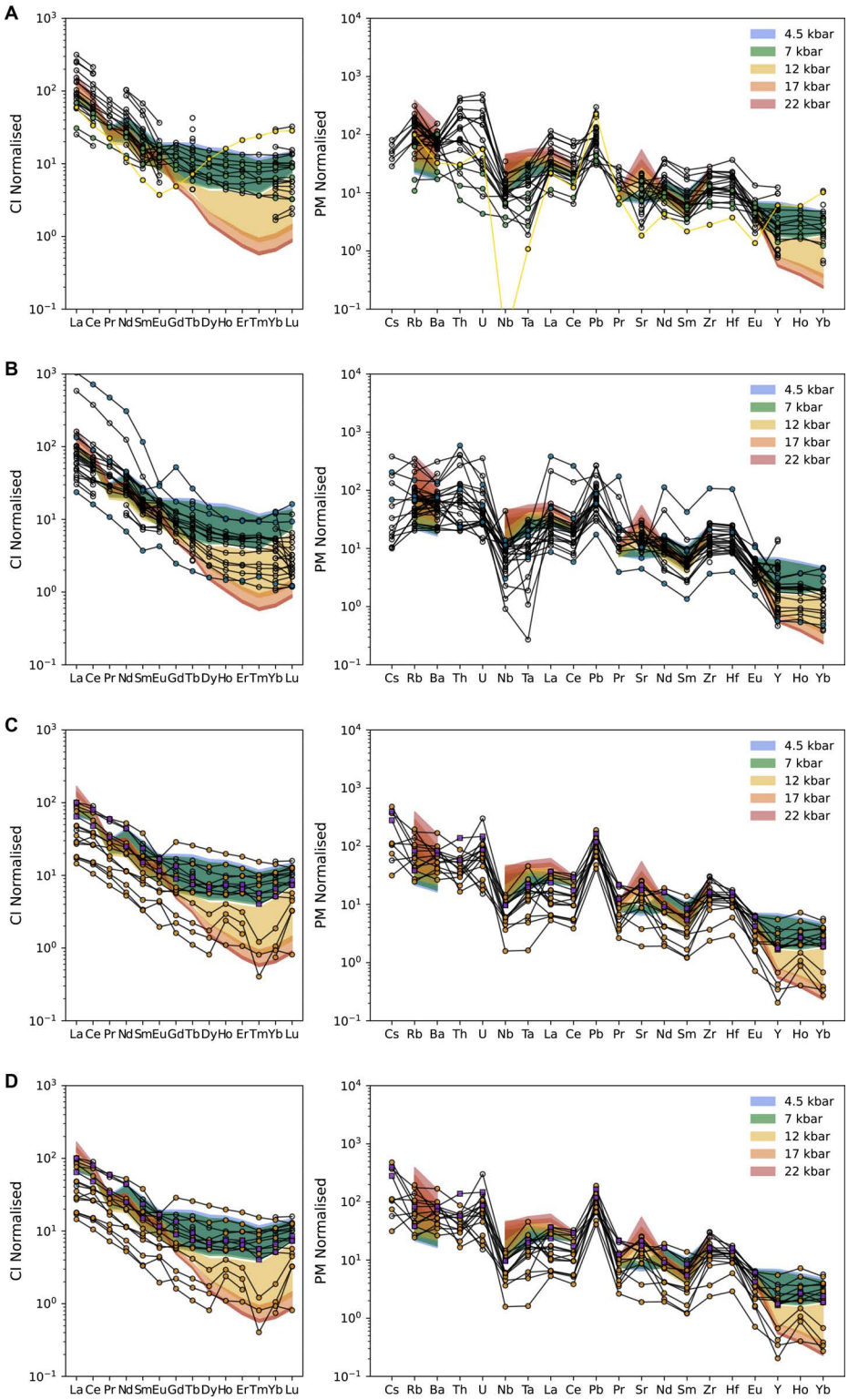


Figure 5.60: Trace element spidergrams (right) and REE plots (left) for all TTG suites in the Zimbabwe craton, with samples collected in this study coloured in. A) Tokwe suite, B) Chingezi suite, C) Sesombi/Wedza suites, D) Northern marginal zone. All plots are underlain by modelled EAT (Condie, 1981) melt compositions, coloured by pressure of the isobaric melt path.

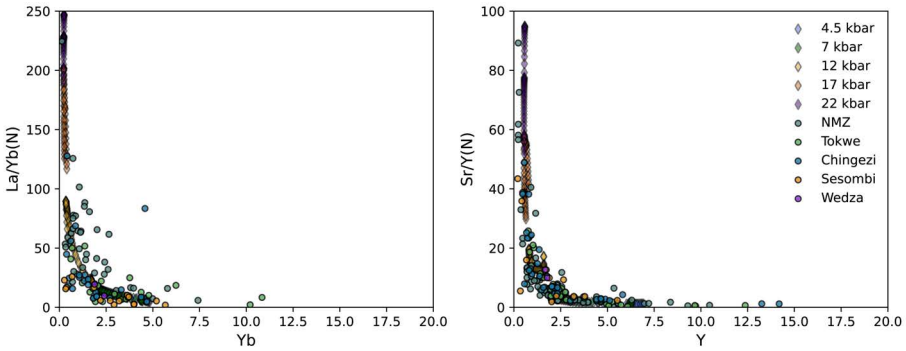


Figure 5.61: La/Yb vs Yb (left) and Sr/Y vs. Y (right), normalised to Primitive Mantle, (McDonough and Sun, 1995), diagrams of all TTG suites in the Zimbabwe craton. The data are underlain by modelled melts by melting EAT (Condie, 1981), colour-coded by pressure at which melting is modelled.

belt in Mozambique (Mantäri, 2008). The Chingezi suite presents elevated La/Yb, Sr/Y and more steeply negative REE plots, suggestive of a source melted at greater depth (>10 kbar, Figures 5.60 and 5.61, Luais and Hawkesworth, 1994), implying the crust substantially thickened prior to magmatism during time period.

This study also reports the first evidence of Chingezi-age magmatism in the Northern Marginal Zone (NMZ), which is preserved as highly deformed and migmatised granulitic basement into which later charnockitic and enderbitic magmas intruded. This discovery lends credence to the interpretation that the NMZ is a deep-crustal equivalent of the Zimbabwe craton (cf. Rollinson, 2022), and extends its magmatic history by 200 Myr. It is highly likely that pre-3.0 Ga felsic magmatism is not preserved in the NMZ, given that early Tokwe-suite melts were derived from sources shallower than reported depths of the currently exposed NMZ (Kamber and Biino, 1995; Rollinson, 1989).

Belingwean group volcanics formed coevally with intrusive magmatism members of the Chingezi suite, and are best exposed in the Belingwe (as the Hokonui, Brooklands, and Bend formations), Filabusi (as the Shamba-Kudu formations), Fort Rixon–Shangani (the "ycc" series of Harrison, 1969), and Gweru greenstone belts (Ranche formation) (Wilson et al., 1995, Figure 5.1). This group is primarily composed of a bimodal mafic extrusive and andesitic-dacitic agglomerate/tuff succession that document multiple major explosive volcanic episodes (Bickle et al., 1993; Martin et al., 1993). Minor chemical sedimentation forming thin banded iron formations occurred during this period, and textures within the agglomerate and tuff horizons suggest the majority of preserved deposition occurred in shallow marine environments

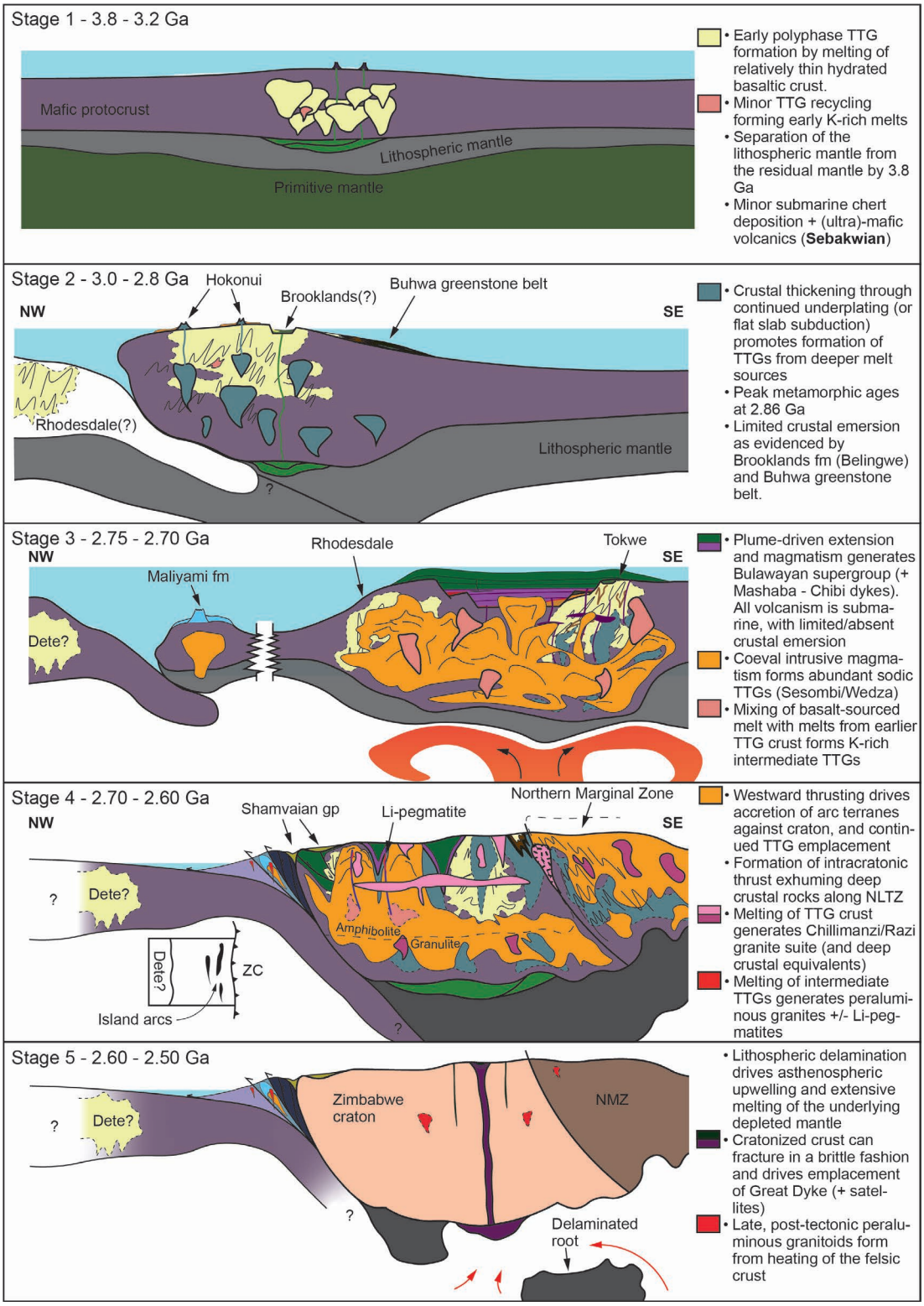


Figure 5.62: Schematic diagram summarizing the major stages of Zimbabwe craton evolution.

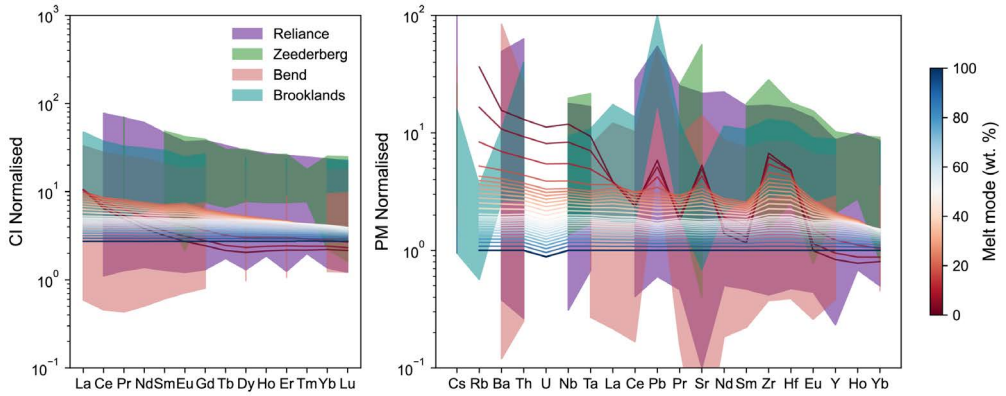


Figure 5.63: Chondrite-normalised REE diagram (left) and trace element spiderplot (right) showing the average composition of mafic volcanics in the central Zimbabwe craton. A model melt of relatively shallow (22 kbar) melting of primitive mantle is overlain, colour-coded by melt mode. Normalisation values are from McDonough and Sun (1995).

(Martin et al., 1993). The andesitic compositions and elevated LILE signatures (Figure 5.56) suggest fluid-rich melting environment, perhaps akin to modern-day mantle wedges situated above dehydrating subducting slabs.

Crustal thickening during this time period coincides with a second amphibolite-facies metamorphic event dated to c. 2.86 Ga (Figure 5.59; Nägler et al., 1997), and emplacement of the Chingezi suite was, at least in part, along major active shear zones (Fedo et al., 1995). These events may have coincided with the accretion of the Rhodesdale terrane onto the Tokwe terrane, with flat slab subduction suggested to promote substantial thickening via underthrusting (Figure 5.62). These processes are thought to have led to the formation of the Sebakwe protocraton (Jelsma et al., 2021), which subsequently evolved as a single cratonic block. In this scenario, the Brooklands formation preserved along the south-eastern margin of the Belingwe greenstone belt may represent a back-arc type rift basin within the Tokwe segment (e.g., Nisbet et al., 1993). In any case, both the Brooklands and Buhwa belt sedimentation indicate that there is some component of crustal emergence present during this time period, both preserving Tokwe-age detritus, however only generating limited sedimentary basins.

### 5.3.3 Plume-related growth of the craton (2.8–2.7 Ga)

Following a short period of quiescence, the last major period of crustal growth in the Zimbabwe craton began at c. 2.75 Ga. Large swaths of the central Zimbabwe craton preserve a coherent Bulawayan group stratigraphy in the greenstone belts, which

is subdivided into the felsic volcanic Koodoovale, shallow sedimentary Manjeri, ultramafic Reliance, mafic Zeederberg, and sedimentary Cheshire formations (Bickle et al., 1993; Jelsma et al., 2021; Wilson et al., 1995). The post-Koodoovale formation succession has been variously suggested to have an autochthonous origin (e.g., Blenkinsop et al., 1993; Hunter, 1998; Wilson et al., 1995), or an allochthonous origin (e.g., Hofmann and Kusky, 2004; Kusky, 1998; Kusky and Winsky, 1995).

Proponents for the allochthonous origin argue that the volcanic pile of the Bulawayan succession was tectonically emplaced along a major décollement onto a stable shelf — now preserved as the Manjeri formation — overlying basement gneisses (Hofmann and Dirks, 2003; Kusky and Kidd, 1992). The contact between the Manjeri formation and overlying volcanics commonly consists of a sulphidic banded iron formation (the Jimmy member of the Manjeri formation), which has been interpreted as a major mylonitic horizon (Hofmann and Dirks, 2003; Hofmann and Kusky, 2004; Kusky and Winsky, 1995). Hofmann et al. (2001; 2024) further argued that the topmost Cheshire formation experienced deformation prior to folding into the current synformal geometry, which they interpret to show that the Belingwe belt underwent an earlier stage of tectonic activity. To these authors, the upper Bulawayan group (Reliance fm. and up) is therefore a segment of an oceanic plateau that was thrust onto the Sebakwe protocraton.

This scenario conflicts with the model (e.g., Blenkinsop et al., 1993) for an autochthonous origin for the Bulawayan group. In the autochthonous model, the Manjeri formation represents a cyclical shallow fluvial–marine transgressive sequence within rifted grabens, capped by banded iron formations formed during sediment-starved deposition (Blenkinsop et al., 1993; Hunter, 1998). A clear nonconformity between the Manjeri formation and 3.35 Ga granitoid gneisses (Hofmann et al., 2022) is exposed at the Basement Unconformity Exposure national monument south of Zvishavane (Blenkinsop et al., 1993; Hunter, 1998; Martin et al., 1993; Nisbet et al., 1977), and similarly as an angular unconformity against the Hokonui formation along the Dohwe river along the western edge of the Belingwe greenstone belt (Martin et al., 1993). Continuous deposition and a transition to volcanic activity is inferred by the presence of isolated quartzose horizons between the basal Reliance formation volcanics (Blenkinsop et al., 1993), and Prendergast (2004b) further suggests that interdigitation between the Koodoovale, Manjeri, and Reliance formation occurs at various points across the central craton. This would eliminate the possibility of an allochthonous origin for the volcanic pile. In addition, trace element (e.g., elevated

Th) and Nd-isotope geochemical evidence suggests that the Bulawayan volcanics experienced a component of crustal assimilation prior to eruption (Bolhar et al., 2003; Chauvel et al., 1993; Shimizu et al., 2005), as also supported by inherited zircons found in felsic volcanic horizons (Wilson et al., 1995). Arguably most convincing is the temporal overlap between the Mashaba-Chibi dyke swarm and associated ultramafic intrusive bodies (e.g., the Shabani and Mashaba sills), interpreted to be the intrusive feeders to the Bulawayan volcanics (Prendergast, 2004a; Prendergast and Wingate, 2007), which are emplaced into the Tokwe segment (Prendergast and Wingate, 2013; Wilson et al., 1995).

It is therefore most likely that the Bulawayan group was deposited onto the Sebakwe proton, and not tectonically juxtaposed. The volcanic succession is generally considered to have formed by plume-driven mantle melting, forming a large igneous province (c. 250 000 km$^2$, Prendergast, 2004a) atop a felsic protocrust, starting at c. 2.75 Ga (Hofmann et al., 2024; Prendergast and Wingate, 2013). A mantle plume origin is invoked to generate the high temperatures required to form the komatiitic successions (Shimizu et al., 2005), and supported by melt inclusion studies by McDonough and Ireland (1993), who showed that incompatible/compatible element ratios in the komatiitic melts are comparable to modern plume-related magmas. Models of primitive mantle melting closely align with the generally observed flat REE profiles of the Reliance and Zeederberg formations, with progressive enrichment inferred to be caused by fractional crystallisation within a magma chamber prior to eruption (Figure 5.63, Bolhar et al., 2003). A very deep ($>$ 150 km) melt origin, as suggested by Shimizu et al. (2005), is not required (Figure 5.63), though the absence of depletion in incompatible elements suggests that the mantle was not extensively depleted prior to this event (e.g., Salters and Stracke, 2004). The upper Cheshire formation, which consists primarily of a basal carbonate ramp grading upwards into a deeper water siliciclastic facies formed by turbidity currents (Hofmann et al., 2001; Martin et al., 1993), must have formed prior to 2.71 Ga, thereby constraining the (ultra)-mafic volcanism to a $<$40 Myr period (Hofmann et al., 2024). This encompasses sufficient time to generate comparable plume-related large-igneous provinces (e.g., Columbia River flood basalts, 210 000 km$^2$ in c. 11 Myr, Reidel et al., 2013; Deccan Traps, 500 000 km$^2$ in c. 3 Myr, Jay and Widdowson, 2008).

Initial plume impingement is expected to have driven partial melting of the lower crust, generating the intermediate–felsic volcanic Koodoovale formation (in the Belingwe greenstone belt) early in the Bulawayan succession (Prendergast, 2004a; Prendergast and Wingate, 2013). Similar stratigraphy is observed in the Filabusi (Eldo-

rado formation), Bulawayo (Lonsdale formation), Gweru (Arizona formation), and Fort Rixon–Shangani (Series formation). Associated with the volcanic activity is extensive intrusive magmatism, generating the Sesombi suite (Figure 5.62). The presence of both high and low La/Yb, Sr/Y, and variably negative REE patterns all suggest that melting of a mafic protolith would have occurred at varying depths in the crust during this time. Some of the protolith may have been underplated equivalents of the Bulawayan volcanic succession. The relative increase in proportion of TTGs with evelated $K_2O/Na_2O$ values in TTGs of this time period (Figure 5.49) in both the NMZ and the Zimbabwe craton suggests that earlier (Tokwe/Chingezi suite) TTGs were also incorporated in the melting environment and mixed with primitive EAT-sourced melts (cf. Rollinson et al., 2024).

### 5.3.4 Accretion of the Western Successions and Shamvaian deposition (2.71–2.60 Ga)

The Western Succession comprises an almost continuous greenstone belt from southwest of Bulawayo towards Shamva in the north-east of Zimbabwe (Figure 5.1). Typifying the succession is extensive calc-alkaline felsic volcanism, and a relatively high proportion of felsic and intermediate volcanics (c. 45% of the stratigraphy) when compared to greenstones of the central craton (Jelsma and Dirks, 2002). Intermediate–felsic volcanism is dated at 2715–2683, with later volcanic activity found in the Harare greenstone belt at 2648–2643 Ma (Jelsma et al., 2021; Wilson et al., 1995).

The stratigraphy within the western succession is often complicated and obscured by later tectonic repetition and shearing. In the Midlands greenstone belt, the Mafic formation (2880 ± 8 Ma, Horstwood, 1998) and What Cheer formation (2683 ± 8 Ma, Wilson et al., 1995) are interdigitated basalt, quartz grits, and siltstones (Jelsma and Dirks, 2002), and are abutted by a major transpressive shear zone against the Maliyami formation; a thick sequence of calc-alkaline andesites and dacites (2702 ± 6 Ma, Wilson et al., 1995). All are intruded by several late TTGs dated to c. 2670 Ma (Jelsma et al., 2021). The Midlands greenstone belt has been shown to have undergone significant west-directed thrusting, forming complex compressional duplexes which were later reactivated as (minor) strike-slip shear zones (Campbell and Pitfield, 1994; Dirks et al., 2002). This deformational event incorporated slivers of Paleoarchean TTGs of the Rhodesdale terrane (Jelsma and Dirks, 2002). Similarly, the Bindura-Shamva and Harare greenstone belts (Figure 5.1) experienced significant west-directed thrusting and imbricate stacking above major layer-parallel shear zones, stacking a 6 km thick tholeiitic basalt succession (Arcturus formation, 2697 ± 9 Ma, Wilson et al.,

1995) on top of a basal andesitic Iron Mask formation (2712 ± 7 Ma, Jelsma et al., 2021). Structurally overlying the Arcturus formation is the andesitic/dacitic volcanic Passaford/Lower Shamva and Mt Hampden (graphitic argillite) formations, dated at 2643 ± 8 Ma (Wilson et al., 1995). The felsic volcanics are closely associated with porphyry stocks and temporally overlaps with late tectonic TTGs of the Wedza suite (2648 ± 6 Ma, Jelsma et al., 1996), and SR01-2, WG02-3 in this study). The felsic volcanic rocks in the Western Succession have relatively unevolved isotopic signatures (e.g., initial Sr-ratios of 0.701 and 0.704, Baldock and Evans, 1988; Jelsma et al., 2021, $\epsilon$Nd 2.5 ± 0.4, Horstwood, 1998), and $\mu_1$ values between 7.7 and 8.6 (Taylor et al., 1991), suggesting a significant juvenile component in the source.

In the Bulawayo greenstone belt (Figure 5.1), the Avalon and Kensington formations are infolded and thrusted mafic volcanic and calc-alkaline successions. The top of the sequence (Umzingwane formation) is a thick volcanic laharic type breccia overlain by volcaniclastic turbidites and containing intercalations of rhyodacitic lava (Garson, 1995). Interestingly, the calc-alkaline succession in the Bulawayo greenstone belt structurally overlies the Westacre and Umganin formations, which can be correlated to the Bulawayan volcanic successions in the central craton. This succession appears to be imbricated in a series of W-NW directed thrust stacks into the Kensington and Avalon formations (2683 ± 8 Ma, Jelsma et al., 2021).

Throughout the Western succession greenstones are a series of fault-bounded siliciclastic successions which are defined as the Shamvaian group. These are primarily preserved in the Midlands and Harare–Shamva greenstone belts, and correlative successions are also found in the Masvingo greenstone belt. The Shamvaian group are predominantly coarse grained fluvial-deltaic successions composed of conglomerates, grits, and poorly sorted sandstones and minor shales (Dirks et al., 2002; Hofmann et al., 2002). Sporadic lenses of intermediate-felsic volcanism exist, which alongside cross-cutting intrusive rocks date Shamvaian deposition to 2.68–2.61 Ga (Jelsma et al., 2021). Importantly, the Shamvaian succession presents the only significant siliciclastic sedimentary basins documented in the craton.

Combined deformation and shear-sense observation suggests that the Western Succession experienced several generations of W-NW directed thrusting (Garson, 1995; Jelsma and Dirks, 2002), and later strike-slip shearing and reactivation (Campbell and Pitfield, 1994; Dirks et al., 2002). The fault-bounded Shamvaian successions at c. 2.68–2.61 Ga coincide with U-Pb titanite ages dating shearing along the Irisvale-Lancaster shear zone (Figures 5.43 and 5.44), suggesting that the major crustal shear

zones (Campbell and Pitfield, 1994; Stowe, 1980) that transect the craton likely developed during the same deformational event.

The calc-alkaline signatures, along with some overlapping ages with the Bulawayan succession of the central craton indicates that the Western Succession volcanics are as a series of accreted volcanic arcs, possibly incorporating small oceanic plateaux (e.g., Mafic formation, Condie and Harrison, 1976; Horstwood, 1998). Lithologies to the west may be a different Archean cratonic block, which today are exposed in the Dete-Kamativi inlier (Glynn et al., 2020, Figure 5.1). If true, this juxtaposition may mark the closure of an early ocean that represents a valuable opportunity for future investigation. Accretion onto the central Sebakwe protocraton (Jelsma et al., 2021) coincided with the continued emplacement of TTGs, and likely aided by the significant density contrast with the overlying (ultra)-mafic volcanics, promoted (at least partially) solid-state diapirism, generating the general dome-and-keel pattern observed throughout the craton (e.g., Copley et al., 2023; Kusky et al., 2021; Weinberg and Podladchikov, 1995). This presents a unique scenario where geological features conventionally attributed to vertical-style tectonic processes may have formed during a horizontal tectonic event. Similar relationships have recently been proposed in the Wabigoon superterrane, Canada (Tóth et al., 2025). A metamorphic event, coupled with the development of major crustal shear zones accommodated strain in the cratonic block c. 2.68–2.61 Ga (Figure 5.62). The onset of exhumation of the NMZ along the Northern Limpopo Thrust Zone, which overlaps in age with this event (Blenkinsop, 2004; Rollinson and Blenkinsop, 1995) may be related to intracratonic basement uplift related to this accretionary event. The NMZ may therefore be similar to the Kapuskasing zone in the Superior Craton, Canada(c. 2.0 Ga, Percival and Card, 1983; Percival and West, 1994).

### 5.3.5 Emplacement of potassic granites (2.68–2.51 Ga)

Neoarchean potassic granites occur throughout the craton and occupy c. 50% of the current level of exposure (Blenkinsop and Treloar, 2001; Chagondah et al., 2023; Jelsma et al., 2021). Commonly characterised by K-feldspar megacrysts, the late granites have historically been grouped into the Chillimanzi (cratonic) and Razi (NMZ and NMZ-craton margin) suites. Most large-scale Chillimanzi suite intrusions were likely fed by thin vertical dykes and emplaced as thick horizontal sheets making them appear voluminous (Blenkinsop and Treloar, 2001). A general younging eastward trend has been noted previously in the granitic suite, from c. 2680 Ma near the Western Succession towards 2517 Ma along the eastern extent of the NMZ (Frei

et al., 1999; Horstwood, 1998; Jelsma et al., 1996; Mkweli et al., 1995). However, the first age of the Nalatale granite (2512 ± 36 Ma, apatite U-Pb, Figure 5.42), which partially bisects the Fort Rixon–Shangani greenstone belt (Figure 5.1), indicates that late Archean felsic magmatism occurs near the Western Succession as well. The older Rb-Sr biotite cooling ages (2602 ± 20 Ma and 2560 ± 28 Ma, Figure 5.46) supports the fact that this is a crystallisation age and not a later thermal resetting.

Compositionally, most Chillimanzi and Razi suite granites are metaluminous to slightly peraluminous (I-type, Figure 5.65), with some highly peraluminous (A/CNK >1.1), and plot along the calc-alkaline trend of Frost et al. (2001, Figure 5.49C). Evolved geochemical (elevated K/Na, Th, U, and ΣREE, Figures 5.49, 5.54) and isotopic ($\epsilon$Nd = -1.6, Horstwood, 1998) characteristics strongly support their formation by melting of pre-existing felsic lower crust. Modelling of potential felsic sources suggest the best match occurs when melting both sodic and potassic Sesombi suite TTGs at mid-lower crustal levels (Figure 5.64). Importantly, the most evolved units, characterised by elevated Th and U, and the lowest Mg #, best fit melting intermediate TTGs (Figure 5.65B), in agreement with observations made by Rollinson et al. (2024).

The wide range of ages (2.68–2.51 Ga) during which the Chillimanzi and Razi suite granites were emplaced suggests that multiple processes may have generated the collective suites. Early granites (both metaluminous and peraluminous) may be associated with final accretion of the Western Succession, followed by late, peraluminous granites (e.g., the Nalatale granite) possibly driven by mantle heating during emplacement of the Great Dyke and final cratonic stabilisation (discussed below).

### 5.3.6 Emplacement of the Great Dyke (2.575 Ga)

The Great Dyke remains a feature unique to the Zimbabwe craton. The main intrusion is intruded as a 550 km long, and up to 11 km wide dyke (Worst, 1960; Wilson, 1990), and is dated to 2574 ± 2 Ma (Armstrong and Wilson, 2000; Wingate, 2000; Oberthür et al., 2002). Two main satellite dykes occur both west (Umvimeela Dyke) and east (East Dyke) of the main intrusion, and are related to the final pulses of magmatism of the suite (Harrison, 1969; Wingate, 2000). The Great Dyke is emplaced along a NNE trending fault set (Worst, 1960; Wilson, 1990), which may have formed by extensional relaxation following the accretion of the Western Succession. The ultramafic compositions of the Great Dyke imply a significant amount of mantle melting must have occurred (Oberthür et al., 2002; Wilson, 1996). Compositionally, there is no evidence of a deep mantle source, and extensive melting of the depleted

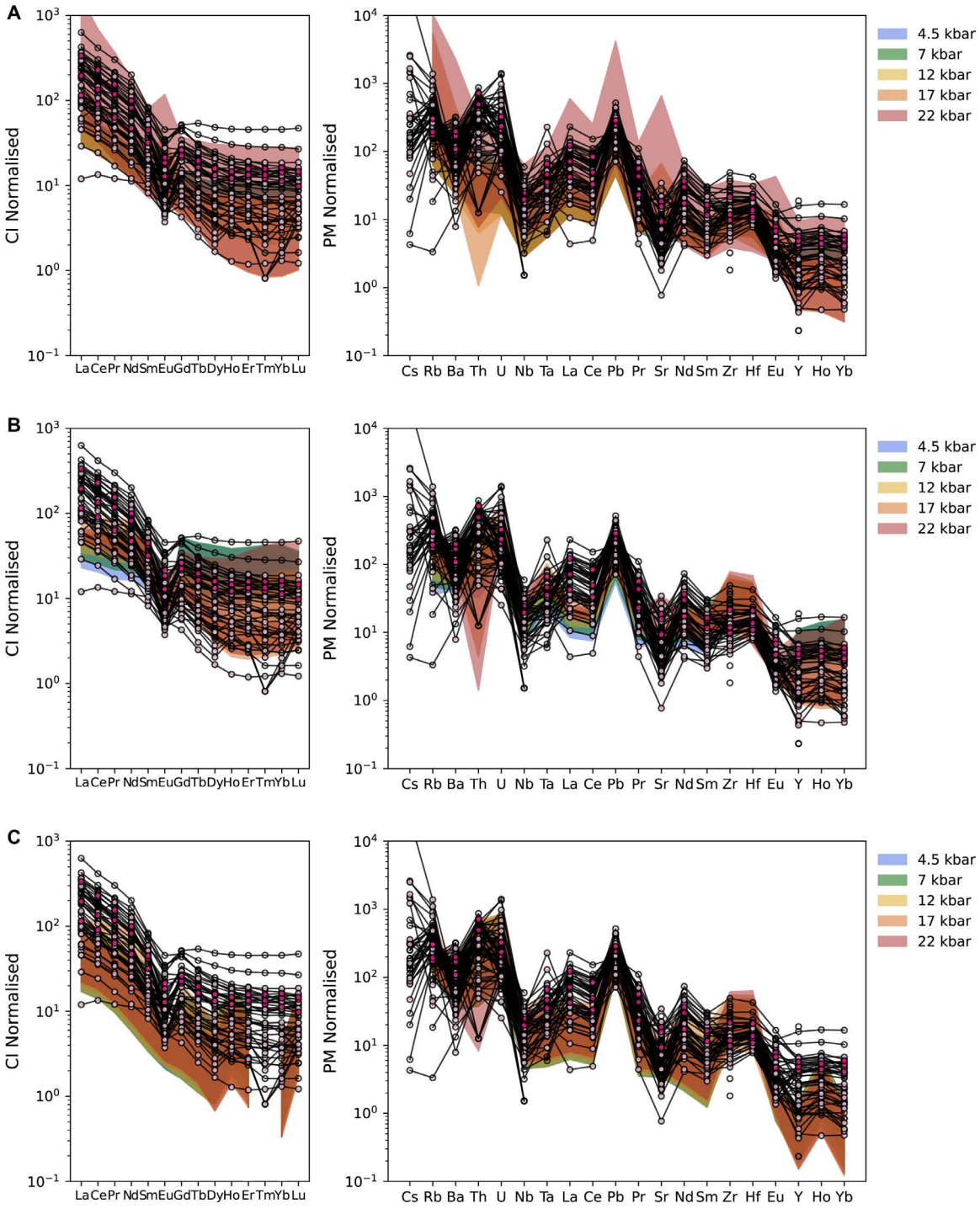


Figure 5.64: Chondrite normalised REE plots (Left) and primitive mantle normalised trace element spidergrams (right) of the Chillimanzi and Razi suite granites overlain onto modelled compositions of direct partial melts of Tokwe suite (TR02, A), Sodic Sesombi suite (GW04, B), and intermediate TTG Sesombi suite (ZB02, C).

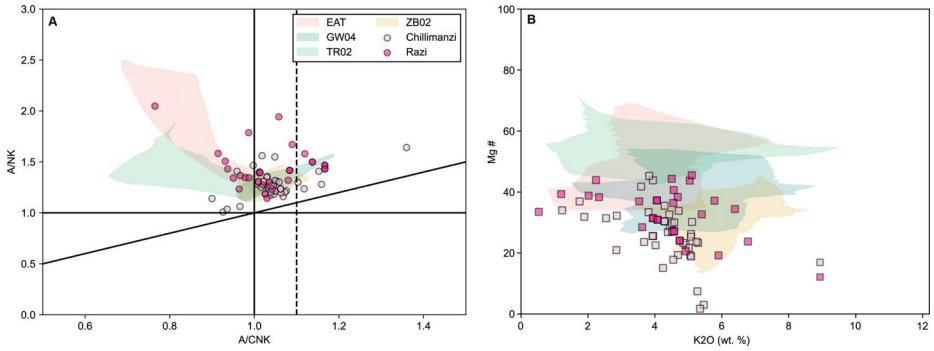


Figure 5.65: A) $Al_2O_3/(Na_2O+K_2O)$ (A/NK) vs. $Al_2O_3/(CaO+Na_2O+K_2O)$ (A/CNK) (molar proportions) diagram, after Maniar and Piccoli (1989). B) Mg # (Mg/(Mg+Fe)×100, molar proportions) vs. $K_2O$ diagram. Both present data from the Chillimanzi and Razi suites overlain on modelled compositions of direct melting of EAT (Condie, 1981), TR02 (Tokwe Suite), GW04 (sodic Sesombi suite), ZB02 (intermediate TTG, Sesombi suite).

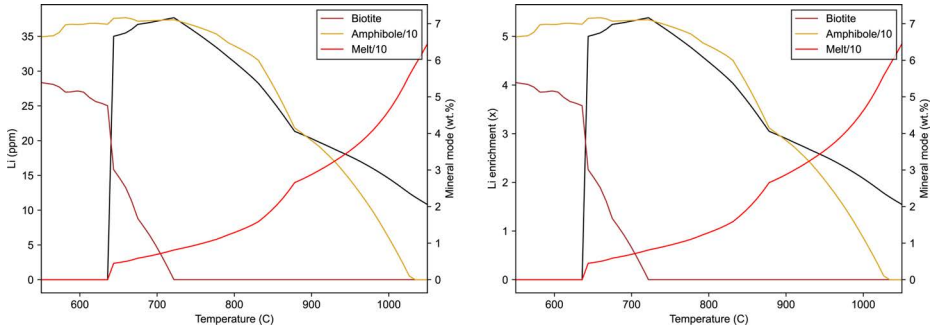


Figure 5.66: Li concentrations (left) and maximum melt enrichment (right) during modelled melting of EAT (Condie, 1981). Modal proportions of melt, biotite, and amphibole are shown.

mantle below the craton is invoked (Oberthür et al., 2002). It is feasible that mantle depletion would have occurred during the Bulawayan volcanic event, and that subsequent melting was driven by significant delamination of the lower crust (Figure 5.62).

Exactly how such a large, effectively singular intrusion was able to form in the craton is unclear, however it is worth noting that this must have been able to occur in the midst of extensive granitic magmatism, given Chillimanzi and Razi suite crystallisation ages straddle the emplacement of the Great Dyke.

### 5.3.7 Lithium fertility during crustal evolution

Compared to other Archean cratons worldwide, the Zimbabwe craton is uniquely endowed in lithium-rich LCT/Group 1 pegmatites (Goodenough et al., 2025). However, unlike other Li pegmatite-rich domains, the Zimbabwe craton lacks the sedimentary successions commonly assumed to be protoliths for such melts (Černý, 1991b; Černý et al., 2012; London, 2008). It is therefore unclear which geological mechanisms allowed such enrichment in Zimbabwe.

The assumption that sedimentary material is needed within a source region undergoing partial melting arises from the compositional affinity that LCT/Group 1-type signatures have with S-type granites (Černý et al., 2012; Chappell and White, 1992, 2001). Enrichment in lithium is a key characteristic of LCT pegmatites (Černý et al., 2012), and is considered to arise from melting a previously unmelted, mica-bearing metapelite or metagreywacke (Acosta-Vigil et al., 2012; Černý et al., 2012; London and Morgan, 2012). Similarly, elevated P contents commonly seen in LCT-type pegmatites are considered diagnostic of a metapelitic protolith (London et al., 1999; Martin and De Vito, 2005). Initial enrichment in Li, Cs, Rb, P, etc. in the metasedimentary source is a product of the relative incompatibility of these elements in granitic minerals (i.e. quartz and two feldspars), thereby promoting their release during weathering, which thus acts as a pre-concentrating step. In this model, the source for LCT/Group 1 pegmatites must form via crustal recycling prior to attaining the required enrichments to form key LCT ore minerals (see also Chapter 3).

If recycling of felsic continental crust is required to generate a fertile source rock, this can be achieved simply through crustal melting–remelting processes. In the Zimbabwe craton, and Archean cratons more generally, the first stage of differentiation occurs during the formation of primitive (sodic) TTGs from a hydrated metabasaltic source. Assuming average EAT concentrations for lithium (c. 7 ppm, Condie, 1981), mid-lower crustal melting of hydrated EAT can generate a melt of TTG composition with Li contents of up to 36 ppm (Figure 5.66). The release of lithium into the melt is primarily controlled by the breakdown of biotite, with minor influence of amphibole. Lithium concentrations of $\leq$36 ppm is within the range of Li concentrations measured in Tokwe suite TTGs.

In the Zimbabwe craton, there is evidence for the mixing of primitive TTG melts (sourced from hydrated metabasalt) and those derived by melting of pre-existing TTG crust, generating intermediate-stage TTGs with elevated K/Na throughout craton evolution (Figure 5.49). Taking *TR02* (Li = 32 ppm) as a typical Tokwe suite TTG, melting of early, sodic TTGs can generate melts with Li up to c. 300 ppm (Figure

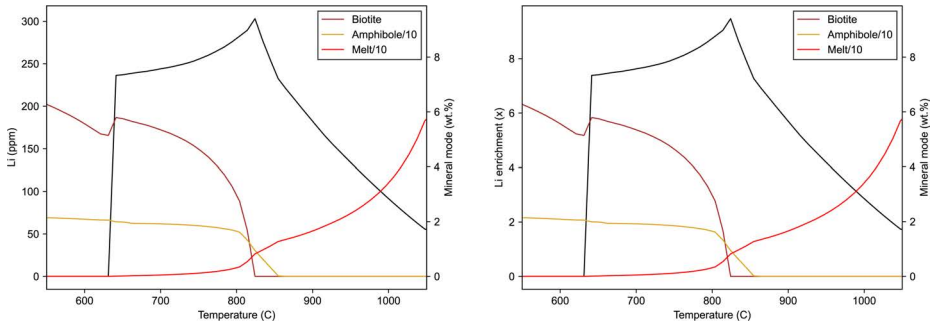


Figure 5.67: Li concentrations (left) and maximum melt enrichment (right) during modelled melting of TR02, as a representative TTG of the Tokwe suite. Modal proportions of melt, biotite, and amphibole are shown.

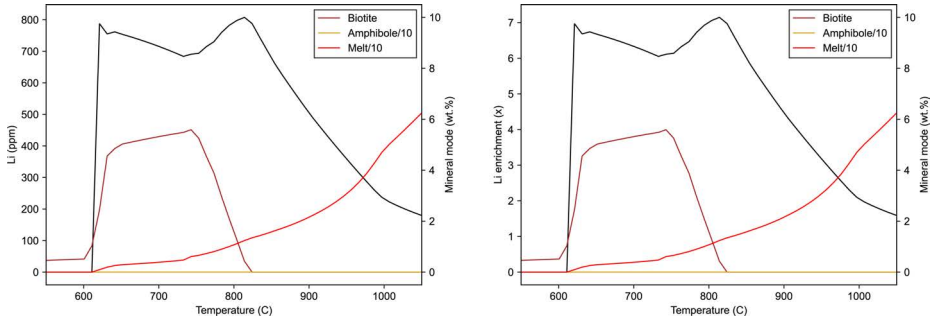


Figure 5.68: Li concentrations (left) and maximum melt enrichment (right) during modelled melting of ZB02, as a representative intermediate TTG of the Sesombi suite. Modal proportions of melt, biotite, and amphibole are shown.

5.67). Mixing of this melt (25%) with a primitive melt (75%) sourced from a hydrated mafic source would therefore generate an intermediate stage TTG ($K_2O/Na_2O \approx 1$) with Li concentrations of ∼100 ppm, which is in line with what is observed in the craton.

Finally, melting of intermediate TTGs (taking *ZB02* as an example, Li = 113 ppm) can generate enriched melts with concentrations of c. 800 ppm Li, with a maximum enrichment factor of c. 7 (Figure 5.68). Whilst this is insufficient to saturate in spodumene or petalite (>5000 ppm Li), subsequent fractional crystallisation of the granitic melt can further enrich Li, either within granitic staging bodies or directly within pegmatites generating strongly zoned pegmatitic bodies (London, 2014). Such strongly zoned bodies are seen in the Zimbabwe craton (e.g., Arcadia, Goodenough et al., 2025; Mistress, Baldock, 1991). Later melting of early formed fertile Chilimanzi/Razi suite granites (cf. Chapter 3) can, alongside fractional crystallisation (owing to the higher starting concentrations), directly form melts with Li contents >5000 ppm, enabling the formation of unzoned pegmatites.

Melting of intermediate TTGs generates peraluminous–highly peraluminous melt compositions (Figure 5.65A), low Mg # (Figure 5.65B), and low degrees of partial melting promotes the formation of melts with distinct fertile characteristics (Figure 5.69). Whilst compositions comparable to Chillimanzi and Razi suite granites can form melting of both primitive (sodic) and intermediate (potassic) TTGs, regions with a prevalence of intermediate TTGs may prove fertile for future exploration for Li pegmatites.

### 5.3.8 Conclusions

The Zimbabwe craton preserves an extensive and complicated history spanning the Eo- to Neoarchean. Detailed geochronology, geochemistry, and modelling suggests that the earliest TTGs of the Tokwe and Rhodesdale segments likely formed through relatively shallow (<10 kbar) melting of a hydrated mafic protocrust. Intrusive TTGs of the Tokwe suite became complexly infolded with small remnants of the early Sebakwian greenstone cycle during an amphibolite-facies metamorphic event which initiated the first cycle of crustal recycling within the craton, forming intrusive sills and larger

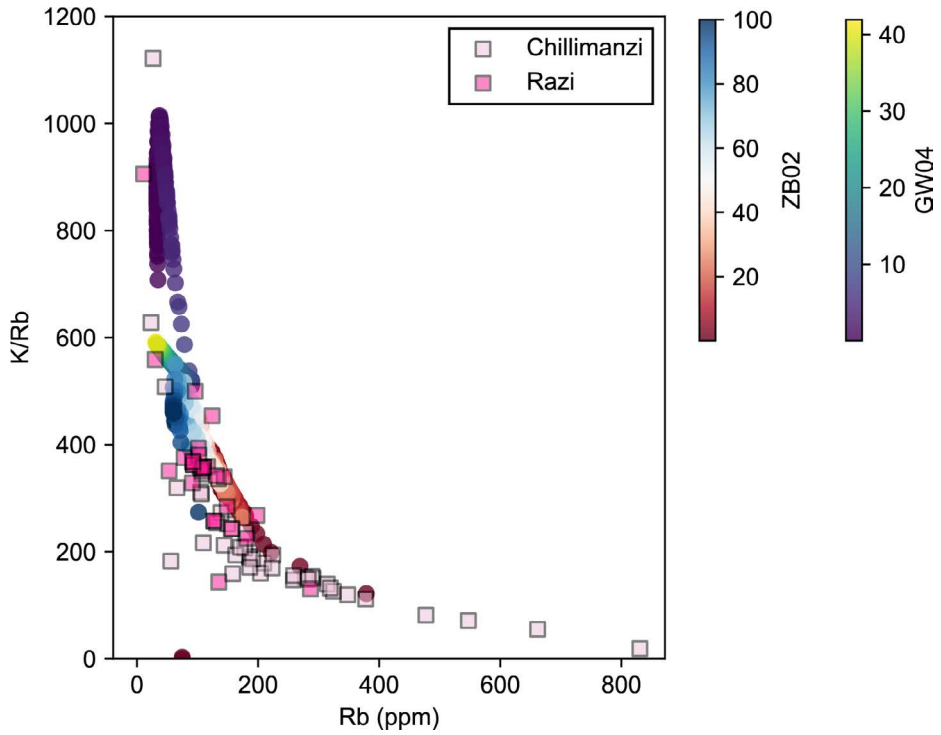


Figure 5.69: K/Rb vs. Rb plot of Chillimanzi and Razi suite granite samples, underlain by model melt compositions of melting intermediate TTG (ZB02) and primitive TTG (GW04) of the Sesombi suite in mid-lower crustal levels (8-10 kbar).

intrusive bodies (e.g., the Mushandike granite).

Following a period of quiescence and relative stability, during which the southern margin of the Tokwe segment developed a passive margin, deeper-seated melting of mafic crust (forming the Chingezi TTG suite) was coupled with extensive bimodal volcanism in the first major generation of greenstone belts (Belingwean) in the craton. This may have been driven by the amalgamation of the Tokwe and Rhodesdale terranes through underthrusting or flat-slab subduction underneath the Tokwe terrane, generating the Sebakwe protocraton during a regional metamorphic event at c. 2.86 Ga (Figure 5.62).

Plume impingement underneath the protocraton first generated felsic volcanism and the initiation of extension, prior to development of a major (c. 250 000 $km^2$) large igneous province (Bulawayan) which covered the majority of the central Zimbabwe craton. Coupled with the extensive volcanism was the emplacement of the Mashaba-Chibi dyke swarm and ultramafic sills as intrusive feeders for the flood-basalt type volcanism under shallow submarine conditions. Heating of the lower crust generated abundant melting of underplated basalts and relatively mafic lower crust, generating the Sesombi TTG suite. Through assimilation and mixing, earlier formed TTG suites were incorporated into the primitive TTG melts to form a suite of intermediate (elevated K/Na) TTGs (Figure 5.62).

Immature and mature volcanic arcs and oceanic plateaux accreted onto the western margin of the Sebakwe protocraton during a major accretionary event c. 2.68–2.61 Ga, which formed the spatially extensive and complexly deformed Western Succession greenstone belts. Coupled with this orogenic event was the doming of TTGs, generating the dome-and-keel style structures seen in the craton today, emplacement of the major Chillimanzi and Razi suite granites, and the thrusting of the deep-crustal Northern Marginal Zone onto the craton (Figure 5.62). Final craton stabilisation was marked by the emplacement of the Great Dyke at c. 2574 Ma during a major delamination event and coincided with continued crustal melting and granitic magmatism. By 2.5 Ga, the Zimbabwe craton became a fully stable cratonic block.

The Zimbabwe craton presents an intriguing case study for the study of LCT pegmatite petrogenesis, as the previously assumed melting protoliths (metasedimentary rocks) are scarce, and therefore the craton presents a markedly different example to Archean pegmatite formation when compared to well-studied cratons such as the Superior. In the Zimbabwe craton, repeated recycling of the early formed crust during repeated crustal melting events likely provided the necessary enrichment of lithium, where models suggest that three to four crustal melting/recycling events is sufficient

to generate the concentrations required to form potentially economic LCT type pegmatites. This can also explain an Archean enigma: lithium-rich pegmatites only appear towards the end of cratonisation in any Archean craton as only at this point has the crust been sufficiently recycled to generate the required lithium enrichment.

# Chapter 6

# Conclusions

## 6.1 Thesis conclusions

This thesis explored the source and structural controls of lithium-rich, LCT/Group 1 type pegmatites, and integrated this understanding into the broader context of the evolution of the Zimbabwe craton. First, I conducted a modelling based study to test whether the two main formation models of lithium pegmatites can generate the necessary lithium enrichment (>5000 ppm Li for spodumene saturation) to form unzoned, albite-spodumene, pegmatites which characterise the majority of economic deposits (Chapter 3). Next, I presented a structural case study on the Zulu pegmatite field to determine the relative timing of emplacement and potential structural controls on the distribution of the pegmatite field (Chapter 4). Finally, I integrated new geochronological and geochemical data from the Zimbabwe craton to propose a refined holistic model of the evolution of the craton during the Archean (Chapter 5).

### 6.1.1 Modelling of pegmatite sources

In Chapter 3, I showed through thermodynamic modelling that the lithium content of a melt generated by anatexis of metasedimentary protoliths is primarily controlled by the breakdown of biotite. When comparing a typical pelite and greywacke as protoliths, greywackes were found to be more fertile given lower mica content. Direct anatexis of metasedimentary rocks was found to have a maximum enrichment factor of c. 4.3. Flux melting (by introduction of external fluids to the system), which has historically been considered a potential source mechanism for pegmatite formation (e.g., Müller et al., 2017), served to depress lithium enrichment in the melt due to persistent mica stability. Given sedimentary rocks with lithium contents >1000 ppm

are exceptionally rare, it is unlikely that direct anatexis of metasedimentary protoliths is a viable mechanism to generate economic albite-spodumene pegmatites.

By comparison, fractional crystallisation was simulated to test the granite fractionation model. Fractionation can enrich lithium in a granitic melt by a factor $\leq$6 at 90% fractionation (above the generally accepted particle locking threshold of Vigneresse et al., 1996, at which separation of crystals from remaining melt becomes untenable). Therefore elevated initial lithium contents of c. 600 ppm (a melt that formed a result of direct anatexis of enriched metasedimentary rocks tested above) generated melts with a maximum lithium of up to 3400 ppm, still below the minimum saturation point for spodumene.

Forming economic albite-spodumene pegmatites through either generally accepted mechanism is therefore considered unlikely. In this study, I proposed a new petrogenetic model, whereby an initial melting event of metasedimentary rocks generated an early generation of granites. Subsequent reheating of the system, either within the same or during a later orogenic event, promotes partial melting of the earlier granitic body, which modelling suggest is an extremely efficient mechanism at concentrating lithium. The resultant melts readily pass the required 5000 ppm threshold, thereby providing a viable mechanism to generate spodumene saturation at initial crystallisation of a pegmatitic melt.

This model accounts for two features observed in several pegmatite fields: 1) economic pegmatites are commonly unzoned, and therefore spodumene saturation must be achieved at the onset of crystallisation, and 2) pegmatites are often significantly younger than spatially related granites (e.g., Brou et al., 2022; Goodenough et al., 2014). It should be noted that the classic fractionation and direct anatectic models can potentially explain the genesis of some (zoned) deposits worldwide.

### 6.1.2 Structural controls on economic deposits

In chapter 4, I presented a field-based case study on the Zulu pegmatite field in the Zimbabwe craton, within which two main pegmatite types were delineated.

Type 1 pegmatites were interpreted to have been emplaced synkinematic to transcurrent shearing ($D_2$) along the Irisvale–Lancaster and Zulu shear zones. This was highlighted by internal deformation within the pegmatites, their lenticular shape subparallel to the main shear fabrics, and the synkinematic growth of exomorphic alteration phases surrounding the pegmatite bodies. The signficant rheological contrast between the weaker serpentinite hanging wall and amphibolitic footwall likely acted as a concentrating mechanism to generate large individual pegmatite intrusions.

Type 2 pegmatites, on the other hand, primarily preserved magmatic textures and were emplaced obliquely to the main deformation fabric. Type 2 pegmatites were therefore interpreted to be syn-to-late kinematic to $D_2$, and emplaced along typical conjugate strike-slip fracture sets and tension gashes.

The study also highlighted that the rheology of the country rock has a strong control on the potential dimensions of individual pegmatite bodies, which provided an explanation for why pegmatites within the Fort Rixon–Shangani greenstone belt are larger than those in the surrounding (more rheologically competent) granitoid basement.

By comparing the Zulu pegmatite field to other major pegmatite fields globally, shear zones are shown to be a critical component in developing large economic deposits, and can enable migration of pegmatitic melt far from the source region. Constraining the structural history surrounding a pegmatite field is therefore shown to be a highly effective method to identify new greenfield and brownfield targets.

### 6.1.3 Tectonic evolution of the Zimbabwe craton

Chapter 5 presented an integrated geochemical, geochronological, and petrological modelling approach to developing a holistic tectonic evolution model of the Zimbabwe craton and summarised below.

Early cratonic nuclei (Tokwe and Rhodesdale terranes) formed through relatively shallow (<10 kbar) partial melting of an early mafic protocrust as a result of an elevated geothermal gradient. This likely coincided with the formation of the first extrusive ultramafic volcanic succession (the Sebakwian group). Early (felsic) crustal recycling is evidenced by the formation of the c. 3300–3375 Ma Mont D'Or and Mushandike granitoids, as well as the associated intrusive sills found cross-cutting the intrusive basement.

Following a period of relative quiescence and limited continental emergence (forming shelf successions of the Buhwa greenstone belt), A second major TTG-forming event (the Chingezi suite, 3.0–2.85 Ga) possibly resulted from the accretion of the Tokwe and Rhodesdale terranes to form the Sebakwe protocraton, and drove andesitic extrusive volcanism to form the Belingwean group along the western and northern margin of the Tokwe terrane. Crustal thickening during this period is suggested from trace element signatures which overlap with models of deeper (>10 kbar) melting of mafic protocrust and coincided with a major metamorphic event and ductile shearing.

The impingement of a plume at the base of the protocraton initiated a period of major extrusive volcanism, generating the Bulawayan large igneous province that

typifies the majority of central cratonic greenstone belts between 2.75–2.71 Ga. Associated melting of the (still predominantly) mafic lower crust formed the Sesombi TTG suite, though earlier felsic crustal melts were locally mixed to generate a series of more potassic (K/Na $\approx$ 1) intermediate TTGs within this suite.

During a major tectonic event c. 2.68–2.61 Ga, a series of volcanic arcs and oceanic plateaux are proposed to have accreted onto the Sebakwe protocraton along its western margin to form the Western Successions. This generated a mixture of more primitive TTG type magmatism (the Wedza suite), and extensive crustal recycling to form the Chillimanzi and Razi suite by melting both sodic (generating metaluminous granites) and intermediate (generating peraluminous granites) TTGs formed previously. Major shear zones developed, and the Northern Marginal Zone – a deep crustal block of the Zimbabwe craton – was thrust onto the central craton during this event. The Shamvaian group, the major siliciclastic supracrustal succession in the Zimbabwe craton, was deposited into major syntectonic basins during this episode, marking extnesive continental emergence.

Final craton stabilisation was marked by the emplacement of the Great Dyke at 2574 Ma, which likely formed by melting of a depleted mantle source during delamination of part of the lower lithosphere underneath the craton. Late state granitic melts, probably formed by coincident elevated geotherms melting the lower crust, continued to be emplaced until c. 2.51 Ga.

### 6.1.4 Implications for lithium enrichment

The proposed tectonic model for Zimbabwe craton highlights its unique position in testing how LCT/Group 1 pegmatites form, as siliciclastic sedimentary rocks are unrealistic source rocks given their concurrent formation with pegmatites. In this way, the lithium-rich pegmatites in the craton are good evidence to indicate that alternative formation mechanisms must exist.

The tectonic model of the Zimbabwe craton highlights the episodic growth of the craton, and indicates felsic crustal recycling initiated early in the cratonic history. Modelling of these recycling events suggest that three to four crustal melting events is sufficient to generate highly peraluminous melts with economic concentrations of lithium. Importantly, this implies that recycling, which can either occur through erosion and sedimentation, or repeated partial melting, is the key factor required to generate lithium-rich melts, obviating the assumed requirement of sedimentary material in the source.

Put differently, the presence of abundant hard rock lithium deposits in the Archean suggests that the enrichment mechanisms driving lithium enrichment must have been active early in Earth history. If sedimentary recycling is a necessary component for LCT/Group 1 pegmatites, we should expect to see major pegmatite deposits later in Earth history as sedimentary processes become more effective (e.g., Bucholz, 2022; Bucholz and Hernández-Montenegro, 2025). The propensity for major hard rock lithium deposits to be Archean in age suggests partial melting, rather than sedimentary recycling, is a more efficient lithium enrichment mechanism. Only in post-Archean terranes which rework significant components of Archean crust, such as the Dete–Kamativi inlier in Zimbabwe (Shaw et al., 2022) or the Kibaran belt (Dewaele et al., 2016) during later orogenic events do we see significant lithium deposits post-Archean.

### 6.1.5 Implications for exploration

The conclusions made above have several key implications for exploration for new lithium deposits. First, desktop studies should not focus on constraining potential sources, as regional structures place a more significant control on the distribution pegmatite fields. Second, transcurrent shear zones are very effective at extracting, vertically migrating, and subsequently emplacing pegmatitic melts, and should therefore be targeted. Finally, Archean terranes, or terranes which significantly rework Archean protoliths, are most likely to host major lithium deposits.

### 6.1.6 Summary

In summary, this thesis has shown: 1) Whilst pegmatites can form through both anatexis and granitic fractionation, a simple single-stage model is unlikely to account for the necessary enrichment required to generate economic hard rock lithium deposits, 2) The Zimbabwe craton grew through episodic periods of growth through various geodynamic mechanisms, and repeated melting events provided a mechanism by which to progressively enrich a source region in lithium through the formation of intermediate-stage TTGs, 3) The absence of siliciclastic sedimentary sources for lithium pegmatites in Zimbabwe, and the feasibility of a melt-driven recycling mechanism implies sedimentary sources are not an essential component of LCT/Group 1 pegmatites, and 4) From an exploration perspective, a focus should therefore be put on delineating structural corridors across Archean or reworked Archean terranes which may have enabled pegmatitic melt migration and emplacement.

## 6.2 Future Work

The results of this thesis present several exciting avenues for further research, some of which are highlighted below.

### 6.2.1 Archean evolution of Zimbabwe

Whilst Chapter 5 presents a reasonable attempt at synthesizing the complex geological history of the Zimbabwe craton, several questions remain and would benefit from further work:

- The recognition of Archean protoliths in the Dete–Kamativi inlier (Glynn et al., 2020) presents an interesting opportunity to test the accretion model for the Western Succession. If the Western Succession is allochtonous, then the Dete–Kamativi block could present the cratonic block which, upon collision with the Sebakwe protocraton, marked the closure of an Archean ocean. Further geochronological and isotopic studies on the Dete–Kamativi block to determine whether it evolved independently to the rest of the Zimbabwe craton is highly recommended.
- Additional structural studies on the Midlands and Bulawayo greenstone belts will help better unravel the complex history of the Western Succession, and better delineate the potential geometries of accretion.
- Our understanding of the evolution of the Zimbabwe craton as a whole will benefit from significantly more coupled geochemical and geochronological analyses of samples across the craton, and extending the database towards Botswana and towards the north-east extent of the craton will help potentially delineate other early protocratonic blocks.

### 6.2.2 Testing source models

Since the publication of Chapter 3 (as Koopmans et al., 2024), several researchers have proposed areas in which the multi-stage mechanism appears to have formed lithium pegmatites. Additional studies are needed to further test and refine our understanding of the exact source requirements for economic lithium pegmatites.

- Modelling of lithium during anatexis will benefit from additional experimental work to better constrain the partition coefficients for lithium across $P-T$ space, and may reveal additional caveats to the presented source models.

- Further field based studies in terranes which expose a larger cross-section of the crust, in order to capture both the source and trap, are recommended to validate the proposed source models.
- Delineating source models would benefit from developing a technique by which to differentiate the various proposed processes. Whilst the source mechanisms proposed result in comparable geochemical signatures, isotopic fractionation may differ, and thus may prove a fruitful avenue for future research.

### 6.2.3 Refining structural model

Detailed structural studies around economic pegmatite fields remain sparse. Our understanding of the structural controls of pegmatite systems would greatly benefit from additional field-based investigations, which may reveal additional factors which will help delineate new exploration targets.

## 6.3 The lithium mineral system model

Whilst this thesis has contributed to a solid foundation for developing a robust mineral system model for hard rock lithium deposits, it is evident more work is needed. At present, the following simple model can be proposed: for the source, the key component appears to be a sufficiently recycled felsic crust, with or without sedimentary processes to drive recycling. Whilst precise mechanisms for how to generate the necessary lithium enrichment have been proposed, these will need to be tested and validated in field-based studies. For the migration and trap, (transcurrent) crustal-scale shear zones appear to be pivotal in initial extraction, migration, and subsequent emplacement of the pegmatitic melt to form large intrusions. Further structural studies on additional pegmatite fields may shed light on additional structural controls which promote the formation of large pegmatitic bodies. Post emplacement, mechanisms must be present to promote late-stage metasomatic fluid migration so as to minimise the effects of albitisation and greisenisation (Goodenough et al., 2025), preserving the magmatic lithium ore-forming minerals for subsequent extraction. The exact controls on what promotes fluid expulsion remains elusive (Sweetapple et al., 2024).

Finding new lithium deposits is critical to meet and supply the growing demand for lithium, therefore detailed geological research to refine the mineral system model remains vital to realize a renewable-based future.

# Appendix A

# List of sample locations

The following tables list and describe the samples that have been referenced in Chapter 5.

# A.1 Surface samples

| Sample | UTM | X | Y | Rock suite | Description |
|---|---|---|---|---|---|
| BL005 | WGS84, 36S | 201758 | 7735901 | Chillimanzi | 30-35% qz, 30-35% ksp (tartan twinning, perthitic), 15-20% plg, 5-10% bt, 5% mu. |
| BL017 | WGS84, 36S | 187143 | 7755960 | Chillimanzi | 30-35% qz, 20-25% ksp, 30-35% plg, 5% bt, <5% mu. |
| CH001 | WGS84, 35S | 849026 | 7778164 | Chillimanzi | 30-35% qz, 25-30% kps (perthitic), 20-25% plg, 5-10% bt, <5% mu. |
| DP01 | WGS84, 35S | 754025 | 7778901 | Chillimanzi | 30-35% qz (undulose extinction), 25-30% ksp (partly sericitised), 20-25% plg (sericitised), 5-10% bt (fabric defining), 5% mu. |
| GH002 | WGS84, 35S | 805135 | 7819670 | Chillimanzi | 40-45% qz, 15-20% ksp (partly sericitised), 25-30% plg (partly sericitised), 5-15% bt (fabric defining), <5% chl (replacing bt). |
| GH003 | WGS84, 35S | 807590 | 7821208 | Chillimanzi | 30-35% qz, 25-30% ksp (perthitic), 20-25% plg, 5-10% bt, <5% tit, <5% opq. |
| GW001 | WGS84, 35S | 801104 | 7811636 | Sesombi | <5% qz, 25-30% plg (partly sericitised), 65-70% amph. |
| GW002 | WGS84, 35S | 801104 | 7811636 | Sesombi | 25-30% qz, 30-35% plg (partly sericitised), 20% amph (fabric defining), 15-20% bt (fabric defining), <5% tit, <5% zrc. |
| GW003 | WGS84, 35S | 801104 | 7811636 | Chillimanzi | 40-45% qz, 35-40% plg (partly sericitised), 5-10% bt (fabric defining), 5% opq, <5% grt. |
| GW004 | WGS84, 35S | 801104 | 7811636 | Sesombi | 30-35% qz, 35-40% plg (partly sericitised), 15-20% bt, 5% tit, <5% opq, |
| GW006 | WGS84, 35S | 801104 | 7811636 | Sesombi | 30-35% qz, 40-45% plg (partly sericitised), 10-15% amph, 5-10% bt, |
| LP002 | WGS84, 36S | 285702 | 7748398 | Chillimanzi | 30-35% qz, 25-30% ksp, 25-30% plg, 5% bt, <5% opq. |
| LP003 | WGS84, 36S | 289653 | 7736345 | Chillimanzi | 30% qz, 25-30% ksp, 20-25% plg, 10-15% bt, <5% opq. |
| LP004 | WGS84, 36S | 289542 | 7736329 | Razi | 30% qz, 20% ksp (tartan twinning), 15-20% plg (partly sericitised), 15-20% bt (fabric defining), 10-15% amph (fabric defining), 5% tit. |
| LP010 | WGS84, 36S | 3144489 | 7718183 | NMZ | 20% qz, 15% ksp (partly sericitised), 30-40% plg (partly sericitised), 5-10% bt (fabric defining), 5% grt. |
| LP011 | WGS84, 36S | 314501 | 7718207 | NMZ | 30% qz, 5-10% ksp (partly sericitised), 25-30% plg (partly sericitised), 25-30% bt (fabric defining, partly altered to chl+mt), 5% grt, <5% opq. |
| MA001 A+B | WGS84, 36S | 218729 | 7783769 | Chingezi | 35-40% qz, 5% ksp (occasionally phenocrystic), 40-45% plg (sericitised), <5% bt, <5% chl (replacmeent) <5% opq. |
| MO01 | WGS84, 36S | 403329 | 7785110 | Bulawayan | 80-85% qz, <5% plg, 5-10% bt, 5% amph. |
| MO03 | WGS84, 36S | 403329 | 7785110 | Bulawayan | 70-75% cpx, 10-15% plg, 10-15% amph. |
| MO04 | WGS84, 36S | 403329 | 7785120 | Bulawayan | <5% qz, 20-25% plg, 55-60% trm, 10-15% chl, 5% chr, 5% opq. |
| MO05 | WGS84, 36S | 403329 | 7785137 | Bulawayan | 5-10% qz, 60-65% clc, 25-30% chl, 5-10% opq. |
| MU001 A+B | WGS84, 35S | 886715 | 7797507 | Tokwe | 20-25% qz, 50-55% plg, 10-15% bt, 5% opq. |
| MU003 | WGS84, 35S | 886715 | 7797507 | Tokwe | 35-40% qz (some polycrystalline), 40-45% plg (sericitised, some porphyroblastic), 10-15% bt (fabric defining), <5% gt, <5% opq. |
| NG01 | WGS84, 35S | 743951 | 7792632 | Chillimanzi | 40% qz, 20-25% ksp, 25-30% plg (partly sericitised), 5% bt (partly chloritised), 5% mu, <5% opq. |
| NG02 | WGS84, 35S | 751515 | 7784631 | Chillimanzi | 35-40% qz, 20-25% ksp, 30-35% plg (partly sericitised), <5% bt (partly chloritised), 5% mu, <5% opq. |
| NM002 | WGS84, 35S | 799792 | 7819146 | Chillimanzi | 25-30% qz, 20-25% ksp (partly sericitised, oscillatory zoning preserved), 30-35% plg (partly sericitised), 15-20% bt (defining weak fabric), <5% chl (replacing bt), <5% opq. |
| NM003A+B | WGS84, 35S | 799783 | 7819130 | Amphibolite | 5% qz, 10% plg, 75% amph (fabric defining), 5% altered grt (to opq+amp+qz). |
| NY01 | WGS84, 36S | 379519 | 7870697 | Chillimanzi | 25-30% qz, 30% ksp (partly sericitised), 25-30% plg (sericitised), 5% chlorite, <5% bt (relict), <5% opq. |
| NY02 | WGS84, 36S | 380107 | 7865946 | Chillimanzi | 35-40% qz, 30% ksp (tartan twinning), 20-25% plg (partly sericitised), 5% bt, <5% mu, <5% opq. |
| NY03 | WGS84, 36S | 376339 | 7877660 | Chillimanzi | 25-30% qz, 20-25% ksp (oscillatory zoning, partly sericitised), 15-20% plg (partly sericitised), 5-10% bt (fabric defining), 5% mu (fabric defining), 5% opq. |
| PG01 | WGS84, 35S | 765196 | 7778059 | Chillimanzi | 30-35% qz, 30-40% ksp (megacrystic (<5cm), tartan twinning, oscillatory zoning), 15-20% plg, 5% bt, 5% mu, <5% opq. |
| SC003 A+B+C | WGS84, 35S | 802312 | 7794971 | Sesombi | 20-25% qz, 35-40% plg, 20-25% amph (fabric defining), 10-15% bt (fabric defining), <5% opq. |
| SC004 | WGS84, 35S | 802312 | 7794971 | Chillimanzi | 30-35% qz, 25-30% ksp (sericitised), 30-35% plg (sericitised), <5% bt. |
| SG01 | WGS84, 36S | 201881 | 7759606 | Chingezi | 30-35% qz, <5% ksp, 15-20% plg, 20-30% bt (fabric defining), 5% chl, 5% zrc, <5% opq. |
| SG02 | WGS84, 36S | 201881 | 7759606 | Chingezi | 30-35% qz, <5% ksp, 25-30% plg, 15-20% bt (fabric defining), 5% mu, <5% tit, 5% opq. |
| SR01 | WGS84, 36S | 394943 | 7881998 | Wedza | 30% qz, 15-20% ksp, 30-35% plg, 10% bt (fabric defining), 5% amph, <5% chl, <5% opq. |
| SR02 | WGS84, 36S | 395955 | 7881592 | Wedza | 30% qz, 10-15% ksp, 25-30% plg, 20-25% bt (fabric defining), <5% chl, 5% tit, 5% opq. |
| TR002 | WGS84, 35S | 856534 | 7781890 | Tokwe | 25-30% qz, 20-25% plg (partly sericitised), 40-45% amph (fabric defining), <5% opq. |
| TR004 | WGS84, 35S | 856534 | 7781890 | Tokwe | 30-35% qz, 25-30% plg (partly sericitised), 35-40% amph (fabric defining), <5% opq. |
| TR006 | WGS84, 35S | 856534 | 7781890 | Tokwe | 30-35% qz, 45-50% plg (partly sericitised), 10-15% bt (fabric defining), 5% chl, <5% opq. |
| TR007 | WGS84, 35S | 856505 | 7781948 | Tokwe | 20-25% qz, 5% ksp, 25-30% plg, 35-40% mu, 5-10% gt, <5% opq. |

Continued on next page

| Sample | UTM | X | Y | Rock suite | Description |
|---|---|---|---|---|---|
| TR008 | WGS84, 35S | 856505 | 7781948 | Tokwe | 25-30% qz, 25-30% plg (partly sericitised), 35-40% amph (fabric defining), <5% opq. |
| WG01 | WGS84, 36S | 377196 | 7871516 | Amphibolite | 90% amph (fabric defining), 5% opq, <5% plg, <5% qz. |
| WG02 | WGS84, 36S | 377196 | 7871516 | Wedza | 25-30% qz, 5-15% ksp, 25-30% plg (partly sericitised), 20% amph, 5-10% bt, <5% opq. |
| WG03 | WGS84, 36S | 377203 | 7871429 | Wedza | 25-30% qz, 5-10% ksp. 25-30% plg (partly sericitised), 5-10% bt, 20-25% chl (fabric defining), <5% opq. |
| ZB01 | WGS84, 35S | 756648 | 7774436 | Sesombi | 35-40% qz (some polycrystalline), <5% ksp, 30-35% plg (partly sericitised), 10-15% bt, 5-10% opq. |
| ZB02 | WGS84, 35S | 757278 | 7772204 | Sesombi | 40-45% qz (some polycrystalline), <5% ksp, 35-40% plg (partly sericitised), 5-10% bt (fabric defining), 5% opq. |
| ZB03 | WGS84, 35S | 752669 | 7770703 | Sesombi | 15-20% qz, 25-30% plg, 30-35% amph (fabric defining), 15-20% chl (fabric defining). |
| ZB04 | WGS84, 35S | 757629 | 7771363 | Sesombi | 30-35% qz, 35-40% plg (partly sericitised), 15-20% bt, 5% tit, <5% opq. |
| ZB05 | WGS84, 35S | 753762 | 7767205 | Chillimanzi | 30-35% qz (undulose extinction), 25-30% ksp (partly sericitised, megacrystic), 20-25% plg (sericitised), 5-10% bt (fabric defining), <5% chl (replacing bt). |
| ZB06 | WGS84, 35S | 747776 | 7769137 | Sesombi | 35-40% qz (undulose extinction), <5% ksp (partly sericitised), 25-30% plg (partly sericitised), 10-15% bt (fabric defining), 5-10% chl (fabric defining, replacing bt), <5% opq. |
| ZB07 | WGS84, 35S | 747441 | 7770096 | Chillimanzi | 40-45% qz, 20-25% ksp (partly sericitised, perthitic), 15-20% plg (partly sericitised), 10% bt (weak fabric defining), 5% mu (weak fabric defining). |
| ZL01 | WGS84, 35S | 751318 | 7780779 | Belingwean | 20-25% qz, 55-60% plg, 5-10% bt (fabric defining), 5-10% amph (fabric defining), <5% opq. |
| ZL09 | WGS84, 35S | 751007 | 7784869 | Bulawayan | <5% qz, 10-15% plg, 70-75% trm, <5% chl, <5% chr. |
| ZL11 | WGS84, 35S | 750368 | 7782271 | Bulawayan | <5% qz, 15-20% plg, 65-70% trm, 5%chl, <5% opq. |
| ZL15 | WGS84, 35S | 751065 | 7783893 | Bulawayan | 10-15% qz, 30-35% plg, 5-10% chl, 35-40% talc, <5% opq. |
| ZL16 | WGS84, 35S | 750515 | 7784006 | Bulawayan | <5% qz, 15-20% plg, 50-55% trm, 20-25% chl, <5% opq. |
| ZL20 | WGS84, 35S | 751072 | 7782166 | Bulawayan | <5% qz, 15-20% plg, 60-65% trm, 10-15% chl (defining shear bands), <5% chr. |

## A.2 Drill core samples

Core samples are collected from core drilled by Premier African Minerals around their Zulu project.

| Sample | Rock suite | Core | UTM | Hole X | Hole Y | Depth | Description |
|---|---|---|---|---|---|---|---|
| ZLC06 | Chillimanzi | ZDD18 | WGS84, 35S | 751222 | 7784390 | 100.68 - 100.87 | 30-35% qz, 25-30%ksp (tartan twinning), 20-25% plg (partly sericitised), 10-15% bt (partially replaced with clay), 5% mu. |
| ZLC07 | Chillimanzi | ZDD18 | WGS84, 35S | 751222 | 7784390 | 102.17 - 102.33 | 25-30% qz, 30-35% ksp (tartan twinning, perthitic), 25-30% plg (partly sericitised), <5% bt, 5% mu. |
| ZLC15 | Belingwean | ZDD64 | WGS84, 35S | 751792 | 7783148 | 63.63 - 63.80 | 35-40% qz, 30-35% plg (partly sericitised), 15-20% amph (fabric defining),<5% bt (fabric defining), 5-10% tit. |
| ZLC17/15 | Belingwean | ZDD64 | WGS84, 35S | 751792 | 7783148 | 85.20 - 85.40 | 20-25% qz, 30-35% plg (partly sericitised), 20-25% amph (fabric defining), 15-20% tit. Melt lens in ZLC15. |
| ZLC20 | Belingwean | ZDD64 | WGS84, 35S | 751792 | 7783148 | 106.57 - 106.67 | 35-40% qz, 30-35% plg (partly sericitised), 20-25% amph (fabric defining), 5-10% tit. |
| ZLC32 | Bulawayan | ZDD142 | WGS84, 35S | 751346 | 7784116 | 159.10 - 159.23 | 5% qz, 20-25% plg, 65-70% trm (fabric defining), 5% tit. |
| ZLD01 | Chillimanzi | ZDD65 | WGS84, 35S | 751889 | 7782800 | 175.60 - 175.80 | 30-35% qz, 15-20% ksp, 30-35% plg (partly sericitised), 10-15% bt, <5% mu. |
| ZLD02 | Chillimanzi | ZDD65 | WGS84, 35S | 751889 | 7782800 | 130.10 - 130.25 | 35-40% qz, 15-20% ksp, 25-30% plg (partly sericitised), 10-15% bt (fabric defining), <5% mu. |
| ZLD03 | Bulawayan | ZDD89 | WGS84, 35S | 751373 | 7783468 | 186.52 - 186.62 | 10% plg, 70-75% serp (atg), 10% cc, 5-10% mt. |
| ZLD05 | Bulawayan | ZDD136 | WGS84, 35S | 751099 | 7782841 | 336.75 - 336.85 | <5% plg, 40-45% serp, 25-30% tlc (rhombic, fabric defining), <5% trm, 5-15% mt, <5% pyr. |
| ZLD06 | Belingwean | MDGT06 | WGS84, 35S | 751070 | 7782109 | 32.43 - 32.53 | 35-40% qz, 30-35% plg (partly sericitised), 10-15% bt (fabric defining), 20-25% chl (fabric defining), 5% gt, <5% opq. Metasomatically altered by nearby pegmatite, protolith equivalent to ZLC15 |
| ZLD07 | Belingwean | ZDD122 | WGS84, 35S | 751128 | 7782511 | 104.20 - 104.30 | 30-35% qz, 35-40% plg (partly sericitised), 15-20% amph, 5-10% bt, <5% tit. |
| ZLD08 | Bulawayan | ZDD102 | WGS84, 35S | 750930 | 7782260 | 50.05 - 50.15 | <5% plg, 65-70% serp (atg dominant), 5% tlc, 15-20% cc, 5-10% mt. |
| ZU06 | Bulawayan | ZDD134 | WGS84, 35S | 750825 | 7781918 | 205.0 - 205.12 | 40-45% qz, 30-35%plg (matrix), 5% plg (phenocrystic), 10-15% bt (fabric defining), <5% chl (replacement of bt). |

# Appendix B

# Field photgraphs of sample locations

The following images are of sample localities that have been referenced in this study in Chapter 5, and described in Appendix A. Where multiple samples were collected in close proximity, the sampled lithologies are labelled.

Figure B.1: Locality BL17, a quarry north of Zvishavane along the Zvishavane – Gweru road.

Figure B.2: Locality CH01, A small granite plug between Masvingo and Zvishavane.

Figure B.3: Locality DP01, sampled near the Deep Purple deposit east of the Fort Rixon – Shangani belt.

Figure B.4: Locality GH02, sampled from a small plug along a side road between Gwenoro dam and Shurugwi.

Figure B.5: Locality GH03, sampled from a small plug east of GH02.

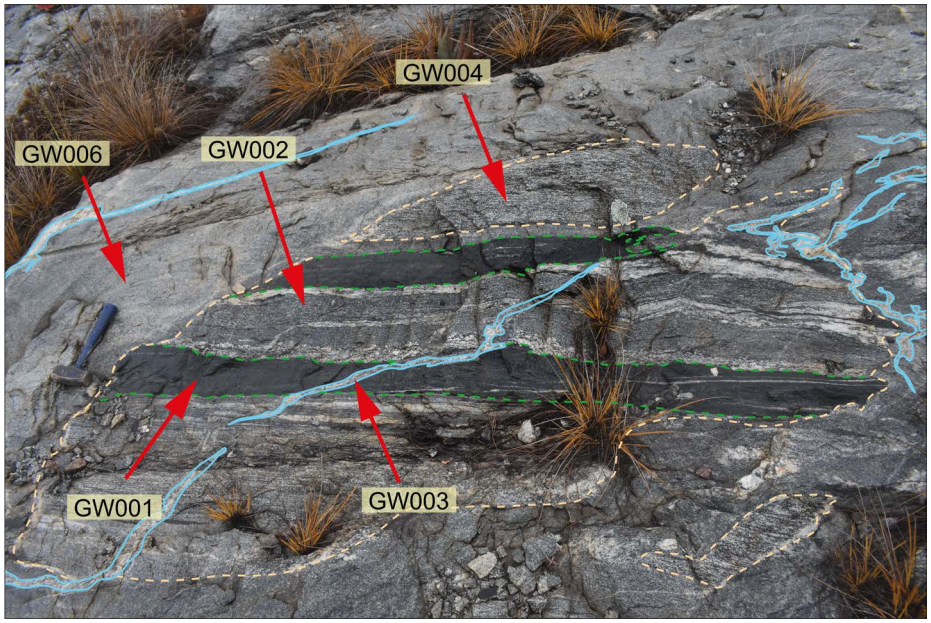


Figure B.6: Gwenoro dam (GW) locality, along the western flank of the Gwenoro Dam spillway.

Figure B.7: Locality LP02, collected south of the Masvingo greenstone belt along the road to Renco.

Figure B.8: Locality LP03, collected south of LP02.

Figure B.9: Locality LP04, collected further south of LP03 along the Renco road.

Figure B.10: Locality LP10, in dry river bed east of Renco.

Figure B.11: Locality LP11, in a dry river bed east of Renco.

Figure B.12: Trench from which MO01-5 were collected, trenched by Li3 in the Odzi greenstone belt.

Figure B.13: Locality MU01, a dry river bed c. 20 km north of Masvingo along the Masvingo – Mvume road.

Figure B.14: Locality MU03, a dry river bed c. 20 km north of Masvingo along the Masvingo – Mvume road.

Figure B.15: Locality NG01, an exposure of the Nalatale granite along the Perlycross road north of Fort Rixon.

Figure B.16: Locality NG02, an exposure of the Nalatale granite in a quarry north of the Zulu mine.

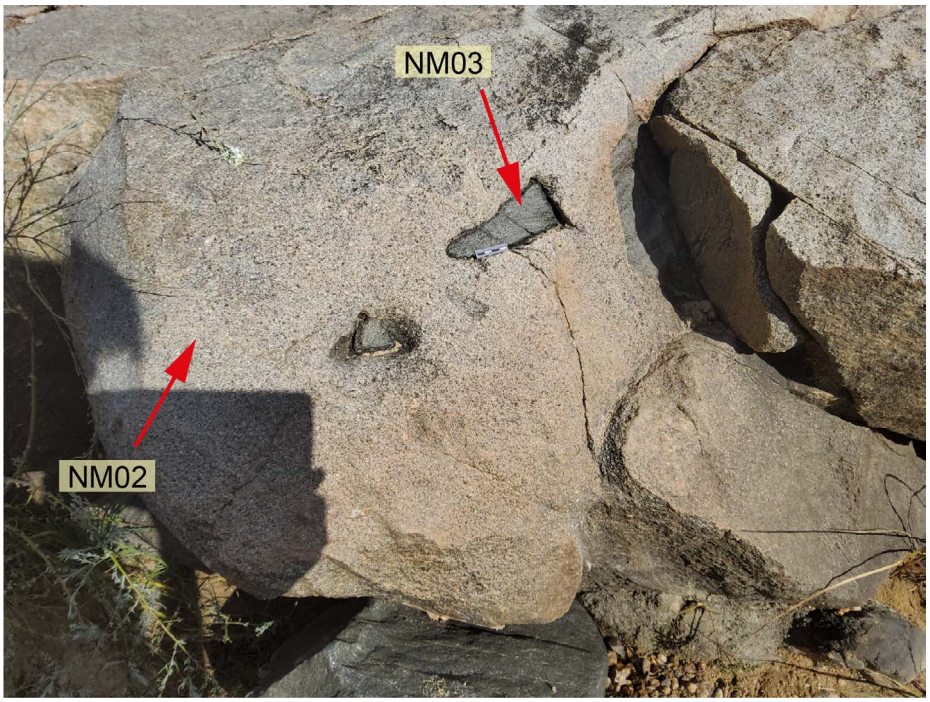


Figure B.17: Locality of NM samples, along the Nyamaziva river at the norther end of Gwenoro dam.

Figure B.18: Locality NY01, a granitic plug south of Nyashanu.

Figure B.19: Locality NY02, a granitic plug north of Nyashanu.

Figure B.20: Locality NY03, a granitic plug north of Nyashanu.

Figure B.21: Locality PG01, a large granite koppie east of the Fort Rixon – Shangani greenstone belt.

Figure B.22: Locality SC03, a dry river bed along the Mapongokwe river south of Gwenoro dam.

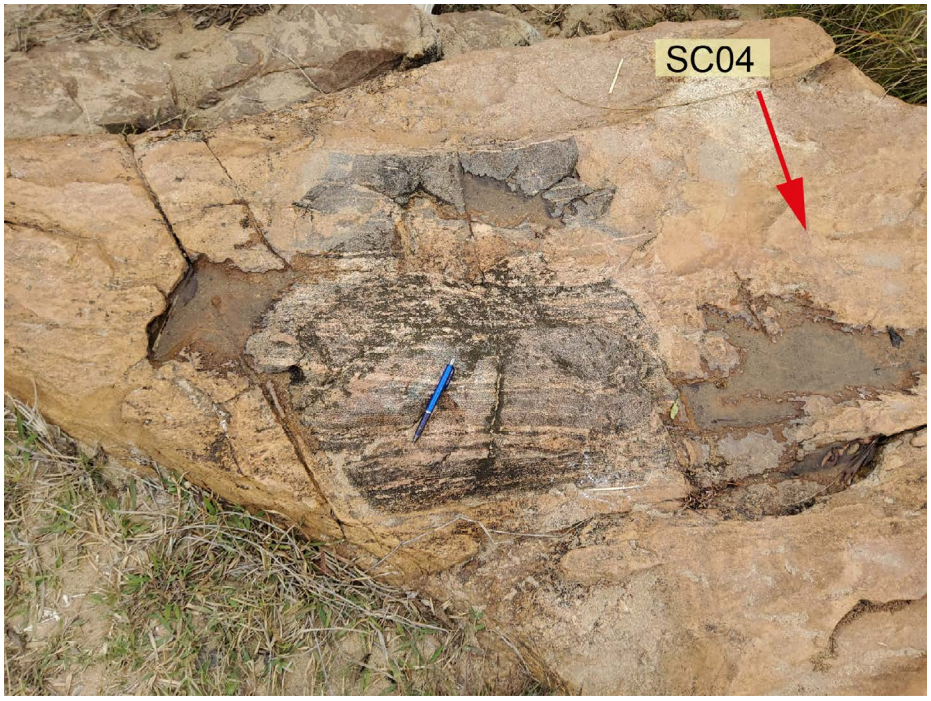


Figure B.23: Locality SC04, a dry river bed along the Mapongokwe river, west of SC03.

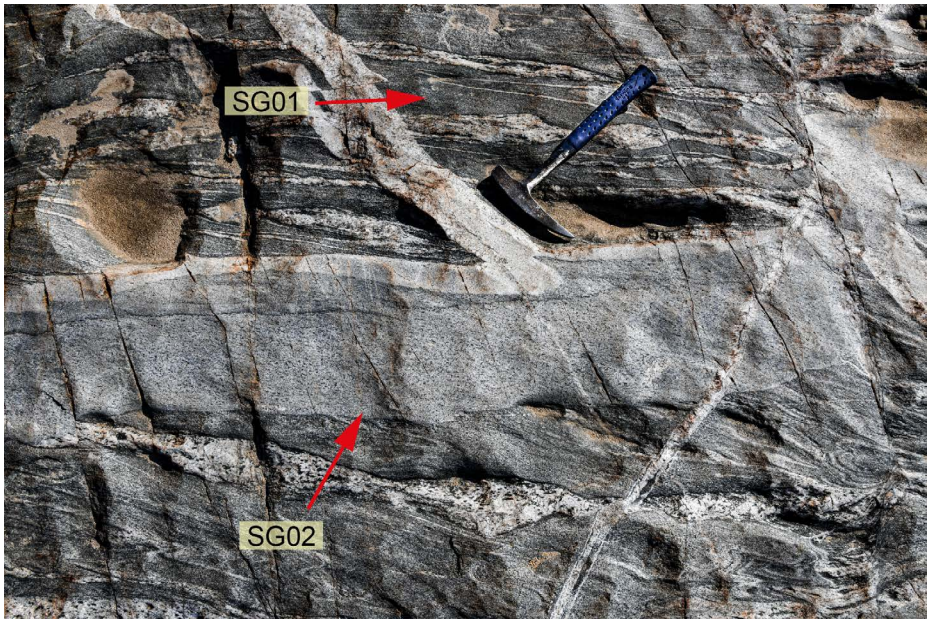


Figure B.24: Locality for SG samples, A dried river bed of the Runde river north of the Zvishavane – Masvingo road.

Figure B.25: Locality SR01, an outcrop along a dried river bed of the Save river where it crosscuts the Odzi greenstone belt.

Figure B.26: Locality SR02, an outcrop southeast of SR01 along a dried river bed of the Save river where it crosscuts the Odzi greenstone belt.

Figure B.27: Locality TR02, an outcrop along the Tokwe river north of the Zvishavane – Masvingo road.

Figure B.28: Locality TR04, sampled near TR02.

Figure B.29: Locality TR06, sampled near TR02.

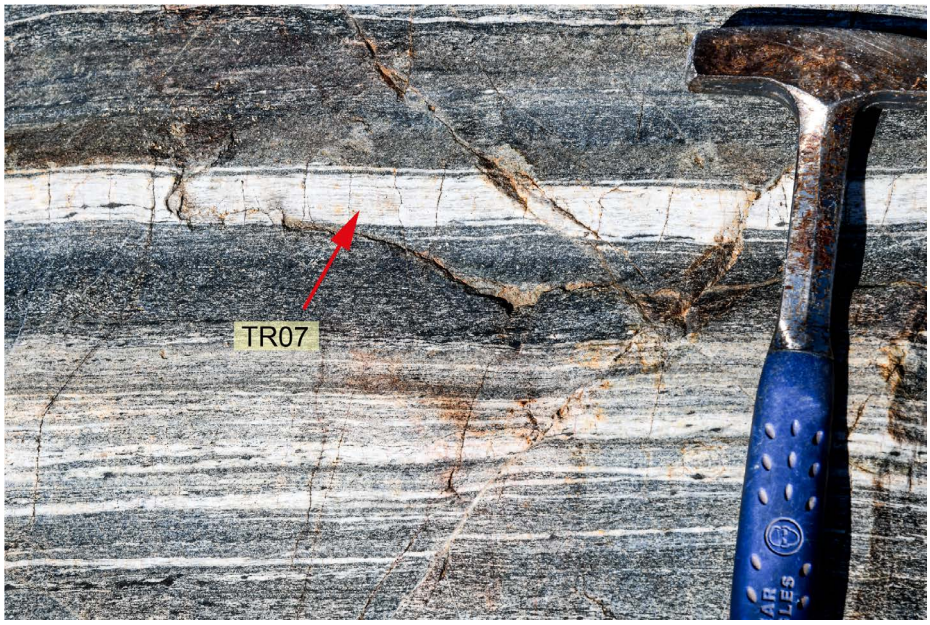


Figure B.30: Locality TR07, sampled near TR02.

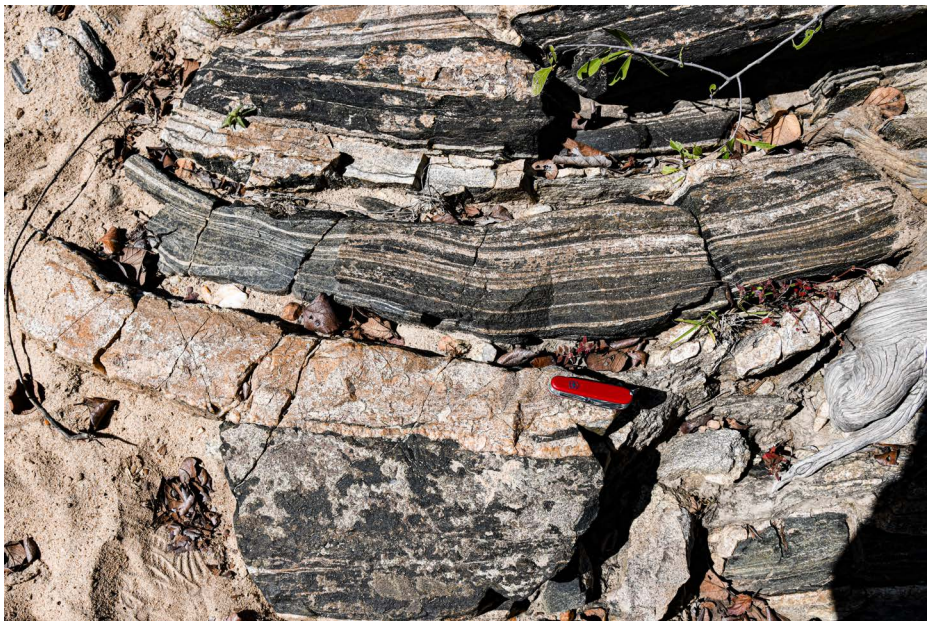

Figure B.31: Locality TR08, sampled near TR02.

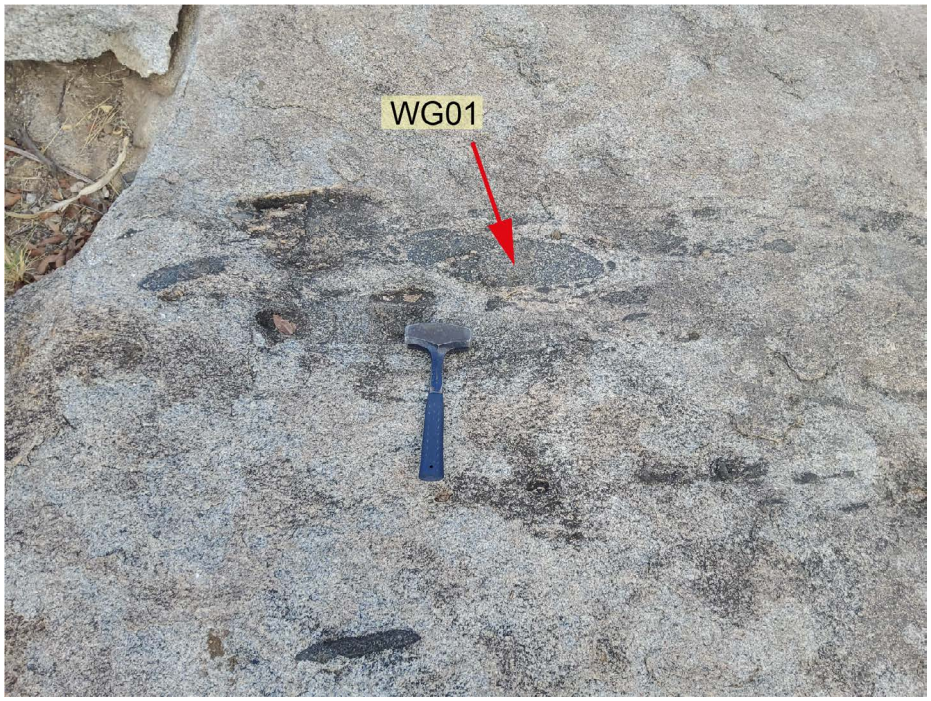


Figure B.32: Locality WG01, an outcrop along the bank of the Murove river.

Figure B.33: Locality WG02, sampled near WG01.

Figure B.34: Locality WG03, sampled 100 m south of WG01 along the Murove river.

Figure B.35: Locality ZB01, an outcropping hill east of the Fort Rixon – Shangani greenstone belt.

Figure B.36: Locality ZB02, an outcropping hill east of the Fort Rixon – Shangani greenstone belt.

Figure B.37: Locality ZB03, a small outcrop in a river bank of the Machakwe river, east of the Fort Rixon – Shangani greenstone belt.

Figure B.38: Locality ZB04, an outcrop along the south-eastern margin of the Fort Rixon – Shangani greenstone belt.

Figure B.39: Locality ZB05, a washed outcrop in the Three Fingers ranch.

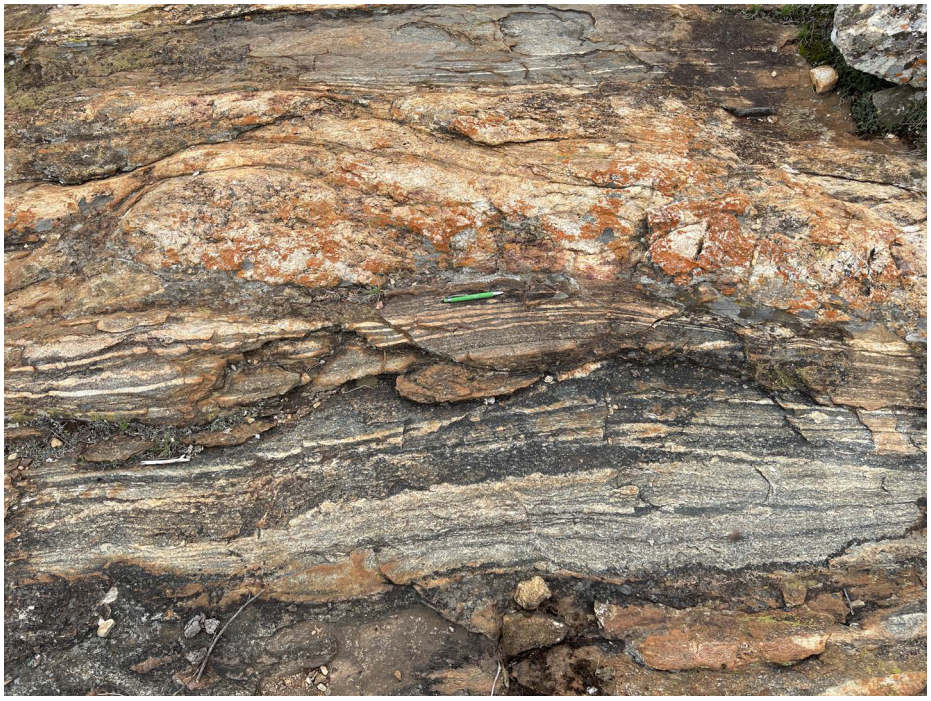

Figure B.40: Locality ZB06, a washed oucrop along the eastern margin of the Fort Rixon – Shangani greenstone belt.


Figure B.41: Locality ZB07, an outcrop 5 km west of the Three Fingers ranch..

Figure B.42: Locality ZL01, a small outcrop within the Machakwe river south of the Zulu mine.

Figure B.43: Locality ZL09, a row of outcrops west of the Zulu mine.

Figure B.44: Locality ZL11, a row of outcrops west of the Zulu mine.

Figure B.45: Locality ZL15, a small patchy outcrop north of the Zulu mine, west of the dam road.

Figure B.46: Locality ZL16, a row of outcrops west of the Zulu mine offices.

Figure B.47: Locality ZL20, a row of outcrops north of the Zulu mine offices.

# Appendix C

# Geochronological data

# C.1 Zircon U-Pb data

| Sample | Spot name | Run | 206/238 | ±2SE | 207/235 | ±2SE | 207/206 | ±2SE | 238/P206 | ±2SE | 206/238 Age | ±2SE | 207/235 Age | ±2SE | 207/206 Age | ±2SE | U/Th | U | Th | Pb |
|---|---|---|---|---|---|---|---|---|---|---|---|---|---|---|---|---|---|---|---|---|
| BL05 | 1 | 4 | 0.07177 | 0.002083 | 2.351663 | 0.112161 | 0.236224 | 0.008098 | 13.944911 | 0.414437 | 446.8 | 12.5 | 1224.1 | 33.5 | 3087 | 54 | 2.5 | 3548 | 1409 | 1551 |
| | 2 | 4 | 0.184585 | 0.007148 | 5.16113 | 0.183013 | 0.202555 | 0.00412 | 5.456537 | 0.220001 | 1091.3 | 39 | 1843.9 | 30.3 | 2845.6 | 33.3 | 2.63 | 1585 | 593 | 558 |
| | 3 | 4 | 0.398949 | 0.016941 | 14.712965 | 0.514466 | 0.269873 | 0.006959 | 2.509665 | 0.106684 | 2163.4 | 78 | 2796.1 | 33.3 | 3303.9 | 40.2 | 1.22 | 623 | 499 | 794 |
| | 4 | 4 | 0.195085 | 0.006423 | 4.674774 | 0.132906 | 0.172814 | 0.0037 | 5.138679 | 0.169799 | 1148.5 | 34.6 | 1762 | 23.5 | 2583.3 | 36 | 2.17 | 1089 | 500 | 449 |
| | 5 | 4 | 0.224867 | 0.007015 | 5.784036 | 0.1709 | 0.186426 | 0.004096 | 4.451857 | 0.134215 | 1307.2 | 36.8 | 1943 | 25.8 | 2708.9 | 35.8 | 1.86 | 1089 | 574 | 530 |
| | 6 | 4 | 0.329597 | 0.01114 | 10.412337 | 0.326099 | 0.229112 | 0.004961 | 3.041418 | 0.099955 | 1835.4 | 53.8 | 2470.6 | 28.9 | 3044.1 | 34.4 | 1.65 | 924 | 548 | 762 |
| | 7 | 4 | 0.633414 | 0.017039 | 23.812648 | 0.643508 | 0.272469 | 0.005455 | 1.576269 | 0.043334 | 3162.6 | 67.5 | 3260.1 | 26.6 | 3319.2 | 31.3 | 1.42 | 242 | 167 | 311 |
| | 8 | 4 | 0.623955 | 0.01727 | 23.527376 | 0.709447 | 0.272334 | 0.005687 | 1.600495 | 0.043558 | 3125 | 68.3 | 3247.6 | 28.7 | 3318.1 | 32.8 | 1.46 | 223 | 150 | 287 |
| | 9 | 4 | 0.655101 | 0.019479 | 24.739397 | 0.74198 | 0.275059 | 0.006301 | 1.525147 | 0.04616 | 3247.1 | 76.1 | 3296.9 | 29.3 | 3333.3 | 36.2 | 1.43 | 123 | 85 | 148 |
| | 10 | 4 | 0.238478 | 0.009673 | 7.321275 | 0.335262 | 0.222679 | 0.004897 | 4.222979 | 0.173697 | 1377.6 | 50.4 | 2145.8 | 40.9 | 2998.3 | 35 | 2.39 | 931 | 395 | 489 |
| | 11 | 4 | 0.347208 | 0.010375 | 11.167332 | 0.400983 | 0.237212 | 0.005781 | 2.887283 | 0.08721 | 1920.8 | 49.7 | 2534.7 | 33.8 | 3098.8 | 39 | 1.54 | 328 | 218 | 344 |
| | 13 | 4 | 0.484458 | 0.016269 | 17.607646 | 0.617011 | 0.272098 | 0.006821 | 2.07193 | 0.071147 | 2545.8 | 70.9 | 2967.1 | 34.3 | 3316.3 | 39.3 | 1.94 | 238 | 125 | 265 |
| | 14 | 4 | 0.67806 | 0.018686 | 24.442413 | 0.626442 | 0.269525 | 0.005575 | 1.4794 | 0.041512 | 3336.2 | 72 | 3285.9 | 25 | 3301.9 | 32.4 | 1.83 | 343 | 192 | 372 |
| | 15 | 4 | 0.278158 | 0.008277 | 6.867361 | 0.242264 | 0.182593 | 0.003929 | 3.609192 | 0.109428 | 1581.8 | 41.8 | 2092.7 | 30.8 | 2675 | 35.8 | 2.91 | 1014 | 391 | 324 |
| | 16 | 4 | 0.174652 | 0.006054 | 6.719375 | 0.226496 | 0.285917 | 0.006261 | 5.750149 | 0.199825 | 1037.5 | 33.2 | 2074.4 | 29.7 | 3394.4 | 33.9 | 2 | 2296 | 1147 | 960 |
| | 17 | 4 | 0.285075 | 0.008652 | 7.700236 | 0.218811 | 0.20173 | 0.004182 | 3.524834 | 0.108623 | 1616.4 | 43.4 | 2195.8 | 25.3 | 2838.8 | 33.7 | 1.94 | 871 | 459 | 549 |
| | 18 | 4 | 0.309789 | 0.009106 | 8.823579 | 0.294415 | 0.212067 | 0.004523 | 3.240661 | 0.098928 | 1739.2 | 45 | 2317.8 | 31.7 | 2919.7 | 34.6 | 1.88 | 967 | 515 | 505 |
| | 19 | 4 | 0.393535 | 0.011102 | 13.000769 | 0.371692 | 0.245638 | 0.00519 | 2.547302 | 0.071723 | 2138.7 | 51.3 | 2678.8 | 27 | 3155.3 | 33.4 | 3.63 | 371 | 105 | 203 |
| | 20 | 4 | 0.516792 | 0.017982 | 19.231088 | 0.646225 | 0.27696 | 0.005869 | 1.926267 | 0.057295 | 2684.2 | 77.1 | 3051.9 | 32.8 | 3344.6 | 32.9 | 0.98 | 277 | 294 | 595 |
| | 21 | 4 | 0.318152 | 0.011721 | 10.66512 | 0.485041 | 0.244 | 0.006622 | 3.129816 | 0.120925 | 1780 | 57.6 | 2491.1 | 43.7 | 3143.8 | 43 | 1.9 | 1014 | 531 | 656 |
| | 22 | 4 | 0.138477 | 0.012139 | 4.652447 | 0.368262 | 0.245033 | 0.005492 | 7.758161 | 0.798521 | 832.8 | 69.1 | 1738.9 | 69.5 | 3150.9 | 35.4 | 2.05 | 2445 | 1197 | 1055 |
| | 23 | 4 | 0.371703 | 0.010651 | 12.344161 | 0.404614 | 0.242894 | 0.005776 | 2.671311 | 0.075851 | 2037.1 | 50 | 2629.8 | 31.2 | 3137.3 | 37.8 | 1.75 | 997 | 571 | 690 |
| | 24 | 4 | 0.245929 | 0.008859 | 7.279933 | 0.328321 | 0.216224 | 0.005029 | 4.053459 | 0.147296 | 1416.9 | 45.8 | 2142.4 | 39.9 | 2950.8 | 37.1 | 2.27 | 1343 | 595 | 697 |
| | 25 | 4 | 0.393294 | 0.01329 | 15.599196 | 0.463368 | 0.289071 | 0.005875 | 2.531307 | 0.082603 | 2137.3 | 61.2 | 2851.8 | 27.9 | 3411.6 | 31.8 | 1.91 | 1130 | 589 | 1418 |
| | 26 | 4 | 0.129291 | 0.004705 | 4.222125 | 0.134127 | 0.241007 | 0.005807 | 7.675939 | 0.30216 | 783.5 | 26.8 | 1677 | 25.9 | 3130.7 | 43.2 | 1.07 | 3903 | 4285 | 4675 |
| | 27 | 4 | 0.490678 | 0.018524 | 17.288457 | 0.673008 | 0.258871 | 0.005345 | 2.038063 | 0.079348 | 2571.4 | 80.5 | 2947.6 | 38.1 | 3238.6 | 32.5 | 1.73 | 669 | 388 | 624 |
| | 28 | 4 | 0.354293 | 0.02397 | 13.385563 | 0.79642 | 0.28156 | 0.0077 | 2.884452 | 0.200231 | 1949.2 | 114.2 | 2698.2 | 57.7 | 3368.6 | 42.1 | 1.36 | 155 | 118 | 169 |
| | 29 | 4 | 0.214932 | 0.006367 | 6.180805 | 0.190681 | 0.213146 | 0.00478 | 4.640499 | 0.14254 | 1254.8 | 33.9 | 2000.4 | 27.2 | 2927.5 | 36.5 | 1.96 | 895 | 460 | 591 |
| | 30 | 4 | 0.184825 | 0.008319 | 6.918807 | 0.303334 | 0.274889 | 0.006678 | 5.42925 | 0.261199 | 1092.7 | 45.4 | 2098.4 | 38.4 | 3342.4 | 48.7 | 4.69 | 430 | 94 | 218 |
| CH01 | 1 | 4 | 0.312999 | 0.00939 | 8.463542 | 0.247232 | 0.191344 | 0.004079 | 3.183461 | 0.096626 | 1755 | 46.1 | 2281 | 26.7 | 2752.1 | 35 | 0.45 | 727 | 1575 | 1876 |
| | 2 | 4 | 0.388709 | 0.011892 | 9.923449 | 0.343912 | 0.181633 | 0.003786 | 2.559239 | 0.075436 | 2116.4 | 54.9 | 2426.4 | 31.5 | 2666.7 | 34.4 | 0.68 | 13735 | 19823 | 13589 |
| | 3 | 4 | 0.121612 | 0.004695 | 2.879279 | 0.129075 | 0.167248 | 0.003346 | 8.230363 | 0.3102 | 739.5 | 26.9 | 1372.8 | 33.5 | 2529.1 | 33.6 | 0.6 | 13149 | 22996 | 10842 |
| | 4 | 4 | 0.274588 | 0.011374 | 7.185476 | 0.242739 | 0.187619 | 0.007729 | 3.63117 | 0.152669 | 1563.4 | 57.6 | 2133.8 | 30 | 2715.8 | 65 | 1.41 | 1213 | 839 | 1159 |
| | 5 | 4 | 0.592343 | 0.016953 | 18.768837 | 0.557982 | 0.223688 | 0.00534 | 1.677499 | 0.047044 | 2998.4 | 68.4 | 3029.3 | 28.8 | 3005.6 | 38 | 2.07 | 299 | 140 | 227 |
| | 6 | 4 | 0.437983 | 0.012864 | 11.341858 | 0.31901 | 0.18428 | 0.004115 | 2.271949 | 0.067246 | 2340.9 | 57.7 | 2550.8 | 26.2 | 2689.7 | 36.7 | 2.04 | 343 | 163 | 255 |
| | 7 | 4 | 0.061298 | 0.001808 | 1.084926 | 0.033077 | 0.126276 | 0.003471 | 16.24066 | 0.478765 | 383.5 | 11 | 745.6 | 15.8 | 2042 | 47.5 | 1.24 | 16112 | 12578 | 6550 |
| | 8 | 4 | 0.36588 | 0.010589 | 8.887612 | 0.26529 | 0.174889 | 0.004128 | 2.718083 | 0.078722 | 2009.8 | 50 | 2326.1 | 27.2 | 2603.5 | 38.7 | 0.3 | 1438 | 4628 | 4409 |
| | 9 | 4 | 0.213684 | 0.005856 | 3.443189 | 0.104868 | 0.114855 | 0.002668 | 4.659344 | 0.129547 | 1248.3 | 31.1 | 1513.7 | 24.1 | 1875.5 | 42.2 | 0.22 | 1508 | 6541 | 4422 |
| | 10 | 4 | 0.119032 | 0.004651 | 4.638297 | 0.1588 | 0.280757 | 0.006784 | 8.443039 | 0.340265 | 724.7 | 26.8 | 1754.3 | 28.4 | 3364.5 | 37.7 | 1.45 | 1623 | 1130 | 1592 |
| | 11 | 4 | 0.131627 | 0.004353 | 3.635378 | 0.134237 | 0.201369 | 0.005118 | 7.649451 | 0.250603 | 797 | 24.8 | 1555.8 | 29.5 | 2834.9 | 41.5 | 1.35 | 10439 | 7957 | 6984 |
| | 12 | 4 | 0.082373 | 0.003427 | 3.039867 | 0.141545 | 0.269849 | 0.006067 | 12.215942 | 0.491822 | 510.2 | 20.4 | 1416.6 | 35.1 | 3304.1 | 35.3 | 2.67 | 12171 | 4721 | 6540 |
| | 13 | 4 | 0.106559 | 0.004874 | 3.357515 | 0.13537 | 0.228179 | 0.004913 | 9.536881 | 0.406835 | 652.3 | 28.3 | 1491.7 | 30.9 | 3037.6 | 34.8 | 0.98 | 2637 | 2793 | 1212 |
| | 14 | 4 | 0.525767 | 0.014895 | 15.893443 | 0.493871 | 0.218733 | 0.005836 | 1.908804 | 0.053628 | 2723.1 | 62.8 | 2869.2 | 30.1 | 2968.3 | 43.1 | 0.52 | 85 | 169 | 176 |
| | 15 | 4 | 0.568915 | 0.02087 | 18.045652 | 0.627199 | 0.226341 | 0.007417 | 1.764335 | 0.061061 | 2902.3 | 84.7 | 2991.2 | 34.1 | 3023.3 | 53.3 | 0.35 | 131 | 383 | 411 |
| | 17 | 4 | 0.203262 | 0.007007 | 5.18389 | 0.252241 | 0.183053 | 0.005613 | 4.934499 | 0.164919 | 1192.5 | 37.4 | 1846 | 41.6 | 2676.4 | 51.5 | 1.83 | 1790 | 1113 | 1324 |
| | 18 | 4 | 0.408701 | 0.011006 | 10.740362 | 0.286034 | 0.187911 | 0.004111 | 2.445621 | 0.06624 | 2208.7 | 50.4 | 2500.4 | 24.7 | 2722.1 | 35.9 | 0.38 | 240 | 646 | 653 |
| | 19 | 4 | 0.201441 | 0.007077 | 6.083441 | 0.189873 | 0.214417 | 0.005819 | 4.964774 | 0.175698 | 1182.8 | 38 | 1987.3 | 27 | 2937 | 43.7 | 1.15 | 696 | 612 | 789 |
| | 20 | 4 | 0.167879 | 0.00485 | 3.597313 | 0.102692 | 0.153155 | 0.003065 | 5.949304 | 0.178755 | 1000.3 | 26.8 | 1548.3 | 23 | 2380.2 | 34.2 | 0.75 | 12150 | 16634 | 10943 |
| | 21 | 4 | 0.377861 | 0.015198 | 9.500062 | 0.324642 | 0.184954 | 0.004424 | 2.64462 | 0.106455 | 2065.4 | 71.1 | 2386.7 | 31.2 | 2696.2 | 39.9 | 0.59 | 723 | 1191 | 1769 |

Continued on next page

| Sample | Spot name | Run | 206/238 | ±2SE | 207/235 | ±2SE | 207/206 | ±2SE | 238/P206 | ±2SE | 206/238 Age | ±2SE | 207/235 Age | ±2SE | 207/206 Age | ±2SE | U/Th | U | Th | Pb |
|---|---|---|---|---|---|---|---|---|---|---|---|---|---|---|---|---|---|---|---|---|
| | 22 | 4 | 0.177725 | 0.004825 | 4.397518 | 0.119316 | 0.180952 | 0.003591 | 5.610899 | 0.150386 | 1054.5 | 26.4 | 1711.4 | 22.3 | 2660.5 | 32.7 | 0.65 | 15640 | 23237 | 17885 |
| | 23 | 4 | 0.521216 | 0.014918 | 15.659446 | 0.499259 | 0.220251 | 0.005379 | 1.91574 | 0.055601 | 2703.6 | 63.3 | 2854.4 | 30.6 | 2979.6 | 39.8 | 0.58 | 123 | 208 | 345 |
| | 24 | 4 | 0.220163 | 0.00622 | 5.25933 | 0.150624 | 0.174406 | 0.004399 | 4.532788 | 0.126872 | 1282.6 | 32.8 | 1861.9 | 24.5 | 2598.3 | 41.7 | 0.39 | 738 | 1884 | 1409 |
| | 25 | 4 | 0.447817 | 0.014573 | 12.696159 | 0.472 | 0.210071 | 0.006539 | 2.214196 | 0.054118 | 2399.5 | 48.6 | 2655.6 | 35.2 | 2902.5 | 50.8 | 0.75 | 85 | 112 | 176 |
| | 26 | 4 | 0.393186 | 0.01067 | 8.972322 | 0.238164 | 0.169005 | 0.003498 | 2.539389 | 0.068608 | 2137.4 | 49.3 | 2334.9 | 24.3 | 2546.6 | 34.8 | 0.26 | 1009 | 3861 | 3194 |
| | 27 | 4 | 0.625468 | 0.016272 | 21.693422 | 0.584871 | 0.255501 | 0.00518 | 1.596387 | 0.041884 | 3131.4 | 64.6 | 3169.5 | 26.3 | 3217.9 | 32.2 | 1.21 | 427 | 352 | 544 |
| | 28 | 4 | 0.517455 | 0.013572 | 12.607933 | 0.355887 | 0.178981 | 0.004085 | 1.929474 | 0.051075 | 2688.2 | 57.7 | 2650.1 | 26.5 | 2641.4 | 37.7 | 0.48 | 360 | 748 | 946 |
| | 29 | 4 | 0.127934 | 0.003548 | 3.562601 | 0.102168 | 0.204842 | 0.004549 | 7.809125 | 0.217354 | 776 | 20.3 | 1540.6 | 22.7 | 2863.2 | 35.9 | 1.69 | 512 | 304 | 245 |
| | 30 | 4 | 0.38744 | 0.011316 | 10.122177 | 0.297742 | 0.19211 | 0.004337 | 2.576769 | 0.075499 | 2110.6 | 52.6 | 2445.3 | 27.6 | 2758.7 | 37.2 | 0.33 | 1000 | 3004 | 3209 |
| DP01 | 1 | 7 | 0.443108 | 0.009033 | 11.333301 | 1.151205 | 0.18546 | 0.006798 | 2.256421 | 0.044941 | 2364 | 40.2 | 2550.1 | 93.6 | 2701.2 | 60.7 | 0.02 | 2734 | 139109 | 162701 |
| | 2 | 7 | 0.435497 | 0.010604 | 10.88055 | 1.117458 | 0.181598 | 0.006678 | 2.300836 | 0.054742 | 2329.4 | 47.4 | 2511.2 | 94.3 | 2666.3 | 60.4 | 0.02 | 1761 | 95776 | 108636 |
| | 3 | 7 | 0.797561 | 0.026274 | 34.42554 | 3.702013 | 0.31175 | 0.013188 | 1.257075 | 0.044095 | 3778.1 | 95.4 | 3619.3 | 110.3 | 3527.1 | 65.7 | 0.01 | 1033 | 87042 | 74469 |
| | 4 | 7 | 1.010966 | 0.066673 | 91.863468 | 10.426001 | 0.660516 | 0.026711 | 1.009881 | 0.066505 | 4486 | 213.5 | 4593.7 | 114 | 4645.1 | 59.1 | 0.02 | 1605 | 90763 | 46283 |
| | 5 | 7 | 0.372607 | 0.009842 | 18.99048 | 1.987618 | 0.369713 | 0.015073 | 2.694953 | 0.072474 | 2040.5 | 46.3 | 3037.4 | 102 | 3786.4 | 62 | 0.01 | 642 | 84263 | 49951 |
| | 6 | 7 | 0.314966 | 0.017605 | 6.864722 | 0.820811 | 0.157334 | 0.006568 | 3.282618 | 0.203509 | 1759.4 | 87.1 | 2076 | 111.4 | 2421.7 | 72.6 | 0.01 | 519 | 47194 | 40558 |
| | 7 | 7 | 0.46508 | 0.008531 | 11.900902 | 1.205265 | 0.185692 | 0.00683 | 2.151923 | 0.03955 | 2461.6 | 37.5 | 2596.1 | 95 | 2705.9 | 54.4 | 0.02 | 1862 | 98346 | 113053 |
| | 8 | 7 | 1.661861 | 0.099236 | 158.728514 | 19.264501 | 0.68876 | 0.026725 | 0.615461 | 0.036618 | 6283.2 | 239.6 | 5135.7 | 124.3 | 4705.7 | 56.3 | 0.02 | 786 | 39302 | 45150 |
| | 9 | 7 | 0.44526 | 0.009609 | 12.414591 | 1.293941 | 0.202196 | 0.008277 | 2.251959 | 0.049265 | 2373.4 | 42.9 | 2632.9 | 98.7 | 2839.6 | 66.9 | 0.01 | 475 | 36496 | 40349 |
| | 10 | 7 | 0.333289 | 0.007458 | 7.371269 | 0.759751 | 0.160454 | 0.006122 | 3.010309 | 0.068035 | 1853.8 | 36.1 | 2155.5 | 92.6 | 2463.2 | 57.2 | 2.83 | 550 | 195 | 153 |
| | 11 | 7 | 0.508454 | 0.010489 | 18.147052 | 1.858306 | 0.258017 | 0.009679 | 1.971321 | 0.040052 | 2649.9 | 44.7 | 2997.1 | 98.5 | 3233.7 | 59.1 | 0.02 | 2339 | 154424 | 188960 |
| | 12 | 7 | 0.505872 | 0.013629 | 12.98836 | 1.364275 | 0.187316 | 0.007953 | 1.984881 | 0.055866 | 2638.2 | 58.7 | 2677.1 | 100.2 | 2716 | 68.6 | 4.88 | 174 | 36 | 52 |
| | 13 | 7 | 0.449081 | 0.009328 | 12.127042 | 1.245265 | 0.195447 | 0.007896 | 2.232893 | 0.045458 | 2391 | 41.4 | 2613.7 | 97.3 | 2786.7 | 66.6 | 0.01 | 767 | 62336 | 70749 |
| | 14 | 7 | 0.527396 | 0.013143 | 27.323713 | 2.980489 | 0.37593 | 0.017743 | 1.902486 | 0.048093 | 2730 | 55.6 | 3392.6 | 108.3 | 3812.5 | 70.9 | 0.01 | 836 | 117315 | 88511 |
| | 15 | 7 | 0.550347 | 0.018242 | 13.820864 | 1.483665 | 0.183557 | 0.00961 | 1.837744 | 0.061728 | 2823 | 75.8 | 2731.1 | 101.6 | 2669.2 | 91.2 | 0 | 22 | 0 | 0 |
| | 16 | 7 | 0.319059 | 0.012171 | 15.984419 | 1.676342 | 0.364429 | 0.013608 | 3.174165 | 0.132761 | 1783.3 | 60 | 2872.7 | 103.1 | 3767.2 | 56.5 | 0.02 | 1788 | 106630 | 55785 |
| | 17 | 7 | 0.443917 | 0.00794 | 11.637219 | 1.178354 | 0.190828 | 0.007243 | 2.259964 | 0.040666 | 2367.9 | 35.5 | 2575.1 | 94.7 | 2747.2 | 61.8 | 0.02 | 2440 | 134629 | 151595 |
| | 18 | 7 | 0.575866 | 0.029932 | 17.977074 | 2.159635 | 0.228437 | 0.013569 | 1.753454 | 0.088914 | 2928.7 | 121.7 | 2982.8 | 113.3 | 3034.5 | 93.5 | 1.97 | 43 | 21 | 47 |
| | 19 | 7 | 0.445525 | 0.011939 | 10.85681 | 1.122488 | 0.178322 | 0.006815 | 2.253243 | 0.060177 | 2374.9 | 53.2 | 2510.3 | 97.6 | 2636.2 | 63.4 | 0.01 | 890 | 81983 | 86577 |
| | 20 | 7 | 0.437492 | 0.008544 | 11.296325 | 1.145574 | 0.188089 | 0.006891 | 2.294922 | 0.044656 | 2339 | 38.3 | 2547.2 | 93.9 | 2724.4 | 60.5 | 0.02 | 2559 | 132126 | 146886 |
| | 21 | 7 | 0.465327 | 0.013021 | 12.856701 | 1.321028 | 0.201456 | 0.007495 | 2.166449 | 0.060122 | 2461.2 | 57.1 | 2667.2 | 97.8 | 2836.5 | 60.5 | 4.29 | 470 | 109 | 210 |
| | 22 | 7 | 0.501924 | 0.012127 | 14.264031 | 1.447248 | 0.207625 | 0.008033 | 1.995068 | 0.053081 | 2620.8 | 51.9 | 2769.6 | 106.7 | 2884.4 | 63.8 | 1.58 | 274 | 178 | 266 |
| | 23 | 7 | 0.529983 | 0.012529 | 15.23771 | 1.585991 | 0.210099 | 0.008508 | 1.897374 | 0.044065 | 2740.1 | 52.6 | 2827 | 97.2 | 2902.3 | 66.2 | 1.85 | 167 | 89 | 157 |
| | 24 | 7 | 0.499241 | 0.019134 | 13.867337 | 1.491186 | 0.203087 | 0.00789 | 2.033858 | 0.078728 | 2605.9 | 82.3 | 2734 | 102.9 | 2848.4 | 62.7 | 3.24 | 296 | 98 | 168 |
| | 25 | 7 | 0.376363 | 0.009537 | 10.248299 | 1.058053 | 0.199216 | 0.007618 | 2.673346 | 0.064725 | 2058.3 | 44.3 | 2455.2 | 94.6 | 2817.5 | 62.6 | 8.31 | 484 | 56 | 201 |
| | 26 | 7 | 0.380736 | 0.009867 | 9.990966 | 1.039852 | 0.191978 | 0.007468 | 2.643544 | 0.06785 | 2078.6 | 46 | 2430.9 | 96.2 | 2756.3 | 64.2 | 11.52 | 631 | 57 | 151 |
| | 27 | 7 | 0.4096 | 0.008869 | 11.06279 | 1.12376 | 0.197996 | 0.007711 | 2.451816 | 0.052503 | 2212.5 | 40.5 | 2527.6 | 95.2 | 2806.9 | 63.4 | 0.02 | 2311 | 132713 | 135181 |
| | 28 | 7 | 0.4191 | 0.009413 | 11.724991 | 1.220304 | 0.204074 | 0.008133 | 2.393291 | 0.05511 | 2256.1 | 42.9 | 2581.3 | 98.7 | 2857.1 | 64.6 | 0.02 | 841 | 52710 | 57221 |
| | 29 | 7 | 0.556549 | 0.012335 | 18.273689 | 1.937545 | 0.241798 | 0.011428 | 1.801132 | 0.040617 | 2852.1 | 51.2 | 3002.9 | 101.5 | 3128.8 | 74.9 | 0.01 | 1387 | 132619 | 144773 |
| | 30 | 7 | 0.709459 | 0.02014 | 45.660446 | 5.18369 | 0.468889 | 0.023475 | 1.42049 | 0.042495 | 3453.1 | 76.7 | 3886.8 | 119.7 | 4135 | 76.3 | 0.01 | 1126 | 110488 | 90492 |
| GH02 | 1 | 3 | 0.509965 | 0.014007 | 12.986798 | 0.725326 | 0.183218 | 0.003975 | 1.960495 | 0.053897 | 2656 | 59.8 | 2677.5 | 51.7 | 2679.3 | 36 | 1.01 | 137 | 220 | 757 |
| | 2 | 3 | 0.448371 | 0.015683 | 12.811393 | 0.82373 | 0.205934 | 0.006991 | 2.230748 | 0.078582 | 2387.4 | 69.9 | 2664 | 61.1 | 2870.3 | 55.7 | 1.37 | 246 | 364 | 446 |
| | 3 | 3 | 0.49768 | 0.015084 | 13.54202 | 0.858659 | 0.195406 | 0.006006 | 2.010642 | 0.062196 | 2602.8 | 65.1 | 2713.4 | 58 | 2781.2 | 49.6 | 0.97 | 209 | 663 | 274 |
| | 4 | 3 | 0.498133 | 0.014334 | 12.660181 | 0.714059 | 0.181908 | 0.004061 | 2.005939 | 0.055559 | 2605.1 | 61.2 | 2653.2 | 53.4 | 2667.1 | 37.3 | 0.97 | 263 | 1996 | 203 |
| | 5 | 3 | 0.498407 | 0.014366 | 12.887179 | 0.718054 | 0.185865 | 0.004238 | 2.004046 | 0.057709 | 2606.3 | 61.8 | 2670.3 | 52.4 | 2702.5 | 37.7 | 0.92 | 330 | 357 | 188 |
| | 7 | 3 | 0.410142 | 0.014704 | 11.039916 | 0.627057 | 0.193674 | 0.004566 | 2.44313 | 0.087154 | 2213.9 | 67.1 | 2524.9 | 53.4 | 2770 | 38.6 | 0.89 | 365 | 412 | 113 |
| | 8 | 3 | 0.527254 | 0.014419 | 13.365617 | 0.739419 | 0.18197 | 0.004105 | 1.88972 | 0.051847 | 2729.4 | 60.9 | 2704.8 | 52.5 | 2667.6 | 37.6 | 1.01 | 352 | 350 | 118 |
| | 9 | 3 | 0.524291 | 0.017793 | 13.687807 | 0.854775 | 0.187683 | 0.00689 | 1.904473 | 0.063919 | 2715.9 | 75 | 2724.8 | 59.1 | 2713.6 | 58.2 | 1.61 | 122 | 76 | 28 |
| | 10 | 3 | 0.336122 | 0.009794 | 10.410252 | 0.686524 | 0.22211 | 0.008289 | 2.94781 | 0.071642 | 1867.7 | 47.4 | 2467.7 | 60.6 | 2988.1 | 60.1 | 1.16 | 1199 | 1032 | 414 |
| GW02 | 1 | 2 | 0.5094 | 0.006078 | 12.953629 | 0.95216 | 0.184314 | 0.004017 | 1.962168 | 0.023054 | 2653.8 | 25.9 | 2675.7 | 69 | 2691 | 36 | 1.1 | 352 | 304 | 407 |
| | 2 | 2 | 0.449635 | 0.011083 | 10.690585 | 0.850695 | 0.172059 | 0.004385 | 2.233248 | 0.05811 | 2392 | 49.6 | 2492 | 77 | 2575 | 42.9 | 2.1 | 291 | 130 | 174 |
| | 3 | 2 | 0.536182 | 0.007658 | 14.000913 | 1.037032 | 0.18931 | 0.004445 | 1.864859 | 0.02618 | 2766.9 | 32 | 2748.8 | 70.7 | 2734.4 | 38.8 | 1.51 | 204 | 130 | 190 |
| | 4 | 2 | 0.580913 | 0.017673 | 15.503582 | 1.267266 | 0.193149 | 0.004835 | 1.732322 | 0.050266 | 2948.9 | 71.3 | 2840.9 | 75.9 | 2766.7 | 41.4 | 1.33 | 161 | 117 | 179 |
| | 5 | 2 | 0.544076 | 0.010187 | 14.092922 | 1.067836 | 0.18767 | 0.004296 | 1.840059 | 0.034506 | 2799.4 | 42.5 | 2754 | 71.9 | 2724.3 | 33.2 | 2.08 | 390 | 178 | 260 |

Continued on next page

| Sample | Spot name | Run | 206/238 | ±2SE | 207/235 | ±2SE | 207/206 | ±2SE | 238/P206 | ±2SE | 206/238 Age | ±2SE | 207/235 Age | ±2SE | 207/206 Age | ±2SE | U/Th | U | Th | Pb |
|---|---|---|---|---|---|---|---|---|---|---|---|---|---|---|---|---|---|---|---|---|
| | 6 | 2 | 0.476491 | 0.006534 | 12.058556 | 0.891157 | 0.18351 | 0.004422 | 2.091213 | 0.025629 | 2517.4 | 25.2 | 2608.2 | 68.4 | 2682.8 | 39.4 | 1.5 | 221 | 151 | 201 |
| | 7 | 2 | 0.461172 | 0.016176 | 13.698981 | 1.159157 | 0.217223 | 0.00571 | 2.187878 | 0.074474 | 2441.2 | 70.9 | 2721.3 | 79.1 | 2957.3 | 41.7 | 17.98 | 3275 | 173 | 2029 |
| | 8 | 2 | 0.374856 | 0.011177 | 8.788918 | 0.711229 | 0.168828 | 0.004413 | 2.684059 | 0.081693 | 2050.3 | 52.5 | 2311.3 | 74.2 | 2543 | 44.3 | 2.56 | 243 | 118 | 131 |
| | 9 | 2 | 0.556694 | 0.009526 | 14.513715 | 1.096037 | 0.18894 | 0.004618 | 1.796729 | 0.031405 | 2852 | 39.6 | 2782 | 72 | 2730.7 | 40.3 | 1.08 | 199 | 179 | 230 |
| | 10 | 2 | 0.505448 | 0.006517 | 12.665303 | 0.924921 | 0.182148 | 0.004121 | 1.976216 | 0.025477 | 2636.8 | 27.9 | 2657 | 77.4 | 2671.1 | 37.6 | 1.82 | 338 | 181 | 259 |
| | 11 | 2 | 0.543572 | 0.006602 | 13.983645 | 1.025314 | 0.186513 | 0.004235 | 1.835933 | 0.022228 | 2798.1 | 27.6 | 2748.1 | 69.9 | 2710.2 | 37.4 | 1.12 | 211 | 189 | 321 |
| | 12 | 2 | 0.298583 | 0.017287 | 7.502844 | 0.961002 | 0.178248 | 0.0096 | 3.436561 | 0.181853 | 1679 | 84.7 | 2135.4 | 106.6 | 2614 | 87.5 | 4.56 | 1583 | 343 | 1624 |
| | 13 | 2 | 0.233904 | 0.003016 | 5.436861 | 0.399456 | 0.168608 | 0.00421 | 4.26657 | 0.056316 | 1354.8 | 15.8 | 1890.2 | 63.1 | 2541.3 | 42.2 | 2.68 | 1717 | 642 | 1072 |
| | 14 | 2 | 0.304032 | 0.005325 | 6.875053 | 0.517542 | 0.163843 | 0.003745 | 3.286484 | 0.057949 | 1710.9 | 26.3 | 2093.9 | 67.7 | 2494.1 | 38.6 | 5.29 | 1492 | 296 | 699 |
| | 15 | 2 | 0.331996 | 0.022277 | 7.412798 | 0.881028 | 0.158874 | 0.006065 | 3.138549 | 0.218977 | 1839.6 | 108.1 | 2127.3 | 111.1 | 2433 | 66.3 | 4.15 | 1198 | 300 | 447 |
| | 16 | 2 | 0.515335 | 0.008317 | 12.945843 | 0.961627 | 0.182115 | 0.004193 | 1.937634 | 0.030811 | 2678.7 | 35.3 | 2674.6 | 70 | 2670.6 | 37.7 | 1.34 | 343 | 257 | 406 |
| | 17 | 2 | 0.472179 | 0.008065 | 11.488233 | 0.852825 | 0.176431 | 0.004127 | 2.115276 | 0.036394 | 2492.4 | 35.3 | 2562.6 | 69.2 | 2617.8 | 39.1 | 1.29 | 582 | 469 | 688 |
| | 18 | 2 | 0.328942 | 0.00839 | 7.041947 | 0.554757 | 0.154604 | 0.003415 | 3.045438 | 0.073117 | 1832.2 | 40.4 | 2113.4 | 68 | 2396.2 | 37.9 | 3.36 | 1194 | 350 | 466 |
| | 19 | 2 | 0.522942 | 0.006893 | 13.199686 | 0.973017 | 0.182979 | 0.004186 | 1.902248 | 0.022588 | 2711.2 | 29.3 | 2693.3 | 69.6 | 2682.4 | 33.5 | 0.99 | 487 | 485 | 694 |
| | 20 | 2 | 0.238177 | 0.00394 | 4.786482 | 0.367355 | 0.144885 | 0.003499 | 4.175529 | 0.076399 | 1377 | 20.5 | 1780.5 | 63.7 | 2284.2 | 41.5 | 3.09 | 1833 | 614 | 625 |
| | 21 | 2 | 0.538292 | 0.008015 | 13.580436 | 1.007843 | 0.18405 | 0.004051 | 1.852993 | 0.028334 | 2775.7 | 33.7 | 2719.8 | 71.1 | 2688.5 | 36.5 | 1.14 | 168 | 147 | 186 |
| | 22 | 2 | 0.361957 | 0.012481 | 8.753835 | 0.751624 | 0.174582 | 0.004515 | 2.784101 | 0.106441 | 1989 | 59.7 | 2303.9 | 82.6 | 2599.1 | 43.6 | 1.81 | 1013 | 552 | 718 |
| | 23 | 2 | 0.524417 | 0.009048 | 13.23554 | 0.983917 | 0.182593 | 0.003997 | 1.903298 | 0.034013 | 2717 | 38.5 | 2695.5 | 71.2 | 2678.5 | 41.1 | 1.74 | 281 | 160 | 203 |
| | 24 | 2 | 0.498862 | 0.009758 | 12.401705 | 0.933535 | 0.180161 | 0.004004 | 2.002535 | 0.041453 | 2607.8 | 42.3 | 2633.6 | 72 | 2653.1 | 36.8 | 1.49 | 413 | 285 | 356 |
| | 25 | 2 | 0.446278 | 0.005823 | 10.899137 | 0.800132 | 0.177064 | 0.004032 | 2.233536 | 0.029403 | 2378.4 | 26 | 2514 | 68.1 | 2624 | 37.9 | 2.37 | 498 | 220 | 330 |
| | 26 | 2 | 0.206539 | 0.004506 | 4.01246 | 0.324569 | 0.139773 | 0.003935 | 4.839839 | 0.105091 | 1210 | 24.1 | 1632.9 | 64.5 | 2228.8 | 53.9 | 3.99 | 3179 | 806 | 858 |
| | 27 | 2 | 0.558508 | 0.006416 | 14.217782 | 1.041853 | 0.184551 | 0.004228 | 1.783966 | 0.020574 | 2860.2 | 26.6 | 2763.9 | 69.4 | 2692.6 | 37.9 | 1.36 | 222 | 163 | 221 |
| | 28 | 2 | 0.78782 | 0.037693 | 22.700886 | 2.136297 | 0.207839 | 0.005906 | 1.290626 | 0.060981 | 3732.2 | 135.3 | 3198.3 | 91.6 | 2884.8 | 46 | 0.84 | 227 | 273 | 530 |
| | 29 | 2 | 0.540336 | 0.006938 | 13.643712 | 1.003699 | 0.183042 | 0.004179 | 1.844468 | 0.023566 | 2784.5 | 29 | 2724.7 | 69.4 | 2679.1 | 37.6 | 1.07 | 370 | 351 | 440 |
| | 30 | 2 | 0.532154 | 0.006194 | 13.481701 | 0.992613 | 0.183222 | 0.004372 | 1.868031 | 0.024205 | 2750.2 | 26 | 2713.3 | 69.1 | 2680.3 | 39 | 1.33 | 190 | 144 | 185 |
| | 31 | 5 | 0.524099 | 0.019361 | 14.618291 | 0.956887 | 0.19149 | 0.006619 | 1.921978 | 0.072127 | 2716 | 82.1 | 2789.5 | 62.7 | 2752.4 | 57.1 | 1.22 | 88 | 63 | 97 |
| | 32 | 5 | 0.517415 | 0.020102 | 14.397854 | 0.9455 | 0.186397 | 0.006644 | 1.952356 | 0.075962 | 2687.7 | 85.4 | 2775.7 | 62.2 | 2708.8 | 59 | 1.16 | 86 | 64 | 100 |
| | 33 | 5 | 0.486346 | 0.021699 | 13.486195 | 0.960829 | 0.184452 | 0.006023 | 2.095644 | 0.095349 | 2552.2 | 94.3 | 2709.7 | 69.3 | 2691.9 | 54.3 | 1.22 | 177 | 125 | 181 |
| | 34 | 5 | 0.527451 | 0.023602 | 15.594259 | 1.13929 | 0.194361 | 0.006672 | 1.935792 | 0.086316 | 2727.8 | 99.4 | 2846.6 | 69.5 | 2777.1 | 56.5 | 1.06 | 147 | 121 | 207 |
| | 35 | 5 | 0.484561 | 0.01858 | 14.036061 | 0.944114 | 0.189182 | 0.00632 | 2.100266 | 0.082585 | 2546.2 | 81 | 2750 | 63.6 | 2733.2 | 54.6 | 1.19 | 141 | 103 | 150 |
| | 36 | 5 | 0.46855 | 0.01775 | 13.505568 | 0.899991 | 0.187574 | 0.006259 | 2.171341 | 0.082074 | 2476.5 | 77.8 | 2713.9 | 62.4 | 2719.2 | 54.9 | 2.34 | 156 | 58 | 108 |
| | 37 | 5 | 0.480114 | 0.017602 | 13.615845 | 0.880674 | 0.185009 | 0.006129 | 2.114957 | 0.07709 | 2527.2 | 76.6 | 2722.6 | 61.3 | 2696.6 | 54.6 | 0.98 | 128 | 113 | 157 |
| | 38 | 5 | 0.484985 | 0.01785 | 13.656916 | 0.888164 | 0.185126 | 0.006182 | 2.087108 | 0.077303 | 2548.5 | 77.5 | 2725.3 | 61.9 | 2697.5 | 55.2 | 1.59 | 136 | 75 | 106 |
| | 39 | 5 | 0.223114 | 0.009246 | 6.46106 | 0.444203 | 0.19445 | 0.00711 | 4.477325 | 0.117754 | 1298.1 | 49 | 2039.5 | 62.1 | 2778.2 | 59.4 | 6.35 | 624 | 86 | 248 |
| | 40 | 5 | 0.495382 | 0.018946 | 13.182154 | 0.859702 | 0.182159 | 0.005937 | 2.025879 | 0.077759 | 2593.2 | 81.7 | 2692 | 61.6 | 2671.4 | 54.1 | 2.01 | 151 | 66 | 92 |
| | 41 | 5 | 0.698883 | 0.025459 | 15.266267 | 0.993303 | 0.183074 | 0.006294 | 1.456023 | 0.054075 | 3416 | 96.9 | 2831.4 | 62.5 | 2679.1 | 57.5 | 1.41 | 86 | 57 | 86 |
| | 42 | 5 | 0.654103 | 0.02331 | 15.074959 | 0.963408 | 0.193661 | 0.006413 | 1.554867 | 0.054512 | 3243.9 | 90.5 | 2819.7 | 60.8 | 2771.9 | 54.4 | 1.17 | 194 | 160 | 263 |
| | 43 | 5 | 0.704726 | 0.028666 | 15.885934 | 1.064764 | 0.186944 | 0.006676 | 1.431012 | 0.043333 | 3437.4 | 109.4 | 2868.9 | 65.9 | 2713.5 | 58.3 | 1.16 | 120 | 97 | 144 |
| | 44 | 5 | 0.375328 | 0.016706 | 7.414469 | 0.55969 | 0.16166 | 0.00568 | 2.707706 | 0.12144 | 2053.4 | 78.3 | 2159 | 68.3 | 2471.1 | 59.8 | 3.43 | 347 | 95 | 110 |
| | 45 | 5 | 0.446091 | 0.017 | 9.540837 | 0.643891 | 0.17286 | 0.005766 | 2.265381 | 0.087254 | 2377.3 | 75.9 | 2389.9 | 62.4 | 2584 | 55.8 | 2.82 | 284 | 95 | 103 |
| | 46 | 5 | 0.732334 | 0.027111 | 18.272201 | 1.19664 | 0.197609 | 0.006851 | 1.373567 | 0.050494 | 3541.7 | 100.7 | 3003.5 | 63.9 | 2804.8 | 56.8 | 1.54 | 174 | 108 | 209 |
| | 47 | 5 | 0.545603 | 0.019949 | 12.683151 | 0.839137 | 0.181732 | 0.00607 | 1.841015 | 0.067398 | 2806.1 | 83.1 | 2654.9 | 63 | 2666.9 | 55.5 | 2.33 | 287 | 117 | 139 |
| | 48 | 5 | 0.581412 | 0.021833 | 14.110966 | 0.926589 | 0.184189 | 0.007537 | 1.720907 | 0.064812 | 2954.3 | 89 | 2756.9 | 62.3 | 2688.6 | 67 | 1.28 | 156 | 115 | 155 |
| | 49 | 5 | 0.412853 | 0.015773 | 9.651972 | 0.647526 | 0.176768 | 0.006209 | 2.422767 | 0.092845 | 2227.5 | 72 | 2401.1 | 61.5 | 2620.8 | 58.1 | 4.25 | 543 | 119 | 218 |
| | 50 | 5 | 0.580664 | 0.020596 | 14.909843 | 0.977988 | 0.18826 | 0.006489 | 1.719753 | 0.061098 | 2951.2 | 84 | 2808.7 | 62.6 | 2725.2 | 57.2 | 1.51 | 146 | 92 | 119 |
| | 51 | 7 | 0.258383 | 0.006123 | 5.208366 | 0.538381 | 0.145145 | 0.005608 | 3.866582 | 0.089037 | 1481.1 | 31.3 | 1852 | 86.9 | 2286.7 | 65.5 | 31.54 | 1019 | 33 | 321 |
| | 52 | 7 | 0.657596 | 0.019501 | 23.768128 | 2.545009 | 0.259964 | 0.010405 | 1.525239 | 0.048451 | 3254.4 | 76.7 | 3252 | 109.7 | 3242.9 | 64.5 | 6.68 | 361 | 54 | 286 |
| | 53 | 7 | 0.605701 | 0.017797 | 16.1885 | 1.688235 | 0.192179 | 0.007479 | 1.643751 | 0.042519 | 3049.8 | 71.5 | 2884.5 | 99.9 | 2758.1 | 63.1 | 1.53 | 174 | 114 | 188 |
| | 54 | 7 | 0.740676 | 0.022302 | 20.400604 | 2.157228 | 0.198846 | 0.007878 | 1.353988 | 0.0408 | 3569.1 | 82.5 | 3105.5 | 102.7 | 2813.4 | 64.3 | 2.28 | 122 | 53 | 119 |
| | 55 | 7 | 0.176287 | 0.005195 | 2.855825 | 0.316756 | 0.1167 | 0.005318 | 5.686961 | 0.168973 | 1046.2 | 28.5 | 1364.2 | 81.8 | 1897 | 79 | 2.94 | 758 | 261 | 123 |
| | 56 | 7 | 0.557472 | 0.014843 | 13.617089 | 1.429669 | 0.176865 | 0.007496 | 1.795178 | 0.046981 | 2854.2 | 61.2 | 2719.4 | 98.3 | 2618 | 70.3 | 2.54 | 122 | 47 | 75 |
| | 57 | 7 | 0.527505 | 0.010659 | 13.633577 | 1.396449 | 0.187328 | 0.007471 | 1.891381 | 0.037965 | 2730.3 | 44.9 | 2723 | 96.1 | 2715.2 | 65.4 | 1.53 | 144 | 95 | 141 |
| | 58 | 7 | 0.526072 | 0.01093 | 13.319537 | 1.382207 | 0.183776 | 0.008166 | 1.897085 | 0.039515 | 2724.1 | 46.2 | 2699.6 | 98.5 | 2679.9 | 72.7 | 1.19 | 104 | 86 | 113 |
| | 59 | 7 | 0.607443 | 0.01973 | 15.723207 | 1.683286 | 0.187627 | 0.007551 | 1.653772 | 0.053789 | 3055.9 | 78.9 | 2854 | 101.5 | 2717.7 | 63.9 | 1.47 | 110 | 75 | 115 |
| | 60 | 7 | 0.534814 | 0.01261 | 13.68377 | 1.414517 | 0.185967 | 0.007738 | 1.868635 | 0.044267 | 2760.4 | 53 | 2725.5 | 98.3 | 2701.8 | 68.3 | 1.76 | 92 | 51 | 72 |

Continued on next page

| Sample | Spot name | Run | 206/238 | ±2SE | 207/235 | ±2SE | 207/206 | ±2SE | 238/P206 | ±2SE | 206/238 Age | ±2SE | 207/235 Age | ±2SE | 207/206 Age | ±2SE | U/Th | U | Th | Pb |
|---|---|---|---|---|---|---|---|---|---|---|---|---|---|---|---|---|---|---|---|---|
| GW03 | 1 | 2 | 0.519445 | 0.008831 | 14.98115 | 1.127047 | 0.20889 | 0.004715 | 1.934429 | 0.033206 | 2696 | 37.5 | 2812.3 | 71.8 | 2895.6 | 36.6 | 0.88 | 507 | 628 | 998 |
| | 2 | 2 | 0.527157 | 0.006445 | 15.566572 | 1.158989 | 0.213939 | 0.005198 | 1.903259 | 0.023438 | 2729.1 | 27.2 | 2849.4 | 70.7 | 2933.5 | 39.5 | 0.84 | 514 | 677 | 1092 |
| | 3 | 2 | 0.86774 | 0.036402 | 44.501783 | 3.739214 | 0.371446 | 0.008443 | 1.162326 | 0.052893 | 4015.4 | 131.2 | 3879.5 | 81.1 | 3796 | 34.5 | 0.95 | 387 | 437 | 2812 |
| | 4 | 2 | 0.430181 | 0.008539 | 28.929336 | 2.111629 | 0.489719 | 0.012932 | 2.336868 | 0.045271 | 2305.6 | 38.3 | 3450.8 | 71.3 | 4207.9 | 39.4 | 0.87 | 2689 | 3349 | 14704 |
| | 5 | 2 | 0.510516 | 0.007083 | 13.589408 | 1.0067 | 0.192982 | 0.004853 | 1.965195 | 0.027092 | 2658.4 | 30.2 | 2720.6 | 69.2 | 2765.2 | 41.1 | 0.65 | 582 | 969 | 1247 |
| | 6 | 2 | 0.50538 | 0.005121 | 13.014769 | 0.950152 | 0.187149 | 0.0042 | 1.978998 | 0.023495 | 2636.7 | 21.9 | 2680.4 | 69.4 | 2715.9 | 37 | 0.61 | 691 | 1221 | 1532 |
| | 7 | 2 | 0.508566 | 0.005674 | 13.019551 | 0.949266 | 0.185555 | 0.00407 | 1.970797 | 0.022095 | 2650.3 | 24.3 | 2680.8 | 68.8 | 2702 | 36.2 | 0.62 | 740 | 1294 | 1660 |
| | 8 | 2 | 0.513413 | 0.005928 | 13.36014 | 0.978989 | 0.188579 | 0.004178 | 1.952 | 0.022636 | 2670.9 | 25.3 | 2705 | 69.7 | 2728.6 | 36.4 | 0.93 | 560 | 640 | 888 |
| | 9 | 2 | 0.329738 | 0.013213 | 7.785524 | 0.755078 | 0.169855 | 0.006876 | 3.083616 | 0.129335 | 1834.2 | 64.3 | 2190.1 | 90.5 | 2543.6 | 71.2 | 2.41 | 456 | 246 | 363 |
| | 10 | 2 | 0.574503 | 0.009784 | 15.667104 | 1.211917 | 0.198525 | 0.005426 | 1.746393 | 0.030252 | 2925.3 | 40.2 | 2860.3 | 65 | 2810.6 | 44.2 | 1.27 | 58 | 47 | 92 |
| GW04 | 1 | 2 | 0.530237 | 0.005975 | 13.614289 | 0.99591 | 0.186083 | 0.004127 | 1.886004 | 0.021508 | 2742.2 | 25.2 | 2722.9 | 69.4 | 2706.6 | 36.6 | 1.31 | 431 | 334 | 477 |
| | 2 | 2 | 0.515233 | 0.006072 | 13.196901 | 0.967039 | 0.185625 | 0.004111 | 1.94057 | 0.023065 | 2678.7 | 25.9 | 2693.4 | 69.1 | 2702.5 | 36.8 | 1.35 | 527 | 397 | 530 |
| | 3 | 2 | 0.53444 | 0.006513 | 13.745034 | 1.004702 | 0.186406 | 0.00407 | 1.87055 | 0.022978 | 2759.8 | 27.4 | 2731.9 | 69.5 | 2709.6 | 36.2 | 0.75 | 634 | 867 | 1189 |
| | 4 | 2 | 0.550116 | 0.00717 | 14.190072 | 1.039146 | 0.186984 | 0.004202 | 1.817139 | 0.0237 | 2825.2 | 29.8 | 2762.1 | 69.3 | 2714.4 | 37 | 0.95 | 459 | 495 | 696 |
| | 5 | 2 | 0.546668 | 0.007615 | 14.311695 | 1.057623 | 0.189712 | 0.004275 | 1.828566 | 0.025848 | 2810.8 | 31.8 | 2769.7 | 70.7 | 2738.2 | 37.3 | 1.09 | 406 | 383 | 525 |
| | 6 | 2 | 0.429071 | 0.012768 | 9.829381 | 0.773188 | 0.165969 | 0.003715 | 2.34554 | 0.074313 | 2299.2 | 58 | 2415.1 | 74.6 | 2516 | 37.9 | 1.39 | 1262 | 932 | 1276 |
| | 7 | 2 | 0.503094 | 0.011318 | 13.002851 | 1.00735 | 0.187151 | 0.00452 | 1.99183 | 0.045241 | 2625.5 | 48.6 | 2676.7 | 73.5 | 2715.2 | 39.7 | 1.56 | 432 | 361 | 435 |
| | 8 | 2 | 0.54983 | 0.006977 | 14.384981 | 1.058222 | 0.189046 | 0.00432 | 1.815956 | 0.02269 | 2824.1 | 28.9 | 2774.8 | 69.2 | 2732.3 | 37.8 | 1.83 | 223 | 127 | 203 |
| | 9 | 2 | 0.499347 | 0.006896 | 13.043161 | 0.960207 | 0.189299 | 0.004187 | 1.999604 | 0.027793 | 2610.5 | 29.7 | 2682.1 | 70.2 | 2734.8 | 36.6 | 2.44 | 489 | 214 | 376 |
| | 10 | 2 | 0.534543 | 0.005922 | 13.801351 | 1.009067 | 0.186628 | 0.004028 | 1.866182 | 0.020772 | 2760.3 | 24.9 | 2735.8 | 69 | 2711.6 | 35.7 | 1.09 | 759 | 730 | 1060 |
| | 11 | 2 | 0.301844 | 0.022377 | 6.738675 | 0.810541 | 0.159273 | 0.005171 | 3.472733 | 0.257393 | 1691.5 | 110.4 | 2043.7 | 107.1 | 2441.4 | 54.9 | 0.55 | 6586 | 15053 | 9760 |
| | 12 | 2 | 0.239417 | 0.020537 | 5.093894 | 0.797191 | 0.145258 | 0.007726 | 4.358326 | 0.355056 | 1403.3 | 117.2 | 1775.3 | 126.2 | 2264.7 | 98.4 | 0.26 | 16984 | 84955 | 39299 |
| | 13 | 2 | 0.430483 | 0.055428 | 11.207914 | 1.899883 | 0.182822 | 0.007219 | 2.685715 | 0.329867 | 2263.7 | 243.4 | 2445.1 | 158.5 | 2667.7 | 65.3 | 2.29 | 2659 | 3542 | 3503 |
| | 14 | 2 | 0.564985 | 0.008509 | 14.580639 | 1.078498 | 0.187033 | 0.004193 | 1.762369 | 0.027598 | 2886.5 | 35.3 | 2787.4 | 70.9 | 2714.9 | 37 | 1.14 | 363 | 336 | 491 |
| | 15 | 2 | 0.453115 | 0.023106 | 11.335161 | 1.087568 | 0.180199 | 0.004763 | 2.250767 | 0.122552 | 2401.4 | 103.3 | 2534.2 | 93.1 | 2651.5 | 44.4 | 1.56 | 580 | 395 | 468 |
| | 16 | 2 | 0.551123 | 0.007588 | 14.736837 | 1.099347 | 0.193154 | 0.004413 | 1.803203 | 0.025592 | 2829.3 | 31.7 | 2797.1 | 70.6 | 2767.7 | 37.4 | 1.17 | 381 | 351 | 551 |
| | 17 | 2 | 0.530076 | 0.005843 | 13.671763 | 0.999319 | 0.187259 | 0.004059 | 1.875402 | 0.020436 | 2741.5 | 24.6 | 2726.9 | 68.9 | 2717.2 | 35.7 | 0.77 | 696 | 934 | 1295 |
| | 18 | 2 | 0.537947 | 0.00651 | 13.956122 | 1.020603 | 0.188026 | 0.004069 | 1.847963 | 0.022429 | 2774.5 | 27.3 | 2746.4 | 69.9 | 2723.9 | 35.8 | 0.98 | 539 | 571 | 823 |
| | 19 | 2 | 0.333313 | 0.019532 | 7.756534 | 0.809691 | 0.167325 | 0.004546 | 3.06318 | 0.154188 | 1848.1 | 92.5 | 2184 | 86.5 | 2527.5 | 44.9 | 1.84 | 793 | 448 | 445 |
| | 20 | 2 | 0.540516 | 0.005385 | 14.097129 | 1.02663 | 0.188956 | 0.004213 | 1.837413 | 0.018294 | 2785.5 | 22.5 | 2756.1 | 69.2 | 2731.8 | 36.6 | 0.84 | 582 | 730 | 1054 |
| | 21 | 2 | 0.537508 | 0.006206 | 14.062005 | 1.034459 | 0.189566 | 0.004213 | 1.844816 | 0.021344 | 2772.7 | 26 | 2753.3 | 69.9 | 2737.1 | 36.7 | 1.24 | 519 | 475 | 636 |
| | 22 | 2 | 0.505935 | 0.008429 | 18.790836 | 1.940215 | 0.270202 | 0.021505 | 1.962395 | 0.034275 | 2638.5 | 36.3 | 3008.3 | 97.5 | 3257.5 | 124.2 | 1.25 | 676 | 706 | 1977 |
| | 23 | 2 | 0.48281 | 0.005438 | 12.187405 | 0.890749 | 0.183412 | 0.004001 | 2.052888 | 0.022888 | 2539.3 | 23.6 | 2621 | 77.6 | 2682.8 | 36.1 | 2.07 | 628 | 342 | 422 |
| | 24 | 2 | 0.630687 | 0.007787 | 20.062937 | 1.471306 | 0.230556 | 0.005077 | 1.571704 | 0.019836 | 3151.9 | 30.9 | 3093.9 | 71.2 | 3054.7 | 35.2 | 0.82 | 651 | 891 | 1301 |
| | 25 | 2 | 0.602792 | 0.008064 | 19.057938 | 1.39774 | 0.229154 | 0.004966 | 1.639851 | 0.019823 | 3040.6 | 32.6 | 3044.2 | 71.6 | 3045.1 | 34.8 | 0.76 | 760 | 1103 | 1533 |
| | 26 | 2 | 0.538942 | 0.006014 | 13.861708 | 1.014888 | 0.186942 | 0.004212 | 1.838135 | 0.020715 | 2778.8 | 25.2 | 2739.9 | 69.3 | 2714 | 37 | 0.91 | 825 | 1005 | 1339 |
| | 27 | 2 | 0.467429 | 0.007328 | 11.805012 | 0.870058 | 0.183151 | 0.00437 | 2.113931 | 0.029571 | 2471.7 | 32.3 | 2588.4 | 68.9 | 2679.6 | 39.1 | 2.6 | 763 | 328 | 448 |
| | 28 | 2 | 0.536875 | 0.007355 | 13.987838 | 1.028059 | 0.18888 | 0.004335 | 1.845761 | 0.024971 | 2769.9 | 30.8 | 2748.3 | 69.5 | 2730.9 | 37.9 | 1.31 | 402 | 335 | 478 |
| | 29 | 2 | 0.236236 | 0.004946 | 5.235789 | 0.401457 | 0.160539 | 0.003823 | 4.204358 | 0.089023 | 1366.7 | 25.8 | 1856.4 | 64.7 | 2459.4 | 39.6 | 1 | 3801 | 4251 | 2644 |
| | 30 | 2 | 0.237038 | 0.008999 | 4.729415 | 0.45322 | 0.143298 | 0.0048 | 4.230234 | 0.162253 | 1369.7 | 46.9 | 1759.5 | 80.8 | 2259.9 | 58.1 | 4.03 | 2245 | 652 | 515 |
| GW06 | 1 | 6 | 0.33876 | 0.007415 | 9.721441 | 0.697464 | 0.21019 | 0.007276 | 2.946037 | 0.062539 | 1880.4 | 35.6 | 2408 | 65.7 | 2905.4 | 56.3 | 7.41 | 528 | 70 | 339 |
| | 2 | 6 | 1.233511 | 0.031439 | 43.931858 | 3.266593 | 0.262254 | 0.009784 | 0.813211 | 0.020404 | 5173.5 | 90.3 | 3859.4 | 72.2 | 3263.5 | 52.7 | 0.76 | 38 | 49 | 153 |
| | 3 | 6 | 0.748724 | 0.02659 | 23.139639 | 1.793594 | 0.226679 | 0.009792 | 1.332521 | 0.04126 | 3594.9 | 99.2 | 3235 | 70.5 | 3019.1 | 68.7 | 0.69 | 35 | 49 | 90 |
| | 4 | 6 | 1.091333 | 0.033119 | 38.089156 | 2.933734 | 0.25731 | 0.010531 | 0.915842 | 0.028655 | 4753.5 | 102.9 | 3720.2 | 76.4 | 3227.5 | 64.2 | 0.77 | 33 | 41 | 112 |
| | 5 | 6 | 0.79683 | 0.033569 | 26.29378 | 2.388169 | 0.238941 | 0.010844 | 1.273856 | 0.053287 | 3766 | 119.9 | 3339.6 | 89.2 | 3101.2 | 73.8 | 0.82 | 44 | 53 | 116 |
| | 6 | 6 | 0.275466 | 0.014169 | 6.222868 | 0.504586 | 0.162461 | 0.005683 | 3.66059 | 0.21311 | 1566.9 | 72.3 | 2004.6 | 73.3 | 2479.5 | 59.3 | 3.19 | 1182 | 376 | 589 |
| | 7 | 6 | 0.571843 | 0.014046 | 14.377218 | 1.025294 | 0.183147 | 0.005632 | 1.745593 | 0.045761 | 2914.7 | 58.3 | 2774.3 | 69.9 | 2680.8 | 50.9 | 0.35 | 341064 | 940552 | 1262252 |
| | 8 | 6 | 0.343901 | 0.013825 | 8.757067 | 0.688011 | 0.183235 | 0.005609 | 2.947735 | 0.119864 | 1901.8 | 66.3 | 2306.4 | 71.7 | 2681.5 | 51 | 0.34 | 309572 | 882040 | 743303 |
| | 9 | 6 | 0.122213 | 0.007637 | 3.003163 | 0.276584 | 0.175735 | 0.005414 | 8.440719 | 0.443976 | 741.7 | 43.3 | 1397.9 | 65.5 | 2614.4 | 43.7 | 0.32 | 317217 | 940228 | 273157 |
| | 10 | 6 | 0.133488 | 0.009486 | 3.273986 | 0.338059 | 0.174254 | 0.005383 | 7.885515 | 0.573632 | 805.4 | 53.9 | 1455.9 | 80.9 | 2597.8 | 51.5 | 0.32 | 304134 | 928912 | 291266 |
| | 11 | 6 | 4.349811 | 0.053062 | 107.586152 | 7.435138 | 0.176859 | 0.005552 | 0.229454 | 0.002763 | 10807.7 | 63.6 | 4759 | 69 | 2622.2 | 52.5 | 6.31 | 8118 | 1969 | 267726 |
| | 12 | 6 | 3.716031 | 0.073684 | 91.851934 | 6.506011 | 0.177086 | 0.005494 | 0.267986 | 0.004822 | 9989.9 | 101.3 | 4598.8 | 71.7 | 2624.6 | 51.2 | 11.75 | 7660 | 706 | 213254 |
| | 13 | 6 | 2.017763 | 0.072156 | 49.020276 | 3.869948 | 0.1756 | 0.005469 | 0.496582 | 0.017733 | 7112.4 | 153.8 | 3969.3 | 78.2 | 2610.8 | 51.7 | 8.1 | 11478 | 1463 | 166074 |
| | 14 | 6 | 3.783938 | 0.047575 | 93.779136 | 6.541918 | 0.177583 | 0.005478 | 0.263 | 0.003689 | 10087 | 64.4 | 4620.3 | 69.5 | 2629.4 | 51.3 | 18.2 | 6686 | 382 | 192383 |

Continued on next page

| Sample | Spot name | Run | 206/238 | ±2SE | 207/235 | ±2SE | 207/206 | ±2SE | 238/P206 | ±2SE | 206/238 Age | ±2SE | 207/235 Age | ±2SE | 207/206 Age | ±2SE | U/Th | U | Th | Pb |
|---|---|---|---|---|---|---|---|---|---|---|---|---|---|---|---|---|---|---|---|---|
| | 15 | 6 | 3.815799 | 0.129051 | 94.815724 | 7.329193 | 0.178314 | 0.005476 | 0.262843 | 0.008987 | 10120.3 | 173.5 | 4628.9 | 78 | 2636.4 | 51.1 | 10.07 | 6660 | 703 | 200477 |
| | 16 | 6 | 3.964096 | 0.096655 | 98.424635 | 7.139622 | 0.178677 | 0.005522 | 0.252806 | 0.006387 | 10317.4 | 127.3 | 4667.2 | 74.8 | 2639.6 | 51.2 | 13.33 | 5628 | 434 | 175026 |
| | 17 | 6 | 3.473075 | 0.237094 | 85.114458 | 8.380377 | 0.177101 | 0.00547 | 0.302735 | 0.022449 | 9558.3 | 352.2 | 4496.1 | 103.7 | 2624.8 | 51.4 | 19.89 | 8906 | 454 | 223598 |
| | 18 | 6 | 3.119095 | 0.083346 | 76.775011 | 5.615624 | 0.177535 | 0.005633 | 0.320694 | 0.008343 | 9118.9 | 129 | 4418.9 | 73.2 | 2628.8 | 52.1 | 9.24 | 9703 | 1082 | 237131 |
| | 19 | 6 | 3.18123 | 0.094603 | 77.588554 | 5.723001 | 0.176477 | 0.005489 | 0.314944 | 0.009315 | 9212.4 | 145.3 | 4428.9 | 74.4 | 2619 | 51.6 | 10.77 | 10165 | 1001 | 250593 |
| | 20 | 6 | 4.30034 | 0.07963 | 105.727704 | 7.47132 | 0.178151 | 0.005517 | 0.232223 | 0.00433 | 10746.9 | 97.1 | 4741.1 | 71.2 | 2634.8 | 51.4 | 15.55 | 5317 | 349 | 177430 |
| LP02 | 1 | 1 | 0.289645 | 0.00561 | 5.889325 | 0.420548 | 0.149728 | 0.005952 | 3.434665 | 0.065384 | 1639.5 | 28 | 1957 | 61.6 | 2337.3 | 67.5 | 2.01 | 30079 | 15817 | 17182 |
| | 2 | 1 | 0.424814 | 0.007666 | 11.1168 | 0.748889 | 0.194552 | 0.006698 | 2.339809 | 0.043045 | 2282.1 | 34.8 | 2532.3 | 64.2 | 2779.4 | 56.1 | 1.56 | 2012 | 1302 | 2224 |
| | 3 | 1 | 0.517897 | 0.009081 | 12.074991 | 0.781681 | 0.172151 | 0.005402 | 1.920635 | 0.03382 | 2689.8 | 38.6 | 2609.8 | 61.5 | 2577.3 | 52.6 | 5.15 | 2359 | 488 | 1180 |
| | 4 | 1 | 0.47648 | 0.007681 | 12.2587 | 0.807619 | 0.190418 | 0.006014 | 2.087958 | 0.033486 | 2511.5 | 33.5 | 2623.2 | 62.4 | 2744.1 | 52.3 | 4.25 | 1616 | 371 | 763 |
| | 5 | 1 | 0.493838 | 0.010235 | 13.041322 | 0.849699 | 0.19662 | 0.006076 | 2.018098 | 0.040949 | 2586.3 | 44 | 2681.8 | 61.1 | 2797.1 | 50.3 | 1.02 | 1221 | 1178 | 1821 |
| | 6 | 1 | 0.369263 | 0.01455 | 8.848236 | 0.670507 | 0.177961 | 0.005518 | 2.732014 | 0.117701 | 2022.7 | 69.1 | 2315.4 | 73 | 2632.6 | 51.6 | 4.3 | 2838 | 760 | 1165 |
| | 7 | 1 | 0.464717 | 0.011549 | 11.583362 | 0.752046 | 0.18536 | 0.005964 | 2.149265 | 0.052693 | 2458.9 | 50.7 | 2570.6 | 60.6 | 2699.4 | 53.1 | 0.9 | 1662 | 1998 | 1058 |
| | 8 | 1 | 0.167531 | 0.007052 | 2.708841 | 0.21799 | 0.119414 | 0.004365 | 5.972776 | 0.250143 | 998.1 | 38.9 | 1328.4 | 60.4 | 1944.9 | 63.9 | 0.3 | 46755 | 156883 | 53260 |
| | 9 | 1 | 0.516163 | 0.007434 | 12.496353 | 0.802666 | 0.179915 | 0.005525 | 1.92849 | 0.028156 | 2682.6 | 31.7 | 2642.1 | 60.5 | 2650.9 | 51.1 | 3.59 | 1828 | 496 | 648 |
| | 10 | 1 | 0.201173 | 0.009715 | 5.612189 | 0.437849 | 0.207051 | 0.007488 | 5.010947 | 0.250826 | 1180.5 | 52.2 | 1913.5 | 69.8 | 2879.6 | 59.7 | 1.08 | 8840 | 8903 | 10770 |
| | 11 | 1 | 0.344073 | 0.006022 | 7.85983 | 0.505448 | 0.170178 | 0.005231 | 2.900994 | 0.051655 | 1905.9 | 28.9 | 2214.8 | 57.7 | 2558.2 | 51.2 | 3.82 | 2218 | 574 | 1468 |
| | 12 | 1 | 0.338787 | 0.014041 | 6.735459 | 0.512449 | 0.147921 | 0.004601 | 2.986366 | 0.12277 | 1877.7 | 67.5 | 2070.9 | 67.3 | 2320.6 | 53.3 | 1.42 | 10192 | 7960 | 6579 |
| | 13 | 1 | 0.245909 | 0.004491 | 5.369169 | 0.351203 | 0.162603 | 0.005329 | 4.06162 | 0.074555 | 1417.1 | 23.2 | 1879.2 | 56.4 | 2480.4 | 56.1 | 2.68 | 4909 | 1855 | 3003 |
| | 14 | 1 | 0.362871 | 0.005824 | 7.953452 | 0.514656 | 0.163091 | 0.005025 | 2.750958 | 0.044109 | 1995.5 | 27.5 | 2225.2 | 58.4 | 2486.7 | 51.7 | 2.67 | 2332 | 1003 | 814 |
| | 15 | 1 | 0.225061 | 0.00504 | 4.038543 | 0.263523 | 0.134119 | 0.004256 | 4.445879 | 0.095495 | 1308.2 | 26.4 | 1644.5 | 59.3 | 2150.7 | 55 | 5.98 | 9858 | 1546 | 3939 |
| | 17 | 1 | 0.38253 | 0.005354 | 8.854732 | 0.56775 | 0.172005 | 0.005315 | 2.60937 | 0.036251 | 2088 | 24.9 | 2322.9 | 58.6 | 2576 | 51.6 | 3.82 | 1705 | 439 | 743 |
| | 18 | 1 | 0.315022 | 0.008861 | 8.036256 | 0.550012 | 0.189456 | 0.005806 | 3.186626 | 0.087788 | 1764.2 | 43.3 | 2232.7 | 60.5 | 2736.3 | 50.4 | 1.1 | 3959 | 3567 | 4661 |
| | 19 | 1 | 0.339179 | 0.010636 | 8.505107 | 0.596458 | 0.186029 | 0.005668 | 2.967183 | 0.098103 | 1881 | 51.5 | 2283 | 65.4 | 2706.3 | 50.3 | 3.18 | 3440 | 1064 | 3108 |
| | 20 | 1 | 0.392731 | 0.005883 | 8.624727 | 0.556734 | 0.162424 | 0.005046 | 2.543401 | 0.038056 | 2135.3 | 27.2 | 2298.7 | 58.5 | 2479.6 | 53.1 | 1.44 | 4918 | 3458 | 3929 |
| | 21 | 1 | 0.501028 | 0.009702 | 11.612991 | 0.755915 | 0.171156 | 0.005742 | 1.995479 | 0.038814 | 2617.8 | 41.7 | 2573.4 | 60.7 | 2567.2 | 55.2 | 4.04 | 3097 | 753 | 1264 |
| | 22 | 1 | 0.448797 | 0.010638 | 10.076265 | 0.744219 | 0.164204 | 0.005667 | 2.234428 | 0.052537 | 2388.7 | 47.2 | 2436.3 | 67 | 2495.9 | 57.3 | 4 | 4150 | 929 | 1835 |
| | 23 | 1 | 0.498291 | 0.010879 | 14.736624 | 0.980807 | 0.216403 | 0.00672 | 2.008006 | 0.044315 | 2605.8 | 46.9 | 2797.5 | 63.7 | 2953.1 | 49.8 | 10.55 | 2773 | 275 | 2326 |
| | 24 | 1 | 0.308893 | 0.008114 | 8.172609 | 0.550586 | 0.193672 | 0.005975 | 3.251785 | 0.089998 | 1734.3 | 40.2 | 2248.4 | 62.3 | 2772.3 | 50.8 | 2 | 2005 | 991 | 2585 |
| | 25 | 1 | 0.249274 | 0.007613 | 4.907223 | 0.372028 | 0.14327 | 0.00484 | 4.041087 | 0.136181 | 1433.7 | 39.6 | 1797.4 | 68 | 2263.9 | 59.4 | 3.13 | 7098 | 3144 | 1899 |
| | 26 | 1 | 0.374856 | 0.006483 | 9.648645 | 0.629363 | 0.187215 | 0.005833 | 2.669258 | 0.046268 | 2051.8 | 30.4 | 2401 | 59.9 | 2716.4 | 51.8 | 1.16 | 1288 | 1092 | 1242 |
| | 27 | 1 | 0.311721 | 0.004768 | 6.809366 | 0.439373 | 0.158758 | 0.004891 | 3.207309 | 0.048658 | 1749 | 23.4 | 2086.6 | 57 | 2441.4 | 52.3 | 4.23 | 2042 | 488 | 477 |
| | 28 | 1 | 0.338817 | 0.008415 | 6.655797 | 0.471426 | 0.142617 | 0.004633 | 2.9463 | 0.066249 | 1880 | 40.6 | 2063.2 | 62.5 | 2256.9 | 56.1 | 1.36 | 4829 | 4197 | 2913 |
| | 29 | 1 | 0.17709 | 0.00653 | 3.965799 | 0.2807 | 0.163087 | 0.005838 | 5.70738 | 0.20605 | 1050.2 | 35.7 | 1624.4 | 56 | 2483.7 | 58.6 | 2.17 | 7046 | 3446 | 6299 |
| | 30 | 1 | 0.194598 | 0.004731 | 5.03329 | 0.329511 | 0.187742 | 0.005863 | 5.159258 | 0.134092 | 1145.9 | 25.7 | 1824.1 | 56.1 | 2721 | 50.5 | 2.29 | 2462 | 1081 | 2005 |
| LP03 | 1 | 1 | 0.501155 | 0.007352 | 12.083997 | 0.779738 | 0.173921 | 0.005312 | 2.001134 | 0.029342 | 2618.5 | 31.6 | 2610.5 | 61.3 | 2594.6 | 50.7 | 0.93 | 1217 | 1199 | 1513 |
| | 2 | 1 | 0.326643 | 0.00897 | 7.705713 | 0.560495 | 0.168316 | 0.005871 | 3.073462 | 0.082823 | 1821.7 | 43.5 | 2195.6 | 64.4 | 2539.1 | 58.6 | 1.32 | 1478 | 1048 | 2201 |
| | 3 | 1 | 0.435056 | 0.0066 | 10.250983 | 0.661713 | 0.169682 | 0.005221 | 2.304198 | 0.035211 | 2328.2 | 29.7 | 2459.8 | 52.6 | 2553.3 | 51.6 | 2.08 | 1494 | 674 | 681 |
| | 4 | 1 | 0.471653 | 0.006365 | 11.459022 | 0.736093 | 0.17464 | 0.005405 | 2.123828 | 0.028714 | 2490.7 | 27.9 | 2560.9 | 60.5 | 2601.3 | 51.4 | 4.34 | 912 | 203 | 293 |
| | 5 | 1 | 0.272154 | 0.007404 | 6.699886 | 0.466152 | 0.176334 | 0.00569 | 3.699987 | 0.104404 | 1550.9 | 37.6 | 2069.7 | 62.2 | 2616.6 | 53.8 | 0.57 | 519 | 888 | 310 |
| | 6 | 1 | 0.269971 | 0.004894 | 5.67683 | 0.372945 | 0.150569 | 0.004667 | 3.713506 | 0.067877 | 1540.4 | 24.9 | 1930.5 | 50.7 | 2351 | 53.3 | 2.05 | 2311 | 1124 | 877 |
| | 7 | 1 | 0.44448 | 0.009314 | 11.249238 | 0.778477 | 0.180938 | 0.005865 | 2.257082 | 0.045972 | 2369.8 | 41.4 | 2541 | 63.6 | 2659.3 | 53.7 | 0.51 | 1010 | 1946 | 2176 |
| | 8 | 1 | 0.527388 | 0.009479 | 12.77144 | 0.822959 | 0.173869 | 0.005562 | 1.898614 | 0.033283 | 2730 | 39.8 | 2662.7 | 60.5 | 2593.7 | 53.4 | 1.38 | 435 | 310 | 427 |
| | 9 | 1 | 0.232079 | 0.00546 | 4.745089 | 0.317654 | 0.146327 | 0.00465 | 4.325412 | 0.101591 | 1344.9 | 28.5 | 1773.8 | 56.8 | 2301.6 | 54.4 | 1.87 | 1702 | 901 | 1144 |
| | 10 | 1 | 0.14497 | 0.005175 | 2.588605 | 0.206159 | 0.12815 | 0.004438 | 6.922701 | 0.245481 | 872.5 | 29.1 | 1295.3 | 58 | 2070.8 | 61.5 | 0.84 | 4226 | 5048 | 2366 |
| | 11 | 1 | 0.515277 | 0.007813 | 12.456973 | 0.800244 | 0.173194 | 0.005271 | 1.937691 | 0.029529 | 2678.9 | 33.3 | 2639.3 | 60.5 | 2587.8 | 50.9 | 4.79 | 1109 | 237 | 370 |
| | 12 | 1 | 0.494336 | 0.009393 | 12.460681 | 0.817947 | 0.181876 | 0.00579 | 2.020563 | 0.037961 | 2589 | 40.4 | 2639.1 | 61.6 | 2668.7 | 52.3 | 1.07 | 1184 | 1127 | 2265 |
| | 13 | 1 | 0.448359 | 0.011238 | 10.964926 | 0.74933 | 0.174049 | 0.006031 | 2.228212 | 0.055207 | 2387.4 | 49.9 | 2519.2 | 64.5 | 2595.2 | 57.1 | 1.29 | 687 | 544 | 817 |
| | 14 | 1 | 0.711082 | 0.011164 | 28.248723 | 1.839539 | 0.282994 | 0.008721 | 1.403014 | 0.022068 | 3462.2 | 42.1 | 3427.3 | 63.8 | 3378.6 | 48 | 1.72 | 1935 | 1194 | 2596 |
| | 15 | 1 | 0.478229 | 0.007152 | 11.79377 | 0.7596 | 0.176478 | 0.005478 | 2.086368 | 0.030856 | 2519.3 | 31.1 | 2587.8 | 60.4 | 2618.7 | 51.9 | 0.8 | 1033 | 1314 | 1896 |
| | 17 | 1 | 0.528527 | 0.008574 | 12.925647 | 0.837461 | 0.174885 | 0.005528 | 1.885491 | 0.030868 | 2735 | 36.2 | 2673.9 | 61.7 | 2603.7 | 52.8 | 0.93 | 671 | 710 | 991 |
| | 18 | 1 | 0.425661 | 0.00619 | 9.870789 | 0.63665 | 0.166269 | 0.005105 | 2.342819 | 0.034356 | 2285.9 | 28 | 2422.3 | 59.5 | 2519.2 | 51.9 | 0.4 | 2238 | 5730 | 5997 |
| | 19 | 1 | 0.328703 | 0.0062 | 7.812043 | 0.508926 | 0.17035 | 0.005302 | 3.037518 | 0.058635 | 1831.7 | 30.1 | 2212 | 52.2 | 2559.7 | 51.5 | 0.79 | 1036 | 1321 | 1133 |
| | 20 | 1 | 0.368987 | 0.01506 | 9.171645 | 0.713597 | 0.17792 | 0.005606 | 2.739748 | 0.110532 | 2021.2 | 70.7 | 2347.3 | 70.5 | 2631.9 | 51.8 | 0.95 | 881 | 955 | 1069 |

Continued on next page

| Sample | Spot name | Run | 206/238 | ±2SE | 207/235 | ±2SE | 207/206 | ±2SE | 238/P206 | ±2SE | 206/238 Age | ±2SE | 207/235 Age | ±2SE | 207/206 Age | ±2SE | U/Th | U | Th | Pb |
|---|---|---|---|---|---|---|---|---|---|---|---|---|---|---|---|---|---|---|---|---|
| | 21 | 1 | 0.302693 | 0.006012 | 8.266061 | 0.538202 | 0.19754 | 0.006204 | 3.292872 | 0.068444 | 1704.2 | 29.9 | 2259.9 | 59.5 | 2804.4 | 51.6 | 1.77 | 1087 | 633 | 896 |
| | 22 | 1 | 0.475448 | 0.009537 | 11.323775 | 0.760466 | 0.172711 | 0.00535 | 2.09592 | 0.043023 | 2506.6 | 41.8 | 2548.2 | 64.2 | 2582.8 | 51.8 | 0.89 | 876 | 938 | 1033 |
| | 23 | 1 | 0.425535 | 0.008033 | 10.320212 | 0.674779 | 0.175801 | 0.005383 | 2.340097 | 0.043738 | 2285 | 36.3 | 2463 | 60.4 | 2612.5 | 51.1 | 2.01 | 1059 | 517 | 728 |
| | 24 | 1 | 0.459572 | 0.011224 | 11.016575 | 0.756114 | 0.173851 | 0.005372 | 2.171234 | 0.052377 | 2436.3 | 49.4 | 2521.9 | 63.4 | 2593.8 | 51.8 | 1.26 | 1328 | 1020 | 1417 |
| | 25 | 1 | 0.495816 | 0.010952 | 11.931321 | 0.804983 | 0.174797 | 0.005411 | 2.010317 | 0.045225 | 2594.6 | 47.3 | 2596.9 | 63.5 | 2602.8 | 51.5 | 1.34 | 846 | 630 | 833 |
| | 26 | 1 | 0.517775 | 0.007509 | 12.849549 | 0.82972 | 0.180032 | 0.005689 | 1.919517 | 0.02722 | 2689.5 | 31.8 | 2668.2 | 60.9 | 2651.5 | 52.9 | 1.14 | 540 | 461 | 712 |
| | 27 | 1 | 0.407797 | 0.007527 | 9.12089 | 0.59201 | 0.163044 | 0.004994 | 2.439979 | 0.045546 | 2204.3 | 34.5 | 2349.5 | 59.9 | 2486.3 | 51.7 | 1.9 | 2027 | 1061 | 1275 |
| | 28 | 1 | 0.312944 | 0.011513 | 7.29126 | 0.593005 | 0.169274 | 0.006063 | 3.2106 | 0.12066 | 1753.1 | 56.6 | 2138.3 | 71.7 | 2546.2 | 58.6 | 0.7 | 882 | 1223 | 1032 |
| | 29 | 1 | 0.226423 | 0.011303 | 4.597943 | 0.415827 | 0.14748 | 0.005196 | 4.477701 | 0.208246 | 1313.3 | 58.9 | 1736.2 | 72.2 | 2312.8 | 59.9 | 2.51 | 2507 | 1011 | 1351 |
| | 30 | 1 | 0.380779 | 0.00862 | 8.736926 | 0.573772 | 0.167269 | 0.00512 | 2.615359 | 0.059205 | 2079.2 | 40.2 | 2310 | 59.7 | 2529.4 | 51.3 | 1.37 | 1166 | 843 | 1816 |
| LP04 | 1 | 1 | 0.475409 | 0.0084 | 11.57126 | 0.755884 | 0.176575 | 0.005434 | 2.108838 | 0.038034 | 2506.7 | 36.8 | 2569.5 | 60.9 | 2619.7 | 50.9 | 1.05 | 379 | 366 | 569 |
| | 2 | 1 | 0.478327 | 0.006979 | 11.834762 | 0.762283 | 0.179446 | 0.005526 | 2.094038 | 0.03047 | 2519.7 | 30.4 | 2591 | 60.2 | 2646.5 | 51 | 1.04 | 448 | 466 | 743 |
| | 3 | 1 | 0.430149 | 0.006884 | 10.147871 | 0.662472 | 0.170213 | 0.005521 | 2.327946 | 0.037571 | 2306.3 | 31.1 | 2448 | 60.6 | 2558.4 | 54.1 | 1.34 | 532 | 380 | 519 |
| | 4 | 1 | 0.245528 | 0.004433 | 5.887242 | 0.398618 | 0.174089 | 0.006046 | 4.082282 | 0.073148 | 1415.2 | 22.9 | 1958 | 57.6 | 2594.5 | 56.8 | 3.45 | 1462 | 422 | 1419 |
| | 5 | 1 | 0.372099 | 0.007673 | 8.311272 | 0.558528 | 0.161739 | 0.004942 | 2.697439 | 0.056241 | 2038.6 | 36.1 | 2263.7 | 61.2 | 2472.8 | 51.5 | 2.24 | 2089 | 1293 | 1775 |
| | 6 | 1 | 0.388342 | 0.014467 | 10.181994 | 0.668572 | 0.192339 | 0.007951 | 2.607043 | 0.093484 | 2112.2 | 66.7 | 2454.3 | 67.5 | 2754.4 | 66.6 | 0.61 | 1076 | 8462 | 1823 |
| | 7 | 1 | 0.357955 | 0.005319 | 8.422593 | 0.541348 | 0.170553 | 0.005557 | 2.798221 | 0.041844 | 1972.3 | 25.3 | 2277.3 | 58.2 | 2560.8 | 53.5 | 1.06 | 1570 | 1577 | 2793 |
| | 8 | 1 | 0.478269 | 0.006821 | 12.09832 | 0.780183 | 0.182418 | 0.005564 | 2.093024 | 0.030008 | 2519.6 | 29.8 | 2611.8 | 60.3 | 2674.1 | 50.2 | 1.24 | 1043 | 937 | 1764 |
| | 9 | 1 | 0.444438 | 0.009161 | 11.351451 | 0.754619 | 0.184365 | 0.005722 | 2.255173 | 0.045238 | 2370 | 40.7 | 2551.5 | 62.6 | 2691.4 | 51.4 | 1.51 | 1122 | 834 | 1824 |
| | 10 | 1 | 0.136305 | 0.011415 | 2.416823 | 0.307579 | 0.126596 | 0.005281 | 7.5929 | 0.59956 | 822.1 | 64.3 | 1232.4 | 87.3 | 2045.9 | 72 | 0.5 | 8875 | 22696 | 6255 |
| | 11 | 1 | 0.277397 | 0.010188 | 7.357197 | 0.512599 | 0.192505 | 0.006527 | 3.638799 | 0.130244 | 1576.5 | 51.2 | 2152.8 | 62.2 | 2760.6 | 56.2 | 1.05 | 10806 | 156082 | 290484 |
| | 12 | 1 | 0.384991 | 0.012845 | 10.524323 | 0.721311 | 0.197197 | 0.006238 | 2.602969 | 0.08979 | 2098.5 | 60 | 2480.8 | 64.9 | 2802 | 51.4 | 1.33 | 5090 | 3829 | 7520 |
| | 13 | 1 | 0.349586 | 0.007737 | 9.513309 | 0.651589 | 0.197907 | 0.006449 | 2.855846 | 0.062793 | 1932.4 | 36.9 | 2388 | 62.9 | 2807.8 | 53.4 | 0.76 | 14065 | 18467 | 6050 |
| | 14 | 1 | 0.443393 | 0.008648 | 10.492958 | 0.676501 | 0.171416 | 0.005289 | 2.253231 | 0.044287 | 2365.1 | 38.6 | 2478.9 | 59.9 | 2570.2 | 51.4 | 0.58 | 3464 | 5944 | 14113 |
| | 15 | 1 | 0.39181 | 0.007959 | 9.865837 | 0.645911 | 0.18181 | 0.005539 | 2.546635 | 0.052328 | 2130.8 | 36.9 | 2421.8 | 60.6 | 2668.5 | 50.4 | 2.27 | 1602 | 706 | 1777 |
| | 16 | 1 | 0.43241 | 0.022873 | 11.448049 | 0.990758 | 0.190915 | 0.006038 | 2.370125 | 0.141903 | 2309 | 104.5 | 2545.1 | 85.9 | 2748.4 | 52.6 | 0.92 | 1545 | 1683 | 2180 |
| | 17 | 1 | 0.227534 | 0.008474 | 5.841257 | 0.451626 | 0.18521 | 0.00593 | 4.434219 | 0.187939 | 1320.2 | 45 | 1945.1 | 71.9 | 2698.1 | 53.4 | 1.21 | 2424 | 1998 | 3748 |
| | 18 | 1 | 0.24164 | 0.0039 | 6.271915 | 0.406135 | 0.187094 | 0.005749 | 4.119455 | 0.066853 | 1395.2 | 20.3 | 2014.3 | 56.7 | 2715.8 | 50.4 | 3.39 | 1501 | 443 | 1849 |
| | 19 | 1 | 0.274114 | 0.011509 | 6.937286 | 0.489789 | 0.182897 | 0.00607 | 3.657281 | 0.152813 | 1560.4 | 58.2 | 2101.6 | 62.2 | 2677.6 | 55 | 1.79 | 711 | 398 | 693 |
| | 20 | 1 | 0.298311 | 0.009775 | 7.656954 | 0.533179 | 0.18593 | 0.005729 | 3.362768 | 0.113553 | 1681.4 | 48.6 | 2188.5 | 63.3 | 2705.2 | 51.2 | 1.82 | 533 | 293 | 417 |
| LP10 | 1 | 1 | 0.537531 | 0.0131 | 16.006518 | 1.083502 | 0.215603 | 0.006633 | 1.852347 | 0.047143 | 2771.4 | 55.3 | 2874.8 | 66.1 | 2947 | 49.9 | 1.61 | 1666 | 988 | 1248 |
| | 2 | 1 | 0.417478 | 0.014089 | 11.560888 | 0.906547 | 0.199585 | 0.006602 | 2.395062 | 0.076843 | 2246.4 | 63.5 | 2561.4 | 70.2 | 2820.3 | 52.9 | 1.84 | 2055 | 1034 | 1252 |
| | 3 | 1 | 0.489384 | 0.008675 | 14.020071 | 0.908062 | 0.206553 | 0.006524 | 2.026252 | 0.036337 | 2567.7 | 37.6 | 2750.7 | 61.2 | 2877.4 | 51.7 | 1.85 | 1287 | 648 | 810 |
| | 4 | 1 | 0.504548 | 0.007812 | 12.190235 | 0.789046 | 0.174622 | 0.005579 | 1.964726 | 0.030149 | 2633 | 33.4 | 2618.6 | 60.6 | 2600.5 | 53.3 | 0.77 | 420 | 510 | 648 |
| | 5 | 1 | 0.381714 | 0.005795 | 9.980466 | 0.647756 | 0.189176 | 0.005828 | 2.596081 | 0.039536 | 2084.1 | 27 | 2432.3 | 60 | 2733.8 | 51 | 1.44 | 1852 | 1213 | 1223 |
| | 6 | 1 | 0.524417 | 0.008633 | 15.11156 | 0.980159 | 0.208899 | 0.006704 | 1.888498 | 0.030918 | 2717.7 | 36.5 | 2822 | 62 | 2895.8 | 52.6 | 2.3 | 1570 | 657 | 850 |
| | 7 | 1 | 0.31713 | 0.010048 | 7.79848 | 0.546807 | 0.178242 | 0.00573 | 3.129878 | 0.098445 | 1775.1 | 49.1 | 2206.8 | 63.2 | 2635.4 | 53.6 | 1.32 | 2314 | 1722 | 1122 |
| | 8 | 1 | 0.602217 | 0.01184 | 19.421444 | 1.268349 | 0.232507 | 0.007191 | 1.646767 | 0.032801 | 3037.7 | 47.7 | 3062 | 64 | 3068.1 | 49.6 | 1.19 | 879 | 740 | 1097 |
| | 9 | 1 | 0.391815 | 0.006588 | 10.384915 | 0.670634 | 0.19099 | 0.005928 | 2.527941 | 0.043078 | 2130.9 | 30.6 | 2469.2 | 60 | 2749.3 | 51.6 | 2.81 | 1084 | 390 | 406 |
| | 10 | 1 | 0.457358 | 0.012321 | 13.14079 | 0.928604 | 0.206589 | 0.00644 | 2.174146 | 0.058102 | 2426.1 | 54.4 | 2686 | 65.7 | 2877.6 | 50.4 | 1.74 | 2054 | 1215 | 1630 |
| | 11 | 1 | 0.868233 | 0.038436 | 34.003075 | 2.981082 | 0.28094 | 0.010177 | 1.143693 | 0.051386 | 4025.1 | 132.9 | 3604.8 | 87.8 | 3366.4 | 56.9 | 1.6 | 944 | 634 | 3026 |
| | 12 | 1 | 0.219734 | 0.003879 | 4.246803 | 0.282001 | 0.138834 | 0.00436 | 4.500753 | 0.078981 | 1280.3 | 20.5 | 1682 | 54.7 | 2211 | 54.7 | 1.64 | 2698 | 1760 | 1077 |
| | 13 | 1 | 0.260576 | 0.008319 | 5.664278 | 0.440331 | 0.155597 | 0.005242 | 3.819672 | 0.118756 | 1491.6 | 42.4 | 1919.1 | 66.1 | 2405.3 | 56.9 | 1.79 | 2137 | 1320 | 767 |
| | 14 | 1 | 0.381137 | 0.008456 | 10.314553 | 0.728325 | 0.195614 | 0.007245 | 2.592205 | 0.057817 | 2081.4 | 39.5 | 2462.4 | 65.4 | 2788.1 | 60.8 | 2.21 | 1354 | 662 | 884 |
| | 15 | 1 | 0.239441 | 0.005391 | 5.001713 | 0.33224 | 0.15045 | 0.005461 | 4.136313 | 0.091683 | 1383.4 | 28 | 1818.4 | 55.8 | 2346.3 | 60.6 | 2.35 | 1880 | 877 | 737 |
| | 16 | 1 | 0.370181 | 0.005893 | 9.496883 | 0.616715 | 0.184447 | 0.00572 | 2.668886 | 0.04209 | 2030 | 27.7 | 2386.6 | 59.5 | 2691.9 | 51.1 | 4.94 | 1757 | 381 | 367 |
| | 17 | 1 | 0.44033 | 0.010418 | 12.25745 | 0.83115 | 0.200076 | 0.006165 | 2.250899 | 0.058044 | 2350.9 | 47.2 | 2621.9 | 66.7 | 2825.6 | 51 | 1.43 | 1720 | 1294 | 1325 |
| | 18 | 1 | 0.236847 | 0.005522 | 4.535428 | 0.337419 | 0.137056 | 0.00516 | 4.174933 | 0.09637 | 1370 | 28.7 | 1734.9 | 60 | 2186.8 | 63.9 | 1.51 | 2044 | 1444 | 900 |
| | 19 | 1 | 0.558794 | 0.017576 | 16.992127 | 1.251946 | 0.218313 | 0.007078 | 1.781238 | 0.060422 | 2858.2 | 73.6 | 2928.1 | 73.7 | 2966.2 | 52.5 | 1.25 | 895 | 769 | 998 |
| | 20 | 1 | 0.48512 | 0.013688 | 13.838117 | 0.979213 | 0.205059 | 0.006469 | 2.046924 | 0.059287 | 2547.4 | 59.6 | 2734.6 | 67.4 | 2865.3 | 51.1 | 3.2 | 1654 | 546 | 652 |
| | 21 | 1 | 0.453786 | 0.013245 | 13.647996 | 0.972378 | 0.216797 | 0.006935 | 2.190339 | 0.068306 | 2409.9 | 59.3 | 2721.2 | 68.4 | 2955.2 | 51.1 | 5.47 | 1125 | 207 | 374 |
| | 22 | 1 | 0.369354 | 0.006214 | 8.993154 | 0.585415 | 0.175258 | 0.00569 | 2.67405 | 0.044643 | 2026.2 | 29.2 | 2336.9 | 59.9 | 2606.9 | 53.8 | 1.88 | 1599 | 858 | 842 |
| | 23 | 1 | 0.358637 | 0.005891 | 8.722531 | 0.574829 | 0.17633 | 0.005703 | 2.753534 | 0.045377 | 1975.6 | 28 | 2308.9 | 60 | 2617.2 | 53.8 | 4.36 | 2110 | 494 | 372 |
| | 24 | 1 | 0.492614 | 0.011909 | 14.030634 | 0.954265 | 0.205667 | 0.006336 | 2.012817 | 0.05207 | 2580.5 | 51.9 | 2749.3 | 66.2 | 2870.5 | 50.2 | 2.67 | 942 | 347 | 438 |

Continued on next page

| Sample | Spot name | Run | 206/238 | ±2SE | 207/235 | ±2SE | 207/206 | ±2SE | 238/P206 | ±2SE | 206/238 Age | ±2SE | 207/235 Age | ±2SE | 207/206 Age | ±2SE | U/Th | U | Th | Pb |
|---|---|---|---|---|---|---|---|---|---|---|---|---|---|---|---|---|---|---|---|---|
| | 25 | 1 | 0.308556 | 0.009872 | 7.643221 | 0.535175 | 0.179923 | 0.005902 | 3.210449 | 0.107694 | 1733 | 48.9 | 2188.6 | 64.9 | 2650.8 | 54.1 | 1.23 | 2067 | 1673 | 1479 |
| | 26 | 1 | 0.383502 | 0.011967 | 10.231156 | 0.801863 | 0.193683 | 0.007285 | 2.580888 | 0.080336 | 2092 | 55.7 | 2453.2 | 73.7 | 2771.5 | 61.8 | 1.73 | 1282 | 727 | 704 |
| | 27 | 1 | 0.287267 | 0.004192 | 6.280679 | 0.412107 | 0.158108 | 0.005096 | 3.439935 | 0.050274 | 1627.7 | 21 | 2014.9 | 56.9 | 2433.4 | 54.4 | 3.73 | 1622 | 432 | 397 |
| | 28 | 1 | 0.302877 | 0.01166 | 8.460246 | 0.603605 | 0.201816 | 0.006579 | 3.300759 | 0.12086 | 1703.4 | 57.3 | 2277.8 | 63.5 | 2838.8 | 51.8 | 1.81 | 2069 | 1131 | 1462 |
| | 29 | 1 | 0.561376 | 0.008697 | 16.526665 | 1.073697 | 0.213063 | 0.006493 | 1.761366 | 0.027316 | 2871.9 | 35.9 | 2907 | 62.8 | 2928 | 49.2 | 1.09 | 916 | 831 | 1157 |
| | 30 | 1 | 0.299461 | 0.004044 | 7.295817 | 0.467829 | 0.176448 | 0.005399 | 3.300792 | 0.044381 | 1688.6 | 20.1 | 2148.1 | 57.4 | 2618.6 | 50.8 | 2.03 | 1941 | 954 | 867 |
| LP11 | 1 | 1 | 0.555427 | 0.011535 | 16.269356 | 1.091803 | 0.212396 | 0.006628 | 1.806198 | 0.037829 | 2846.6 | 47.9 | 2890.8 | 65.1 | 2922.5 | 50.5 | 2.51 | 607 | 247 | 602 |
| | 2 | 1 | 0.507672 | 0.015119 | 14.594182 | 1.056022 | 0.208529 | 0.006484 | 1.983695 | 0.056176 | 2644.1 | 64.1 | 2784.3 | 66.6 | 2892.8 | 50.6 | 3.23 | 908 | 297 | 713 |
| | 3 | 1 | 0.411277 | 0.01758 | 11.502155 | 0.971235 | 0.202302 | 0.006773 | 2.471131 | 0.105627 | 2216.4 | 80.1 | 2552.1 | 79.5 | 2842.1 | 55 | 2.37 | 1838 | 827 | 1483 |
| | 4 | 1 | 0.555413 | 0.01213 | 16.873273 | 1.129835 | 0.22128 | 0.006892 | 1.806335 | 0.039594 | 2846.3 | 50.3 | 2925.8 | 64.4 | 2988.7 | 50.1 | 1.83 | 1101 | 655 | 1651 |
| | 5 | 1 | 0.488518 | 0.015604 | 14.46801 | 1.090368 | 0.215417 | 0.006954 | 2.063686 | 0.06468 | 2561.4 | 67.3 | 2774.1 | 70.8 | 2944.8 | 52.4 | 1.77 | 1112 | 695 | 1482 |
| | 6 | 1 | 0.508376 | 0.01058 | 14.455779 | 0.975711 | 0.208899 | 0.006906 | 1.967901 | 0.041521 | 2649.4 | 45.3 | 2779.6 | 65.5 | 2895.9 | 54.1 | 2.96 | 1257 | 479 | 1128 |
| | 7 | 1 | 0.458794 | 0.010906 | 12.522823 | 0.842309 | 0.199575 | 0.006093 | 2.187754 | 0.052432 | 2432.9 | 48.2 | 2642.5 | 63.1 | 2821.6 | 49.9 | 2.43 | 1203 | 562 | 1114 |
| | 8 | 1 | 0.407545 | 0.008459 | 10.991114 | 0.732205 | 0.198525 | 0.006462 | 2.454441 | 0.050301 | 2203.5 | 38.7 | 2521.9 | 61.9 | 2813 | 52.8 | 1.98 | 1388 | 797 | 1291 |
| | 9 | 1 | 0.468504 | 0.014738 | 12.972683 | 0.97596 | 0.202422 | 0.006695 | 2.149621 | 0.064395 | 2474.4 | 64.1 | 2671.3 | 68.5 | 2843.3 | 53.1 | 1.44 | 1090 | 873 | 1356 |
| | 10 | 1 | 0.57889 | 0.009437 | 17.522556 | 1.130571 | 0.222133 | 0.006886 | 1.728235 | 0.028386 | 2943.7 | 38.6 | 2963.4 | 61.8 | 2994.9 | 49.6 | 1.61 | 1657 | 1152 | 1969 |
| | 11 | 1 | 0.151181 | 0.005693 | 2.189151 | 0.196218 | 0.105674 | 0.004542 | 6.693332 | 0.276891 | 906.9 | 32 | 1168 | 65.3 | 1714.7 | 80.8 | 15.05 | 3300 | 224 | 161 |
| | 12 | 1 | 0.178105 | 0.00528 | 2.749075 | 0.20213 | 0.113521 | 0.003728 | 5.650409 | 0.190169 | 1056.1 | 29.1 | 1338.1 | 57.1 | 1853.8 | 59.8 | 18.84 | 3417 | 183 | 160 |
| | 13 | 1 | 0.103536 | 0.002437 | 1.20245 | 0.091471 | 0.085905 | 0.003382 | 9.657963 | 0.229461 | 635.1 | 14.2 | 800.7 | 41.6 | 1332 | 74.9 | 11.99 | 5673 | 465 | 290 |
| | 14 | 1 | 0.586188 | 0.012208 | 17.930392 | 1.175205 | 0.226762 | 0.007609 | 1.704557 | 0.034799 | 2973.5 | 49.4 | 2985.6 | 62.4 | 3027.9 | 54.1 | 2.1 | 968 | 455 | 560 |
| | 15 | 1 | 0.472122 | 0.017738 | 12.982958 | 1.014062 | 0.202157 | 0.006692 | 2.141168 | 0.084752 | 2488.8 | 78.2 | 2669.5 | 75.9 | 2841.2 | 54.1 | 2.84 | 1349 | 496 | 510 |
| | 16 | 1 | 0.55914 | 0.009699 | 16.480206 | 1.090026 | 0.217203 | 0.006737 | 1.7876 | 0.031147 | 2862.4 | 40.1 | 2903.7 | 63.7 | 2958.7 | 50.2 | 2.09 | 856 | 410 | 589 |
| | 17 | 1 | 0.460973 | 0.008872 | 13.416914 | 0.877868 | 0.214643 | 0.00672 | 2.169429 | 0.041537 | 2443.1 | 39.1 | 2708.5 | 61.5 | 2939.5 | 50.8 | 1.98 | 1243 | 653 | 707 |
| | 18 | 1 | 0.563252 | 0.00865 | 16.288029 | 1.05093 | 0.213188 | 0.006639 | 1.773004 | 0.026939 | 2879.7 | 35.6 | 2893.4 | 61.4 | 2928.5 | 51.1 | 1.48 | 478 | 334 | 453 |
| | 19 | 1 | 0.471363 | 0.010504 | 13.044221 | 0.881464 | 0.203803 | 0.006296 | 2.123708 | 0.047866 | 2488.4 | 46.1 | 2680.7 | 64.3 | 2855.6 | 50.3 | 1.7 | 1642 | 991 | 1207 |
| | 20 | 1 | 0.247659 | 0.004743 | 5.680474 | 0.383446 | 0.168869 | 0.005532 | 4.035975 | 0.075068 | 1426.1 | 24.4 | 1926.7 | 57.3 | 2544.1 | 54.8 | 1.9 | 3704 | 2013 | 1688 |
| | 21 | 1 | 0.524135 | 0.008334 | 15.30012 | 0.995286 | 0.214203 | 0.006671 | 1.902222 | 0.030463 | 2716.3 | 35.3 | 2833.3 | 61.8 | 2936.2 | 50.3 | 2.07 | 999 | 528 | 786 |
| | 22 | 1 | 0.423211 | 0.00729 | 11.523742 | 0.765461 | 0.199569 | 0.006361 | 2.356181 | 0.041112 | 2274.6 | 33.1 | 2565 | 62.1 | 2820.9 | 51.7 | 1.59 | 1283 | 898 | 1059 |
| | 23 | 1 | 0.187528 | 0.004789 | 4.549127 | 0.416741 | 0.177294 | 0.009848 | 5.324396 | 0.1365 | 1107.7 | 26 | 1730.7 | 79.1 | 2613.4 | 97.2 | 3.06 | 4073 | 1490 | 2580 |
| | 24 | 1 | 0.228752 | 0.004255 | 5.490699 | 0.359335 | 0.175822 | 0.005618 | 4.358714 | 0.080477 | 1327.7 | 22.3 | 1898.3 | 56.3 | 2611.9 | 52.7 | 2.02 | 2769 | 1551 | 1600 |
| | 25 | 1 | 0.503034 | 0.013421 | 15.115945 | 1.043366 | 0.219797 | 0.006949 | 1.988597 | 0.053657 | 2624.8 | 57.6 | 2819.5 | 66.5 | 2977.6 | 51.1 | 1.1 | 702 | 741 | 903 |
| | 26 | 1 | 0.573378 | 0.012877 | 17.67286 | 1.176263 | 0.225368 | 0.006958 | 1.740741 | 0.04009 | 2920.2 | 53 | 2970.4 | 64.7 | 3018.2 | 49.7 | 1.47 | 539 | 421 | 641 |
| | 27 | 1 | 0.536154 | 0.00927 | 16.037104 | 1.048996 | 0.218484 | 0.006723 | 1.857373 | 0.033113 | 2766.7 | 39.1 | 2878 | 63.1 | 2968.4 | 49.9 | 1.86 | 999 | 607 | 923 |
| | 28 | 1 | 0.469034 | 0.018892 | 12.655867 | 0.940238 | 0.197022 | 0.006137 | 2.151683 | 0.093403 | 2474.6 | 83.7 | 2648 | 72.7 | 2800.3 | 50.8 | 5.35 | 857 | 278 | 407 |
| | 29 | 1 | 0.453952 | 0.00995 | 12.845747 | 0.865573 | 0.206283 | 0.006371 | 2.19647 | 0.050572 | 2411.8 | 44.4 | 2666.3 | 64.8 | 2875.3 | 50.1 | 1.16 | 1520 | 1468 | 1676 |
| | 30 | 1 | 0.219175 | 0.008558 | 6.317234 | 0.44859 | 0.210759 | 0.007247 | 4.596707 | 0.191723 | 1276.1 | 45.5 | 2017.2 | 62.7 | 2908.1 | 55.5 | 34.31 | 3826 | 131 | 2709 |
| MA01 | 1 | 4 | 0.052411 | 0.002129 | 3.521528 | 0.107745 | 0.483872 | 0.012094 | 19.121477 | 0.741138 | 329.2 | 13 | 1531.1 | 24 | 4190 | 37.5 | 3.73 | 28790 | 7426 | 17327 |
| | 2 | 4 | 0.096495 | 0.004085 | 4.784704 | 0.173959 | 0.356093 | 0.008221 | 10.404859 | 0.439833 | 593.6 | 24 | 1779.8 | 30.9 | 3731.1 | 35.7 | 9.93 | 8930 | 910 | 5776 |
| | 3 | 4 | 0.107319 | 0.004298 | 2.749701 | 0.158322 | 0.184368 | 0.005312 | 9.289564 | 0.367204 | 657 | 25 | 1339.1 | 42.6 | 2690 | 47.6 | 13.93 | 13675 | 981 | 4519 |
| | 4 | 4 | 0.162525 | 0.004926 | 11.355456 | 0.41326 | 0.499547 | 0.012588 | 6.129268 | 0.183033 | 970.6 | 27.3 | 2549.7 | 34.7 | 4237 | 37.8 | 0.27 | 7563 | 30276 | 14592 |
| | 5 | 4 | 0.240569 | 0.006684 | 12.577219 | 0.390336 | 0.374095 | 0.008507 | 4.136633 | 0.114332 | 1389.5 | 34.7 | 2647 | 29 | 3806.1 | 34.2 | 17.87 | 3715 | 210 | 7876 |
| | 6 | 4 | 0.583096 | 0.015657 | 20.710966 | 0.584909 | 0.256406 | 0.005702 | 1.705504 | 0.045831 | 2961.2 | 63.8 | 3124.8 | 27.2 | 3223.5 | 35.4 | 5.89 | 4514 | 817 | 6318 |
| | 7 | 4 | 0.489344 | 0.016475 | 19.697146 | 0.620539 | 0.287783 | 0.005672 | 2.040118 | 0.070661 | 2566.5 | 71.6 | 3075.2 | 30.7 | 3404.7 | 30.8 | 1.51 | 3018 | 2039 | 2626 |
| | 8 | 4 | 0.492879 | 0.014146 | 19.242039 | 0.582833 | 0.28044 | 0.005572 | 2.020489 | 0.059505 | 2582.8 | 61.3 | 3053.3 | 29.4 | 3364.5 | 31.1 | 1.13 | 3956 | 3563 | 3407 |
| | 9 | 4 | 0.150883 | 0.004344 | 3.785954 | 0.111027 | 0.179139 | 0.004942 | 6.601884 | 0.185563 | 905.9 | 24.3 | 1589.4 | 23.6 | 2642.6 | 45.5 | 2.22 | 7711 | 3537 | 2588 |
| | 10 | 4 | 0.218355 | 0.006198 | 9.678085 | 0.276468 | 0.318197 | 0.006494 | 4.565842 | 0.131666 | 1273 | 32.8 | 2404 | 26.3 | 3560 | 31.4 | 8.25 | 3672 | 557 | 5337 |
| | 11 | 4 | 0.302429 | 0.009022 | 14.768342 | 0.576695 | 0.358394 | 0.009488 | 3.313032 | 0.100169 | 1703.1 | 44.7 | 2798.4 | 36.4 | 3740.9 | 39.4 | 5.39 | 2470 | 450 | 5176 |
| | 12 | 4 | 0.24846 | 0.00705 | 10.918103 | 0.334457 | 0.326058 | 0.006933 | 4.03866 | 0.117309 | 1430.3 | 36.5 | 2514.7 | 28.8 | 3597.1 | 32.7 | 11.9 | 2464 | 206 | 3692 |
| | 13 | 4 | 0.273875 | 0.007818 | 15.035284 | 0.404155 | 0.406584 | 0.008096 | 3.664237 | 0.103765 | 1560.3 | 39.5 | 2817.1 | 25.7 | 3932.7 | 29.8 | 12.85 | 2472 | 188 | 6853 |
| | 14 | 4 | 0.263365 | 0.007986 | 11.662232 | 0.399925 | 0.329926 | 0.006693 | 3.819401 | 0.117022 | 1506.6 | 40.8 | 2575.3 | 31.8 | 3615.5 | 30.9 | 12.67 | 2734 | 214 | 4850 |
| | 15 | 4 | 0.171216 | 0.005188 | 5.833727 | 0.177178 | 0.254576 | 0.005721 | 5.868208 | 0.177154 | 1018.7 | 28.5 | 1950.9 | 26.1 | 3212.1 | 35.7 | 13.15 | 2821 | 210 | 2451 |
| | 16 | 4 | 0.226131 | 0.006152 | 13.183562 | 0.35994 | 0.435061 | 0.008968 | 4.44256 | 0.122577 | 1314.1 | 32.4 | 2692.2 | 25.9 | 4033.7 | 30.7 | 2.76 | 3112 | 1093 | 7272 |
| | 17 | 4 | 0.264029 | 0.007267 | 14.429201 | 0.414 | 0.406922 | 0.008473 | 3.804506 | 0.104063 | 1510.2 | 37 | 2777.4 | 26.9 | 3933.5 | 31.2 | 5.65 | 3092 | 651 | 8255 |
| | 18 | 4 | 0.15724 | 0.004706 | 8.185146 | 0.256002 | 0.382741 | 0.009411 | 6.380391 | 0.182811 | 941.4 | 26.1 | 2251.2 | 28.1 | 3841.2 | 37.4 | 4.74 | 8395 | 1740 | 12249 |

Continued on next page

| Sample | Spot name | Run | 206/238 | ±2SE | 207/235 | ±2SE | 207/206 | ±2SE | 238/P206 | ±2SE | 206/238 Age | ±2SE | 207/235 Age | ±2SE | 207/206 Age | ±2SE | U/Th | U | Th | Pb |
|---|---|---|---|---|---|---|---|---|---|---|---|---|---|---|---|---|---|---|---|---|
| | 19 | 4 | 0.18866 | 0.005742 | 7.070546 | 0.210448 | 0.276488 | 0.006017 | 5.322337 | 0.161893 | 1113.9 | 31.1 | 2119.2 | 26.5 | 3341.5 | 33.6 | 14.85 | 3212 | 213 | 3214 |
| | 20 | 4 | 0.151947 | 0.006008 | 5.335103 | 0.317761 | 0.255586 | 0.009196 | 6.637084 | 0.257308 | 911.4 | 33.5 | 1865 | 48.7 | 3210.8 | 57.7 | 3.26 | 6018 | 2039 | 3555 |
| | 22 | 4 | 0.212953 | 0.006149 | 11.153436 | 0.369803 | 0.358478 | 0.00754 | 4.656393 | 0.13449 | 1244.3 | 32.7 | 2534 | 30.8 | 3742 | 32 | 12.53 | 4196 | 345 | 6896 |
| | 23 | 4 | 0.583802 | 0.016537 | 23.336614 | 0.656119 | 0.271238 | 0.005617 | 1.696398 | 0.048888 | 2963.8 | 67.5 | 3240.5 | 27.2 | 3312.1 | 32.6 | 3.62 | 790 | 227 | 335 |
| | 24 | 4 | 0.270528 | 0.007536 | 16.159084 | 0.69824 | 0.40728 | 0.016205 | 3.661663 | 0.104464 | 1543.3 | 38.3 | 2880.8 | 41.1 | 3926.3 | 57.8 | 3.28 | 4120 | 1946 | 9840 |
| | 25 | 4 | 0.381884 | 0.015252 | 14.054737 | 0.635426 | 0.250542 | 0.005162 | 2.614446 | 0.1074 | 2082.8 | 71.4 | 2747.2 | 43.2 | 3186.8 | 32.8 | 16.24 | 3054 | 194 | 1761 |
| | 26 | 4 | 0.146486 | 0.004124 | 3.125507 | 0.112665 | 0.144966 | 0.005011 | 6.756346 | 0.188885 | 881.2 | 23.2 | 1438 | 27.6 | 2282.4 | 58 | 15.73 | 4308 | 285 | 866 |
| | 27 | 4 | 0.205815 | 0.005767 | 10.053791 | 0.31092 | 0.334385 | 0.007109 | 4.812386 | 0.137509 | 1206.3 | 30.9 | 2438.2 | 28.9 | 3635.8 | 32.6 | 17.58 | 2935 | 174 | 4920 |
| | 28 | 4 | 0.179287 | 0.005289 | 7.231029 | 0.337866 | 0.276589 | 0.009737 | 5.529318 | 0.159727 | 1062.9 | 28.9 | 2134.7 | 40.1 | 3336.1 | 52.5 | 14.38 | 2165 | 158 | 2263 |
| | 29 | 4 | 0.178448 | 0.005296 | 4.838201 | 0.156684 | 0.18829 | 0.005028 | 5.549919 | 0.156514 | 1058.4 | 28.8 | 1790.8 | 27 | 2724.8 | 43.6 | 14.51 | 3808 | 274 | 1955 |
| | 30 | 4 | 0.231729 | 0.006639 | 11.559997 | 0.392676 | 0.345287 | 0.008405 | 4.277426 | 0.120875 | 1343.3 | 34.7 | 2567.4 | 31.9 | 3683.9 | 37.7 | 15.53 | 2532 | 170 | 4521 |
| MU03 | 1 | 4 | 0.363259 | 0.011133 | 13.38306 | 0.389366 | 0.26641 | 0.005933 | 2.745148 | 0.083422 | 1997.1 | 52.6 | 2706.3 | 27.5 | 3283.5 | 34.8 | 4.31 | 1079 | 272 | 354 |
| | 2 | 4 | 0.263522 | 0.008141 | 10.341623 | 0.32163 | 0.285065 | 0.007561 | 3.780406 | 0.116053 | 1507.6 | 41.5 | 2465.1 | 28.6 | 3388.8 | 41 | 3.48 | 894 | 286 | 462 |
| | 3 | 4 | 0.386691 | 0.011367 | 14.637869 | 0.44944 | 0.271842 | 0.006355 | 2.576139 | 0.078064 | 2107 | 53.1 | 2790.9 | 29 | 3314.8 | 36.9 | 4.25 | 606 | 158 | 242 |
| | 4 | 4 | 0.173235 | 0.005619 | 4.516824 | 0.132492 | 0.188379 | 0.004561 | 5.764075 | 0.189889 | 1029.6 | 30.9 | 1733.2 | 24.6 | 2725.2 | 40.1 | 6.24 | 2633 | 472 | 457 |
| NG01 | 1 | 3 | 0.329285 | 0.009666 | 7.95531 | 0.444468 | 0.173788 | 0.002777 | 3.010711 | 0.088844 | 1834.8 | 46.9 | 2225.6 | 50.7 | 2593.6 | 26.6 | 0.03 | 3776 | 116777 | 62915 |
| | 2 | 3 | 0.349128 | 0.009145 | 10.196257 | 0.55168 | 0.210545 | 0.003535 | 2.84095 | 0.075019 | 1930.3 | 43.7 | 2452.3 | 50.2 | 2908.5 | 27.5 | 2.16 | 679 | 316 | 437 |
| | 3 | 3 | 0.356093 | 0.010026 | 10.794644 | 0.595695 | 0.219813 | 0.004241 | 2.788799 | 0.080292 | 1963.4 | 47.8 | 2504.9 | 51.8 | 2977.6 | 31.1 | 2.09 | 454 | 219 | 306 |
| | 4 | 3 | 0.252386 | 0.007563 | 9.202339 | 0.517605 | 0.262468 | 0.004285 | 3.939318 | 0.117906 | 1450.5 | 38.9 | 2357.4 | 50.9 | 3260.6 | 25.6 | 0.54 | 3028 | 5755 | 3698 |
| | 5 | 3 | 0.225485 | 0.006459 | 8.119248 | 0.44824 | 0.259464 | 0.004395 | 4.411698 | 0.126049 | 1310.6 | 33.9 | 2243.5 | 49.9 | 3242.3 | 26.7 | 0.66 | 1748 | 2868 | 1701 |
| | 6 | 3 | 0.827946 | 0.078532 | 35.323565 | 3.791943 | 0.306775 | 0.00505 | 1.310409 | 0.134472 | 3835 | 280.5 | 3604.9 | 112.3 | 3503.7 | 25.3 | 0.01 | 649 | 95419 | 4498 |
| | 7 | 3 | 0.178858 | 0.005208 | 5.40703 | 0.297838 | 0.217794 | 0.003663 | 5.569374 | 0.160589 | 1060.6 | 28.4 | 1885.3 | 46.7 | 2963.3 | 27 | 2.07 | 1398 | 673 | 586 |
| | 11 | 7 | 0.469616 | 0.026663 | 12.727583 | 1.691673 | 0.200559 | 0.015325 | 2.188676 | 0.130808 | 2471.6 | 117 | 2646.4 | 116.8 | 2785.4 | 125.4 | 18.12 | 10 | 1 | 4 |
| | 12 | 7 | 0.429709 | 0.029684 | 10.261383 | 1.28756 | 0.180236 | 0.015332 | 2.369876 | 0.139447 | 2290.8 | 132.5 | 2447.4 | 126.1 | 2592.9 | 145.1 | 9.47 | 9 | 1 | 3 |
| | 13 | 7 | 0.314344 | 0.040165 | 8.758185 | 1.910531 | 0.198163 | 0.024571 | 3.378134 | 0.441089 | 1744.1 | 198.6 | 2219.3 | 204.9 | 2723.8 | 222.1 | 6.89 | 13 | 2 | 5 |
| | 14 | 7 | 0.18838 | 0.013568 | 4.573578 | 0.557895 | 0.175898 | 0.006692 | 5.541319 | 0.490137 | 1109.3 | 74.5 | 1729.9 | 110.8 | 2612.7 | 63.2 | 0.03 | 1966 | 60771 | 28966 |
| | 15 | 7 | 0.137977 | 0.005993 | 3.050895 | 0.327742 | 0.159741 | 0.006109 | 7.32419 | 0.313185 | 832.4 | 33.8 | 1416.2 | 81.9 | 2450.5 | 65.6 | 0.03 | 1481 | 57908 | 24220 |
| NG02 | 1 | 3 | 0.377963 | 0.02314 | 15.04535 | 1.284488 | 0.281713 | 0.006574 | 2.719355 | 0.185429 | 2059.5 | 109.1 | 2797.7 | 86.4 | 3369.1 | 36.5 | 6.9 | 11676 | 1717 | 23453 |
| | 2 | 3 | 0.102712 | 0.004401 | 2.199584 | 0.16291 | 0.154489 | 0.003657 | 9.705788 | 0.422281 | 630.2 | 25.7 | 1179.9 | 51.9 | 2395 | 40.2 | 12.94 | 4965 | 393 | 978 |
| | 3 | 3 | 0.090406 | 0.003124 | 3.046203 | 0.252013 | 0.240677 | 0.010776 | 11.070747 | 0.37866 | 557.8 | 18.5 | 1408.5 | 62.6 | 3108.5 | 71.7 | 4.2 | 9439 | 2337 | 3698 |
| | 4 | 3 | 0.104645 | 0.004904 | 4.335673 | 0.258628 | 0.300137 | 0.008684 | 9.634235 | 0.465746 | 641.3 | 28.6 | 1698.4 | 49.7 | 3466.7 | 43.8 | 3.75 | 6624 | 1746 | 4221 |
| | 5 | 3 | 0.234248 | 0.007465 | 6.75159 | 0.382761 | 0.206534 | 0.005521 | 4.261251 | 0.134381 | 1356.6 | 38.9 | 2078.8 | 49.9 | 2876.1 | 43.1 | 7 | 737 | 111 | 477 |
| NM02 | 1 | 2 | 0.293705 | 0.043726 | 7.389117 | 1.181568 | 0.188389 | 0.005231 | 4.528124 | 0.862504 | 1624.3 | 221.8 | 2069.5 | 162.1 | 2724.4 | 45.7 | 1.56 | 736 | 498 | 535 |
| | 2 | 2 | 0.361817 | 0.019097 | 9.238843 | 0.824773 | 0.185182 | 0.004485 | 2.801655 | 0.142084 | 1985 | 89.7 | 2351.5 | 80.8 | 2697.7 | 39.9 | 0.91 | 545 | 817 | 419 |
| | 3 | 2 | 0.207132 | 0.011421 | 5.169219 | 0.471089 | 0.180808 | 0.004142 | 4.918529 | 0.287766 | 1210.8 | 61.1 | 1836.7 | 80.5 | 2658.7 | 38.1 | 1.39 | 1479 | 1186 | 952 |
| | 4 | 2 | 0.413043 | 0.005507 | 9.8112 | 0.722472 | 0.172174 | 0.0039 | 2.396173 | 0.032106 | 2228.5 | 25.1 | 2416.6 | 67.5 | 2577.4 | 37.6 | 1.12 | 816 | 806 | 834 |
| | 5 | 2 | 0.524827 | 0.009451 | 13.643369 | 1.030663 | 0.188415 | 0.004742 | 1.888347 | 0.034103 | 2718.7 | 39.9 | 2723.4 | 71.1 | 2725.8 | 41.4 | 0.83 | 266 | 353 | 493 |
| | 6 | 2 | 0.511211 | 0.006108 | 12.734235 | 0.932746 | 0.180557 | 0.004002 | 1.935214 | 0.022905 | 2661.5 | 26 | 2659.8 | 69.4 | 2656.7 | 37 | 0.93 | 663 | 792 | 1101 |
| | 7 | 2 | 0.538059 | 0.007401 | 15.044797 | 1.152656 | 0.20268 | 0.006242 | 1.839421 | 0.025216 | 2774.8 | 31 | 2815.6 | 71.2 | 2842.7 | 49 | 1.25 | 211 | 186 | 424 |
| | 8 | 2 | 0.395583 | 0.005115 | 9.513185 | 0.695516 | 0.174379 | 0.00399 | 2.501333 | 0.031992 | 2148.4 | 23.6 | 2388.5 | 66.7 | 2598.5 | 38.3 | 1.95 | 680 | 383 | 551 |
| | 9 | 2 | 0.482978 | 0.007094 | 12.304329 | 0.912018 | 0.183956 | 0.004171 | 2.042572 | 0.034215 | 2539.7 | 30.9 | 2627 | 68.6 | 2687.4 | 37.6 | 0.88 | 545 | 713 | 928 |
| | 10 | 2 | 0.518092 | 0.006401 | 13.060326 | 0.960185 | 0.182804 | 0.004104 | 1.909584 | 0.023447 | 2690.8 | 27.1 | 2683.4 | 69 | 2677.1 | 37.2 | 1.02 | 578 | 632 | 844 |
| | 11 | 2 | 0.438258 | 0.005864 | 10.817003 | 0.800076 | 0.178871 | 0.004049 | 2.258535 | 0.030434 | 2342.5 | 26.3 | 2506.7 | 69.3 | 2641 | 37.4 | 1.04 | 652 | 637 | 688 |
| | 12 | 2 | 0.305269 | 0.004321 | 6.81577 | 0.506873 | 0.16179 | 0.00372 | 3.243356 | 0.046437 | 1717.1 | 21.4 | 2086.8 | 66.4 | 2472.8 | 39.2 | 1.84 | 989 | 549 | 509 |
| | 13 | 2 | 0.3567 | 0.012018 | 8.292176 | 0.675544 | 0.168277 | 0.003834 | 2.804109 | 0.106006 | 1964.2 | 57.8 | 2257.7 | 78.4 | 2539 | 38.3 | 1.39 | 817 | 583 | 537 |
| | 14 | 2 | 0.207585 | 0.003713 | 3.846322 | 0.286295 | 0.134366 | 0.003199 | 4.77552 | 0.084881 | 1215.7 | 19.8 | 1601.7 | 59.4 | 2153.7 | 41.2 | 0.63 | 2593 | 4100 | 2074 |
| | 15 | 2 | 0.236894 | 0.003241 | 4.584877 | 0.335975 | 0.140356 | 0.003256 | 4.179841 | 0.057677 | 1370.4 | 16.9 | 1746.2 | 60.7 | 2229.8 | 40.2 | 0.61 | 2991 | 4893 | 2821 |
| | 16 | 2 | 0.505764 | 0.00621 | 12.828539 | 0.938629 | 0.183982 | 0.004373 | 1.952451 | 0.026652 | 2643.9 | 30.1 | 2666.8 | 68.6 | 2691.9 | 35 | 1.44 | 300 | 204 | 275 |
| | 17 | 2 | 0.439678 | 0.008361 | 10.857707 | 0.815517 | 0.178972 | 0.003985 | 2.256408 | 0.044618 | 2348.3 | 37.6 | 2509.5 | 70.2 | 2642.1 | 36.7 | 1.24 | 583 | 463 | 525 |
| | 18 | 2 | 0.481403 | 0.012586 | 12.115913 | 0.929643 | 0.182471 | 0.004117 | 2.06787 | 0.05734 | 2531.3 | 55.3 | 2610.7 | 74.4 | 2674 | 37.3 | 1.23 | 454 | 364 | 450 |
| | 19 | 2 | 0.499332 | 0.006579 | 12.804553 | 0.940431 | 0.185947 | 0.004377 | 1.98342 | 0.025676 | 2610.5 | 28.2 | 2664.8 | 69.8 | 2704.8 | 39 | 1.02 | 325 | 309 | 416 |
| | 20 | 2 | 0.410154 | 0.007427 | 9.901121 | 0.737433 | 0.175066 | 0.004192 | 2.418606 | 0.044402 | 2214.9 | 34 | 2424.5 | 69.1 | 2604.6 | 40.1 | 1.44 | 339 | 231 | 271 |

Continued on next page

| Sample | Spot name | Run | 206/238 | ±2SE | 207/235 | ±2SE | 207/206 | ±2SE | 238/P206 | ±2SE | 206/238 Age | ±2SE | 207/235 Age | ±2SE | 207/206 Age | ±2SE | U/Th | U | Th | Pb |
|---|---|---|---|---|---|---|---|---|---|---|---|---|---|---|---|---|---|---|---|---|
| NY01 | 1 | 3 | 0.520592 | 0.014039 | 12.87205 | 0.694122 | 0.178879 | 0.003153 | 1.96174 | 0.053827 | 2701.3 | 59.7 | 2670 | 50.9 | 2641 | 29.5 | 0.51 | 296 | 641 | 683 |
| | 2 | 3 | 0.520804 | 0.013774 | 12.823504 | 0.68993 | 0.17813 | 0.003026 | 1.959415 | 0.050676 | 2702.3 | 58.1 | 2666.5 | 50.5 | 2634.2 | 28.1 | 0.59 | 231 | 421 | 427 |
| | 3 | 3 | 0.483458 | 0.013502 | 12.853714 | 0.791515 | 0.192889 | 0.006984 | 2.109304 | 0.059357 | 2542.2 | 58.7 | 2668.3 | 57.4 | 2764.4 | 59.2 | 0.62 | 293 | 511 | 596 |
| | 4 | 3 | 0.527775 | 0.014736 | 12.978145 | 0.712996 | 0.178014 | 0.003587 | 1.93371 | 0.054615 | 2731.5 | 62.3 | 2677.3 | 51.8 | 2632.1 | 33.4 | 0.46 | 120 | 283 | 299 |
| | 5 | 3 | 0.510879 | 0.013927 | 12.87341 | 0.702042 | 0.182363 | 0.003172 | 1.996365 | 0.055147 | 2660 | 59.5 | 2669.8 | 51.5 | 2673.1 | 28.7 | 0.66 | 516 | 837 | 868 |
| | 7 | 3 | 0.392058 | 0.010838 | 13.234723 | 0.796586 | 0.243979 | 0.005959 | 2.600697 | 0.072228 | 2132 | 50.2 | 2693.2 | 57.6 | 3142.2 | 39.5 | 3.82 | 686 | 188 | 864 |
| | 8 | 3 | 0.40891 | 0.013701 | 11.295573 | 0.735506 | 0.199382 | 0.004468 | 2.498766 | 0.080066 | 2208.9 | 62.3 | 2543.5 | 58.6 | 2818.5 | 36.2 | 0.9 | 575 | 660 | 1069 |
| | 9 | 3 | 0.500968 | 0.014139 | 12.423953 | 0.671917 | 0.179979 | 0.003152 | 2.035559 | 0.059771 | 2617.4 | 61.1 | 2636.6 | 51.3 | 2651.2 | 29.1 | 0.63 | 232 | 372 | 432 |
| | 10 | 3 | 0.207003 | 0.009134 | 5.799911 | 0.472683 | 0.202411 | 0.006464 | 4.935841 | 0.216911 | 1212.5 | 48.8 | 1942.5 | 71 | 2843 | 52.4 | 9.7 | 2168 | 223 | 2239 |
| | 11 | 3 | 0.475451 | 0.013112 | 11.454097 | 0.626547 | 0.174641 | 0.002832 | 2.147595 | 0.061632 | 2507 | 57.6 | 2560.2 | 51.9 | 2601.6 | 26.9 | 0.74 | 538 | 690 | 998 |
| | 12 | 3 | 0.425939 | 0.011553 | 10.245493 | 0.55624 | 0.174689 | 0.002751 | 2.397483 | 0.065335 | 2287.1 | 52.2 | 2456.7 | 50.4 | 2602.1 | 26.3 | 0.78 | 505 | 615 | 865 |
| | 13 | 3 | 0.506394 | 0.01377 | 13.222481 | 0.714847 | 0.189365 | 0.003188 | 2.016611 | 0.054956 | 2640.9 | 58.9 | 2695.4 | 51 | 2735.6 | 27.6 | 0.59 | 295 | 483 | 797 |
| | 14 | 3 | 0.455835 | 0.012823 | 13.082729 | 0.712497 | 0.208411 | 0.004507 | 2.242681 | 0.063409 | 2420.7 | 56.8 | 2685.1 | 51.6 | 2890.3 | 35.7 | 0.54 | 366 | 659 | 1108 |
| | 16 | 3 | 0.367415 | 0.011349 | 9.513369 | 0.544749 | 0.187523 | 0.00316 | 2.78403 | 0.087398 | 2016.8 | 53.6 | 2387.9 | 52.2 | 2719.5 | 27.9 | 1.8 | 584 | 314 | 525 |
| | 17 | 3 | 0.466845 | 0.012324 | 11.35414 | 0.614863 | 0.176469 | 0.003003 | 2.18885 | 0.057747 | 2469.5 | 54.1 | 2552.2 | 50.7 | 2618.7 | 28.4 | 0.59 | 349 | 571 | 718 |
| | 18 | 3 | 0.507254 | 0.013317 | 12.975148 | 0.699908 | 0.185214 | 0.003143 | 2.014346 | 0.052913 | 2644.7 | 56.9 | 2677.5 | 50.8 | 2698.8 | 27.8 | 0.67 | 356 | 515 | 725 |
| | 19 | 3 | 0.44055 | 0.01214 | 11.451814 | 0.620975 | 0.188754 | 0.003504 | 2.320777 | 0.066409 | 2352.7 | 54.6 | 2560.2 | 50.7 | 2729.6 | 30.4 | 3.21 | 477 | 144 | 287 |
| | 20 | 3 | 0.471198 | 0.016249 | 12.487359 | 0.758473 | 0.192218 | 0.004675 | 2.172117 | 0.076216 | 2488 | 71.4 | 2640.1 | 57.5 | 2759 | 39.5 | 1.38 | 70 | 49 | 85 |
| | 22 | 3 | 0.325245 | 0.010738 | 9.233157 | 0.569443 | 0.205962 | 0.004859 | 3.133165 | 0.106769 | 1814.4 | 52.4 | 2357.5 | 57.7 | 2870.4 | 38.2 | 6.09 | 786 | 128 | 640 |
| | 23 | 3 | 0.160954 | 0.004393 | 3.474162 | 0.194251 | 0.15645 | 0.003441 | 6.298597 | 0.169843 | 962.1 | 24.4 | 1521.1 | 43.8 | 2416.1 | 37.3 | 10.46 | 1092 | 102 | 411 |
| | 24 | 3 | 0.432645 | 0.011783 | 12.038917 | 0.681883 | 0.202018 | 0.004061 | 2.342631 | 0.063782 | 2317.3 | 53 | 2605.9 | 53.4 | 2840.3 | 32.8 | 2.31 | 503 | 221 | 502 |
| | 25 | 3 | 0.424644 | 0.011264 | 11.301492 | 0.62366 | 0.192915 | 0.003975 | 2.382277 | 0.062468 | 2281.5 | 50.9 | 2548 | 52 | 2765.8 | 33.8 | 2.91 | 236 | 79 | 157 |
| | 26 | 3 | 0.502055 | 0.013994 | 12.635458 | 0.684888 | 0.182806 | 0.003082 | 2.015078 | 0.05658 | 2622.2 | 60.1 | 2652.5 | 51.4 | 2677.3 | 28 | 0.77 | 286 | 363 | 467 |
| | 27 | 3 | 0.462134 | 0.01539 | 11.96292 | 0.660487 | 0.18863 | 0.003612 | 2.195001 | 0.075263 | 2447.5 | 68.1 | 2600.6 | 52.1 | 2728.3 | 31.3 | 0.82 | 280 | 334 | 454 |
| | 28 | 3 | 0.18694 | 0.006375 | 5.529441 | 0.352068 | 0.215372 | 0.004549 | 5.424823 | 0.191227 | 1104.4 | 34.7 | 1900.6 | 57.7 | 2943.7 | 35.1 | 2.72 | 1973 | 713 | 1633 |
| | 29 | 3 | 0.3949 | 0.011636 | 14.028854 | 0.771508 | 0.258583 | 0.006277 | 2.557034 | 0.07436 | 2144.9 | 53.7 | 2750.8 | 52 | 3234.4 | 37.5 | 1.33 | 236 | 168 | 473 |
| | 30 | 3 | 0.40937 | 0.011231 | 10.796405 | 0.584504 | 0.191677 | 0.003273 | 2.465458 | 0.067166 | 2211.7 | 51.3 | 2505.3 | 50.2 | 2755.3 | 28.2 | 0.75 | 508 | 668 | 870 |
| NY02 | 1 | 4 | 0.331085 | 0.009621 | 7.262073 | 0.204556 | 0.162921 | 0.003377 | 3.017986 | 0.089209 | 1843.2 | 46.7 | 2143.4 | 25.1 | 2484.7 | 34.8 | 0.62 | 1368 | 2257 | 1437 |
| | 2 | 4 | 0.167291 | 0.005626 | 9.806918 | 0.335769 | 0.435118 | 0.010966 | 5.989945 | 0.211079 | 996.8 | 31.1 | 2414.5 | 31.6 | 4032.2 | 38 | 1.26 | 818 | 675 | 2019 |
| | 3 | 4 | 0.229824 | 0.006001 | 8.49968 | 0.237068 | 0.273069 | 0.005886 | 4.340429 | 0.112584 | 1333.5 | 31.4 | 2285.2 | 25.2 | 3322 | 34.1 | 1.29 | 2808 | 2227 | 4488 |
| | 4 | 4 | 0.245661 | 0.007348 | 7.329241 | 0.252048 | 0.221359 | 0.005142 | 4.065031 | 0.122833 | 1415.8 | 38 | 2150.9 | 31.2 | 2988.8 | 37.4 | 1.43 | 1121 | 793 | 1686 |
| | 5 | 4 | 0.49611 | 0.018746 | 15.739515 | 0.750738 | 0.232151 | 0.006547 | 2.017888 | 0.077094 | 2595.5 | 80.9 | 2857.3 | 44.5 | 3064.1 | 44.7 | 0.5 | 223 | 456 | 764 |
| | 6 | 4 | 0.52411 | 0.015303 | 12.487056 | 0.390595 | 0.175186 | 0.004264 | 1.906167 | 0.056917 | 2715.7 | 64.9 | 2640.1 | 29.5 | 2604.8 | 40.6 | 0.36 | 118 | 327 | 316 |
| | 7 | 4 | 0.200248 | 0.005954 | 6.408695 | 0.203643 | 0.234567 | 0.005115 | 4.990491 | 0.153481 | 1176.4 | 32.1 | 2031.9 | 27.9 | 3081.7 | 35 | 1.52 | 1823 | 1208 | 1785 |
| | 8 | 4 | 0.279429 | 0.008127 | 5.681274 | 0.190356 | 0.149036 | 0.003214 | 3.572225 | 0.101214 | 1588.2 | 40.8 | 1927.2 | 28.5 | 2333.3 | 36.8 | 5.43 | 1113 | 203 | 194 |
| | 9 | 4 | 0.51537 | 0.014518 | 12.475308 | 0.373873 | 0.176439 | 0.004231 | 1.936791 | 0.053601 | 2678.9 | 61.6 | 2639.6 | 28 | 2616.8 | 40.4 | 0.31 | 171 | 559 | 590 |
| | 10 | 4 | 0.508991 | 0.016531 | 13.297516 | 0.446749 | 0.189456 | 0.006016 | 1.963827 | 0.063496 | 2651.2 | 70.5 | 2699.2 | 32.7 | 2732.1 | 53.3 | 0.6 | 78 | 128 | 170 |
| | 11 | 4 | 0.506684 | 0.014331 | 12.603406 | 0.390745 | 0.176595 | 0.004361 | 1.96552 | 0.054997 | 2641.8 | 61.2 | 2648.9 | 29.4 | 2617.9 | 42 | 0.47 | 111 | 234 | 413 |
| | 12 | 4 | 0.320662 | 0.008575 | 8.466882 | 0.23896 | 0.186962 | 0.00419 | 3.101882 | 0.084016 | 1792.8 | 41.9 | 2281.6 | 25.9 | 2713.5 | 37 | 1.21 | 730 | 610 | 1161 |
| | 13 | 4 | 0.27745 | 0.008979 | 7.557048 | 0.304973 | 0.191524 | 0.006408 | 3.588961 | 0.117667 | 1578.1 | 45.4 | 2177.5 | 36.7 | 2750.5 | 55.9 | 0.79 | 119 | 152 | 258 |
| | 14 | 4 | 0.404564 | 0.011546 | 9.439032 | 0.26557 | 0.165541 | 0.003587 | 2.450452 | 0.062515 | 2189.5 | 53.1 | 2384.4 | 29.2 | 2511.2 | 36.4 | 0.76 | 390 | 516 | 772 |
| | 15 | 4 | 0.342095 | 0.010454 | 10.261108 | 0.283039 | 0.211352 | 0.004699 | 2.908965 | 0.087406 | 1896.3 | 50.1 | 2458.1 | 25.7 | 2914.3 | 36.4 | 0.5 | 410 | 821 | 1513 |
| | 16 | 4 | 0.334876 | 0.009864 | 11.244168 | 0.45938 | 0.236956 | 0.006373 | 2.972222 | 0.088603 | 1861.5 | 47.7 | 2539.2 | 37.9 | 3095.8 | 42.3 | 0.24 | 739 | 4289 | 1754 |
| | 17 | 4 | 0.39274 | 0.012183 | 11.450612 | 0.318104 | 0.207037 | 0.005124 | 2.537183 | 0.080581 | 2134.7 | 56.5 | 2559.8 | 26 | 2879.4 | 40.1 | 0.32 | 240 | 755 | 947 |
| | 18 | 4 | 0.235275 | 0.00819 | 5.292793 | 0.154083 | 0.16033 | 0.003543 | 4.247485 | 0.153651 | 1361.4 | 42.9 | 1866.8 | 25.1 | 2457.1 | 37.8 | 1.12 | 2013 | 1818 | 1451 |
| | 19 | 4 | 0.23473 | 0.00829 | 8.62364 | 0.370604 | 0.261345 | 0.00693 | 4.254587 | 0.152315 | 1358.7 | 43.3 | 2295.3 | 39.2 | 3251.9 | 41.4 | 1.05 | 1535 | 1469 | 2548 |
| | 20 | 4 | 0.510639 | 0.0146 | 12.566461 | 0.38478 | 0.177027 | 0.004392 | 1.944645 | 0.049387 | 2666.3 | 55 | 2646.3 | 29.1 | 2622 | 41 | 0.3 | 157 | 526 | 666 |
| | 23 | 4 | 0.311355 | 0.012605 | 6.903249 | 0.239469 | 0.168339 | 0.003763 | 3.24622 | 0.132178 | 1746.7 | 62 | 2098.2 | 30.8 | 2539.9 | 37.5 | 3.05 | 1120 | 359 | 594 |
| | 24 | 4 | 0.244044 | 0.006929 | 7.882145 | 0.223451 | 0.24311 | 0.005773 | 4.135076 | 0.118634 | 1407.5 | 35.9 | 2216.8 | 25.6 | 3137.9 | 37.3 | 0.88 | 1091 | 1208 | 2326 |
| | 25 | 4 | 0.247242 | 0.006674 | 6.415594 | 0.18485 | 0.195022 | 0.004856 | 4.079286 | 0.112163 | 1424.1 | 34.6 | 2033.5 | 25.4 | 2781.9 | 40.1 | 0.59 | 1135 | 1876 | 1571 |
| | 26 | 4 | 0.489211 | 0.013199 | 11.64276 | 0.333417 | 0.177749 | 0.003974 | 2.060506 | 0.05624 | 2567 | 57.2 | 2575.5 | 26.8 | 2630.4 | 37 | 0.65 | 378 | 565 | 769 |
| | 27 | 4 | 0.319312 | 0.012523 | 8.203678 | 0.242086 | 0.19232 | 0.005363 | 3.177018 | 0.125796 | 1785 | 61.2 | 2252.8 | 26.6 | 2758.2 | 45.3 | 3.22 | 1336 | 411 | 849 |
| | 28 | 4 | 0.269945 | 0.008221 | 6.948432 | 0.219557 | 0.190581 | 0.005221 | 3.733758 | 0.11666 | 1540.3 | 41.8 | 2104 | 28.5 | 2744.4 | 43.9 | 0.42 | 353 | 821 | 867 |
| | 29 | 4 | 0.537874 | 0.014989 | 12.783562 | 0.353996 | 0.176176 | 0.003836 | 1.871823 | 0.053087 | 2773.9 | 63 | 2663.1 | 26.2 | 2620 | 32.3 | 0.36 | 124 | 339 | 491 |

Continued on next page

| Sample | Spot name | Run | 206/238 | ±2SE | 207/235 | ±2SE | 207/206 | ±2SE | 238/P206 | ±2SE | 206/238 Age | ±2SE | 207/235 Age | ±2SE | 207/206 Age | ±2SE | U/Th | U | Th | Pb |
|---|---|---|---|---|---|---|---|---|---|---|---|---|---|---|---|---|---|---|---|---|
| | 30 | 4 | 0.441056 | 0.013355 | 10.435542 | 0.375359 | 0.174904 | 0.004697 | 2.280432 | 0.069775 | 2354.8 | 59.8 | 2472.2 | 34 | 2602.1 | 44.3 | 0.51 | 122 | 234 | 347 |
| NY03 | 1 | 4 | 0.398987 | 0.010519 | 9.475941 | 0.258259 | 0.172328 | 0.003551 | 2.51144 | 0.066775 | 2164.2 | 48.5 | 2384.6 | 25 | 2578.9 | 34.6 | 0.61 | 1190 | 2009 | 1736 |
| | 2 | 4 | 0.447133 | 0.012531 | 10.928903 | 0.33031 | 0.177888 | 0.003676 | 2.241974 | 0.062936 | 2382 | 55.8 | 2515.7 | 28.7 | 2631.8 | 34.7 | 1.12 | 659 | 645 | 680 |
| | 3 | 4 | 0.431901 | 0.011891 | 10.973345 | 0.293562 | 0.184744 | 0.004204 | 2.319475 | 0.064097 | 2313.9 | 53.6 | 2520.4 | 25 | 2693.7 | 37.5 | 2.29 | 502 | 247 | 355 |
| | 4 | 4 | 0.483349 | 0.014204 | 12.353505 | 0.392679 | 0.184231 | 0.004116 | 2.072777 | 0.061726 | 2541.2 | 61.8 | 2630.2 | 30.3 | 2689.5 | 36.1 | 4.36 | 382 | 87 | 164 |
| | 5 | 4 | 0.325843 | 0.011769 | 7.148095 | 0.321998 | 0.158416 | 0.003899 | 3.080424 | 0.113435 | 1817.4 | 57.3 | 2126.6 | 40.4 | 2436.5 | 41.5 | 1.88 | 1332 | 704 | 595 |
| | 6 | 4 | 0.332256 | 0.008896 | 7.583575 | 0.224732 | 0.166898 | 0.00359 | 3.008182 | 0.082206 | 1849.2 | 43.2 | 2182.5 | 26.7 | 2525.6 | 35.9 | 1.52 | 1501 | 986 | 758 |
| | 7 | 4 | 0.14454 | 0.003838 | 2.403626 | 0.076347 | 0.121612 | 0.00348 | 6.912175 | 0.181162 | 870.3 | 21.6 | 1243.1 | 22.9 | 1976.4 | 50.7 | 0.84 | 3044 | 3600 | 1625 |
| | 8 | 5 | 0.140579 | 0.004689 | 2.901431 | 0.083704 | 0.149193 | 0.003931 | 7.11719 | 0.242334 | 847.8 | 26.5 | 1382 | 21.9 | 2334.3 | 45.1 | 1.91 | 3210 | 1688 | 1206 |
| | 9 | 5 | 0.071834 | 0.002613 | 1.008906 | 0.040441 | 0.101394 | 0.002106 | 13.943896 | 0.511929 | 447.1 | 15.7 | 707.6 | 20.5 | 1648.4 | 38.6 | 0.77 | 27492 | 36280 | 6979 |
| | 10 | 5 | 0.15413 | 0.004179 | 3.383295 | 0.103078 | 0.159725 | 0.003757 | 6.476565 | 0.172995 | 924 | 23.3 | 1504.3 | 27.4 | 2458 | 45.4 | 0.77 | 2783 | 3725 | 2709 |
| | 13 | 5 | 0.24763 | 0.007847 | 6.177713 | 0.200563 | 0.180631 | 0.003892 | 4.030623 | 0.131837 | 1426.1 | 40.7 | 2000.6 | 28.3 | 2657.5 | 35.6 | 2.77 | 1060 | 387 | 681 |
| | 14 | 5 | 0.309487 | 0.009127 | 7.397873 | 0.211507 | 0.17289 | 0.003444 | 3.224556 | 0.095094 | 1738 | 44.9 | 2160.3 | 25.6 | 2584.8 | 33.5 | 1.25 | 1470 | 1202 | 1360 |
| | 15 | 5 | 0.368232 | 0.010268 | 9.238641 | 0.250094 | 0.182592 | 0.004219 | 2.709253 | 0.076724 | 2020.9 | 48.5 | 2361.6 | 24.8 | 2674.9 | 38.1 | 3.31 | 818 | 254 | 496 |
| | 16 | 5 | 0.16815 | 0.004701 | 3.769647 | 0.124208 | 0.164299 | 0.004291 | 5.934865 | 0.166054 | 1001.8 | 25.9 | 1585.3 | 25.8 | 2497.5 | 42.7 | 1.33 | 2784 | 2141 | 2195 |
| | 17 | 5 | 0.422229 | 0.01079 | 11.574997 | 0.308799 | 0.198881 | 0.004384 | 2.361636 | 0.06054 | 2270.5 | 48.9 | 2570.3 | 25 | 2815.3 | 36.3 | 1.92 | 457 | 243 | 573 |
| | 18 | 5 | 0.467792 | 0.012197 | 11.503528 | 0.300155 | 0.179036 | 0.003719 | 2.132368 | 0.056119 | 2473.7 | 53.6 | 2564.5 | 24.3 | 2642.5 | 34.7 | 0.93 | 679 | 743 | 908 |
| | 20 | 5 | 0.241815 | 0.007115 | 11.191873 | 0.367178 | 0.336991 | 0.007343 | 4.12704 | 0.119555 | 1396 | 36.9 | 2538.2 | 30.5 | 3648 | 33.3 | 1.02 | 1406 | 1393 | 3758 |
| | 21 | 5 | 0.378132 | 0.010489 | 9.915436 | 0.25325 | 0.182449 | 0.003669 | 2.640686 | 0.074232 | 2067.2 | 49.1 | 2426.7 | 23.6 | 2677.4 | 37.6 | 1.67 | 1159 | 684 | 1040 |
| | 22 | 5 | 0.253052 | 0.008487 | 7.452328 | 0.288985 | 0.202183 | 0.005054 | 3.956811 | 0.131878 | 1453.8 | 43.6 | 2165 | 33.9 | 2841.5 | 40.9 | 1.63 | 1721 | 951 | 1281 |
| | 23 | 5 | 0.382797 | 0.010185 | 10.699587 | 0.324139 | 0.193275 | 0.004311 | 2.607854 | 0.069943 | 2089.1 | 47.5 | 2496.1 | 28.1 | 2768.2 | 36.4 | 1.04 | 732 | 683 | 764 |
| | 24 | 5 | 0.279781 | 0.008407 | 6.692759 | 0.22185 | 0.163643 | 0.003797 | 3.570339 | 0.106462 | 1590.1 | 42.3 | 2070.7 | 29.6 | 2492 | 39.3 | 1.1 | 1996 | 1739 | 1626 |
| | 25 | 5 | 0.345683 | 0.010283 | 9.464224 | 0.344242 | 0.186641 | 0.005022 | 2.889797 | 0.086337 | 1913.7 | 49.3 | 2382.7 | 33.5 | 2710.4 | 44.4 | 1.57 | 1839 | 1107 | 1571 |
| | 26 | 5 | 0.382705 | 0.01051 | 9.463812 | 0.250605 | 0.169513 | 0.003569 | 2.610833 | 0.071885 | 2088.6 | 49 | 2383.6 | 24.2 | 2551.2 | 35.2 | 1.69 | 934 | 508 | 552 |
| | 27 | 5 | 0.369926 | 0.011584 | 9.834785 | 0.291769 | 0.181728 | 0.003875 | 2.707469 | 0.085784 | 2028.2 | 54.6 | 2418.2 | 27.9 | 2667 | 35.4 | 0.83 | 1495 | 1596 | 1976 |
| | 28 | 5 | 0.427646 | 0.011907 | 11.327309 | 0.301911 | 0.180942 | 0.003628 | 2.337421 | 0.066278 | 2294.7 | 53.9 | 2549.9 | 25.2 | 2660.3 | 33.1 | 0.36 | 1097 | 2647 | 3365 |
| | 29 | 5 | 0.305388 | 0.009405 | 11.172112 | 0.473755 | 0.250497 | 0.007591 | 3.275552 | 0.102034 | 1717.6 | 46.5 | 2533.7 | 41.4 | 3183.6 | 48.6 | 1.36 | 1686 | 1111 | 1910 |
| | 30 | 5 | 0.163699 | 0.005183 | 4.663799 | 0.141086 | 0.194159 | 0.004975 | 6.108928 | 0.194517 | 977.2 | 28.7 | 1760.1 | 25.2 | 2775.3 | 42.5 | 3.21 | 2382 | 623 | 1098 |
| PG01 | 3.01 | 3 | 0.269514 | 0.007489 | 6.240093 | 0.338338 | 0.165935 | 0.002747 | 3.703135 | 0.104534 | 1538.1 | 38.1 | 2009.7 | 47.6 | 2515.9 | 28 | 5.33 | 1409 | 265 | 479 |
| | 6.01 | 6 | 0.568894 | 0.005522 | 14.597697 | 1.006167 | 0.187909 | 0.005988 | 1.749475 | 0.018673 | 2902.9 | 22.6 | 2788.9 | 65.6 | 2726.1 | 47.2 | 2.51 | 601 | 236 | 337 |
| | 3.02 | 3 | 0.368146 | 0.011523 | 8.772155 | 0.492775 | 0.171174 | 0.002977 | 2.697736 | 0.074082 | 2020.1 | 54.7 | 2313.7 | 52.2 | 2567.9 | 28.9 | 6.06 | 965 | 160 | 301 |
| | 6.02 | 6 | 0.546617 | 0.007026 | 13.914737 | 0.968499 | 0.186172 | 0.00596 | 1.826685 | 0.023669 | 2810.4 | 29.3 | 2742.9 | 66.5 | 2706.9 | 53 | 2.94 | 626 | 212 | 296 |
| | 3.03 | 3 | 0.517015 | 0.013991 | 13.225553 | 0.712906 | 0.18416 | 0.003464 | 1.928405 | 0.05244 | 2686.3 | 59.5 | 2695.7 | 50.7 | 2689.2 | 31.5 | 5.69 | 866 | 155 | 295 |
| | 6.03 | 6 | 0.551004 | 0.009007 | 13.828231 | 0.97015 | 0.183353 | 0.005914 | 1.814216 | 0.030451 | 2828.2 | 37.6 | 2736.7 | 66.9 | 2681.5 | 53.4 | 2.4 | 592 | 245 | 345 |
| | 3.04 | 3 | 0.386479 | 0.010843 | 9.85868 | 0.540223 | 0.18337 | 0.003113 | 2.581398 | 0.073127 | 2106.1 | 50.5 | 2420.9 | 50.9 | 2682.3 | 28 | 6.07 | 962 | 160 | 387 |
| | 6.04 | 6 | 0.5722 | 0.007267 | 14.428652 | 0.996626 | 0.184618 | 0.005963 | 1.744968 | 0.022159 | 2916.1 | 29.8 | 2777.7 | 65.9 | 2692.9 | 52.9 | 2.43 | 580 | 233 | 308 |
| | 3.05 | 3 | 0.263978 | 0.007406 | 7.296074 | 0.400485 | 0.198698 | 0.003636 | 3.778419 | 0.105621 | 1510 | 37.7 | 2147.6 | 49.6 | 2813.9 | 29.7 | 5.78 | 1386 | 242 | 806 |
| | 6.05 | 6 | 0.52115 | 0.008325 | 12.975312 | 0.908935 | 0.181308 | 0.005797 | 1.917873 | 0.030981 | 2703 | 35.3 | 2676.6 | 66.3 | 2663.1 | 52.9 | 3.13 | 949 | 303 | 420 |
| | 3.06 | 3 | 0.271558 | 0.007382 | 9.539577 | 0.515282 | 0.252503 | 0.004091 | 3.670414 | 0.100053 | 1548.6 | 37.4 | 2391 | 49.7 | 3199.5 | 25.6 | 0.87 | 8052 | 9870 | 14368 |
| | 6.06 | 6 | 0.18278 | 0.003827 | 3.980951 | 0.301179 | 0.156787 | 0.005682 | 5.461335 | 0.11362 | 1082 | 20.8 | 1629.2 | 60.8 | 2419.3 | 61.7 | 4.24 | 2735 | 632 | 1013 |
| | 3.07 | 3 | 0.28137 | 0.009581 | 9.229508 | 0.512896 | 0.23619 | 0.004634 | 3.555933 | 0.122819 | 1597.5 | 48.3 | 2360 | 50.6 | 3092.4 | 31.4 | 1.08 | 3762 | 5046 | 6067 |
| | 6.07 | 6 | 0.169872 | 0.003938 | 2.696871 | 0.197817 | 0.115082 | 0.003652 | 5.903017 | 0.144182 | 1011 | 21.8 | 1325.5 | 55.6 | 1879.4 | 57.4 | 6.53 | 2993 | 454 | 467 |
| | 3.08 | 3 | 0.468751 | 0.016685 | 11.289661 | 0.700354 | 0.172966 | 0.003867 | 2.135793 | 0.075713 | 2476.1 | 73.1 | 2543.2 | 57.5 | 2583.3 | 37.3 | 4.63 | 149 | 33 | 54 |
| | 6.08 | 6 | 0.298791 | 0.009491 | 6.940071 | 0.559538 | 0.167616 | 0.005568 | 3.371774 | 0.107303 | 1683.5 | 47 | 2096.4 | 70.4 | 2531.4 | 55.5 | 5.06 | 932 | 192 | 152 |
| | 3.09 | 3 | 0.524551 | 0.014203 | 13.504171 | 0.732747 | 0.185618 | 0.003597 | 1.895081 | 0.051267 | 2718.1 | 60 | 2717.9 | 57.8 | 2701.7 | 31.7 | 3.26 | 156 | 47 | 64 |
| | 6.09 | 6 | 0.251671 | 0.008314 | 5.40297 | 0.448661 | 0.154963 | 0.005445 | 3.972748 | 0.130548 | 1445.6 | 42.3 | 1887.1 | 73.8 | 2397.4 | 59.4 | 3.51 | 993 | 287 | 260 |
| | 3.1 | 3 | 0.534682 | 0.014463 | 13.693292 | 0.748722 | 0.183999 | 0.003132 | 1.858642 | 0.051138 | 2760.8 | 60.9 | 2728 | 52.1 | 2688 | 28.1 | 14.99 | 1190 | 78 | 176 |
| | 6.1 | 6 | 0.224958 | 0.002976 | 4.724372 | 0.354294 | 0.151346 | 0.005788 | 4.439542 | 0.059087 | 1307.8 | 15.7 | 1767.9 | 64 | 2354.5 | 67.7 | 4.02 | 1282 | 321 | 462 |
| | 3.11 | 3 | 0.780496 | 0.026 | 23.636308 | 1.439572 | 0.217297 | 0.005402 | 1.274067 | 0.043585 | 3717.8 | 94.7 | 3252 | 59.2 | 2958.7 | 40.4 | 20.28 | 905 | 44 | 311 |
| | 6.11 | 6 | 0.10736 | 0.00392 | 3.635192 | 0.281218 | 0.246114 | 0.011021 | 9.347276 | 0.354864 | 657.2 | 22.8 | 1555.3 | 61.7 | 3154.8 | 69.5 | 19.09 | 893 | 49 | 376 |
| | 3.12 | 3 | 0.576139 | 0.016167 | 14.19352 | 0.761221 | 0.177414 | 0.003075 | 1.723522 | 0.048306 | 2932.7 | 66.1 | 2762.6 | 51 | 2627.8 | 29 | 12.21 | 2790 | 233 | 392 |
| | 6.12 | 6 | 0.479199 | 0.01496 | 12.7528 | 0.945583 | 0.193392 | 0.007779 | 2.090928 | 0.06381 | 2522.1 | 64.9 | 2659.6 | 69.3 | 2767 | 67 | 2.36 | 129 | 55 | 77 |
| | 3.13 | 3 | 0.430823 | 0.011688 | 9.938434 | 0.540307 | 0.166278 | 0.002719 | 2.305186 | 0.06281 | 2309.1 | 52.7 | 2428.6 | 50.9 | 2519.4 | 27.6 | 19.41 | 3003 | 156 | 312 |
| | 6.13 | 6 | 0.105686 | 0.007804 | 2.98048 | 0.290353 | 0.205269 | 0.006956 | 9.974881 | 0.712526 | 646 | 45.3 | 1388.6 | 72.3 | 2865.6 | 55.6 | 7.98 | 654 | 81 | 141 |

Continued on next page

| Sample | Spot name | Run | 206/238 | ±2SE | 207/235 | ±2SE | 207/206 | ±2SE | 238/P206 | ±2SE | 206/238 Age | ±2SE | 207/235 Age | ±2SE | 207/206 Age | ±2SE | U/Th | U | Th | Pb |
|---|---|---|---|---|---|---|---|---|---|---|---|---|---|---|---|---|---|---|---|---|
| | 3.14 | 3 | 0.227512 | 0.006996 | 4.680593 | 0.269642 | 0.147774 | 0.002646 | 4.37281 | 0.13394 | 1321.1 | 36.7 | 1762.2 | 48.3 | 2318.7 | 31.1 | 4.58 | 1162 | 259 | 252 |
| | 6.14 | 6 | 0.211974 | 0.00702 | 5.725659 | 0.441405 | 0.195097 | 0.006724 | 4.761058 | 0.166594 | 1238.2 | 37.5 | 1930.1 | 67.2 | 2782.3 | 56.4 | 5.3 | 326 | 62 | 98 |
| | 3.15 | 3 | 0.205443 | 0.005996 | 4.27474 | 0.241731 | 0.149524 | 0.003645 | 4.835028 | 0.143454 | 1204.3 | 32.1 | 1687.6 | 47.1 | 2337 | 42 | 4.67 | 1074 | 238 | 314 |
| | 6.15 | 6 | 0.526652 | 0.006547 | 13.060855 | 0.902596 | 0.179793 | 0.005923 | 1.895856 | 0.02304 | 2726.8 | 27.5 | 2686.5 | 73.9 | 2654.2 | 48.2 | 1.51 | 424 | 282 | 392 |
| | 3.16 | 3 | 0.314154 | 0.00954 | 6.876911 | 0.387773 | 0.157648 | 0.003024 | 3.159964 | 0.097755 | 1760.9 | 46.9 | 2095.1 | 50.3 | 2429.3 | 32.8 | 6.39 | 1122 | 181 | 180 |
| | 6.16 | 6 | 0.502318 | 0.00547 | 12.690575 | 0.874928 | 0.182965 | 0.00586 | 1.987384 | 0.021944 | 2623.3 | 23.5 | 2656.4 | 65.1 | 2678.2 | 53 | 1.48 | 477 | 322 | 450 |
| | 3.17 | 3 | 0.345718 | 0.012247 | 8.656897 | 0.508767 | 0.178768 | 0.003262 | 2.877545 | 0.103966 | 1913.4 | 58.8 | 2301.1 | 54.4 | 2640.2 | 30.4 | 4.37 | 841 | 206 | 404 |
| | 6.17 | 6 | 0.46603 | 0.005136 | 11.68245 | 0.808435 | 0.181748 | 0.005868 | 2.142198 | 0.023625 | 2465.7 | 22.6 | 2578.6 | 64.4 | 2666.9 | 53.8 | 1.47 | 433 | 291 | 402 |
| | 3.18 | 3 | 0.50272 | 0.013984 | 12.337985 | 0.672421 | 0.176431 | 0.002808 | 1.974316 | 0.055112 | 2625 | 60 | 2629.9 | 51.1 | 2618.6 | 26.5 | 6.16 | 695 | 117 | 139 |
| | 6.18 | 6 | 0.481909 | 0.006432 | 12.235378 | 0.855147 | 0.184295 | 0.006043 | 2.072932 | 0.028073 | 2534.9 | 28 | 2621.5 | 66.4 | 2689.6 | 54.1 | 2.02 | 264 | 129 | 201 |
| | 6.19 | 6 | 0.525947 | 0.009566 | 15.200167 | 1.101213 | 0.21029 | 0.008278 | 1.902139 | 0.033301 | 2723 | 40.1 | 2825 | 68.8 | 2900.9 | 64.1 | 2.01 | 73 | 37 | 75 |
| | 6.2 | 6 | 0.531502 | 0.008404 | 13.495155 | 0.963509 | 0.185582 | 0.006641 | 1.880909 | 0.029592 | 2746.8 | 35.3 | 2717.8 | 60.7 | 2699.1 | 58.9 | 1.43 | 118 | 81 | 114 |
| | 6.21 | 6 | 0.528641 | 0.008039 | 13.694032 | 0.973758 | 0.188926 | 0.007235 | 1.890984 | 0.029022 | 2734.8 | 33.9 | 2726.8 | 67.9 | 2736.1 | 55.9 | 1.68 | 92 | 57 | 71 |
| | 6.22 | 6 | 0.339592 | 0.012945 | 11.45851 | 0.930046 | 0.243466 | 0.007987 | 2.953735 | 0.120436 | 1883.6 | 62.8 | 2557.9 | 78.5 | 3141.5 | 52 | 0.69 | 783 | 1205 | 884 |
| | 6.23 | 6 | 0.52225 | 0.009207 | 13.074587 | 0.953919 | 0.182554 | 0.007213 | 1.915766 | 0.033851 | 2707.5 | 39 | 2681.9 | 69.6 | 2668.9 | 66.9 | 1.95 | 56 | 30 | 37 |
| | 6.24 | 6 | 0.506527 | 0.007433 | 12.977412 | 0.941697 | 0.187745 | 0.007738 | 1.97329 | 0.029084 | 2641 | 31.8 | 2675.1 | 68.8 | 2714.1 | 67.4 | 1.37 | 65 | 50 | 58 |
| | 6.25 | 6 | 0.534121 | 0.012655 | 13.720222 | 1.010287 | 0.18608 | 0.007244 | 1.878007 | 0.043832 | 2756.5 | 53 | 2727 | 69.5 | 2701.2 | 64.2 | 1.45 | 59 | 44 | 53 |
| | 6.26 | 6 | 0.201549 | 0.004499 | 4.656262 | 0.371203 | 0.167053 | 0.006226 | 4.963696 | 0.107274 | 1183.3 | 24.1 | 1755.7 | 65.3 | 2524.6 | 62.4 | 5.8 | 1828 | 341 | 604 |
| | 6.27 | 6 | 0.212739 | 0.003436 | 4.41814 | 0.316724 | 0.151221 | 0.004953 | 4.700835 | 0.075951 | 1243.1 | 18.3 | 1713.9 | 60.1 | 2357.4 | 55.9 | 3.95 | 1487 | 533 | 395 |
| | 6.31 | 7 | 0.46251 | 0.012863 | 12.939356 | 1.3593 | 0.202123 | 0.008852 | 2.153661 | 0.061495 | 2449.8 | 56.9 | 2673.3 | 99.3 | 2839.8 | 71.3 | 0.48 | 126 | 266 | 364 |
| | 6.32 | 7 | 0.494752 | 0.015973 | 14.884829 | 1.599679 | 0.217007 | 0.010335 | 2.011697 | 0.065727 | 2590.4 | 69 | 2806.1 | 104.1 | 2955.5 | 76.4 | 0.38 | 120 | 322 | 473 |
| | 6.33 | 7 | 0.479001 | 0.013308 | 12.231697 | 1.279551 | 0.184883 | 0.00716 | 2.084292 | 0.058552 | 2521.1 | 58 | 2618.7 | 98.4 | 2694.5 | 62.8 | 1.94 | 309 | 163 | 238 |
| | 6.34 | 7 | 0.529661 | 0.01346 | 13.793576 | 1.441122 | 0.188498 | 0.007512 | 1.881734 | 0.047542 | 2738.4 | 56.6 | 2738.5 | 89.7 | 2725.4 | 67.3 | 1.86 | 90 | 49 | 72 |
| | 6.35 | 7 | 0.359033 | 0.010015 | 8.372698 | 0.868933 | 0.168917 | 0.006418 | 2.778617 | 0.074897 | 1976.3 | 47.2 | 2269.6 | 92.7 | 2544.7 | 64.4 | 1.58 | 916 | 593 | 793 |
| | 6.36 | 7 | 0.432972 | 0.011223 | 10.865037 | 1.137451 | 0.181366 | 0.007255 | 2.301528 | 0.061258 | 2317.8 | 50.6 | 2507.8 | 100.5 | 2661.6 | 67.3 | 3.76 | 624 | 212 | 378 |
| SC03 | 1 | 2 | 0.30465 | 0.01134 | 7.314658 | 0.608137 | 0.173904 | 0.004053 | 3.31694 | 0.118991 | 1712.1 | 55.8 | 2144.5 | 73.3 | 2593.8 | 38.7 | 1.47 | 1283 | 879 | 643 |
| | 2 | 2 | 0.49262 | 0.007994 | 12.720507 | 0.961305 | 0.188027 | 0.004208 | 2.030645 | 0.032846 | 2581.3 | 34.5 | 2662.7 | 61.7 | 2723.6 | 36.8 | 5.98 | 400 | 62 | 98 |
| | 3 | 2 | 0.290134 | 0.01035 | 6.297777 | 0.538539 | 0.156873 | 0.003897 | 3.481566 | 0.124259 | 1640.3 | 51.7 | 2010.7 | 75.4 | 2419.7 | 42.4 | 4.89 | 1482 | 450 | 253 |
| | 4 | 2 | 0.364508 | 0.004056 | 8.549357 | 0.622719 | 0.169677 | 0.00373 | 2.735695 | 0.026824 | 2003.4 | 19.2 | 2291 | 66.1 | 2553.2 | 37.1 | 136.4 | 1123 | 8 | 46 |
| | 5 | 2 | 0.321838 | 0.006431 | 7.078341 | 0.540565 | 0.159378 | 0.003779 | 3.113534 | 0.063615 | 1798.1 | 31.4 | 2119.2 | 68.4 | 2447.1 | 40.4 | 17.73 | 870 | 48 | 62 |
| | 6 | 2 | 0.289293 | 0.003154 | 6.072568 | 0.443198 | 0.151931 | 0.003334 | 3.454749 | 0.038053 | 1637.9 | 15.8 | 1986.1 | 63.7 | 2369.7 | 42.1 | 20.45 | 1228 | 57 | 60 |
| | 7 | 2 | 0.558806 | 0.00745 | 14.981469 | 1.101565 | 0.194386 | 0.004239 | 1.78972 | 0.024249 | 2861.2 | 30.9 | 2813.4 | 70.6 | 2778.5 | 35.6 | 1.87 | 872 | 438 | 485 |
| | 8 | 2 | 0.16214 | 0.002517 | 2.244613 | 0.168132 | 0.100334 | 0.002312 | 6.172373 | 0.095584 | 968.5 | 14 | 1194.3 | 52.5 | 1628.4 | 42.9 | 224.83 | 2904 | 13 | 25 |
| | 9 | 2 | 0.127427 | 0.005316 | 8.338067 | 0.687529 | 0.473882 | 0.010417 | 7.966358 | 0.330755 | 772.5 | 30.3 | 2262.7 | 73.1 | 4160.9 | 32.2 | 1.89 | 6424 | 3211 | 13541 |
| | 10 | 2 | 0.168765 | 0.003213 | 10.398282 | 0.7814 | 0.44761 | 0.009856 | 5.938385 | 0.114965 | 1005.1 | 17.7 | 2469.3 | 70.6 | 4076.2 | 32.8 | 2.57 | 5607 | 2064 | 15879 |
| | 11 | 2 | 0.169947 | 0.002911 | 3.692959 | 0.302744 | 0.157365 | 0.005877 | 5.895989 | 0.099223 | 1011.7 | 16 | 1565.6 | 64.4 | 2417.7 | 63.3 | 19.44 | 3265 | 156 | 2213 |
| | 12 | 2 | 0.314401 | 0.005142 | 7.76505 | 0.587277 | 0.17894 | 0.004177 | 3.186431 | 0.051096 | 1762 | 25.1 | 2202.5 | 67 | 2641.3 | 38.7 | 5.37 | 739 | 128 | 412 |
| | 13 | 2 | 0.547653 | 0.007415 | 14.716262 | 1.080095 | 0.194808 | 0.004296 | 1.828012 | 0.025202 | 2814.9 | 31 | 2796.5 | 70.2 | 2782 | 36.3 | 2.11 | 450 | 199 | 423 |
| | 14 | 2 | 0.395002 | 0.006226 | 9.528818 | 0.702987 | 0.174176 | 0.003773 | 2.526699 | 0.036544 | 2151.8 | 25.5 | 2389.6 | 69.6 | 2597.1 | 36.2 | 22.62 | 1030 | 43 | 88 |
| | 15 | 2 | 0.500974 | 0.005708 | 12.692056 | 0.92995 | 0.183691 | 0.004097 | 1.997442 | 0.022945 | 2617.7 | 24.5 | 2656.6 | 69.2 | 2685.2 | 37 | 15.36 | 577 | 58 | 114 |
| | 16 | 2 | 0.494815 | 0.005705 | 12.541174 | 0.917789 | 0.18375 | 0.003953 | 2.022425 | 0.023594 | 2591.2 | 24.6 | 2645.4 | 69.1 | 2686 | 35.6 | 1.34 | 1039 | 760 | 754 |
| | 17 | 2 | 0.495236 | 0.006857 | 12.432351 | 0.913829 | 0.181792 | 0.004058 | 2.021815 | 0.027521 | 2592.8 | 29.5 | 2637 | 68.4 | 2668 | 36.9 | 14.3 | 467 | 37 | 97 |
| | 18 | 2 | 0.351781 | 0.007058 | 8.058627 | 0.607653 | 0.166058 | 0.003709 | 2.852712 | 0.060925 | 1942.4 | 33.9 | 2235.9 | 69.9 | 2516.9 | 37.3 | 24.35 | 1273 | 54 | 69 |
| | 19 | 2 | 0.350022 | 0.0191 | 8.140205 | 0.80351 | 0.167639 | 0.004483 | 2.929468 | 0.143362 | 1928.8 | 89.7 | 2230.6 | 85.3 | 2530.9 | 44.3 | 11.6 | 804 | 66 | 92 |
| | 20 | 2 | 0.282145 | 0.018301 | 8.793949 | 0.687245 | 0.2325 | 0.013649 | 3.674065 | 0.214624 | 1596.1 | 90.8 | 2313.5 | 72.7 | 3043 | 92.9 | 1.61 | 1141 | 883 | 1590 |
| | 21 | 2 | 0.373166 | 0.014145 | 8.772771 | 0.757531 | 0.169891 | 0.004133 | 2.714364 | 0.101029 | 2041.2 | 66.2 | 2306.2 | 78.3 | 2554.4 | 40.7 | 18.13 | 1138 | 74 | 80 |
| | 22 | 2 | 0.34534 | 0.021382 | 7.856422 | 0.870637 | 0.162691 | 0.005478 | 3.005935 | 0.192341 | 1904.7 | 102.7 | 2186.7 | 103.7 | 2476.3 | 58 | 19.63 | 1065 | 135 | 89 |
| | 23 | 2 | 0.480975 | 0.012197 | 12.085703 | 0.938931 | 0.182006 | 0.003943 | 2.090974 | 0.056 | 2529.6 | 53.5 | 2607.7 | 75.3 | 2670.2 | 36.1 | 8.97 | 1363 | 146 | 160 |
| | 24 | 2 | 0.505164 | 0.007119 | 12.815233 | 0.941029 | 0.183949 | 0.004036 | 1.981709 | 0.027582 | 2635.5 | 30.4 | 2665.6 | 68.9 | 2687.6 | 36.5 | 0.91 | 723 | 767 | 862 |
| | 25 | 2 | 0.521254 | 0.007584 | 13.758737 | 1.036976 | 0.191191 | 0.00443 | 1.920747 | 0.028377 | 2703.9 | 32.2 | 2731.5 | 72.2 | 2750.8 | 38.2 | 2.1 | 511 | 237 | 550 |
| | 26 | 2 | 0.332752 | 0.005467 | 10.352519 | 1.020233 | 0.224303 | 0.013179 | 3.010461 | 0.051251 | 1851.3 | 26.5 | 2449.6 | 88.6 | 2986 | 91.6 | 0.8 | 1077 | 1307 | 3553 |
| | 27 | 2 | 0.252241 | 0.003376 | 4.69528 | 0.343339 | 0.135062 | 0.003303 | 3.967403 | 0.053121 | 1449.9 | 17.4 | 1766.1 | 61.2 | 2162.4 | 42.4 | 120.68 | 2808 | 24 | 382 |
| | 28 | 2 | 0.432314 | 0.006771 | 10.524106 | 0.780653 | 0.176484 | 0.003962 | 2.307833 | 0.032877 | 2315.6 | 30.7 | 2481.1 | 69.3 | 2618.7 | 37.7 | 1.52 | 560 | 360 | 385 |
| | 29 | 2 | 0.306682 | 0.003226 | 7.868711 | 0.573128 | 0.186406 | 0.003983 | 3.260559 | 0.034083 | 1724.3 | 15.9 | 2215.9 | 65.6 | 2709.8 | 35.1 | 31.56 | 5174 | 160 | 1881 |
| | 30 | 2 | 0.31769 | 0.004624 | 7.1494 | 0.53217 | 0.163077 | 0.003614 | 3.150469 | 0.046838 | 1778.2 | 22.7 | 2129.2 | 67.1 | 2486.5 | 37.3 | 96.6 | 1461 | 15 | 20 |

Continued on next page

| Sample | Spot name | Run | 206/238 | ±2SE | 207/235 | ±2SE | 207/206 | ±2SE | 238/P206 | ±2SE | 206/238 Age | ±2SE | 207/235 Age | ±2SE | 207/206 Age | ±2SE | U/Th | U | Th | Pb |
|---|---|---|---|---|---|---|---|---|---|---|---|---|---|---|---|---|---|---|---|---|
| | 31 | 2 | 0.545758 | 0.008937 | 14.617862 | 1.088298 | 0.194127 | 0.004537 | 1.836561 | 0.029676 | 2806.7 | 37.2 | 2789.5 | 71.3 | 2775.7 | 38.6 | 1.36 | 265 | 240 | 334 |
| | 32 | 2 | 0.379457 | 0.003942 | 9.410973 | 0.686705 | 0.179736 | 0.003878 | 2.637826 | 0.027213 | 2073.6 | 18.4 | 2378.6 | 66.8 | 2649.4 | 35.8 | 3.55 | 1618 | 501 | 473 |
| | 33 | 2 | 0.47964 | 0.010911 | 11.913296 | 0.944167 | 0.179685 | 0.004613 | 2.095652 | 0.050008 | 2524.2 | 47.8 | 2593.3 | 75.7 | 2647.2 | 42.1 | 1.79 | 1308 | 955 | 1356 |
| | 34 | 2 | 0.508878 | 0.006543 | 12.864621 | 0.943657 | 0.183221 | 0.004011 | 1.968479 | 0.025628 | 2651.5 | 28 | 2669.3 | 69.6 | 2681.1 | 36.1 | 4.24 | 771 | 202 | 343 |
| | 35 | 2 | 0.325045 | 0.026333 | 7.671221 | 1.032792 | 0.167011 | 0.006297 | 3.26198 | 0.24441 | 1802.6 | 126.2 | 2147.3 | 116 | 2518.1 | 62.4 | 2.51 | 1191 | 532 | 414 |
| | 36 | 2 | 0.368987 | 0.035227 | 9.023304 | 1.297683 | 0.171561 | 0.007373 | 2.998278 | 0.327344 | 2004.2 | 167.5 | 2271 | 146.4 | 2558.2 | 75.8 | 2.41 | 1209 | 612 | 456 |
| | 37 | 2 | 0.161952 | 0.008382 | 4.065813 | 0.727573 | 0.174566 | 0.018168 | 6.319947 | 0.293339 | 966.1 | 46 | 1585.1 | 117.8 | 2526 | 144.3 | 0.73 | 3138 | 4801 | 3909 |
| | 38 | 2 | 0.282993 | 0.004912 | 6.426333 | 0.47912 | 0.164534 | 0.00355 | 3.546035 | 0.063611 | 1606.1 | 24.8 | 2034.8 | 66.7 | 2501.7 | 36.2 | 3.42 | 1192 | 461 | 281 |
| | 39 | 2 | 0.347877 | 0.005137 | 8.149109 | 0.604484 | 0.169715 | 0.003702 | 2.882618 | 0.044252 | 1924.1 | 24.7 | 2246.8 | 68.4 | 2553.7 | 36.7 | 29.76 | 844 | 37 | 81 |
| | 40 | 2 | 0.32763 | 0.04046 | 6.954704 | 1.252898 | 0.14637 | 0.007655 | 3.488553 | 0.389639 | 1799.6 | 191.2 | 2007.8 | 157.7 | 2279.7 | 93.9 | 0.44 | 5156 | 17445 | 8501 |
| | 42 | 5 | 0.353722 | 0.029541 | 8.85667 | 1.069792 | 0.181328 | 0.007878 | 2.987815 | 0.253824 | 1940.3 | 140.5 | 2279.7 | 115.1 | 2655.8 | 74.7 | 4.12 | 816 | 213 | 274 |
| | 43 | 5 | 0.41476 | 0.015986 | 10.26099 | 0.672959 | 0.182471 | 0.005857 | 2.413431 | 0.0971 | 2235.9 | 73.2 | 2457.4 | 62.4 | 2674.4 | 53.1 | 2.98 | 1211 | 485 | 391 |
| | 44 | 5 | 0.53569 | 0.019909 | 13.859379 | 0.894573 | 0.190749 | 0.006112 | 1.864888 | 0.070984 | 2764.9 | 83.9 | 2739.6 | 61.7 | 2747.7 | 52.7 | 60.16 | 1070 | 16 | 35 |
| | 45 | 5 | 0.159347 | 0.006286 | 10.789417 | 0.709716 | 0.492466 | 0.015917 | 6.266388 | 0.249776 | 953.1 | 35 | 2504.6 | 61.6 | 4218 | 47.9 | 69.37 | 3309 | 39 | 4103 |
| | 46 | 5 | 0.238227 | 0.008645 | 5.571814 | 0.358757 | 0.170173 | 0.005466 | 4.187722 | 0.152781 | 1377.4 | 45 | 1911.4 | 55.6 | 2558.3 | 53.5 | 3.85 | 1964 | 464 | 658 |
| | 47 | 5 | 0.39226 | 0.014412 | 9.674902 | 0.629346 | 0.179493 | 0.005768 | 2.544512 | 0.095512 | 2132.9 | 66.9 | 2403.4 | 60.6 | 2647.2 | 53.3 | 4.75 | 1419 | 258 | 365 |
| | 48 | 5 | 0.267157 | 0.018266 | 8.385937 | 1.138991 | 0.226117 | 0.01725 | 3.760728 | 0.265857 | 1525.2 | 93.2 | 2259.6 | 129.2 | 3013.6 | 127.5 | 139.04 | 1705 | 10 | 1354 |
| | 49 | 5 | 0.469163 | 0.020261 | 12.141687 | 0.832781 | 0.187752 | 0.006134 | 2.138409 | 0.096321 | 2477.8 | 89.4 | 2612.4 | 66.3 | 2721.2 | 53.7 | 1.71 | 407 | 221 | 265 |
| | 50 | 5 | 0.278697 | 0.01404 | 4.924615 | 0.383573 | 0.127885 | 0.004288 | 3.602948 | 0.19479 | 1583.8 | 71.3 | 1802.7 | 67.7 | 2067.6 | 59 | 52.92 | 3450 | 54 | 3848 |
| SG01 | 1 | 4 | 0.622889 | 0.044279 | 20.094873 | 1.526099 | 0.246764 | 0.005661 | 1.648531 | 0.12833 | 3112.3 | 178.5 | 3085 | 77.6 | 3162.7 | 36.6 | 0.25 | 2841 | 11264 | 8119 |
| | 2 | 4 | 0.285244 | 0.013654 | 6.103593 | 0.408896 | 0.163808 | 0.005098 | 3.583981 | 0.161927 | 1615.2 | 68 | 1977.5 | 56.4 | 2488.8 | 52.2 | 1.45 | 1801 | 1321 | 308 |
| | 3 | 4 | 0.318755 | 0.009986 | 7.010094 | 0.252638 | 0.169854 | 0.004306 | 3.1722 | 0.099523 | 1783 | 48.8 | 2110.1 | 32.3 | 2552.7 | 42.7 | 7.44 | 1550 | 230 | 548 |
| | 4 | 4 | 0.344155 | 0.011421 | 7.743551 | 0.272085 | 0.174612 | 0.003887 | 2.935601 | 0.09848 | 1906.1 | 54.8 | 2200.4 | 32.2 | 2600.9 | 37.4 | 36.21 | 2130 | 67 | 64 |
| | 5 | 4 | 0.303582 | 0.008843 | 7.037752 | 0.196573 | 0.178003 | 0.003735 | 3.323867 | 0.096829 | 1708.8 | 43.7 | 2115.8 | 24.8 | 2633.1 | 34.9 | 3.12 | 1891 | 605 | 465 |
| | 6 | 4 | 0.30359 | 0.009495 | 6.720311 | 0.248088 | 0.169604 | 0.003849 | 3.325756 | 0.103477 | 1708.7 | 46.9 | 2073.3 | 32.3 | 2551.9 | 37.9 | 1.24 | 3193 | 2671 | 1459 |
| | 7 | 4 | 0.278416 | 0.007821 | 5.799518 | 0.200719 | 0.159463 | 0.003725 | 3.620797 | 0.104522 | 1583.1 | 39.5 | 1944.1 | 30.6 | 2447.4 | 39.5 | 1.7 | 2199 | 1312 | 646 |
| | 8 | 4 | 0.516329 | 0.014602 | 13.765166 | 0.413804 | 0.202414 | 0.004046 | 1.949264 | 0.055262 | 2683 | 62.1 | 2732.6 | 28.5 | 2844.6 | 32.5 | 10.78 | 908 | 94 | 83 |
| | 9 | 4 | 0.219321 | 0.007235 | 4.224152 | 0.151387 | 0.145555 | 0.003389 | 4.556089 | 0.138013 | 1278 | 38.6 | 1677.1 | 30.3 | 2292.3 | 39.7 | 1.04 | 3009 | 3971 | 1561 |
| | 10 | 4 | 0.372021 | 0.011586 | 9.359027 | 0.284207 | 0.187027 | 0.00374 | 2.697174 | 0.085107 | 2038.3 | 54.5 | 2372.8 | 27.6 | 2715.1 | 33.2 | 8.41 | 1769 | 334 | 848 |
| | 11 | 4 | 0.252434 | 0.008609 | 5.792718 | 0.274283 | 0.161814 | 0.004253 | 3.955454 | 0.136915 | 1450.3 | 44.4 | 1939.4 | 41.5 | 2470.7 | 44.9 | 2.56 | 2544 | 990 | 1125 |
| | 12 | 4 | 0.239672 | 0.015948 | 5.475199 | 0.476381 | 0.161073 | 0.004577 | 4.258719 | 0.294006 | 1381.9 | 83.1 | 1879.4 | 75.6 | 2463.1 | 47.8 | 4.49 | 2155 | 659 | 534 |
| | 13 | 4 | 0.281304 | 0.007753 | 7.003459 | 0.195215 | 0.177728 | 0.003701 | 3.539173 | 0.097874 | 1597.7 | 39 | 2111.2 | 24.8 | 2630.3 | 34.6 | 3.1 | 2168 | 714 | 571 |
| | 14 | 4 | 0.455277 | 0.012097 | 13.176475 | 0.345959 | 0.207783 | 0.004335 | 2.187354 | 0.058192 | 2418.4 | 53.6 | 2691.9 | 24.8 | 2886.8 | 33.7 | 7.09 | 1064 | 150 | 170 |
| | 15 | 4 | 0.278848 | 0.009367 | 6.664909 | 0.257746 | 0.171891 | 0.003594 | 3.585676 | 0.125495 | 1585 | 47.4 | 2065.2 | 35.1 | 2574.7 | 35.1 | 2.44 | 2034 | 947 | 1469 |
| | 16 | 4 | 0.332167 | 0.009077 | 8.788868 | 0.235127 | 0.191747 | 0.003816 | 3.003688 | 0.082732 | 1848.7 | 44 | 2315.9 | 24.4 | 2756.1 | 32.6 | 3.19 | 1737 | 552 | 558 |
| | 17 | 4 | 0.256948 | 0.007487 | 5.41995 | 0.186015 | 0.153728 | 0.003601 | 3.886328 | 0.110228 | 1474 | 38.3 | 1886.8 | 28.5 | 2385.9 | 39.2 | 2.09 | 2221 | 1079 | 1272 |
| | 18 | 4 | 0.225464 | 0.005881 | 4.286352 | 0.111814 | 0.139204 | 0.00284 | 4.42833 | 0.114503 | 1310.6 | 30.9 | 1690.5 | 21.4 | 2215.9 | 35.5 | 1.71 | 2801 | 1643 | 1073 |
| | 19 | 4 | 0.465544 | 0.013179 | 12.751282 | 0.414869 | 0.200397 | 0.004228 | 2.1471 | 0.06099 | 2463.5 | 58 | 2659.8 | 30.6 | 2828 | 34.5 | 23.6 | 1354 | 58 | 481 |
| | 20 | 4 | 0.238423 | 0.007984 | 4.79654 | 0.236349 | 0.148547 | 0.004442 | 4.193399 | 0.140702 | 1378.3 | 41.6 | 1781.9 | 41.3 | 2326.4 | 51.1 | 2.67 | 2531 | 950 | 1176 |
| | 21 | 4 | 0.251741 | 0.01153 | 5.777068 | 0.348445 | 0.162337 | 0.004178 | 4.007317 | 0.198503 | 1445.6 | 59.8 | 1931.6 | 54.8 | 2476.4 | 44.2 | 10.41 | 2144 | 221 | 232 |
| | 22 | 4 | 0.424807 | 0.02854 | 16.30206 | 1.187222 | 0.272455 | 0.009731 | 2.364117 | 0.159761 | 2279.2 | 129 | 2888.7 | 71.3 | 3317.2 | 57.1 | 4.1 | 3535 | 854 | 8301 |
| | 23 | 4 | 0.237871 | 0.008115 | 5.14962 | 0.231874 | 0.153321 | 0.003939 | 4.199185 | 0.144085 | 1375 | 42.3 | 1839.4 | 38.6 | 2379.5 | 44.6 | 0.79 | 2292 | 3078 | 1045 |
| | 24 | 4 | 0.141788 | 0.003735 | 2.021315 | 0.054826 | 0.101196 | 0.002077 | 7.014555 | 0.18598 | 854.7 | 21.1 | 1124.4 | 16.4 | 1644.5 | 38.3 | 85.44 | 5196 | 59 | 514 |
| | 25 | 4 | 0.37993 | 0.011782 | 10.375007 | 0.371773 | 0.19494 | 0.004094 | 2.621047 | 0.082141 | 2075.5 | 55.1 | 2467.3 | 33.7 | 2783.1 | 34.5 | 8.99 | 2045 | 218 | 308 |
| | 26 | 4 | 0.572134 | 0.016888 | 17.400999 | 0.5384 | 0.215509 | 0.004394 | 1.74185 | 0.052835 | 2915.7 | 69.6 | 2955.8 | 30.2 | 2946.2 | 32.8 | 25.06 | 1111 | 43 | 124 |
| | 27 | 4 | 0.201611 | 0.005854 | 3.94106 | 0.11629 | 0.139285 | 0.002956 | 4.943182 | 0.154683 | 1183.8 | 31.6 | 1626.4 | 17.9 | 2216.7 | 36.9 | 2.81 | 4782 | 1793 | 2984 |
| | 28 | 4 | 0.407134 | 0.01123 | 11.269433 | 0.310317 | 0.19686 | 0.003923 | 2.447533 | 0.068553 | 2201.4 | 51.5 | 2545 | 25.8 | 2799.2 | 32.6 | 9.72 | 1265 | 124 | 331 |
| | 29 | 4 | 0.328213 | 0.008668 | 8.535743 | 0.225555 | 0.185172 | 0.003663 | 3.035288 | 0.079628 | 1829.6 | 42 | 2289.3 | 24 | 2698.6 | 32.7 | 2.47 | 1857 | 724 | 908 |
| | 30 | 4 | 0.216555 | 0.006206 | 4.198966 | 0.143316 | 0.138126 | 0.003109 | 4.607302 | 0.1333 | 1263.4 | 32.9 | 1672.1 | 27.4 | 2201.5 | 38.5 | 2.78 | 4074 | 1421 | 2208 |
| SG02 | 1 | 4 | 0.207614 | 0.005665 | 4.460247 | 0.125113 | 0.155445 | 0.003264 | 4.806721 | 0.133879 | 1216 | 30.3 | 1723 | 23.3 | 2405.1 | 35.8 | 1.6 | 3214 | 2118 | 1556 |
| | 2 | 4 | 0.247111 | 0.009306 | 5.449608 | 0.241934 | 0.159071 | 0.003603 | 4.057962 | 0.155566 | 1422.8 | 48.2 | 1889.1 | 38.1 | 2443.9 | 38 | 1.57 | 2739 | 1795 | 1770 |
| | 3 | 4 | 0.364718 | 0.011425 | 9.567816 | 0.330662 | 0.190204 | 0.00382 | 2.743199 | 0.088795 | 2003.7 | 54.2 | 2391.7 | 32 | 2742.7 | 33.1 | 1.37 | 2090 | 1548 | 1394 |
| | 5 | 4 | 0.125268 | 0.003916 | 1.673977 | 0.057171 | 0.097564 | 0.002427 | 7.975226 | 0.249217 | 760.7 | 22.4 | 998.1 | 21.5 | 1575.6 | 46 | 7.66 | 6539 | 852 | 958 |
| | 6 | 4 | 0.237525 | 0.013261 | 6.9977 | 0.537928 | 0.214783 | 0.007782 | 4.217435 | 0.243964 | 1373.3 | 69.3 | 2107.4 | 70.4 | 2939.6 | 60.2 | 2.95 | 4198 | 1417 | 6048 |

Continued on next page

| Sample | Spot name | Run | 206/238 | ±2SE | 207/235 | ±2SE | 207/206 | ±2SE | 238/P206 | ±2SE | 206/238 Age | ±2SE | 207/235 Age | ±2SE | 207/206 Age | ±2SE | U/Th | U | Th | Pb |
|---|---|---|---|---|---|---|---|---|---|---|---|---|---|---|---|---|---|---|---|---|
| | 7 | 4 | 0.53065 | 0.014469 | 16.917387 | 0.443031 | 0.232608 | 0.004707 | 1.881587 | 0.052014 | 2743.7 | 61.1 | 2929.7 | 25.3 | 3068.8 | 32.2 | 0.79 | 1024 | 1284 | 2470 |
| | 8 | 4 | 0.606795 | 0.018173 | 17.85032 | 0.514476 | 0.215906 | 0.004437 | 1.646063 | 0.049174 | 3056.4 | 72.8 | 2981.1 | 27.7 | 2949.3 | 33.5 | 5.56 | 1781 | 318 | 808 |
| | 9 | 4 | 0.29609 | 0.0086 | 7.486539 | 0.219219 | 0.184587 | 0.003579 | 3.375211 | 0.102876 | 1671.5 | 43 | 2170.3 | 26.7 | 2693.5 | 32 | 1.58 | 2163 | 1359 | 1629 |
| | 10 | 4 | 0.389305 | 0.01122 | 10.538034 | 0.304798 | 0.196156 | 0.004109 | 2.56299 | 0.073562 | 2119.4 | 52 | 2482.8 | 26.9 | 2793.4 | 34.3 | 14.36 | 1519 | 108 | 212 |
| | 11 | 4 | 0.344335 | 0.009837 | 8.911715 | 0.256203 | 0.188694 | 0.004022 | 2.897479 | 0.084497 | 1907.1 | 47.3 | 2328.1 | 26.4 | 2729.1 | 35 | 2.87 | 1420 | 532 | 771 |
| | 12 | 4 | 0.259474 | 0.006814 | 5.685401 | 0.147673 | 0.159826 | 0.003154 | 3.84092 | 0.099711 | 1487.1 | 34.8 | 1928.9 | 22.4 | 2452.7 | 33.2 | 10.21 | 2799 | 277 | 504 |
| | 13 | 4 | 0.407298 | 0.010695 | 11.265894 | 0.28807 | 0.201909 | 0.004074 | 2.447292 | 0.063313 | 2202.4 | 48.9 | 2545.1 | 23.9 | 2840.4 | 33.1 | 2.17 | 1881 | 900 | 728 |
| | 14 | 4 | 0.432047 | 0.011924 | 11.667261 | 0.325567 | 0.195606 | 0.004231 | 2.307281 | 0.063665 | 2314.8 | 53.7 | 2577.8 | 26 | 2788.7 | 35.5 | 12.05 | 1086 | 101 | 127 |
| | 15 | 4 | 0.552297 | 0.014786 | 16.285749 | 0.450401 | 0.214162 | 0.004219 | 1.805283 | 0.047977 | 2834.5 | 61.3 | 2893.3 | 26.6 | 2936.4 | 31.8 | 3.23 | 1270 | 403 | 532 |
| | 16 | 4 | 0.572559 | 0.017984 | 16.387994 | 0.477632 | 0.207185 | 0.004663 | 1.742421 | 0.054488 | 2917.9 | 73.6 | 2899.4 | 27.7 | 2882.6 | 36.2 | 1.71 | 1749 | 1038 | 941 |
| | 17 | 4 | 0.292077 | 0.009138 | 7.43899 | 0.236643 | 0.187637 | 0.003886 | 3.418008 | 0.109016 | 1651.7 | 45.7 | 2165 | 28.7 | 2720.5 | 34.3 | 2.25 | 1804 | 821 | 864 |
| | 18 | 4 | 0.384792 | 0.013172 | 10.014177 | 0.345935 | 0.190188 | 0.003755 | 2.605248 | 0.092751 | 2097.3 | 61.6 | 2433.6 | 32.6 | 2742.7 | 32.5 | 3.7 | 2001 | 593 | 783 |
| | 19 | 4 | 0.307933 | 0.010967 | 7.599517 | 0.298449 | 0.180123 | 0.003845 | 3.258441 | 0.118207 | 1729.4 | 54.1 | 2181.2 | 35.4 | 2652.3 | 35.3 | 4.16 | 2040 | 496 | 487 |
| | 20 | 4 | 0.595504 | 0.015866 | 18.901101 | 0.500117 | 0.231711 | 0.004606 | 1.675811 | 0.043917 | 3011.3 | 63.9 | 3036.3 | 25.6 | 3065.5 | 27.9 | 1.45 | 497 | 339 | 547 |
| | 21 | 4 | 0.26423 | 0.008747 | 6.406185 | 0.226512 | 0.173906 | 0.003659 | 3.781616 | 0.127089 | 1510.8 | 44.7 | 2030.7 | 31.1 | 2594 | 35 | 3 | 1998 | 745 | 709 |
| | 22 | 4 | 0.377856 | 0.00984 | 10.239192 | 0.265579 | 0.194695 | 0.003849 | 2.632068 | 0.068518 | 2066.2 | 46 | 2456.4 | 24 | 2781.2 | 32.4 | 2.26 | 2155 | 966 | 965 |
| | 23 | 4 | 0.621872 | 0.016605 | 20.51915 | 0.536494 | 0.235762 | 0.004779 | 1.599421 | 0.042916 | 3116.9 | 66.1 | 3115.7 | 25.2 | 3090.3 | 32.4 | 1.22 | 414 | 337 | 505 |
| | 24 | 4 | 0.369499 | 0.011254 | 9.7533 | 0.295411 | 0.187785 | 0.003788 | 2.694762 | 0.082288 | 2026.5 | 53 | 2410.7 | 28 | 2721.7 | 33.2 | 3.55 | 2119 | 604 | 707 |
| | 25 | 4 | 0.375657 | 0.01228 | 10.930793 | 0.356937 | 0.207381 | 0.00403 | 2.653076 | 0.08678 | 2055.1 | 57.5 | 2515.7 | 30.5 | 2884.2 | 31.7 | 1.91 | 1202 | 626 | 756 |
| | 26 | 4 | 0.303913 | 0.0091 | 7.82842 | 0.232628 | 0.183232 | 0.003905 | 3.274141 | 0.098981 | 1710.3 | 45 | 2210.6 | 26.7 | 2680.9 | 35.2 | 2.94 | 1471 | 525 | 558 |
| | 27 | 4 | 0.238475 | 0.006211 | 5.818998 | 0.146144 | 0.174722 | 0.003449 | 4.166649 | 0.107531 | 1378.7 | 32.3 | 1949.1 | 21.7 | 2602.3 | 32.8 | 0.24 | 2459 | 13462 | 1038 |
| | 28 | 4 | 0.17092 | 0.006111 | 3.577754 | 0.13395 | 0.149113 | 0.00307 | 5.831069 | 0.195492 | 1016.9 | 33.5 | 1543.3 | 29 | 2334.6 | 35.4 | 9.8 | 2371 | 243 | 542 |
| | 29 | 4 | 0.268386 | 0.007461 | 6.599934 | 0.204041 | 0.176221 | 0.003909 | 3.706456 | 0.104304 | 1532.5 | 38 | 2058.4 | 27.7 | 2615.9 | 37.4 | 24.37 | 2066 | 85 | 424 |
| | 30 | 4 | 0.602797 | 0.016441 | 19.237676 | 0.507615 | 0.231184 | 0.004807 | 1.65175 | 0.044302 | 3040.5 | 65.9 | 3053.3 | 25.3 | 3058.8 | 33.2 | 1.35 | 416 | 311 | 522 |
| SR01 | 1 | 3 | 0.405318 | 0.010641 | 10.150466 | 0.54759 | 0.182616 | 0.003194 | 2.475251 | 0.064603 | 2193.3 | 48.8 | 2448.2 | 49.8 | 2675.3 | 28.9 | 1.02 | 374 | 360 | 372 |
| | 2 | 3 | 0.38315 | 0.010902 | 9.33467 | 0.538062 | 0.17743 | 0.003728 | 2.620657 | 0.075835 | 2090.7 | 50.9 | 2370.1 | 52.5 | 2626.9 | 34.7 | 1.29 | 288 | 217 | 250 |
| | 3 | 3 | 0.496433 | 0.013801 | 12.223668 | 0.665343 | 0.179587 | 0.00307 | 2.022831 | 0.05588 | 2598 | 59.4 | 2621.2 | 50.8 | 2647.8 | 28.5 | 1.35 | 223 | 161 | 209 |
| | 4 | 3 | 0.492709 | 0.014883 | 12.388721 | 0.687217 | 0.183571 | 0.003413 | 2.04139 | 0.061731 | 2581.4 | 64.3 | 2633.3 | 51.7 | 2683.6 | 30.6 | 1.15 | 87 | 74 | 99 |
| | 5 | 3 | 0.574471 | 0.016893 | 23.132324 | 1.356253 | 0.293572 | 0.006048 | 1.750317 | 0.052303 | 2925.2 | 69.3 | 3229.8 | 57.7 | 3434.3 | 31.8 | 1.46 | 336 | 225 | 338 |
| | 6 | 3 | 0.417251 | 0.014936 | 10.229719 | 0.611911 | 0.178889 | 0.002901 | 2.419995 | 0.088862 | 2246.3 | 68.2 | 2452.7 | 56 | 2641.5 | 26.9 | 1.88 | 347 | 181 | 221 |
| | 7 | 3 | 0.459179 | 0.014147 | 11.259799 | 0.654984 | 0.178912 | 0.003329 | 2.192182 | 0.070002 | 2435 | 62.8 | 2542.6 | 54.9 | 2641 | 30.8 | 2.32 | 165 | 70 | 93 |
| | 9 | 3 | 0.272758 | 0.00799 | 7.517817 | 0.479353 | 0.201599 | 0.006487 | 3.682832 | 0.107473 | 1554.7 | 40.4 | 2173.2 | 56.7 | 2835.5 | 51.6 | 1.53 | 568 | 372 | 413 |
| | 10 | 3 | 0.319407 | 0.009672 | 7.325575 | 0.424267 | 0.167295 | 0.002941 | 3.14879 | 0.097421 | 1786.5 | 47.4 | 2150.5 | 52.1 | 2529.5 | 29.4 | 0.77 | 550 | 713 | 584 |
| | 11 | 3 | 0.243899 | 0.009165 | 5.604224 | 0.360623 | 0.167662 | 0.003157 | 4.135192 | 0.152426 | 1406.3 | 47.4 | 1913.8 | 54.7 | 2532.9 | 31.6 | 1.94 | 1189 | 638 | 521 |
| | 12 | 3 | 0.508848 | 0.013553 | 12.569187 | 0.68222 | 0.180744 | 0.00329 | 1.973914 | 0.052397 | 2651.4 | 57.9 | 2647.4 | 51.5 | 2658 | 30.2 | 1.22 | 283 | 242 | 315 |
| | 13 | 3 | 0.516512 | 0.013878 | 12.81557 | 0.691919 | 0.18138 | 0.00312 | 1.944698 | 0.052314 | 2684 | 59 | 2665.8 | 50.2 | 2664.2 | 28.7 | 1.34 | 261 | 203 | 270 |
| | 14 | 3 | 0.293614 | 0.007707 | 7.523043 | 0.443786 | 0.187573 | 0.005701 | 3.419571 | 0.090932 | 1659.5 | 38.5 | 2173.2 | 53.7 | 2713.7 | 52 | 1.25 | 624 | 528 | 490 |
| | 15 | 3 | 0.428356 | 0.011597 | 10.750212 | 0.579158 | 0.183645 | 0.00331 | 2.344517 | 0.062991 | 2298 | 52.3 | 2501.5 | 50.1 | 2688.5 | 26.5 | 2.3 | 217 | 99 | 141 |
| | 16 | 3 | 0.362243 | 0.00981 | 8.78086 | 0.472174 | 0.177243 | 0.002987 | 2.770989 | 0.076049 | 1992.6 | 46.5 | 2315.3 | 49.1 | 2626.2 | 28.1 | 1.99 | 774 | 408 | 409 |
| | 17 | 3 | 0.418723 | 0.012723 | 9.795147 | 0.538345 | 0.171143 | 0.003016 | 2.399858 | 0.0724 | 2254.1 | 57.7 | 2415.2 | 50.4 | 2567.6 | 29.4 | 1.62 | 485 | 312 | 308 |
| | 18 | 3 | 0.345327 | 0.01031 | 8.334314 | 0.462859 | 0.176999 | 0.003116 | 2.906735 | 0.085751 | 1912 | 49.3 | 2267.6 | 50.5 | 2623.9 | 29.6 | 0.9 | 664 | 763 | 744 |
| | 19 | 3 | 0.382648 | 0.0113 | 9.288755 | 0.511884 | 0.177799 | 0.003254 | 2.625646 | 0.078813 | 2088.1 | 52.8 | 2366.1 | 50.7 | 2630.7 | 30.2 | 1.57 | 404 | 264 | 311 |
| | 20 | 3 | 0.405898 | 0.010609 | 9.334125 | 0.500368 | 0.168374 | 0.002799 | 2.469837 | 0.065424 | 2196 | 48.7 | 2371.2 | 49.4 | 2540.3 | 28 | 2.53 | 640 | 256 | 252 |
| | 21 | 3 | 0.378998 | 0.011928 | 10.749281 | 0.686585 | 0.207159 | 0.005326 | 2.641049 | 0.082946 | 2070.8 | 55.7 | 2496.6 | 59.4 | 2878.9 | 42.2 | 0.82 | 518 | 611 | 660 |
| | 22 | 3 | 0.639134 | 0.027388 | 28.076605 | 2.113113 | 0.320633 | 0.008127 | 1.572215 | 0.065882 | 3181.5 | 107.1 | 3413 | 70.1 | 3569.8 | 37.8 | 1.55 | 195 | 120 | 304 |
| | 23 | 3 | 0.614972 | 0.01691 | 24.885245 | 1.350007 | 0.295912 | 0.005144 | 1.620323 | 0.044444 | 3089.5 | 67.5 | 3303.4 | 52.9 | 3447.9 | 27.1 | 1.08 | 212 | 187 | 304 |
| | 24 | 3 | 0.509838 | 0.014271 | 12.434596 | 0.675084 | 0.178657 | 0.003501 | 1.954091 | 0.056248 | 2655.4 | 61.2 | 2637.3 | 51.3 | 2638.3 | 32.3 | 0.97 | 75 | 73 | 107 |
| | 25 | 3 | 0.521555 | 0.014812 | 12.864631 | 0.719996 | 0.180662 | 0.004172 | 1.908697 | 0.053854 | 2705.1 | 62.7 | 2668.5 | 52.2 | 2655.4 | 38.4 | 1.07 | 59 | 53 | 81 |
| | 26 | 3 | 0.422324 | 0.012514 | 10.036277 | 0.560794 | 0.174098 | 0.002955 | 2.354573 | 0.069501 | 2270.6 | 56.7 | 2437.4 | 51.4 | 2596.3 | 28.2 | 9.61 | 496 | 50 | 75 |
| | 27 | 3 | 0.46973 | 0.013107 | 11.957801 | 0.643873 | 0.185787 | 0.003155 | 2.10752 | 0.066665 | 2481.9 | 57.5 | 2600.8 | 50.3 | 2703.9 | 28.1 | 1.66 | 443 | 260 | 367 |
| | 28 | 3 | 0.451987 | 0.01289 | 10.948978 | 0.610441 | 0.177213 | 0.003142 | 2.196199 | 0.06328 | 2403.5 | 57.3 | 2517.7 | 52.2 | 2625.4 | 29.4 | 1.42 | 412 | 283 | 347 |
| | 29 | 3 | 0.427835 | 0.01146 | 10.182674 | 0.549057 | 0.174188 | 0.003113 | 2.315763 | 0.06187 | 2295.7 | 51.7 | 2451.2 | 49.9 | 2596.7 | 29.9 | 1.18 | 548 | 456 | 513 |
| | 30 | 3 | 0.289837 | 0.008791 | 6.025213 | 0.342701 | 0.152015 | 0.00263 | 3.421581 | 0.105876 | 1640.3 | 44 | 1978 | 50.3 | 2367.3 | 29.7 | 2.24 | 801 | 358 | 327 |
| SR02 | 1 | 4 | 0.441832 | 0.012936 | 10.656304 | 0.337819 | 0.174284 | 0.003571 | 2.257819 | 0.068386 | 2358.2 | 58.1 | 2491.9 | 30.1 | 2597.8 | 34 | 1.96 | 469 | 245 | 313 |

Continued on next page

| Sample | Spot name | Run | 206/238 | ±2SE | 207/235 | ±2SE | 207/206 | ±2SE | 238/P206 | ±2SE | 206/238 Age | ±2SE | 207/235 Age | ±2SE | 207/206 Age | ±2SE | U/Th | U | Th | Pb |
|---|---|---|---|---|---|---|---|---|---|---|---|---|---|---|---|---|---|---|---|---|
| | 2 | 4 | 0.348557 | 0.010315 | 8.448334 | 0.230748 | 0.176242 | 0.004274 | 2.864378 | 0.084848 | 1927.2 | 49.3 | 2279.8 | 24.8 | 2614.9 | 40.5 | 2.04 | 883 | 439 | 694 |
| | 3 | 4 | 0.424592 | 0.011549 | 10.306057 | 0.291001 | 0.175982 | 0.003772 | 2.34891 | 0.064506 | 2281.1 | 52.3 | 2462.1 | 25.9 | 2614 | 35.5 | 1.58 | 607 | 390 | 566 |
| | 4 | 4 | 0.368413 | 0.010276 | 8.50741 | 0.233533 | 0.168882 | 0.003426 | 2.711286 | 0.076828 | 2021.6 | 48.5 | 2286.1 | 25.2 | 2545.3 | 34 | 3.21 | 773 | 246 | 368 |
| | 5 | 4 | 0.24023 | 0.008497 | 5.206252 | 0.182623 | 0.159004 | 0.003289 | 4.178901 | 0.14548 | 1387.2 | 44.1 | 1851.5 | 29.7 | 2443.6 | 34.9 | 0.77 | 1887 | 2474 | 1867 |
| | 6 | 4 | 0.486103 | 0.013811 | 11.529377 | 0.339318 | 0.174407 | 0.003602 | 2.058028 | 0.05935 | 2553.2 | 60 | 2565.8 | 27.6 | 2598.9 | 34.6 | 1.73 | 515 | 301 | 485 |
| | 7 | 4 | 0.177651 | 0.008901 | 4.627544 | 0.21692 | 0.192877 | 0.004103 | 5.691091 | 0.278554 | 1053.2 | 48.6 | 1750.7 | 38.5 | 2765.5 | 35.1 | 3.2 | 1081 | 336 | 700 |
| | 8 | 4 | 0.358798 | 0.011464 | 8.165723 | 0.271746 | 0.167612 | 0.0036 | 2.794983 | 0.0872 | 1975.6 | 54.2 | 2247.6 | 30 | 2532.1 | 36.3 | 1.97 | 328 | 174 | 279 |
| | 9 | 4 | 0.393938 | 0.01102 | 8.866793 | 0.258193 | 0.1656 | 0.003893 | 2.539524 | 0.071849 | 2140.6 | 51 | 2323.4 | 26.6 | 2511 | 39.1 | 1.87 | 295 | 160 | 244 |
| | 10 | 4 | 0.189723 | 0.010665 | 3.898191 | 0.282163 | 0.150546 | 0.003942 | 5.342971 | 0.306789 | 1118.6 | 57.8 | 1604.5 | 57.7 | 2349.4 | 43.9 | 4.03 | 1427 | 351 | 518 |
| | 11 | 4 | 0.43297 | 0.012894 | 12.999537 | 0.460093 | 0.210284 | 0.005879 | 2.300057 | 0.068763 | 2318.8 | 58 | 2678.6 | 33.5 | 2905.6 | 45.1 | 1.44 | 242 | 168 | 387 |
| | 12 | 4 | 0.343062 | 0.009423 | 8.321308 | 0.292008 | 0.169642 | 0.004395 | 2.904738 | 0.080104 | 1901.3 | 45.3 | 2265.7 | 31.5 | 2552.3 | 43.4 | 2.55 | 432 | 169 | 184 |
| | 13 | 4 | 0.306792 | 0.009331 | 7.841801 | 0.25327 | 0.181407 | 0.004596 | 3.25493 | 0.09956 | 1724.6 | 46 | 2212 | 29.2 | 2663.5 | 41.7 | 2.35 | 301 | 130 | 162 |
| | 14 | 4 | 0.48409 | 0.013035 | 12.25357 | 0.327798 | 0.17865 | 0.003777 | 2.06384 | 0.056583 | 2544.7 | 56.8 | 2623.5 | 25.3 | 2638.7 | 35.3 | 0.8 | 649 | 811 | 881 |
| | 15 | 4 | 0.479886 | 0.012617 | 12.183961 | 0.328256 | 0.178026 | 0.003827 | 2.082795 | 0.055276 | 2526.6 | 55 | 2618.4 | 25.2 | 2633.3 | 35.8 | 1.52 | 464 | 303 | 381 |
| | 16 | 4 | 0.267372 | 0.00855 | 6.805626 | 0.339481 | 0.178999 | 0.005109 | 3.754281 | 0.116137 | 1526.9 | 43.3 | 2079.9 | 42.3 | 2638.8 | 45.7 | 2.48 | 1342 | 544 | 885 |
| | 17 | 4 | 0.19772 | 0.0054 | 3.986998 | 0.106907 | 0.142446 | 0.002933 | 5.067634 | 0.136247 | 1162.9 | 29 | 1631.1 | 22 | 2255.6 | 35.7 | 1.71 | 3787 | 2196 | 1633 |
| | 18 | 4 | 0.16026 | 0.005643 | 4.96758 | 0.19252 | 0.222206 | 0.005161 | 6.257397 | 0.208463 | 958.1 | 31.2 | 1813 | 32.1 | 2995.5 | 37.5 | 2.04 | 3866 | 1875 | 2674 |
| | 19 | 4 | 0.21056 | 0.005747 | 3.596409 | 0.099393 | 0.120526 | 0.002482 | 4.747924 | 0.145399 | 1235.3 | 34.7 | 1548.2 | 21.8 | 1962.4 | 36.7 | 0.31 | 5014 | 15902 | 9496 |
| | 20 | 4 | 0.428808 | 0.012925 | 10.392702 | 0.359421 | 0.172424 | 0.005273 | 2.338899 | 0.06837 | 2299.8 | 58 | 2468.7 | 32.3 | 2576.7 | 52.8 | 2.33 | 116 | 50 | 65 |
| | 21 | 4 | 0.20879 | 0.006432 | 6.8162 | 0.217649 | 0.228051 | 0.005286 | 4.770443 | 0.144106 | 1222.3 | 34.2 | 2087.3 | 27.9 | 3037.1 | 37.4 | 3.35 | 983 | 292 | 1002 |
| | 22 | 4 | 0.290768 | 0.01054 | 8.130446 | 0.295095 | 0.198141 | 0.004037 | 3.435237 | 0.128258 | 1644.7 | 52.8 | 2243.9 | 33.1 | 2809.8 | 33.4 | 2.85 | 959 | 334 | 1279 |
| | 23 | 4 | 0.304593 | 0.008753 | 7.842495 | 0.240085 | 0.182215 | 0.003963 | 3.270103 | 0.093799 | 1713.8 | 43.2 | 2212.1 | 27.7 | 2671.6 | 36.3 | 1.57 | 662 | 414 | 535 |
| | 24 | 4 | 0.387494 | 0.010587 | 9.251559 | 0.251641 | 0.168493 | 0.003608 | 2.57007 | 0.070171 | 2110.9 | 49.2 | 2362.6 | 24.9 | 2541 | 35.8 | 1.44 | 570 | 395 | 427 |
| | 25 | 4 | 0.455789 | 0.012915 | 11.671757 | 0.332351 | 0.180812 | 0.003642 | 2.186331 | 0.061107 | 2420.4 | 57 | 2577.5 | 26.4 | 2659.1 | 33.3 | 0.95 | 558 | 584 | 780 |
| | 26 | 4 | 0.419171 | 0.01221 | 10.871411 | 0.326391 | 0.181989 | 0.004655 | 2.375861 | 0.069509 | 2256.5 | 55.5 | 2511.7 | 27.9 | 2669.2 | 42.6 | 2.17 | 259 | 118 | 133 |
| | 27 | 4 | 0.21433 | 0.008669 | 5.636366 | 0.208091 | 0.186797 | 0.004093 | 4.682953 | 0.197704 | 1251 | 46.2 | 1919.4 | 32.4 | 2712.4 | 36.6 | 1.29 | 2209 | 1679 | 1515 |
| | 28 | 4 | 0.296499 | 0.016902 | 11.752442 | 0.959438 | 0.278004 | 0.011413 | 3.384724 | 0.197048 | 1672.6 | 84.1 | 2576.5 | 80.1 | 3347.3 | 67.3 | 3.01 | 1213 | 395 | 2617 |
| | 29 | 4 | 0.256427 | 0.006919 | 5.993261 | 0.19585 | 0.165839 | 0.003704 | 3.887451 | 0.104602 | 1471.4 | 35.5 | 1973.2 | 28.1 | 2513.9 | 37.2 | 3.86 | 1760 | 464 | 456 |
| | 30 | 4 | 0.332346 | 0.01178 | 8.491415 | 0.396253 | 0.180606 | 0.004599 | 3.009882 | 0.113595 | 1849 | 57.4 | 2280.8 | 44.7 | 2655.9 | 42.9 | 2.86 | 846 | 288 | 450 |
| TR02 | 1 | 4 | 0.571731 | 0.016381 | 20.974232 | 0.620723 | 0.264218 | 0.006075 | 1.737182 | 0.048058 | 2914.6 | 66.7 | 3137 | 28.2 | 3270.8 | 35.4 | 1.84 | 101 | 55 | 73 |
| | 2 | 4 | 0.597618 | 0.015535 | 23.071929 | 0.585549 | 0.275294 | 0.00558 | 1.661667 | 0.043004 | 3020 | 62.6 | 3229.7 | 24.8 | 3335.2 | 31.9 | 1.68 | 127 | 76 | 125 |
| | 3 | 4 | 0.245954 | 0.008988 | 5.739004 | 0.264705 | 0.165854 | 0.004237 | 4.065183 | 0.157106 | 1416.7 | 46.7 | 1931.6 | 41.2 | 2512.6 | 43.4 | 4.1 | 857 | 211 | 185 |
| | 4 | 4 | 0.659967 | 0.017487 | 25.486757 | 0.681746 | 0.275359 | 0.005578 | 1.502173 | 0.03471 | 3266.6 | 68 | 3326.5 | 26.5 | 3335.6 | 31.4 | 1.8 | 140 | 78 | 121 |
| | 5 | 4 | 0.501735 | 0.014555 | 17.625449 | 0.494317 | 0.251524 | 0.005561 | 1.983308 | 0.055985 | 2620.6 | 62.2 | 2968.8 | 27.1 | 3192.7 | 35.3 | 1.92 | 295 | 155 | 210 |
| | 6 | 4 | 0.372169 | 0.018081 | 12.911824 | 0.44282 | 0.248405 | 0.006349 | 2.705078 | 0.130539 | 2036.6 | 84.8 | 2671.4 | 32.2 | 3172 | 40.3 | 1.92 | 463 | 248 | 381 |
| | 7 | 4 | 0.684633 | 0.017806 | 26.481742 | 0.693295 | 0.27679 | 0.005528 | 1.453754 | 0.037868 | 3361.8 | 68.1 | 3364.1 | 25.9 | 3343.8 | 31.3 | 1.1 | 238 | 218 | 361 |
| | 8 | 4 | 0.517955 | 0.026103 | 19.650128 | 0.84025 | 0.27399 | 0.005807 | 1.942975 | 0.096781 | 2686.4 | 110.5 | 3071 | 41.3 | 3327.8 | 33.6 | 1.95 | 315 | 166 | 268 |
| | 9 | 4 | 0.682714 | 0.018122 | 25.848722 | 0.679237 | 0.27197 | 0.005428 | 1.46031 | 0.039001 | 3354.3 | 69.5 | 3340.4 | 25.8 | 3316.3 | 31.4 | 1.96 | 210 | 107 | 178 |
| | 10 | 4 | 0.246746 | 0.008238 | 9.810777 | 0.3072 | 0.287727 | 0.006095 | 4.051038 | 0.125641 | 1421.3 | 42.3 | 2416.2 | 28.2 | 3404.1 | 32.7 | 4.89 | 776 | 159 | 531 |
| | 11 | 4 | 0.224807 | 0.006385 | 6.146026 | 0.163567 | 0.197737 | 0.004711 | 4.447719 | 0.125244 | 1307.1 | 33.6 | 1996.6 | 23.2 | 2805.9 | 39.4 | 1.55 | 1020 | 665 | 585 |
| | 12 | 4 | 0.610107 | 0.016727 | 21.747389 | 0.60467 | 0.259721 | 0.005584 | 1.639497 | 0.044523 | 3069.8 | 66.8 | 3171.7 | 27 | 3243.3 | 33.9 | 1.72 | 90 | 53 | 92 |
| | 13 | 4 | 0.685168 | 0.019357 | 26.302749 | 0.761449 | 0.281036 | 0.006058 | 1.459705 | 0.04185 | 3363.5 | 74.2 | 3357.1 | 28.6 | 3367.3 | 33.7 | 1.85 | 118 | 64 | 111 |
| | 16 | 4 | 0.606398 | 0.015973 | 22.081054 | 0.564692 | 0.267367 | 0.005698 | 1.647354 | 0.043711 | 3055.4 | 64.2 | 3187.2 | 24.8 | 3289.6 | 33.3 | 2.18 | 304 | 142 | 263 |
| | 17 | 4 | 0.686053 | 0.019423 | 25.921927 | 0.711597 | 0.275284 | 0.006261 | 1.457651 | 0.041606 | 3366.7 | 74.4 | 3343 | 27 | 3334.5 | 35.3 | 0.71 | 51 | 73 | 131 |
| | 18 | 4 | 0.695657 | 0.018185 | 26.148396 | 0.683606 | 0.2742 | 0.005371 | 1.436118 | 0.037714 | 3403.8 | 69.2 | 3351.7 | 25.7 | 3329.2 | 30.5 | 2.13 | 235 | 111 | 191 |
| | 19 | 4 | 0.700082 | 0.018334 | 26.949451 | 0.71833 | 0.280688 | 0.005627 | 1.426916 | 0.037684 | 3420.6 | 69.6 | 3381.1 | 26.1 | 3365.6 | 31.2 | 1.83 | 164 | 90 | 163 |
| | 20 | 4 | 0.674108 | 0.018152 | 25.333116 | 0.676153 | 0.273899 | 0.005533 | 1.482281 | 0.039824 | 3321.2 | 69.8 | 3320.6 | 26 | 3327.3 | 31.9 | 2.81 | 146 | 52 | 91 |
| | 21 | 4 | 0.546675 | 0.017058 | 20.182068 | 0.680584 | 0.263184 | 0.00546 | 1.82915 | 0.05955 | 2809.9 | 71.6 | 3097.6 | 33.5 | 3264.5 | 32.4 | 3.09 | 200 | 95 | 158 |
| | 22 | 4 | 0.682531 | 0.018138 | 26.771277 | 0.70594 | 0.278294 | 0.005511 | 1.460587 | 0.040077 | 3353.6 | 69.9 | 3374.6 | 26.2 | 3352.3 | 31 | 3.41 | 163 | 81 | 141 |
| | 23 | 4 | 0.683407 | 0.018671 | 26.780105 | 0.726727 | 0.278536 | 0.00556 | 1.458017 | 0.040314 | 3357 | 71.7 | 3375.1 | 26.9 | 3353.8 | 31.3 | 2.38 | 142 | 122 | 211 |
| | 24 | 4 | 0.679952 | 0.019269 | 26.840367 | 0.755411 | 0.27762 | 0.005481 | 1.466075 | 0.042812 | 3343.4 | 74.4 | 3376.9 | 27.8 | 3348.6 | 30.9 | 4.9 | 96 | 54 | 95 |
| | 25 | 4 | 0.435151 | 0.02575 | 15.449951 | 1.099492 | 0.25021 | 0.006481 | 2.310814 | 0.139888 | 2325.9 | 116 | 2836.2 | 68.8 | 3184.4 | 40.8 | 2.11 | 185 | 88 | 77 |
| | 26 | 4 | 0.64271 | 0.018182 | 24.940263 | 0.73785 | 0.270615 | 0.006013 | 1.550954 | 0.04456 | 3198.8 | 71.5 | 3304.6 | 28.9 | 3312.4 | 30.7 | 2.39 | 19 | 60 | 104 |
| | 27 | 4 | 0.592397 | 0.017118 | 23.60352 | 0.693218 | 0.276941 | 0.005557 | 1.682977 | 0.048865 | 2998.2 | 69.3 | 3250.9 | 29 | 3347.5 | 27.6 | 1.74 | 98 | 56 | 90 |
| | 28 | 4 | 0.639286 | 0.016783 | 25.309578 | 0.66651 | 0.274509 | 0.00538 | 1.557312 | 0.041512 | 3185.9 | 66.2 | 3319.8 | 26.1 | 3331 | 30.6 | 2.08 | 122 | 58 | 99 |

Continued on next page

| Sample | Spot name | Run | 206/238 | ±2SE | 207/235 | ±2SE | 207/206 | ±2SE | 238/P206 | ±2SE | 206/238 Age | ±2SE | 207/235 Age | ±2SE | 207/206 Age | ±2SE | U/Th | U | Th | Pb |
|---|---|---|---|---|---|---|---|---|---|---|---|---|---|---|---|---|---|---|---|---|
| | 29 | 4 | 0.239474 | 0.010697 | 11.810756 | 0.432765 | 0.339726 | 0.008194 | 4.180646 | 0.180875 | 1383.2 | 55.4 | 2588 | 34.3 | 3659.9 | 36.4 | 0.99 | 303 | 304 | 329 |
| | 30 | 4 | 0.544181 | 0.01805 | 20.219 | 0.688015 | 0.257221 | 0.006204 | 1.836803 | 0.062506 | 2799.1 | 75.7 | 3099.4 | 32.8 | 3227.1 | 37.3 | 0.54 | 27 | 50 | 84 |
| TR06 | 1 | 4 | 0.292492 | 0.012779 | 8.526129 | 0.529841 | 0.206306 | 0.005932 | 3.461031 | 0.159443 | 1651.9 | 64.1 | 2275.2 | 59.3 | 2871.7 | 47.6 | 2.55 | 606 | 341 | 247 |
| | 2 | 4 | 0.235744 | 0.006312 | 5.224355 | 0.163886 | 0.157466 | 0.003682 | 4.241506 | 0.11394 | 1364.4 | 32.9 | 1855.5 | 26.7 | 2426.4 | 39.4 | 2.17 | 993 | 454 | 382 |
| | 3 | 4 | 0.278024 | 0.008403 | 8.704783 | 0.26846 | 0.223122 | 0.00456 | 3.587575 | 0.099471 | 1581 | 42.6 | 2306.1 | 28.5 | 3002 | 32.7 | 1.38 | 665 | 484 | 408 |
| | 4 | 4 | 0.287794 | 0.009237 | 7.775249 | 0.292187 | 0.191563 | 0.004137 | 3.480754 | 0.111336 | 1630 | 46.2 | 2203.1 | 33.8 | 2754.1 | 35.5 | 1.58 | 627 | 392 | 300 |
| | 5 | 4 | 0.344083 | 0.010159 | 10.926615 | 0.346062 | 0.226792 | 0.004919 | 2.90877 | 0.084312 | 1905.8 | 48.6 | 2515.5 | 29.4 | 3027.9 | 34.8 | 1.72 | 471 | 274 | 269 |
| | 6 | 4 | 0.668341 | 0.017689 | 25.602002 | 0.730317 | 0.272947 | 0.005962 | 1.49543 | 0.039315 | 3299.1 | 68.2 | 3330.5 | 28.2 | 3321.3 | 34.3 | 1.19 | 73 | 61 | 108 |
| | 7 | 4 | 0.650364 | 0.018126 | 24.554843 | 0.681811 | 0.270797 | 0.006021 | 1.537827 | 0.043571 | 3228.9 | 71 | 3293.5 | 30.3 | 3308.7 | 34.8 | 1.21 | 48 | 40 | 69 |
| | 9 | 4 | 0.382386 | 0.012881 | 11.858994 | 0.446311 | 0.221538 | 0.0048 | 2.618363 | 0.091655 | 2086.7 | 60.4 | 2591.4 | 35.7 | 2990.6 | 34.4 | 2.27 | 511 | 232 | 302 |
| | 10 | 4 | 0.251939 | 0.010566 | 7.558298 | 0.45085 | 0.214531 | 0.006643 | 4.005618 | 0.166217 | 1447.1 | 54.3 | 2168.8 | 53.2 | 2934.1 | 49.6 | 2.65 | 676 | 259 | 357 |
| | 11 | 4 | 0.391075 | 0.011254 | 10.919138 | 0.401388 | 0.202551 | 0.005879 | 2.553855 | 0.072158 | 2127.5 | 52 | 2514.1 | 34.1 | 2843 | 47.2 | 4.18 | 1175 | 282 | 559 |
| | 12 | 4 | 0.352917 | 0.009236 | 10.329213 | 0.278982 | 0.213012 | 0.004888 | 2.827002 | 0.074472 | 1948.4 | 44 | 2464.2 | 24.9 | 2926.3 | 36.8 | 2.69 | 1148 | 429 | 609 |
| | 13 | 4 | 0.573893 | 0.015536 | 21.574166 | 0.591411 | 0.273233 | 0.006307 | 1.73885 | 0.047244 | 2923.3 | 63.7 | 3164 | 26.6 | 3322.4 | 36.3 | 1.49 | 59 | 40 | 62 |
| | 14 | 4 | 0.274331 | 0.009386 | 8.321618 | 0.324092 | 0.222261 | 0.005228 | 3.637374 | 0.123772 | 1562.6 | 47.4 | 2265.8 | 35.8 | 2996 | 38.3 | 2.26 | 827 | 366 | 344 |
| | 15 | 4 | 0.306644 | 0.009496 | 8.77674 | 0.328165 | 0.206925 | 0.004865 | 3.259713 | 0.098094 | 1723.6 | 46.7 | 2312 | 33.6 | 2879.1 | 38.3 | 2.57 | 675 | 263 | 246 |
| | 16 | 4 | 0.464631 | 0.012742 | 15.636169 | 0.425003 | 0.243249 | 0.004948 | 2.147159 | 0.05771 | 2459.6 | 55.9 | 2854.2 | 25.6 | 3140.1 | 32.5 | 1.61 | 355 | 221 | 154 |
| | 17 | 4 | 0.23963 | 0.007088 | 6.011956 | 0.224492 | 0.180747 | 0.003995 | 4.168092 | 0.12094 | 1384.5 | 36.8 | 1974.8 | 31.9 | 2657.7 | 36.5 | 2.92 | 924 | 314 | 319 |
| | 18 | 4 | 0.554429 | 0.019431 | 32.269721 | 1.111125 | 0.424279 | 0.010286 | 1.805095 | 0.06373 | 2841.8 | 80.5 | 3556.6 | 33.7 | 3995.4 | 35.8 | 6.11 | 29 | 5 | 73 |
| | 19 | 4 | 0.336936 | 0.009036 | 9.907897 | 0.271275 | 0.213245 | 0.004583 | 2.959901 | 0.079339 | 1871.8 | 43.6 | 2425.9 | 25.3 | 2929.1 | 35 | 2.16 | 561 | 269 | 242 |
| | 20 | 4 | 0.27787 | 0.007877 | 8.991872 | 0.244354 | 0.23351 | 0.005117 | 3.592172 | 0.100307 | 1580.5 | 39.7 | 2336.9 | 25.1 | 3074.9 | 34.8 | 2.57 | 434 | 169 | 267 |
| | 21 | 4 | 0.220141 | 0.006067 | 5.120926 | 0.147894 | 0.170428 | 0.003685 | 4.564372 | 0.128542 | 1282.5 | 32.1 | 1839.1 | 24.5 | 2560.5 | 36.2 | 5.33 | 1532 | 288 | 380 |
| | 22 | 4 | 0.224132 | 0.00654 | 4.829717 | 0.167238 | 0.160065 | 0.004374 | 4.48973 | 0.129989 | 1303.5 | 34.4 | 1789 | 28.9 | 2453.7 | 45.2 | 2.95 | 1057 | 381 | 301 |
| | 23 | 4 | 0.63236 | 0.020937 | 22.483328 | 0.780706 | 0.263704 | 0.005803 | 1.598064 | 0.052496 | 3156.7 | 82.5 | 3202.1 | 33.8 | 3267.1 | 34.6 | 1.48 | 78 | 51 | 83 |
| | 24 | 4 | 0.408071 | 0.012686 | 13.067398 | 0.506521 | 0.236309 | 0.005302 | 2.471375 | 0.077312 | 2205.6 | 58.1 | 2682.5 | 36.6 | 3093.9 | 35.6 | 1.78 | 778 | 435 | 525 |
| | 25 | 4 | 0.209307 | 0.005585 | 3.843672 | 0.10242 | 0.136602 | 0.00304 | 4.815711 | 0.127604 | 1225 | 29.7 | 1601.6 | 21.3 | 2182.5 | 38.8 | 3.41 | 1522 | 449 | 322 |
| | 26 | 4 | 0.382089 | 0.011811 | 11.427317 | 0.363768 | 0.223888 | 0.004835 | 2.641832 | 0.082278 | 2085.5 | 55.1 | 2557.5 | 29.6 | 3007.5 | 34.5 | 1.82 | 351 | 193 | 188 |
| | 28 | 4 | 0.385215 | 0.011802 | 12.160664 | 0.383482 | 0.233859 | 0.004906 | 2.618239 | 0.08034 | 2100.1 | 54.9 | 2615.7 | 29.4 | 3077.4 | 33.1 | 1.69 | 739 | 434 | 453 |
| | 29 | 4 | 0.358899 | 0.014265 | 12.713778 | 0.739191 | 0.263015 | 0.007988 | 2.814362 | 0.121605 | 1976 | 68.3 | 2652.7 | 58.2 | 3261.8 | 48.8 | 1.26 | 1084 | 857 | 1133 |
| | 30 | 4 | 0.338444 | 0.009746 | 10.063138 | 0.316609 | 0.220993 | 0.004926 | 2.953217 | 0.067295 | 1879 | 47.3 | 2439.7 | 29.3 | 2986.5 | 35.5 | 1.46 | 602 | 411 | 284 |
| TR07 | 1 | 3 | 0.244367 | 0.006571 | 4.368916 | 0.236119 | 0.130145 | 0.002178 | 4.043451 | 0.108649 | 1409.3 | 34 | 1706.2 | 44.7 | 2098.6 | 29.3 | 4.28 | 1581 | 370 | 277 |
| | 2 | 3 | 0.24623 | 0.006603 | 4.891955 | 0.270384 | 0.144405 | 0.002516 | 4.008859 | 0.107065 | 1418.9 | 34.1 | 1800.4 | 46.5 | 2279.5 | 29.9 | 9.78 | 1754 | 180 | 261 |
| | 3 | 3 | 0.538587 | 0.018926 | 19.317992 | 1.252229 | 0.261361 | 0.006254 | 1.835786 | 0.061074 | 2776.5 | 78.4 | 3055.1 | 60.3 | 3252.9 | 37.2 | 5.33 | 2602 | 483 | 2357 |
| | 4 | 3 | 0.514448 | 0.023417 | 17.016417 | 1.239598 | 0.240165 | 0.00659 | 1.924056 | 0.085741 | 2674 | 99.3 | 2932.5 | 67.8 | 3118.9 | 44.1 | 2.17 | 1287 | 583 | 1114 |
| | 5 | 3 | 0.511803 | 0.015654 | 24.210807 | 1.321821 | 0.344901 | 0.006152 | 1.930522 | 0.057879 | 2663.3 | 66.5 | 3276.2 | 53.2 | 3683.2 | 27.6 | 1.81 | 423 | 232 | 575 |
| | 7 | 3 | 0.412127 | 0.012621 | 14.782259 | 0.841524 | 0.261893 | 0.005303 | 2.391202 | 0.072933 | 2224.4 | 57.6 | 2800.7 | 54.9 | 3256.9 | 32 | 7.18 | 5087 | 692 | 5220 |
| | 8 | 3 | 0.651372 | 0.018324 | 22.074877 | 1.215595 | 0.246939 | 0.004469 | 1.511534 | 0.041306 | 3233.3 | 71.1 | 3186.8 | 53 | 3164.3 | 28.8 | 12.9 | 5482 | 396 | 9612 |
| | 9 | 3 | 0.713168 | 0.020318 | 35.462473 | 1.959108 | 0.36206 | 0.006417 | 1.381341 | 0.039557 | 3469.7 | 76.5 | 3650.8 | 54.5 | 3761.4 | 22.5 | 1.95 | 163 | 82 | 364 |
| | 10 | 3 | 0.322476 | 0.008355 | 17.08744 | 0.916094 | 0.386194 | 0.006284 | 3.051531 | 0.078859 | 1801.7 | 40.7 | 2939.6 | 51.3 | 3855.2 | 24.6 | 12.84 | 3054 | 252 | 6574 |
| | 11 | 3 | 0.548561 | 0.016174 | 37.024797 | 2.059177 | 0.490921 | 0.007941 | 1.794919 | 0.053136 | 2818.9 | 67.4 | 3693.8 | 55.3 | 4213.4 | 23.8 | 5.44 | 1248 | 223 | 5863 |
| | 13 | 3 | 0.344804 | 0.009064 | 14.187455 | 0.768455 | 0.300161 | 0.005307 | 2.856414 | 0.075715 | 1909.6 | 43.5 | 2761.9 | 51.1 | 3469.7 | 27.2 | 12.39 | 1263 | 100 | 1491 |
| | 14 | 3 | 0.683264 | 0.01869 | 31.323903 | 1.696901 | 0.33431 | 0.005804 | 1.442603 | 0.039724 | 3356.3 | 71.6 | 3528.8 | 53.7 | 3635.7 | 26.6 | 2.82 | 130 | 43 | 118 |
| | 15 | 3 | 0.286849 | 0.008312 | 8.498111 | 0.498107 | 0.215556 | 0.00441 | 3.437758 | 0.099327 | 1625.6 | 41.6 | 2284.2 | 53.2 | 2946 | 32.9 | 5.88 | 2145 | 335 | 965 |
| | 16 | 3 | 0.272399 | 0.011295 | 7.56672 | 0.52062 | 0.202066 | 0.004149 | 3.632832 | 0.147669 | 1552.3 | 57.1 | 2177.7 | 61.5 | 2841.4 | 33.7 | 4.91 | 5746 | 1099 | 2703 |
| | 17 | 3 | 0.629705 | 0.021076 | 22.839625 | 1.345501 | 0.264996 | 0.005038 | 1.566668 | 0.053023 | 3147.8 | 83.5 | 3219.4 | 57.9 | 3275.7 | 29.8 | 5.02 | 486 | 90 | 203 |
| | 18 | 3 | 0.472878 | 0.013462 | 17.540556 | 0.997173 | 0.270467 | 0.006053 | 2.086048 | 0.059595 | 2495.9 | 58.9 | 2964 | 54.3 | 3306.9 | 35 | 0.98 | 759 | 718 | 1075 |
| | 19 | 3 | 0.392242 | 0.011905 | 15.633507 | 0.903899 | 0.290532 | 0.005582 | 2.516268 | 0.074973 | 2132.9 | 55 | 2853.7 | 55.3 | 3419.3 | 29.9 | 14.42 | 2019 | 130 | 2369 |
| | 20 | 3 | 0.659908 | 0.017626 | 24.743646 | 1.335452 | 0.273295 | 0.00471 | 1.495528 | 0.040183 | 3266.4 | 68.5 | 3297.8 | 52.8 | 3323.8 | 27.1 | 1.26 | 148 | 110 | 189 |
| | 21 | 3 | 5.535242 | 1.738246 | 660.589185 | 216.406123 | 0.735363 | 0.061836 | 0.871034 | 0.284312 | 9385.1 | 2014.9 | 5605.3 | 548.5 | 4328 | 154 | 5.32 | 2093 | 452 | 195547 |
| | 22 | 3 | 0.328213 | 0.008926 | 16.699945 | 0.918017 | 0.371126 | 0.008039 | 3.009014 | 0.082474 | 1829.6 | 43.4 | 2917.4 | 53 | 3794.5 | 32.8 | 11.2 | 4505 | 464 | 9013 |
| | 23 | 3 | 0.379043 | 0.010652 | 17.836512 | 0.970088 | 0.342508 | 0.005599 | 2.608339 | 0.073742 | 2071.4 | 49.8 | 2980.4 | 52.2 | 3673 | 24.9 | 14.55 | 2453 | 195 | 4817 |
| | 24 | 3 | 0.154249 | 0.005837 | 3.407959 | 0.233607 | 0.161223 | 0.00909 | 6.425888 | 0.259395 | 924.5 | 32.7 | 1503.5 | 54.3 | 2453.3 | 98.4 | 2.24 | 11941 | 7577 | 4066 |
| | 25 | 3 | 0.195578 | 0.005718 | 4.890671 | 0.290124 | 0.181645 | 0.003694 | 5.057988 | 0.145839 | 1151.3 | 30.8 | 1798.4 | 49.4 | 2665.5 | 33.6 | 1.45 | 1402 | 1102 | 745 |
| | 26 | 3 | 0.198538 | 0.006034 | 6.535528 | 0.388714 | 0.238791 | 0.005188 | 4.976768 | 0.148968 | 1167.4 | 32.4 | 2049.8 | 51.7 | 3110.5 | 34.3 | 2.59 | 3239 | 1391 | 2732 |

Continued on next page

| Sample | Spot name | Run | 206/238 | ±2SE | 207/235 | ±2SE | 207/206 | ±2SE | 238/P206 | ±2SE | 206/238 Age | ±2SE | 207/235 Age | ±2SE | 207/206 Age | ±2SE | U/Th | U | Th | Pb |
|---|---|---|---|---|---|---|---|---|---|---|---|---|---|---|---|---|---|---|---|---|
| | 27 | 3 | 0.39477 | 0.011046 | 15.172603 | 0.834944 | 0.279277 | 0.00526 | 2.503338 | 0.070322 | 2144.6 | 51.1 | 2825.5 | 52.8 | 3357.4 | 29 | 2.9 | 251 | 94 | 185 |
| | 28 | 3 | 0.319757 | 0.01422 | 18.98821 | 1.151538 | 0.433341 | 0.013125 | 3.096884 | 0.128191 | 1787.9 | 68.8 | 3040.2 | 58.2 | 4026.9 | 46.5 | 5.73 | 6859 | 1289 | 17914 |
| | 29 | 3 | 0.179921 | 0.01177 | 9.23031 | 0.822017 | 0.373011 | 0.007338 | 5.545884 | 0.355058 | 1065.7 | 64.2 | 2355 | 79.8 | 3802.6 | 29.4 | 6.34 | 8284 | 1426 | 10094 |
| | 30 | 3 | 1.009751 | 0.081215 | 52.212145 | 6.673454 | 0.365699 | 0.017286 | 1.028723 | 0.075365 | 4456.3 | 253 | 3974.2 | 125.3 | 3757.1 | 72 | 2.67 | 2243 | 880 | 11400 |
| | 31 | 5 | 0.458375 | 0.029347 | 14.720028 | 1.31631 | 0.21869 | 0.007518 | 2.220821 | 0.140411 | 2427.3 | 129.2 | 2787.7 | 84 | 2969.4 | 55.2 | 2.57 | 1476 | 639 | 893 |
| | 32 | 5 | 0.632741 | 0.027786 | 45.427771 | 3.273909 | 0.487396 | 0.016321 | 1.592359 | 0.070106 | 3157.9 | 109.7 | 3892.8 | 71.6 | 4202.2 | 49.2 | 17.59 | 2849 | 181 | 17289 |
| | 33 | 5 | 0.489438 | 0.027205 | 17.688546 | 1.521078 | 0.245946 | 0.008986 | 2.083425 | 0.111403 | 2562.1 | 116.9 | 2958.8 | 80.4 | 3155.3 | 57.5 | 0.61 | 455 | 2638 | 990 |
| | 34 | 5 | 0.389638 | 0.039756 | 15.640771 | 1.711464 | 0.276928 | 0.009376 | 2.734542 | 0.28212 | 2106 | 184 | 2831.1 | 107 | 3344.2 | 52.9 | 3.13 | 224 | 81 | 150 |
| | 35 | 5 | 0.615112 | 0.024411 | 25.889506 | 1.711939 | 0.288117 | 0.009317 | 1.634236 | 0.06573 | 3088.7 | 97.7 | 3340.7 | 65 | 3406.4 | 50.3 | 0.73 | 278 | 428 | 445 |
| | 36 | 5 | 0.301926 | 0.011035 | 8.411282 | 0.540166 | 0.191686 | 0.006119 | 3.319695 | 0.120619 | 1700.6 | 54.6 | 2276 | 58.1 | 2755.7 | 52.2 | 6.15 | 3635 | 656 | 711 |
| | 37 | 5 | 0.757455 | 0.028968 | 27.441844 | 1.776893 | 0.248816 | 0.008152 | 1.322232 | 0.050478 | 3634.2 | 106.2 | 3399 | 63.2 | 3176.3 | 51.7 | 1.31 | 613 | 510 | 1719 |
| | 38 | 5 | 0.598441 | 0.024336 | 22.951268 | 1.534507 | 0.266111 | 0.008628 | 1.67864 | 0.073397 | 3021.5 | 99.4 | 3222.7 | 67.4 | 3282.1 | 50.9 | 2.07 | 169 | 90 | 169 |
| | 39 | 5 | 0.320142 | 0.022433 | 9.969942 | 1.050267 | 0.218221 | 0.011346 | 3.153146 | 0.219046 | 1788.5 | 109.2 | 2423.5 | 100.1 | 2962.6 | 83.6 | 9.36 | 2913 | 424 | 1717 |
| | 40 | 5 | 0.28259 | 0.016622 | 8.277 | 0.822002 | 0.204035 | 0.009508 | 3.581307 | 0.214979 | 1602.4 | 83.6 | 2247.9 | 91.4 | 2851.6 | 77.4 | 13.44 | 3255 | 261 | 1509 |
| TR08 | 1 | 3 | 0.660966 | 0.017679 | 25.003773 | 1.348583 | 0.273198 | 0.004766 | 1.510369 | 0.040456 | 3270.5 | 68.6 | 3308 | 53.1 | 3323.1 | 27.2 | 1 | 91 | 88 | 125 |
| | 2 | 3 | 0.678926 | 0.017992 | 25.611704 | 1.382322 | 0.272405 | 0.004648 | 1.468479 | 0.038877 | 3339.9 | 69.1 | 3331.4 | 52.4 | 3318.7 | 26.6 | 0.69 | 163 | 232 | 346 |
| | 3 | 3 | 0.684598 | 0.019222 | 25.818447 | 1.41524 | 0.272549 | 0.005867 | 1.45551 | 0.040838 | 3361.4 | 73.5 | 3339.1 | 53.1 | 3318.7 | 33.2 | 0.98 | 106 | 106 | 164 |
| | 4 | 3 | 0.689765 | 0.018652 | 26.317826 | 1.423518 | 0.274955 | 0.004619 | 1.443158 | 0.03818 | 3381.2 | 70.8 | 3358 | 52.6 | 3333.4 | 26.2 | 1.74 | 120 | 68 | 108 |
| | 5 | 3 | 0.509768 | 0.014283 | 17.636833 | 0.986077 | 0.250348 | 0.0045 | 1.950354 | 0.055188 | 2655.5 | 61.1 | 2969.7 | 54 | 3186 | 28.6 | 5.97 | 554 | 93 | 118 |
| | 6 | 3 | 0.313026 | 0.01071 | 8.14676 | 0.481908 | 0.187854 | 0.003197 | 3.188972 | 0.113662 | 1754.6 | 52.8 | 2244.8 | 54.1 | 2722.2 | 28 | 8.63 | 1654 | 193 | 226 |
| | 7 | 3 | 0.685241 | 0.018079 | 25.834279 | 1.39326 | 0.272312 | 0.004804 | 1.448943 | 0.037965 | 3364.1 | 69 | 3339.9 | 52.6 | 3318 | 27.6 | 0.75 | 153 | 205 | 336 |
| | 8 | 3 | 0.561698 | 0.016455 | 20.267309 | 1.127155 | 0.260124 | 0.004203 | 1.769251 | 0.051116 | 2872.7 | 67.7 | 3103 | 53.3 | 3246.5 | 25.4 | 6.94 | 568 | 83 | 136 |
| | 9 | 3 | 0.192421 | 0.005472 | 4.310976 | 0.238274 | 0.161809 | 0.00282 | 5.159624 | 0.146245 | 1134.3 | 29.6 | 1694.7 | 45.6 | 2473.2 | 29.5 | 2.1 | 951 | 456 | 244 |
| | 10 | 3 | 0.234415 | 0.006421 | 5.174237 | 0.286938 | 0.159053 | 0.0032 | 4.227451 | 0.117109 | 1357.6 | 33.6 | 1848.1 | 47.7 | 2444.4 | 34 | 5.62 | 882 | 158 | 180 |
| | 11 | 3 | 0.692449 | 0.018693 | 26.607742 | 1.453376 | 0.278622 | 0.004979 | 1.431196 | 0.038243 | 3391.4 | 71 | 3368.4 | 53.6 | 3353.8 | 27.7 | 0.79 | 66 | 81 | 132 |
| | 12 | 3 | 0.21321 | 0.006147 | 3.131171 | 0.177227 | 0.10631 | 0.002171 | 4.64727 | 0.13194 | 1245.8 | 32.6 | 1440.1 | 43.5 | 1735.7 | 37.5 | 8.33 | 2641 | 309 | 181 |
| | 13 | 3 | 0.67687 | 0.01924 | 25.240136 | 1.369498 | 0.269254 | 0.005117 | 1.464726 | 0.042032 | 3331.9 | 74.1 | 3317.3 | 53 | 3300.5 | 29.8 | 0.71 | 259 | 358 | 556 |
| | 14 | 3 | 0.675803 | 0.017783 | 25.179085 | 1.356035 | 0.269455 | 0.004424 | 1.467134 | 0.039446 | 3327.9 | 68.7 | 3314.9 | 52.5 | 3301.8 | 25.7 | 0.74 | 275 | 362 | 542 |
| | 15 | 3 | 0.690601 | 0.018945 | 25.989435 | 1.407981 | 0.272249 | 0.004787 | 1.436947 | 0.039517 | 3384.3 | 72.2 | 3345.7 | 52.7 | 3317.6 | 27.7 | 0.98 | 96 | 96 | 145 |
| | 16 | 3 | 0.678677 | 0.017983 | 25.509576 | 1.390158 | 0.271194 | 0.004859 | 1.461959 | 0.038339 | 3338.9 | 68.9 | 3327.3 | 53.4 | 3311.5 | 28.1 | 0.94 | 93 | 98 | 146 |
| | 17 | 3 | 0.686289 | 0.019168 | 25.836759 | 1.409403 | 0.272496 | 0.004917 | 1.447293 | 0.04111 | 3367.7 | 73.5 | 3339.7 | 53.2 | 3318.9 | 28.4 | 0.84 | 202 | 237 | 354 |
| | 18 | 3 | 0.679668 | 0.01892 | 25.618026 | 1.392914 | 0.272952 | 0.005312 | 1.46173 | 0.04052 | 3342.4 | 72.5 | 3331.5 | 53.2 | 3321.1 | 30.3 | 0.95 | 98 | 103 | 154 |
| | 19 | 3 | 0.682563 | 0.017873 | 25.819807 | 1.392281 | 0.273791 | 0.004472 | 1.454736 | 0.038079 | 3353.9 | 68.5 | 3339.4 | 52.7 | 3326.8 | 25.7 | 5.75 | 444 | 75 | 118 |
| | 20 | 3 | 0.683303 | 0.018585 | 25.703849 | 1.396586 | 0.272348 | 0.00453 | 1.454319 | 0.039415 | 3356.5 | 71.1 | 3334.8 | 52.9 | 3318.5 | 25.9 | 1.27 | 166 | 129 | 200 |
| | 21 | 3 | 0.67568 | 0.017926 | 26.465041 | 1.460386 | 0.283338 | 0.005722 | 1.467646 | 0.044311 | 3327.4 | 69 | 3362.9 | 54 | 3379.2 | 31.9 | 1 | 101 | 101 | 195 |
| | 22 | 3 | 0.69619 | 0.01924 | 27.309404 | 1.490717 | 0.284615 | 0.005267 | 1.428373 | 0.038813 | 3405.5 | 72.8 | 3393.9 | 53.9 | 3386.8 | 28.6 | 0.76 | 92 | 120 | 236 |
| | 23 | 3 | 0.681966 | 0.018133 | 25.750583 | 1.396735 | 0.273937 | 0.004639 | 1.45721 | 0.039157 | 3351.5 | 69.6 | 3336.6 | 52.8 | 3327.5 | 26.6 | 4.33 | 417 | 96 | 175 |
| | 24 | 3 | 0.684151 | 0.018555 | 25.914567 | 1.40266 | 0.274213 | 0.004829 | 1.452646 | 0.039062 | 3359.7 | 70.9 | 3342.9 | 52.4 | 3328.9 | 27.7 | 0.93 | 138 | 147 | 255 |
| | 25 | 3 | 0.685718 | 0.018503 | 25.752735 | 1.398259 | 0.272624 | 0.00471 | 1.448889 | 0.038745 | 3365.8 | 70.6 | 3336.7 | 53 | 3319.9 | 27.1 | 0.86 | 165 | 192 | 331 |
| | 26 | 3 | 0.461789 | 0.012975 | 16.052147 | 0.877273 | 0.253379 | 0.004183 | 2.152032 | 0.058566 | 2447 | 56.9 | 2879.2 | 51.7 | 3204.9 | 26 | 0.81 | 651 | 810 | 937 |
| | 27 | 3 | 0.569039 | 0.015418 | 20.678999 | 1.124674 | 0.263902 | 0.004455 | 1.745098 | 0.047528 | 2903.5 | 63.4 | 3123.1 | 53.2 | 3269 | 26.5 | 1.01 | 540 | 536 | 747 |
| | 28 | 3 | 0.602015 | 0.015913 | 21.998806 | 1.188577 | 0.265414 | 0.00434 | 1.648391 | 0.043367 | 3037.7 | 64 | 3183.3 | 52.4 | 3278.1 | 25.6 | 0.74 | 361 | 487 | 750 |
| | 29 | 3 | 0.695761 | 0.019537 | 26.775809 | 1.460564 | 0.279725 | 0.005166 | 1.426967 | 0.039774 | 3403.7 | 74.1 | 3377.6 | 47.5 | 3359.8 | 28.9 | 0.99 | 178 | 181 | 332 |
| | 30 | 3 | 0.677579 | 0.018726 | 26.836254 | 1.476726 | 0.287541 | 0.005515 | 1.464277 | 0.040352 | 3334.4 | 71.9 | 3376.6 | 54.4 | 3402.5 | 30.4 | 1.12 | 89 | 81 | 169 |
| WG02 | 1 | 3 | 0.289276 | 0.009928 | 7.248308 | 0.437885 | 0.182855 | 0.005303 | 3.404056 | 0.118232 | 1637.5 | 49.7 | 2141.1 | 54.9 | 2675.7 | 48.6 | 1.27 | 106 | 82 | 104 |
| | 2 | 3 | 0.410401 | 0.011539 | 10.105105 | 0.562318 | 0.179725 | 0.003414 | 2.394561 | 0.067685 | 2216.4 | 52.8 | 2443.6 | 51.1 | 2648.7 | 31.5 | 0.92 | 74 | 78 | 99 |
| | 3 | 3 | 0.436264 | 0.011868 | 10.485639 | 0.570151 | 0.175578 | 0.003077 | 2.250879 | 0.06054 | 2333.6 | 53.2 | 2478.1 | 50.3 | 2610.1 | 29.5 | 1.6 | 329 | 198 | 166 |
| | 4 | 3 | 0.513643 | 0.01493 | 12.748886 | 0.73359 | 0.18146 | 0.004356 | 1.911326 | 0.055342 | 2671.6 | 63.5 | 2659.9 | 54.9 | 2663.3 | 40 | 1.07 | 42 | 37 | 47 |
| | 5 | 3 | 0.518711 | 0.01425 | 12.891151 | 0.701625 | 0.181486 | 0.003207 | 1.885683 | 0.045208 | 2693.3 | 60.4 | 2671.2 | 51.3 | 2665 | 29.3 | 0.98 | 321 | 313 | 428 |
| | 6 | 3 | 0.330075 | 0.010992 | 7.726725 | 0.446674 | 0.170868 | 0.002911 | 2.980484 | 0.101137 | 1837.8 | 53.4 | 2197.7 | 52.5 | 2564.8 | 28.5 | 1.14 | 485 | 403 | 385 |
| | 7 | 3 | 0.412957 | 0.012327 | 9.706259 | 0.537387 | 0.171406 | 0.003184 | 2.374284 | 0.072436 | 2228 | 56.4 | 2406.7 | 50.9 | 2569.9 | 31.1 | 1.89 | 334 | 167 | 187 |
| | 8 | 3 | 0.365239 | 0.011022 | 8.857325 | 0.495619 | 0.176934 | 0.002916 | 2.685971 | 0.081486 | 2006.3 | 52.1 | 2322.2 | 51 | 2623.2 | 27.5 | 2.53 | 378 | 140 | 177 |
| | 9 | 3 | 0.510546 | 0.013984 | 12.581329 | 0.688539 | 0.179765 | 0.003169 | 1.917889 | 0.052552 | 2658.5 | 59.7 | 2648.1 | 51.4 | 2649.2 | 29.3 | 2.32 | 257 | 105 | 146 |
| | 10 | 3 | 0.492023 | 0.014541 | 12.906101 | 0.716863 | 0.191621 | 0.003979 | 1.990024 | 0.058525 | 2578.9 | 62.8 | 2672.2 | 52.7 | 2754.3 | 34.6 | 1.19 | 87 | 70 | 101 |

Continued on next page

| Sample | Spot name | Run | 206/238 | ±2SE | 207/235 | ±2SE | 207/206 | ±2SE | 238/P206 | ±2SE | 206/238 Age | ±2SE | 207/235 Age | ±2SE | 207/206 Age | ±2SE | U/Th | U | Th | Pb |
|---|---|---|---|---|---|---|---|---|---|---|---|---|---|---|---|---|---|---|---|---|
| | 11 | 3 | 0.33478 | 0.010657 | 7.922051 | 0.445654 | 0.172294 | 0.002911 | 2.932422 | 0.094206 | 1860.8 | 51.5 | 2220.9 | 51.1 | 2578.8 | 28.4 | 1.82 | 456 | 263 | 263 |
| | 12 | 3 | 0.361613 | 0.010075 | 8.879038 | 0.483099 | 0.177651 | 0.003142 | 2.708514 | 0.075787 | 1989.6 | 47.7 | 2325.3 | 49.5 | 2629.8 | 29.3 | 1.06 | 269 | 266 | 300 |
| | 13 | 3 | 0.408786 | 0.012174 | 10.054247 | 0.547752 | 0.179077 | 0.003274 | 2.400539 | 0.074522 | 2208.7 | 56 | 2439.2 | 50.6 | 2642.6 | 30.4 | 1.89 | 243 | 135 | 175 |
| | 14 | 3 | 0.223575 | 0.007835 | 4.715162 | 0.266435 | 0.1538 | 0.003626 | 4.391714 | 0.149604 | 1300.4 | 41.2 | 1769.3 | 47.1 | 2386.3 | 40.1 | 1.23 | 809 | 691 | 458 |
| | 15 | 3 | 0.207663 | 0.007657 | 4.738711 | 0.279797 | 0.166271 | 0.003308 | 4.73136 | 0.181331 | 1216.1 | 41 | 1773.2 | 50 | 2519.1 | 33 | 2.23 | 561 | 261 | 204 |
| | 16 | 3 | 0.461216 | 0.0124 | 11.063636 | 0.603281 | 0.173819 | 0.003053 | 2.126654 | 0.05641 | 2444.6 | 54.6 | 2527.9 | 50.9 | 2593.3 | 29.2 | 2 | 249 | 128 | 166 |
| | 17 | 3 | 0.482156 | 0.013262 | 11.797167 | 0.6404 | 0.178428 | 0.003263 | 2.035788 | 0.05732 | 2536.2 | 57.9 | 2588 | 50.3 | 2636.6 | 30.1 | 1.86 | 143 | 83 | 120 |
| | 18 | 3 | 0.470405 | 0.013445 | 11.29326 | 0.620495 | 0.174392 | 0.002962 | 2.081254 | 0.053707 | 2484.7 | 59.2 | 2546.9 | 51.5 | 2598.9 | 28.5 | 1.67 | 247 | 150 | 180 |
| | 19 | 3 | 0.29168 | 0.007812 | 7.062097 | 0.383465 | 0.17546 | 0.003213 | 3.364819 | 0.090778 | 1649.9 | 39 | 2119.1 | 48.2 | 2609.3 | 30.6 | 2.12 | 369 | 175 | 215 |
| | 20 | 3 | 0.324939 | 0.010553 | 7.754544 | 0.478337 | 0.173585 | 0.004622 | 3.024189 | 0.101075 | 1813.6 | 51.5 | 2201.8 | 54.3 | 2590.4 | 43.3 | 1.47 | 511 | 349 | 337 |
| | 21 | 3 | 0.34966 | 0.010561 | 8.397225 | 0.465616 | 0.173958 | 0.002931 | 2.816216 | 0.086115 | 1932.4 | 50.5 | 2273.9 | 50.4 | 2594.8 | 28.2 | 1.62 | 671 | 396 | 331 |
| | 22 | 3 | 0.290486 | 0.009341 | 6.571107 | 0.361613 | 0.163966 | 0.002982 | 3.393577 | 0.111766 | 1643.3 | 46.8 | 2054.7 | 49 | 2495.3 | 30.6 | 4.11 | 871 | 203 | 157 |
| | 23 | 3 | 0.507277 | 0.013595 | 12.553222 | 0.686279 | 0.179074 | 0.003222 | 1.93702 | 0.051772 | 2644.7 | 58.1 | 2646 | 51.8 | 2642.7 | 29.8 | 0.69 | 290 | 401 | 417 |
| | 25 | 3 | 0.167062 | 0.004809 | 4.010668 | 0.222183 | 0.173345 | 0.003033 | 5.88064 | 0.173373 | 995.8 | 26.6 | 1636 | 45.2 | 2589.1 | 29.2 | 2.65 | 1078 | 381 | 270 |
| | 26 | 3 | 0.504988 | 0.014905 | 12.455521 | 0.710771 | 0.178406 | 0.004083 | 1.947623 | 0.058562 | 2634.4 | 64 | 2637.6 | 52.9 | 2634.7 | 37.8 | 1.01 | 58 | 54 | 53 |
| | 27 | 3 | 0.447203 | 0.012836 | 11.034743 | 0.603979 | 0.178394 | 0.002977 | 2.197781 | 0.063255 | 2382.2 | 57.2 | 2525.4 | 51.1 | 2636.8 | 27.7 | 1.78 | 466 | 249 | 254 |
| | 28 | 3 | 0.427334 | 0.01143 | 10.347165 | 0.558328 | 0.174981 | 0.002887 | 2.297107 | 0.061628 | 2293.5 | 51.6 | 2466 | 50 | 2604.7 | 27.5 | 1.9 | 480 | 239 | 226 |
| | 29 | 3 | 0.427117 | 0.014078 | 10.414045 | 0.602989 | 0.176672 | 0.002928 | 2.301352 | 0.079139 | 2292 | 64 | 2471.2 | 54.2 | 2620.9 | 27.6 | 1.17 | 470 | 381 | 403 |
| | 30 | 3 | 0.511708 | 0.013925 | 12.726086 | 0.701758 | 0.179607 | 0.003404 | 1.91792 | 0.050917 | 2663.5 | 59.1 | 2658.7 | 51.8 | 2647.3 | 31.5 | 1.21 | 131 | 102 | 110 |
| WG03 | 1 | 3 | 0.200015 | 0.008452 | 4.609222 | 0.327719 | 0.167647 | 0.004021 | 5.058552 | 0.214045 | 1175.1 | 45.4 | 1748.4 | 59.4 | 2532.4 | 40.7 | 1.36 | 822 | 612 | 400 |
| | 2 | 3 | 0.193196 | 0.006722 | 4.393427 | 0.272359 | 0.165534 | 0.003604 | 5.232582 | 0.181133 | 1138.5 | 36.3 | 1709.7 | 51 | 2511.3 | 36.6 | 1.44 | 806 | 564 | 409 |
| | 3 | 3 | 0.242504 | 0.010424 | 5.504225 | 0.356884 | 0.164829 | 0.003014 | 4.197653 | 0.177238 | 1398.6 | 54 | 1897.6 | 55.5 | 2504.3 | 30.9 | 1.35 | 672 | 504 | 374 |
| | 4 | 3 | 0.50641 | 0.014055 | 12.604027 | 0.699408 | 0.181006 | 0.003897 | 1.996431 | 0.055936 | 2640.8 | 60.2 | 2649.5 | 52.1 | 2659.2 | 35.4 | 1.1 | 58 | 53 | 69 |
| | 5 | 3 | 0.508047 | 0.015077 | 12.556759 | 0.695266 | 0.180108 | 0.004171 | 1.990237 | 0.059161 | 2647.9 | 64.4 | 2646.6 | 51.6 | 2651.9 | 38.4 | 1.26 | 66 | 53 | 70 |
| | 6 | 3 | 0.148596 | 0.007208 | 3.788978 | 0.279185 | 0.184685 | 0.00345 | 6.912441 | 0.331664 | 892.2 | 40.4 | 1582.6 | 58.8 | 2693.6 | 31 | 5.85 | 1418 | 240 | 217 |
| | 7 | 3 | 0.468438 | 0.018769 | 11.515104 | 0.675805 | 0.178594 | 0.00396 | 2.167402 | 0.088906 | 2475.3 | 82.6 | 2564.7 | 55.2 | 2638 | 37.2 | 1.97 | 195 | 100 | 128 |
| | 8 | 3 | 0.516629 | 0.01431 | 12.704099 | 0.688669 | 0.179355 | 0.003173 | 1.959912 | 0.054094 | 2684.4 | 60.8 | 2660.2 | 57.8 | 2645.4 | 29.4 | 1.75 | 215 | 125 | 159 |
| | 9 | 3 | 0.186083 | 0.005513 | 4.181382 | 0.239314 | 0.163591 | 0.002823 | 5.440683 | 0.159138 | 1100 | 29.9 | 1669.7 | 46.8 | 2492.1 | 29.1 | 2.24 | 1305 | 584 | 347 |
| | 10 | 3 | 0.186671 | 0.006759 | 4.376886 | 0.27984 | 0.17034 | 0.00389 | 5.432247 | 0.192404 | 1103.1 | 36.6 | 1706.3 | 52 | 2559.1 | 38.4 | 2.39 | 1082 | 449 | 227 |
| | 12 | 3 | 0.184879 | 0.007489 | 4.271739 | 0.27994 | 0.167537 | 0.003784 | 5.456716 | 0.231813 | 1093.3 | 40.9 | 1686.1 | 54.4 | 2531.4 | 38.3 | 2.68 | 827 | 299 | 264 |
| | 13 | 3 | 0.205384 | 0.006492 | 4.817341 | 0.273271 | 0.17056 | 0.003175 | 4.895498 | 0.15806 | 1204 | 34.8 | 1787.3 | 48.3 | 2561.9 | 31.3 | 1.64 | 766 | 456 | 300 |
| | 14 | 3 | 0.234715 | 0.006605 | 5.592721 | 0.307098 | 0.173062 | 0.003075 | 4.275795 | 0.121699 | 1359.1 | 34.5 | 1914.6 | 47.5 | 2586.2 | 29.6 | 2.49 | 821 | 322 | 243 |
| | 15 | 3 | 0.383184 | 0.011492 | 9.230329 | 0.533208 | 0.175448 | 0.003569 | 2.615729 | 0.077579 | 2091 | 53.5 | 2360.6 | 52.4 | 2609.1 | 33.7 | 2.61 | 481 | 181 | 166 |
| | 17 | 3 | 0.35028 | 0.010188 | 8.346463 | 0.463304 | 0.173157 | 0.003012 | 2.858524 | 0.084176 | 1935.5 | 48.7 | 2268.4 | 50.8 | 2587 | 29.2 | 1.31 | 457 | 347 | 261 |
| | 18 | 3 | 0.277736 | 0.007342 | 6.565542 | 0.352651 | 0.171801 | 0.002891 | 3.59629 | 0.094509 | 1579.9 | 37 | 2054.5 | 47.4 | 2574 | 28 | 1.93 | 586 | 303 | 252 |
| | 19 | 3 | 0.078077 | 0.002149 | 1.567234 | 0.084634 | 0.145904 | 0.002532 | 12.787809 | 0.358201 | 484.6 | 12.9 | 957.2 | 33.5 | 2297 | 29.7 | 3.34 | 1965 | 589 | 357 |
| | 20 | 3 | 0.169211 | 0.00583 | 3.699507 | 0.218274 | 0.159099 | 0.002681 | 5.90171 | 0.196418 | 1007.6 | 32.1 | 1570.4 | 46.8 | 2445.1 | 28.5 | 2.35 | 1062 | 449 | 335 |
| | 21 | 3 | 0.278464 | 0.008688 | 6.643476 | 0.375086 | 0.173242 | 0.002985 | 3.579716 | 0.11441 | 1583.1 | 43.9 | 2063.8 | 50.6 | 2587.8 | 28.9 | 1.56 | 704 | 458 | 487 |
| | 22 | 3 | 0.311521 | 0.011851 | 7.298676 | 0.436071 | 0.170506 | 0.003192 | 3.198029 | 0.124545 | 1747.7 | 58.4 | 2147.7 | 53.8 | 2561.5 | 31.3 | 1.7 | 642 | 378 | 364 |
| | 23 | 3 | 0.349332 | 0.013557 | 8.303263 | 0.502782 | 0.172946 | 0.003449 | 2.853859 | 0.111044 | 1930.7 | 64.8 | 2263.4 | 54.6 | 2585 | 33.7 | 1.08 | 375 | 349 | 344 |
| | 24 | 3 | 0.249639 | 0.007461 | 5.605246 | 0.329844 | 0.162599 | 0.003738 | 3.985142 | 0.123475 | 1436.5 | 38.6 | 1916.1 | 51.5 | 2481.1 | 38.7 | 1.71 | 623 | 368 | 345 |
| | 25 | 3 | 0.322524 | 0.009419 | 7.655648 | 0.425831 | 0.172164 | 0.003064 | 3.08765 | 0.091111 | 1801.7 | 46 | 2190.6 | 50.2 | 2577.4 | 29.9 | 1.59 | 543 | 348 | 308 |
| | 26 | 3 | 0.372301 | 0.010143 | 8.940743 | 0.486235 | 0.174299 | 0.003004 | 2.674104 | 0.072713 | 2040 | 47.6 | 2331.5 | 49.7 | 2598 | 28.7 | 1.55 | 596 | 395 | 335 |
| | 27 | 3 | 0.370398 | 0.011203 | 9.007895 | 0.500559 | 0.176345 | 0.0034 | 2.690812 | 0.08098 | 2030.9 | 52.7 | 2338.1 | 50.2 | 2617.2 | 32.5 | 1.6 | 597 | 386 | 369 |
| | 28 | 3 | 0.424772 | 0.011844 | 10.349678 | 0.569198 | 0.176773 | 0.002999 | 2.34663 | 0.067442 | 2281.7 | 53.8 | 2465.7 | 51.7 | 2621.5 | 28.3 | 1.39 | 611 | 457 | 398 |
| | 29 | 3 | 0.272424 | 0.007938 | 6.322923 | 0.34451 | 0.168551 | 0.003304 | 3.663125 | 0.106812 | 1552.8 | 40.2 | 2021.1 | 47.9 | 2541.1 | 32.6 | 1.5 | 969 | 680 | 526 |
| | 30 | 3 | 0.187301 | 0.005158 | 4.254545 | 0.231193 | 0.165133 | 0.003123 | 5.322384 | 0.148822 | 1106.7 | 28 | 1684.5 | 44.8 | 2507.7 | 31.7 | 1.78 | 1360 | 805 | 401 |
| ZB01 | 1 | 2 | 0.34677 | 0.004407 | 7.794743 | 0.571995 | 0.163061 | 0.003648 | 2.887601 | 0.036591 | 1918.9 | 21.1 | 2207.1 | 65.7 | 2486.3 | 37.7 | 2.15 | 1870 | 8485 | 4128 |
| | 2 | 2 | 0.503446 | 0.006133 | 12.623988 | 0.927169 | 0.181891 | 0.004108 | 1.988881 | 0.024438 | 2628.3 | 26.3 | 2651.5 | 69.2 | 2668.7 | 37.6 | 1.48 | 1103 | 745 | 1957 |
| | 3 | 2 | 0.249902 | 0.00681 | 4.995834 | 0.404418 | 0.144695 | 0.003683 | 4.032196 | 0.12071 | 1437.1 | 35.4 | 1814.1 | 70.9 | 2281.3 | 43.2 | 1.41 | 4478 | 3178 | 3571 |
| | 4 | 2 | 0.286357 | 0.005123 | 6.65676 | 0.490592 | 0.168743 | 0.003826 | 3.502936 | 0.063967 | 1622.9 | 25.7 | 2066.3 | 64.8 | 2543.7 | 38 | 3.24 | 4289 | 1324 | 2444 |
| | 5 | 2 | 0.226103 | 0.005961 | 4.469432 | 0.371825 | 0.142848 | 0.004001 | 4.45445 | 0.12705 | 1313.4 | 31.5 | 1719.6 | 72.4 | 2257.7 | 49.7 | 1.33 | 8132 | 6133 | 5248 |
| | 6 | 2 | 0.531303 | 0.006411 | 13.386105 | 0.98212 | 0.182756 | 0.004045 | 1.884994 | 0.023096 | 2746.6 | 27.1 | 2706.8 | 70.1 | 2676.8 | 36.8 | 2.81 | 1879 | 669 | 1255 |
| | 7 | 2 | 0.438857 | 0.005745 | 10.719085 | 0.783042 | 0.177217 | 0.003835 | 2.282744 | 0.030414 | 2345.2 | 25.8 | 2498.8 | 68.4 | 2625.9 | 36.1 | 2.48 | 3548 | 1432 | 3588 |

Continued on next page

| Sample | Spot name | Run | 206/238 | ±2SE | 207/235 | ±2SE | 207/206 | ±2SE | 238/P206 | ±2SE | 206/238 Age | ±2SE | 207/235 Age | ±2SE | 207/206 Age | ±2SE | U/Th | U | Th | Pb |
|---|---|---|---|---|---|---|---|---|---|---|---|---|---|---|---|---|---|---|---|---|
| | 8 | 2 | 0.542928 | 0.007495 | 13.698572 | 1.004594 | 0.183064 | 0.004042 | 1.845588 | 0.025783 | 2795.2 | 31.4 | 2728.6 | 69.6 | 2679.6 | 36.4 | 1.82 | 1283 | 706 | 695 |
| | 9 | 2 | 0.526792 | 0.007869 | 13.349557 | 0.989747 | 0.183867 | 0.004431 | 1.902752 | 0.028393 | 2727.3 | 33.2 | 2703.7 | 71.2 | 2686 | 39.7 | 2.64 | 476 | 701 | 672 |
| | 10 | 2 | 0.522506 | 0.007482 | 13.266064 | 0.976323 | 0.184224 | 0.004188 | 1.918163 | 0.02806 | 2709.3 | 31.8 | 2698.1 | 69.6 | 2689.8 | 37.5 | 1.88 | 540 | 459 | 560 |
| | 11 | 2 | 0.329909 | 0.005842 | 7.206819 | 0.549453 | 0.158354 | 0.003769 | 3.041542 | 0.054841 | 1837.5 | 28.4 | 2135.4 | 66.4 | 2436.2 | 39.8 | 1.35 | 682 | 383 | 299 |
| | 12 | 2 | 0.248494 | 0.008767 | 4.736877 | 0.403087 | 0.138937 | 0.003561 | 4.068925 | 0.128482 | 1429.3 | 44.7 | 1767.9 | 66.1 | 2211.1 | 43.4 | 1.69 | 916 | 412 | 246 |
| | 13 | 2 | 0.26176 | 0.007506 | 5.768163 | 0.525025 | 0.158884 | 0.005538 | 3.850091 | 0.103439 | 1497.8 | 38.1 | 1931.9 | 74 | 2436.1 | 56.5 | 2.43 | 938 | 293 | 260 |
| | 14 | 2 | 0.157164 | 0.002776 | 1.984986 | 0.151641 | 0.091697 | 0.002237 | 6.384377 | 0.113617 | 940.9 | 15.5 | 1113.6 | 57.6 | 1458.4 | 46.1 | 1.16 | 2046 | 1353 | 577 |
| | 15 | 2 | 0.314983 | 0.007085 | 6.948495 | 0.528099 | 0.160049 | 0.00367 | 3.191161 | 0.07077 | 1764.4 | 34.6 | 2103 | 67.1 | 2454.5 | 38.8 | 2.02 | 409 | 158 | 128 |
| | 16 | 2 | 0.540256 | 0.007446 | 13.635199 | 0.998726 | 0.183173 | 0.00409 | 1.849561 | 0.023322 | 2784 | 31.4 | 2724.3 | 69.9 | 2680.5 | 37.1 | 3.91 | 299 | 61 | 87 |
| | 17 | 2 | 0.38439 | 0.006444 | 9.40561 | 0.705339 | 0.177448 | 0.003972 | 2.609659 | 0.045193 | 2096.2 | 30.1 | 2376.9 | 69.6 | 2627.8 | 37.1 | 2.66 | 631 | 194 | 213 |
| | 18 | 2 | 0.418332 | 0.006626 | 10.13941 | 0.748118 | 0.175897 | 0.003926 | 2.396992 | 0.037587 | 2252.4 | 30.1 | 2446.8 | 67.8 | 2613.2 | 37.1 | 2.18 | 549 | 211 | 231 |
| | 19 | 2 | 0.342819 | 0.00681 | 8.434261 | 0.630558 | 0.178528 | 0.003904 | 2.92883 | 0.057199 | 1899.6 | 32.6 | 2277.6 | 67.6 | 2638.1 | 36 | 1.73 | 1153 | 572 | 560 |
| | 20 | 2 | 0.524367 | 0.006263 | 13.387453 | 0.980103 | 0.18529 | 0.004261 | 1.910285 | 0.022689 | 2717.4 | 26.4 | 2707 | 69.2 | 2699.2 | 37.7 | 1.43 | 179 | 110 | 143 |
| | 21 | 2 | 0.27671 | 0.016323 | 7.158302 | 0.687537 | 0.188366 | 0.00507 | 3.691552 | 0.22355 | 1592 | 92.1 | 2117.1 | 83.3 | 2724.6 | 44 | 4.09 | 2080 | 466 | 2093 |
| | 22 | 2 | 0.327552 | 0.013123 | 7.677353 | 0.709384 | 0.168938 | 0.004833 | 3.10113 | 0.126128 | 1823.6 | 63.8 | 2181.4 | 84 | 2542.8 | 48.1 | 2 | 832 | 368 | 383 |
| | 23 | 2 | 0.307335 | 0.006632 | 7.261153 | 0.548591 | 0.171448 | 0.00385 | 3.269215 | 0.073961 | 1726.9 | 32.8 | 2142.3 | 68.8 | 2570.4 | 37.6 | 2.57 | 857 | 292 | 374 |
| | 24 | 2 | 0.542981 | 0.007549 | 13.889635 | 1.023511 | 0.185625 | 0.004121 | 1.845244 | 0.025457 | 2795.4 | 31.5 | 2741.5 | 70.1 | 2702.5 | 36.4 | 1.09 | 510 | 409 | 503 |
| | 25 | 2 | 0.481643 | 0.010336 | 11.980723 | 0.910614 | 0.180011 | 0.00404 | 2.085745 | 0.04617 | 2533.1 | 45.2 | 2600.7 | 72.5 | 2651.6 | 37.5 | 2.53 | 319 | 112 | 139 |
| | 26 | 2 | 0.337365 | 0.014675 | 7.721974 | 0.696136 | 0.165479 | 0.003973 | 3.013104 | 0.118406 | 1870.5 | 69.7 | 2189.2 | 76.3 | 2510.3 | 40.3 | 1.92 | 1067 | 514 | 353 |
| | 27 | 2 | 0.523633 | 0.007028 | 13.751676 | 1.043426 | 0.190465 | 0.00501 | 1.913045 | 0.025429 | 2714.1 | 29.7 | 2730.7 | 70.2 | 2743.1 | 42.9 | 2.98 | 280 | 90 | 163 |
| | 28 | 2 | 0.374288 | 0.019412 | 8.653054 | 0.852065 | 0.166577 | 0.004439 | 2.738543 | 0.136279 | 2043.6 | 90.4 | 2285.4 | 88 | 2520.2 | 44.8 | 2.31 | 932 | 354 | 324 |
| | 29 | 2 | 0.48711 | 0.014294 | 12.227712 | 0.97399 | 0.181991 | 0.00437 | 2.070857 | 0.065021 | 2555.5 | 62.5 | 2617.3 | 78.5 | 2669.1 | 39.3 | 2.01 | 488 | 211 | 278 |
| | 30 | 2 | 0.531052 | 0.008228 | 13.364829 | 0.990033 | 0.182622 | 0.004002 | 1.88739 | 0.030139 | 2745.2 | 34.8 | 2704.8 | 70.2 | 2675.7 | 36.3 | 1.2 | 363 | 267 | 346 |
| ZB02 | 1 | 2 | 0.992977 | 0.037391 | 27.230564 | 2.279314 | 0.198742 | 0.004449 | 1.020008 | 0.036841 | 4435.5 | 119.2 | 3384.3 | 79.5 | 2814.6 | 36.6 | 0.76 | 6396 | 7997 | 94128 |
| | 2 | 2 | 0.175466 | 0.003653 | 4.067725 | 0.309405 | 0.168242 | 0.004083 | 5.722261 | 0.122273 | 1041.9 | 20.1 | 1646.2 | 62.3 | 2538 | 40.3 | 3.3 | 1161 | 313 | 356 |
| | 3 | 2 | 0.533549 | 0.006766 | 13.459698 | 0.985815 | 0.183141 | 0.004134 | 1.876795 | 0.023682 | 2756 | 28.4 | 2712 | 69 | 2680.1 | 37 | 1.89 | 336 | 160 | 229 |
| | 4 | 2 | 0.356527 | 0.005518 | 9.092966 | 0.672897 | 0.185131 | 0.004171 | 2.810743 | 0.043489 | 1965.3 | 26.2 | 2346.6 | 67.1 | 2698 | 37.5 | 2.84 | 499 | 161 | 222 |
| | 5 | 2 | 0.1594 | 0.004666 | 4.761418 | 0.350741 | 0.217894 | 0.006409 | 6.324317 | 0.187272 | 953 | 26 | 1777.6 | 62.6 | 2960.7 | 47.8 | 0.95 | 5187 | 5240 | 4057 |
| | 6 | 2 | 0.453825 | 0.026464 | 11.337013 | 1.072984 | 0.181075 | 0.004114 | 2.290167 | 0.15986 | 2402 | 120 | 2534.6 | 95.1 | 2661.2 | 37.5 | 1.44 | 777 | 465 | 623 |
| | 7 | 2 | 0.15754 | 0.002172 | 2.750059 | 0.208279 | 0.12665 | 0.003355 | 6.357801 | 0.087848 | 943 | 12.1 | 1340.9 | 55.9 | 2048.5 | 46.7 | 2.68 | 6492 | 2225 | 1558 |
| | 8 | 2 | 0.418934 | 0.011202 | 10.840467 | 0.842779 | 0.187159 | 0.004739 | 2.387475 | 0.06377 | 2253.9 | 51.7 | 2506.3 | 74.3 | 2721.1 | 46.1 | 1.84 | 530 | 273 | 371 |
| | 9 | 2 | 0.519394 | 0.007894 | 13.174939 | 0.967353 | 0.184209 | 0.004173 | 1.929114 | 0.029322 | 2696 | 33.5 | 2691.7 | 69.1 | 2689.7 | 37.3 | 2.51 | 302 | 109 | 149 |
| | 10 | 2 | 0.437141 | 0.006966 | 10.539022 | 0.782253 | 0.174987 | 0.003881 | 2.292653 | 0.037317 | 2337.3 | 31.3 | 2482.4 | 68.9 | 2604.6 | 36.6 | 1.99 | 701 | 319 | 353 |
| | 11 | 2 | 0.316779 | 0.007175 | 8.003661 | 0.608978 | 0.183471 | 0.004516 | 3.170851 | 0.071282 | 1773.2 | 35.1 | 2229.4 | 69.1 | 2682.2 | 40 | 0.84 | 420 | 454 | 250 |
| | 12 | 2 | 0.511713 | 0.006755 | 12.863041 | 0.942733 | 0.182529 | 0.00409 | 1.956631 | 0.025887 | 2663.5 | 28.8 | 2669.2 | 69.1 | 2674.6 | 37.3 | 1.26 | 425 | 315 | 394 |
| | 13 | 2 | 0.373688 | 0.005541 | 9.344563 | 0.690571 | 0.181562 | 0.004159 | 2.680424 | 0.039918 | 2046.4 | 26 | 2371.6 | 67.9 | 2665.6 | 37.8 | 2.08 | 459 | 207 | 184 |
| | 14 | 2 | 0.280439 | 0.006585 | 6.396087 | 0.514275 | 0.165187 | 0.004343 | 3.583376 | 0.08707 | 1592.8 | 33.2 | 2027.3 | 71.7 | 2506.3 | 44.3 | 1.95 | 671 | 326 | 200 |
| | 15 | 2 | 0.329182 | 0.016245 | 8.038668 | 0.786389 | 0.175907 | 0.005073 | 3.110489 | 0.159403 | 1829.9 | 79.1 | 2218.4 | 90.3 | 2610.3 | 47.9 | 2.03 | 637 | 335 | 341 |
| | 16 | 2 | 0.490272 | 0.009726 | 12.567416 | 0.934886 | 0.186197 | 0.004169 | 2.046462 | 0.042449 | 2570.7 | 42.3 | 2646.6 | 71 | 2707.5 | 37.1 | 1.82 | 430 | 228 | 295 |
| | 17 | 2 | 0.361273 | 0.00612 | 8.398775 | 0.620835 | 0.168852 | 0.003856 | 2.774062 | 0.048516 | 1987.7 | 29.1 | 2274.2 | 68 | 2544.7 | 38.1 | 3.15 | 633 | 195 | 168 |
| | 18 | 2 | 0.371274 | 0.011493 | 9.105373 | 0.758133 | 0.177527 | 0.004619 | 2.718681 | 0.092888 | 2033.3 | 54.6 | 2341.7 | 80.1 | 2626.9 | 43.3 | 3.23 | 620 | 186 | 218 |
| | 19 | 2 | 0.133379 | 0.004132 | 2.383961 | 0.193266 | 0.129545 | 0.003099 | 7.564087 | 0.246027 | 806.7 | 23.6 | 1234.5 | 60.1 | 2089.6 | 43.1 | 5.04 | 3001 | 564 | 565 |
| | 20 | 2 | 0.315356 | 0.004444 | 7.499649 | 0.557347 | 0.172018 | 0.003984 | 3.174562 | 0.04395 | 1766.8 | 21.7 | 2172 | 65.3 | 2575.7 | 38.7 | 1.99 | 679 | 320 | 318 |
| | 21 | 2 | 0.4551 | 0.014178 | 11.173613 | 0.88769 | 0.178164 | 0.003888 | 2.216919 | 0.075972 | 2415.1 | 63.6 | 2533.2 | 77.4 | 2634.7 | 36.1 | 1.7 | 992 | 447 | 794 |
| | 22 | 2 | 0.171335 | 0.009381 | 4.297204 | 0.416087 | 0.181209 | 0.004499 | 5.995573 | 0.322707 | 1017.5 | 51.5 | 1679.8 | 79.7 | 2661.5 | 41.4 | 3.91 | 2296 | 441 | 1263 |
| | 23 | 2 | 0.302461 | 0.010138 | 7.154848 | 0.591275 | 0.171479 | 0.00413 | 3.335581 | 0.10682 | 1701.8 | 49.8 | 2125.3 | 71.8 | 2570 | 40.5 | 0.35 | 1197 | 2537 | 528 |
| | 24 | 2 | 0.301081 | 0.010744 | 7.200278 | 0.617969 | 0.173021 | 0.004394 | 3.359551 | 0.127926 | 1694.7 | 53.5 | 2128.3 | 79.3 | 2584.4 | 42.5 | 2.45 | 906 | 272 | 352 |
| | 25 | 2 | 0.533415 | 0.007429 | 13.466377 | 0.991006 | 0.183359 | 0.004182 | 1.875352 | 0.026556 | 2755.3 | 31.3 | 2712.3 | 69.7 | 2682 | 37.9 | 1.54 | 517 | 245 | 417 |
| | 26 | 2 | 0.262085 | 0.008731 | 7.927223 | 0.675044 | 0.218829 | 0.005577 | 3.851309 | 0.133143 | 1499.1 | 44.7 | 2215 | 78.2 | 2969.5 | 41 | 3.19 | 2273 | 512 | 1566 |
| | 27 | 2 | 0.461871 | 0.005298 | 11.754383 | 0.868309 | 0.185244 | 0.004234 | 2.164205 | 0.025573 | 2447.6 | 23.5 | 2584.2 | 70.7 | 2698.8 | 37.9 | 2.88 | 402 | 102 | 158 |
| | 28 | 2 | 0.454464 | 0.014087 | 11.073715 | 0.894563 | 0.17623 | 0.003985 | 2.21762 | 0.072221 | 2412.4 | 62.8 | 2524 | 77.3 | 2620.3 | 42.8 | 1.15 | 1314 | 862 | 1135 |
| | 29 | 2 | 0.34334 | 0.009721 | 8.917689 | 0.688499 | 0.18868 | 0.004192 | 2.929239 | 0.082281 | 1901.2 | 46.6 | 2326.9 | 70.8 | 2729.4 | 36.8 | 2.35 | 814 | 260 | 458 |
| | 30 | 2 | 0.472447 | 0.008468 | 11.990681 | 0.887006 | 0.184388 | 0.004109 | 2.119089 | 0.038712 | 2493.5 | 37.2 | 2602.8 | 69.9 | 2691.4 | 36.5 | 1.32 | 1209 | 706 | 1036 |
| ZB03 | 1 | 3 | 0.27643 | 0.007541 | 11.607059 | 0.646441 | 0.304507 | 0.005955 | 3.634344 | 0.100045 | 1573.2 | 38.1 | 2572.5 | 52.1 | 3491.7 | 30.4 | 3.01 | 1040 | 343 | 1615 |

Continued on next page

| Sample | Spot name | Run | 206/238 | ±2SE | 207/235 | ±2SE | 207/206 | ±2SE | 238/P206 | ±2SE | 206/238 Age | ±2SE | 207/235 Age | ±2SE | 207/206 Age | ±2SE | U/Th | U | Th | Pb |
|---|---|---|---|---|---|---|---|---|---|---|---|---|---|---|---|---|---|---|---|---|
| | 2 | 3 | 0.459329 | 0.012874 | 11.413782 | 0.625116 | 0.180564 | 0.003345 | 2.18761 | 0.061403 | 2436.4 | 56.9 | 2557.3 | 51 | 2656.9 | 30.7 | 2.79 | 350 | 125 | 181 |
| | 3 | 3 | 0.375971 | 0.011902 | 8.890218 | 0.507825 | 0.171955 | 0.003251 | 2.676776 | 0.086212 | 2057 | 55.9 | 2325.9 | 52.8 | 2575.4 | 31.7 | 3.15 | 356 | 113 | 144 |
| | 4 | 3 | 0.347516 | 0.010437 | 8.207497 | 0.477931 | 0.17163 | 0.003801 | 2.894031 | 0.087017 | 1922.5 | 49.9 | 2253.3 | 52.8 | 2571.9 | 37.2 | 2.26 | 438 | 194 | 210 |
| | 5 | 3 | 0.264616 | 0.006941 | 7.496507 | 0.424653 | 0.205623 | 0.004721 | 3.799431 | 0.099205 | 1513.3 | 35.4 | 2171.1 | 51.3 | 2868 | 37.7 | 6.26 | 1108 | 184 | 648 |
| | 6 | 3 | 0.192511 | 0.005775 | 3.451892 | 0.208083 | 0.129957 | 0.002761 | 5.233497 | 0.157802 | 1134.8 | 31.2 | 1513.9 | 47.9 | 2094.4 | 37.3 | 1.7 | 879 | 521 | 295 |
| | 7 | 3 | 0.483347 | 0.014075 | 12.125895 | 0.669098 | 0.182042 | 0.003165 | 2.082725 | 0.062593 | 2541.2 | 61.4 | 2613.5 | 51.9 | 2670.3 | 28.7 | 2.02 | 392 | 196 | 269 |
| | 8 | 3 | 0.521557 | 0.014641 | 13.2809 | 0.72156 | 0.184823 | 0.003194 | 1.929247 | 0.055141 | 2705.3 | 62.2 | 2702.3 | 44.7 | 2699.1 | 24.4 | 2.15 | 325 | 153 | 219 |
| | 9 | 3 | 0.146515 | 0.004079 | 1.872408 | 0.102184 | 0.092728 | 0.001525 | 6.866146 | 0.193804 | 881.3 | 22.9 | 1071.1 | 36.2 | 1481.1 | 31.1 | 14.38 | 3592 | 253 | 272 |
| | 10 | 3 | 0.273385 | 0.007928 | 5.621986 | 0.324281 | 0.149064 | 0.002718 | 3.680819 | 0.106202 | 1557.7 | 40.1 | 1918 | 49.1 | 2333.6 | 30.9 | 15.25 | 914 | 61 | 64 |
| | 11 | 3 | 0.339876 | 0.008943 | 7.956085 | 0.427472 | 0.169829 | 0.002779 | 2.949559 | 0.078168 | 1885.9 | 43.1 | 2225.8 | 48.4 | 2554.8 | 27.3 | 18.63 | 670 | 37 | 59 |
| | 12 | 3 | 0.317372 | 0.009816 | 7.129427 | 0.409578 | 0.162836 | 0.002679 | 3.165115 | 0.101326 | 1776.3 | 48.2 | 2125.9 | 52 | 2484.2 | 27.9 | 1.67 | 671 | 409 | 341 |
| | 13 | 3 | 0.315163 | 0.010167 | 7.153519 | 0.411875 | 0.164498 | 0.002903 | 3.186029 | 0.107001 | 1765.5 | 50.1 | 2129.2 | 52.4 | 2501 | 29.8 | 1.65 | 760 | 470 | 406 |
| | 14 | 3 | 0.377005 | 0.011044 | 9.28923 | 0.538465 | 0.178282 | 0.003605 | 2.655662 | 0.078327 | 2062 | 51.7 | 2366 | 53.7 | 2635.5 | 33.5 | 2.55 | 593 | 238 | 289 |
| | 15 | 3 | 0.342545 | 0.00939 | 7.759425 | 0.433502 | 0.164104 | 0.002894 | 2.921491 | 0.082134 | 1898.7 | 45.2 | 2202.5 | 51.3 | 2496.9 | 30.1 | 2.09 | 739 | 361 | 341 |
| | 17 | 3 | 0.244343 | 0.006619 | 5.251349 | 0.29291 | 0.15552 | 0.003837 | 4.08788 | 0.111575 | 1409.2 | 34.3 | 1860.6 | 47.7 | 2405.3 | 41.8 | 6.62 | 991 | 153 | 232 |
| | 18 | 3 | 0.352948 | 0.010384 | 8.076443 | 0.449326 | 0.165753 | 0.002863 | 2.832585 | 0.085901 | 1948.3 | 49.6 | 2238.8 | 51 | 2513.9 | 28.8 | 1.75 | 735 | 429 | 400 |
| | 19 | 3 | 0.414324 | 0.012244 | 9.947723 | 0.557126 | 0.173831 | 0.002848 | 2.411472 | 0.074038 | 2234.2 | 56.1 | 2428.9 | 52.6 | 2593.8 | 27.3 | 1.82 | 670 | 373 | 413 |
| | 21 | 3 | 0.504281 | 0.017204 | 12.869569 | 0.732244 | 0.185121 | 0.004207 | 1.970288 | 0.069175 | 2631.5 | 74 | 2669.6 | 53.7 | 2697.7 | 37.3 | 2.35 | 297 | 127 | 168 |
| | 22 | 3 | 0.497354 | 0.013642 | 12.592491 | 0.692201 | 0.182885 | 0.003056 | 1.994016 | 0.054987 | 2602.2 | 58.8 | 2649.2 | 52 | 2678.2 | 27.7 | 2.05 | 503 | 248 | 345 |
| | 23 | 3 | 0.184415 | 0.005126 | 3.19523 | 0.175306 | 0.125336 | 0.002199 | 5.378547 | 0.145766 | 1090.9 | 27.8 | 1455.5 | 42 | 2032 | 30.9 | 10.29 | 849 | 90 | 68 |
| | 24 | 3 | 0.236246 | 0.007882 | 5.999 | 0.38151 | 0.183575 | 0.004257 | 4.203662 | 0.140272 | 1366.8 | 41.1 | 1972.8 | 55.9 | 2682.8 | 39 | 2.16 | 871 | 416 | 530 |
| | 25 | 3 | 0.211981 | 0.005842 | 4.899146 | 0.264918 | 0.167242 | 0.003319 | 4.674298 | 0.128508 | 1239.2 | 31.1 | 1801.8 | 45.8 | 2527.9 | 33.3 | 4.12 | 1096 | 337 | 452 |
| | 26 | 3 | 0.489678 | 0.013505 | 17.088807 | 0.978834 | 0.251994 | 0.005456 | 2.021654 | 0.057232 | 2569 | 58.7 | 2938.7 | 56.4 | 3195.4 | 34.4 | 2.78 | 609 | 227 | 867 |
| | 27 | 3 | 0.323046 | 0.010046 | 9.892276 | 0.622273 | 0.221071 | 0.00542 | 3.0693 | 0.098099 | 1804.1 | 49.1 | 2421.1 | 59.5 | 2985.2 | 40 | 3.3 | 1775 | 573 | 1683 |
| | 28 | 3 | 0.331179 | 0.009493 | 7.98339 | 0.448445 | 0.174237 | 0.003668 | 2.980484 | 0.077259 | 1843.7 | 46.1 | 2227.9 | 50.1 | 2596.1 | 34.8 | 1.86 | 776 | 430 | 560 |
| | 29 | 3 | 0.471024 | 0.012537 | 11.725184 | 0.635901 | 0.179542 | 0.003216 | 2.099485 | 0.056063 | 2487.9 | 55 | 2582.5 | 50.9 | 2647.5 | 29.9 | 1.75 | 473 | 278 | 376 |
| | 30 | 3 | 0.346446 | 0.009405 | 7.670867 | 0.417449 | 0.159847 | 0.002752 | 2.855639 | 0.077845 | 1917.4 | 45 | 2192.8 | 49 | 2452.7 | 28.9 | 1.84 | 688 | 379 | 387 |
| | 31 | 7 | 0.349219 | 0.010105 | 7.91745 | 0.835712 | 0.166379 | 0.006424 | 2.875406 | 0.078893 | 1929.5 | 47.9 | 2217.6 | 92.8 | 2525.7 | 54.9 | 1.74 | 384 | 223 | 201 |
| | 32 | 7 | 0.345032 | 0.009496 | 7.386237 | 0.7685 | 0.156331 | 0.005939 | 2.908577 | 0.081078 | 1909.7 | 45.5 | 2156.5 | 91.2 | 2414.1 | 64.2 | 1.57 | 477 | 322 | 281 |
| | 33 | 7 | 0.357846 | 0.006975 | 7.840954 | 0.796005 | 0.159835 | 0.006037 | 2.792723 | 0.053797 | 1971.6 | 33.1 | 2212.2 | 91.7 | 2451.9 | 64.4 | 1.5 | 554 | 374 | 355 |
| | 34 | 7 | 0.410406 | 0.008961 | 9.244543 | 0.94799 | 0.163921 | 0.006191 | 2.437298 | 0.054466 | 2216.1 | 41.1 | 2360.9 | 95.1 | 2494.5 | 63.7 | 1.3 | 631 | 492 | 507 |
| | 35 | 7 | 0.181242 | 0.003507 | 3.8405 | 0.39896 | 0.153288 | 0.006591 | 5.507052 | 0.106974 | 1073.7 | 19.1 | 1600.5 | 82.9 | 2380.1 | 72.8 | 11.66 | 1681 | 143 | 426 |
| | 36 | 7 | 0.432712 | 0.009286 | 10.975278 | 1.128884 | 0.183919 | 0.007188 | 2.310236 | 0.049584 | 2317.3 | 41.8 | 2519.1 | 95.5 | 2685.5 | 65.9 | 2.42 | 368 | 152 | 199 |
| | 37 | 7 | 0.475248 | 0.012735 | 14.71925 | 1.584815 | 0.223849 | 0.010943 | 2.105848 | 0.058897 | 2505.4 | 56 | 2792.7 | 100.8 | 3000.5 | 80.5 | 2.36 | 178 | 76 | 195 |
| | 38 | 7 | 0.603337 | 0.012089 | 17.420299 | 1.771889 | 0.208653 | 0.007768 | 1.655271 | 0.033696 | 3042.5 | 48.7 | 2957.3 | 97.5 | 2893.6 | 60.3 | 1.5 | 522 | 356 | 527 |
| | 39 | 7 | 0.592371 | 0.011002 | 17.182708 | 1.74043 | 0.209341 | 0.00795 | 1.684546 | 0.031324 | 2998.6 | 44.5 | 2944.5 | 97.5 | 2898.3 | 62.3 | 2.22 | 337 | 159 | 227 |
| | 40 | 7 | 0.598058 | 0.011422 | 17.715253 | 1.803006 | 0.213262 | 0.008025 | 1.668552 | 0.031869 | 3021.5 | 46.1 | 2973.3 | 97.8 | 2928.7 | 60.7 | 2.81 | 361 | 132 | 235 |
| | 41 | 7 | 0.296393 | 0.006358 | 8.400439 | 0.855999 | 0.202774 | 0.008621 | 3.367765 | 0.072876 | 1673 | 31.6 | 2274.2 | 93.4 | 2842.9 | 70 | 2.22 | 861 | 394 | 712 |
| | 42 | 7 | 0.406587 | 0.01213 | 11.711969 | 1.225792 | 0.204828 | 0.007864 | 2.460325 | 0.075615 | 2198.1 | 55.8 | 2579.2 | 101.1 | 2863.2 | 62.7 | 1.03 | 758 | 731 | 1207 |
| | 43 | 7 | 0.567316 | 0.01112 | 15.51512 | 1.574559 | 0.194853 | 0.007353 | 1.757849 | 0.034511 | 2896.2 | 45.7 | 2846.7 | 96.9 | 2781.6 | 62.3 | 1.1 | 377 | 339 | 512 |
| | 44 | 7 | 0.481097 | 0.045089 | 24.335347 | 3.767231 | 0.361069 | 0.029606 | 2.114034 | 0.194966 | 2524.8 | 195.5 | 3264.3 | 160.9 | 3743.3 | 116.5 | 10.04 | 3015 | 295 | 10140 |
| | 45 | 7 | 0.226655 | 0.009068 | 5.463601 | 0.652726 | 0.16999 | 0.007988 | 4.423305 | 0.169184 | 1316.2 | 47.4 | 1887.2 | 101.1 | 2552.2 | 77.9 | 16.73 | 2915 | 171 | 2351 |
| | 46 | 7 | 0.208685 | 0.004738 | 4.148043 | 0.434037 | 0.141199 | 0.005757 | 4.776785 | 0.111189 | 1221.7 | 25.3 | 1662.7 | 86.7 | 2239.7 | 71.1 | 10.63 | 2775 | 256 | 1167 |
| | 47 | 7 | 0.212595 | 0.00514 | 6.257508 | 0.701451 | 0.208733 | 0.010608 | 4.694092 | 0.114645 | 1242.4 | 27.3 | 2006.5 | 99.6 | 2887.3 | 82.4 | 9.95 | 3190 | 315 | 3123 |
| | 48 | 7 | 0.202103 | 0.005626 | 4.013835 | 0.41759 | 0.141121 | 0.005727 | 4.953585 | 0.135038 | 1186.1 | 30.1 | 1634.7 | 82.2 | 2236.6 | 69.8 | 1.96 | 942 | 586 | 399 |
| | 49 | 7 | 0.219513 | 0.005523 | 4.243459 | 0.448554 | 0.136966 | 0.005548 | 4.553639 | 0.109637 | 1278.9 | 29.1 | 1679 | 84.3 | 2184.8 | 70 | 1.3 | 849 | 647 | 402 |
| | 50 | 7 | 0.285731 | 0.006668 | 6.027966 | 0.625626 | 0.14956 | 0.005853 | 3.49604 | 0.084064 | 1619.7 | 33.5 | 1977.3 | 92.9 | 2337.7 | 67.1 | 1.28 | 781 | 601 | 472 |
| | 51 | 7 | 0.159188 | 0.004986 | 3.399943 | 0.352789 | 0.151851 | 0.005666 | 6.305061 | 0.204091 | 951.8 | 27.8 | 1502.3 | 82.2 | 2365.2 | 63.9 | 6.49 | 9473 | 1479 | 4296 |
| | 52 | 7 | 0.172779 | 0.003597 | 3.856289 | 0.405314 | 0.158441 | 0.006676 | 5.774093 | 0.117913 | 1027.3 | 19.7 | 1601.7 | 81.4 | 2433.6 | 69.8 | 7.89 | 7820 | 991 | 4020 |
| | 53 | 7 | 0.323052 | 0.00859 | 8.151984 | 0.837085 | 0.179848 | 0.007368 | 3.097214 | 0.082743 | 1803.7 | 41.8 | 2246.3 | 93.3 | 2646.9 | 68.4 | 1.96 | 800 | 418 | 614 |
| | 54 | 7 | 0.511782 | 0.014151 | 14.595049 | 1.526615 | 0.203708 | 0.009209 | 1.952696 | 0.054215 | 2662.9 | 60.3 | 2786.7 | 99.8 | 2850.5 | 74.3 | 2.02 | 103 | 54 | 77 |
| | 55 | 7 | 0.565358 | 0.01378 | 14.530418 | 1.51001 | 0.18201 | 0.007279 | 1.767949 | 0.045153 | 2887.2 | 57.2 | 2781.9 | 98.3 | 2667.5 | 67.5 | 2.99 | 169 | 58 | 71 |
| | 56 | 7 | 0.1869 | 0.004097 | 3.016027 | 0.311362 | 0.115488 | 0.004949 | 5.333868 | 0.117597 | 1104.5 | 22.3 | 1410.9 | 77.6 | 1883.8 | 76.6 | 1.49 | 998 | 669 | 337 |
| | 57 | 7 | 0.367366 | 0.009637 | 8.367091 | 0.871652 | 0.162401 | 0.006253 | 2.723126 | 0.072035 | 2015.9 | 45.5 | 2268.5 | 95.5 | 2478.2 | 64.9 | 2.73 | 509 | 185 | 184 |
| | 58 | 7 | 0.290136 | 0.012314 | 11.170441 | 1.222724 | 0.276727 | 0.010869 | 3.491039 | 0.156027 | 1639.5 | 61.6 | 2529 | 103.7 | 3341.6 | 62.1 | 0.99 | 2025 | 2117 | 3739 |
| | 59 | 7 | 0.165906 | 0.003221 | 2.284249 | 0.233228 | 0.098398 | 0.003714 | 5.993214 | 0.106141 | 989.4 | 17.8 | 1206.7 | 72.1 | 1591.6 | 69.7 | 10.31 | 3751 | 363 | 280 |

Continued on next page

| Sample | Spot name | Run | 206/238 | ±2SE | 207/235 | ±2SE | 207/206 | ±2SE | 238/P206 | ±2SE | 206/238 Age | ±2SE | 207/235 Age | ±2SE | 207/206 Age | ±2SE | U/Th | U | Th | Pb |
|---|---|---|---|---|---|---|---|---|---|---|---|---|---|---|---|---|---|---|---|---|
| | 60 | 7 | 0.118461 | 0.002631 | 1.446093 | 0.14923 | 0.086962 | 0.003399 | 8.394087 | 0.209338 | 721.6 | 15.2 | 907.3 | 60.9 | 1355.9 | 76 | 10.29 | 4939 | 478 | 223 |
| ZB05 | 1 | 7 | 0.480675 | 0.010073 | 11.751159 | 1.202318 | 0.178037 | 0.006791 | 2.076867 | 0.044002 | 2529.5 | 43.9 | 2583.3 | 97 | 2632.4 | 64.2 | 2.08 | 391 | 190 | 251 |
| | 2 | 7 | 0.458689 | 0.011747 | 10.960441 | 1.141459 | 0.174028 | 0.00689 | 2.181547 | 0.056952 | 2432.4 | 52 | 2516.7 | 95.4 | 2593.4 | 65.3 | 1.99 | 294 | 150 | 190 |
| | 3 | 7 | 0.465364 | 0.010296 | 11.129457 | 1.136711 | 0.174309 | 0.006657 | 2.146552 | 0.049042 | 2462.4 | 45.5 | 2532.7 | 95.6 | 2597.1 | 63.5 | 1.95 | 407 | 213 | 296 |
| | 4 | 7 | 0.488633 | 0.013925 | 11.951775 | 1.239175 | 0.178261 | 0.006757 | 2.051729 | 0.061296 | 2562.7 | 60.7 | 2597.8 | 99.8 | 2634.7 | 63.1 | 1.82 | 393 | 222 | 298 |
| | 5 | 7 | 0.528453 | 0.011745 | 13.236433 | 1.354202 | 0.182595 | 0.007114 | 1.890339 | 0.042329 | 2733.9 | 49.6 | 2695.2 | 96 | 2673.7 | 63.8 | 1.86 | 294 | 164 | 252 |
| | 6 | 7 | 0.522934 | 0.010955 | 12.909287 | 1.311686 | 0.180029 | 0.007013 | 1.909234 | 0.040263 | 2710.9 | 46.4 | 2672.2 | 96.4 | 2650.2 | 64.4 | 1.63 | 348 | 219 | 307 |
| | 7 | 7 | 0.517039 | 0.011241 | 12.663045 | 1.291256 | 0.178495 | 0.006814 | 1.931729 | 0.042085 | 2685.7 | 47.8 | 2653.7 | 96.1 | 2636.7 | 62.8 | 1.8 | 379 | 218 | 309 |
| | 8 | 7 | 0.454681 | 0.011675 | 11.557204 | 1.184553 | 0.185382 | 0.007276 | 2.201117 | 0.057047 | 2414.7 | 51.8 | 2567.6 | 95.7 | 2698.5 | 64.9 | 2.07 | 346 | 173 | 266 |
| | 9 | 7 | 0.51088 | 0.012005 | 12.495895 | 1.271238 | 0.179043 | 0.006822 | 1.95701 | 0.047637 | 2659.2 | 51.5 | 2641.4 | 97.2 | 2641.8 | 63.7 | 1.7 | 389 | 235 | 330 |
| | 10 | 7 | 0.53528 | 0.011306 | 13.105567 | 1.331845 | 0.178384 | 0.006858 | 1.865594 | 0.039295 | 2762.9 | 47.4 | 2686.4 | 96.2 | 2635.4 | 64.1 | 1.56 | 333 | 225 | 326 |
| | 11 | 7 | 0.496957 | 0.010153 | 12.219695 | 1.249811 | 0.178624 | 0.0069 | 2.009765 | 0.042009 | 2600.1 | 43.9 | 2619.9 | 96.5 | 2637.5 | 63.7 | 1.82 | 377 | 206 | 280 |
| | 12 | 7 | 0.490004 | 0.012462 | 12.138222 | 1.24571 | 0.180573 | 0.006834 | 2.043143 | 0.050981 | 2569.2 | 53.7 | 2613.4 | 94.8 | 2656.1 | 62.6 | 1.91 | 366 | 193 | 289 |
| | 13 | 7 | 0.524512 | 0.011129 | 13.164512 | 1.341833 | 0.182254 | 0.006995 | 1.90511 | 0.040277 | 2717.5 | 47 | 2690.3 | 96.7 | 2671 | 64.2 | 1.93 | 299 | 155 | 229 |
| | 14 | 7 | 0.476098 | 0.01099 | 12.73268 | 1.347943 | 0.193768 | 0.00831 | 2.100896 | 0.048676 | 2509.2 | 48 | 2655.3 | 97.9 | 2768.5 | 68.9 | 1.67 | 425 | 256 | 458 |
| | 15 | 7 | 0.478357 | 0.01081 | 12.018988 | 1.234051 | 0.182275 | 0.007117 | 2.090746 | 0.047658 | 2519.2 | 47.2 | 2604 | 96.2 | 2670.7 | 64.7 | 2.13 | 313 | 174 | 134 |
| | 16 | 7 | 0.451604 | 0.009294 | 11.824407 | 1.201321 | 0.189938 | 0.00724 | 2.212756 | 0.045193 | 2401.8 | 41.2 | 2589.8 | 95 | 2739.4 | 63.4 | 1.52 | 401 | 268 | 359 |
| | 17 | 7 | 0.485305 | 0.00999 | 12.018519 | 1.220156 | 0.179589 | 0.006827 | 2.059369 | 0.041945 | 2549.7 | 43.2 | 2605.1 | 94.2 | 2646.9 | 62.8 | 1.91 | 491 | 260 | 441 |
| | 18 | 7 | 0.47522 | 0.016846 | 12.820307 | 1.459241 | 0.194575 | 0.009085 | 2.122199 | 0.07645 | 2502.9 | 73.6 | 2654.1 | 104 | 2772 | 74.9 | 1.51 | 539 | 355 | 760 |
| | 19 | 7 | 0.363972 | 0.010405 | 9.282413 | 0.972715 | 0.184658 | 0.007227 | 2.758052 | 0.078586 | 1999.6 | 49.1 | 2362.7 | 94.9 | 2692.1 | 65.2 | 1.62 | 763 | 513 | 619 |
| | 20 | 7 | 0.313975 | 0.006357 | 7.042053 | 0.716075 | 0.162498 | 0.006251 | 3.184167 | 0.064479 | 1759.9 | 31.2 | 2115.9 | 89.6 | 2479.2 | 65.1 | 2.25 | 632 | 286 | 277 |
| | 21 | 7 | 0.524077 | 0.009537 | 12.9605 | 1.313464 | 0.178973 | 0.006749 | 1.908484 | 0.034583 | 2716.1 | 40.3 | 2676.2 | 96 | 2641.4 | 63.2 | 1.63 | 373 | 230 | 314 |
| | 22 | 7 | 0.526344 | 0.012175 | 12.996171 | 1.326168 | 0.179192 | 0.006811 | 1.902451 | 0.043879 | 2725.3 | 51.4 | 2678.6 | 95.5 | 2643.8 | 63.2 | 1.54 | 369 | 241 | 352 |
| | 23 | 7 | 0.562756 | 0.012585 | 13.967394 | 1.438314 | 0.179643 | 0.007156 | 1.781279 | 0.039742 | 2876.9 | 51.8 | 2745.3 | 97 | 2645.9 | 67.1 | 2.41 | 133 | 56 | 82 |
| | 24 | 7 | 0.523185 | 0.010027 | 13.077179 | 1.336531 | 0.180192 | 0.006949 | 1.913789 | 0.036883 | 2712.2 | 42.5 | 2683.8 | 95.8 | 2652 | 64.4 | 1.39 | 335 | 249 | 351 |
| | 25 | 7 | 0.524304 | 0.009585 | 13.053657 | 1.325682 | 0.180201 | 0.006821 | 1.909387 | 0.034899 | 2717.1 | 40.5 | 2682.7 | 95.4 | 2652.7 | 63.3 | 1.73 | 449 | 262 | 370 |
| | 26 | 7 | 0.399067 | 0.010965 | 11.222262 | 1.148129 | 0.204001 | 0.008057 | 2.521294 | 0.075044 | 2163.3 | 51 | 2544.4 | 86 | 2855.2 | 64.8 | 1.1 | 663 | 660 | 826 |
| | 27 | 7 | 0.21083 | 0.005876 | 4.3328 | 0.447768 | 0.148824 | 0.005612 | 4.771551 | 0.129735 | 1232.7 | 31.2 | 1697.7 | 84.7 | 2330.4 | 65.1 | 2.48 | 1658 | 684 | 626 |
| | 28 | 7 | 0.466244 | 0.010029 | 11.433512 | 1.176482 | 0.178179 | 0.007295 | 2.148627 | 0.046666 | 2466.7 | 44.2 | 2558.2 | 96.8 | 2633.5 | 66.6 | 1.68 | 531 | 314 | 371 |
| | 29 | 7 | 0.432397 | 0.011156 | 10.746164 | 1.104516 | 0.179348 | 0.007109 | 2.31891 | 0.059098 | 2316 | 50.1 | 2500.6 | 96.6 | 2644.9 | 66.9 | 1.24 | 420 | 338 | 355 |
| | 30 | 7 | 0.279236 | 0.006519 | 5.941197 | 0.617799 | 0.153913 | 0.005853 | 3.592899 | 0.085542 | 1587.2 | 32.9 | 1965.3 | 91.2 | 2388 | 65.2 | 1.55 | 2016 | 1362 | 892 |
| ZB06 | 1 | 7 | 0.454855 | 0.014486 | 12.345324 | 1.301339 | 0.199548 | 0.008231 | 2.217522 | 0.0702 | 2414.3 | 64 | 2626.7 | 97.8 | 2817.9 | 66.4 | 1.83 | 138 | 75 | 96 |
| | 2 | 7 | 0.553246 | 0.011879 | 15.242222 | 1.551118 | 0.202548 | 0.007695 | 1.812377 | 0.039101 | 2837.7 | 49.3 | 2829.5 | 97.8 | 2844.7 | 62.9 | 1.73 | 236 | 136 | 201 |
| | 3 | 7 | 0.518619 | 0.012482 | 14.535627 | 1.504528 | 0.206848 | 0.008992 | 1.931905 | 0.046205 | 2692.7 | 52.9 | 2784.1 | 98.4 | 2877.5 | 71.9 | 1.51 | 149 | 99 | 152 |
| | 4 | 7 | 0.338125 | 0.007212 | 8.624834 | 0.877377 | 0.186738 | 0.007035 | 2.964448 | 0.065914 | 1877.2 | 34.9 | 2298.3 | 92.4 | 2711.8 | 61.3 | 1.53 | 692 | 458 | 459 |
| | 5 | 7 | 0.544908 | 0.010346 | 14.738072 | 1.49807 | 0.198923 | 0.007681 | 1.837144 | 0.034579 | 2803.5 | 43.1 | 2797.6 | 97.2 | 2814.8 | 63.4 | 1.71 | 239 | 143 | 202 |
| | 6 | 7 | 0.565389 | 0.011345 | 15.272772 | 1.560097 | 0.198694 | 0.00781 | 1.771081 | 0.03569 | 2888.2 | 46.7 | 2831 | 96.5 | 2812.4 | 65 | 1.49 | 165 | 112 | 159 |
| | 7 | 7 | 0.369849 | 0.00852 | 9.357463 | 0.95707 | 0.185484 | 0.007134 | 2.710365 | 0.061164 | 2028 | 39.9 | 2372.3 | 92.7 | 2700 | 63.4 | 1.24 | 399 | 325 | 329 |
| | 8 | 7 | 0.18376 | 0.00643 | 4.96211 | 0.520992 | 0.197757 | 0.007973 | 5.454012 | 0.17473 | 1087.2 | 34.7 | 1811.9 | 87.7 | 2806 | 66.2 | 1.47 | 1304 | 898 | 802 |
| | 9 | 7 | 0.156438 | 0.005065 | 2.991897 | 0.324883 | 0.140229 | 0.005623 | 6.438932 | 0.201572 | 936.5 | 28.1 | 1400.8 | 80.4 | 2226 | 68.8 | 3.03 | 2908 | 970 | 641 |
| | 10 | 7 | 0.477349 | 0.011982 | 13.096168 | 1.352011 | 0.201151 | 0.007869 | 2.097998 | 0.053421 | 2514.9 | 52.4 | 2685.1 | 97 | 2842.1 | 76.8 | 1.89 | 266 | 142 | 208 |
| | 11 | 7 | 0.546271 | 0.010264 | 14.717408 | 1.492831 | 0.197731 | 0.007418 | 1.828349 | 0.03471 | 2809.2 | 42.9 | 2796.4 | 96.4 | 2805.8 | 61.3 | 1.54 | 280 | 181 | 247 |
| | 12 | 7 | 0.514338 | 0.010438 | 14.069047 | 1.426051 | 0.201292 | 0.007645 | 1.942571 | 0.03923 | 2674.5 | 44.4 | 2753.7 | 95.5 | 2834.6 | 62.5 | 1.79 | 379 | 210 | 280 |
| | 13 | 7 | 0.532559 | 0.011818 | 14.616286 | 1.493503 | 0.201221 | 0.007886 | 1.877343 | 0.041875 | 2751.2 | 49.7 | 2789.2 | 97.3 | 2833.1 | 63.8 | 1.6 | 180 | 112 | 143 |
| | 14 | 7 | 0.54757 | 0.011615 | 14.808753 | 1.506989 | 0.197519 | 0.007508 | 1.824714 | 0.039297 | 2814.2 | 48.5 | 2802 | 98.2 | 2808.5 | 69 | 1.31 | 326 | 249 | 339 |
| | 15 | 7 | 0.391161 | 0.009704 | 10.84909 | 1.11456 | 0.202216 | 0.007996 | 2.547899 | 0.071198 | 2136.1 | 50.2 | 2512.9 | 86.4 | 2840.9 | 64.1 | 1.87 | 249 | 132 | 179 |
| | 16 | 7 | 0.474796 | 0.01489 | 12.183225 | 1.29862 | 0.187341 | 0.007299 | 2.116117 | 0.069381 | 2502 | 65.5 | 2612.9 | 101.8 | 2716.1 | 64 | 45.78 | 659 | 14 | 28 |
| | 17 | 7 | 0.44416 | 0.020205 | 12.401839 | 1.349038 | 0.204298 | 0.007616 | 2.289241 | 0.109694 | 2363.4 | 90.7 | 2627.4 | 103.9 | 2859.2 | 61 | 1.48 | 1221 | 838 | 642 |
| | 18 | 7 | 0.563358 | 0.010603 | 15.368723 | 1.559938 | 0.199547 | 0.007489 | 1.765902 | 0.036897 | 2880 | 43.7 | 2837.6 | 97.5 | 2820.7 | 61.6 | 1.96 | 348 | 177 | 269 |
| | 19 | 7 | 0.544005 | 0.01388 | 15.118974 | 1.549534 | 0.203851 | 0.008479 | 1.834415 | 0.046724 | 2799.5 | 57.9 | 2822 | 95.8 | 2854.8 | 67.4 | 1.22 | 214 | 175 | 256 |
| | 20 | 7 | 0.543281 | 0.009995 | 14.819314 | 1.506047 | 0.199009 | 0.007476 | 1.834966 | 0.033874 | 2796.8 | 41.8 | 2802.8 | 95.6 | 2816.3 | 61.6 | 1.65 | 238 | 144 | 198 |
| | 21 | 7 | 0.515714 | 0.013756 | 14.131239 | 1.472221 | 0.199489 | 0.007877 | 1.939742 | 0.054171 | 2679.1 | 58.9 | 2755.2 | 99.8 | 2818.7 | 65.1 | 1.75 | 215 | 125 | 180 |
| | 22 | 7 | 0.452568 | 0.010261 | 19.299352 | 1.967688 | 0.310481 | 0.01236 | 2.200817 | 0.050495 | 2406.4 | 45.6 | 3056.5 | 97.8 | 3521.9 | 61.3 | 1.45 | 361 | 253 | 783 |
| | 23 | 7 | 0.468736 | 0.009298 | 12.841137 | 1.307024 | 0.199566 | 0.007889 | 2.126337 | 0.042353 | 2477.5 | 40.8 | 2667 | 96.3 | 2819.4 | 64.7 | 1.33 | 182 | 140 | 162 |

Continued on next page

| Sample | Spot name | Run | 206/238 | ±2SE | 207/235 | ±2SE | 207/206 | ±2SE | 238/P206 | ±2SE | 206/238 Age | ±2SE | 207/235 Age | ±2SE | 207/206 Age | ±2SE | U/Th | U | Th | Pb |
|---|---|---|---|---|---|---|---|---|---|---|---|---|---|---|---|---|---|---|---|---|
| | 24 | 7 | 0.522576 | 0.01306 | 14.542623 | 1.507317 | 0.203107 | 0.008198 | 1.90877 | 0.047612 | 2709.2 | 55.3 | 2784.1 | 98.5 | 2848.7 | 66.1 | 1.24 | 160 | 131 | 177 |
| | 25 | 7 | 0.421037 | 0.014193 | 11.021376 | 1.204822 | 0.189533 | 0.008437 | 2.36986 | 0.080604 | 2264.4 | 64.4 | 2522.6 | 101.7 | 2735.4 | 75.2 | 1.78 | 290 | 166 | 215 |
| | 26 | 7 | 0.543365 | 0.012738 | 14.777435 | 1.516428 | 0.198613 | 0.007862 | 1.834258 | 0.042432 | 2796.9 | 53.1 | 2800.1 | 99.7 | 2812.8 | 64.8 | 1.5 | 324 | 217 | 307 |
| | 27 | 7 | 0.453242 | 0.015646 | 11.95067 | 1.289493 | 0.191418 | 0.007433 | 2.218625 | 0.080682 | 2406.5 | 69.9 | 2593.3 | 105.1 | 2751.6 | 63.3 | 1.5 | 416 | 299 | 322 |
| | 28 | 7 | 0.511464 | 0.012736 | 14.042957 | 1.443577 | 0.199799 | 0.007498 | 1.953343 | 0.049039 | 2661.4 | 54.3 | 2750.6 | 97.9 | 2822.8 | 61.4 | 2.19 | 316 | 149 | 195 |
| | 29 | 7 | 0.488717 | 0.010586 | 13.277849 | 1.359439 | 0.197785 | 0.007805 | 2.033868 | 0.040565 | 2564.3 | 46 | 2698 | 96.4 | 2804.8 | 64.7 | 1.76 | 199 | 112 | 145 |
| | 30 | 7 | 0.521429 | 0.011235 | 14.185768 | 1.449104 | 0.198044 | 0.00774 | 1.912987 | 0.041207 | 2704.4 | 47.6 | 2760.8 | 98.4 | 2807.2 | 64.1 | 1.38 | 185 | 134 | 182 |
| ZB07 | 1 | 7 | 0.483216 | 0.012014 | 11.964418 | 1.220127 | 0.18019 | 0.006855 | 2.068844 | 0.051403 | 2539.9 | 52.2 | 2600.4 | 96.4 | 2652.4 | 62.7 | 2.21 | 291 | 132 | 171 |
| | 2 | 7 | 0.476347 | 0.010726 | 12.170814 | 1.246962 | 0.185876 | 0.007508 | 2.096648 | 0.047925 | 2510.4 | 46.9 | 2616 | 95.5 | 2702 | 65.8 | 2.87 | 171 | 59 | 73 |
| | 3 | 7 | 0.369863 | 0.009595 | 9.287256 | 0.964072 | 0.182367 | 0.007003 | 2.7056 | 0.07233 | 2027.7 | 45.3 | 2363.9 | 96.3 | 2672.1 | 62.4 | 4.65 | 472 | 101 | 113 |
| | 4 | 7 | 0.529817 | 0.012023 | 13.192588 | 1.368471 | 0.180929 | 0.007538 | 1.885654 | 0.042752 | 2739.6 | 50.6 | 2690.6 | 98.2 | 2656.2 | 70.8 | 3.55 | 107 | 30 | 42 |
| | 5 | 7 | 0.476873 | 0.013842 | 11.980188 | 1.235532 | 0.182851 | 0.00784 | 2.101804 | 0.063689 | 2511.7 | 60.8 | 2600.8 | 97.1 | 2673.3 | 70.6 | 3.44 | 122 | 37 | 35 |
| | 6 | 7 | 0.47888 | 0.012239 | 12.791832 | 1.308075 | 0.193522 | 0.007286 | 2.089716 | 0.052455 | 2521 | 53.2 | 2663 | 96.7 | 2770.5 | 61.5 | 3.33 | 420 | 140 | 221 |
| | 7 | 7 | 0.433754 | 0.011685 | 12.440188 | 1.295455 | 0.20881 | 0.008477 | 2.287815 | 0.051323 | 2321.8 | 52.9 | 2636.4 | 98.4 | 2893.7 | 65.6 | 1.31 | 299 | 224 | 304 |
| | 8 | 7 | 0.362218 | 0.018741 | 9.933954 | 1.094171 | 0.199799 | 0.007998 | 2.820804 | 0.141114 | 1986.9 | 88 | 2420.3 | 98.5 | 2820.9 | 65.8 | 5.55 | 595 | 102 | 320 |
| | 9 | 7 | 0.42877 | 0.009808 | 11.14647 | 1.145414 | 0.188698 | 0.007493 | 2.331753 | 0.052986 | 2299.3 | 44.2 | 2533.6 | 95.2 | 2727.4 | 64.8 | 0.01 | 226 | 32104 | 33991 |
| | 10 | 7 | 0.861815 | 0.03169 | 47.914615 | 5.039751 | 0.405596 | 0.016341 | 1.159865 | 0.044113 | 4005.1 | 110.5 | 3948.9 | 105.8 | 3928.7 | 60.4 | 0.01 | 406 | 33120 | 36706 |
| | 11 | 7 | 0.455661 | 0.01439 | 12.343845 | 1.286451 | 0.196053 | 0.008377 | 2.198212 | 0.068029 | 2419 | 63.5 | 2629 | 99.3 | 2789.9 | 70.4 | 0.01 | 235 | 33985 | 38866 |
| | 12 | 7 | 0.488265 | 0.014353 | 15.376579 | 1.58831 | 0.227277 | 0.009425 | 2.045726 | 0.059765 | 2562.6 | 62.1 | 2838.2 | 98.7 | 3031.2 | 66 | 0.01 | 162 | 29238 | 31916 |
| | 13 | 7 | 0.44028 | 0.008445 | 13.396495 | 1.380779 | 0.220182 | 0.008922 | 2.267027 | 0.043512 | 2351.6 | 37.8 | 2706.2 | 98.2 | 2978.6 | 66.3 | 0.01 | 231 | 42230 | 44175 |
| | 14 | 7 | 0.449607 | 0.010303 | 11.798714 | 1.212205 | 0.190305 | 0.00756 | 2.223932 | 0.050461 | 2392.6 | 45.7 | 2586.6 | 96.8 | 2741.3 | 66.2 | 0 | 182 | 48265 | 50949 |
| | 15 | 7 | 0.446431 | 0.009433 | 11.222275 | 1.155961 | 0.182902 | 0.007582 | 2.235248 | 0.047777 | 2379.1 | 42.1 | 2540.8 | 96.3 | 2676.7 | 68.9 | 0.01 | 358 | 56553 | 58261 |
| | 16 | 7 | 0.467805 | 0.008429 | 14.026964 | 1.442937 | 0.217275 | 0.008766 | 2.132485 | 0.038009 | 2473.7 | 36.9 | 2749.5 | 96.9 | 2956.8 | 64.9 | 0.01 | 655 | 54451 | 60048 |
| | 17 | 7 | 0.457311 | 0.010654 | 11.933722 | 1.235666 | 0.188985 | 0.007148 | 2.186213 | 0.051308 | 2426.7 | 47.2 | 2596.6 | 97 | 2731.3 | 62.6 | 0.01 | 900 | 75992 | 84564 |
| | 18 | 7 | 0.414961 | 0.010985 | 10.728936 | 1.093712 | 0.187913 | 0.007526 | 2.413019 | 0.064659 | 2236.2 | 50 | 2498.8 | 93.4 | 2720.3 | 65.7 | 0.01 | 304 | 44396 | 46809 |
| | 19 | 7 | 0.437911 | 0.016687 | 13.689998 | 1.526451 | 0.226509 | 0.009454 | 2.295691 | 0.089388 | 2338.7 | 75 | 2721 | 107.4 | 3023.9 | 67.5 | 0.01 | 258 | 46075 | 48437 |
| | 20 | 7 | 0.484621 | 0.016299 | 17.568653 | 1.852639 | 0.26347 | 0.011358 | 2.075272 | 0.072032 | 2544.2 | 71 | 2961.8 | 100.3 | 3261.8 | 66.8 | 0.01 | 276 | 38433 | 41236 |

# C.2 Apatite U-Pb data

| Sample | Spot name | 238/206 | ±2σ | 207/206 | ±2σ | Err. Corr | 207/235 | ±2σ | 206/238 | ±2σ | Err. Corr | 207/235 Age | ±2σ | 206/238 Age | ±2σ | 207/206 Age | ±2σ | 206/238* Age | ±2σ |
|---|---|---|---|---|---|---|---|---|---|---|---|---|---|---|---|---|---|---|---|
| GW06 | 1 | 1.752 | 0.115 | 0.248 | 0.004 | 0.471 | 19.01 | 1.233 | 0.556 | 0.036 | 0.376 | 3068.4 | 57.49 | 2910.82 | 153.35 | 3173.25 | 26.1 | 2762.38 | 137.87 |
| | 2 | 1.759 | 0.109 | 0.247 | 0.003 | 0.508 | 18.755 | 1.198 | 0.553 | 0.035 | 0.198 | 3058.1 | 54.8 | 2901.74 | 145.43 | 3162.48 | 20.58 | 2756.27 | 131 |
| | 3 | 1.827 | 0.117 | 0.233 | 0.004 | 0.554 | 17.123 | 1.123 | 0.534 | 0.036 | 0.71 | 2966.61 | 54.64 | 2813.71 | 145.87 | 3071.98 | 24.76 | 2686.76 | 132.82 |
| | 4 | 1.779 | 0.119 | 0.239 | 0.005 | -0.017 | 18.023 | 1.232 | 0.548 | 0.036 | 0.704 | 3015.64 | 67.42 | 2875.54 | 155.42 | 3110.41 | 30.43 | 2750.44 | 141.99 |
| | 5 | 1.851 | 0.117 | 0.219 | 0.003 | 0.391 | 15.944 | 1.026 | 0.526 | 0.033 | 0.483 | 2895.2 | 56.67 | 2783.95 | 142.74 | 2973.51 | 21.25 | 2696.66 | 133.81 |
| | 6 | 1.595 | 0.101 | 0.336 | 0.004 | 0.202 | 28.463 | 1.855 | 0.611 | 0.039 | 0.53 | 3454.76 | 60.83 | 3137.26 | 157.13 | 3644.4 | 17.3 | 2704.53 | 116.19 |
| | 8 | 1.687 | 0.111 | 0.286 | 0.004 | 0.188 | 22.83 | 1.506 | 0.579 | 0.038 | 0.684 | 3243.21 | 62.78 | 3000.08 | 157.38 | 3397.2 | 22.62 | 2732.81 | 130.19 |
| | 9 | 1.819 | 0.12 | 0.213 | 0.004 | 0.584 | 15.728 | 1.022 | 0.536 | 0.034 | 0.07 | 2884.59 | 53.95 | 2824.63 | 150.47 | 2926.72 | 32.68 | 2776.26 | 145.28 |
| | 10 | 1.817 | 0.116 | 0.217 | 0.003 | 0.281 | 16.075 | 1.042 | 0.538 | 0.035 | 0.68 | 2904.02 | 58.9 | 2826.3 | 146.03 | 2958.36 | 19.47 | 2762.95 | 139.46 |
| | 11 | 1.768 | 0.115 | 0.253 | 0.002 | 0.443 | 19.28 | 1.236 | 0.553 | 0.035 | 0.727 | 3078.95 | 59.19 | 2890.22 | 150.95 | 3204.49 | 14.79 | 2714.71 | 132.91 |
| | 12 | 1.785 | 0.112 | 0.25 | 0.004 | 0.153 | 18.785 | 1.227 | 0.547 | 0.035 | 0.493 | 3056.92 | 60 | 2867.91 | 144.92 | 3183.61 | 24.52 | 2697.04 | 127.92 |
| | 13 | 1.687 | 0.12 | 0.287 | 0.007 | -0.114 | 22.939 | 1.593 | 0.577 | 0.037 | 0.513 | 3246.64 | 76.44 | 3000.41 | 171.17 | 3402.46 | 39.82 | 2729.26 | 141.19 |
| | 14 | 1.784 | 0.123 | 0.256 | 0.004 | 0.645 | 19.309 | 1.27 | 0.548 | 0.037 | 0.727 | 3079.37 | 57.63 | 2868.32 | 160.2 | 3220.07 | 26.97 | 2675.49 | 139.08 |
| | 15 | 1.665 | 0.116 | 0.28 | 0.007 | 0.145 | 22.633 | 1.639 | 0.587 | 0.04 | 0.688 | 3233.01 | 68.94 | 3031.69 | 168.32 | 3360.39 | 41.66 | 2804.65 | 143.67 |
| | 16 | 1.769 | 0.117 | 0.248 | 0.004 | 0.131 | 18.933 | 1.269 | 0.553 | 0.036 | 0.694 | 3059.68 | 63.87 | 2888.34 | 154.17 | 3174.2 | 26.4 | 2730.62 | 137.55 |
| | 17 | 1.758 | 0.111 | 0.254 | 0.003 | 0.447 | 19.467 | 1.248 | 0.556 | 0.036 | 0.548 | 3087.42 | 56.84 | 2903.21 | 147.45 | 3209.53 | 18.47 | 2729.36 | 130.07 |
| | 18 | 1.753 | 0.112 | 0.256 | 0.004 | 0.428 | 19.688 | 1.289 | 0.558 | 0.036 | 0.529 | 3098.12 | 56.93 | 2909.66 | 150.15 | 3222.66 | 27.11 | 2729.97 | 131.91 |
| | 19 | 1.617 | 0.105 | 0.322 | 0.006 | 0.231 | 26.872 | 1.777 | 0.605 | 0.039 | 0.522 | 3400.37 | 61.98 | 3103.38 | 159.97 | 3580.34 | 27.94 | 2719.95 | 122.33 |
| | 20 | 1.603 | 0.106 | 0.321 | 0.006 | 0.456 | 26.949 | 1.758 | 0.61 | 0.039 | 0.392 | 3404.15 | 59.09 | 3124.74 | 164.14 | 3572.98 | 27.27 | 2755.78 | 127.11 |
| | 21 | 1.76 | 0.116 | 0.262 | 0.003 | 0.331 | 20.03 | 1.309 | 0.556 | 0.036 | 0.773 | 3114.61 | 60.97 | 2899.83 | 153.91 | 3256.14 | 18.71 | 2695.22 | 132.65 |
| | 22 | 1.815 | 0.117 | 0.23 | 0.004 | 0 | 17.039 | 1.128 | 0.539 | 0.034 | 0.569 | 2959.21 | 64.12 | 2829.79 | 147.81 | 3048.4 | 27.41 | 2721.32 | 136.53 |
| | 23 | 1.81 | 0.113 | 0.234 | 0.003 | 0.458 | 17.416 | 1.119 | 0.54 | 0.034 | 0.314 | 2981.19 | 55.27 | 2834.91 | 143.66 | 3081.41 | 22.96 | 2710.55 | 131.15 |
| | 24 | 1.775 | 0.113 | 0.243 | 0.004 | 0.515 | 18.42 | 1.187 | 0.55 | 0.035 | 0.241 | 3035.43 | 55.16 | 2880.41 | 148.08 | 3139.73 | 25.29 | 2740.2 | 133.8 |
| | 25 | 1.84 | 0.116 | 0.224 | 0.004 | 0.368 | 16.388 | 1.064 | 0.531 | 0.034 | 0.382 | 2922.94 | 56.76 | 2797.46 | 143.5 | 3010.52 | 25.86 | 2696.67 | 133.2 |
| | 26 | 1.797 | 0.117 | 0.231 | 0.004 | 0.493 | 17.268 | 1.123 | 0.543 | 0.035 | 0.479 | 2973.55 | 56.42 | 2851.72 | 150.16 | 3057.02 | 27.03 | 2747.08 | 139.18 |
| | 27 | 1.819 | 0.116 | 0.228 | 0.003 | 0.571 | 16.95 | 1.085 | 0.537 | 0.034 | 0.522 | 2952.29 | 55.34 | 2824.29 | 146.34 | 3040.71 | 20.47 | 2717.84 | 135.35 |
| | 28 | 1.71 | 0.114 | 0.284 | 0.01 | -0.695 | 22.45 | 1.948 | 0.572 | 0.039 | 0.906 | 3222.99 | 92.57 | 2968.1 | 158.61 | 3385.68 | 55.88 | 2698.1 | 130.66 |
| | 29 | 1.891 | 0.121 | 0.201 | 0.002 | 0.154 | 14.323 | 0.924 | 0.516 | 0.033 | 0.797 | 2795.06 | 60.04 | 2736.75 | 142.53 | 2837.41 | 14.89 | 2694.66 | 138.12 |
| | 30 | 1.874 | 0.118 | 0.207 | 0.003 | -0.327 | 14.881 | 0.989 | 0.521 | 0.033 | 0.839 | 2830.65 | 64.57 | 2756.49 | 140.68 | 2883.9 | 20.05 | 2701.21 | 135.01 |
| | 31 | 1.848 | 0.118 | 0.205 | 0.003 | 0.398 | 14.878 | 0.956 | 0.527 | 0.034 | 0.47 | 2832.42 | 57.19 | 2788.33 | 144.73 | 2863.95 | 20.73 | 2754.61 | 141.2 |
| | 32 | 1.757 | 0.113 | 0.247 | 0.003 | 0.597 | 18.904 | 1.216 | 0.555 | 0.036 | 0.423 | 3062.46 | 56.27 | 2904.94 | 149.88 | 3167.49 | 17.17 | 2757.68 | 134.85 |
| | 34 | 1.77 | 0.112 | 0.251 | 0.003 | 0.045 | 19.023 | 1.235 | 0.55 | 0.035 | 0.694 | 3068.53 | 61.91 | 2886.63 | 147.85 | 3189.87 | 18.54 | 2718.76 | 130.91 |
| | 35 | 1.738 | 0.112 | 0.276 | 0.006 | -0.09 | 21.292 | 1.449 | 0.56 | 0.036 | 0.574 | 3177.39 | 67.66 | 2930.15 | 151.52 | 3337.47 | 33.77 | 2681.63 | 126.56 |
| | 36 | 1.793 | 0.112 | 0.236 | 0.005 | 0.214 | 17.635 | 1.166 | 0.542 | 0.034 | 0.181 | 2996.94 | 59.3 | 2857.1 | 144.6 | 3092.14 | 32.99 | 2735.19 | 132.34 |
| | 38 | 1.783 | 0.116 | 0.238 | 0.004 | -0.309 | 17.887 | 1.225 | 0.546 | 0.035 | 0.757 | 3009.44 | 70.27 | 2870.25 | 150.74 | 3103.78 | 29.57 | 2746.87 | 137.86 |
| | 39 | 1.827 | 0.12 | 0.229 | 0.003 | -0.046 | 16.901 | 1.111 | 0.533 | 0.034 | 0.583 | 2952.08 | 64.87 | 2814.12 | 149.39 | 3047.5 | 22.19 | 2700.31 | 137.38 |
| | 40 | 1.761 | 0.114 | 0.249 | 0.003 | 0.352 | 18.989 | 1.228 | 0.552 | 0.035 | 0.433 | 3065.43 | 59.22 | 2899.4 | 150.8 | 3176.12 | 19.74 | 2744.73 | 134.91 |
| | 41 | 1.281 | 0.083 | 0.49 | 0.015 | 0.076 | 51.217 | 3.66 | 0.758 | 0.049 | 0.399 | 4045.05 | 69.22 | 3719.03 | 182.33 | 4210.98 | 45.98 | 2654.28 | 91.62 |
| | 42 | 1.163 | 0.089 | 0.543 | 0.014 | 0.572 | 62.161 | 4.114 | 0.833 | 0.056 | 0.458 | 4243.68 | 65.43 | 4000.37 | 228.84 | 4361.08 | 38.31 | 2662.56 | 99.59 |
| | 43 | 1.167 | 0.076 | 0.532 | 0.014 | 0.7 | 60.94 | 4.01 | 0.835 | 0.056 | 0.289 | 4219.01 | 50.29 | 3988.82 | 193.31 | 4330.6 | 38.3 | 2730.12 | 89.04 |
| | 44 | 1.312 | 0.087 | 0.466 | 0.01 | 0.046 | 47.616 | 3.304 | 0.741 | 0.049 | 0.679 | 3971.37 | 68.31 | 3652.05 | 184.19 | 4136.81 | 32.51 | 2714.23 | 100.53 |
| | 45 | 1.745 | 0.116 | 0.239 | 0.006 | 0.556 | 18.27 | 1.21 | 0.556 | 0.036 | 0.271 | 3033.85 | 54.41 | 2919.93 | 155.42 | 3110.21 | 38.64 | 2813.32 | 144.1 |
| | 46 | 1.812 | 0.114 | 0.231 | 0.003 | 0.024 | 17.036 | 1.1 | 0.535 | 0.034 | 0.743 | 2967.1 | 61.35 | 2833.3 | 144.69 | 3059.1 | 18.2 | 2720.44 | 133.23 |
| | 47 | 1.757 | 0.117 | 0.242 | 0.005 | 0.511 | 18.437 | 1.204 | 0.552 | 0.036 | 0.349 | 3042.92 | 56.89 | 2904.47 | 155.42 | 3135.67 | 30.74 | 2776.2 | 141.79 |
| | 48 | 1.762 | 0.117 | 0.249 | 0.004 | 0.414 | 18.89 | 1.236 | 0.55 | 0.036 | 0.457 | 3066.64 | 58.85 | 2897.16 | 154.3 | 3179.61 | 28.33 | 2739.5 | 137.72 |
| | 50 | 1.754 | 0.109 | 0.267 | 0.004 | 0.251 | 20.379 | 1.354 | 0.551 | 0.035 | 0.343 | 3137.27 | 58.22 | 2908.88 | 145.29 | 3286.84 | 25.72 | 2687.4 | 123.7 |
| NG01 | 3 | 1.537 | 0.099 | 0.399 | 0.008 | 0.159 | 34.598 | 2.326 | 0.629 | 0.041 | 0.534 | 3661.32 | 63.45 | 3230.69 | 163.31 | 3906.11 | 30.39 | 2534.03 | 99.67 |
| | 4 | 1.524 | 0.099 | 0.385 | 0.011 | -0.337 | 33.628 | 2.471 | 0.634 | 0.041 | 0.702 | 3632.56 | 78.17 | 3252.63 | 165.6 | 3849.26 | 43.21 | 2631.46 | 107.6 |
| | 6 | 0.56 | 0.04 | 0.834 | 0.018 | 0.294 | 199.567 | 14.448 | 1.739 | 0.126 | 0.819 | 5410.84 | 68.59 | 6602.39 | 293.35 | 4980.66 | 31.31 | 292.59 | 0.53 |

Continued on next page

| Sample | Spot name | 238/206 | ±2σ | 207/206 | ±2σ | Err. Corr | 207/235 | ±2σ | 206/238 | ±2σ | Err. Corr | 207/235 Age | ±2σ | 206/238 Age | ±2σ | 207/206 Age | ±2σ | 206/238* Age | ±2σ |
|---|---|---|---|---|---|---|---|---|---|---|---|---|---|---|---|---|---|---|---|
| | 7 | 0.377 | 0.025 | 0.896 | 0.013 | 0.252 | 317.482 | 21.929 | 2.574 | 0.177 | 0.881 | 5883.63 | 65.59 | 8351.04 | 313.2 | 5081.6 | 20.04 | 2479.99 | 24.36 |
| | 8 | 0.519 | 0.034 | 0.84 | 0.015 | 0.063 | 216.44 | 15.478 | 1.87 | 0.131 | 0.842 | 5494.77 | 68.19 | 6921.19 | 280.73 | 4990.48 | 25.51 | 3653.1 | 73.03 |
| | 9 | 0.195 | 0.017 | 0.973 | 0.019 | 0.375 | 686.169 | 61.397 | 5.14 | 0.479 | 0.959 | 6635.99 | 83.56 | 11691.42 | 473.54 | 5197.99 | 27.78 | 2492.97 | 16.69 |
| | 10 | 0.209 | 0.018 | 0.98 | 0.028 | 0.083 | 645.848 | 61.53 | 4.789 | 0.441 | 0.906 | 6573.19 | 90.01 | 11321.22 | 461.4 | 5207.93 | 39.98 | 2688.47 | 20.54 |
| | 11 | 0.207 | 0.02 | 0.974 | 0.031 | 0.486 | 652.109 | 62.678 | 4.802 | 0.478 | 0.928 | 6573.86 | 87.84 | 11356.1 | 521.07 | 5199.67 | 45.34 | 2591.26 | 21.37 |
| | 15 | 1.446 | 0.094 | 0.425 | 0.009 | 0.363 | 39.053 | 2.575 | 0.667 | 0.043 | 0.291 | 3783.37 | 59.82 | 3387.99 | 170.46 | 3999.93 | 30.24 | 2601.79 | 99.59 |
| | 16 | 1.377 | 0.093 | 0.491 | 0.009 | 0.021 | 47.546 | 3.313 | 0.702 | 0.047 | 0.768 | 3976.31 | 69.55 | 3520.05 | 183.42 | 4215.16 | 28.23 | 2403.98 | 84.43 |
| | 17 | 0.902 | 0.069 | 0.675 | 0.019 | -0.61 | 101.63 | 8.977 | 1.085 | 0.082 | 0.937 | 4717.94 | 96.28 | 4810.15 | 258.69 | 4678.54 | 39.87 | 2492.97 | 67.18 |
| | 18 | 1.306 | 0.084 | 0.492 | 0.009 | 0.594 | 50.038 | 3.248 | 0.739 | 0.048 | 0.376 | 4029.47 | 55.04 | 3664.61 | 179.2 | 4216.48 | 26.95 | 2573.85 | 87.21 |
| | 19 | 0.91 | 0.072 | 0.659 | 0.022 | 0.19 | 96.532 | 7.859 | 1.064 | 0.083 | 0.781 | 4683.9 | 80.15 | 4778.68 | 266.39 | 4643.14 | 48.68 | 2650.48 | 79.41 |
| | 20 | 1.074 | 0.09 | 0.621 | 0.021 | 0.728 | 77.481 | 5.553 | 0.897 | 0.068 | 0.756 | 4458.77 | 63.93 | 4243.5 | 260.27 | 4557.64 | 48.18 | 2335.89 | 76.91 |
| | 22 | 0.829 | 0.067 | 0.701 | 0.014 | -0.199 | 113.049 | 8.913 | 1.185 | 0.094 | 0.934 | 4840.21 | 87.54 | 5099.76 | 285.25 | 4732.82 | 28.01 | 2563.02 | 69.31 |
| | 24 | 0.844 | 0.093 | 0.704 | 0.03 | -0.264 | 115.98 | 14.346 | 1.188 | 0.124 | 0.914 | 4826.89 | 129.47 | 5038.83 | 385.53 | 4738.75 | 62.03 | 2426.43 | 85.99 |
| | 25 | 1.316 | 0.095 | 0.487 | 0.02 | -0.492 | 49.595 | 4.578 | 0.737 | 0.055 | 0.855 | 4012.62 | 98.33 | 3644.33 | 200.82 | 4202.25 | 60.1 | 2577.15 | 99.1 |
| | 26 | 1.597 | 0.103 | 0.36 | 0.007 | 0.121 | 29.969 | 2.006 | 0.605 | 0.039 | 0.604 | 3520.08 | 64.07 | 3134.89 | 160.75 | 3747.19 | 27.98 | 2597.12 | 109.65 |
| | 27 | 1.898 | 0.122 | 0.333 | 0.012 | -0.464 | 23.38 | 1.827 | 0.508 | 0.033 | 0.705 | 3276.31 | 86.03 | 2728.37 | 143.52 | 3631.18 | 57.08 | 2223.37 | 94.83 |
| | 29 | 1.405 | 0.092 | 0.446 | 0.008 | 0.346 | 42.17 | 2.764 | 0.687 | 0.044 | 0.427 | 3858.29 | 60.89 | 3464.38 | 174.67 | 4069.75 | 26.36 | 2589.93 | 96.59 |
| | 30 | 1.639 | 0.106 | 0.375 | 0.005 | 0.347 | 30.414 | 1.954 | 0.591 | 0.038 | 0.518 | 3536.1 | 60.26 | 3069.95 | 157.92 | 3811.87 | 21.13 | 2449.41 | 99.85 |
| | 31 | 0.234 | 0.021 | 0.964 | 0.025 | 0.412 | 551.632 | 42.666 | 4.163 | 0.324 | 0.894 | 6439.87 | 82.01 | 10713.29 | 460.02 | 5184.92 | 36.63 | 2619.53 | 22.26 |
| | 32 | 0.24 | 0.02 | 0.795 | 0.022 | -0.029 | 446.93 | 40.564 | 4.078 | 0.352 | 0.902 | 6218.57 | 88.02 | 10578.04 | 422.66 | 4912.38 | 40.3 | 0.00 | 0.00 |
| | 33 | 0.18 | 0.017 | 0.959 | 0.026 | 0.1 | 695.437 | 54.279 | 5.508 | 0.609 | 0.958 | 6704.08 | 95.42 | 12136.17 | 507.53 | 5177.23 | 38.12 | 2200.18 | 12.64 |
| | 34 | 0.07 | 0.012 | 1.054 | 0.026 | 0.203 | 2434.883 | 459.086 | 16.963 | 3.161 | 0.979 | 7750.98 | 174.8 | 17549.66 | 1057.45 | 5310.71 | 35.1 | 2800.89 | 15.27 |
| | 35 | 2.015 | 0.132 | 0.22 | 0.002 | 0.076 | 14.636 | 0.963 | 0.482 | 0.031 | 0.862 | 2819.13 | 62.34 | 2597.57 | 139.97 | 2981.65 | 16.01 | 2450.25 | 124.36 |
| | 36 | 0.09 | 0.013 | 1.007 | 0.043 | -0.157 | 1679.125 | 257.772 | 11.985 | 1.684 | 0.954 | 7455.65 | 160.67 | 16086.7 | 863.5 | 5246.19 | 59.7 | 2379.07 | 11.65 |
| | 37 | 0.091 | 0.012 | 1.032 | 0.035 | 0.205 | 1652.849 | 204.698 | 11.635 | 1.535 | 0.973 | 7473.19 | 128.38 | 16040.17 | 762.86 | 5281.49 | 47.4 | 2667.52 | 13.09 |
| | 38 | 0.167 | 0.029 | 0.967 | 0.052 | -0.282 | 984.315 | 235.074 | 6.777 | 1.292 | 0.977 | 6787.79 | 201.18 | 12539.06 | 974.01 | 5190.23 | 75.87 | 2259.76 | 23.54 |
| | 39 | 0.27 | 0.022 | 0.954 | 0.016 | 0.152 | 481.805 | 37.903 | 3.669 | 0.287 | 0.93 | 6285.85 | 82.22 | 9983.75 | 416.09 | 5170.36 | 24.08 | 2734.69 | 26.05 |
| | 40 | 0.236 | 0.019 | 0.976 | 0.019 | 0.192 | 566.727 | 47.78 | 4.219 | 0.356 | 0.942 | 6444.72 | 78.65 | 10671.13 | 411.67 | 5203.03 | 27.59 | 2845.01 | 23.79 |
| | 41 | 0.109 | 0.01 | 1.036 | 0.023 | -0.127 | 1319.57 | 126.87 | 9.226 | 0.851 | 0.948 | 7286.58 | 94.61 | 14938.84 | 509.35 | 5287.04 | 31.7 | 2815.56 | 11.97 |
| | 42 | 1.704 | 0.11 | 0.324 | 0.006 | -0.123 | 25.267 | 1.7 | 0.572 | 0.038 | 0.741 | 3353.26 | 68.04 | 2977.29 | 153.29 | 3586.34 | 30.43 | 2551.27 | 112.03 |
| | 43 | 0.301 | 0.021 | 0.942 | 0.021 | 0.284 | 419.844 | 33.062 | 3.243 | 0.256 | 0.904 | 6160.49 | 66.91 | 9428.06 | 340.9 | 5152.13 | 31.42 | 2792.79 | 25.5 |
| | 44 | 0.97 | 0.101 | 0.653 | 0.058 | -0.789 | 93.241 | 16.264 | 1.021 | 0.11 | 0.936 | 4611 | 183.8 | 4566.36 | 341.77 | 4630.64 | 128.44 | 2420.99 | 93.24 |
| | 46 | 1.503 | 0.098 | 0.416 | 0.008 | 0.364 | 37.142 | 2.46 | 0.649 | 0.042 | 0.412 | 3723.38 | 60.44 | 3288.32 | 168.58 | 3966.51 | 30.01 | 2525.76 | 98.58 |
| | 47 | 1.372 | 0.088 | 0.472 | 0.007 | 0.154 | 46.234 | 3.094 | 0.711 | 0.047 | 0.733 | 3938.87 | 63.42 | 3529.34 | 174.75 | 4154.45 | 22.93 | 2525.88 | 88.42 |
| | 49 | 0.271 | 0.04 | 0.932 | 0.051 | 0.323 | 473.423 | 58.262 | 3.703 | 0.481 | 0.856 | 6259.33 | 140.65 | 9967.04 | 743.06 | 5138.1 | 76.69 | 2329 | 33.74 |
| | 50 | 0.285 | 0.022 | 0.955 | 0.022 | 0.159 | 457.757 | 38.237 | 3.481 | 0.286 | 0.912 | 6230.64 | 77.17 | 9701.07 | 382.69 | 5172.51 | 32.96 | 2916.36 | 29.23 |
| | 51 | 1.464 | 0.095 | 0.479 | 0.011 | 0.133 | 43.992 | 2.979 | 0.666 | 0.043 | 0.44 | 3889.93 | 65.48 | 3355.68 | 169.94 | 4177.95 | 33.74 | 2286.24 | 77.94 |
| | 52 | 1.219 | 0.085 | 0.619 | 0.022 | 0.426 | 68.261 | 4.963 | 0.802 | 0.057 | 0.451 | 4327.71 | 63.17 | 3862.26 | 201.5 | 4551.82 | 52.3 | 1955.02 | 50.5 |
| | 53 | 0.954 | 0.078 | 0.659 | 0.022 | 0.391 | 93.135 | 7.346 | 1.028 | 0.08 | 0.762 | 4635.91 | 75.49 | 4621.54 | 269.14 | 4642.19 | 48.71 | 2435.45 | 72.48 |
| | 54 | 1.28 | 0.074 | 0.519 | 0.009 | 0.001 | 54.376 | 3.678 | 0.76 | 0.05 | 0.7 | 4103.79 | 59.9 | 3722.48 | 162.5 | 4295.98 | 25.67 | 2475.36 | 70.75 |
| | 55 | 1.862 | 0.119 | 0.273 | 0.004 | 0.371 | 19.735 | 1.269 | 0.524 | 0.033 | 0.315 | 3102.75 | 58.45 | 2770.8 | 144.43 | 3325.22 | 21.36 | 2485.11 | 115.83 |
| | 56 | 1.814 | 0.123 | 0.287 | 0.004 | 0.362 | 21.343 | 1.407 | 0.539 | 0.036 | 0.737 | 3176.31 | 62 | 2830.25 | 154.88 | 3402.84 | 22.15 | 2508.13 | 121.21 |
| | 57 | 1.764 | 0.113 | 0.307 | 0.004 | 0.266 | 23.435 | 1.516 | 0.553 | 0.035 | 0.512 | 3268.82 | 60.31 | 2894.47 | 149.41 | 3507.22 | 20.76 | 2512.21 | 112.09 |
| | 58 | 0.538 | 0.036 | 0.835 | 0.016 | 0.148 | 209.852 | 14.743 | 1.826 | 0.127 | 0.782 | 5452.95 | 68.13 | 6773.13 | 282.9 | 4981.58 | 27.63 | 423.41 | 1.01 |
| | 59 | 0.206 | 0.021 | 1 | 0.043 | 0.085 | 674.37 | 72.811 | 4.891 | 0.477 | 0.889 | 6608.5 | 110.56 | 11396.96 | 555.37 | 5236.95 | 60.62 | 2984.06 | 30.06 |
| | 60 | 0.355 | 0.032 | 0.884 | 0.023 | 0.32 | 339.344 | 28.295 | 2.789 | 0.23 | 0.891 | 5932.18 | 86.9 | 8637.66 | 430.81 | 5063.53 | 36.28 | 1866.37 | 17.48 |
| | 61 | 0.242 | 0.02 | 0.968 | 0.025 | 0.166 | 553.137 | 48.658 | 4.153 | 0.36 | 0.907 | 6412.92 | 85.19 | 10550.46 | 438.03 | 5191.51 | 36.59 | 2754.36 | 24.36 |
| | 62 | 1.456 | 0.098 | 0.435 | 0.007 | 0.422 | 40.17 | 2.619 | 0.671 | 0.044 | 0.588 | 3798.96 | 61.87 | 3369.86 | 176.57 | 4033.73 | 22.64 | 2529.42 | 98.5 |
| | 63 | 0.256 | 0.034 | 0.954 | 0.021 | -0.128 | 553.834 | 69.318 | 4.086 | 0.461 | 0.979 | 6339.33 | 140.16 | 10250.88 | 686.12 | 5170.98 | 31.31 | 2624.87 | 37.1 |
| | 64 | 0.208 | 0.016 | 0.986 | 0.017 | 0.321 | 645.19 | 55.718 | 4.762 | 0.419 | 0.954 | 6584.94 | 72.81 | 11349.67 | 403.1 | 5216.74 | 24.91 | 2775.06 | 19.02 |
| | 65 | 0.138 | 0.013 | 1 | 0.02 | 0.447 | 1000.646 | 85.995 | 7.294 | 0.661 | 0.957 | 7010.96 | 84.77 | 13583.27 | 512.18 | 5237.22 | 27.43 | 2540.3 | 12.7 |
| | 66 | 0.101 | 0.011 | 1.033 | 0.023 | 0.344 | 1462.546 | 162.037 | 10.322 | 1.16 | 0.971 | 7358.9 | 105.25 | 15372.36 | 639.65 | 5282.76 | 31.53 | 2735.14 | 13.06 |
| | 67 | 0.083 | 0.008 | 1.008 | 0.021 | 0.152 | 1674.769 | 167.82 | 12.068 | 1.214 | 0.965 | 7533.43 | 98.57 | 16532.11 | 583.83 | 5248.39 | 28.74 | 2368.06 | 7.2 |
| | 68 | 0.374 | 0.026 | 0.907 | 0.021 | 0.248 | 323.941 | 22.349 | 2.619 | 0.182 | 0.724 | 5903.22 | 68.6 | 8383.23 | 326.85 | 5099.25 | 32.64 | 2813.26 | 32.54 |
| | 69 | 0.203 | 0.018 | 0.981 | 0.02 | 0.423 | 664.711 | 54.641 | 4.936 | 0.414 | 0.938 | 6603.85 | 81.89 | 11478.2 | 467.48 | 5209.17 | 28.45 | 2659.43 | 19.67 |
| | 71 | 0.582 | 0.045 | 0.808 | 0.019 | -0.195 | 187.173 | 15.78 | 1.684 | 0.133 | 0.94 | 5340.73 | 87.02 | 6448.49 | 318.67 | 4935.32 | 34.17 | 2651.65 | 50.31 |

Continued on next page

| Sample | Spot name | 238/206 | ±2σ | 207/206 | ±2σ | Err. Corr | 207/235 | ±2σ | 206/238 | ±2σ | Err. Corr | 207/235 Age | ±2σ | 206/238 Age | ±2σ | 207/206 Age | ±2σ | 206/238* Age | ±2σ |
|---|---|---|---|---|---|---|---|---|---|---|---|---|---|---|---|---|---|---|---|
| | 72 | 1.08 | 0.1 | 0.587 | 0.016 | -0.147 | 71.751 | 5.121 | 0.892 | 0.061 | 0.861 | 4396.69 | 100.58 | 4226.2 | 287.53 | 4475.79 | 39.44 | 2607.88 | 107.1 |
| | 73 | 1.89 | 0.121 | 0.254 | 0.004 | 0.335 | 18.015 | 1.17 | 0.515 | 0.033 | 0.525 | 3017.13 | 58.71 | 2737.94 | 143.39 | 3208.79 | 23.33 | 2513.01 | 120.51 |
| | 74 | 1.881 | 0.118 | 0.258 | 0.003 | 0.174 | 18.413 | 1.192 | 0.517 | 0.033 | 0.608 | 3038.36 | 59.68 | 2748.18 | 140.59 | 3236.33 | 19.1 | 2510.2 | 117 |
| | 76 | 1.562 | 0.102 | 0.411 | 0.007 | 0.275 | 35.322 | 2.364 | 0.624 | 0.041 | 0.69 | 3674.11 | 61.99 | 3189.24 | 164.13 | 3950.16 | 25.49 | 2429.28 | 94.42 |
| | 77 | 1.418 | 0.094 | 0.446 | 0.008 | 0.355 | 42.188 | 2.795 | 0.687 | 0.045 | 0.601 | 3850.7 | 61.57 | 3440.28 | 176.27 | 4071.79 | 27.13 | 2556.79 | 96.33 |

# C.3 Titanite U-Pb data

| Sample | Spot name | 238/206 | ±2σ | 207/206 | ±2σ | Err. Corr | 207/235 | ±2σ | 206/238 | ±2σ | Err. Corr | 207/235 Age | ±2σ | 206/238 Age | ±2σ | 207/206 Age | ±2σ | 207/206* Age | ±2σ |
|---|---|---|---|---|---|---|---|---|---|---|---|---|---|---|---|---|---|---|---|
| ZL181 | g1.001 | 1.905 | 0.088 | 0.224 | 0.01 | 0.371 | 0.526 | 0.026 | 16.231 | 0.848 | 0.536 | 2888.79 | 52 | 2723.65 | 107.57 | 3006.3 | 69.24 | 2594.01 | 95.95 |
| | g1.002 | 1.786 | 0.062 | 0.225 | 0.004 | 0.217 | 0.562 | 0.02 | 17.401 | 0.64 | 0.75 | 2954.81 | 35.09 | 2872.55 | 81.1 | 3012.35 | 27.79 | 2789.66 | 33.47 |
| | g1.003 | 1.847 | 0.064 | 0.21 | 0.004 | 0.375 | 0.543 | 0.018 | 15.744 | 0.55 | 0.578 | 2859.43 | 34.01 | 2795.74 | 76.76 | 2905.25 | 33.75 | 2737.14 | 34.73 |
| | g1.004 | 1.853 | 0.06 | 0.21 | 0.004 | 0.292 | 0.541 | 0.018 | 15.647 | 0.561 | 0.583 | 2853.28 | 34.26 | 2787.15 | 74.65 | 2900.73 | 33.98 | 2726.93 | 34.98 |
| | g1.005 | 1.844 | 0.064 | 0.213 | 0.004 | 0.415 | 0.544 | 0.019 | 15.976 | 0.558 | 0.609 | 2873.43 | 33.55 | 2798.85 | 77.71 | 2926.92 | 32.77 | 2731.38 | 34.87 |
| | g1.006 | 1.776 | 0.057 | 0.248 | 0.005 | 0.053 | 0.565 | 0.019 | 19.429 | 0.787 | 0.781 | 3059.77 | 38.81 | 2884.48 | 77.47 | 3165.92 | 30.83 | 2719.89 | 43.94 |
| | g1.007 | 1.858 | 0.06 | 0.221 | 0.004 | 0.108 | 0.54 | 0.017 | 16.37 | 0.603 | 0.625 | 2896.12 | 36.43 | 2780.42 | 72.82 | 2988.84 | 26.55 | 2679.03 | 36.17 |
| | g1.008 | 1.839 | 0.065 | 0.234 | 0.005 | 0.337 | 0.546 | 0.019 | 17.6 | 0.652 | 0.695 | 2965.58 | 35.14 | 2807.96 | 81.01 | 3075.53 | 32.04 | 2663.53 | 45.71 |
| | g1.009 | 1.816 | 0.062 | 0.235 | 0.005 | 0.186 | 0.553 | 0.019 | 17.919 | 0.677 | 0.601 | 2982.66 | 36.62 | 2834.56 | 77.67 | 3084.66 | 35.33 | 2698.67 | 44.6 |
| | g1.010 | 1.734 | 0.064 | 0.257 | 0.007 | 0.36 | 0.58 | 0.021 | 20.491 | 0.834 | 0.52 | 3111.27 | 39.17 | 2944.88 | 87.11 | 3221.59 | 44.87 | 2762.19 | 59.72 |
| | g1.011 | 1.885 | 0.065 | 0.224 | 0.005 | 0.248 | 0.532 | 0.018 | 16.414 | 0.616 | 0.578 | 2899.32 | 36.16 | 2748.04 | 75.59 | 3006.31 | 36.71 | 2624.97 | 46.95 |
| | g1.012 | 1.8 | 0.064 | 0.243 | 0.005 | 0.32 | 0.558 | 0.02 | 18.715 | 0.695 | 0.72 | 3024.7 | 35.57 | 2857.5 | 83.01 | 3139.06 | 30.7 | 2696.49 | 44.67 |
| | g1.013 | 1.759 | 0.065 | 0.254 | 0.006 | 0.25 | 0.571 | 0.02 | 20.012 | 0.785 | 0.607 | 3088.66 | 38.99 | 2910.28 | 83.38 | 3218.85 | 32.69 | 2727.5 | 52.45 |
| | g1.014 | 1.55 | 0.067 | 0.335 | 0.011 | 0.329 | 0.65 | 0.028 | 29.986 | 1.428 | 0.559 | 3481.31 | 46.68 | 3225.61 | 108.73 | 3633.93 | 53.75 | 2808.05 | 90.88 |
| | g1.015 | 1.615 | 0.058 | 0.339 | 0.009 | 0.221 | 0.622 | 0.023 | 28.747 | 1.088 | 0.593 | 3442.08 | 37.21 | 3116.33 | 89.89 | 3652.13 | 40.85 | 2651.46 | 82.97 |
| | g1.016 | 1.742 | 0.082 | 0.296 | 0.012 | 0.276 | 0.579 | 0.026 | 23.56 | 1.289 | 0.551 | 3243.98 | 52.71 | 2940.88 | 107.37 | 3439.24 | 64.33 | 2594.12 | 115.13 |
| | g1.017 | 1.732 | 0.065 | 0.28 | 0.011 | 0.243 | 0.58 | 0.021 | 22.328 | 1.063 | 0.353 | 3192.23 | 46.15 | 2946.65 | 84.51 | 3350.61 | 59.83 | 2674.75 | 99.77 |
| | g1.018 | 1.856 | 0.068 | 0.226 | 0.005 | 0.485 | 0.541 | 0.02 | 16.854 | 0.592 | 0.589 | 2924.95 | 34 | 2785.86 | 82.27 | 3023.1 | 34.92 | 2664.39 | 45.68 |
| | g1.019 | 1.922 | 0.083 | 0.211 | 0.004 | 0.333 | 0.523 | 0.022 | 15.244 | 0.632 | 0.825 | 2828.06 | 39.36 | 2711.24 | 92.54 | 2914.38 | 30.76 | 2612.72 | 37.88 |
| | g1.020 | 1.886 | 0.063 | 0.2 | 0.004 | 0.372 | 0.532 | 0.017 | 14.664 | 0.498 | 0.202 | 2792.03 | 32.27 | 2748.12 | 73.44 | 2822.86 | 37.37 | 2707.58 | 35.46 |
| | g2.001 | 1.815 | 0.074 | 0.211 | 0.006 | 0.249 | 0.553 | 0.022 | 16.084 | 0.724 | 0.59 | 2879.87 | 42.75 | 2834.7 | 91.73 | 2911.97 | 48.19 | 2789.67 | 50.21 |
| | g2.002 | 1.813 | 0.064 | 0.223 | 0.004 | -0.005 | 0.554 | 0.02 | 17.029 | 0.681 | 0.776 | 2933.11 | 38.64 | 2839.7 | 81.74 | 2998.94 | 30.34 | 2748.47 | 34.46 |
| | g2.003 | 1.845 | 0.069 | 0.218 | 0.005 | 0.421 | 0.545 | 0.019 | 16.322 | 0.605 | 0.619 | 2893.25 | 35.57 | 2800.53 | 81.87 | 2959.68 | 37.05 | 2711.53 | 44.2 |
| | g2.004 | 1.863 | 0.061 | 0.216 | 0.004 | 0.107 | 0.538 | 0.018 | 16.04 | 0.599 | 0.652 | 2876.68 | 35.35 | 2775.13 | 73.69 | 2948.89 | 32.46 | 2688.68 | 35.93 |
| | g2.005 | 1.805 | 0.064 | 0.224 | 0.006 | 0.372 | 0.556 | 0.019 | 17.111 | 0.645 | 0.537 | 2938.46 | 35.93 | 2848.85 | 80.18 | 3001.14 | 39.26 | 2758.94 | 51.31 |
| | g2.006 | 1.784 | 0.063 | 0.238 | 0.008 | -0.264 | 0.563 | 0.02 | 18.435 | 0.949 | 0.695 | 3017.38 | 54.08 | 2877.19 | 83.13 | 3112.15 | 56.99 | 2743.7 | 69.14 |
| | g2.007 | 1.827 | 0.065 | 0.231 | 0.005 | 0.318 | 0.549 | 0.019 | 17.474 | 0.655 | 0.537 | 2958.61 | 36 | 2820.02 | 78.32 | 3054.88 | 38.1 | 2694.62 | 44.72 |
| | g2.008 | 1.829 | 0.056 | 0.228 | 0.006 | 0.21 | 0.548 | 0.017 | 17.177 | 0.678 | 0.366 | 2941.61 | 37.73 | 2814.39 | 70.06 | 3029.23 | 45.21 | 2702.23 | 53.38 |
| | g2.009 | 1.806 | 0.054 | 0.247 | 0.006 | 0.28 | 0.552 | 0.019 | 18.738 | 0.729 | 0.552 | 3025.42 | 37.33 | 2831.95 | 79.83 | 3157.34 | 39.41 | 2671.21 | 54.55 |
| | g2.010 | 1.758 | 0.057 | 0.261 | 0.006 | 0.453 | 0.57 | 0.018 | 20.512 | 0.714 | 0.33 | 3113.84 | 34.2 | 2907.13 | 75.72 | 3250.12 | 39.05 | 2702.15 | 53.39 |
| | g2.011 | 1.788 | 0.063 | 0.262 | 0.007 | 0.072 | 0.562 | 0.021 | 20.296 | 0.909 | 0.655 | 3100.59 | 43.15 | 2871.21 | 84.26 | 3253.67 | 43.55 | 2645.7 | 64.79 |
| | g2.012 | 1.769 | 0.068 | 0.27 | 0.014 | -0.083 | 0.568 | 0.022 | 21.191 | 1.445 | 0.504 | 3133.55 | 63.13 | 2898.71 | 88.57 | 3287.01 | 80.65 | 2648 | 129.37 |
| | g2.013 | 1.696 | 0.077 | 0.29 | 0.011 | -0.242 | 0.589 | 0.024 | 23.337 | 1.276 | 0.784 | 3233.08 | 50.72 | 3004.24 | 111.34 | 3408.1 | 57.83 | 2701.33 | 97.93 |
| | g2.014 | 1.759 | 0.065 | 0.271 | 0.017 | -0.487 | 0.572 | 0.022 | 21.47 | 1.842 | 0.789 | 3141.02 | 67.17 | 2911.33 | 88.69 | 3315.48 | 95.15 | 2661.65 | 155.6 |
| | g2.015 | 1.85 | 0.065 | 0.236 | 0.005 | 0.163 | 0.542 | 0.019 | 17.643 | 0.682 | 0.726 | 2967.58 | 36.81 | 2791.43 | 79.02 | 3090.17 | 31.9 | 2638.26 | 46.52 |
| | g2.016 | 1.874 | 0.061 | 0.228 | 0.006 | 0.219 | 0.535 | 0.017 | 16.807 | 0.653 | 0.482 | 2920.77 | 37.55 | 2759.44 | 73.04 | 3033.94 | 41.73 | 2628.26 | 56.21 |
| | g2.017 | 1.627 | 0.06 | 0.315 | 0.009 | 0.302 | 0.616 | 0.023 | 26.701 | 1.091 | 0.5 | 3369.77 | 40.02 | 3093.51 | 90.54 | 3539.14 | 43.39 | 2731.88 | 78.43 |
| | g2.018 | 1.822 | 0.064 | 0.25 | 0.005 | 0.165 | 0.551 | 0.02 | 19 | 0.775 | 0.714 | 3038.31 | 38.59 | 2827.33 | 83.5 | 3182.26 | 34.86 | 2633.23 | 46.68 |
| | g2.019 | 1.846 | 0.071 | 0.23 | 0.005 | 0.357 | 0.544 | 0.021 | 17.239 | 0.685 | 0.662 | 2945.84 | 37.7 | 2796.64 | 88.4 | 3050.72 | 37.54 | 2666.44 | 45.61 |
| | g2.020 | 1.678 | 0.07 | 0.286 | 0.011 | -0.506 | 0.598 | 0.026 | 23.649 | 1.659 | 0.86 | 3246.32 | 64.14 | 3019.4 | 104.28 | 3390.44 | 56.17 | 2752.66 | 94.48 |
| | g2.021 | 1.83 | 0.066 | 0.225 | 0.004 | 0.363 | 0.549 | 0.02 | 17.004 | 0.625 | 0.732 | 2932.54 | 35.24 | 2817.12 | 84.25 | 3014.38 | 30.47 | 2711.52 | 35.36 |
| | g2.022 | 1.836 | 0.055 | 0.239 | 0.007 | 0.318 | 0.545 | 0.017 | 17.97 | 0.686 | 0.242 | 2985.34 | 36.19 | 2804 | 69.59 | 3109.36 | 44.75 | 2650.32 | 64.58 |
| | g2.023 | 1.67 | 0.067 | 0.278 | 0.014 | -0.352 | 0.6 | 0.024 | 22.995 | 1.679 | 0.744 | 3220.48 | 68.98 | 3027.07 | 97.68 | 3342.92 | 75.51 | 2802.25 | 116.13 |
| | g2.024 | 1.117 | 0.042 | 0.57 | 0.013 | -0.224 | 0.899 | 0.035 | 70.77 | 3.459 | 0.85 | 4332.82 | 47.14 | 4130.7 | 116.79 | 4429.56 | 32.62 | 2611.73 | 123.21 |
| | g2.025 | 1.341 | 0.05 | 0.46 | 0.01 | 0.325 | 0.747 | 0.028 | 47.314 | 1.821 | 0.698 | 3935.54 | 38.17 | 3594.41 | 102.07 | 4114.79 | 31.96 | 2671.13 | 90.93 |
| | g2.026 | 1.671 | 0.071 | 0.314 | 0.011 | -0.201 | 0.602 | 0.025 | 26.08 | 1.54 | 0.736 | 3340.84 | 56.85 | 3033.32 | 99.78 | 3532.36 | 54.17 | 2649.72 | 101.53 |
| | g2.027 | 1.528 | 0.068 | 0.359 | 0.012 | 0.01 | 0.658 | 0.028 | 32.53 | 1.835 | 0.749 | 3560.25 | 53.5 | 3254.72 | 111.08 | 3738.61 | 49.95 | 2744.29 | 103.67 |
| | g2.028 | 1.711 | 0.067 | 0.306 | 0.011 | -0.318 | 0.588 | 0.024 | 24.904 | 1.492 | 0.781 | 3293.99 | 56.74 | 2977.05 | 95.41 | 3494.43 | 52.99 | 2608.97 | 104.45 |
| | g2.029 | 1.809 | 0.06 | 0.235 | 0.005 | 0.08 | 0.554 | 0.019 | 18.055 | 0.745 | 0.653 | 2988.93 | 39.82 | 2839.75 | 79.2 | 3080.37 | 32.34 | 2710.76 | 44.22 |
| | g2.030 | 1.892 | 0.083 | 0.226 | 0.01 | -0.053 | 0.53 | 0.023 | 16.53 | 1.076 | 0.638 | 2901.8 | 57.85 | 2740.08 | 96.71 | 3016.65 | 66.89 | 2607.06 | 95.08 |

Continued on next page

| Sample | Spot name | 238/206 | ±2σ | 207/206 | ±2σ | Err. Corr | 207/235 | ±2σ | 206/238 | ±2σ | Err. Corr | 207/235 Age | ±2σ | 206/238 Age | ±2σ | 207/206 Age | ±2σ | 207/206* Age | ±2σ |
|---|---|---|---|---|---|---|---|---|---|---|---|---|---|---|---|---|---|---|---|
| | g2.031 | 1.732 | 0.062 | 0.256 | 0.008 | -0.267 | 0.579 | 0.021 | 20.479 | 1.052 | 0.763 | 3107.04 | 49.64 | 2943.11 | 86.55 | 3215.45 | 46.89 | 2769.97 | 67.88 |
| | g2.032 | 1.866 | 0.064 | 0.204 | 0.005 | 0.477 | 0.537 | 0.019 | 14.983 | 0.486 | 0.498 | 2812.84 | 30.95 | 2769.5 | 78.58 | 2854.94 | 36.38 | 2726.55 | 43.74 |
| | g2.033 | 1.826 | 0.066 | 0.213 | 0.006 | -0.636 | 0.549 | 0.021 | 15.866 | 0.791 | 0.909 | 2878.89 | 55.54 | 2818.09 | 86.88 | 2922.24 | 43.74 | 2762.63 | 51.17 |
| | g2.034 | 1.869 | 0.068 | 0.208 | 0.004 | 0.638 | 0.537 | 0.02 | 15.335 | 0.5 | 0.545 | 2834.88 | 31.45 | 2766.79 | 81.8 | 2885.08 | 35.04 | 2707.28 | 35.46 |
| | g2.035 | 1.635 | 0.102 | 0.342 | 0.023 | -0.523 | 0.617 | 0.04 | 29.358 | 3.351 | 0.872 | 3444.68 | 113.73 | 3094 | 156.51 | 3657.73 | 109.39 | 2599.63 | 219.83 |
| | g2.036 | 1.817 | 0.062 | 0.26 | 0.007 | 0.19 | 0.551 | 0.019 | 19.716 | 0.82 | 0.566 | 3074.07 | 39.88 | 2828.72 | 80.16 | 3239.08 | 42.38 | 2604.65 | 66.67 |
| | g2.037 | 1.679 | 0.063 | 0.3 | 0.009 | 0.116 | 0.597 | 0.022 | 24.706 | 1.118 | 0.619 | 3291.62 | 43.76 | 3017.14 | 89.54 | 3464.49 | 44.49 | 2692.6 | 80.62 |
| | g2.038 | 1.765 | 0.061 | 0.279 | 0.006 | -0.042 | 0.564 | 0.017 | 21.795 | 0.854 | 0.654 | 3171.51 | 37.75 | 2892.9 | 82.2 | 3352.9 | 34.47 | 2620.38 | 56.52 |
| | g2.039 | 1.713 | 0.063 | 0.255 | 0.005 | 0.546 | 0.585 | 0.021 | 20.553 | 0.691 | 0.647 | 3116.32 | 32.72 | 2967.12 | 85.86 | 3215.03 | 30.31 | 2810.93 | 41.22 |
| | g2.040 | 1.79 | 0.071 | 0.23 | 0.006 | 0.496 | 0.561 | 0.021 | 17.727 | 0.681 | 0.562 | 2972.2 | 36.79 | 2868.54 | 88.88 | 3044.85 | 42.48 | 2763.29 | 51.15 |
| | g3.001 | 1.813 | 0.067 | 0.228 | 0.006 | 0.387 | 0.553 | 0.02 | 17.365 | 0.669 | 0.516 | 2952.14 | 38.41 | 2836.37 | 82.91 | 3032.96 | 43.79 | 2729.85 | 52.36 |
| | g3.002 | 1.912 | 0.064 | 0.206 | 0.004 | 0.264 | 0.524 | 0.017 | 14.838 | 0.536 | 0.574 | 2802.74 | 33.8 | 2713.14 | 72.73 | 2868.21 | 33.76 | 2645.23 | 37.03 |
| | g3.003 | 1.841 | 0.061 | 0.213 | 0.004 | 0.185 | 0.544 | 0.018 | 15.987 | 0.583 | 0.653 | 2873.71 | 34.1 | 2798.27 | 74.34 | 2927.43 | 31.22 | 2736.53 | 34.75 |
| | g3.004 | 1.85 | 0.078 | 0.22 | 0.006 | 0.38 | 0.538 | 0.019 | 16.446 | 0.665 | 0.529 | 2899.67 | 38.65 | 2774 | 80.19 | 2976.07 | 45.55 | 2695.9 | 53.62 |
| | g3.005 | 1.767 | 0.068 | 0.237 | 0.004 | 0.336 | 0.568 | 0.021 | 18.497 | 0.684 | 0.817 | 3013.41 | 35.99 | 2896.63 | 87.92 | 3094.16 | 25.5 | 2778.69 | 33.73 |
| | g3.006 | 1.742 | 0.062 | 0.253 | 0.006 | 0.304 | 0.575 | 0.02 | 20.079 | 0.777 | 0.554 | 3092.12 | 37.02 | 2928.27 | 83.28 | 3201.29 | 38.87 | 2762.92 | 51.16 |
| | g3.007 | 1.702 | 0.062 | 0.275 | 0.008 | 0.1 | 0.589 | 0.021 | 22.31 | 0.881 | 0.084 | 3194.03 | 38.8 | 2982.88 | 84.43 | 3330.05 | 47.54 | 2751.03 | 68.79 |
| | g3.008 | 1.586 | 0.054 | 0.325 | 0.009 | 0.282 | 0.628 | 0.024 | 28.071 | 1.18 | 0.582 | 3417.41 | 41.88 | 3137.85 | 95.08 | 3587.25 | 43.04 | 2773.93 | 76.15 |
| | g3.009 | 1.588 | 0.067 | 0.361 | 0.011 | 0.277 | 0.633 | 0.025 | 31.472 | 1.373 | 0.619 | 3528.93 | 44.24 | 3159.29 | 100.31 | 3748.17 | 44.01 | 2607.8 | 104.54 |
| | g3.010 | 1.522 | 0.065 | 0.349 | 0.013 | -0.075 | 0.66 | 0.026 | 31.8 | 1.774 | 0.652 | 3535.68 | 56.7 | 3263.98 | 102.52 | 3694.5 | 59.08 | 2806.22 | 107.54 |
| | g3.011 | 1.625 | 0.066 | 0.347 | 0.01 | 0.12 | 0.619 | 0.025 | 29.574 | 1.411 | 0.729 | 3466.83 | 46.3 | 3100.91 | 100.06 | 3687.85 | 42.21 | 2597.17 | 95.74 |
| | g3.012 | 1.76 | 0.081 | 0.25 | 0.01 | -0.131 | 0.569 | 0.028 | 19.667 | 1.296 | 0.742 | 3070.55 | 62.97 | 2903.1 | 113.59 | 3182.8 | 62.29 | 2741.2 | 86.58 |
| | g3.013 | 1.847 | 0.086 | 0.251 | 0.009 | 0.167 | 0.543 | 0.024 | 18.785 | 1.022 | 0.613 | 3026.97 | 52.18 | 2794.24 | 102.82 | 3186.51 | 58.93 | 2589.07 | 86.65 |
| | g3.014 | 1.56 | 0.086 | 0.313 | 0.016 | -0.027 | 0.646 | 0.035 | 27.911 | 2.149 | 0.707 | 3406.33 | 73.85 | 3206.52 | 135.87 | 3528.19 | 78.56 | 2888.49 | 124.91 |
| | g3.015 | 1.797 | 0.068 | 0.225 | 0.007 | 0.492 | 0.558 | 0.02 | 17.3 | 0.661 | 0.349 | 2948.79 | 36.09 | 2857.21 | 83.95 | 3012.88 | 47.68 | 2769.57 | 59.41 |
| | g3.016 | 0.768 | 0.04 | 0.747 | 0.038 | 0.328 | 1.322 | 0.071 | 132.081 | 6.702 | 0.558 | 4958.3 | 52.93 | 5410.96 | 195.27 | 4752.94 | 51.3 | 2193.14 | 480.92 |
| | g3.017 | 0.981 | 0.053 | 0.624 | 0.027 | -0.067 | 1.021 | 0.048 | 89.064 | 6.121 | 0.77 | 4552.26 | 72.41 | 4524.13 | 153.55 | 4551.07 | 64.67 | 2680.36 | 243.93 |
| | g3.018 | 0.918 | 0.044 | 0.66 | 0.019 | 0.221 | 1.101 | 0.055 | 100.008 | 5.084 | 0.765 | 4678.41 | 52.23 | 4774.72 | 165.55 | 4640.57 | 42.36 | 2595.78 | 182.08 |
| | g3.019 | 1.856 | 0.058 | 0.219 | 0.006 | 0.105 | 0.539 | 0.017 | 16.303 | 0.648 | 0.53 | 2891.56 | 37.7 | 2778.02 | 71.32 | 2971.35 | 41.19 | 2689.51 | 53.86 |
| | g3.020 | 1.772 | 0.054 | 0.264 | 0.006 | 0.083 | 0.562 | 0.019 | 20.406 | 0.824 | 0.686 | 3107.13 | 39.6 | 2872.3 | 81.08 | 3263.5 | 35.25 | 2665.75 | 54.76 |
| | g3.021 | 0.479 | 0.045 | 0.898 | 0.045 | 0.338 | 2.227 | 0.214 | 272.04 | 25.399 | 0.819 | 5664.69 | 92.3 | 7450.5 | 419.12 | 4788.39 | 98.83 | | |
| | g3.022 | 1.067 | 0.046 | 0.565 | 0.026 | 0.227 | 0.937 | 0.046 | 72.629 | 4.219 | 0.554 | 4354.07 | 60.18 | 4250.32 | 153.14 | 4405.98 | 65.53 | 2852.22 | 208.23 |
| | g3.023 | 1.721 | 0.059 | 0.281 | 0.007 | 0.226 | 0.581 | 0.019 | 22.664 | 0.917 | 0.549 | 3209.06 | 39.51 | 2953.22 | 77.17 | 3362.01 | 41.54 | 2690.91 | 62.78 |
| | g3.024 | 1.812 | 0.062 | 0.237 | 0.007 | 0.272 | 0.553 | 0.019 | 18.045 | 0.75 | 0.418 | 2988.05 | 41.25 | 2834.99 | 79.09 | 3092.95 | 50.11 | 2698.13 | 62.46 |
| | g3.025 | 1.861 | 0.06 | 0.222 | 0.006 | 0.312 | 0.537 | 0.017 | 16.409 | 0.612 | 0.387 | 2898.43 | 35.25 | 2770.96 | 70.94 | 2987.98 | 41.28 | 2670.53 | 54.58 |
| ZL182 | 1.001 | 1.907 | 0.07 | 0.2 | 0.003 | 0.226 | 0.525 | 0.019 | 14.421 | 0.524 | 0.802 | 2775.52 | 35.11 | 2716.85 | 79.43 | 2819.84 | 25.13 | 2673.76 | 27.23 |
| | 1.002 | 1.783 | 0.054 | 0.263 | 0.005 | 0.331 | 0.559 | 0.017 | 20.261 | 0.664 | 0.555 | 3102.79 | 31.28 | 2863.78 | 71.23 | 3261.25 | 27.15 | 2650.49 | 46.12 |
| | 1.003 | 1.664 | 0.056 | 0.307 | 0.006 | 0.232 | 0.601 | 0.021 | 25.437 | 0.951 | 0.684 | 3322.48 | 36.36 | 3030.76 | 83.52 | 3504.38 | 31.08 | 2692.34 | 53.75 |
| | 1.004 | 1.73 | 0.059 | 0.283 | 0.006 | 0.249 | 0.578 | 0.02 | 22.541 | 0.846 | 0.597 | 3204.58 | 36.24 | 2937.27 | 79.91 | 3377.14 | 34.56 | 2666.5 | 54.73 |
| | 1.005 | 1.919 | 0.067 | 0.21 | 0.004 | 0.249 | 0.521 | 0.019 | 15.052 | 0.566 | 0.671 | 2815.81 | 37.16 | 2702.52 | 78.84 | 2899.03 | 35.11 | 2620.72 | 37.67 |
| | 1.006 | 1.883 | 0.063 | 0.217 | 0.004 | 0.531 | 0.531 | 0.018 | 15.847 | 0.509 | 0.592 | 2866.39 | 30.72 | 2742.21 | 75.11 | 2955.65 | 28.69 | 2652.7 | 36.84 |
| | 1.007 | 1.913 | 0.06 | 0.214 | 0.004 | 0.31 | 0.522 | 0.017 | 15.369 | 0.523 | 0.54 | 2836.68 | 32.71 | 2705.61 | 70.55 | 2931.4 | 31.31 | 2616.2 | 37.79 |
| | 1.008 | 1.846 | 0.06 | 0.214 | 0.003 | 0.442 | 0.541 | 0.018 | 15.956 | 0.513 | 0.735 | 2872.87 | 30.89 | 2786.65 | 74.49 | 2934.57 | 23.24 | 2724.34 | 26.28 |
| | 1.009 | 1.815 | 0.068 | 0.215 | 0.005 | 0.334 | 0.551 | 0.02 | 16.285 | 0.621 | 0.608 | 2891.39 | 36.63 | 2826.19 | 82.1 | 2937.86 | 37.75 | 2774.74 | 42.28 |
| | 1.01 | 1.87 | 0.067 | 0.222 | 0.005 | 0.279 | 0.535 | 0.019 | 16.357 | 0.612 | 0.588 | 2895.19 | 36.24 | 2759.17 | 78.5 | 2992.14 | 36.03 | 2655.9 | 45.95 |
| | 1.011 | 1.865 | 0.055 | 0.222 | 0.004 | 0.261 | 0.533 | 0.018 | 16.273 | 0.59 | 0.634 | 2890.63 | 34.83 | 2751.27 | 75.24 | 2989.84 | 32.71 | 2664 | 36.55 |
| | 1.012 | 1.848 | 0.058 | 0.225 | 0.004 | 0.342 | 0.54 | 0.017 | 16.761 | 0.547 | 0.569 | 2919.87 | 31.25 | 2781.67 | 70.36 | 3016.71 | 27.35 | 2681.18 | 36.12 |
| | 1.013 | 1.831 | 0.06 | 0.228 | 0.004 | 0.474 | 0.546 | 0.018 | 17.115 | 0.565 | 0.619 | 2939.8 | 31.52 | 2805.29 | 75.54 | 3033.89 | 28.83 | 2698.83 | 35.67 |
| | 1.014 | 1.842 | 0.06 | 0.232 | 0.004 | 0.284 | 0.542 | 0.017 | 17.32 | 0.586 | 0.631 | 2951.04 | 32.87 | 2789.62 | 72.51 | 3063.34 | 28 | 2665.81 | 36.51 |
| | 1.015 | 1.923 | 0.068 | 0.201 | 0.004 | 0.368 | 0.52 | 0.018 | 14.414 | 0.513 | 0.679 | 2775.25 | 33.54 | 2696.68 | 76.94 | 2833.97 | 30.75 | 2645.3 | 37.03 |
| | 1.016 | 1.948 | 0.067 | 0.199 | 0.004 | 0.202 | 0.513 | 0.017 | 14.054 | 0.512 | 0.687 | 2751.08 | 34.5 | 2666.96 | 73.33 | 2814.02 | 30.73 | 2614.09 | 37.85 |
| | 1.017 | 1.828 | 0.066 | 0.216 | 0.004 | 0.042 | 0.546 | 0.02 | 16.285 | 0.676 | 0.804 | 2891.62 | 39.44 | 2807.74 | 84.12 | 2951.07 | 31.36 | 2748.05 | 34.47 |
| | 1.018 | 1.936 | 0.063 | 0.2 | 0.003 | 0.319 | 0.515 | 0.017 | 14.212 | 0.475 | 0.639 | 2762.33 | 31.93 | 2678.69 | 70.76 | 2824.45 | 27.81 | 2628.8 | 28.1 |
| | 1.019 | 1.859 | 0.064 | 0.227 | 0.004 | 0.243 | 0.537 | 0.018 | 16.835 | 0.598 | 0.751 | 2923.41 | 34.05 | 2771.15 | 76.84 | 3030.88 | 26.34 | 2655.92 | 36.76 |
| | 1.02 | 1.808 | 0.06 | 0.231 | 0.004 | 0.135 | 0.552 | 0.018 | 17.611 | 0.644 | 0.696 | 2966.29 | 34.91 | 2832.64 | 75.61 | 3058.72 | 29.38 | 2727.43 | 34.97 |

Continued on next page

| Sample | Spot name | 238/206 | ±2σ | 207/206 | ±2σ | Err. Corr | 207/235 | ±2σ | 206/238 | ±2σ | Err. Corr | 207/235 Age | ±2σ | 206/238 Age | ±2σ | 207/206 Age | ±2σ | 207/206* Age | ±2σ |
|---|---|---|---|---|---|---|---|---|---|---|---|---|---|---|---|---|---|---|---|
| | 1.021 | 1.851 | 0.061 | 0.225 | 0.004 | 0.292 | 0.54 | 0.019 | 16.705 | 0.604 | 0.693 | 2915.8 | 34.34 | 2780.9 | 77.3 | 3011.12 | 30.43 | 2676.21 | 36.24 |
| | 1.022 | 1.828 | 0.062 | 0.216 | 0.004 | 0.431 | 0.546 | 0.018 | 16.277 | 0.556 | 0.575 | 2891.46 | 32.46 | 2808.17 | 76.45 | 2950.67 | 31.86 | 2748.05 | 34.47 |
| | 1.023 | 1.834 | 0.065 | 0.217 | 0.004 | 0.319 | 0.545 | 0.019 | 16.284 | 0.577 | 0.665 | 2891.53 | 34.33 | 2801.59 | 78.69 | 2955.71 | 30.43 | 2733.97 | 34.81 |
| | 1.024 | 1.848 | 0.059 | 0.216 | 0.003 | 0.456 | 0.54 | 0.017 | 16.125 | 0.512 | 0.572 | 2883.06 | 30.62 | 2782.19 | 72.41 | 2947.35 | 22.79 | 2713.71 | 26.48 |
| | 1.025 | 1.86 | 0.062 | 0.217 | 0.004 | 0.33 | 0.537 | 0.018 | 16.006 | 0.544 | 0.644 | 2875.42 | 33.27 | 2768.09 | 74.3 | 2952.03 | 29.1 | 2690.05 | 35.89 |
| | 1.026 | 1.878 | 0.065 | 0.204 | 0.004 | 0.363 | 0.532 | 0.019 | 14.942 | 0.53 | 0.721 | 2809.53 | 33.43 | 2749.15 | 78.08 | 2854.21 | 28.94 | 2706.61 | 35.48 |
| | 1.027 | 1.832 | 0.076 | 0.214 | 0.007 | 0.268 | 0.546 | 0.022 | 16.075 | 0.745 | 0.595 | 2877.74 | 43.54 | 2806.96 | 93.09 | 2928.88 | 50.03 | 2748.44 | 60.3 |
| | 1.028 | 1.854 | 0.065 | 0.215 | 0.004 | 0.267 | 0.539 | 0.018 | 15.942 | 0.578 | 0.606 | 2871.02 | 35.02 | 2776.5 | 76.2 | 2938.64 | 33.57 | 2707.22 | 35.47 |
| | 1.029 | 1.833 | 0.06 | 0.214 | 0.005 | 0.529 | 0.545 | 0.018 | 16.026 | 0.531 | 0.385 | 2876.81 | 31.98 | 2801.37 | 75.16 | 2930.48 | 36.39 | 2746.7 | 43.12 |
| | 1.03 | 1.86 | 0.061 | 0.22 | 0.004 | 0.277 | 0.537 | 0.018 | 16.264 | 0.572 | 0.561 | 2890.41 | 33.8 | 2768.57 | 73.53 | 2976.81 | 32.63 | 2679.32 | 36.16 |
| | 1.031 | 1.839 | 0.056 | 0.22 | 0.006 | 0.478 | 0.542 | 0.017 | 16.412 | 0.568 | 0.17 | 2899.29 | 33.11 | 2791.76 | 69.08 | 2974.43 | 40.7 | 2714.44 | 52.93 |
| | 1.032 | 1.843 | 0.074 | 0.205 | 0.004 | 0.212 | 0.543 | 0.022 | 15.349 | 0.64 | 0.76 | 2834.93 | 41.05 | 2792.28 | 93.02 | 2866.55 | 35.52 | 2762.23 | 34.13 |
| | 1.033 | 1.846 | 0.055 | 0.218 | 0.005 | 0.234 | 0.54 | 0.016 | 16.12 | 0.575 | 0.458 | 2881.85 | 33.87 | 2782.6 | 67.13 | 2959.52 | 35.19 | 2709.85 | 44.25 |
| | 1.034 | 1.853 | 0.061 | 0.217 | 0.004 | 0.503 | 0.539 | 0.018 | 16.135 | 0.516 | 0.599 | 2883.59 | 30.22 | 2777.92 | 73.63 | 2958.82 | 27.12 | 2701.69 | 35.6 |
| | 1.035 | 1.851 | 0.06 | 0.217 | 0.003 | 0.602 | 0.539 | 0.017 | 16.149 | 0.49 | 0.509 | 2884.82 | 29.07 | 2778.85 | 71.63 | 2959.99 | 26.74 | 2705.04 | 26.64 |
| | 1.036 | 1.903 | 0.066 | 0.22 | 0.004 | -0.023 | 0.525 | 0.018 | 15.969 | 0.643 | 0.768 | 2871.61 | 38.05 | 2719.67 | 76.93 | 2980.82 | 31.28 | 2610.89 | 37.93 |
| | 1.037 | 1.892 | 0.063 | 0.215 | 0.004 | 0.417 | 0.528 | 0.018 | 15.656 | 0.53 | 0.564 | 2854.34 | 32.13 | 2731.3 | 74.02 | 2943.01 | 31.19 | 2645.41 | 37.03 |
| | 1.038 | 1.882 | 0.064 | 0.218 | 0.005 | 0.569 | 0.531 | 0.017 | 15.898 | 0.533 | 0.26 | 2869.13 | 32.02 | 2742.92 | 73.82 | 2959.29 | 40.12 | 2650.78 | 46.11 |
| | 1.039 | 1.86 | 0.068 | 0.223 | 0.005 | 0.388 | 0.538 | 0.02 | 16.531 | 0.609 | 0.63 | 2905.52 | 35.26 | 2773.15 | 82.1 | 2999.98 | 35.06 | 2668.59 | 45.54 |
| | 1.04 | 1.809 | 0.066 | 0.219 | 0.004 | 0.41 | 0.553 | 0.02 | 16.79 | 0.629 | 0.623 | 2920.86 | 36.46 | 2834.56 | 84.53 | 2981.79 | 37.74 | 2770.53 | 33.93 |
| | 1.041 | 1.78 | 0.059 | 0.232 | 0.007 | 0.253 | 0.561 | 0.019 | 17.946 | 0.729 | 0.456 | 2983.16 | 39.49 | 2870.53 | 77.81 | 3060.1 | 46.31 | 2773.91 | 59.23 |
| | 1.042 | 1.818 | 0.06 | 0.222 | 0.004 | 0.549 | 0.55 | 0.018 | 16.768 | 0.545 | 0.473 | 2920.31 | 31.14 | 2821.84 | 75.74 | 2989.43 | 32.9 | 2743.38 | 34.58 |
| | 1.043 | 1.737 | 0.071 | 0.272 | 0.014 | -0.295 | 0.577 | 0.025 | 21.681 | 1.567 | 0.707 | 3157.71 | 71.25 | 2932.92 | 99.79 | 3303.91 | 80.29 | 2697.24 | 125 |
| | 1.044 | 1.825 | 0.066 | 0.221 | 0.005 | 0.529 | 0.548 | 0.02 | 16.685 | 0.579 | 0.636 | 2915.06 | 33.11 | 2816.35 | 82.74 | 2985.33 | 33.26 | 2734.85 | 43.48 |
| | 1.045 | 1.831 | 0.064 | 0.223 | 0.005 | 0.152 | 0.546 | 0.019 | 16.794 | 0.66 | 0.663 | 2920.01 | 38.08 | 2807.55 | 79.78 | 2999.31 | 35.63 | 2717.14 | 44.02 |
| | 1.046 | 1.844 | 0.059 | 0.219 | 0.003 | 0.228 | 0.542 | 0.018 | 16.237 | 0.562 | 0.695 | 2889.01 | 33.29 | 2788.7 | 74.06 | 2968 | 22.93 | 2709.6 | 26.55 |
| | 1.047 | 1.888 | 0.062 | 0.219 | 0.005 | 0.481 | 0.529 | 0.017 | 15.941 | 0.538 | 0.402 | 2871.64 | 32.42 | 2736.73 | 73.45 | 2968.08 | 36.32 | 2637.75 | 46.54 |
| | 1.048 | 1.845 | 0.064 | 0.215 | 0.004 | 0.561 | 0.542 | 0.019 | 16.065 | 0.54 | 0.647 | 2879.06 | 31.69 | 2791.13 | 79.9 | 2942.39 | 31.16 | 2722.42 | 35.09 |
| | 1.049 | 1.844 | 0.063 | 0.223 | 0.004 | 0.39 | 0.542 | 0.018 | 16.668 | 0.568 | 0.566 | 2914.13 | 32.96 | 2790.32 | 74.96 | 3001.37 | 31.58 | 2695.1 | 35.77 |
| | 1.05 | 1.8 | 0.068 | 0.223 | 0.005 | 0.13 | 0.555 | 0.02 | 17.104 | 0.719 | 0.702 | 2938.08 | 40.91 | 2845.7 | 85.05 | 3002.55 | 38.91 | 2771.7 | 42.37 |
| | 1.051 | 1.831 | 0.068 | 0.221 | 0.005 | 0.061 | 0.547 | 0.02 | 16.655 | 0.707 | 0.717 | 2911.23 | 40.11 | 2809.26 | 81.8 | 2983.52 | 37.3 | 2724.48 | 43.8 |
| | 1.052 | 1.89 | 0.063 | 0.217 | 0.004 | 0.533 | 0.529 | 0.017 | 15.818 | 0.51 | 0.499 | 2864.6 | 30.96 | 2734.13 | 73.63 | 2958.26 | 31.26 | 2641.59 | 37.13 |
| | 1.053 | 1.828 | 0.065 | 0.219 | 0.006 | 0.416 | 0.547 | 0.02 | 16.467 | 0.64 | 0.439 | 2902.12 | 37.84 | 2810.39 | 83.11 | 2966.86 | 46.79 | 2737.01 | 52.1 |
| | 1.054 | 1.85 | 0.059 | 0.215 | 0.004 | 0.327 | 0.54 | 0.017 | 15.999 | 0.533 | 0.637 | 2875.19 | 31.94 | 2781.47 | 72.17 | 2941.83 | 27.59 | 2713.95 | 35.3 |
| | 1.055 | 1.852 | 0.06 | 0.214 | 0.004 | -0.045 | 0.54 | 0.018 | 15.872 | 0.574 | 0.65 | 2866.83 | 34.44 | 2780.27 | 73.45 | 2943.3 | 37.42 | 2714.19 | 35.29 |
| | 1.056 | 1.898 | 0.058 | 0.204 | 0.004 | -0.188 | 0.524 | 0.018 | 14.596 | 0.575 | 0.77 | 2793.94 | 43.2 | 2712.73 | 76.37 | 2853.68 | 35.19 | 2674.21 | 36.29 |
| | 1.057 | 1.866 | 0.068 | 0.212 | 0.005 | 0.191 | 0.536 | 0.019 | 15.501 | 0.581 | 0.61 | 2843.9 | 35.44 | 2766.62 | 80.83 | 2914.16 | 40.46 | 2698 | 44.62 |
| | 1.058 | 1.929 | 0.062 | 0.206 | 0.004 | 0.212 | 0.518 | 0.017 | 14.664 | 0.522 | 0.669 | 2791.63 | 33.28 | 2688.82 | 71.82 | 2867.21 | 29.54 | 2619.1 | 37.72 |
| | 1.059 | 1.897 | 0.062 | 0.211 | 0.004 | 0.647 | 0.526 | 0.017 | 15.263 | 0.47 | 0.376 | 2830.84 | 29.09 | 2725.48 | 72.35 | 2907.25 | 32.04 | 2651.45 | 36.87 |
| | 1.06 | 1.776 | 0.06 | 0.234 | 0.006 | 0.599 | 0.562 | 0.02 | 18.142 | 0.629 | 0.31 | 2995.96 | 33.4 | 2875.24 | 80.53 | 3078.29 | 43.13 | 2773.6 | 50.78 |
| | 1.061 | 1.869 | 0.063 | 0.204 | 0.004 | 0.112 | 0.535 | 0.018 | 15.05 | 0.57 | 0.707 | 2815.63 | 35.95 | 2760.29 | 77.01 | 2856.29 | 31.2 | 2721.53 | 35.11 |
| | 1.062 | 1.87 | 0.059 | 0.209 | 0.003 | 0.184 | 0.534 | 0.017 | 15.411 | 0.513 | 0.674 | 2839.53 | 31.07 | 2756.54 | 69.73 | 2899.12 | 24.23 | 2702.07 | 26.69 |
| | 1.063 | 1.743 | 0.054 | 0.28 | 0.005 | 0.063 | 0.57 | 0.02 | 21.97 | 0.856 | 0.748 | 3179.14 | 38.37 | 2906.45 | 80.91 | 3365.64 | 25.91 | 2654.98 | 45.98 |
| | 1.064 | 1.885 | 0.065 | 0.205 | 0.005 | 0.11 | 0.53 | 0.018 | 14.956 | 0.611 | 0.563 | 2809.49 | 38.81 | 2740.13 | 74.71 | 2859.67 | 41.82 | 2691.64 | 44.82 |
| | 2.001 | 1.826 | 0.085 | 0.238 | 0.01 | 0.115 | 0.549 | 0.028 | 18.003 | 1.119 | 0.688 | 2984.79 | 59.86 | 2816.9 | 115.28 | 3101.39 | 67.02 | 2670.62 | 90.96 |
| | 2.002 | 1.82 | 0.064 | 0.219 | 0.004 | 0.43 | 0.548 | 0.019 | 16.517 | 0.557 | 0.718 | 2906.11 | 32.44 | 2817.77 | 78.58 | 2968.36 | 26.49 | 2750.99 | 34.39 |
| | 2.003 | 1.868 | 0.065 | 0.209 | 0.004 | 0.14 | 0.535 | 0.018 | 15.402 | 0.571 | 0.684 | 2837.92 | 35.96 | 2761.72 | 76.5 | 2893.19 | 31.15 | 2705.38 | 35.51 |
| | 2.006 | 1.655 | 0.062 | 0.273 | 0.007 | 0.502 | 0.603 | 0.023 | 22.684 | 0.835 | 0.543 | 3212.47 | 35.93 | 3040.32 | 91.32 | 3322.04 | 39.38 | 2854.9 | 55.96 |
| | 2.007 | 1.801 | 0.076 | 0.262 | 0.007 | -0.271 | 0.552 | 0.021 | 19.848 | 0.981 | 0.858 | 3077.91 | 45.59 | 2831.5 | 87.18 | 3252.85 | 43.47 | 2623.71 | 65.79 |
| | 2.008 | 1.727 | 0.088 | 0.281 | 0.009 | 0.126 | 0.584 | 0.033 | 22.561 | 1.332 | 0.819 | 3200.97 | 57.71 | 2957.24 | 130.85 | 3361.96 | 49.19 | 2679.89 | 81.34 |
| | 2.009 | 1.74 | 0.049 | 0.262 | 0.005 | -0.07 | 0.57 | 0.019 | 20.555 | 0.823 | 0.772 | 3115.28 | 39.1 | 2904.94 | 80.46 | 3254.22 | 30.29 | 2731.15 | 43.6 |
| | 2.01 | 1.702 | 0.078 | 0.267 | 0.012 | -0.526 | 0.589 | 0.027 | 21.739 | 1.739 | 0.857 | 3160.24 | 74.53 | 2981.29 | 109.47 | 3276.83 | 70.61 | 2783.7 | 100.85 |
| | 2.011 | 1.724 | 0.057 | 0.267 | 0.004 | 0.081 | 0.579 | 0.019 | 21.261 | 0.771 | 0.759 | 3148.17 | 35.94 | 2945 | 78.49 | 3288.88 | 22.07 | 2741.25 | 34.63 |
| | 2.012 | 1.828 | 0.067 | 0.223 | 0.005 | 0.332 | 0.547 | 0.019 | 16.787 | 0.631 | 0.596 | 2920.09 | 36 | 2811.14 | 81.58 | 2997.17 | 36.73 | 2722.3 | 43.87 |
| | 2.013 | 1.831 | 0.079 | 0.204 | 0.006 | 0.256 | 0.545 | 0.024 | 15.343 | 0.714 | 0.756 | 2835.29 | 44.82 | 2802.98 | 100.17 | 2858.77 | 43.74 | 2787.01 | 50.31 |
| | 2.014 | 1.845 | 0.087 | 0.22 | 0.007 | 0.242 | 0.541 | 0.026 | 16.424 | 0.85 | 0.706 | 2900 | 49.8 | 2786.63 | 107.75 | 2980.23 | 52.8 | 2704.29 | 62.19 |

Continued on next page

| Sample | Spot name | 238/206 | ±2σ | 207/206 | ±2σ | Err. Corr | 207/235 | ±2σ | 206/238 | ±2σ | Err. Corr | 207/235 Age | ±2σ | 206/238 Age | ±2σ | 207/206 Age | ±2σ | 207/206* Age | ±2σ |
|---|---|---|---|---|---|---|---|---|---|---|---|---|---|---|---|---|---|---|---|
| | 2.015 | 1.981 | 0.085 | 0.207 | 0.005 | 0.226 | 0.505 | 0.021 | 14.404 | 0.653 | 0.732 | 2774.08 | 43.31 | 2632.48 | 91.77 | 2880.03 | 41.75 | 2539.75 | 49.82 |
| | 2.016 | 1.742 | 0.067 | 0.286 | 0.011 | -0.402 | 0.57 | 0.02 | 22.748 | 1.419 | 0.766 | 3204.59 | 59.54 | 2906.11 | 80.38 | 3385.42 | 62.03 | 2633.26 | 102.7 |
| | 2.017 | 1.785 | 0.057 | 0.239 | 0.007 | -0.011 | 0.559 | 0.018 | 18.446 | 0.796 | 0.554 | 3009 | 40.42 | 2861.33 | 74.74 | 3109.03 | 43.68 | 2738.09 | 60.74 |
| | 2.018 | 1.735 | 0.066 | 0.255 | 0.009 | -0.403 | 0.577 | 0.021 | 20.347 | 1.181 | 0.792 | 3098.56 | 54.29 | 2932.43 | 87.38 | 3208.6 | 52.24 | 2768.24 | 76.46 |
| | 2.019 | 1.864 | 0.067 | 0.217 | 0.004 | 0.231 | 0.536 | 0.02 | 15.986 | 0.624 | 0.734 | 2874.02 | 37.88 | 2763.53 | 84.16 | 2953.15 | 33.15 | 2683.46 | 36.06 |
| | 2.02 | 1.854 | 0.081 | 0.245 | 0.007 | -0.183 | 0.54 | 0.023 | 18.248 | 1.021 | 0.791 | 2996.5 | 52.15 | 2781.58 | 95.17 | 3145.75 | 45.84 | 2599.52 | 66.91 |
| | 3.001 | 1.807 | 0.061 | 0.233 | 0.005 | 0.43 | 0.553 | 0.019 | 17.704 | 0.62 | 0.538 | 2971.82 | 33.44 | 2835.15 | 78.21 | 3066.39 | 34.54 | 2721.71 | 43.88 |
| | 3.002 | 1.884 | 0.064 | 0.225 | 0.007 | -0.304 | 0.53 | 0.018 | 16.407 | 0.794 | 0.699 | 2895.16 | 44.34 | 2740.33 | 76.36 | 3024.18 | 53.74 | 2623.04 | 65.82 |
| | 3.003 | 1.869 | 0.076 | 0.216 | 0.004 | 0.308 | 0.531 | 0.019 | 15.937 | 0.613 | 0.731 | 2870.08 | 36.83 | 2761.05 | 91.97 | 2949.48 | 32.31 | 2678.83 | 36.18 |
| | 3.004 | 1.891 | 0.065 | 0.228 | 0.004 | 0.362 | 0.528 | 0.018 | 16.555 | 0.569 | 0.616 | 2907.76 | 32.9 | 2729.77 | 74.46 | 3034 | 30.05 | 2601.63 | 38.18 |
| | 3.005 | 1.816 | 0.069 | 0.238 | 0.008 | -0.424 | 0.546 | 0.018 | 17.917 | 0.852 | 0.732 | 2979.9 | 42.65 | 2807.55 | 73.31 | 3097.95 | 48.71 | 2687.56 | 71.91 |
| | 3.006 | 1.928 | 0.067 | 0.208 | 0.003 | 0.461 | 0.517 | 0.017 | 14.823 | 0.482 | 0.726 | 2802.96 | 31.23 | 2684.66 | 73.78 | 2889.69 | 24.31 | 2613.83 | 28.39 |
| | 3.007 | 1.916 | 0.062 | 0.206 | 0.004 | -0.075 | 0.52 | 0.017 | 14.804 | 0.568 | 0.716 | 2799.68 | 37.69 | 2699.68 | 72.25 | 2872.81 | 32.71 | 2639.02 | 37.2 |
| | 3.008 | 1.852 | 0.057 | 0.223 | 0.005 | 0.414 | 0.538 | 0.017 | 16.495 | 0.562 | 0.323 | 2904.21 | 32.61 | 2773.87 | 70.82 | 2995.82 | 36.74 | 2681.76 | 45.13 |
| | 3.009 | 1.847 | 0.059 | 0.228 | 0.004 | 0.085 | 0.54 | 0.017 | 16.941 | 0.609 | 0.63 | 2929.15 | 35.2 | 2780.74 | 71.52 | 3032.89 | 30.99 | 2672.01 | 36.35 |
| | 3.01 | 1.948 | 0.06 | 0.188 | 0.003 | 0.515 | 0.511 | 0.016 | 13.268 | 0.404 | 0.635 | 2698.04 | 29.2 | 2662.08 | 68.67 | 2725.41 | 23.64 | 2650.95 | 27.67 |
| | 3.011 | 1.898 | 0.067 | 0.201 | 0.004 | 0.671 | 0.526 | 0.019 | 14.421 | 0.43 | 0.521 | 2777.11 | 28.3 | 2722.95 | 78.17 | 2827.24 | 34.12 | 2684.64 | 36.03 |
| | 3.012 | 1.895 | 0.07 | 0.2 | 0.004 | 0.564 | 0.527 | 0.019 | 14.484 | 0.495 | 0.705 | 2780.2 | 32.05 | 2728.5 | 81.53 | 2819.61 | 30.42 | 2692.95 | 35.82 |
| | 3.013 | 1.916 | 0.066 | 0.201 | 0.004 | 0.527 | 0.521 | 0.018 | 14.482 | 0.484 | 0.511 | 2780.25 | 32.05 | 2701.53 | 76.99 | 2838.87 | 34.66 | 2656.17 | 36.75 |
| | 3.014 | 1.827 | 0.064 | 0.229 | 0.005 | 0.492 | 0.546 | 0.019 | 17.241 | 0.6 | 0.506 | 2946.44 | 33.4 | 2807.55 | 79.4 | 3043.61 | 36.44 | 2701.97 | 44.49 |
| | 3.015 | 1.932 | 0.065 | 0.209 | 0.004 | 0.332 | 0.516 | 0.018 | 14.878 | 0.517 | 0.687 | 2805.97 | 33.01 | 2680.32 | 74.46 | 2898.11 | 28.52 | 2604.4 | 38.1 |
| | 3.016 | 1.888 | 0.062 | 0.22 | 0.005 | 0.38 | 0.528 | 0.017 | 15.989 | 0.557 | 0.535 | 2874.28 | 32.78 | 2731.32 | 72.72 | 2976.41 | 33.34 | 2634.26 | 46.65 |
| | 3.017 | 1.855 | 0.063 | 0.217 | 0.005 | 0.313 | 0.538 | 0.018 | 16.057 | 0.581 | 0.585 | 2877.96 | 34.62 | 2771.71 | 76.13 | 2953.79 | 34.51 | 2698.36 | 44.61 |
| | 3.018 | 1.879 | 0.067 | 0.218 | 0.003 | 0.527 | 0.532 | 0.019 | 15.93 | 0.539 | 0.784 | 2870.91 | 32.11 | 2745.91 | 80.41 | 2961.39 | 25.3 | 2655.57 | 27.58 |
| | 3.019 | 1.895 | 0.07 | 0.223 | 0.006 | 0.272 | 0.527 | 0.02 | 16.172 | 0.686 | 0.587 | 2884.02 | 40.42 | 2725.43 | 83.45 | 2997.5 | 45.15 | 2612.85 | 56.82 |
| | 3.02 | 1.879 | 0.059 | 0.224 | 0.003 | 0.323 | 0.53 | 0.017 | 16.277 | 0.553 | 0.752 | 2891.44 | 32.61 | 2741.3 | 70.33 | 3008.13 | 24.02 | 2634.44 | 27.99 |
| | 3.021 | 1.913 | 0.064 | 0.22 | 0.004 | -0.197 | 0.521 | 0.018 | 15.791 | 0.653 | 0.789 | 2861.35 | 39.31 | 2702.13 | 74.28 | 2975.68 | 32.31 | 2595.6 | 38.34 |
| | 3.022 | 1.895 | 0.06 | 0.226 | 0.005 | 0.345 | 0.526 | 0.016 | 16.342 | 0.575 | 0.377 | 2894.94 | 33.59 | 2721.75 | 69.19 | 3017.6 | 37.19 | 2602.42 | 47.7 |
| | 3.023 | 1.861 | 0.063 | 0.215 | 0.006 | 0.448 | 0.536 | 0.018 | 15.857 | 0.566 | 0.354 | 2866.11 | 33.81 | 2764.92 | 75.33 | 2938.41 | 40.5 | 2695.56 | 53.63 |
| | 3.024 | 1.912 | 0.058 | 0.197 | 0.003 | -0.391 | 0.521 | 0.016 | 14.451 | 0.833 | 0.958 | 2772.87 | 43.8 | 2701.26 | 67.21 | 2795.38 | 27.65 | 2676.2 | 27.18 |
| | 3.025 | 1.92 | 0.063 | 0.206 | 0.004 | 0.356 | 0.519 | 0.017 | 14.702 | 0.505 | 0.553 | 2794.35 | 32.4 | 2694.4 | 71.25 | 2867.66 | 32.04 | 2632.85 | 37.36 |
| | 4.001 | 1.966 | 0.069 | 0.206 | 0.006 | 0.581 | 0.506 | 0.018 | 14.365 | 0.525 | 0.231 | 2773.24 | 34.64 | 2639.78 | 76.2 | 2871.64 | 49.54 | 2564.4 | 58.77 |
| | 4.002 | 1.796 | 0.062 | 0.252 | 0.005 | 0.465 | 0.556 | 0.019 | 19.243 | 0.648 | 0.611 | 3052.43 | 32.79 | 2846.88 | 79.08 | 3191.59 | 30.18 | 2669.64 | 45.51 |
| | 4.003 | 1.731 | 0.066 | 0.274 | 0.006 | 0.673 | 0.578 | 0.022 | 21.77 | 0.738 | 0.587 | 3171.81 | 32.52 | 2936.92 | 90.15 | 3325.87 | 36.39 | 2700.33 | 53.45 |
| | 4.004 | 1.801 | 0.055 | 0.262 | 0.007 | 0.454 | 0.55 | 0.019 | 19.802 | 0.745 | 0.454 | 3079.49 | 36.19 | 2822.44 | 81.49 | 3252.44 | 42.18 | 2623.71 | 65.79 |
| | 4.005 | 1.744 | 0.06 | 0.249 | 0.006 | 0.56 | 0.572 | 0.019 | 19.627 | 0.67 | 0.407 | 3071.31 | 33.13 | 2915.16 | 79.91 | 3175.77 | 38.18 | 2774.94 | 50.73 |
| | 4.006 | 1.752 | 0.063 | 0.249 | 0.007 | 0.149 | 0.57 | 0.021 | 19.558 | 0.887 | 0.596 | 3064.96 | 42.32 | 2906.25 | 84.29 | 3171.44 | 46.36 | 2759.9 | 59.82 |
| | 4.007 | 1.759 | 0.066 | 0.241 | 0.007 | 0.361 | 0.568 | 0.021 | 18.868 | 0.778 | 0.586 | 3031.27 | 39.63 | 2898.2 | 87.76 | 3122.11 | 44.62 | 2778.08 | 59.06 |
| | 4.008 | 1.932 | 0.067 | 0.21 | 0.006 | -0.249 | 0.513 | 0.02 | 14.85 | 0.791 | 0.817 | 2799.33 | 50.05 | 2665.48 | 86.21 | 2898.52 | 44.04 | 2601.01 | 57.29 |
| | 4.009 | 1.856 | 0.085 | 0.231 | 0.007 | 0.367 | 0.532 | 0.019 | 17.111 | 0.76 | 0.611 | 2938.26 | 41.43 | 2775.41 | 107.13 | 3052.99 | 48.06 | 2646.47 | 64.75 |
| | 4.01 | 1.869 | 0.065 | 0.22 | 0.004 | 0.393 | 0.534 | 0.018 | 16.165 | 0.549 | 0.668 | 2884.9 | 32.74 | 2757.74 | 76.23 | 2975.76 | 28.33 | 2664.62 | 36.54 |
| | 4.011 | 1.9 | 0.065 | 0.199 | 0.003 | 0.143 | 0.526 | 0.019 | 14.404 | 0.536 | 0.805 | 2774.25 | 35.06 | 2722.8 | 78.31 | 2813.07 | 25.67 | 2688.39 | 26.95 |
| | 4.012 | 1.885 | 0.065 | 0.211 | 0.004 | 0.215 | 0.53 | 0.018 | 15.373 | 0.549 | 0.732 | 2836.5 | 33.79 | 2738.41 | 75.31 | 2907.77 | 27.09 | 2670.56 | 36.39 |
| | 4.013 | 1.876 | 0.071 | 0.23 | 0.006 | 0.492 | 0.532 | 0.021 | 16.883 | 0.625 | 0.585 | 2926.73 | 35.61 | 2750.15 | 86.23 | 3051.36 | 39.21 | 2618.04 | 56.62 |
| | 4.014 | 1.803 | 0.067 | 0.218 | 0.005 | 0.352 | 0.554 | 0.02 | 16.611 | 0.625 | 0.634 | 2910.36 | 35.81 | 2841.47 | 83.63 | 2959.42 | 35.38 | 2785.12 | 41.98 |
| | 4.015 | 1.888 | 0.064 | 0.227 | 0.005 | 0.51 | 0.529 | 0.017 | 16.542 | 0.566 | 0.368 | 2906.9 | 32.41 | 2735.85 | 73.84 | 3028.03 | 38.07 | 2609.78 | 47.45 |
| | 4.016 | 1.94 | 0.067 | 0.202 | 0.005 | 0.016 | 0.514 | 0.018 | 14.291 | 0.615 | 0.665 | 2767.65 | 40.72 | 2672.03 | 76.91 | 2837.93 | 41.21 | 2616.01 | 47.25 |
| | 4.017 | 1.89 | 0.062 | 0.197 | 0.004 | 0.305 | 0.528 | 0.017 | 14.308 | 0.495 | 0.568 | 2768.53 | 32.89 | 2733.05 | 72.46 | 2794.82 | 31.93 | 2711.57 | 35.36 |
| | 4.018 | 1.948 | 0.079 | 0.186 | 0.003 | 0.108 | 0.513 | 0.021 | 13.171 | 0.576 | 0.871 | 2689.76 | 40.45 | 2668.67 | 89.35 | 2706.79 | 28.16 | 2657.66 | 27.54 |
| | 4.019 | 1.876 | 0.071 | 0.201 | 0.003 | 0.362 | 0.534 | 0.02 | 14.688 | 0.509 | 0.839 | 2793.4 | 32.13 | 2754.73 | 84.2 | 2835.36 | 25.19 | 2720.54 | 26.35 |
| | 4.02 | 1.796 | 0.076 | 0.256 | 0.008 | 0.061 | 0.551 | 0.018 | 19.651 | 0.917 | 0.612 | 3070.59 | 44.77 | 2828.56 | 74.56 | 3218.4 | 47.62 | 2654.62 | 73.59 |
| | 4.021 | 1.965 | 0.069 | 0.187 | 0.003 | 0.462 | 0.509 | 0.018 | 13.124 | 0.442 | 0.709 | 2687.04 | 31.85 | 2649.9 | 75.95 | 2716.26 | 27.71 | 2628.71 | 28.1 |
| | 4.022 | 1.767 | 0.059 | 0.256 | 0.006 | -0.046 | 0.566 | 0.019 | 19.757 | 0.766 | 0.679 | 3076.51 | 37.03 | 2888.59 | 78.35 | 3216.65 | 39.16 | 2705.31 | 53.27 |
| | 4.023 | 1.783 | 0.083 | 0.227 | 0.007 | 0.182 | 0.56 | 0.026 | 17.504 | 0.917 | 0.693 | 2960.75 | 50.73 | 2866.83 | 106.98 | 3025.73 | 54 | 2787.55 | 58.67 |
| | 4.024 | 1.883 | 0.061 | 0.214 | 0.005 | 0.24 | 0.53 | 0.018 | 15.601 | 0.599 | 0.463 | 2851.1 | 36.43 | 2740.32 | 73.58 | 2930.13 | 41.01 | 2663.24 | 45.72 |
| | 4.025 | 1.703 | 0.072 | 0.292 | 0.012 | -0.228 | 0.59 | 0.025 | 23.805 | 1.479 | 0.721 | 3247.38 | 65.15 | 2985.5 | 100.79 | 3433.41 | 59.02 | 2680.04 | 108.44 |

Continued on next page

| Sample | Spot name | 238/206 | ±2σ | 207/206 | ±2σ | Err. Corr | 207/235 | ±2σ | 206/238 | ±2σ | Err. Corr | 207/235 Age | ±2σ | 206/238. | ±2σ | 207/206 Age | ±2σ | 207/206* Age | ±2σ |
|---|---|---|---|---|---|---|---|---|---|---|---|---|---|---|---|---|---|---|---|
| | 5.001 | 1.849 | 0.058 | 0.217 | 0.005 | 0.439 | 0.54 | 0.017 | 16.225 | 0.57 | 0.308 | 2888.22 | 32.8 | 2783.09 | 71.52 | 2962.3 | 39.18 | 2708.41 | 44.29 |
| | 5.002 | 1.839 | 0.082 | 0.217 | 0.013 | 0.513 | 0.543 | 0.024 | 16.201 | 0.94 | 0.098 | 2886.85 | 56.32 | 2793.4 | 99.14 | 2952.21 | 96.54 | 2725.38 | 113.81 |
| | 5.003 | 1.824 | 0.06 | 0.237 | 0.007 | -0.041 | 0.548 | 0.018 | 17.862 | 0.797 | 0.543 | 2977.46 | 42.86 | 2814.45 | 74.08 | 3089.16 | 47.94 | 2677.66 | 63.36 |
| | 5.004 | 1.754 | 0.075 | 0.264 | 0.006 | 0.325 | 0.57 | 0.024 | 20.749 | 0.908 | 0.739 | 3125.42 | 41.31 | 2905.76 | 99.38 | 3270.33 | 37.85 | 2697.71 | 53.55 |
| | 5.005 | 1.871 | 0.063 | 0.215 | 0.004 | 0.392 | 0.534 | 0.018 | 15.823 | 0.53 | 0.691 | 2864.54 | 31.84 | 2759.02 | 74.73 | 2940.37 | 26.49 | 2679.12 | 36.17 |
| | 5.006 | 1.865 | 0.059 | 0.214 | 0.004 | 0.282 | 0.536 | 0.017 | 15.753 | 0.539 | 0.504 | 2860.15 | 32.83 | 2763.81 | 69.95 | 2928.7 | 32.15 | 2692.52 | 35.83 |
| | 5.007 | 1.862 | 0.063 | 0.214 | 0.004 | 0.381 | 0.537 | 0.018 | 15.813 | 0.541 | 0.646 | 2863.83 | 32.7 | 2770.25 | 75.91 | 2931.08 | 29.47 | 2697.48 | 35.71 |
| | 5.008 | 1.837 | 0.065 | 0.218 | 0.004 | 0.174 | 0.545 | 0.019 | 16.347 | 0.613 | 0.72 | 2894.66 | 36.46 | 2802.1 | 79.44 | 2960.67 | 30.77 | 2725.15 | 35.02 |
| | 5.009 | 1.883 | 0.065 | 0.213 | 0.004 | 0.127 | 0.532 | 0.018 | 15.59 | 0.583 | 0.628 | 2856.84 | 40.43 | 2746.4 | 76.43 | 2936.18 | 38.44 | 2666.75 | 36.48 |
| | 5.01 | 1.946 | 0.1 | 0.201 | 0.008 | -0.68 | 0.512 | 0.025 | 13.968 | 0.866 | 0.906 | 2738.75 | 53.16 | 2660.23 | 102 | 2851.15 | 86.17 | 2610.38 | 75.89 |
| | 5.011 | 1.821 | 0.059 | 0.221 | 0.005 | 0.535 | 0.549 | 0.018 | 16.732 | 0.548 | 0.469 | 2918.19 | 31.5 | 2820.94 | 74.97 | 2986.41 | 33.32 | 2741.83 | 43.27 |
| | 5.012 | 1.888 | 0.067 | 0.217 | 0.004 | 0.449 | 0.531 | 0.019 | 15.816 | 0.55 | 0.657 | 2863.83 | 32.92 | 2742.21 | 78.19 | 2951.67 | 30.9 | 2644.75 | 37.05 |
| | 5.013 | 1.851 | 0.062 | 0.218 | 0.004 | 0.303 | 0.541 | 0.018 | 16.217 | 0.566 | 0.716 | 2887.71 | 33.91 | 2785.02 | 76.54 | 2960.9 | 28.28 | 2701.44 | 35.61 |
| | 5.014 | 1.911 | 0.072 | 0.221 | 0.005 | 0.342 | 0.525 | 0.02 | 15.949 | 0.618 | 0.678 | 2870.78 | 36.42 | 2718.27 | 83.47 | 2981.38 | 35.1 | 2595.21 | 47.94 |
| | 5.015 | 1.86 | 0.061 | 0.22 | 0.004 | 0.3 | 0.539 | 0.018 | 16.342 | 0.569 | 0.574 | 2895.03 | 34.04 | 2776.26 | 73.95 | 2979.1 | 32.34 | 2679.32 | 36.16 |
| | 5.016 | 1.928 | 0.063 | 0.198 | 0.003 | 0.236 | 0.52 | 0.017 | 14.18 | 0.474 | 0.74 | 2760.31 | 31.71 | 2696.23 | 71.12 | 2807.97 | 23.38 | 2647.81 | 27.73 |
| | 5.017 | 1.917 | 0.069 | 0.195 | 0.003 | 0.522 | 0.52 | 0.016 | 14.058 | 0.442 | 0.74 | 2752.58 | 29.7 | 2697.13 | 69.02 | 2785.21 | 22.72 | 2675.19 | 27.2 |
| | 5.018 | 1.919 | 0.07 | 0.201 | 0.004 | -0.296 | 0.523 | 0.019 | 14.641 | 0.708 | 0.84 | 2786.52 | 43.86 | 2711.44 | 81.76 | 2832.4 | 29.53 | 2651.5 | 36.87 |
| | 5.019 | 1.966 | 0.065 | 0.196 | 0.003 | 0.33 | 0.51 | 0.017 | 13.8 | 0.469 | 0.718 | 2734.43 | 32.09 | 2654.78 | 72.64 | 2794.52 | 26.23 | 2597.46 | 28.72 |
| | 5.02 | 1.798 | 0.061 | 0.228 | 0.005 | 0.37 | 0.557 | 0.019 | 17.514 | 0.637 | 0.453 | 2961.11 | 34.63 | 2854.67 | 77.42 | 3034.68 | 38.45 | 2756.43 | 42.83 |
| | 5.021 | 1.881 | 0.059 | 0.212 | 0.004 | 0.342 | 0.533 | 0.017 | 15.526 | 0.515 | 0.564 | 2846.53 | 31.62 | 2751.21 | 70.44 | 2914.91 | 28.97 | 2673.49 | 36.31 |
| | 5.022 | 1.897 | 0.063 | 0.209 | 0.004 | -0.215 | 0.528 | 0.017 | 15.258 | 0.599 | 0.822 | 2829.15 | 37.71 | 2732.23 | 73.77 | 2899.12 | 28.2 | 2658.41 | 36.7 |
| | 5.023 | 1.831 | 0.052 | 0.236 | 0.005 | -0.132 | 0.544 | 0.018 | 17.685 | 0.692 | 0.744 | 2969.6 | 38.19 | 2799.81 | 75.15 | 3087.12 | 30.58 | 2669.56 | 45.51 |
| | 5.024 | 1.927 | 0.066 | 0.204 | 0.005 | 0.243 | 0.517 | 0.016 | 14.498 | 0.488 | 0.451 | 2787.27 | 37.19 | 2697.08 | 77.4 | 2853.14 | 36.64 | 2628.94 | 46.82 |
| | 5.025 | 1.861 | 0.071 | 0.211 | 0.003 | 0.695 | 0.54 | 0.021 | 15.657 | 0.518 | 0.807 | 2854.6 | 31.51 | 2782.82 | 86.74 | 2907.98 | 26.86 | 2709.88 | 26.55 |
| ZLC32 | 1.001 | 1.969 | 0.098 | 0.21 | 0.01 | 0.699 | 0.508 | 0.026 | 14.658 | 0.664 | 0.304 | 2792.08 | 43.02 | 2648.71 | 109.82 | 2897.98 | 79.07 | 2546.89 | 99.15 |
| | 1.002 | 1.48 | 0.066 | 0.409 | 0.039 | -0.164 | 0.676 | 0.029 | 38.234 | 4.166 | 0.478 | 3712.46 | 108.35 | 3328.44 | 113.51 | 3925.34 | 140.9 | 2607.98 | 370.59 |
| | 1.003 | 0.757 | 0.073 | 0.716 | 0.06 | 0.384 | 1.431 | 0.163 | 136.974 | 14.341 | 0.66 | 4960.64 | 107.96 | 5626.31 | 400.45 | 4598.3 | 117.75 | 2906.58 | 462.49 |
| | 1.005 | 0.662 | 0.089 | 0.835 | 0.085 | 0.077 | 1.751 | 0.284 | 184.559 | 26.813 | 0.754 | 5273.7 | 169.75 | 6311.35 | 603.43 | 4649.97 | 132.02 | 39.27 | 4343.14 |
| | 1.006 | 0.701 | 0.114 | 0.775 | 0.063 | 0.41 | 1.704 | 0.277 | 177.374 | 27.573 | 0.797 | 5163.73 | 161.1 | 6143.48 | 659.57 | 4626.41 | 125.81 | 2084.45 | 858.77 |
| | 1.007 | 0.786 | 0.08 | 0.726 | 0.046 | 0.274 | 1.342 | 0.149 | 133.058 | 15.146 | 0.902 | 4955.9 | 119.2 | 5399.41 | 377.57 | 4685.73 | 78.35 | 2458.4 | 484.97 |
| | 1.009 | 0.808 | 0.083 | 0.664 | 0.034 | -0.386 | 1.305 | 0.137 | 117.502 | 14.244 | 0.888 | 4848.43 | 142.28 | 5324.29 | 377.65 | 4643.23 | 73.67 | 3403.33 | 184.1 |
| | 1.01 | 1.555 | 0.107 | 0.408 | 0.028 | -0.043 | 0.651 | 0.042 | 36.703 | 3.715 | 0.658 | 3667.67 | 93.96 | 3225.97 | 164.21 | 3922.87 | 102.47 | 2458.38 | 295.2 |
| | 1.011 | 0.995 | 0.095 | 0.598 | 0.046 | -0.666 | 1.039 | 0.1 | 87.366 | 13.433 | 0.94 | 4500.01 | 159.17 | 4562.2 | 313.49 | 4482.23 | 114.52 | 2879.86 | 361.31 |
| | 1.012 | 1.849 | 0.069 | 0.231 | 0.007 | 0.144 | 0.543 | 0.021 | 17.257 | 0.802 | 0.65 | 2944.12 | 43.2 | 2791.62 | 86.96 | 3051.46 | 46.34 | 2657.89 | 64.24 |
| | 1.013 | 1.912 | 0.082 | 0.207 | 0.01 | -0.397 | 0.525 | 0.023 | 15.047 | 1.124 | 0.793 | 2808.85 | 68.59 | 2716.09 | 98.06 | 2876.38 | 73.09 | 2641.79 | 92.81 |
| | 1.014 | 1.868 | 0.081 | 0.22 | 0.012 | -0.216 | 0.536 | 0.024 | 16.254 | 1.281 | 0.687 | 2885.16 | 74.24 | 2763.68 | 100.03 | 2970.59 | 91.1 | 2666.24 | 109.49 |
| | 1.015 | 1.915 | 0.087 | 0.215 | 0.011 | 0.359 | 0.524 | 0.023 | 15.204 | 0.703 | 0.287 | 2839.87 | 56.02 | 2713.62 | 97.13 | 2931.47 | 81.05 | 2609.71 | 104.4 |
| | 2.001 | 1.439 | 0.107 | 0.345 | 0.026 | 0.325 | 0.69 | 0.043 | 33.439 | 3.107 | 0.504 | 3609.84 | 104.15 | 3443.91 | 222.28 | 3709.54 | 144.16 | 3045.88 | 181.63 |
| | 2.005 | 1.473 | 0.1 | 0.387 | 0.023 | 0.359 | 0.697 | 0.054 | 36.86 | 2.821 | 0.708 | 3673.04 | 77.92 | 3391.42 | 196.7 | 3840.69 | 88.32 | 2734.33 | 200.09 |
| | 2.006 | 1.584 | 0.076 | 0.303 | 0.024 | 0.507 | 0.631 | 0.031 | 26.254 | 1.888 | -0.001 | 3353.05 | 67.59 | 3152.09 | 120.7 | 3475.1 | 115.21 | 2878.93 | 188.64 |
| | 2.008 | 1.873 | 0.065 | 0.233 | 0.007 | -0.29 | 0.535 | 0.019 | 17.19 | 0.848 | 0.743 | 2939.16 | 47.41 | 2758.99 | 78.92 | 3065.24 | 45.96 | 2612.18 | 66.32 |
| | 2.009 | 1.978 | 0.067 | 0.196 | 0.004 | 0.325 | 0.506 | 0.017 | 13.664 | 0.486 | 0.606 | 2724.64 | 33.87 | 2636.81 | 73.73 | 2791.13 | 33.12 | 2580.05 | 38.76 |
| | 2.01 | 1.921 | 0.069 | 0.206 | 0.004 | -0.082 | 0.522 | 0.02 | 14.96 | 0.749 | 0.713 | 2806.61 | 45.38 | 2704.16 | 83.33 | 2866.63 | 33.66 | 2631.32 | 37.4 |
| | 2.011 | 1.912 | 0.075 | 0.216 | 0.008 | 0.089 | 0.52 | 0.018 | 15.56 | 0.765 | 0.455 | 2844.02 | 46.41 | 2697.93 | 75.79 | 2937.86 | 58.2 | 2610.86 | 75.87 |
| | 2.012 | 1.922 | 0.058 | 0.193 | 0.004 | 0.222 | 0.519 | 0.016 | 13.843 | 0.483 | 0.49 | 2737.12 | 32.89 | 2695.89 | 66.99 | 2767.39 | 33.77 | 2674.18 | 36.29 |
| | 2.015 | 1.282 | 0.079 | 0.484 | 0.025 | 0.083 | 0.789 | 0.052 | 52.565 | 4.093 | 0.713 | 4030.01 | 78.97 | 3739.39 | 184.86 | 4182.75 | 77.12 | 2690.16 | 224.32 |
| | 3.001 | 1.903 | 0.123 | 0.237 | 0.02 | -0.529 | 0.528 | 0.039 | 17.366 | 2.482 | 0.867 | 2937.06 | 127.51 | 2730.41 | 161.54 | 3082.89 | 134.85 | 2552.13 | 197.58 |
| | 3.002 | 1.653 | 0.098 | 0.293 | 0.02 | -0.432 | 0.607 | 0.04 | 24.64 | 2.825 | 0.843 | 3281.73 | 106.89 | 3055.27 | 157.28 | 3424.37 | 107.53 | 2773.42 | 169.29 |
| | 3.003 | 1.94 | 0.066 | 0.198 | 0.005 | 0.524 | 0.516 | 0.018 | 14.04 | 0.49 | 0.442 | 2750.48 | 33.35 | 2678.52 | 76.49 | 2804.52 | 40.34 | 2629.48 | 46.8 |
| | 3.004 | 1.735 | 0.078 | 0.251 | 0.009 | -0.41 | 0.577 | 0.026 | 20.53 | 1.716 | 0.719 | 3104.38 | 77.42 | 2935.65 | 104.54 | 3215.47 | 84.05 | 2784.15 | 75.61 |
| | 3.005 | 1.68 | 0.08 | 0.296 | 0.018 | -0.433 | 0.601 | 0.03 | 24.779 | 2.332 | 0.781 | 3270.61 | 88.31 | 3028 | 119.18 | 3424.49 | 93.65 | 2707.24 | 159.59 |
| | 3.006 | 1.512 | 0.122 | 0.371 | 0.033 | -0.732 | 0.67 | 0.057 | 34.784 | 5.632 | 0.925 | 3600.11 | 155.29 | 3297.02 | 216.86 | 3777.43 | 133.75 | 2722.81 | 289.41 |
| | 3.007 | 0.68 | 0.062 | 0.715 | 0.04 | -0.251 | 1.512 | 0.123 | 149.578 | 14.776 | 0.835 | 5066.43 | 112.24 | 5903.51 | 324.5 | 4709.28 | 56.91 | 5830.5 | 35.87 |

Continued on next page

| Sample | Spot name | 238/206 | ±2σ | 207/206 | ±2σ | Err. Corr | 207/235 | ±2σ | 206/238 | ±2σ | Err. Corr | 207/235 Age | ±2σ | 206/238 Age | ±2σ | 207/206 Age | ±2σ | 207/206* Age | ±2σ |
|---|---|---|---|---|---|---|---|---|---|---|---|---|---|---|---|---|---|---|---|
| | 3.008 | 1.782 | 0.086 | 0.275 | 0.019 | -0.16 | 0.562 | 0.027 | 21.342 | 1.939 | 0.569 | 3143.12 | 82.03 | 2873.82 | 112.51 | 3320.06 | 100.66 | 2606.71 | 180.7 |
| | 3.009 | 0.875 | 0.095 | 0.621 | 0.043 | -0.661 | 1.193 | 0.139 | 104.025 | 16.95 | 0.953 | 4673.39 | 167.49 | 5015.52 | 392.38 | 4541.08 | 105.59 | 3459.72 | 223.6 |
| | 3.012 | 0.775 | 0.07 | 0.685 | 0.089 | 0.587 | 1.322 | 0.131 | 120.981 | 14.628 | 0.271 | 4824.42 | 113.66 | 5453.57 | 399.08 | 4396.44 | 177.18 | 3371.12 | 493.17 |
| | 3.014 | 1.102 | 0.096 | 0.54 | 0.046 | 0.464 | 0.952 | 0.08 | 69.175 | 6.18 | 0.49 | 4288.29 | 88.02 | 4273.3 | 262.7 | 4287.97 | 116.19 | 2916.89 | 352.01 |
| | 3.015 | 1.417 | 0.122 | 0.459 | 0.033 | 0.274 | 0.739 | 0.06 | 46.114 | 4.431 | 0.594 | 3878.39 | 96.54 | 3539.09 | 223.09 | 4074.95 | 117.04 | 2490.78 | 340.19 |
| | 4.001 | 1.854 | 0.064 | 0.215 | 0.007 | -0.083 | 0.539 | 0.018 | 15.952 | 0.925 | 0.7 | 2864.02 | 55.36 | 2778.08 | 74.49 | 2946.07 | 57.44 | 2707.22 | 62.06 |
| | 4.002 | 1.828 | 0.07 | 0.23 | 0.006 | 0.051 | 0.544 | 0.018 | 17.134 | 0.678 | 0.65 | 2939.26 | 37.29 | 2812.66 | 87.83 | 3044.37 | 43.97 | 2696.59 | 53.59 |
| | 4.003 | 1.844 | 0.073 | 0.217 | 0.009 | 0.36 | 0.542 | 0.02 | 16.213 | 0.78 | 0.322 | 2886.06 | 44.9 | 2790.69 | 84.79 | 2953.27 | 63.81 | 2716.86 | 79.26 |
| | 4.004 | 1.962 | 0.067 | 0.194 | 0.005 | 0.016 | 0.51 | 0.018 | 13.608 | 0.589 | 0.444 | 2718.84 | 39.17 | 2654.15 | 74.85 | 2767.85 | 41.49 | 2609.96 | 47.45 |
| | 4.005 | 2.016 | 0.069 | 0.187 | 0.003 | 0.205 | 0.496 | 0.016 | 12.773 | 0.456 | 0.696 | 2660.98 | 33.62 | 2594.25 | 70.83 | 2712.65 | 29.4 | 2555.5 | 29.57 |
| | 4.006 | 2.014 | 0.068 | 0.192 | 0.005 | 0.475 | 0.496 | 0.017 | 13.077 | 0.48 | 0.285 | 2683 | 33.8 | 2596.56 | 71.48 | 2748.95 | 45.57 | 2542.28 | 49.73 |
| | 4.007 | 1.956 | 0.077 | 0.215 | 0.007 | -0.156 | 0.513 | 0.021 | 15.257 | 0.862 | 0.753 | 2822.68 | 51.71 | 2666.68 | 86.96 | 2937.39 | 53.66 | 2548.95 | 69.31 |
| | 4.008 | 1.68 | 0.075 | 0.275 | 0.012 | -0.21 | 0.592 | 0.023 | 22.437 | 1.258 | 0.741 | 3193.26 | 55.11 | 2994.64 | 93.7 | 3339.28 | 76.01 | 2794.52 | 100.08 |
| | 4.009 | 1.893 | 0.067 | 0.206 | 0.007 | -0.142 | 0.529 | 0.019 | 15.055 | 0.813 | 0.671 | 2811.31 | 48.79 | 2734.77 | 80.99 | 2866.85 | 54.59 | 2675.23 | 63.47 |
| | 4.01 | 1.93 | 0.078 | 0.207 | 0.008 | -0.121 | 0.52 | 0.021 | 14.903 | 0.929 | 0.678 | 2798.89 | 54.51 | 2697.53 | 89.86 | 2873.87 | 61.83 | 2614.2 | 75.69 |
| | 4.011 | 1.929 | 0.062 | 0.192 | 0.007 | -0.699 | 0.518 | 0.017 | 13.755 | 0.778 | 0.895 | 2725.01 | 48.42 | 2689.62 | 70.96 | 2750.21 | 55.56 | 2666.66 | 63.85 |
| | 4.012 | 1.894 | 0.061 | 0.209 | 0.006 | 0.431 | 0.528 | 0.017 | 15.154 | 0.552 | 0.311 | 2822.62 | 34.52 | 2730.48 | 73.14 | 2889.24 | 43.15 | 2663.17 | 54.86 |
| | 4.013 | 1.907 | 0.081 | 0.22 | 0.009 | -0.482 | 0.522 | 0.02 | 16.077 | 1.15 | 0.834 | 2866.03 | 65.07 | 2705.09 | 84.15 | 2967.92 | 66.54 | 2604.75 | 85.71 |
| | 4.014 | 1.921 | 0.079 | 0.215 | 0.011 | 0.231 | 0.523 | 0.022 | 15.272 | 0.808 | 0.41 | 2836.44 | 55.38 | 2708.84 | 91.36 | 2929.11 | 76.62 | 2600.59 | 105.06 |
| | 4.015 | 1.983 | 0.062 | 0.193 | 0.003 | 0.253 | 0.504 | 0.016 | 13.395 | 0.454 | 0.553 | 2706.27 | 32.11 | 2628.93 | 67.62 | 2764.58 | 30.61 | 2582.68 | 29.01 |
| | 4.016 | 1.993 | 0.081 | 0.204 | 0.007 | 0.332 | 0.503 | 0.02 | 14.14 | 0.629 | 0.526 | 2755.84 | 41.95 | 2623.29 | 85.22 | 2855.43 | 52.15 | 2532.71 | 70.09 |
| | 4.017 | 1.875 | 0.068 | 0.202 | 0.006 | 0.44 | 0.535 | 0.02 | 14.833 | 0.57 | 0.504 | 2801.72 | 37.09 | 2758.53 | 84.02 | 2834.24 | 44.88 | 2718.65 | 52.77 |
| | 4.018 | 1.849 | 0.052 | 0.209 | 0.006 | 0.002 | 0.537 | 0.017 | 15.521 | 0.662 | 0.573 | 2843.75 | 39.67 | 2783.22 | 63.2 | 2895.17 | 42.9 | 2737.35 | 52.09 |
| | 4.019 | 1.863 | 0.062 | 0.221 | 0.007 | -0.104 | 0.537 | 0.018 | 16.402 | 0.805 | 0.634 | 2894.5 | 46 | 2769.52 | 76.36 | 2982.39 | 51.53 | 2670.83 | 63.66 |
| | 4.02 | 1.756 | 0.078 | 0.24 | 0.009 | 0.063 | 0.567 | 0.022 | 18.946 | 1.067 | 0.658 | 3029.85 | 53.64 | 2890.82 | 89.3 | 3108.58 | 59.72 | 2787.63 | 75.43 |
| | 5.001 | 1.964 | 0.069 | 0.18 | 0.003 | 0.28 | 0.509 | 0.017 | 12.536 | 0.416 | 0.655 | 2643.95 | 31.06 | 2652.53 | 73.01 | 2648.48 | 30.15 | 2653.4 | 27.62 |
| | 5.002 | 1.957 | 0.064 | 0.181 | 0.003 | 0.118 | 0.511 | 0.016 | 12.767 | 0.451 | 0.697 | 2660.62 | 33.42 | 2658.37 | 70.32 | 2662.62 | 28.23 | 2660.67 | 27.48 |
| | 5.003 | 1.934 | 0.065 | 0.18 | 0.003 | 0.435 | 0.517 | 0.017 | 12.822 | 0.423 | 0.68 | 2665.18 | 30.98 | 2686.04 | 72.7 | 2650.07 | 27.22 | 2700 | 26.73 |
| | 5.004 | 1.876 | 0.063 | 0.184 | 0.004 | -0.174 | 0.533 | 0.018 | 13.492 | 0.546 | 0.856 | 2711.56 | 36.81 | 2754.19 | 76.13 | 2686.79 | 38.08 | 2782.6 | 33.64 |
| | 5.005 | 1.91 | 0.097 | 0.19 | 0.004 | 0.281 | 0.524 | 0.025 | 13.739 | 0.671 | 0.843 | 2729.84 | 46.41 | 2715.68 | 107.76 | 2741.75 | 37.52 | 2703.52 | 35.56 |
| | 5.006 | 1.906 | 0.07 | 0.182 | 0.004 | 0.507 | 0.524 | 0.018 | 13.13 | 0.454 | 0.552 | 2688.05 | 32.77 | 2716.34 | 77.6 | 2667.07 | 36.12 | 2738.54 | 34.7 |
| | 5.007 | 1.904 | 0.064 | 0.177 | 0.003 | 0.307 | 0.526 | 0.018 | 12.806 | 0.446 | 0.76 | 2663.62 | 32.98 | 2721.21 | 76.3 | 2621.12 | 26.55 | 2761.84 | 25.6 |
| | 5.008 | 1.931 | 0.065 | 0.178 | 0.003 | 0.466 | 0.518 | 0.018 | 12.719 | 0.412 | 0.743 | 2658.04 | 30.93 | 2688.89 | 74.96 | 2635.27 | 24.22 | 2712.22 | 26.51 |
| | 5.01 | 1.932 | 0.061 | 0.182 | 0.003 | 0.036 | 0.517 | 0.016 | 12.954 | 0.451 | 0.742 | 2674.47 | 32.64 | 2686.4 | 68.99 | 2665.59 | 25.46 | 2696.07 | 26.81 |
| | 5.011 | 1.949 | 0.067 | 0.177 | 0.003 | 0.436 | 0.514 | 0.018 | 12.546 | 0.43 | 0.777 | 2644.47 | 31.91 | 2671.31 | 77.58 | 2625.39 | 25.59 | 2686.98 | 26.98 |
| | 5.012 | 1.94 | 0.067 | 0.182 | 0.004 | 0.345 | 0.516 | 0.018 | 12.943 | 0.47 | 0.602 | 2673.25 | 33.92 | 2680.31 | 74.88 | 2668.6 | 35.46 | 2683.47 | 36.06 |
| | 5.013 | 1.886 | 0.071 | 0.186 | 0.003 | 0.186 | 0.532 | 0.02 | 13.62 | 0.545 | 0.794 | 2720.42 | 37.75 | 2747.23 | 84.83 | 2702.36 | 30.85 | 2757.37 | 25.68 |
| | 5.014 | 1.987 | 0.063 | 0.181 | 0.002 | 0.408 | 0.503 | 0.016 | 12.547 | 0.389 | 0.702 | 2649.53 | 25.21 | 2625.38 | 67.14 | 2660.73 | 21.92 | 2616.06 | 18.9 |
| | 5.015 | 1.879 | 0.072 | 0.185 | 0.004 | 0.204 | 0.533 | 0.021 | 13.609 | 0.57 | 0.781 | 2720.33 | 39 | 2752.71 | 88.24 | 2697.62 | 34.09 | 2773.33 | 33.86 |
| | 5.016 | 1.912 | 0.064 | 0.183 | 0.004 | 0.074 | 0.523 | 0.018 | 13.237 | 0.51 | 0.716 | 2693.94 | 35.69 | 2712.13 | 74.6 | 2680.84 | 32.32 | 2724.84 | 35.03 |
| | 5.017 | 1.916 | 0.067 | 0.186 | 0.005 | -0.027 | 0.523 | 0.018 | 13.401 | 0.59 | 0.699 | 2703.9 | 40.94 | 2709.54 | 77.31 | 2700.15 | 41.84 | 2707.69 | 44.32 |
| | 5.018 | 1.978 | 0.081 | 0.177 | 0.005 | 0.309 | 0.506 | 0.02 | 12.337 | 0.541 | 0.594 | 2628.48 | 40.15 | 2638 | 86.37 | 2621.68 | 47.44 | 2642.42 | 46.38 |
| | 5.019 | 1.924 | 0.104 | 0.182 | 0.005 | 0.451 | 0.521 | 0.026 | 13.038 | 0.615 | 0.76 | 2680.3 | 45.91 | 2703.18 | 113.37 | 2665.05 | 47.88 | 2708.89 | 44.28 |

# C.4 Dioctahedral (White) mica Rb–Sr data

| Sample | Spot name | Rb ppm | Sr | $^{87}Rb/^{87}Sr$ | ±2SE (%) | $^{87}Rb/^{86}Sr$ | ±2SE (%) | $^{87}Sr/^{86}Sr$ | ±2SE (%) | $\rho$ |
|---|---|---|---|---|---|---|---|---|---|---|
| Z6007 | Fs-1 | 15.8 | 35 | 2.08 | 6.2 | 0 | 6.6 | 0.7302 | 0.72 | 0.33 |
| | Fs-2 | 24 | 30 | 2.11 | 4.5 | 0 | 4.3 | 1.232 | 1.5 | 0.036 |
| | Fs-3 | 1.04 | 10 | 0.278 | 22 | 0 | 22 | 1.942 | 1.2 | 0.02 |
| | Fs-5 | 1.15 | 4.1 | 0.79 | 23 | 0 | 23 | 1.746 | 2 | 0.18 |
| | Fs-6 | 18.5 | 4.7 | 6.5 | 14 | 0 | 15 | 1.982 | 2.6 | 0.43 |
| | Fs-7 | 0.688 | 7.5 | 0.33 | 14 | 0 | 13 | 1.659 | 1.3 | 0.028 |
| | Fs-8 | 0.556 | 14 | 0.1759 | 4 | 0 | 4.1 | 1.712 | 0.82 | 0.13 |
| | Fs-9 | 25.7 | 4 | 8.2 | 13 | 0 | 13 | 2.535 | 1.5 | 0.071 |
| | Mc-1 | 7510 | 0.065 | 28.8 | 3.7 | 288200 | 9.8 | 12400 | 9.1 | 0.98 |
| | Mc-2 | 7350 | 0.24 | 30.26 | 2.5 | 81500 | 10 | 3410 | 10 | 0.95 |
| | Mc-3 | 9520 | 0.068 | 30.45 | 0.91 | 364300 | 7.2 | 15000 | 7.4 | 0.99 |
| | Mc-4 | 8740 | 0.19 | 31.3 | 0.93 | 119800 | 5.7 | 4780 | 5.8 | 0.99 |
| | Mc-5 | 8190 | 0.1 | 29.39 | 3.2 | 208200 | 6.5 | 8920 | 7.5 | 0.87 |
| | Mc-6 | 9980 | 0.087 | 30.97 | 1.2 | 286800 | 4.6 | 11570 | 4.5 | 0.97 |
| | Mc-7 | 5070 | 0.32 | 32.24 | 0.82 | 40280 | 4.6 | 1562 | 4.8 | 0.98 |
| | Mc-8 | 7870 | 0.079 | 29.85 | 3.3 | 276600 | 29 | 11500 | 28 | 1 |
| | Mc-9 | 9210 | 0.18 | 30.46 | 0.79 | 139700 | 9.9 | 5740 | 10 | 1 |
| | Fs-10 | 75.3 | 18 | 7.23 | 6.8 | 0 | 10 | 1.795 | 1.7 | 0.38 |
| | Fs-11 | 53.2 | 13 | 7.15 | 9.2 | 0 | 9.5 | 1.775 | 1.5 | 0.36 |
| | Fs-12 | 0.788 | 8.6 | 0.431 | 4 | 0 | 4.1 | 1.214 | 0.97 | 0.26 |
| | Fs-13 | 4.12 | 15 | 0.79 | 18 | 0 | 19 | 1.267 | 1.2 | 0.42 |
| | Fs-15 | 0.252 | 1.3 | 1.677 | 4.5 | 0 | 3.7 | 1.367 | 2.3 | -0.11 |
| | Mc-10 | 10900 | 0.22 | 30.52 | 0.98 | 127700 | 11 | 5230 | 11 | 1 |
| | Mc-11 | 5920 | 0.12 | 29.1 | 5.3 | 129300 | 13 | 5490 | 9.4 | 0.95 |
| | Mc-12 | 8310 | 0.11 | 30.68 | 2.1 | 200100 | 8.6 | 7910 | 6.4 | 0.97 |
| | Mc-13 | 8300 | 0.18 | 31.91 | 1.1 | 114000 | 3.8 | 4460 | 3.8 | 0.97 |
| | Mc-14 | 5290 | 0.57 | 33.55 | 0.97 | 23600 | 5.2 | 879 | 4.7 | 0.99 |
| | Mc-15 | 6370 | 0.13 | 30.7 | 4.5 | 128300 | 10 | 5240 | 9.6 | 0.9 |
| | Mc-16 | 9920 | 0.13 | 30.19 | 1.4 | 192500 | 8.2 | 8000 | 7.2 | 0.98 |
| | Mc-17 | 8510 | 0.24 | 30.34 | 2.2 | 90700 | 8.7 | 3730 | 7.7 | 0.97 |
| | Mc-18 | 5210 | 0.16 | 29 | 10 | 81340 | 8.9 | 3550 | 11 | 0.54 |
| | Mc-19 | 8120 | 0.23 | 31.14 | 1.9 | 89400 | 5 | 3640 | 5.5 | 0.86 |
| | Mc-20 | 12500 | 0.44 | 31.9 | 0.7 | 71300 | 6.2 | 2800 | 6.2 | 0.99 |
| | Mc-21 | 10400 | 0.23 | 30.9 | 0.98 | 112500 | 4.6 | 4560 | 4.7 | 0.98 |
| | Mc-22 | 11800 | 0.066 | 31.42 | 0.75 | 444760 | 5.9 | 17650 | 5.5 | 0.99 |
| | Mc-23 | 8770 | 13 | 29.33 | 2.4 | 1700 | 6.9 | 72.7 | 5.9 | 0.96 |
| | Mc-24 | 10700 | 0.075 | 30.64 | 1.3 | 361900 | 7.7 | 14800 | 7.8 | 0.99 |
| | Mc-25 | 10900 | 0.087 | 31.42 | 1.1 | 353800 | 12 | 14200 | 12 | 0.99 |
| | Mc-26 | 11800 | 0.11 | 31.28 | 0.88 | 263552.846 | 8.8 | 10520 | 8.4 | 1 |
| | Mc-27 | 12200 | 0.084 | 31.88 | 1 | 358337.67 | 5.7 | 14070 | 5.8 | 0.99 |
| | Mc-28 | 6380 | 0.27 | 32.02 | 0.75 | 59198.53 | 3.7 | 2314 | 3.7 | 0.98 |
| | Mc-29 | 9230 | 0.12 | 31.57 | 2.3 | 196311.13 | 5.8 | 7630 | 5 | 0.84 |
| | Mc-30 | 8130 | 0.2 | 31.4 | 0.84 | 103045.9 | 4.7 | 4130 | 4.5 | 0.96 |
| | Mc-31 | 6190 | 0.24 | 32.39 | 0.77 | 63520.617 | 3.8 | 2459 | 3.4 | 0.97 |
| | Mc-32 | 10000 | 0.16 | 31.72 | 0.66 | 157791.661 | 4.9 | 6220 | 4.9 | 0.99 |
| | Mc-33 | 12100 | 0.29 | 32.38 | 2.9 | 106582 | 6.5 | 4040 | 3.6 | 0.77 |
| | Mc-34 | 9990 | 0.18 | 32.13 | 0.95 | 137299.5 | 4.6 | 5340 | 4.3 | 0.98 |
| | Mc-35 | 8700 | 0.25 | 31.45 | 0.83 | 89159.3 | 4.1 | 3540 | 4.1 | 0.97 |
| | Mc-36 | 10000 | 0.45 | 32.06 | 1 | 55884.973 | 3.5 | 2179 | 3.4 | 0.95 |
| | Mc-37 | 5240 | 0.27 | 32.85 | 0.91 | 48363.06 | 4.4 | 1838 | 4 | 0.96 |
| | Mc-38 | 8350 | 0.39 | 32.44 | 0.58 | 52314.547 | 3.4 | 2013 | 3.5 | 0.98 |
| | Mc-39 | 5440 | 0.24 | 31.95 | 0.98 | 55500 | 4.1 | 2171 | 3.6 | 0.97 |
| | Mc-40 | 8370 | 0.099 | 30.97 | 1.5 | 210100 | 8.6 | 8480 | 8.5 | 0.99 |
| | Mc-41 | 7660 | 0.21 | 32.49 | 0.96 | 90200 | 6.7 | 3480 | 7.1 | 0.99 |
| | Mc-42 | 5380 | 1.1 | 28.2 | 6.4 | 12400 | 7.4 | 556 | 10 | 0.74 |
| | Mc-43 | 11100 | 0.35 | 31.1 | 1.2 | 80800 | 5.8 | 3260 | 6.3 | 0.98 |
| | Mc-44 | 9980 | 0.23 | 30.55 | 1 | 109000 | 4.6 | 4460 | 4.7 | 0.97 |
| | Mc-45 | 5010 | 0.26 | 31.91 | 1 | 48200 | 4.7 | 1861 | 4.4 | 0.98 |
| | Mc-47 | 8330 | 0.5 | 32.7 | 4.3 | 42400 | 8.2 | 1630 | 8.1 | 0.87 |
| | Mc-48 | 11700 | 0.49 | 31.13 | 1.2 | 59900 | 7.1 | 2410 | 7.6 | 0.99 |
| | Mc-49 | 7880 | 0.37 | 31.66 | 1.1 | 53500 | 3.9 | 2112 | 3.7 | 0.96 |
| | Mc-50 | 11100 | 0.66 | 33.85 | 0.85 | 41800 | 3 | 1543 | 3.2 | 0.72 |
| | Mc-51 | 6410 | 0.21 | 32.65 | 1.1 | 77900 | 4.3 | 2980 | 4.4 | 0.97 |
| | Mc-52 | 8560 | 0.32 | 30.25 | 1.2 | 65800 | 5.7 | 2650 | 6.6 | 0.69 |
| | Mc-53 | 11800 | 0.047 | 30.54 | 1.4 | 634600 | 7.7 | 26000 | 7.5 | 0.98 |
| | Mc-54 | 12200 | 0.28 | 31.46 | 1.1 | 109130 | 4.3 | 4320 | 4.5 | 0.95 |
| | Mc-55 | 11000 | 1.4 | 31.83 | 0.94 | 19375 | 2.8 | 761 | 2.9 | 0.95 |
| | Mc-56 | 11600 | 0.091 | 31.16 | 0.94 | 315128 | 4.6 | 12650 | 5 | 0.99 |
| | Mc-57 | 7440 | 0.2 | 31.12 | 0.98 | 91400 | 3.8 | 3700 | 4.5 | 0.95 |
| | Mc-58 | 8850 | 0.22 | 31.54 | 0.91 | 98200 | 4.5 | 3890 | 4.2 | 0.98 |
| | Mc-59 | 4410 | 0.25 | 32.02 | 0.74 | 43600 | 3.1 | 1703 | 3.2 | 0.98 |
| | Mc-61 | 1750 | 0.72 | 25.2 | 14 | 6400 | 12 | 332 | 21 | 0.84 |
| | Mc-62 | 5340 | 0.41 | 31 | 3.4 | 32600 | 6.7 | 1311 | 5.9 | 0.88 |
| | Mc-65 | 10600 | 0.11 | 31.5 | 0.92 | 247800 | 6.4 | 9810 | 5.9 | 0.99 |
| | Mc-66 | 8230 | 0.27 | 31.8 | 0.73 | 76000 | 3.6 | 2990 | 3.6 | 0.98 |
| | Mc-68 | 7610 | 0.19 | 30 | 3.9 | 101600 | 7.4 | 4250 | 7.8 | 0.84 |
| Z6029 | Fs-1 | 5930 | 0.35 | 33.54 | 0.8 | 42400 | 3.7 | 1580 | 3.8 | 0.98 |
| | Fs-2 | 5620 | 0.34 | 33.37 | 1.1 | 40700 | 3.4 | 1529 | 3.7 | 0.95 |
| | Fs-3 | 4810 | 0.36 | 30.8 | 7.2 | 33200 | 7.2 | 1352 | 6.9 | 0.52 |
| | Mc-1 | 7020 | 0.14 | 31.7 | 1.1 | 129700 | 5.6 | 5120 | 6.1 | 0.99 |

Continued on next page

| Sample | Spot name | Rb ppm | Sr | $^{87}Rb/^{87}Sr$ | ±2SE | $^{87}Rb/^{86}Sr$ | ±2SE | $^{87}Sr/^{86}Sr$ | ±2SE | $\rho$ |
|---|---|---|---|---|---|---|---|---|---|---|
| | Mc-3 | 4810 | 0.24 | 31.42 | 1.8 | 51000 | 4.2 | 2030 | 5.3 | 0.95 |
| | Mc-4 | 5340 | 0.2 | 32.46 | 1.3 | 66100 | 3.6 | 2541 | 3.2 | 0.93 |
| | Mc-5 | 5820 | 0.21 | 33.42 | 0.74 | 68200 | 4.2 | 2530 | 4 | 0.93 |
| | Mc-6 | 5350 | 0.23 | 32.58 | 1.3 | 58100 | 3.2 | 2231 | 3.2 | 0.92 |
| | Mc-7 | 6070 | 0.19 | 32.31 | 0.88 | 77600 | 4.3 | 3010 | 4 | 0.98 |
| | Mc-9 | 5930 | 0.17 | 32.93 | 1.3 | 89600 | 4.2 | 3410 | 4.9 | 0.97 |
| | Mc-10 | 4950 | 0.16 | 32.83 | 1.2 | 77900 | 5.5 | 2960 | 5.2 | 0.98 |
| | Mc-11 | 7250 | 0.38 | 33.4 | 0.96 | 47500 | 2.4 | 1765 | 2.2 | 0.92 |
| | Mc-12 | 4880 | 0.28 | 33.74 | 0.96 | 43400 | 4.4 | 1622 | 4.7 | 0.93 |
| | Mc-13 | 6950 | 0.23 | 33.54 | 0.93 | 73900 | 3.2 | 2778 | 3.4 | 0.96 |
| | Mc-14 | 8160 | 0.15 | 33.88 | 0.92 | 137700 | 5.2 | 5080 | 4.9 | 0.98 |
| | Mc-15 | 5450 | 0.28 | 33.75 | 0.81 | 48700 | 2.6 | 1804 | 2.6 | 0.98 |
| | Mc-16 | 8190 | 0.11 | 32.26 | 0.97 | 180000 | 5 | 6970 | 4.9 | 0.98 |
| | Mc-17 | 4750 | 0.62 | 31.79 | 1.4 | 18900 | 2.9 | 743 | 3 | 0.89 |
| | Mc-18 | 6580 | 6.2 | 32.87 | 1.2 | 2600 | 1.3 | 99.3 | 1.4 | 0.56 |
| | Mc-19 | 4650 | 5.5 | 32.6 | 1 | 2100 | 1.1 | 79.75 | 0.94 | 0.54 |
| | Mc-20 | 5500 | 0.31 | 32.01 | 1 | 43700 | 3.1 | 1688 | 2.6 | 0.96 |
| | Mc-21 | 10100 | 0.11 | 32.37 | 0.95 | 222400 | 4.1 | 8490 | 3.7 | 0.97 |
| | Mc-22 | 5710 | 0.18 | 33.13 | 1 | 79700 | 4.3 | 3010 | 4.3 | 0.97 |
| | Mc-23 | 8970 | 0.16 | 33.05 | 0.91 | 137100 | 5.1 | 5110 | 4.1 | 0.98 |
| | Mc-24 | 8570 | 0.16 | 32.33 | 1.8 | 137800 | 7.2 | 5320 | 6.8 | 0.97 |
| | Mc-25 | 8620 | 0.28 | 32.7 | 0.64 | 78100 | 7.5 | 2990 | 7.8 | 1 |
| | Mc-26 | 5880 | 0.25 | 33.01 | 0.82 | 58600 | 4.1 | 2219 | 4 | 0.98 |
| | Mc-27 | 4350 | 0.36 | 30.4 | 4.9 | 29400 | 4.2 | 1215 | 5.5 | 0.41 |
| | Mc-28 | 6990 | 0.52 | 34.7 | 3.3 | 33800 | 9.6 | 1188 | 5.6 | 0.86 |
| | Mc-29 | 6140 | 0.44 | 31.68 | 0.93 | 35200 | 4.1 | 1388 | 4.4 | 0.98 |
| | Mc-30 | 5240 | 0.16 | 33.23 | 1 | 80500 | 5.6 | 3030 | 5.5 | 0.98 |
| | Mc-31 | 7040 | 0.18 | 32.75 | 1.1 | 99800 | 4.3 | 3810 | 4.3 | 0.97 |
| | Mc-32 | 5620 | 0.15 | 33.09 | 0.94 | 94500 | 3.8 | 3570 | 3.8 | 0.97 |
| | Mc-33 | 6000 | 0.35 | 33.55 | 0.78 | 43500 | 4.2 | 1614 | 3.9 | 0.97 |
| | Mc-34 | 5480 | 0.19 | 33.14 | 1 | 74500 | 4.7 | 2810 | 4.8 | 0.98 |
| | Mc-35 | 5180 | 0.19 | 32.63 | 1.1 | 69000 | 4.4 | 2640 | 4.4 | 0.97 |
| | Mc-36 | 8840 | 0.12 | 32.04 | 1.3 | 181800 | 5.4 | 7000 | 4.8 | 0.97 |
| | Mc-37 | 5480 | 0.21 | 33.74 | 0.74 | 65800 | 4.7 | 2420 | 4.3 | 0.95 |
| | Mc-38 | 5290 | 0.19 | 33.68 | 0.86 | 69600 | 4.5 | 2610 | 4.8 | 0.91 |
| | Mc-39 | 4950 | 0.19 | 32.5 | 1.1 | 66200 | 3.1 | 2545 | 3 | 0.93 |
| | Mc-40 | 5910 | 0.23 | 32.86 | 1.2 | 63100 | 3.5 | 2400 | 3.3 | 0.96 |
| | Mc-41 | 5070 | 0.18 | 32.93 | 0.76 | 70200 | 4.3 | 2660 | 4.2 | 0.99 |
| | Mc-42 | 5370 | 0.11 | 32.8 | 1.1 | 127400 | 8.9 | 4860 | 9.2 | 0.99 |
| | Mc-43 | 7970 | 0.19 | 32.76 | 0.88 | 106900 | 6.1 | 4080 | 5.9 | 0.99 |
| | Mc-44 | 5890 | 0.2 | 33.38 | 0.8 | 72800 | 2.8 | 2731 | 3.1 | 0.97 |
| | Mc-45 | 4940 | 0.21 | 32.69 | 1.2 | 58800 | 4.4 | 2246 | 3.8 | 0.97 |
| | Mc-46 | 5690 | 0.16 | 32.79 | 1.1 | 92200 | 4.7 | 3520 | 4.6 | 0.97 |
| | Mc-47 | 5530 | 0.24 | 33.05 | 1.1 | 57400 | 4.1 | 2198 | 4.3 | 0.97 |
| | Mc-48 | 5230 | 0.27 | 32.8 | 1.1 | 48300 | 3.6 | 1842 | 3.3 | 0.95 |
| | Mc-49 | 9130 | 0.14 | 32.58 | 1.1 | 167700 | 6 | 6420 | 5.2 | 0.99 |
| | Mc-50 | 4720 | 0.16 | 32.38 | 1.1 | 73600 | 4.6 | 2840 | 4.1 | 0.97 |
| | Mc-51 | 5250 | 0.22 | 32.21 | 1.1 | 60100 | 5.4 | 2330 | 5.1 | 0.98 |
| | Mc-52 | 4870 | 0.24 | 32.25 | 1.3 | 51400 | 3.9 | 1989 | 3.1 | 0.95 |
| | Mc-53 | 5190 | 0.24 | 33.31 | 1 | 54900 | 4.3 | 2061 | 4.3 | 0.97 |
| | Mc-54 | 5310 | 0.2 | 32.35 | 1.1 | 66400 | 4.6 | 2560 | 4.1 | 0.98 |
| | Mc-55 | 4860 | 0.12 | 31.84 | 0.98 | 100200 | 5.1 | 3930 | 4.8 | 0.98 |
| | Mc-56 | 6400 | 0.55 | 33.07 | 0.93 | 28900 | 4.5 | 1097 | 4.1 | 0.97 |
| | Mc-57 | 5540 | 0.21 | 31.72 | 1.4 | 65400 | 4.2 | 2580 | 3.9 | 0.95 |
| | Mc-58 | 5110 | 0.18 | 32.65 | 0.71 | 70900 | 3.7 | 2694 | 3.4 | 0.9 |
| | Mc-59 | 5770 | 0.17 | 32.33 | 1 | 81500 | 4.5 | 3150 | 4.3 | 0.98 |
| | Mc-60 | 6410 | 0.19 | 32.1 | 1.1 | 85800 | 4.4 | 3340 | 4.3 | 0.96 |
| | Mc-61 | 6220 | 0.21 | 32.97 | 0.82 | 74700 | 5.1 | 2830 | 5 | 0.99 |
| | Mc-62 | 5470 | 0.19 | 32.45 | 0.72 | 71400 | 3.6 | 2732 | 3.2 | 0.96 |
| | Mc-63 | 6960 | 0.46 | 31.91 | 0.87 | 38200 | 3.8 | 1496 | 3.4 | 0.98 |
| | Mc-64 | 5710 | 0.22 | 32.81 | 0.81 | 65800 | 5.1 | 2480 | 4.2 | 0.9 |
| | Mc-65 | 5930 | 0.19 | 32.55 | 1 | 77900 | 4.2 | 2990 | 4.2 | 0.97 |
| | Mc-66 | 7480 | 0.18 | 33.3 | 0.78 | 103200 | 3.9 | 3890 | 4 | 0.87 |
| | Mc-67 | 5690 | 0.2 | 33.04 | 1 | 70100 | 4.1 | 2650 | 3.9 | 0.97 |
| | Mc-68 | 9910 | 0.08 | 31.32 | 1.1 | 294800 | 4.9 | 11760 | 5 | 0.98 |
| | Mc-69 | 4910 | 0.17 | 32.71 | 0.94 | 71400 | 5.2 | 2730 | 5.3 | 0.99 |
| | Mc-70 | 5000 | 0.13 | 32.3 | 1 | 93600 | 5.4 | 3620 | 5.3 | 0.98 |
| | Mc-71 | 5520 | 0.26 | 32.95 | 0.92 | 54400 | 3.9 | 2061 | 3.6 | 0.97 |
| ZU008 | Fs-1 | 14.1 | 37 | 1.72 | 6.4 | 1.168813848 | 6.9 | 0.726 | 1.4 | 0.45 |
| | Fs-2 | 0.992 | 4.6 | 0.3587 | 1.4 | 1.090329689 | 2 | 3.258 | 1.9 | 0.75 |
| | Fs-3 | 9.57 | 34 | 1.334 | 1.1 | 0.879647093 | 0.7 | 0.7103 | 0.75 | 0.3 |
| | Fs-4 | 6210 | 14 | 40.8 | 3 | 1090.749327 | 2.6 | 33.37 | 1.7 | 0.084 |
| | Fs-5 | 27.2 | 7.8 | 5.23 | 14 | 10.46710974 | 14 | 2.146 | 2.9 | 0.19 |
| | Fs-6 | 5460 | 7.6 | 35 | 2.9 | 1785.788175 | 2.9 | 63.6 | 4.1 | 0.69 |
| | Fs-7 | 9.84 | 34 | 1.362 | 1.3 | 0.901275809 | 0.91 | 0.7098 | 0.79 | -0.12 |
| | Fs-8 | 12.3 | 38 | 1.456 | 3.4 | 0.972432526 | 3.2 | 0.7163 | 0.97 | -0.019 |
| | Fs-9 | 12.2 | 21 | 1.97 | 12 | 1.766197769 | 12 | 0.966 | 1.7 | -0.091 |
| | Mc-1 | 6290 | 0.26 | 32.17 | 0.68 | 60900 | 6 | 2370 | 5.9 | 0.99 |
| | Mc-2 | 5800 | 0.19 | 31.79 | 0.86 | 76800 | 4 | 3050 | 4.3 | 0.98 |
| | Mc-3 | 8060 | 0.18 | 32.22 | 0.84 | 113600 | 4.7 | 4410 | 4.6 | 0.99 |
| | Mc-4 | 6450 | 0.2 | 32.22 | 0.82 | 80000 | 4.2 | 3100 | 4.1 | 0.98 |
| | Mc-5 | 7820 | 0.21 | 32.56 | 0.86 | 92100 | 4.4 | 3540 | 4.3 | 0.98 |
| | Mc-6 | 7610 | 0.18 | 32.35 | 0.88 | 106800 | 4.7 | 4120 | 4.4 | 0.98 |
| | Mc-7 | 8390 | 0.24 | 31.98 | 0.74 | 88900 | 4.2 | 3480 | 4.3 | 0.99 |
| | Mc-8 | 9410 | 0.15 | 32.74 | 0.87 | 158900 | 4.1 | 6070 | 4.2 | 0.98 |

Continued on next page

| Sample | Spot name | Rb ppm | Sr | $^{87}Rb/^{87}Sr$ | ±2SE | $^{87}Rb/^{86}Sr$ | ±2SE | $^{87}Sr/^{86}Sr$ | ±2SE | $\rho$ |
|---|---|---|---|---|---|---|---|---|---|---|
| | Mc-9 | 8180 | 0.093 | 31.67 | 0.79 | 222290 | 5.4 | 8770 | 5.2 | 0.99 |
| | Fs-10 | 28.2 | 33 | 3.24 | 16 | 2.474576304 | 20 | 0.758 | 2.4 | 0.37 |
| | Fs-11 | 11.2 | 36 | 1.424 | 1.5 | 0.945789146 | 1.5 | 0.7134 | 0.8 | 0.34 |
| | Fs-12 | 10.7 | 32 | 1.459 | 5.7 | 1.000188231 | 7.1 | 0.7192 | 1.1 | 0.14 |
| | Mc-10 | 7030 | 0.21 | 32.82 | 0.66 | 84338.891 | 4.9 | 3210 | 4.9 | 0.99 |
| | Mc-11 | 8530 | 0.12 | 31.85 | 0.75 | 175094.626 | 4.8 | 6810 | 4.6 | 0.91 |
| | Mc-12 | 6680 | 0.21 | 32.77 | 0.77 | 79376.8445 | 4.1 | 3030 | 3.9 | 0.99 |
| | Mc-13 | 6060 | 0.25 | 33 | 0.94 | 59425 | 3.8 | 2254 | 4 | 0.97 |
| | Mc-14 | 6900 | 0.17 | 32.44 | 0.94 | 103673.9 | 5.5 | 3990 | 5.3 | 0.99 |
| | Mc-15 | 6990 | 0.18 | 32.43 | 0.97 | 95206 | 3.7 | 3670 | 3.5 | 0.98 |
| | Mc-16 | 6060 | 0.23 | 30.94 | 1.3 | 67534.7163 | 8.6 | 2750 | 8.5 | 0.98 |
| | Mc-17 | 7290 | 0.1 | 31.46 | 0.91 | 174334.482 | 5.7 | 6930 | 5.8 | 0.99 |
| | Mc-18 | 6120 | 0.17 | 32.77 | 1.3 | 89013.45 | 3.7 | 3370 | 3.5 | 0.91 |
| | Mc-19 | 8210 | 0.13 | 31.81 | 0.79 | 155406.72 | 6.8 | 6100 | 6.5 | 0.99 |
| | Mc-20 | 5260 | 0.29 | 32.75 | 0.67 | 45162.701 | 3.1 | 1725 | 3.1 | 0.98 |
| | Mc-21 | 5150 | 0.29 | 32.72 | 0.76 | 44177.146 | 4 | 1687 | 3.6 | 0.99 |
| | Mc-22 | 6010 | 0.15 | 34.09 | 2 | 97978.19227 | 6.7 | 3600 | 7.1 | 0.96 |
| | Mc-23 | 4790 | 0.28 | 32.04 | 0.95 | 43955.74819 | 5 | 1716 | 5 | 0.98 |
| | Mc-24 | 3610 | 0.17 | 31.61 | 0.94 | 52047.25055 | 3.6 | 2060 | 3.5 | 0.98 |
| | Mc-27 | 5130 | 0.19 | 31.95 | 0.89 | 68016.29746 | 3.7 | 2681 | 3.7 | 0.91 |
| | Mc-28 | 6240 | 0.09 | 31.74 | 1 | 174287.0152 | 5.1 | 6860 | 4.9 | 0.99 |
| | Mc-29 | 7410 | 0.11 | 31.6 | 1 | 175896.8561 | 3.8 | 6970 | 3.9 | 0.96 |
| | Mc-30 | 5460 | 0.12 | 31.6 | 0.88 | 114962.6728 | 5.7 | 4540 | 5.4 | 0.99 |
| | Mc-31 | 8420 | 0.08 | 31.12 | 1.2 | 258298.6845 | 4.7 | 10370 | 4.4 | 0.97 |
| | Mc-32 | 3880 | 0.22 | 37.12 | 2.6 | 45348.38162 | 6.4 | 1528 | 6 | 0.92 |
| | Mc-33 | 6830 | 0.15 | 32.07 | 0.8 | 113681.7929 | 4.2 | 4450 | 4.1 | 0.85 |
| | Mc-34 | 7150 | 0.22 | 31.62 | 1.3 | 81566.62112 | 4.9 | 3230 | 5.2 | 0.97 |
| | Mc-35 | 8210 | 0.22 | 32.82 | 0.52 | 96332.65221 | 4.4 | 3660 | 4.3 | 0.98 |
| | Mc-36 | 8320 | 0.11 | 31.37 | 1.1 | 195812.8116 | 7.1 | 7810 | 7.1 | 0.99 |
| | Mc-37 | 6830 | 0.24 | 31.92 | 1.1 | 72515.75379 | 3.9 | 2836 | 3.2 | 0.97 |
| | Mc-38 | 6460 | 0.21 | 32.46 | 1 | 80252.5535 | 5.4 | 3110 | 5.9 | 0.97 |
| | Mc-39 | 7760 | 0.13 | 31.5 | 1.1 | 151146.5473 | 5.3 | 6010 | 5.7 | 0.98 |
| | Mc-40 | 8600 | 0.058 | 30.91 | 1.1 | 371261.6918 | 9.1 | 15000 | 8.6 | 0.99 |
| | Mc-41 | 5070 | 0.51 | 33.07 | 0.74 | 24868.28128 | 5 | 940 | 5.1 | 0.99 |
| | Mc-42 | 8260 | 0.11 | 32.13 | 1.2 | 188385.338 | 5.4 | 7320 | 5.4 | 0.98 |
| | Mc-43 | 6680 | 0.14 | 31.65 | 0.93 | 120786.3163 | 4.1 | 4770 | 4 | 0.97 |
| | Mc-44 | 7440 | 0.12 | 31.7 | 1.1 | 159627.83 | 5.9 | 6310 | 6.3 | 0.99 |
| | Mc-45 | 6380 | 0.19 | 31.46 | 0.89 | 85090.98504 | 4.2 | 3370 | 3.8 | 0.98 |
| | Mc-46 | 7130 | 0.11 | 31.39 | 0.8 | 169921.4256 | 5.8 | 6770 | 6.1 | 0.99 |
| | Mc-47 | 8390 | 0.12 | 31.67 | 0.97 | 186198.7409 | 7.2 | 7310 | 6.9 | 0.99 |
| | Mc-48 | 6560 | 0.12 | 31.37 | 0.9 | 137369.5624 | 4.6 | 5510 | 4.5 | 0.95 |
| | Mc-49 | 7690 | 0.19 | 31.59 | 1.1 | 100074.8584 | 4.2 | 3930 | 4.4 | 0.9 |
| | Mc-50 | 7710 | 0.12 | 31.66 | 0.89 | 154571.7999 | 4.4 | 6100 | 4.6 | 0.98 |
| | Mc-51 | 6890 | 0.13 | 31.2 | 0.85 | 126104.4531 | 7.2 | 5050 | 7.3 | 1 |
| | Mc-52 | 7430 | 0.096 | 31.59 | 0.66 | 198874.0853 | 4.7 | 7860 | 4.9 | 0.99 |
| | Mc-53 | 5420 | 0.15 | 32.72 | 0.84 | 89543.49045 | 5.2 | 3410 | 4.9 | 0.99 |
| | Mc-54 | 8430 | 0.31 | 31.68 | 1.1 | 67119.13124 | 3.7 | 2650 | 3.9 | 0.98 |
| | Mc-55 | 7780 | 0.08 | 31.25 | 0.9 | 240476.7026 | 5 | 9670 | 4.6 | 0.95 |
| | Mc-56 | 8300 | 0.084 | 31.89 | 0.57 | 246017.1776 | 5.8 | 9520 | 5.5 | 0.97 |
| | Mc-57 | 5620 | 0.12 | 32.7 | 0.69 | 115674.7034 | 4 | 4410 | 4 | 0.99 |
| | Mc-58 | 8610 | 0.085 | 31.22 | 0.89 | 257416.0338 | 5.7 | 10290 | 5.7 | 0.99 |
| | Mc-59 | 7910 | 0.2 | 31.59 | 0.82 | 98075.5794 | 4.4 | 3870 | 4.1 | 0.98 |
| | Mc-60 | 6170 | 0.18 | 31.37 | 1.1 | 84334.92262 | 3.4 | 3350 | 3.3 | 0.96 |
| | Mc-61 | 6130 | 0.22 | 31.56 | 0.97 | 70091.81242 | 3.1 | 2772 | 3 | 0.97 |
| | Mc-62 | 6250 | 0.18 | 31.57 | 1.1 | 89094.76061 | 4.3 | 3520 | 4.2 | 0.96 |
| | Mc-63 | 3460 | 0.33 | 32.01 | 0.87 | 26244.32412 | 2.4 | 1033 | 3.5 | 0.97 |
| Z6035 | 1 | 2620 | 0.36 | 19218 | 3.4 | | | 753 | 3.5 | 0.97 |
| | 2 | 5440 | 0.26 | 54180 | 2.8 | | | 2010 | 2.6 | 0.96 |
| | 3 | 2760 | 0.42 | 16965 | 4 | | | 735 | 4 | 0.99 |
| | 4 | 2930 | 1.2 | 6500 | 2.9 | | | 281.8 | 2.8 | 0.99 |
| | 5 | 2520 | 0.73 | 8950 | 2.5 | | | 337.2 | 2.6 | 0.89 |
| | 6 | 2310 | 0.65 | 9204 | 2.2 | | | 354.4 | 2 | 0.94 |
| | 7 | 2430 | 0.67 | 9330 | 2.4 | | | 354.7 | 1.8 | 0.91 |
| | 8 | 2710 | 0.4 | 17566 | 2.7 | | | 642 | 2.5 | 0.96 |
| | 9 | 2660 | 0.34 | 20520 | 3.5 | | | 746 | 2.9 | 0.86 |
| | 10 | 2650 | 0.78 | 8830 | 2.8 | | | 372.9 | 2.5 | 0.83 |
| | 11 | 3160 | 0.38 | 21400 | 3.6 | | | 920 | 3.2 | 0.99 |
| | 12 | 2970 | 0.52 | 14660 | 2.5 | | | 627 | 2.6 | 0.96 |
| | 13 | 2570 | 2.4 | 2780 | 3.8 | | | 126 | 3.5 | 0.98 |
| | 14 | 1010 | 0.55 | 4750 | 3.3 | | | 267.6 | 3 | 0.99 |
| | 15 | 2960 | 0.98 | 7860 | 2.3 | | | 287 | 2 | 0.94 |
| | 16 | 2790 | 1 | 7050 | 2 | | | 261.7 | 1.3 | 0.6 |
| | 17 | 3710 | 0.98 | 9740 | 1.8 | | | 355.7 | 2.1 | 0.89 |
| | 18 | 2840 | 0.92 | 7900 | 1.9 | | | 283.7 | 1.8 | 0.92 |
| | 19 | 2580 | 0.64 | 10420 | 2.2 | | | 384.8 | 2 | 0.96 |
| | 20 | 2120 | 1 | 5260 | 1.3 | | | 192.6 | 1.6 | 0.87 |
| | 21 | 2160 | 0.96 | 5830 | 1.7 | | | 213.2 | 1.5 | 0.84 |
| | 22 | 2640 | 0.47 | 14570 | 3.2 | | | 541 | 2.9 | 0.95 |
| | 23 | 2290 | 1.8 | 3325 | 1.6 | | | 122 | 1.2 | 0.79 |
| | 24 | 2180 | 1.2 | 4860 | 2.2 | | | 183.5 | 1.6 | 0.87 |
| | 25 | 2740 | 0.51 | 13970 | 2.8 | | | 521 | 3 | 0.93 |
| | 26 | 2490 | 1.6 | 4010 | 1.6 | | | 144.7 | 1.5 | 0.91 |
| | 27 | 2320 | 0.48 | 12340 | 2.2 | | | 451.3 | 2 | 0.94 |
| | 28 | 2570 | 1.8 | 3630 | 1.3 | | | 129.2 | 1.2 | 0.91 |
| | 29 | 2770 | 0.74 | 9605 | 1.9 | | | 350.5 | 1.9 | 0.91 |

Continued on next page

| Sample | Spot name | Rb ppm | Sr | $^{87}Rb/^{87}Sr$ | ±2SE | $^{87}Rb/^{86}Sr$ | ±2SE | $^{87}Sr/^{86}Sr$ | ±2SE | $\rho$ |
|---|---|---|---|---|---|---|---|---|---|---|
| | 30 | 2750 | 1 | 7100 | 3 | | | 256.2 | 2.8 | 0.96 |
| | 31 | 2600 | 0.46 | 14680 | 2.6 | | | 555 | 2.3 | 0.94 |
| | 32 | 2660 | 0.65 | 10600 | 2.9 | | | 397.4 | 2.5 | 0.95 |
| | 33 | 2470 | 0.5 | 12710 | 2.8 | | | 473 | 2.6 | 0.96 |
| | 34 | 2990 | 0.63 | 12270 | 2.6 | | | 459 | 2.4 | 0.95 |
| | 35 | 2300 | 0.96 | 6260 | 1.9 | | | 227.7 | 1.7 | 0.85 |
| | 36 | 2480 | 0.78 | 8230 | 2 | | | 299.2 | 1.8 | 0.92 |
| | 37 | 2450 | 0.93 | 6795 | 2.5 | | | 248.6 | 2.2 | 0.97 |
| | 38 | 2520 | 0.64 | 10075 | 2.9 | | | 374.2 | 2.6 | 0.96 |
| | 39 | 3700 | 0.56 | 17160 | 2.4 | | | 621 | 2.4 | 0.96 |
| | 40 | 2760 | 0.75 | 9540 | 2.1 | | | 359.2 | 1.9 | 0.93 |
| | 41 | 2180 | 0.59 | 9470 | 3.1 | | | 360.5 | 2.4 | 0.91 |
| | 42 | 2610 | 0.96 | 7100 | 2.6 | | | 257.4 | 1.7 | 0.94 |
| | 43 | 2410 | 1.4 | 4610 | 1.8 | | | 171.6 | 1.2 | 0.91 |
| | 44 | 2400 | 1.2 | 5335 | 1.6 | | | 200.9 | 1.8 | 0.77 |
| | 45 | 2490 | 1 | 6190 | 1.9 | | | 224.1 | 1.9 | 0.91 |
| | 46 | 2300 | 0.56 | 10590 | 2.3 | | | 385.1 | 2.1 | 0.95 |
| | 47 | 2930 | 0.47 | 15970 | 1.5 | | | 578.2 | 1.6 | 0.91 |
| | 48 | 2380 | 0.83 | 7470 | 2 | | | 272.8 | 2.1 | 0.94 |
| | 49 | 2660 | 1.6 | 4330 | 1.8 | | | 157.5 | 1.3 | 0.89 |
| | 50 | 3280 | 0.26 | 33020 | 3.2 | | | 1198 | 3.3 | 0.91 |
| | 51 | 2680 | 0.88 | 7817.584 | 1.9 | | | 289.8 | 1.9 | 0.79 |
| | 52 | 2500 | 0.95 | 6797.821 | 2.1 | | | 257.1 | 1.8 | 0.9 |
| | 53 | 3030 | 0.72 | 10866.4 | 2.1 | | | 392.6 | 2.1 | 0.79 |
| | 54 | 2160 | 0.82 | 6870.32 | 2.7 | | | 250 | 2.3 | 0.95 |
| | 55 | 2650 | 0.6 | 11562.709 | 2.2 | | | 424.1 | 1.9 | 0.87 |
| | 56 | 2640 | 0.72 | 9418.897 | 2 | | | 349.6 | 1.7 | 0.89 |
| | 57 | 2170 | 1.5 | 3711.682 | 1.5 | | | 135.6 | 1.5 | 0.89 |
| | 58 | 2100 | 2.2 | 2477.64 | 1.2 | | | 94 | 1.1 | 0.85 |
| | 59 | 2470 | 0.55 | 11774.385 | 2.4 | | | 429 | 2.4 | 0.97 |
| | 60 | 2860 | 0.6 | 12382.047 | 2.9 | | | 447 | 2.8 | 0.98 |
| | 61 | 2090 | 0.84 | 6438.58 | 2.2 | | | 242.9 | 2 | 0.94 |
| | 62 | 2960 | 1.1 | 7113.249 | 1.9 | | | 253.5 | 2 | 0.93 |
| | 63 | 2670 | 0.86 | 8063.66 | 2.4 | | | 294.5 | 2.4 | 0.82 |
| | 64 | 2220 | 1.7 | 3350 | 1.8 | | | 126.2 | 1.6 | 0.93 |
| | 65 | 2590 | 0.43 | 15759.53 | 3.3 | | | 584 | 3.3 | 0.99 |
| | 66 | 2730 | 0.61 | 11609 | 2.5 | | | 420 | 2.5 | 0.97 |
| | 67 | 2640 | 0.56 | 12016 | 2.7 | | | 440 | 2.7 | 0.91 |
| | 68 | 2950 | 1.1 | 7140.6 | 2.8 | | | 258.5 | 1.8 | 0.92 |
| | 69 | 2510 | 0.98 | 6638.2 | 1.8 | | | 252.4 | 1.8 | 0.93 |
| | 70 | 3020 | 0.56 | 13895 | 2.7 | | | 510 | 2.6 | 0.86 |

# C.5 Trioctahedral (Brown) mica Rb–Sr data

| Sample | Spot name | Rb ppm | Sr | $^{87}Rb/^{87}Sr$ | ±2SE (%) | $^{87}Rb/^{86}Sr$ | ±2SE (%) | $^{87}Sr/^{86}Sr$ | ±2SE (%) | rho | Fe ppm | Mg | Ti | Mg# | Ti (a.p.f.u.) | Ti in Biotite Temperature |
|---|---|---|---|---|---|---|---|---|---|---|---|---|---|---|---|---|
| ZU001 | 1 | 660 | 7.1 | 27.83 | 1.2 | 3840 | 6.3 | 158.9 | 6 | 0.98 | 154659 | 30549 | 16102 | 0.16 | 0.32 | 635 |
| | 3 | 634 | 5.8 | 32.24 | 1.7 | 6390 | 5.1 | 223 | 7.9 | 0.99 | 166352 | 32162 | 15599 | 0.16 | 0.31 | 629 |
| | 5 | 5.49 | 4.5 | 4.21 | 3.3 | 3.145 | 3.1 | 0.866 | 3.4 | 0.47 | 155012 | 20488 | 2758 | 0.12 | 0.05 | |
| | 6 | 621 | 6.6 | 32.51 | 1.6 | 1290 | 9.8 | 45.7 | 9.7 | 0.99 | 183793 | 34641 | 17125 | 0.16 | 0.34 | 645 |
| | 7 | 568 | 4.3 | 38.8 | 3.1 | 13100 | 15 | 390 | 15 | 0.98 | 178281 | 35661 | 15282 | 0.17 | 0.3 | 626 |
| | 8 | 614 | 14 | 29.84 | 2.7 | 179.8 | 4.8 | 6.93 | 3.9 | 0.84 | 164923 | 26290 | 12755 | 0.14 | 0.25 | 591 |
| | 9 | 571 | 5.3 | 32.4 | 5.5 | 7800 | 15 | 274 | 12 | 0.92 | 188305 | 38456 | 19198 | 0.17 | 0.38 | 664 |
| | 10 | 668 | 6.3 | 31.3 | 2.2 | 5170 | 10 | 190 | 10 | 0.98 | 156258 | 33099 | 18884 | 0.17 | 0.37 | 662 |
| | 11 | 598 | 5.4 | 31.95 | 2.5 | 8070 | 7.1 | 291 | 6.7 | 0.94 | 174149 | 34381 | 15949 | 0.16 | 0.31 | 633 |
| | 12 | 633 | 6 | 30.44 | 1.4 | 10360 | 6.1 | 392 | 6.3 | 0.98 | 168959 | 34663 | 16321 | 0.17 | 0.32 | 637 |
| | 13 | 508 | 4.9 | 32.78 | 1.6 | 2130 | 6.8 | 74.6 | 6.6 | 0.97 | 176578 | 35158 | 16178 | 0.17 | 0.32 | 636 |
| | 14 | 626 | 6.2 | 29.16 | 0.89 | 7710 | 8.3 | 302 | 8.2 | 0.99 | 175167 | 30595 | 16661 | 0.15 | 0.33 | 641 |
| | 15 | 638 | 5.8 | 33.03 | 1.8 | 3650 | 5.7 | 126.6 | 5.6 | 0.95 | 160320 | 30793 | 14241 | 0.16 | 0.28 | 613 |
| | 17 | 557 | 5 | 32.76 | 1.6 | 5350 | 7.8 | 188 | 8.3 | 0.98 | 176820 | 33546 | 15079 | 0.16 | 0.3 | 623 |
| | 18 | 589 | 5.7 | 30.58 | 1.5 | 4460 | 5.9 | 165.5 | 5 | 0.92 | 163137 | 31844 | 15174 | 0.16 | 0.3 | 624 |
| | 19 | 576 | 5.3 | 32.05 | 1.9 | 6350 | 5 | 231 | 5.6 | 0.94 | 175732 | 33870 | 17587 | 0.16 | 0.34 | 650 |
| | 20 | 578 | 5.2 | 32.82 | 1.4 | 6250 | 8 | 218 | 7.5 | 0.99 | 161435 | 32307 | 18801 | 0.17 | 0.37 | 661 |
| | 21 | 459 | 5.3 | 31.34 | 1.5 | 951 | 4 | 34.8 | 4.2 | 0.93 | 207658 | 33858 | 15999 | 0.14 | 0.31 | 633 |
| | 22 | 489 | 42 | 19.07 | 1.3 | 33.12 | 1.8 | 1.991 | 1.9 | 0.71 | 129982 | 25451 | 12757 | 0.16 | 0.25 | 591 |
| | 25 | 633 | 6 | 32.02 | 1.3 | 3510 | 4.6 | 125.5 | 4.6 | 0.96 | 156458 | 31194 | 14734 | 0.17 | 0.29 | 619 |
| | 27 | 589 | 5.2 | 35.53 | 2 | 2590 | 5.5 | 83.6 | 5.6 | 0.93 | 186743 | 36751 | 16762 | 0.16 | 0.33 | 642 |
| | 28 | 600 | 5.5 | 31.08 | 1.2 | 11260 | 6.6 | 415 | 6.5 | 0.99 | 182268 | 35868 | 15249 | 0.16 | 0.3 | 625 |
| | 29 | 628 | 6.1 | 30.09 | 1.5 | 6940 | 12 | 261 | 12 | 0.97 | 178610 | 32747 | 14259 | 0.15 | 0.28 | 613 |
| | 30 | 623 | 6.2 | 28.76 | 1.3 | 7390 | 5.1 | 295 | 5.4 | 0.97 | 170821 | 29590 | 13700 | 0.15 | 0.27 | 605 |
| | 31 | 614 | 6.1 | 28.73 | 1.9 | 8990 | 8.8 | 359 | 8.5 | 0.98 | 181471 | 32339 | 14764 | 0.15 | 0.29 | 619 |
| | 32 | 695 | 6.8 | 31.33 | 1.6 | 2650 | 8.9 | 97.3 | 9.2 | 0.99 | 190102 | 33936 | 16707 | 0.15 | 0.33 | 641 |
| | 33 | 660 | 9.6 | 28.25 | 1.2 | 498 | 3.2 | 20.06 | 2.8 | 0.93 | 177122 | 32253 | 15397 | 0.15 | 0.3 | 627 |
| | 34 | 668 | 13 | 27.86 | 1.5 | 254 | 4 | 10.45 | 3.6 | 0.93 | 182439 | 33222 | 16001 | 0.15 | 0.31 | 634 |
| | 35 | 574 | 12 | 28.57 | 2.8 | 215 | 5.6 | 8.63 | 5 | 0.85 | 155918 | 26526 | 12373 | 0.15 | 0.24 | 585 |
| | 36 | 619 | 6.3 | 29.54 | 1.6 | 3090 | 4.5 | 120.6 | 5.2 | 0.96 | 181832 | 31629 | 15488 | 0.15 | 0.3 | 628 |
| | 37 | 611 | 5.9 | 29.28 | 1.6 | 9350 | 6.8 | 367 | 6.8 | 0.97 | 166406 | 28918 | 15411 | 0.15 | 0.3 | 627 |
| | 38 | 462 | 34 | 20.92 | 1.9 | 38.4 | 2.9 | 2.108 | 2.1 | 0.75 | 128043 | 22789 | 10743 | 0.15 | 0.21 | 554 |
| | 39 | 615 | 6.8 | 36.86 | 2.4 | 656 | 3.3 | 20.55 | 4.4 | 0.85 | 181396 | 32075 | 16086 | 0.15 | 0.32 | 635 |
| | 40 | 607 | 21 | 24.66 | 2.1 | 97.5 | 2.5 | 4.549 | 2.1 | 0.58 | 160336 | 26607 | 13402 | 0.14 | 0.26 | 601 |
| | 41 | 649 | 6.1 | 30.5 | 1.8 | 6540 | 7.7 | 246 | 7.2 | 0.98 | 165961 | 28185 | 15635 | 0.15 | 0.31 | 629 |
| | 42 | 724 | 6.9 | 29.98 | 1.2 | 6580 | 6.7 | 251 | 7 | 0.97 | 205278 | 34196 | 18266 | 0.14 | 0.36 | 656 |
| | 44 | 690 | 7 | 29.36 | 1.3 | 4180 | 19 | 164 | 19 | 1 | 166191 | 28657 | 14082 | 0.15 | 0.28 | 610 |
| | 46 | 685 | 6.7 | 29.14 | 1.3 | 8150 | 11 | 323 | 11 | 0.99 | 181899 | 32451 | 15135 | 0.15 | 0.3 | 624 |
| | 47 | 609 | 6.2 | 30.14 | 1.2 | 2280 | 6.1 | 87.4 | 6.1 | 0.98 | 183633 | 31725 | 19477 | 0.15 | 0.38 | 666 |
| | 48 | 619 | 5.5 | 31.83 | 1.7 | 10200 | 11 | 370 | 12 | 0.99 | 190323 | 35666 | 16832 | 0.16 | 0.33 | 642 |
| | 49 | 510 | 32 | 22.83 | 1.3 | 45.92 | 1.7 | 2.325 | 1.9 | 0.72 | 150214 | 24724 | 12400 | 0.14 | 0.24 | 585 |
| | 50 | 651 | 6.6 | 29.05 | 1.5 | 3890 | 5.6 | 155 | 5.2 | 0.98 | 179936 | 31448 | 14845 | 0.15 | 0.29 | 620 |
| | 51 | 588 | 25 | 23.87 | 2.1 | 75.3 | 3 | 3.646 | 2 | 0.76 | 163521 | 26577 | 14743 | 0.14 | 0.29 | 619 |
| | 52 | 705 | 7.4 | 29.23 | 1.4 | 2170 | 7 | 85.8 | 6.9 | 0.98 | 186199 | 31571 | 14575 | 0.14 | 0.29 | 617 |
| | 53 | 691 | 6.5 | 30.36 | 1.5 | 6240 | 5.4 | 237 | 4.7 | 0.97 | 187342 | 31265 | 16498 | 0.14 | 0.32 | 639 |
| | 54 | 637 | 6 | 30.1 | 1.4 | 7150 | 6 | 274 | 5.9 | 0.98 | 173068 | 29655 | 13876 | 0.15 | 0.27 | 607 |
| | 55 | 654 | 6.5 | 28.75 | 1.4 | 6580 | 5.5 | 265 | 5.5 | 0.98 | 188979 | 31286 | 16678 | 0.14 | 0.33 | 641 |
| | 56 | 598 | 5.6 | 30.8 | 1.9 | 4980 | 7.8 | 187 | 7.4 | 0.97 | 178346 | 32910 | 14611 | 0.16 | 0.29 | 617 |
| | 58 | 524 | 18 | 29.38 | 1.7 | 91.5 | 1.8 | 3.627 | 2.2 | 0.64 | 148886 | 25648 | 12174 | 0.15 | 0.24 | 581 |
| | 59 | 682 | 11 | 30.36 | 2.2 | 327.1 | 2.3 | 12.48 | 2.2 | 0.5 | 176301 | 31630 | 17048 | 0.15 | 0.33 | 645 |

Continued on next page

| Sample | Spot name | Rb ppm | Sr | $^{87}Rb/^{87}Sr$ | ±2SE (%) | $^{87}Rb/^{86}Sr$ | ±2SE (%) | $^{87}Sr/^{86}Sr$ | ±2SE (%) | rho | Fe ppm | Mg | Ti | Mg# | Ti (a.p.f.u.) | Ti in Biotite Temperature |
|---|---|---|---|---|---|---|---|---|---|---|---|---|---|---|---|---|
| | 60 | 621 | 16 | 25.41 | 2 | 145.6 | 1.9 | 6.65 | 2.1 | 0.49 | 167644 | 27673 | 14136 | 0.14 | 0.28 | 611 |
| | 61 | 632 | 6.3 | 28.59 | 1.7 | 6480 | 8.1 | 263 | 8.2 | 0.98 | 180963 | 28792 | 17487 | 0.14 | 0.34 | 649 |
| | 62 | 668 | 6.6 | 28.72 | 1.3 | 9110 | 7.8 | 367 | 7.8 | 0.99 | 197119 | 33065 | 16226 | 0.14 | 0.32 | 636 |
| | 63 | 688 | 6.5 | 30.07 | 1.9 | 6840 | 9.7 | 264 | 9.4 | 0.98 | 182885 | 30555 | 16485 | 0.14 | 0.32 | 639 |
| | 64 | 666 | 6.6 | 28.7 | 1.5 | 9010 | 4.8 | 363 | 4.8 | 0.97 | 181179 | 31463 | 16120 | 0.15 | 0.32 | 635 |
| | 65 | 673 | 6.1 | 31.16 | 1.4 | 11120 | 5.8 | 411 | 5.9 | 0.94 | 182266 | 29921 | 14908 | 0.14 | 0.29 | 621 |
| | 66 | 657 | 6.6 | 28.06 | 1.1 | 10270 | 6.7 | 424 | 7 | 0.99 | 175838 | 29626 | 15938 | 0.14 | 0.31 | 633 |
| | 67 | 660 | 6.8 | 31.59 | 1.3 | 1516 | 3.7 | 55.6 | 3.3 | 0.94 | 176282 | 29925 | 17552 | 0.15 | 0.34 | 649 |
| | 68 | 740 | 6.5 | 32.94 | 1.8 | 5820 | 6.2 | 205 | 6.1 | 0.95 | 182629 | 32610 | 16679 | 0.15 | 0.33 | 641 |
| | 69 | 610 | 5.3 | 32.81 | 1.9 | 6480 | 7 | 228 | 7.2 | 0.95 | 184514 | 30875 | 13890 | 0.14 | 0.27 | 608 |
| | 70 | 526 | 4 | 37.37 | 1.6 | 7960 | 7.6 | 247 | 7.8 | 0.98 | 194803 | 29753 | 12826 | 0.13 | 0.25 | 592 |
| | 71 | 621 | 6.5 | 28.63 | 1.7 | 3000 | 5.5 | 121.4 | 5.7 | 0.95 | 184364 | 29809 | 16768 | 0.14 | 0.33 | 641 |
| | 73 | 679 | 6.4 | 29.74 | 1.3 | 11760 | 6.4 | 458 | 6.1 | 0.99 | 180122 | 31404 | 15585 | 0.15 | 0.31 | 629 |
| | 74 | 549 | 4.9 | 33.09 | 1.5 | 4050 | 5.3 | 141.8 | 5.2 | 0.96 | 199684 | 36134 | 15132 | 0.15 | 0.3 | 624 |
| | 75 | 701 | 11 | 28.61 | 2.9 | 360 | 5.2 | 14.55 | 3.7 | 0.84 | 182374 | 32890 | 17319 | 0.15 | 0.34 | 647 |
| | 78 | 670 | 5.6 | 33.67 | 1 | 15500 | 6.8 | 532 | 6.6 | 0.99 | 187209 | 34135 | 16055 | 0.15 | 0.31 | 634 |
| | 79 | 712 | 9.9 | 27.65 | 1.9 | 628 | 2.9 | 26.23 | 3.2 | 0.8 | 175222 | 30918 | 15703 | 0.15 | 0.31 | 630 |
| | 80 | 666 | 8 | 30.51 | 1.7 | 801 | 2.3 | 30.3 | 2.4 | 0.71 | 176410 | 30946 | 14631 | 0.15 | 0.29 | 617 |
| | 81 | 670 | 6.1 | 31.53 | 1.7 | 10340 | 7.9 | 378 | 7.7 | 0.97 | 187178 | 34425 | 16593 | 0.16 | 0.33 | 640 |
| | 82 | 624 | 14 | 27.23 | 1.5 | 180 | 7 | 7.78 | 5.1 | 0.73 | 175123 | 32150 | 15194 | 0.16 | 0.3 | 624 |
| | 83 | 701 | 6.7 | 31.08 | 1.8 | 4850 | 7.3 | 180 | 6.7 | 0.97 | 187278 | 34566 | 15701 | 0.16 | 0.31 | 630 |
| | 84 | 684 | 6.5 | 30.54 | 1.5 | 6430 | 5.8 | 243 | 6.2 | 0.98 | 173061 | 32265 | 14673 | 0.16 | 0.29 | 618 |
| | 85 | 696 | 6.7 | 30.43 | 1.3 | 6980 | 7.8 | 264 | 7.8 | 0.99 | 193327 | 36368 | 16466 | 0.16 | 0.32 | 639 |
| | 86 | 748 | 7.2 | 29.81 | 1.7 | 9760 | 6.7 | 377 | 6.5 | 0.97 | 178559 | 34745 | 16403 | 0.16 | 0.32 | 638 |
| | 87 | 710 | 6.6 | 31.31 | 2.6 | 6670 | 12 | 245 | 13 | 0.98 | 175942 | 31717 | 13320 | 0.15 | 0.26 | 600 |
| | 88 | 728 | 6.6 | 32.6 | 2.4 | 6510 | 6.3 | 229 | 5.7 | 0.92 | 189095 | 34433 | 17449 | 0.15 | 0.34 | 648 |
| | 89 | 735 | 7.9 | 28.34 | 2.2 | 2990 | 4.8 | 123.7 | 5.4 | 0.96 | 190030 | 37308 | 18611 | 0.16 | 0.36 | 659 |
| | 90 | 723 | 7.6 | 31.71 | 2.6 | 1519 | 5.5 | 55 | 5.3 | 0.9 | 181884 | 34031 | 15895 | 0.16 | 0.31 | 633 |
| | 91 | 686 | 6.5 | 31.97 | 1.9 | 5480 | 6.5 | 195 | 5.8 | 0.96 | 182836 | 34632 | 15326 | 0.16 | 0.3 | 626 |
| | 92 | 6.38 | 5.9 | 3.87 | 2.7 | 2.809 | 1.8 | 0.828 | 2.6 | 0.31 | 163408 | 23891 | 3837 | 0.13 | 0.08 | |
| | 93 | 6.67 | 5.8 | 4.22 | 3.2 | 2.989 | 2 | 0.814 | 2.8 | 0.14 | 167452 | 23531 | 3697 | 0.12 | 0.07 | |
| | 94 | 4.82 | 5.2 | 3.44 | 3.4 | 2.434 | 2.6 | 0.813 | 3 | 0.23 | 157846 | 22425 | 3060 | 0.12 | 0.06 | |
| | 95 | 6.72 | 5.7 | 4.28 | 3.1 | 3.07 | 2.9 | 0.82 | 2.9 | 0.4 | 156948 | 23454 | 3999 | 0.13 | 0.08 | |
| | 96 | 6.4 | 5.8 | 3.85 | 3.3 | 2.875 | 2.3 | 0.857 | 3 | 0.19 | 154013 | 21543 | 3654 | 0.12 | 0.07 | |
| | 97 | 5.67 | 5.2 | 3.88 | 3.2 | 2.842 | 2.6 | 0.838 | 2.6 | 0.15 | 154907 | 21869 | 3573 | 0.12 | 0.07 | |
| | 98 | 5.7 | 5.4 | 3.94 | 2.8 | 2.776 | 2.2 | 0.805 | 2.8 | 0.35 | 152694 | 21652 | 3435 | 0.12 | 0.07 | |
| | 99 | 5.91 | 5.1 | 4.25 | 3.5 | 3.062 | 1.7 | 0.83 | 3.7 | 0.32 | 165907 | 21897 | 3367 | 0.12 | 0.07 | |
| | 100 | 6.43 | 5.6 | 4.05 | 2.9 | 3.014 | 2 | 0.846 | 3 | 0.086 | 170075 | 23361 | 3801 | 0.12 | 0.07 | |
| | 101 | 7.61 | 6 | 4.55 | 2.6 | 3.334 | 2.2 | 0.836 | 2.9 | 0.45 | 157835 | 21870 | 3745 | 0.12 | 0.07 | |
| | 102 | 6.74 | 5.4 | 4.54 | 3 | 3.259 | 2.1 | 0.821 | 3.4 | 0.44 | 159107 | 21456 | 3376 | 0.12 | 0.07 | |
| | 103 | 7.02 | 5.6 | 4.36 | 2.8 | 3.286 | 2.1 | 0.855 | 3.1 | 0.29 | 158519 | 20604 | 3221 | 0.12 | 0.06 | |
| | 104 | 6.91 | 5.7 | 4.43 | 3.4 | 3.173 | 2.3 | 0.821 | 2.9 | 0.22 | 157179 | 21422 | 3388 | 0.12 | 0.07 | |
| | 105 | 7.17 | 5.7 | 4.4 | 3.2 | 3.308 | 2.3 | 0.857 | 3 | 0.23 | 163400 | 23332 | 3778 | 0.12 | 0.07 | |
| ZU005 | 1 | 1030 | 9.4 | 31.3 | 1.4 | 21100 | 9.9 | 814 | 11 | 0.99 | 129614 | 54746 | 10678 | 0.3 | 0.21 | 562 |
| | 2 | 1020 | 9.6 | 30.24 | 1.4 | 16200 | 6.9 | 627 | 6.8 | 0.98 | 125331 | 56797 | 11306 | 0.31 | 0.22 | 576 |
| | 3 | 1490 | 11 | 38.63 | 1.9 | 18600 | 11 | 565 | 10 | 0.98 | 124404 | 56597 | 11035 | 0.31 | 0.22 | 571 |
| | 4 | 1160 | 11 | 31.04 | 1.8 | 14300 | 8.4 | 542 | 8.7 | 0.97 | 141758 | 65955 | 11461 | 0.32 | 0.22 | 579 |
| | 5 | 1350 | 12 | 32.48 | 1.5 | 25500 | 8 | 921 | 7.9 | 0.99 | 133599 | 62403 | 10368 | 0.32 | 0.2 | 558 |
| | 6 | 1320 | 12 | 30.61 | 1.1 | 20200 | 7.8 | 770 | 7.6 | 0.99 | 129513 | 59788 | 10215 | 0.32 | 0.2 | 554 |
| | 7 | 1090 | 9.7 | 32.1 | 1.8 | 18600 | 8.7 | 683 | 8.1 | 0.99 | 128829 | 59442 | 11276 | 0.32 | 0.22 | 576 |
| | 8 | 867 | 8.2 | 30.73 | 1.4 | 10260 | 6.7 | 392 | 6.3 | 0.98 | 123648 | 56287 | 11218 | 0.31 | 0.22 | 574 |
| | 9 | 915 | 7.9 | 34.5 | 1.4 | 4970 | 6.3 | 172 | 6.6 | 0.98 | 134078 | 64236 | 9286 | 0.32 | 0.18 | 532 |
| | 10 | 1300 | 11 | 32.74 | 1.4 | 15500 | 7.1 | 556 | 6.9 | 0.99 | 128359 | 58800 | 10460 | 0.31 | 0.2 | 559 |
| | 11 | 1300 | 11 | 34.95 | 1.8 | 9590 | 5.2 | 325 | 5.1 | 0.94 | 127715 | 55140 | 8541 | 0.3 | 0.17 | 508 |

Continued on next page

| Sample | Spot name | Rb ppm | Sr | $^{87}Rb/^{87}Sr$ | ±2SE (%) | $^{87}Rb/^{86}Sr$ | ±2SE (%) | $^{87}Sr/^{86}Sr$ | ±2SE (%) | rho | Fe ppm | Mg | Ti | Mg# | Ti (a.p.f.u.) | Ti in Biotite Temperature |
|---|---|---|---|---|---|---|---|---|---|---|---|---|---|---|---|---|
| | 12 | 1380 | 12 | 33.46 | 1.8 | 18800 | 7.8 | 663 | 6.9 | 0.97 | 121810 | 53253 | 9318 | 0.3 | 0.18 | 531 |
| | 13 | 1190 | 12 | 29.38 | 1.2 | 13210 | 7.2 | 531 | 6.8 | 0.98 | 134740 | 60967 | 11682 | 0.31 | 0.23 | 583 |
| | 14 | 1370 | 11 | 34.77 | 1.5 | 20600 | 6.8 | 702 | 7.1 | 0.99 | 129297 | 59101 | 10434 | 0.31 | 0.2 | 558 |
| | 15 | 1230 | 12 | 30.36 | 1.4 | 20100 | 8.6 | 779 | 7.9 | 0.99 | 129860 | 58429 | 11019 | 0.31 | 0.22 | 570 |
| | 16 | 1280 | 11 | 32.53 | 1.3 | 23000 | 7.3 | 830 | 6.6 | 0.96 | 134633 | 62421 | 9964 | 0.32 | 0.2 | 548 |
| | 17 | 1220 | 11 | 31.89 | 1.2 | 15690 | 6.3 | 581 | 5.9 | 0.98 | 125373 | 56975 | 9800 | 0.31 | 0.19 | 544 |
| | 18 | 1370 | 12 | 33.64 | 1.1 | 19900 | 6.5 | 699 | 6.2 | 0.98 | 131226 | 62745 | 10925 | 0.32 | 0.21 | 570 |
| | 19 | 1010 | 9.1 | 31.63 | 1.4 | 24200 | 9.2 | 907 | 9.1 | 0.99 | 116217 | 56246 | 9318 | 0.33 | 0.18 | 533 |
| | 20 | 1300 | 12 | 30.42 | 1.4 | 24600 | 11 | 960 | 11 | 0.99 | 129001 | 57225 | 9896 | 0.31 | 0.19 | 546 |
| | 21 | 1360 | 10 | 37.34 | 1.4 | 52300 | 14 | 1650 | 13 | 1 | 150964 | 50135 | 8941 | 0.25 | 0.18 | 514 |
| | 22 | 1080 | 9.4 | 32.95 | 1.5 | 15600 | 10 | 545 | 8.9 | 0.99 | 157482 | 51839 | 11505 | 0.25 | 0.23 | 574 |
| | 23 | 1300 | 12 | 31.81 | 1.3 | 14500 | 7.4 | 541 | 7.4 | 0.99 | 146024 | 47896 | 10307 | 0.25 | 0.2 | 549 |
| | 24 | 1380 | 11 | 36.94 | 1.2 | 14040 | 7 | 451 | 7 | 0.99 | 150145 | 47809 | 10279 | 0.24 | 0.2 | 548 |
| | 25 | 1140 | 9.7 | 33.75 | 1.4 | 14900 | 9.5 | 522 | 9.2 | 0.99 | 141821 | 48461 | 9495 | 0.25 | 0.19 | 530 |
| | 26 | 1110 | 10 | 31.55 | 1.1 | 20300 | 11 | 756 | 11 | 1 | 128401 | 61737 | 9545 | 0.32 | 0.19 | 539 |
| | 27 | 1300 | 11 | 33.84 | 1.1 | 22800 | 9.5 | 800 | 9 | 0.99 | 147651 | 52823 | 8783 | 0.26 | 0.17 | 511 |
| | 28 | 1430 | 11 | 35.78 | 1.3 | 11690 | 7.2 | 389 | 7 | 0.98 | 142636 | 51137 | 9639 | 0.26 | 0.19 | 535 |
| | 29 | 772 | 7.4 | 30.37 | 1.3 | 6720 | 8.6 | 263 | 8.3 | 0.99 | 136966 | 63569 | 11642 | 0.32 | 0.23 | 583 |
| | 30 | 914 | 8.5 | 31.05 | 1.6 | 11700 | 9 | 447 | 8.7 | 0.98 | 126248 | 61882 | 10424 | 0.33 | 0.2 | 560 |
| | 31 | 1350 | 11 | 33.19 | 2 | 30200 | 12 | 1080 | 11 | 0.98 | 135305 | 64425 | 9194 | 0.32 | 0.18 | 530 |
| | 32 | 890 | 8.1 | 31.39 | 1.5 | 12700 | 7.9 | 481 | 7.7 | 0.99 | 129337 | 62519 | 11136 | 0.33 | 0.22 | 574 |
| | 33 | 1380 | 12 | 33.55 | 2 | 27800 | 14 | 990 | 14 | 0.99 | 133713 | 62077 | 8602 | 0.32 | 0.17 | 512 |
| | 34 | 1330 | 11 | 35.88 | 1.6 | 13820 | 6.2 | 456 | 6.1 | 0.95 | 140962 | 63331 | 10981 | 0.31 | 0.22 | 569 |
| | 35 | 1290 | 9.9 | 37.65 | 1.4 | 11410 | 7.9 | 360 | 7.2 | 0.98 | 128690 | 58839 | 8006 | 0.31 | 0.16 | 491 |
| | 36 | 1040 | 8.8 | 34.38 | 1.3 | 8710 | 5.3 | 302 | 5.2 | 0.97 | 142867 | 56769 | 9246 | 0.28 | 0.18 | 526 |
| | 37 | 1280 | 11 | 33.31 | 1.6 | 15400 | 6.6 | 552 | 6.6 | 0.98 | 143628 | 55179 | 10235 | 0.28 | 0.2 | 550 |
| | 38 | 1270 | 11 | 31.46 | 1.2 | 19900 | 11 | 752 | 11 | 1 | 146899 | 58888 | 11868 | 0.29 | 0.23 | 583 |
| | 39 | 1390 | 11 | 36 | 1.6 | 24000 | 10 | 795 | 9.9 | 0.98 | 138892 | 57655 | 10336 | 0.29 | 0.2 | 554 |
| | 40 | 1150 | 10 | 32.29 | 1.3 | 22400 | 12 | 817 | 11 | 0.98 | 138751 | 57264 | 10876 | 0.29 | 0.21 | 565 |
| | 41 | 1190 | 11 | 30.57 | 1.6 | 21300 | 8.2 | 830 | 8.3 | 0.99 | 145004 | 55066 | 11606 | 0.28 | 0.23 | 578 |
| | 42 | 786 | 7.2 | 32.13 | 1.4 | 9170 | 6.6 | 339 | 6 | 0.97 | 137451 | 52814 | 11190 | 0.28 | 0.22 | 570 |
| | 43 | 1010 | 8.7 | 34.63 | 1 | 7120 | 4.7 | 245 | 4.5 | 0.97 | 136091 | 50224 | 9153 | 0.27 | 0.18 | 522 |
| | 44 | 941 | 8.8 | 31.47 | 1.1 | 9600 | 7.5 | 361 | 6.9 | 0.96 | 145669 | 56531 | 12124 | 0.28 | 0.24 | 587 |
| | 45 | 1030 | 9.6 | 31.2 | 1.2 | 17000 | 7.7 | 659 | 8.4 | 0.98 | 140600 | 50916 | 10164 | 0.27 | 0.2 | 548 |
| | 46 | 882 | 8.3 | 31.03 | 1.3 | 11110 | 6.6 | 426 | 6.5 | 0.99 | 132856 | 53319 | 10313 | 0.29 | 0.2 | 553 |
| | 47 | 1250 | 11 | 34 | 1.4 | 28700 | 9 | 998 | 8.8 | 0.99 | 134314 | 49530 | 10179 | 0.27 | 0.2 | 548 |
| | 48 | 1100 | 10 | 32.23 | 1.6 | 11300 | 9.3 | 420 | 9.6 | 0.98 | 136590 | 52733 | 10520 | 0.28 | 0.21 | 557 |
| | 49 | 1590 | 13 | 35.87 | 1.4 | 35100 | 10 | 1160 | 9.6 | 0.99 | 144762 | 59403 | 11886 | 0.29 | 0.23 | 584 |
| | 50 | 1450 | 12 | 34.42 | 1.3 | 32700 | 10 | 1130 | 10 | 0.99 | 130374 | 53205 | 10861 | 0.29 | 0.21 | 565 |
| | 51 | 1080 | 9.9 | 32.1 | 1.5 | 14900 | 8.1 | 553 | 8.1 | 0.99 | 131772 | 53528 | 11374 | 0.29 | 0.22 | 575 |
| | 52 | 1190 | 11 | 33.29 | 1.1 | 9300 | 9.6 | 329 | 9.1 | 0.98 | 138972 | 60968 | 8760 | 0.3 | 0.17 | 515 |
| | 53 | 1190 | 11 | 31.18 | 1.1 | 15100 | 7.4 | 576 | 7.1 | 0.99 | 136773 | 56034 | 12096 | 0.29 | 0.24 | 588 |
| | 54 | 1330 | 13 | 31.2 | 1.9 | 9590 | 8 | 356 | 6.4 | 0.96 | 128864 | 53976 | 11698 | 0.3 | 0.23 | 581 |
| | 55 | 1440 | 13 | 32.82 | 1.5 | 21300 | 12 | 775 | 12 | 1 | 130212 | 54672 | 11432 | 0.3 | 0.22 | 577 |
| | 56 | 1080 | 9.6 | 33.09 | 1.5 | 10800 | 11 | 387 | 11 | 0.99 | 129817 | 55810 | 11824 | 0.3 | 0.23 | 584 |
| | 57 | 1350 | 13 | 30.89 | 1.4 | 18200 | 9.8 | 702 | 9.7 | 0.99 | 130213 | 56803 | 12140 | 0.3 | 0.24 | 590 |
| | 58 | 1390 | 12 | 33.59 | 1.4 | 15400 | 10 | 546 | 10 | 0.99 | 136432 | 58854 | 11463 | 0.3 | 0.22 | 578 |
| | 59 | 1280 | 11 | 32.48 | 1.4 | 21800 | 9.6 | 798 | 9.3 | 0.99 | 133450 | 58133 | 10792 | 0.3 | 0.21 | 565 |
| | 60 | 1150 | 10 | 31.85 | 1.4 | 18300 | 9.4 | 662 | 7.4 | 0.99 | 139323 | 61147 | 12162 | 0.31 | 0.24 | 590 |
| | 61 | 902 | 8 | 33.06 | 1.6 | 11900 | 9.4 | 434 | 9.8 | 0.94 | 129002 | 53600 | 10626 | 0.29 | 0.21 | 560 |
| | 62 | 943 | 8.6 | 31.96 | 1.3 | 9380 | 7.3 | 349 | 7.2 | 0.98 | 132828 | 57682 | 10653 | 0.3 | 0.21 | 562 |
| | 63 | 1340 | 11 | 35.7 | 1.3 | 16400 | 7.7 | 544 | 7.5 | 0.99 | 129176 | 59514 | 11287 | 0.32 | 0.22 | 576 |
| | 64 | 998 | 9.5 | 31.14 | 1.3 | 5890 | 5.2 | 225 | 4.9 | 0.96 | 131574 | 57076 | 11633 | 0.3 | 0.23 | 581 |
| | 65 | 1360 | 11 | 34.72 | 1.3 | 24000 | 11 | 826 | 12 | 0.99 | 133944 | 61103 | 11515 | 0.31 | 0.23 | 580 |
| | 66 | 1090 | 9.8 | 32.43 | 1.4 | 9480 | 5.9 | 354 | 6.7 | 0.98 | 134651 | 63583 | 12163 | 0.32 | 0.24 | 592 |

Continued on next page

| Sample | Spot name | Rb ppm | Sr | $^{87}Rb/^{87}Sr$ | ±2SE (%) | $^{87}Rb/^{86}Sr$ | ±2SE (%) | $^{87}Sr/^{86}Sr$ | ±2SE (%) | rho | Fe ppm | Mg | Ti | Mg# | Ti (a.p.f.u.) | Ti in Biotite Temperature |
|---|---|---|---|---|---|---|---|---|---|---|---|---|---|---|---|---|
| | 67 | 1290 | 12 | 31.72 | 1.3 | 16600 | 11 | 619 | 10 | 0.99 | 127682 | 54701 | 11260 | 0.3 | 0.22 | 574 |
| | 68 | 1150 | 9.8 | 33.65 | 1.3 | 12800 | 8 | 451 | 7.7 | 0.98 | 128755 | 58604 | 10994 | 0.31 | 0.22 | 570 |
| | 69 | 816 | 7.8 | 29.95 | 1.5 | 8610 | 7.5 | 340 | 7.4 | 0.98 | 133561 | 61520 | 12220 | 0.32 | 0.24 | 592 |
| | 70 | 1520 | 11 | 38.33 | 1.5 | 26400 | 10 | 819 | 10 | 0.99 | 129839 | 60047 | 10270 | 0.32 | 0.2 | 555 |
| | 71 | 1130 | 10 | 31.24 | 1.6 | 14600 | 7.7 | 552 | 7.1 | 0.98 | 125727 | 55594 | 12534 | 0.31 | 0.25 | 596 |
| | 72 | 1120 | 9.8 | 32.34 | 1.2 | 12040 | 6.2 | 442 | 5.7 | 0.99 | 131683 | 56659 | 11742 | 0.3 | 0.23 | 583 |
| | 73 | 1040 | 9.9 | 30.86 | 1.5 | 3910 | 4.3 | 150.1 | 4 | 0.94 | 121976 | 54938 | 25761 | 0.31 | 0.5 | 714 |
| | 74 | 1260 | 11 | 32.12 | 1.4 | 14770 | 6.5 | 545 | 6.3 | 0.98 | 125695 | 52351 | 12143 | 0.29 | 0.24 | 589 |
| | 75 | 1150 | 10 | 31.03 | 1.3 | 23900 | 5.6 | 909 | 5.4 | 0.98 | 134998 | 56229 | 11792 | 0.29 | 0.23 | 583 |
| | 76 | 1160 | 10 | 32.52 | 1.2 | 19000 | 7.6 | 691 | 7.4 | 0.99 | 136815 | 58816 | 11651 | 0.3 | 0.23 | 581 |
| | 77 | 792 | 6.6 | 33.94 | 1.4 | 10050 | 5.9 | 358 | 6.4 | 0.98 | 146813 | 51524 | 9766 | 0.26 | 0.19 | 538 |
| | 78 | 1100 | 9.5 | 32.75 | 1.5 | 14700 | 9.2 | 533 | 8.8 | 0.99 | 153897 | 55456 | 10311 | 0.26 | 0.2 | 551 |
| | 79 | 871 | 170 | 12.49 | 1.4 | 12.84 | 2.5 | 1.217 | 1.6 | 0.7 | 137239 | 64538 | 8921 | 0.32 | 0.17 | 521 |
| | 80 | 1210 | 9.9 | 34.46 | 1.3 | 15900 | 11 | 545 | 11 | 0.99 | 128107 | 54774 | 11341 | 0.3 | 0.22 | 575 |
| | 81 | 1090 | 10 | 30.44 | 1.3 | 16400 | 8.4 | 625 | 7.5 | 0.99 | 130062 | 54675 | 11708 | 0.3 | 0.23 | 582 |
| | 82 | 906 | 7.9 | 32.51 | 1.3 | 10430 | 5.6 | 379 | 5.1 | 0.97 | 152025 | 54691 | 16210 | 0.26 | 0.32 | 640 |
| | 83 | 942 | 8.3 | 32.03 | 1.5 | 11740 | 7.1 | 436 | 7.3 | 0.98 | 145193 | 53291 | 11413 | 0.27 | 0.22 | 574 |
| | 84 | 818 | 6.8 | 34.6 | 1.6 | 8040 | 5.8 | 275 | 5.7 | 0.97 | 158457 | 62339 | 11597 | 0.28 | 0.23 | 578 |
| | 85 | 1180 | 11 | 30.65 | 1.6 | 18000 | 9.1 | 718 | 10 | 0.99 | 139473 | 51154 | 12069 | 0.27 | 0.24 | 585 |
| | 86 | 1090 | 9.3 | 34 | 1.7 | 7520 | 6.5 | 261 | 6.2 | 0.96 | 137909 | 53870 | 13141 | 0.28 | 0.26 | 603 |
| | 87 | 792 | 7.5 | 30.19 | 1.9 | 12800 | 8.7 | 500 | 8.8 | 0.98 | 131550 | 59914 | 13062 | 0.31 | 0.26 | 605 |
| | 88 | 1430 | 12 | 34.22 | 1.9 | 16100 | 11 | 554 | 11 | 0.99 | 137094 | 61057 | 11265 | 0.31 | 0.22 | 575 |
| | 89 | 1140 | 9.8 | 32.84 | 1.5 | 25000 | 8.8 | 898 | 8.5 | 0.99 | 135194 | 64698 | 12398 | 0.32 | 0.24 | 596 |
| | 90 | 945 | 8.7 | 31.07 | 1.4 | 16600 | 7.8 | 630 | 7.5 | 0.99 | 136065 | 58235 | 12842 | 0.3 | 0.25 | 601 |
| | 91 | 0.147 | 240 | 0.00238 | 28 | 0.00142 | 28 | 0.7032 | 1 | 0.13 | 304 | 10 | 42 | 0.032 | 0 | |
| | 93 | 0.0384 | 220 | 0.00073 | 81 | 0.00044 | 81 | 0.7093 | 0.87 | -0.066 | 230 | 3 | 1 | 0.013 | 0 | |
| | 94 | 5.64 | 240 | 0.098 | 11 | 0.0589 | 11 | 0.7118 | 1.1 | 0.13 | 360 | 27 | 6 | 0.07 | 0 | |
| | 96 | 0.401 | 210 | 0.00782 | 11 | 0.00467 | 11 | 0.7034 | 1.3 | -0.06 | 207 | 3 | 79 | 0.012 | 0 | |
| | 97 | 0.202 | 230 | 0.00358 | 18 | 0.00216 | 18 | 0.7125 | 1.1 | 0.034 | 150 | 3 | 36 | 0.018 | 0 | |
| | 98 | 0.0867 | 240 | 0.00148 | 28 | 0.00089 | 28 | 0.7095 | 0.97 | -0.11 | 254 | 3 | 38 | 0.011 | 0 | |
| | 99 | 0.0542 | 220 | 0.001 | 42 | 0.0006 | 42 | 0.7048 | 0.97 | 0.13 | 223 | 3 | 46 | 0.013 | 0 | |
| | 100 | 0.0105 | 220 | 0.00018 | 260 | 0.00011 | 260 | 0.7066 | 0.83 | | 162 | 3 | 28 | 0.016 | 0 | |
| | 102 | 0.158 | 240 | 0.00269 | 24 | 0.00161 | 24 | 0.7071 | 0.98 | -0.21 | 210 | 4 | 9 | 0.02 | 0 | |
| | 103 | 0.86 | 210 | 0.0162 | 12 | 0.0098 | 12 | 0.7119 | 1.1 | -0.09 | 178 | 4 | | 0.022 | 0 | |
| | 104 | 0.0447 | 240 | 0.00075 | 41 | 0.00046 | 41 | 0.7187 | 1.1 | 0.11 | 90 | 2 | | 0.016 | 0 | |
| | 105 | 0.117 | 210 | 0.0022 | 20 | 0.00138 | 21 | 0.7059 | 0.96 | -0.087 | 213 | 3 | 9 | 0.015 | 0 | |

# Appendix D

# Geochemical data

The following tables list the geochemical data from samples that have collected during this study. Type corresponds to whether the sample was collected from the basement (bas) or a greenstone belt (gst).

| Sample | BL05 | BL17 | CH01 | DP01 | GH02 | GH03 | GW01 | GW02 | GW03 | GW04 |
|---|---|---|---|---|---|---|---|---|---|---|
| Type | bas | bas | bas | bas | bas | bas | bas | bas | bas | bas |
| *wt. %* | | | | | | | | | | |
| $SiO_2$ | 75.94 | 76 | 75.54 | 75.44 | 72.9 | 72.66 | 50.32 | 63.18 | 74.79 | 69.34 |
| $TiO_2$ | 0.14 | 0.08 | 0.07 | 0.12 | 0.26 | 0.19 | 1.36 | 0.44 | 0.02 | 0.42 |
| $Al_2O_3$ | 12.07 | 13.03 | 13.6 | 14.72 | 14.13 | 13.84 | 13.05 | 15.41 | 13.74 | 16.67 |
| $Fe_2O_3$ | 1.27 | 0.67 | 0.67 | 0.89 | 2.32 | 1.73 | 15.96 | 5.61 | 0.59 | 2.18 |
| MnO | 0.02 | 0.03 | 0.03 | 0.03 | 0.04 | 0.04 | 0.21 | 0.09 | 0.02 | 0.02 |
| MgO | 0.02 | n.d. | 0.06 | 0.21 | 0.31 | 0.3 | 5.1 | 3.38 | n.d. | 0.95 |
| CaO | 0.58 | 0.74 | 0.55 | 1.02 | 1.81 | 1.78 | 8.16 | 4.46 | 0.98 | 3.58 |
| $Na_2O$ | 3.69 | 4.66 | 4.34 | 4.21 | 4.46 | 4.78 | 2.54 | 4 | 4.84 | 4.97 |
| $K_2O$ | 5.46 | 4.54 | 4.24 | 1.89 | 2.85 | 3.95 | 1.49 | 1.88 | 4.44 | 1.08 |
| $P_2O_5$ | 0.05 | n.d. | 0.06 | 0.05 | 0.1 | 0.07 | 0.1 | 0.32 | 0.03 | 0.09 |
| LOI | 0.53 | 0.11 | 0.67 | 1.16 | 0.6 | 0.44 | 0.84 | 0.92 | 0.36 | 0.5 |
| Sum | 99.77 | 99.84 | 99.84 | 99.73 | 99.77 | 99.77 | 99.13 | 99.68 | 99.82 | 99.81 |
| *ppm* | | | | | | | | | | |
| Li | 12 | 18 | 37 | 700 | 28 | 33 | 18 | 33 | 1 | 17 |
| B | | | | | | | | | | |
| Sc | 2 | 1 | 2 | 1 | 3 | 2 | 14 | 7 | 1 | 3 |
| V | | | | | 13 | 11 | 348 | 62 | 1 | 43 |
| Cr | | | | | 35 | 62 | 57 | 173 | 32 | 41 |
| Co | | | | | 5 | 5 | 54 | 21 | 3 | 10 |
| Ni | | | | | 4 | 6 | 59 | 75 | 3 | 10 |
| Cu | 3 | 1 | 1 | 3 | 4 | 8 | 308 | 20 | 1 | 9 |
| Zn | | | | | 58 | 38 | 122 | 85 | 16 | 40 |
| Ga | | | | | | | | | | |
| Ge | 2 | 1 | 2 | 2 | 1 | 1 | 3 | 2 | 1 | 1 |
| As | 2 | 1 | 1 | 3 | 1 | 1 | 1 | 1 | 0 | 0 |
| Rb | 135 | 150 | 186 | 831 | 47 | 105 | 41 | 26 | 117 | 15 |
| Sr | 44 | 86 | 88 | 346 | 286 | 178 | 98 | 259 | 75 | 373 |
| Y | 28 | 2 | 8 | 11 | 12 | 8 | 29 | 24 | 9 | 8 |
| Zr | 184 | 62 | 50 | 76 | 215 | 101 | 99 | 105 | 39 | 155 |
| Nb | 12 | 6 | 10 | 5 | 6 | 6 | 318 | 9 | 3 | 4 |
| Mo | 1 | 1 | 0 | 0 | 0 | 0 | 9 | 0 | 0 | 0 |
| Sn | 8 | 7 | 8 | 7 | 1 | 1 | 3 | 2 | 1 | 1 |

Continued on next page

| Sample | BL05 | BL17 | CH01 | DP01 | GH02 | GH03 | GW01 | GW02 | GW03 | GW04 |
|---|---|---|---|---|---|---|---|---|---|---|
| Cs | 2 | 2 | 3 | 451 | n.d | n.d | 0 | n.d | n.d | n.d |
| Ba | 448 | 292 | 440 | 448 | 737 | 655 | 229 | 433 | 348 | 273 |
| La | 70 | 12 | 11 | 87 | 36 | 23 | 7 | 18 | 8 | 4 |
| Ce | 136 | 25 | 22 | 90 | 66 | 42 | 20 | 45 | 16 | 9 |
| Pr | 15 | 3 | 2 | 18 | 7 | 5 | 3 | 6 | 2 | 1 |
| Nd | 51 | 8 | 8 | 58 | 26 | 17 | 15 | 24 | 5 | 5 |
| Sm | 8 | 1 | 2 | 9 | 4 | 3 | 4 | 6 | 1 | 1 |
| Eu | 1 | 0 | 0 | 2 | 1 | 1 | 1 | 1 | 0 | 1 |
| Gd | 6 | 1 | 2 | 5 | 3 | 2 | 5 | 6 | 1 | 1 |
| Tb | 1 | 0 | 0 | 1 | 0 | 0 | 1 | 1 | 0 | 0 |
| Dy | 5 | 0 | 1 | 3 | 2 | 2 | 6 | 5 | 1 | 1 |
| Ho | 1 | 0 | 0 | 0 | 0 | 0 | 1 | 1 | 0 | 0 |
| Er | 3 | 0 | 1 | 1 | 1 | 1 | 4 | 3 | 1 | 1 |
| Tm | 0 | 0 | 0 | 0 | 0 | 0 | 1 | 0 | 0 | 0 |
| Yb | 3 | 0 | 1 | 1 | 1 | 1 | 4 | 2 | 1 | 1 |
| Lu | 0 | 0 | 0 | 0 | 0 | 0 | 1 | 0 | 0 | 0 |
| Hf | 6 | 2 | 2 | 3 | 5 | 3 | 3 | 3 | 2 | 3 |
| Ta | 1 | 1 | 1 | 1 | 0 | 1 | 2 | 1 | 1 | 1 |
| W | | | | | 0 | 0 | 1 | 0 | 0 | 0 |
| Pb | 25 | 46 | 38 | 36 | 16 | 21 | 6 | 10 | 28 | 7 |
| Th | 22 | 25 | 12 | 7 | 5 | 8 | 1 | 4 | 5 | 2 |
| U | 3 | 9 | 6 | 2 | 1 | 2 | 2 | 2 | 2 | 1 |

| Sample | GW06 | LP02 | LP03 | LP04 | LP10 | LP11 | MA01 | MO01 | MO03 | MO04 |
|---|---|---|---|---|---|---|---|---|---|---|
| Type | bas | bas | bas | bas | bas | bas | bas | gst | gst | gst |
| *wt. %* | | | | | | | | | | |
| $SiO_2$ | 75.28 | 73.15 | 69.51 | 73.86 | 65.75 | 66.89 | 74.68 | 87.38 | 54.97 | 41.4 |
| $TiO_2$ | 0.12 | 0.26 | 0.4 | 0.21 | 0.53 | 0.49 | 0.03 | 0 | 0.27 | 0.42 |
| $Al_2O_3$ | 13.99 | 13.5 | 14.46 | 13.87 | 14.28 | 14.55 | 14.62 | 0.16 | 4.97 | 17.85 |
| $Fe_2O_3$ | 1.07 | 2.91 | 3.06 | 1.07 | 5.73 | 4.87 | 0.45 | 9.39 | 7.04 | 16.51 |
| MnO | 0.01 | 0.03 | 0.04 | 0.01 | 0.1 | 0.13 | 0.01 | 0.31 | 1 | 2.44 |
| MgO | 0.23 | 0.38 | 1.23 | 0.42 | 3.8 | 1.98 | 0.2 | 1.94 | 10.23 | 17.51 |
| CaO | 1.15 | 1.25 | 2.22 | 1.49 | 3.03 | 3.76 | 0.18 | 0.78 | 18.48 | 3.71 |
| $Na_2O$ | 3.3 | 2.98 | 3.57 | 3.3 | 2.77 | 2.72 | 7.71 | 0 | 0.07 | 0.03 |
| $K_2O$ | 4.21 | 4.92 | 4.5 | 5.04 | 2.33 | 1.68 | 1.36 | 0.01 | 2.83 | 0.05 |
| $P_2O_5$ | 0.03 | 0.04 | 0.18 | 0.09 | 0.03 | 0.08 | 0.02 | 0.01 | 0.01 | 0.01 |
| LOI | 0.45 | 0.35 | 0.51 | 0.35 | 1.4 | 1.4 | 0.59 | 2.82 | 0.82 | 11.35 |
| Sum | 99.83 | 99.76 | 99.66 | 99.72 | 99.74 | 98.55 | 99.86 | 99.98 | 99.87 | 99.93 |
| *ppm* | | | | | | | | | | |
| Li | 2 | 11 | 14 | 8 | 19 | 21 | 3 | 12 | 141 | 228 |
| B | | | | | | | | 8 | 36 | 1 |
| Sc | 0 | 1 | 5 | 1 | 6 | 9 | 1 | 0 | 4 | 63 |
| V | 2 | 43 | 38 | 13 | 92 | | 3 | 2 | 66 | 153 |
| Cr | 9 | 48 | 39 | 29 | 59 | | 14 | 54 | 744 | 4539 |
| Co | 1 | 7 | 10 | 5 | 17 | | 3 | 2 | 28 | 913 |
| Ni | 1 | 9 | 17 | 10 | 21 | | 4 | 32 | 201 | 3657 |
| Cu | 1 | 2 | 10 | 9 | 0 | 104 | 8 | 1 | 0 | 126 |
| Zn | 5 | 38 | 59 | 23 | 140 | | 11 | 9 | 48 | 123 |
| Ga | | | | | | | | 1 | 48 | 60 |
| Ge | 0 | 2 | 2 | 2 | 2 | 2 | 0 | 1 | 1 | 2 |
| As | 0 | 1 | 2 | 1 | 1 | 1 | 0 | 14 | 67 | 159 |
| Rb | 23 | 182 | 104 | 116 | 82 | 109 | 47 | 1 | 212 | 2 |
| Sr | 38 | 185 | 370 | 312 | 108 | 120 | 89 | 2 | 27 | 5 |
| Y | 1 | 19 | 21 | 25 | 10 | 16 | 2 | 1 | 8 | 10 |
| Zr | 25 | 103 | 228 | 125 | 172 | 185 | 39 | 1 | 116 | 9 |
| Nb | 1 | 16 | 14 | 13 | 7 | 8 | 2 | n.d | 2 | 2 |
| Mo | 0 | 0 | 1 | 0 | 1 | 3 | 0 | 0 | 0 | 0 |
| Sn | 0 | 3 | 3 | 2 | 3 | 12 | 0 | n.d | 5 | 1 |
| Cs | n.d | n.d | n.d | n.d | n.d | 1 | n.d | 1 | 43 | 5 |
| Ba | 175 | 720 | 1107 | 1307 | 291 | 248 | 528 | 5 | 259 | 325 |
| La | 3 | 27 | 79 | 46 | 28 | 24 | 6 | 0 | 6 | 3 |
| Ce | 6 | 56 | 142 | 82 | 48 | 43 | 10 | n.d | 11 | 44 |
| Pr | 1 | 6 | 14 | 11 | 5 | 5 | 1 | 0 | 1 | 1 |
| Nd | 2 | 22 | 45 | 37 | 17 | 16 | 3 | n.d | 4 | 7 |
| Sm | 0 | 5 | 6 | 7 | 3 | 3 | 1 | 0 | 1 | 2 |
| Eu | 0 | 1 | 1 | 1 | 1 | 1 | 0 | 0 | 0 | 1 |
| Gd | 0 | 4 | 4 | 5 | 2 | 3 | 0 | 0 | 1 | 2 |
| Tb | 0 | 1 | 1 | 1 | 0 | 0 | 0 | 0 | 0 | 0 |
| Dy | 0 | 4 | 3 | 4 | 2 | 3 | 0 | 0 | 1 | 3 |
| Ho | 0 | 1 | 1 | 1 | 0 | 1 | 0 | 0 | 0 | 1 |
| Er | 0 | 2 | 2 | 3 | 1 | 2 | 0 | 0 | 1 | 2 |
| Tm | 0 | 0 | 0 | 0 | 0 | 0 | 0 | n.d | 0 | 0 |
| Yb | 0 | 2 | 2 | 3 | 1 | 2 | 0 | n.d | 1 | 2 |
| Lu | 0 | 0 | 0 | 0 | 0 | 0 | 0 | 0 | 0 | 0 |
| Hf | 1 | 3 | 6 | 4 | 4 | 5 | 1 | n.d | 3 | 0 |
| Ta | 0 | 1 | 2 | 2 | 1 | 1 | 0 | 0 | 0 | 1 |
| W | 0 | 0 | 0 | 0 | 1 | | 0 | 0 | 1 | 28 |
| Pb | 6 | 42 | 37 | 43 | 28 | 49 | 3 | 0 | 8 | 0 |
| Th | 2 | 58 | 39 | 57 | 7 | 7 | 2 | n.d | 5 | 0 |
| U | 2 | 5 | 5 | 7 | 0 | 1 | 1 | 0 | 2 | 2 |

| Sample | MO05 | MU01 | MU03 | NG01 | NG02 | NG03 | NM02 | NM03 | NY01 | NY02 |
|---|---|---|---|---|---|---|---|---|---|---|
| Type | gst | bas | bas | bas | bas | bas | bas | bas | bas | bas |
| *wt. %* | | | | | | | | | | |
| $SiO_2$ | 18.64 | 76 | 73.12 | 75.63 | 77.1 | 75.32 | 70.35 | 48.76 | 74.81 | 73.79 |
| $TiO_2$ | 0.26 | 0.01 | 0.2 | 0.11 | 0.07 | 0.09 | 0.39 | 2.52 | 0.12 | 0.22 |
| $Al_2O_3$ | 5.11 | 13.56 | 14.44 | 13.38 | 12.82 | 13.6 | 15.29 | 11.58 | 13.52 | 14.03 |
| $Fe_2O_3$ | 18.57 | 0.36 | 1.85 | 1.24 | 0.81 | 0.93 | 2.71 | 21.18 | 1.1 | 1.71 |
| MnO | 0.84 | 0.01 | 0.04 | 0.05 | 0.04 | 0.04 | 0.03 | 0.26 | 0.02 | 0.03 |
| MgO | 10.37 | n.d. | 0.3 | 0.15 | 0.15 | 0.24 | 0.8 | 3.85 | 0.24 | 0.35 |
| CaO | 45.81 | 0.81 | 2.15 | 0.74 | 0.6 | 0.8 | 2.59 | 8.47 | 1.18 | 1.45 |
| $Na_2O$ | 0 | 3.54 | 5.85 | 3.68 | 3.42 | 3.7 | 4.85 | 1.36 | 3.25 | 3.58 |
| $K_2O$ | 0.07 | 5.13 | 1.01 | 4.69 | 4.39 | 4.71 | 1.75 | 0.81 | 5.11 | 4.44 |
| $P_2O_5$ | 0.02 | n.d. | 0.06 | 0.04 | 0.03 | 0.03 | 0.1 | 0.13 | 0.04 | 0.06 |
| LOI | 29.72 | 0.44 | 0.81 | 0.6 | 0.55 | 1.1 | 0.9 | 0.68 | 0.52 | 0.7 |
| Sum | 99.69 | 99.84 | 99.83 | 99.71 | 99.43 | 99.46 | 99.76 | 99.6 | 99.39 | 99.66 |
| *ppm* | | | | | | | | | | |
| Li | 14 | 2 | 2 | 106 | 234 | 80 | 22 | 10 | 18 | 23 |
| B | 1 | | | 6 | 6 | | | | 5 | 4 |
| Sc | 3 | 0 | 2 | 2 | 2 | 2 | 3 | 30 | 2 | 2 |
| V | 103 | 1 | 15 | 6 | 5 | 5 | 28 | 746 | 6 | 12 |
| Cr | 3463 | 12 | 12 | 39 | 31 | 18 | 20 | 36 | 41 | 26 |
| Co | 137 | 3 | 6 | 1 | 1 | 3 | 9 | 68 | 2 | 2 |
| Ni | 1749 | 3 | 5 | 2 | 2 | 11 | 10 | 34 | 2 | 2 |
| Cu | 57 | 5 | 1 | 2 | 19 | 6 | 4 | 78 | 1 | 5 |
| Zn | 62 | 4 | 45 | 40 | 39 | 43 | 54 | 149 | 20 | 44 |
| Ga | 41 | | | 54 | 49 | | | | 84 | 221 |
| Ge | 1 | 2 | 1 | 4 | 3 | 2 | 1 | 2 | 3 | 3 |
| As | 185 | 0 | 1 | 1 | 1 | 1 | 1 | 2 | 1 | 1 |
| Rb | 1 | 141 | 56 | 477 | 662 | 547 | 23 | 21 | 180 | 107 |
| Sr | 16 | 67 | 245 | 47 | 48 | 54 | 401 | 95 | 89 | 144 |
| Y | 10 | 40 | 5 | 21 | 16 | 22 | 6 | 40 | 4 | 2 |
| Zr | 6 | 46 | 149 | 103 | 84 | 100 | 159 | 105 | 139 | 197 |
| Nb | 0 | 2 | 3 | 24 | 21 | 17 | 4 | 5 | 6 | 4 |
| Mo | 0 | 0 | 0 | 1 | 1 | 1 | 0 | 0 | 1 | 1 |
| Sn | 0 | 1 | 1 | 5 | 7 | 5 | 1 | 1 | 1 | 1 |
| Cs | 1 | n.d | n.d | 30 | 53 | 55 | n.d | n.d | 1 | 2 |
| Ba | 221 | 645 | 351 | 215 | 184 | 228 | 699 | 115 | 397 | 1169 |
| La | 3 | 7 | 15 | 27 | 20 | 25 | 21 | 5 | 23 | 23 |
| Ce | 2 | 13 | 28 | 53 | 39 | 52 | 44 | 15 | 49 | 43 |
| Pr | 1 | 1 | 3 | 6 | 5 | 6 | 5 | 2 | 5 | 4 |
| Nd | 3 | 4 | 10 | 21 | 16 | 20 | 15 | 13 | 18 | 14 |
| Sm | 1 | 2 | 2 | 4 | 3 | 4 | 3 | 4 | 3 | 2 |
| Eu | 0 | 0 | 0 | 0 | 0 | 0 | 1 | 1 | 0 | 0 |
| Gd | 1 | 3 | 1 | 4 | 3 | 4 | 2 | 5 | 2 | 1 |
| Tb | 0 | 1 | 0 | 1 | 1 | 1 | 0 | 1 | 0 | 0 |
| Dy | 1 | 5 | 1 | 4 | 3 | 4 | 1 | 6 | 1 | 0 |
| Ho | 0 | 1 | 0 | 1 | 1 | 1 | 0 | 1 | 0 | 0 |
| Er | 1 | 4 | 0 | 2 | 2 | 2 | 1 | 4 | 1 | 0 |
| Tm | 0 | 1 | 0 | 0 | 0 | 0 | 0 | 1 | 0 | 0 |
| Yb | 1 | 5 | 0 | 2 | 2 | 3 | 1 | 4 | 1 | 0 |
| Lu | 0 | 1 | 0 | 0 | 0 | 0 | 0 | 1 | 0 | 0 |
| Hf | 0 | 3 | 4 | 4 | 4 | 4 | 4 | 2 | 4 | 6 |
| Ta | 0 | 0 | 0 | 5 | 8 | 3 | 1 | 1 | 0 | 1 |
| W | 4 | 0 | 0 | 1 | 1 | 1 | 0 | 0 | 1 | 0 |
| Pb | 1 | 25 | 15 | 42 | 41 | 40 | 11 | 4 | 46 | 38 |
| Th | 0 | 9 | 4 | 24 | 25 | 25 | 5 | 1 | 31 | 23 |
| U | 0 | 3 | 1 | 13 | 22 | 16 | 1 | 0 | 7 | 4 |

| Sample | NY03 | PG01 | SC03 | SC04 | SG01 | SG02 | SR01 | SR02 | TR02 | TR04 |
|---|---|---|---|---|---|---|---|---|---|---|
| Type | bas | bas | bas | bas | bas | bas | bas | bas | bas | bas |
| *wt. %* | | | | | | | | | | |
| $SiO_2$ | 75.52 | 73.3 | 66.75 | 75.4 | 73.42 | 71.97 | 69.24 | 68.25 | 64.26 | 51.22 |
| $TiO_2$ | 0.15 | 0.15 | 0.43 | 0.04 | 0.86 | 0.28 | 0.38 | 0.52 | 0.42 | 0.72 |
| $Al_2O_3$ | 13.28 | 14.92 | 15.42 | 13.46 | 9.31 | 14.73 | 15.7 | 15.37 | 15 | 9.84 |
| $Fe_2O_3$ | 0.95 | 0.94 | 4.23 | 0.73 | 5.67 | 2.6 | 3.1 | 3.91 | 4.72 | 13.36 |
| MnO | 0.03 | 0.02 | 0.05 | 0.02 | 0.03 | 0.02 | 0.04 | 0.05 | 0.09 | 0.24 |
| MgO | 0.17 | 0.37 | 2.06 | n.d. | 2.09 | 0.69 | 1.29 | 1.59 | 3.42 | 9.37 |
| CaO | 0.77 | 1.47 | 4.2 | 0.7 | 2 | 3.28 | 3.68 | 3.57 | 5.78 | 11.47 |
| $Na_2O$ | 3.4 | 4.46 | 4.61 | 4.69 | 2.7 | 4.6 | 4.56 | 3.81 | 4.33 | 1.44 |
| $K_2O$ | 5.08 | 3.94 | 1.08 | 4.57 | 2.41 | 1.05 | 1.58 | 2.21 | 0.76 | 0.56 |
| $P_2O_5$ | 0.07 | 0.07 | 0.1 | n.d. | 0.13 | 0.11 | 0.15 | 0.19 | 0.06 | 0.08 |
| LOI | 0.58 | 0.41 | 0.79 | 0.28 | 0.82 | 0.44 | 0.72 | 0.87 | 0.95 | 1.29 |
| Sum | 99.42 | 99.64 | 99.72 | 99.89 | 99.43 | 99.78 | 99.72 | 99.47 | 99.78 | 99.59 |
| *ppm* | | | | | | | | | | |
| Li | 46 | 40 | 12 | n.d | 33 | 14 | 120 | 346 | 9 | 5 |
| B | 5 | 9 | | | | | 7 | 6 | | |
| Sc | 2 | 1 | 8 | 2 | 7 | 3 | 3 | 5 | 16 | 7 |
| V | 6 | 11 | | 1 | | | 39 | 59 | 122 | 194 |
| Cr | 23 | 20 | | 9 | | | 49 | 70 | 248 | 812 |
| Co | 1 | 3 | | 3 | | | 8 | 10 | 28 | 66 |
| Ni | 1 | 5 | | 4 | | | 15 | 17 | 104 | 258 |
| Cu | 5 | 2 | 33 | 1 | 2 | 3 | 1 | 2 | 55 | 45 |
| Zn | 26 | 32 | | 13 | | | 52 | 62 | 54 | 109 |
| Ga | 60 | 332 | | | | | 104 | 115 | | |
| Ge | 3 | 3 | 1 | 2 | 3 | 1 | 2 | 4 | 1 | 3 |
| As | 1 | 1 | 0 | 0 | 4 | 1 | 6 | 3 | 0 | 1 |
| Rb | 278 | 106 | 37 | 139 | 90 | 41 | 23 | 50 | 37 | 21 |
| Sr | 45 | 682 | 436 | 15 | 136 | 209 | 423 | 352 | 234 | 220 |
| Y | 6 | 3 | 7 | 11 | 13 | 14 | 7 | 8 | 9 | 17 |
| Zr | 141 | 106 | 114 | 72 | 1131 | 220 | 161 | 170 | 61 | 142 |
| Nb | 14 | 4 | 4 | 5 | 9 | 7 | 7 | 6 | 2 | 3 |
| Mo | 1 | 0 | 0 | 0 | 0 | 0 | 1 | 1 | 0 | 0 |
| Sn | 2 | 4 | 7 | 1 | 7 | 7 | 2 | 1 | 1 | 1 |
| Cs | 2 | 7 | 1 | n.d | 4 | 1 | 6 | 8 | n.d | n.d |
| Ba | 263 | 1752 | 460 | 52 | 925 | 494 | 488 | 554 | 150 | 126 |
| La | 19 | 14 | 20 | 3 | 248 | 32 | 15 | 24 | 7 | 10 |
| Ce | 53 | 29 | 35 | 8 | 440 | 55 | 29 | 49 | 14 | 27 |
| Pr | 5 | 3 | 3 | 1 | 44 | 6 | 3 | 5 | 2 | 3 |
| Nd | 15 | 13 | 13 | 5 | 141 | 21 | 11 | 20 | 6 | 14 |
| Sm | 2 | 2 | 2 | 2 | 17 | 4 | 2 | 3 | 1 | 4 |
| Eu | 0 | 1 | 1 | 0 | 2 | 2 | 1 | 1 | 1 | 1 |
| Gd | 2 | 1 | 2 | 2 | 10 | 3 | 2 | 3 | 2 | 4 |
| Tb | 0 | 0 | 0 | 0 | 1 | 1 | 0 | 0 | 0 | 1 |
| Dy | 1 | 1 | 2 | 2 | 4 | 3 | 2 | 2 | 2 | 4 |
| Ho | 0 | 0 | 0 | 0 | 1 | 1 | 0 | 0 | 0 | 1 |
| Er | 1 | 0 | 1 | 1 | 2 | 2 | 1 | 1 | 1 | 2 |
| Tm | 0 | 0 | 0 | 0 | 0 | 0 | 0 | 0 | 0 | 0 |
| Yb | 1 | 0 | 1 | 1 | 2 | 1 | 1 | 1 | 1 | 2 |
| Lu | 0 | 0 | 0 | 0 | 0 | 0 | 0 | 0 | 0 | 0 |
| Hf | 5 | 3 | 3 | 3 | 30 | 5 | 4 | 5 | 2 | 3 |
| Ta | 1 | 0 | 0 | 1 | 1 | 1 | 1 | 1 | 0 | 0 |
| W | 0 | 0 | | 0 | | | 1 | 0 | 0 | 0 |
| Pb | 52 | 67 | 10 | 30 | 13 | 9 | 18 | 25 | 7 | 4 |
| Th | 29 | 7 | 3 | 7 | 47 | 8 | 5 | 11 | 1 | 1 |
| U | 5 | 2 | 0 | 2 | 3 | 1 | 2 | 3 | 0 | 0 |

| Sample | TR06 | TR07 | TR08 | WG01 | WG02 | WG03 | ZB01 | ZB02 | ZB03 | ZB04 |
|---|---|---|---|---|---|---|---|---|---|---|
| Type | bas | bas | bas | bas | bas | bas | bas | bas | bas | bas |
| *wt. %* | | | | | | | | | | |
| $SiO_2$ | 66.09 | 76.79 | 65.14 | 53.36 | 69.44 | 65.66 | 72.39 | 73.6 | 70 | 72.06 |
| $TiO_2$ | 0.53 | 0.01 | 0.62 | 0.16 | 0.36 | 0.42 | 0.29 | 0.21 | 0.34 | 0.3 |
| $Al_2O_3$ | 15.5 | 14.51 | 15.25 | 2.9 | 15.68 | 16.9 | 15.01 | 14.76 | 14.98 | 15.5 |
| $Fe_2O_3$ | 4.21 | 0.99 | 4.87 | 12.86 | 2.75 | 2.62 | 2.07 | 1.55 | 3.68 | 2.1 |
| MnO | 0.06 | 0.04 | 0.08 | 0.48 | 0.04 | 0.05 | 0.03 | 0.02 | 0.06 | 0.03 |
| MgO | 1.32 | 0.13 | 2.23 | 17.24 | 1.33 | 2.19 | 0.68 | 0.48 | 1.67 | 0.73 |
| CaO | 4.23 | 0.84 | 6.9 | 12.3 | 3.53 | 2.31 | 3.03 | 2.09 | 3.29 | 2.75 |
| $Na_2O$ | 4.68 | 1.68 | 3.27 | 0.37 | 4.38 | 6.11 | 4.43 | 3.89 | 3.97 | 4.75 |
| $K_2O$ | 1.02 | 3.23 | 0.43 | 0.32 | 2.31 | 3.12 | 1.63 | 3.34 | 1.8 | 1.34 |
| $P_2O_5$ | 1.12 | 0.02 | 0.07 | 0.01 | 0.14 | 0.15 | 0.09 | 0.08 | 0.1 | 0.11 |
| LOI | 0.97 | 1.59 | 0.94 | 0.93 | 0.73 | 2.24 | 0.53 | 0.69 | 1.54 | 0.96 |
| Sum | 99.72 | 99.84 | 99.8 | 100 | 99.96 | 99.53 | 99.65 | 100.02 | 99.89 | 99.67 |
| *ppm* | | | | | | | | | | |
| Li | 12 | 1 | 2 | 12 | 23 | 10 | 46 | 113 | 36 | 37 |
| B | | | | 5 | 6 | 6 | 6 | 5 | 7 | 6 |
| Sc | 5 | 4 | 6 | 12 | 3 | 3 | 2 | 2 | 9 | 2 |
| V | 56 | 3 | 94 | 65 | 42 | 32 | 23 | 19 | 50 | 30 |
| Cr | 42 | 15 | 122 | 1705 | 49 | 37 | 36 | 46 | 115 | 40 |
| Co | 13 | 4 | 21 | 43 | 8 | 6 | 5 | 4 | 10 | 5 |
| Ni | 14 | 11 | 62 | 1206 | 16 | 14 | 6 | 4 | 28 | 11 |
| Cu | 16 | 3 | 23 | 1 | 3 | 1 | 1 | 1 | 13 | 8 |
| Zn | 69 | 4 | 53 | 260 | 43 | 46 | 48 | 34 | 61 | 27 |
| Ga | | | | 11 | 142 | 226 | 77 | 119 | 58 | 213 |
| Ge | 1 | 2 | 1 | 5 | 2 | 3 | 2 | 2 | 3 | 2 |
| As | 0 | 0 | 0 | 0 | 1 | 1 | 1 | 0 | 1 | 0 |
| Rb | 6 | 60 | 10 | 16 | 24 | 21 | 27 | 60 | 16 | 106 |
| Sr | 319 | 37 | 145 | 13 | 404 | 186 | 213 | 177 | 235 | 172 |
| Y | 6 | 26 | 13 | 6 | 6 | 9 | 3 | 1 | 14 | 10 |
| Zr | 136 | 30 | 74 | 13 | 145 | 146 | 144 | 121 | 130 | 124 |
| Nb | 2 | 0 | 4 | 2 | 6 | 7 | 4 | 3 | 8 | 10 |
| Mo | 0 | 1 | 0 | 0 | 1 | 0 | 1 | 4 | 1 | 0 |
| Sn | 1 | 0 | 1 | 2 | 1 | 2 | 1 | 0 | 2 | 1 |
| Cs | n.d | n.d | n.d | 1 | 1 | 0 | 2 | 10 | 2 | 8 |
| Ba | 670 | 215 | 113 | 15 | 714 | 1179 | 344 | 572 | 232 | 1116 |
| La | 16 | 14 | 14 | 2 | 11 | 20 | 11 | 4 | 6 | 7 |
| Ce | 30 | 21 | 26 | 9 | 26 | 43 | 24 | 9 | 16 | 21 |
| Pr | 3 | 2 | 3 | 1 | 3 | 5 | 3 | 1 | 2 | 2 |
| Nd | 12 | 5 | 11 | 6 | 13 | 17 | 9 | 3 | 9 | 5 |
| Sm | 2 | 1 | 2 | 2 | 3 | 3 | 2 | 0 | 3 | 1 |
| Eu | 1 | 0 | 1 | 0 | 1 | 1 | 0 | 0 | 1 | 0 |
| Gd | 2 | 1 | 3 | 1 | 2 | 2 | 1 | 0 | 3 | 1 |
| Tb | 0 | 0 | 0 | 0 | 0 | 0 | 0 | 0 | 1 | 0 |
| Dy | 1 | 3 | 2 | 1 | 2 | 2 | 1 | 0 | 3 | 2 |
| Ho | 0 | 1 | 1 | 0 | 0 | 0 | 0 | 0 | 1 | 1 |
| Er | 1 | 3 | 2 | 1 | 1 | 1 | 1 | 0 | 2 | 2 |
| Tm | 0 | 1 | 0 | 0 | 0 | 0 | 0 | n.d | 0 | 0 |
| Yb | 1 | 4 | 1 | 1 | 1 | 1 | 0 | 0 | 2 | 2 |
| Lu | 0 | 1 | 0 | 0 | 0 | 0 | 0 | 0 | 0 | 0 |
| Hf | 3 | 1 | 2 | 0 | 4 | 4 | 4 | 3 | 4 | 4 |
| Ta | 0 | 0 | 0 | 0 | 1 | 1 | 0 | 0 | 1 | 2 |
| W | 0 | 0 | 0 | 0 | 0 | 0 | 1 | n.d | 0 | 0 |
| Pb | 6 | 34 | 5 | 1 | 20 | 12 | 10 | 15 | 12 | 21 |
| Th | 1 | 2 | 2 | 0 | 7 | 11 | 4 | 3 | 3 | 7 |
| U | 0 | 1 | 0 | 0 | 2 | 2 | 0 | 2 | 1 | 1 |

| Sample | ZB05 | ZB06 | ZB07 | ZL01 | ZL011 | ZL015 | ZL09 | ZL16 | ZL20 | ZLC06 |
|---|---|---|---|---|---|---|---|---|---|---|
| Type | bas | bas | bas | gst | gst | gst | gst | gst | gst | gst |
| *wt. %* | | | | | | | | | | |
| $SiO_2$ | 73.15 | 73.11 | 74.57 | 65.04 | 50.89 | 79.28 | 51.5 | 48.23 | 48.64 | 65.46 |
| $TiO_2$ | 0.21 | 0.25 | 0.11 | 0.61 | 0.6 | 0.43 | 0.53 | 0.32 | 0.32 | 0.13 |
| $Al_2O_3$ | 14.49 | 14.18 | 15.11 | 14.54 | 13.54 | 13.24 | 13.12 | 8.52 | 8.37 | 19.56 |
| $Fe_2O_3$ | 1.38 | 1.99 | 1 | 6.76 | 10.65 | 0.42 | 10.59 | 11.88 | 11.76 | 0.78 |
| MnO | 0.02 | 0.03 | 0.01 | 0.08 | 0.17 | 0.02 | 0.18 | 0.2 | 0.21 | 0.03 |
| MgO | 0.5 | 0.71 | 0.24 | 4.13 | 8.61 | 0.04 | 9.05 | 21.65 | 20.86 | 0.29 |
| CaO | 1.68 | 2.13 | 1.31 | 2.82 | 11.65 | 0.03 | 10.96 | 8.59 | 9.28 | 1.52 |
| $Na_2O$ | 4.4 | 3.57 | 4.64 | 4.02 | 2.21 | 0.78 | 1.7 | 0.26 | 0.24 | 4.92 |
| $K_2O$ | 3.59 | 3.31 | 2.86 | 1.33 | 0.06 | 3.67 | 0.06 | 0.02 | 0.03 | 7.3 |
| $P_2O_5$ | 0.09 | 0.08 | 0.05 | 0.15 | 0.03 | 0.04 | 0.01 | 0.02 | 0.02 | 0.03 |
| LOI | 0.61 | 0.8 | 0.98 | 1.08 | 0.98 | 1.8 | 1.81 | 4.63 | 4.31 | 1.96 |
| Sum | 99.51 | 99.36 | 99.9 | 99.48 | 99.4 | 99.75 | 99.5 | 99.69 | 99.73 | 100.02 |
| *ppm* | | | | | | | | | | |
| Li | 866 | 38 | 48 | 123 | 5 | 21 | 22 | 30 | 53 | 104 |
| B | 7 | 6 | 9 | 6 | | | | 0 | 0 | 5 |
| Sc | 2 | 1 | 1 | 7 | 45 | 9 | 44 | 28 | 30 | 2 |
| V | 21 | 8 | 20 | 109 | 229 | 77 | 243 | 146 | 144 | 12 |
| Cr | 55 | 44 | 55 | 51 | 452 | 89 | 463 | 3079 | 2638 | 5 |
| Co | 5 | 2 | 4 | 22 | 55 | 5 | 48 | 87 | 78 | 1 |
| Ni | 5 | 2 | 8 | 54 | 151 | 9 | 138 | 921 | 777 | 2 |
| Cu | 4 | 2 | 6 | 111 | 93 | 1 | 108 | 17 | 38 | 1 |
| Zn | 62 | 35 | 44 | 66 | 78 | 4 | 74 | 71 | 74 | 7 |
| Ga | 39 | 133 | 160 | 130 | | | | 7 | 7 | 64 |
| Ge | 2 | 1 | 3 | 3 | 0 | 2 | 1 | 1 | 1 | 4 |
| As | 0 | 1 | 2 | 1 | 1 | 1 | 1 | 0 | 0 | 1 |
| Rb | 27 | 64 | 110 | 44 | 1 | 346 | 3 | 1 | 1 | 653 |
| Sr | 196 | 302 | 438 | 296 | 100 | 62 | 106 | 28 | 19 | 52 |
| Y | 4 | 2 | 4 | 17 | 12 | 8 | 14 | 7 | 7 | 18 |
| Zr | 206 | 84 | 120 | 152 | 16 | 122 | 14 | 9 | 11 | 133 |
| Nb | 8 | 2 | 5 | 6 | 1 | 4 | 1 | 1 | 1 | 25 |
| Mo | 3 | 1 | 1 | 1 | 0 | 0 | 0 | 0 | 0 | 1 |
| Sn | 1 | 1 | 1 | 1 | 0 | 3 | 0 | 0 | 0 | 6 |
| Cs | 26 | 2 | 6 | 78 | n.d | 13 | n.d | 1 | 0 | 33 |
| Ba | 123 | 659 | 792 | 673 | 27 | 170 | 18 | 3 | 6 | 272 |
| La | 7 | 4 | 24 | 16 | 1 | 29 | 2 | 1 | 1 | 18 |
| Ce | 15 | 9 | 38 | 29 | 4 | 24 | 4 | 2 | 2 | 40 |
| Pr | 2 | 1 | 4 | 4 | 1 | 5 | 1 | 0 | 0 | 5 |
| Nd | 6 | 3 | 15 | 14 | 3 | 18 | 4 | 1 | 1 | 16 |
| Sm | 1 | 1 | 2 | 3 | 1 | 3 | 1 | 1 | 1 | 4 |
| Eu | 0 | 0 | 1 | 1 | 0 | 1 | 1 | 0 | 0 | 0 |
| Gd | 1 | 1 | 2 | 4 | 1 | 2 | 2 | 1 | 1 | 4 |
| Tb | 0 | 0 | 0 | 1 | 0 | 0 | 0 | 0 | 0 | 1 |
| Dy | 1 | 0 | 1 | 3 | 2 | 2 | 2 | 1 | 1 | 4 |
| Ho | 0 | 0 | 0 | 1 | 0 | 0 | 0 | 0 | 0 | 1 |
| Er | 1 | 0 | 0 | 2 | 1 | 1 | 1 | 1 | 1 | 3 |
| Tm | 0 | 0 | 0 | 0 | 0 | 0 | 0 | 0 | 0 | 0 |
| Yb | 1 | 0 | 0 | 2 | 1 | 1 | 1 | 1 | 1 | 3 |
| Lu | 0 | 0 | 0 | 0 | 0 | 0 | 0 | 0 | 0 | 0 |
| Hf | 5 | 3 | 4 | 4 | 0 | 3 | 0 | 0 | 0 | 5 |
| Ta | 1 | 0 | 1 | 1 | 0 | 0 | 0 | 0 | 0 | 6 |
| W | 0 | 0 | 1 | 1 | 0 | 6 | 0 | 0 | 0 | 1 |
| Pb | 16 | 17 | 47 | 19 | 1 | 7 | 1 | 0 | 0 | 39 |
| Th | 4 | 1 | 15 | 4 | 0 | 6 | 0 | n.d | n.d | 26 |
| U | 1 | 1 | 5 | 1 | 0 | 2 | 0 | n.d | 0 | 17 |

| Sample | ZLC07 | ZLC15 | ZLC17/15 | ZLC20 | ZLC32 | ZLD01 | ZLD02 | ZLD03 | ZLD05 | ZLD06 |
|---|---|---|---|---|---|---|---|---|---|---|
| Type | gst | gst | gst | gst | gst | bas | bas | gst | gst | gst |
| *wt. %* | | | | | | | | | | |
| $SiO_2$ | 66.98 | 48.76 | 64.22 | 64.65 | 50.08 | 75.45 | 76.58 | 34 | 43.9 | 65 |
| $TiO_2$ | 0.01 | 0.95 | 0.76 | 0.67 | 0.71 | 0.05 | 0.03 | 0.07 | 0.29 | 0.55 |
| $Al_2O_3$ | 18.81 | 21.55 | 14.66 | 14.84 | 12.27 | 14 | 13.97 | 0.6 | 5.74 | 15.01 |
| $Fe_2O_3$ | 0.44 | 10.03 | 4.75 | 6.11 | 15.57 | 0.74 | 0.32 | 7.58 | 11.8 | 6.87 |
| MnO | 0.02 | 0.18 | 0.11 | 0.11 | 0.23 | 0.02 | 0.02 | 0.15 | 0.19 | 0.2 |
| MgO | 0.08 | 3.75 | 2.29 | 2.92 | 7.68 | 0.03 | n.d. | 39.4 | 25.78 | 0.96 |
| CaO | 1.26 | 9.78 | 5.37 | 5.57 | 11.44 | 0.63 | 1.05 | 2.34 | 5.8 | 4.69 |
| $Na_2O$ | 7.85 | 2.49 | 1.8 | 3.54 | 1.19 | 3.18 | 4.55 | 0.33 | 0.29 | 3.3 |
| $K_2O$ | 4.6 | 2.08 | 5.52 | 1.29 | 0.44 | 5.27 | 3.02 | 0.01 | 0.01 | 2.16 |
| $P_2O_5$ | 0.09 | 0.24 | 0.06 | 0.16 | 0.19 | 0.02 | 0.04 | n.d. | 0.03 | 0.13 |
| LOI | 0.97 | 1.75 | 0.67 | 1.04 | 0.86 | 0.4 | 0.22 | 14.61 | 5.34 | 0.65 |
| Sum | 100.14 | 99.81 | 99.54 | 99.86 | 99.8 | 99.79 | 99.79 | 99.07 | 99.18 | 99.51 |
| *ppm* | | | | | | | | | | |
| Li | 11 | 287 | 42 | 131 | 156 | 248 | 69 | n.d | 28 | 352 |
| B | 6 | 6 | 7 | 5 | 1 | | | | | |
| Sc | 0 | 6 | 9 | 3 | 19 | 3 | 2 | 5 | 14 | 12 |
| V | 3 | 137 | 79 | 103 | 194 | | | 15 | 100 | 85 |
| Cr | 2 | 98 | 22 | 92 | 282 | | | 1021 | 2276 | 55 |
| Co | 1 | 31 | 18 | 17 | 52 | | | 114 | 68 | 23 |
| Ni | 1 | 61 | 19 | 57 | 207 | | | 2686 | 1027 | 32 |
| Cu | 2 | 51 | 22 | 3 | 50 | 5 | 10 | 4 | 19 | 36 |
| Zn | 4 | 164 | 93 | 296 | 106 | | | 17 | 82 | 67 |
| Ga | 22 | 74 | 257 | 88 | 30 | | | | | |
| Ge | 4 | 5 | 2 | 5 | 4 | 2 | 2 | 0 | 3 | 1 |
| As | 1 | 1 | 0 | 1 | 1 | 0 | 0 | 5 | 0 | 0 |
| Rb | 692 | 100 | 38 | 55 | 29 | 291 | 158 | 0 | 1 | 81 |
| Sr | 27 | 294 | 187 | 199 | 197 | 36 | 54 | 68 | 21 | 111 |
| Y | 8 | 16 | 7 | 17 | 21 | 17 | 18 | 1 | 12 | 11 |
| Zr | 57 | 216 | 58 | 195 | 110 | 57 | 66 | 7 | 25 | 143 |
| Nb | 14 | 5 | 13 | 7 | 4 | 12 | 9 | 1 | 2 | 5 |
| Mo | 12 | 1 | 6 | 1 | 0 | 0 | 5 | 0 | 0 | 2 |
| Sn | 1 | 1 | 2 | 1 | 0 | 9 | 7 | 1 | 2 | 1 |
| Cs | 39 | 33 | 4 | 10 | 5 | 31 | 35 | n.d | n.d | 90 |
| Ba | 59 | 299 | 1401 | 418 | 104 | 223 | 155 | n.d | n.d | 326 |
| La | 9 | 25 | 3 | 25 | 22 | 14 | 11 | 0 | 4 | 12 |
| Ce | 20 | 52 | 7 | 52 | 45 | 29 | 22 | 0 | 10 | 24 |
| Pr | 2 | 6 | 1 | 6 | 5 | 3 | 3 | 0 | 1 | 3 |
| Nd | 8 | 24 | 3 | 24 | 22 | 12 | 9 | n.d | 6 | 10 |
| Sm | 2 | 5 | 1 | 5 | 4 | 2 | 2 | 0 | 2 | 2 |
| Eu | 0 | 1 | 0 | 1 | 1 | 0 | 0 | 0 | 1 | 1 |
| Gd | 2 | 4 | 1 | 4 | 4 | 3 | 3 | 0 | 2 | 2 |
| Tb | 0 | 1 | 0 | 1 | 1 | 0 | 0 | 0 | 0 | 0 |
| Dy | 2 | 4 | 1 | 4 | 4 | 3 | 3 | 0 | 2 | 2 |
| Ho | 0 | 1 | 0 | 1 | 1 | 1 | 1 | 0 | 0 | 0 |
| Er | 1 | 2 | 1 | 2 | 3 | 2 | 2 | 0 | 1 | 1 |
| Tm | 0 | 0 | 0 | 0 | 0 | 0 | 0 | 0 | 0 | 0 |
| Yb | 1 | 2 | 2 | 2 | 2 | 2 | 2 | 0 | 1 | 1 |
| Lu | 0 | 0 | 0 | 0 | 0 | 0 | 0 | 0 | 0 | 0 |
| Hf | 4 | 5 | 2 | 5 | 3 | 2 | 3 | 0 | 1 | 4 |
| Ta | 37 | 1 | 1 | 1 | 0 | 2 | 3 | 0 | 0 | 1 |
| W | 0 | 1 | 3 | 3 | 9 | | | 8 | 0 | 1 |
| Pb | 24 | 27 | 49 | 69 | 5 | 37 | 31 | 1 | 1 | 13 |
| Th | 13 | 5 | 1 | 6 | 4 | 15 | 11 | 0 | 1 | 5 |
| U | 19 | 2 | 1 | 2 | 1 | 5 | 11 | 0 | 0 | 1 |

| Sample | ZLD07 | ZLD08 | ZU06 |
|---|---|---|---|
| Type | gst | gst | gst |
| *wt. %* | | | |
| $SiO_2$ | 63.51 | 39.4 | 74.09 |
| $TiO_2$ | 0.65 | 0.38 | 0.31 |
| $Al_2O_3$ | 15.66 | 14.64 | 14.28 |
| $Fe_2O_3$ | 5.81 | 4.63 | 1.77 |
| MnO | 0.08 | 0.12 | 0.02 |
| MgO | 1.97 | 3.87 | 0.81 |
| CaO | 5.21 | 15.97 | 1.18 |
| $Na_2O$ | 3.84 | 3.83 | 6.31 |
| $K_2O$ | 1.47 | 3.08 | 0.77 |
| $P_2O_5$ | 0.17 | 0.07 | 0.08 |
| LOI | 0.94 | 13.33 | 0.49 |
| Sum | 99.33 | 99.32 | 99.62 |
| *ppm* | | | |
| Li | 347 | 216 | 304 |
| B | | | 6 |
| Sc | 9 | 11 | 3 |
| V | 112 | 125 | 42 |
| Cr | 17 | 95 | 13 |
| Co | 17 | 16 | 3 |
| Ni | 14 | 60 | 76 |
| Cu | 36 | 2 | 9 |
| Zn | 97 | 40 | 30 |
| Ga | | | 30 |
| Ge | 1 | 0 | 3 |
| As | 0 | 1 | 1 |
| Rb | 85 | 299 | 28 |
| Sr | 239 | 146 | 74 |
| Y | 12 | 12 | 12 |
| Zr | 158 | 80 | 164 |
| Nb | 6 | 3 | 6 |
| Mo | 0 | 0 | 1 |
| Sn | 1 | 1 | 1 |
| Cs | 58 | 15 | 9 |
| Ba | 288 | 524 | 101 |
| La | 13 | 15 | 16 |
| Ce | 29 | 29 | 36 |
| Pr | 3 | 3 | 4 |
| Nd | 13 | 13 | 16 |
| Sm | 3 | 2 | 3 |
| Eu | 1 | 1 | 1 |
| Gd | 3 | 2 | 3 |
| Tb | 0 | 0 | 0 |
| Dy | 3 | 2 | 2 |
| Ho | 1 | 0 | 1 |
| Er | 2 | 1 | 2 |
| Tm | 0 | 0 | 0 |
| Yb | 2 | 1 | 2 |
| Lu | 0 | 0 | 0 |
| Hf | 4 | 2 | 4 |
| Ta | 1 | 1 | 1 |
| W | 1 | 3 | 1 |
| Pb | 18 | 2 | 20 |
| Th | 4 | 3 | 10 |
| U | 2 | 1 | 3 |

# References


A. Acosta-Vigil, I. Buick, B. Cesare, D. London, and G. B. Morgan. The extent of equilibration between melt and residuum during regional anatexis and its implications for differentiation of the continental crust: a study of partially melted metapelitic enclaves. *J. Petrol.*, 53(7):1319–1356, 1 July 2012.

J. J. Ague. Evidence for major mass transfer and volume strain during regional metamorphism of pelites. *Geology*, 19(8):855–858, 1991.

J. Aitchison. The statistical analysis of compositional data. *J. R. Stat. Soc.*, 44(2): 139–177, 1982.

J. N. Aleinikoff, R. P. Wintsch, R. P. Tollo, D. M. Unruh, C. M. Fanning, and M. D. Schmitz. Ages and origins of rocks of the killingworth dome, south-central connecticut: Implications for the tectonic evolution of southern new england. *Am. J. Sci.*, 307(1):63–118, 1 Jan. 2007.

M. N. C. Araújo, F. C. A. da Silva, and E. F. J. de Sá. Pegmatite emplacement in the seridó belt, northeastern brazil: Late stage kinematics of the brasiliano orogen. *Gondwana Res.*, 4(1):75–85, 1 Jan. 2001.

R. J. Arculus and L. J. Ruff. Genesis of continental crust: Evidence from island arcs, granulites, and exospheric processes. In *Granulites and Crustal Evolution*, pages 7–23. Springer Netherlands, Dordrecht, 1990.

R. Armstrong and A. H. Wilson. A SHRIMP U–pb study of zircons from the layered sequence of the great dyke, zimbabwe, and a granitoid anatectic dyke. *Earth Planet. Sci. Lett.*, 180(1-2):1–12, 30 July 2000.

N. T. Arndt. Formation and evolution of the continental crust. *Geochemical Perspectives*, 2(3), 2013.

H. Baadsgard and P. Černý. Geochronological studies in the winnipeg river pegmatite populations, southeastern manitoba. In *Program with Abstracts*, 18, page 5, 1993.

D. R. Baker. The escape of pegmatite dikes from granitic plutons; constraints from new models of viscosity and dike propagation. *Can. Mineral.*, 36(2):255–263, 1 Apr. 1998.

J. W. Baldock. The geology of the harare greenstone belt and surrounding granitic terrain. Technical Report 94, Zimbabwe Geological Survey, 1991.

J. W. Baldock and J. A. Evans. Constraints on the age of the bulawayan group metavolcanic sequence, harare greenstone belt, zimbabwe. *J. Afr. Earth Sci. (Middle East)*, 7(5-6):795–804, 1 Jan. 1988.

C. Ballouard, M. A. Elburg, S. Tappe, C. Reinke, H. Ueckermann, and S. Doggart. Magmatic-hydrothermal evolution of rare metal pegmatites from the mesoproterozoic orange river pegmatite belt (namaqualand, south africa). *Ore Geology Reviews*, 116:103252, 1 Jan. 2020.

J. H. Bédard. Evidence for regional-scale, pluton-driven, high-grade metamorphism in the archaean minto block, northern superior province, canada. *J. Geol.*, 111(2): 183–205, Mar. 2003.

J. H. Bédard. A catalytic delamination-driven model for coupled genesis of archaean crust and sub-continental lithospheric mantle. *Geochim. Cosmochim. Acta*, 70(5): 1188–1214, 1 Mar. 2006.

J. H. Bédard. Stagnant lids and mantle overturns: Implications for archaean tectonics, magmagenesis, crustal growth, mantle evolution, and the start of plate tectonics. *Geoscience Frontiers*, 9(1):19–49, 1 Jan. 2018.

J. H. Bédard, L. B. Harris, and P. C. Thurston. The hunting of the snArc. *Precambrian Res.*, 229:20–48, May 2013.

T. R. Benson, S. M. Jowitt, and A. C. Simon. Special issues on the geology and origin of lithium deposits–introduction: Lithium deposit types, sizes, and global distribution. *Econ. Geol.*, 12 Apr. 2025.

M. Berger, J. Kramers, and T. Nägler. Geochemistry and geochronology of charnoenderbites in the northern marginal zone of the limpopo belt, southern africa, and

genetic models. *Schweizerische Mineralogische und Petrographische Mitteilungen*, 75(1):17–42, 1995.

S. Bhatt, V. Rana, S. Lahiri, and M. A. Mamtani. Pegmatite dyke emplacement and the state of stress during cratonization – an example from the dharwar craton (south india). *J. Struct. Geol.*, 123:67–80, 1 June 2019.

M. J. Bickle, A. Martin, and E. G. Nisbet. Basaltic and peridotitic komatiites and stromatolites above a basal unconformity in the belingwe greenstone belt, rhodesia. *Earth Planet. Sci. Lett.*, 27(2):155–162, 1 Sept. 1975.

M. J. Bickle, A. Martin, E. G. Nisbet, and J. L. Orpen. *The Geology of the Belingwe Greenstone Belt, Zimbabwe: A study of Archaean continental crust.* Taylor & Francis, 1 Jan. 1993.

W. Bleeker. The late archean record: a puzzle in ca. 35 pieces. *Lithos*, 71(2):99–134, 1 Dec. 2003.

T. G. Blenkinsop. Single stage, late archaean exhumation of granulites in the northern marginal zone, limpopo belt, zimbabwe, and relevance to gold mineralization at renco mine. *South Afr. J. Geol.*, 107(3):377–396, 1 Sept. 2004.

T. G. Blenkinsop and P. J. Treloar. Tabular intrusion and folding of the late archaean murehwa granite, zimbabwe, during regional shortening. *J. Geol. Soc. London*, 158 (4):653–664, July 2001.

T. G. Blenkinsop, C. M. Fedo, M. J. Bickle, K. A. Eriksson, A. Martin, E. G. Nisbet, and J. F. Wilson. Ensialic origin for the ngezi group, belingwe greenstone belt, zimbabwe. *Geology*, 21(12):1135–1138, 1 Dec. 1993.

T. G. Blenkinsop, C. M. Fedo, M. J. Bickle, K. A. Eriksson, A. Martin, E. G. Nisbet, and J. F. Wilson. The zimbabwe craton, southern africa. In M. J. de Wit and L. D. Ashwal, editors, *Greenstone Belts*, pages 562–574. Oxford University Press, Oxford, England, 1997.

R. Bolhar, J. D. Woodhead, and J. M. Hergt. Continental setting inferred for emplacement of the 2.9–2.7 ga belingwe greenstone belt, zimbabwe. *Geology*, 31(4): 295–298, 1 Apr. 2003.

R. Bolhar, A. Hofmann, A. I. S. Kemp, M. J. Whitehouse, S. Wind, and B. S. Kamber. Juvenile crust formation in the zimbabwe craton deduced from the O-hf isotopic record of 3.8–3.1 ga detrital zircons. *Geochim. Cosmochim. Acta*, 215:432–446, 2017.

R. J. Bowell, L. Lagos, C. R. de los Hoyos, and J. Declercq. Classification and characteristics of natural lithium resources. *Elements*, 16(4):259–264, 1 Aug. 2020.

D. Bradley and A. Mccauley. A preliminary deposit model for lithium-cesium-tantalum (LCT) pegmatites. Technical report, US Geological Survey, 2017.

C. M. Breasley, T. Martins, R. L. Linnen, C. Deveau, L. A. Groat, L. Koopmans, E. Landry, and D. Moser. The geochemistry, origins and metallurgical implications of different textural types of spodumene-quartz intergrowths (SQUI) from the tanco pegmatite, manitoba, canada. *Ore Geol. Rev.*, 180(106577):106577, 1 May 2025.

L. A. Brengman, C. M. Fedo, M. J. Whitehouse, I. Jabeen, and N. R. Banerjee. Evaluating the geochemistry and paired silicon and oxygen isotope record of quartz in siliceous rocks from the 3 ga buhwa greenstone belt, zimbabwe, a critical link to deciphering the mesoarchean silica cycle. *Chem. Geol.*, 577(April):120300, 2021.

W. C. Brisbin. Mechanics of pegmatite intrusion. *Am. Mineral.*, 71(3-4):644–651, 1 Apr. 1986.

W. C. Brisbin and D. L. Trueman. Dilational mechanics of fractures during pegmatite emplacement, winnipeg river area, manitoba. In *Geological Association of Canada, Mineralogical Association of Canada, 1982 Annual Meeting, Program with Abstracts*, 7, page 40, 1982.

J. K. Brou, M. Van Lichtervelde, N. A. Kouamelan, D. Baratoux, and N. Thébaud. Petrogenetic relationships between peraluminous granites and li- cs-ta rich pegmatites in south issia zone (central-west of côte d'ivoire): Petrography, mineralogy, geochemistry and zircon U–pb geochronology. *Mineral. Petrol.*, 116(6):443–471, 1 Dec. 2022.

M. Brown. Granite: From genesis to emplacement. *Bulletin of the Geological Society of America*, 125(7-8):1079–1113, July 2013.

M. Brown and G. S. Solar. Shear-zone systems and melts: feedback relations and self-organization in orogenic belts. *J. Struct. Geol.*, 20(2):211–227, 1 Feb. 1998.

M. Brown, F. J. Korhonen, and C. S. Siddoway. Organizing melt flow through the crust. *Elements*, 7(4):261–266, Aug. 2011.

M. Brown, T. Johnson, and N. J. Gardiner. Plate tectonics and the archean earth. *Annu. Rev. Earth Planet. Sci.*, 2020.

C. E. Bucholz. Coevolution of sedimentary and strongly peraluminous granite phosphorus records. *Earth Planet. Sci. Lett.*, 596(117795):117795, 15 Oct. 2022.

C. E. Bucholz and J. D. Hernández-Montenegro. Temporal variation in oxygen isotopes of peraluminous granites derived from sedimentary sources. *Lithos*, 492-493 (107864):107864, 1 Jan. 2025.

R. F. Butler, G. E. Gehrels, S. L. Baldwin, and C. Davidson. Paleomagnetism and geochronology of the ecstall pluton in the coast mountains of british columbia: Evidence for local deformation rather than large-scale transport: ECSTALL PLUTON. *J. Geophys. Res.*, 107(B1):EPM 3–1–EPM 3–13, 1 Jan. 2002.

A. Camacho, H. Baadsgaard, D. W. Davis, and P. Cerny. Radiogenic isotope systematics of the tanco and silverleaf granitic pegmatites, winnipeg river pegmatite district, manitoba. *Can. Mineral.*, 50(6):1775–1792, 1 Dec. 2012.

A. Camacho, J. K. W. Lee, J. Zhao, Y. A. Abdu, M. Fayek, and R. A. Creaser. A test of the interlayer ionic porosity model as a measure of argon diffusivity in trioctahedral micas. *Geochim. Cosmochim. Acta*, 288:341–368, 1 Nov. 2020.

E. N. Cameron, R. H. Jahns, A. H. McNair, and L. R. Page. *Internal Structure of Granitic Pegmatites*. Society of Economic Geologists, 1949.

S. D. G. Campbell and P. E. J. Pitfield. Structural controls of gold mineralization in the zimbabwe craton - exploration guidelines. Technical Report 101, Zimbabwe Geological Survey, 1994.

C. A. Carlson. Spatial distribution of ore deposits. *Geology*, 19(2):111, 1 Feb. 1991.

P. R. Castillo. Adakite petrogenesis. *Lithos*, 134-135:304–316, 1 Mar. 2012.

G. C. G. Cavalcante, G. Viegas, C. J. Archanjo, and M. E. da Silva. The influence of partial melting and melt migration on the rheology of the continental crust. *J. Geodyn.*, 101:186–199, 1 Nov. 2016.

P. A. Cawood, C. J. Hawkesworth, S. A. Pisarevsky, B. Dhuime, F. A. Capitanio, and O. Nebel. Geological archive of the onset of plate tectonics. In *Philosophical Transactions of the Royal Society A: Mathematical, Physical and Engineering Sciences*, volume 376. Royal Society Publishing, 13 Nov. 2018.

P. A. Cawood, P. Chowdhury, J. A. Mulder, C. J. Hawkesworth, F. A. Capitanio, P. M. Gunawardana, and O. Nebel. Secular evolution of continents and the earth system. *Rev. Geophys.*, 60(4), Dec. 2022.

P. Černý and S. T. Ercit. THE CLASSIFICATION OF GRANITIC PEGMATITES REVISITED. *Can. Mineral.*, 43(6):2005–2026, 1 Dec. 2005.

P. Černý, M. Masau, B. E. Goad, and K. Ferreira. The greer lake leucogranite, manitoba, and the origin of lepidolite-subtype granitic pegmatites. *Lithos*, 80(1-4 SPEC. ISS.):305–321, Mar. 2005.

G. S. Chagondah, A. Hofmann, M. A. Elburg, L. M. Iaccheri, J. D. Kramers, and A. H. Wilson. Petrogenesis of potassic granite suites along the southern margin of the zimbabwe craton. *South Afr. J. Geol.*, 126(1):1–28, 1 Mar. 2023.

G. S. Chagondah, J. D. Kramers, A. Hofmann, and H. Rollinson. Neoarchaean and palaeoproterozoic tectono-metamorphic events along the southern margin of the zimbabwe craton: Insights from muscovite 40Ar/39Ar geochronology from rare-metal pegmatites, zimbabwe. *J. Afr. Earth. Sci.*, 217:105333, 1 Sept. 2024.

T. Chakraborty and D. Upadhyay. The geochemical differentiation of S-type pegmatites: constraints from major–trace element and li–B isotopic composition of muscovite and tourmaline. *Contrib. Mineral. Petrol.*, 175(7):1–25, 1 July 2020.

B. W. Chappell and A. J. R. White. I- and S-type granites in the lachlan fold belt. In *Geological Society of America Special Papers*, Geological Society of America Special Papers, pages 1–26. Geological Society of America, 1992.

B. W. Chappell and A. J. R. White. Two contrasting granite types: 25 years later. *Aust. J. Earth Sci.*, 48(4):489–499, 1 Aug. 2001.

F. R. Chaúque, U. G. Cordani, D. L. Jamal, and A. T. Onoe. The zimbabwe craton in mozambique: A brief review of its geochronological pattern and its relation to the mozambique belt. *J. Afr. Earth Sci.*, 129:366–379, 1 May 2017.

C. Chauvel, B. Dupré, and N. T. Arndt. Pb and nd isotopic correlation in belingwe komatiites and basalts. In *The Geology of the Belingwe Greenstone Belt, Zimbabwe*, pages 167–174. CRC Press, 1st edition edition, 26 Aug. 1993.

D. M. Chew, P. J. Sylvester, and M. N. Tubrett. U–pb and th–pb dating of apatite by LA-ICPMS. *Chem. Geol.*, 280(1-2):200–216, 7 Jan. 2011.

D. M. Chew, J. A. Petrus, and B. S. Kamber. U–pb LA–ICPMS dating using accessory mineral standards with variable common pb. *Chem. Geol.*, 363:185–199, 10 Jan. 2014.

J. I. Chowdhury, N. Balta-Ozkan, P. Goglio, Y. Hu, L. Varga, and L. McCabe. Techno-environmental analysis of battery storage for grid level energy services. *Renew. Sustain. Energy Rev.*, 131(110018):110018, 1 Oct. 2020.

P. Chowdhury, J. A. Mulder, P. A. Cawood, S. Bhattacharjee, S. Roy, A. N. Wainwright, O. Nebel, and S. Mukherjee. Magmatic thickening of crust in non-plate tectonic settings initiated the subaerial rise of earth's first continents 3.3 to 3.2 billion years ago. *Proc. Natl. Acad. Sci. U. S. A.*, 118(46):e2105746118, 16 Nov. 2021.

K. C. Condie. *Archean Greenstone Belts*, volume 3 of *Developments in Precambrian Geology*. Elsevier Science & Technology, 1 Jan. 1981.

K. C. Condie and N. M. Harrison. Geochemistry of the archean bulawayan group, midlands greenstone belt, rhodesia. *Precambrian Res.*, 3(3):253–271, 1 May 1976.

A. Copley, O. Weller, and H. Bain. Diapirs of crystal-rich slurry explain granite emplacement temperature and duration. *Sci. Rep.*, 13(1):13730, 23 Aug. 2023.

L. J. Crisp and A. J. Berry. A new model for zircon saturation in silicate melts. *Contrib. Mineral. Petrol.*, 177(7):71, 2022.

N. Culshaw and P. Reynolds. 40Ar/39Ar age of shear zones in the southwest meguma zone between yarmouth and meteghan, nova scotia. *Can. J. Earth Sci.*, 34(6):848–853, 1 June 1997.

C. D. P. Dana, A. Agangi, A. Idrus, C. Chelle-Michou, C.-K. Lai, M. Ishida, M. Guillong, I. González-Álvarez, R. Takahashi, M. Yano, K. Mimura, J. Ohta, Y. Kato, D. R. Simbolon, and X.-P. Xia. The age and origin of the ruwai polymetallic skarn

deposit, indonesia: Evidence of cretaceous mineralization in the central borneo metallogenic belt. *Econ. Geol.*, 118(6):1341–1370, 1 Sept. 2023.

C. De Capitani and K. Petrakakis. The computation of equilibrium assemblage diagrams with theriak/domino software. *Am. Mineral.*, 95:1006–1016, 2010.

M. A. Delgado, C. Valencia, M. C. Sánchez, J. M. Franco, and C. Gallegos. Thermorheological behaviour of a lithium lubricating grease. *Tribol. Lett.*, 23(1):47–54, 19 Sept. 2006.

M. Demartis, L. P. Pinotti, J. E. Coniglio, F. J. D'Eramo, J. M. Tubía, E. Aragón, and L. A. Agulleiro Insúa. Ascent and emplacement of pegmatitic melts in a major reverse shear zone (sierras de córdoba, argentina). *J. Struct. Geol.*, 33(9):1334–1346, 1 Sept. 2011.

S. Deveaud, C. Gumiaux, E. Gloaguen, and Y. Branquet. Spatial statistical analysis applied to rare-element LCT-type pegmatite fields: an original approach to constrain faults-pegmatites-granites relationships. *J. Geosci.*, 58:163–182, 15 July 2013.

S. Dewaele, N. Hulsbosch, Y. Cryns, A. Boyce, R. Burgess, and P. Muchez. Geological setting and timing of the world-class sn, nb–ta and li mineralization of manono-kitotolo (katanga, democratic republic of congo). *Ore Geol. Rev.*, 72:373–390, 1 Jan. 2016.

B. Dhuime, C. J. Hawkesworth, P. A. Cawood, and C. D. Storey. A change in the geodynamics of continental growth 3 billion years ago. *Science*, 335(6074):1334–1336, 16 Mar. 2012.

H. G. Dill, R. Škoda, B. Weber, Z. A. Berner, A. Müller, and R. J. Bakker. A newly discovered swarm of shear-zone-hosted bi–as–fe–mg–P-rich aplites and pegmatites in the hagendorf–pleystein pegmatite province, southeastern germany: A step closer to the metamorphic root of pegmatites. *Can. Mineral.*, 50(4):943–974, 1 Aug. 2012.

P. H. G. M. Dirks, H. A. Jelsma, and A. Hofmann. Thrust-related accretion of an archaean greenstone belt in the midlands of zimbabwe. *J. Struct. Geol.*, 24(11): 1707–1727, Nov. 2002.

T. Dittrich, T. Seifert, B. Schulz, S. Hagemann, A. Gerdes, and J. Pfänder. Introduction to archean rare-metal pegmatites. In T. Dittrich, T. Seifert, B. Schulz,

S. Hagemann, A. Gerdes, and J. Pfänder, editors, *Archean Rare-Metal Pegmatites in Zimbabwe and Western Australia: Geology and Metallogeny of Pollucite Mineralisations*, pages 1–21. Springer International Publishing, Cham, 2019.

M. H. Dodson, W. Compston, I. S. Williams, and J. F. Wilson. A search for ancient detrital zircons in zimbabwean sediments. *Journal - Geological Society (London)*, 145(6):977–983, 1988.

M. H. Dodson, I. S. Williams, and J. D. Kramers. The mushandike granite: Further evidence for 3.4 ga magmatism in the zimbabwe craton. *Geol. Mag.*, 138(1):31–38, 2001.

M. S. Drummond and M. J. Defant. A model for trondhjemite-tonalite-dacite genesis and crustal growth via slab melting: Archean to modern comparisons. *J. Geophys. Res.*, 95(B13):21503–21521, 10 Dec. 1990.

M. Duguet, S. Lin, D. W. Davis, M. T. Corkery, and J. McDonald. Long-lived transpression in the archean bird river greenstone belt, western superior province, southeastern manitoba. *Precambrian Res.*, 174(3-4):381–407, 1 Nov. 2009.

M. A. Etheridge, N. R. Daczko, T. Chapman, and C. A. Stuart. Mechanisms of melt extraction during lower crustal partial melting. *J. Metamorph. Geol.*, 39(1):57–75, Jan. 2021.

European Commission. Critical raw materials resilience: Charting a path towards greater security and sustainability. Technical report, European Commission, 2020.

J. M. Evensen and D. London. Experimental partitioning of be, cs, and other trace elements between cordierite and felsic melt, and the chemical signature of S-type granite. *Contrib. Mineral. Petrol.*, 144(6):739–757, 1 Mar. 2003.

Ú. C. Farrell, R. Samawi, S. Anjanappa, R. Klykov, O. O. Adeboye, H. Agic, A. S. C. Ahm, T. H. Boag, F. Bowyer, J. J. Brocks, T. N. Brunoir, D. E. Canfield, X. Chen, M. Cheng, M. O. Clarkson, D. B. Cole, D. R. Cordie, P. W. Crockford, H. Cui, T. W. Dahl, L. D. Mouro, K. Dewing, S. Q. Dornbos, N. Drabon, J. A. Dumoulin, J. F. Emmings, C. R. Endriga, T. A. Fraser, R. R. Gaines, R. M. Gaschnig, T. M. Gibson, G. J. Gilleaudeau, B. C. Gill, K. Goldberg, R. Guilbaud, G. P. Halverson, E. U. Hammarlund, K. G. Hantsoo, M. A. Henderson, M. S. W. Hodgskiss, T. J. Horner, J. M. Husson, B. Johnson, P. Kabanov, C. Brenhin Keller, J. Kimmig, M. A. Kipp, A. H. Knoll, T. Kreitsmann, M. Kunzmann, F. Kurzweil, M. A. LeRoy,

C. Li, A. G. Lipp, D. K. Loydell, X. Lu, F. A. Macdonald, J. M. Magnall, K. Mänd, A. Mehra, M. J. Melchin, A. J. Miller, N. T. Mills, C. N. Mwinde, B. O'Connell, L. M. Och, F. Ossa Ossa, A. Pagès, K. Paiste, C. A. Partin, S. E. Peters, P. Petrov, T. L. Playter, S. Plaza-Torres, S. M. Porter, S. W. Poulton, S. B. Pruss, S. Richoz, S. R. Ritzer, A. D. Rooney, S. K. Sahoo, S. D. Schoepfer, J. A. Sclafani, Y. Shen, O. Shorttle, S. P. Slotznick, E. F. Smith, S. Spinks, R. G. Stockey, J. V. Strauss, E. E. Stüeken, S. Tecklenburg, D. Thomson, N. J. Tosca, G. J. Uhlein, M. N. Vizcaíno, H. Wang, T. White, P. R. Wilby, C. R. Woltz, R. A. Wood, L. Xiang, I. A. Yurchenko, T. Zhang, N. J. Planavsky, K. V. Lau, D. T. Johnston, and E. A. Sperling. The sedimentary geochemistry and paleoenvironments project. *Geobiology*, 19(6):545–556, 1 Nov. 2021.

C. M. Fedo and K. A. Eriksson. Stratigraphic framework of the $\sim$ 3.0 ga buhwa greenstone belt: A unique stable-shelf succession in the zimbabwe archean craton. *Precambrian Res.*, 77(3-4):161–178, 1996.

C. M. Fedo, K. A. Eriksson, and T. G. Blenkinsop. Geologic history of the archean buhwa greenstone belt and surrounding granite-gneiss terrane, zimbabwe, with implications for the evolution of the limpopo belt. *Can. J. Earth Sci.*, 32(11):1977–1990, 1995.

C. M. Fedo, K. A. Eriksson, and E. J. Krogstad. Geochemistry of shales from the archean ( -3 . 0 ga ) buhwa greenstone zimbabwe : Implications for provenance and source-area weathering. *Geochimica et Cosmochimica Acta*, 60(10):1751–1763, 1996.

S. Foley, M. Tiepolo, and R. Vannucci. Growth of early continental crust controlled by melting of amphibolite in subduction zones. *Nature*, 417(6891):837–840, 20 June 2002.

R. Frei, T. Blenkinsop, and R. Schonberg. Geochronology of the late archaean razi and chilimanzi suites of granites in zimbabwe; implications for the late archaean tectonics of the limpopo belt and zimbabwe craton. *South African Journal of Geology*, 102(1):55–63, 1 Mar. 1999.

B. R. Frost, C. G. Barnes, W. J. Collins, R. J. Arculus, D. J. Ellis, and C. D. Frost. A geochemical classification for granitic rocks. *J. Petrol.*, 42(11):2033–2048, 1 Nov. 2001.

W. C. Fuchsloch, P. A. M. Nex, and J. A. Kinnaird. Classification, mineralogical and geochemical variations in pegmatites of the cape cross-uis pegmatite belt, namibia. *Lithos*, 296-299:79–95, 1 Jan. 2018.

N. J. Gardiner, S. M. Jowitt, and J. P. Sykes. Lithium: critical, or not so critical? *Geoenergy*, 2(1):geoenergy2023–045, 31 Dec. 2024a.

N. J. Gardiner, R. M. Palin, L. Koopmans, M. F. Mangler, and L. J. Robb. On tin and lithium granite systems: A crustal evolution perspective. *Earth Sci. Rev.*, 258 (104947):104947, 1 Oct. 2024b.

M. S. Garson. The geology of the bulawayo greenstone belt and the surrounding granitic terrain. Technical Report 93, Zimbabwe Geological Survey, 1995.

A. Getsinger, T. Rushmer, M. D. Jackson, and D. Baker. Generating high mg-numbers and chemical diversity in tonalite-trondhjemite-granodiorite (TTG) magmas during melting and melt segregation in the continental crust. *J. Petrol.*, 50 (10):1935–1954, 1 Oct. 2009.

H. P. Gilbert, D. W. Davis, M. Duguet, P. D. Kremer, C. A. Mealin, and J. Macdonald. *Geology of the Bird River Belt, southeastern Manitoba (parts of NTS 52L5, 6)*. Manitoba Science, Technology, Energy and Mines, Winnipeg, 2008.

A. I. Ginsburg. The geological condition of the location and the forma - tion of granitic pegmatites. In *Proceedings*, pages 245–260, 1984.

A. I. Ginsburg and G. G. Rodionov. On the depth of formation of granitic pegmatites. *Geologiya Rudnykh Mestorozhdenii*, 2:45–54, 1960.

S. M. Glynn, S. Master, D. Frei, and M. Wiedenbeck. U-pb zircon geochronology of the dete-kamativi inlier , NW zimbabwe , with implications for the western margin of the archaean zimbabwe craton. *Precambrian Res.*, 346(June):105824, 2020.

K. M. Goodenough, P. A. J. Lusty, N. M. W. Roberts, R. M. Key, and A. Garba. Post-collisional pan-african granitoids and rare metal pegmatites in western nigeria: Age, petrogenesis, and the 'pegmatite conundrum'. *Lithos*, 200-201:22–34, 1 July 2014.

K. M. Goodenough, R. A. Shaw, A. M. Borst, P. A. M. Nex, J. A. Kinnaird, M. van Lichtervelde, A. Essaifi, L. Koopmans, and E. A. Deady. Lithium pegmatites in africa: A review. *Econ. Geol.*, 10 Mar. 2025.

A. M. Goodwin. Chapter 5 archaean plates and greenstone belts. In A. Kröner, editor, *Developments in Precambrian Geology*, volume 4 of *Developments in precambrian geology*, pages 105–135. Elsevier, 1981.

B. Goscombe, D. A. Foster, D. Gray, and B. Wade. Assembly of central gondwana along the zambezi belt: Metamorphic response and basement reactivation during the kuunga orogeny. *Gondwana Res.*, 80:410–465, 1 Apr. 2020.

E. C. R. Green, R. W. White, J. F. A. Diener, R. Powell, T. J. B. Holland, and R. M. Palin. Activity–composition relations for the calculation of partial melting equilibria in metabasic rocks. *J. Metamorph. Geol.*, 34(9):845–869, 1 Dec. 2016.

E. C. R. Green, T. J. B. Holland, R. Powell, O. M. Weller, and N. Riel. Corrigendum to: Melting of peridotites through to granites: A simple thermodynamic model in the system KNCFMASHTOCr, and, a thermodynamic model for the subsolidus evolution and .... *Journal of Petrology*, 66(1):egae079, Jan. 2025.

M. Guillong, K. Hametner, E. Reusser, S. A. Wilson, and D. Günther. Preliminary characterisation of new glass reference materials (GSA-1G, GSC-1G, GSD-1G and GSE-1G) by laser ablation-inductively coupled plasma-mass spectrometry using 193 nm, 213 nm and 266 nm wavelengths. *Geostandards and Geoanalytical Research*, 29(3):315–331, 1 Nov. 2005.

M. Guitreau, J. Blichert-Toft, H. Martin, S. J. Mojzsis, and F. Albarède. Hafnium isotope evidence from archean granitic rocks for deep-mantle origin of continental crust. *Earth Planet. Sci. Lett.*, 337-338:211–223, July 2012.

S. G. Hagemann, V. A. Lisitsin, and D. L. Huston. Mineral system analysis: Quo vadis. *Ore Geol. Rev.*, 76:504–522, 1 July 2016.

D. Hall and A. Kisters. The stabilization of self-organised leucogranite networks–implications for melt segregation and far-field melt transfer in the continental crust. *Earth Planet. Sci. Lett.*, 355-356:1–12, 15 Nov. 2012.

W. B. Hamilton. Archean magmatism and deformation were not products of plate tectonics. *Precambrian Res.*, 91(1-2):143–179, Aug. 1998.

R. E. Hanson, T. J. Wilson, and H. Munyanyiwa. Geologic evolution of the neoproterozoic zambezi orogenic belt in zambia. *J. Afr. Earth Sci.*, 18(2):135–150, 1 Feb. 1994.

N. M. Harrison. The geology of the country around fort rixon and shangani. Technical Report 61, Zimbabwe Geological Survey, 1969.

M. I. H. Hartnady, T. E. Johnson, S. Schorn, R. Hugh Smithies, C. L. Kirkland, and S. H. Richardson. Fluid processes in the early earth and the growth of continents. *Earth Planet. Sci. Lett.*, 594(117695):117695, Sept. 2022.

C. J. Hawkesworth and A. I. S. Kemp. Using hafnium and oxygen isotopes in zircons to unravel the record of crustal evolution. *Chem. Geol.*, 226(3):144–162, 28 Feb. 2006.

C. J. Hawkesworth, P. A. Cawood, and B. Dhuime. Tectonics and crustal evolution. *GSA Today*, 26(9):4–11, 1 Sept. 2016.

C. Herzberg, K. Condie, and J. Korenaga. Thermal history of the earth and its petrological expression. *Earth Planet. Sci. Lett.*, 292(1-2):79–88, 15 Mar. 2010.

M. H. Hickman. 3,500-myr-old granite in southern africa. *Nature*, 251(5473):295–296, Sept. 1974.

J. E. Hoffmann, T. J. Nagel, C. Münker, T. Næraa, and M. T. Rosing. Constraining the process of eoarchean TTG formation in the itsaq gneiss complex, southern west greenland. *Earth Planet. Sci. Lett.*, 388:374–386, Feb. 2014.

A. Hofmann and P. H. G. M. Dirks. Continental setting inferred for emplacement of the 2.9–2.7 ga belingwe greenstone belt, zimbabwe: Comment and reply. *Geology*, 31(1):e30–e31, Jan. 2003.

A. Hofmann and T. Kusky. The belingwe greenstone belt: Ensialic or oceanic? In *Precambrian Ophiolites and Related Rocks*, volume 13 of *Developments in precambrian geology*, pages 487–538. Elsevier, 1 Jan. 2004.

A. Hofmann, P. H. G. Dirks, and H. A. Jelsma. Horizontal tectonic deformation geometries in a late archaean sedimentary sequence, belingwe greenstone belt, zimbabwe. *Tectonics*, 20(6):909–932, 1 Dec. 2001.

A. Hofmann, P. H. G. M. Dirks, and H. A. Jelsma. Late archaean clastic sedimentary rocks (shamvaian group) of the zimbabwe craton: first observations from the bindura-shamva greenstone belt. *Can. J. Earth Sci.*, 39(11):1689–1708, 1 Nov. 2002.

A. Hofmann, A. Kröner, L. M. Iaccheri, J. Wong, H. Geng, and H. Xie. 3.63 ga grey gneisses reveal the eoarchaean history of the zimbabwe craton. *South Afr. J. Geol.*, 125(1):1–12, 1 Mar. 2022.

A. Hofmann, X.-H. Li, D. C. Bradley, and F. Humbert. The belingwe greenstone belt, zimbabwe – some new age constraints and implications for greenstone belt evolution. *Int. Geol. Rev.*, 66(16):2940–2959, 7 Sept. 2024.

K. J. Hogmalm, T. Zack, A. K.-O. Karlsson, A. S. L. Sjöqvist, and D. Garbe-Schönberg. In situ rb–sr and K–ca dating by LA-ICP-MS/MS: an evaluation of N2O and SF6 as reaction gases. *J. Anal. At. Spectrom.*, 32(2):305–313, 8 Feb. 2017.

T. J. B. Holland and R. Powell. An improved and extended internally consistent thermodynamic dataset for phases of petrological interest, involving a new equation of state for solids. *J. Metamorph. Geol.*, 29(3):333–383, Apr. 2011.

T. J. B. Holland, E. C. R. Green, and R. Powell. Melting of peridotites through to granites: A simple thermodynamic model in the system KNCFMASHTOCr. *J. Petrol.*, 59(5):881–900, 2018.

T. J. B. Holland, E. C. R. Green, and R. Powell. A thermodynamic model for feldspars in $KAlSi_3O_8$-$NaAlSi_3O_8$-$CaAl_2Si_2O_8$ for mineral equilibrium calculations. *J. Metamorph. Geol.*, 40(4):587–600, May 2022.

M. S. A. Horstwood. *Stratigraphy, geochemistry and zircon geochronology of the midlands greenstone belt, Zimbabwe*. PhD thesis, University of Southampton, 1998.

M. S. A. Horstwood, R. W. Nesbitt, S. R. Noble, and J. F. Wilson. U-pb zircon evidence for an extensive early archean craton in zimbabwe: A reassessment of the timing of craton formation, stabilization, and growth. *Geology*, 27(8):707–710, 1999.

M. S. A. Horstwood, J. Košler, G. Gehrels, S. E. Jackson, N. M. McLean, C. Paton, N. J. Pearson, K. Sircombe, P. Sylvester, P. Vermeesch, J. F. Bowring, D. J. Condon, and B. Schoene. Community-derived standards for LA - ICP - MS U-(th-)pb geochronology – uncertainty propagation, age interpretation and data reporting. *Geostand. Geoanal. Res.*, 40(3):311–332, 1 Sept. 2016.

M. A. Hunter. Continental extensional setting for the archean belingwe greenstone belt, zimbabwe. *Geology*, 26(10):883–886, 1998.

J. Icenhower and D. London. An experimental study of element partitioning among biotite, muscovite, and coexisting peraluminous silicic melt at 200 MPa (H2 O). *Am. Mineral.*, 80(11-12):1229–1251, 1995.

B. M. Intelligence. How many mines are needed for the energy transition? `https://source.benchmarkminerals.com/article/how-many-mines-are-needed-for-the-energy-transition`, 2025. Accessed: 2025-5-22.

O. Jagoutz and P. B. Kelemen. Role of arc processes in the formation of continental crust. *Annu. Rev. Earth Planet. Sci.*, 43(1):363–404, 30 May 2015.

R. H. Jahns. The genesis of pegmatites: I. occurrence and origin of giant crystals. *Am. Mineral.*, 38(7-8):563–598, 1 Aug. 1953.

R. H. Jahns and C. Wayne Burnham. Experimental studies of pegmatite genesis; l, a model for the derivation and crystallization of granitic pegmatites. *Econ. Geol.*, 64(8):843–864, 1 Dec. 1969.

A. E. Jay and M. Widdowson. Stratigraphy, structure and volcanology of the SE deccan continental flood basalt province: implications for eruptive extent and volumes. *J. Geol. Soc. London*, 165(1):177–188, 1 Jan. 2008.

H. A. Jelsma and P. H. G. M. Dirks. Neoarchaean tectonic evolution of the zimbabwe craton. *Geol. Soc. Spec. Publ.*, 199:183–211, 2002.

H. A. Jelsma, M. L. Vinyu, J. R. Wijbrans, E. A. T. Verdurmen, P. J. Valbracht, G. R. Davies, and P. J. Valbracht. Constraints on archaean crustal evolution of the zimbabwe craton: a U-pb zircon, sm-nd and pb-pb whole-rock isotope study. *Contrib. Mineral. Petrol.*, 124(1):55–70, 24 June 1996.

H. A. Jelsma, R. W. Nesbitt, and C. M. Fanning. Exploring our current understanding of the geological evolution and mineral endowment of the zimbabwe craton. *South Afr. J. Geol.*, 124(1):279–310, 1 Mar. 2021.

K. P. Jochum, U. Weis, B. Stoll, D. Kuzmin, Q. Yang, I. Raczek, D. E. Jacob, A. Stracke, K. Birbaum, D. A. Frick, D. Günther, and J. Enzweiler. Determination of reference values for NIST SRM 610-617 glasses following ISO guidelines. *Geostandards and Geoanalytical Research*, 35(4):397–429, Dec. 2011.

T. E. Johnson, M. Brown, N. J. Gardiner, C. L. Kirkland, and R. H. Smithies. Earth's first stable continents did not form by subduction. *Nature*, 543(7644): 239–242, 9 Mar. 2017.

B. L. Jolliff, J. J. Papike, and C. K. Shearer. Petrogenetic relationships between pegmatite and granite based on geochemistry of muscovite in pegmatite wall zones, black hills, south dakota, USA. *Geochim. Cosmochim. Acta*, 56(5):1915–1939, 1 May 1992.

S. Kadir, T. Külah, H. Erkoyun, C. Helvacı, M. Eren, and B. Demiral. Mineralogy, geochemistry, and genesis of lithium-bearing argillaceous sediments associated with the neogene bigadiç borate deposits, balıkesir, western anatolia, türkiye. *Appl. Clay Sci.*, 242:107015, 15 Sept. 2023.

D. Kaeter, R. Barros, J. F. Menuge, and D. M. Chew. The magmatic–hydrothermal transition in rare-element pegmatites from southeast ireland: LA-ICP-MS chemical mapping of muscovite and columbite–tantalite. *Geochim. Cosmochim. Acta*, 240: 98–130, 1 Nov. 2018.

B. Kamber. The evolving nature of terrestrial crust from the hadean, through the archaean, into the proterozoic. *Precambrian Res.*, 258:48–82, Mar. 2015.

B. S. Kamber. Archean mafic–ultramafic volcanic landmasses and their effect on ocean–atmosphere chemistry. *Chem. Geol.*, 274(1-2):19–28, June 2010.

B. S. Kamber and G. G. Biino. The evolution of high T- low P granulites in the northern marginal zone sensu stricto, limpopo belt, zimbabwe - the case for petrography. *Schweiz. Mineral. Petrogr. Mitt.*, 75:427–454, 1995.

B. S. Kamber, T. G. Blenkinsop, I. M. Villa, and P. S. Dahl. Proterozoic transpressive deformation in the northern marginal zone, limpopo belt, zimbabwe. *https://doi.org/10.1086/629772*, 103(5):493–508, 29 Sept. 2015.

L. A. Kendall-Langley, A. I. S. Kemp, J. L. Grigson, and J. Hammerli. U-pb and reconnaissance lu-hf isotope analysis of cassiterite and columbite group minerals

from archean li-cs-ta type pegmatites of western australia. *Lithos*, 352-353:105231, 1 Jan. 2020.

J. Kendrick and C. Yakymchuk. Garnet fractionation, progressive melt loss and bulk composition variations in anatectic metabasites: Complications for interpreting the geodynamic significance of TTGs. *Geosci. Front.*, 11(3):745–763, 1 May 2020.

S. E. Kesler and A. C. Simon. *Mineral resources, economics and the environment*. Cambridge University Press, Cambridge, England, 2 edition, 26 Oct. 2015.

W. Keyser, A. Müller, R. Steiner, M. Erambert, M. Kristoffersen, and T. Unterweissacher. Alpine eclogite-facies modification of li-cs-ta pegmatite from the wolfsberg lithium deposit, austria. *Miner. Deposita*, 58(7):1191–1210, 19 Apr. 2023.

T. Knoll, B. Huet, R. Schuster, H. Mali, T. Ntaflos, and C. Hauzenberger. Lithium pegmatite of anatectic origin - a case study from the austroalpine unit pegmatite province (eastern european alps): geological data and geochemical model. *Ore Geol. Rev.*, page 105298, 12 Jan. 2023.

D. J. Kontak. Nature and origin of an LCT-suite pegmatite with late-stage sodium enrichment, brazil lake, yarmouth county, nova scotia. I. geological setting and petrology. *Can. Mineral.*, 44(3):563–598, 1 June 2006.

D. J. Kontak, R. A. Creaser, L. M. Heaman, and D. A. Archibald. U-pb tantalite, re-os molybdenite, and 40Ar/39Ar muscovite dating of the brazil lake pegmatite, nova scotia: a possible shear-zone related origin for an LCT-type pegmatite. *atlgeo*, 41(1), 1 Jan. 2005.

L. Koopmans, R. M. Palin, and N. J. Gardiner. TDMelts: A theriak-domino wrapper for 2-dimensional batch melting models. In *Goldschmidt 2023 Conference*. GOLDSCHMIDT, 11 July 2023.

L. Koopmans, T. Martins, R. Linnen, N. J. Gardiner, C. M. Breasley, R. M. Palin, L. A. Groat, D. Silva, and L. J. Robb. The formation of lithium-rich pegmatites through multi-stage melting. *Geology*, 52(1):7–11, 1 Jan. 2024.

J. Korenaga. Archean geodynamics and the thermal evolution of earth. In *Archean Geodynamics and Environments*, pages 7–32. American Geophysical Union (AGU), 18 Mar. 2006.

J. Korenaga. Initiation and evolution of plate tectonics on earth: Theories and observations. *Annu. Rev. Earth Planet. Sci.*, 41(1):117–151, 30 May 2013.

P. Kremer. *Structural geology and geochronology of the bernic lake area in the Bird River Greenstone belt, Manitoba: Evidence for syn-deformational emplacement of the bernic lake pegmatite group.* PhD thesis, University of Waterloo, Waterloo, Ontario, Canada, 31 Aug. 2010.

B. E. Kunz, C. J. Warren, F. E. Jenner, N. B. W. Harris, and T. W. Argles. Critical metal enrichment in crustal melts: The role of metamorphic mica. *Geology*, 50(11): 1219–1223, 1 Nov. 2022.

Y. Kuribara, T. Tsunogae, Y. Takamura, and Y. Tsutsumi. Petrology, geochemistry, and zircon U-pb geochronology of the zambezi belt in zimbabwe: Implications for terrane assembly in southern africa. *Geosci. Front.*, 10(6):2021–2044, 1 Nov. 2019.

T. Kusky, B. F. Windley, A. Polat, L. Wang, W. Ning, and Y. Zhong. Archean dome-and-basin style structures form during growth and death of intraoceanic and continental margin arcs in accretionary orogens. *Earth Sci. Rev.*, 220(103725): 103725, 1 Sept. 2021.

T. M. Kusky. Tectonic setting and terrane accretion of the archean zimbabwe craton. *Geology*, 26(2):163–166, 1998.

T. M. Kusky and W. S. F. Kidd. Remnants of an archean oceanic plateau, belingwe greenstone belt, zimbabwe. *Geology*, 20(1):43, 1992.

T. M. Kusky and P. A. Winsky. Structural relationships along a greenstone/shallow water shelf contact, belingwe greenstone belt, zimbabwe. *Tectonics*, 14(2):448–471, Apr. 1995.

K. Landes. Origin and classification of pegmatites. *American Mineralogist*, 18(3): 33–56, 1 Feb. 1933.

K. P. Larson. LA-QQQ-ICP-MS RbSr data reduction scheme, 18 Jan. 2024.

K. P. Larson, M. Button, S. Shrestha, and A. Camacho. A comparison of $^{87}Rb/^{87}Sr$ and $^{40}Ar/^{39}Ar$ dates: Evaluating the problem of excess $^{40}Ar$ in himalayan mica. *Earth Planet. Sci. Lett.*, 609, 1 May 2023.

K. P. Larson, B. Dyck, S. Shrestha, M. Button, and Y. Najman. On the viability of detrital biotite rb–sr geochronology. *Geochronology*, 6(3):303–312, 2 July 2024.

J. N. Lauerdale. The geology of the country around dorowa - shawa. Technical Report 95, Zimbabwe Geological Survey, 1988.

O. Laurent. *Les changements géodynamiques à la transition Archéen-Protérozoïque: étude des granitoïdes de la marge Nord du craton du Kaapvaal (Afrique du Sud)*. PhD thesis, Université Blaise Pascal-Clermont-Ferrand II, 2012.

O. Laurent, H. Martin, J. F. Moyen, and R. Doucelance. The diversity and evolution of late-archean granitoids: Evidence for the onset of "modern-style" plate tectonics between 3.0 and 2.5Ga. *Lithos*, 205:208–235, 15 Sept. 2014.

A. Laurie, G. Stevens, and J. van Hunen. The end of continental growth by TTG magmatism: Modelling water-present melting during archaean subduction. *Terra Nova*, 25(2):130–136, 1 Apr. 2013.

A. L. Lee, G. E. Lloyd, T. Torvela, and A. M. Walker. Evolution of a shear zone before, during and after melting. *J. Geol. Soc. London*, 177(4):738–751, 1 July 2020.

A. Lindroos, R. L. Romer, C. Ehlers, and R. Alviola. Late-orogenic svecofennian deformation in SW finland constrained by pegmatite emplacement ages. *Terra Nova*, 8(6):567–574, Nov. 1996.

R. L. Linnen. The solubility of nb-ta-zr-hf-W in granitic melts with li and li+ F; constraints for mineralization in rare metal granites and pegmatites. *Econ. Geol.*, 1998.

R. L. Linnen, M. Van Lichtervelde, and P. Černý. Granitic pegmatites as sources of strategic metals. *Elements*, 8(4):275–280, 1 Aug. 2012.

C. Liu, R.-C. Wang, R. L. Linnen, F.-Y. Wu, L. Xie, and X.-C. Liu. Continuous be mineralization from two-mica granite to pegmatite: Critical element enrichment processes in a himalayan leucogranite pluton. *Am. Mineral.*, 108(1):31–41, 3 Jan. 2023.

S. Liu, R. Wang, R. E. Botcharnikov, and H. Sha. Formation of rare-element pegmatites in the chinese altai: Contribution of two-stage melting. *Geology*, 53(3): 207–211, 1 Mar. 2025.

D. London. Experimental phase equilibria in the system LiAlSiO4–SiO2–H2O: a petrogenetic grid for lithium-rich pegmatites. *Am. Mineral.*, 69(11-12):995–1004, 1 Dec. 1984.

D. London. Granitic pegmatites: an assessment of current concepts and directions for the future. *Lithos*, 80(1-4):281–303, 1 Mar. 2005.

D. London. *Pegmatites*. Mineralogical Association of Canada, 2008.

D. London. A petrologic assessment of internal zonation in granitic pegmatites. *Lithos*, 184-187:74–104, 1 Jan. 2014.

D. London. Ore-forming processes within granitic pegmatites. *Ore Geol. Rev.*, 101: 349–383, 1 Oct. 2018.

D. London and G. B. Morgan. The pegmatite puzzle. *Elements*, 8(4):263–268, 1 Aug. 2012.

D. London, M. B. Wolf, G. B. Morgan, and M. G. Garrido. Experimental silicate–phosphate equilibria in peraluminous granitic magmas, with a case study of the alburquerque batholith at tres arroyos, badajoz, spain. *J. Petrol.*, 40(1):215–240, 1 Jan. 1999.

B. Luais and C. J. Hawkesworth. The generation of continental crust: An integrated study of crust-forming processes in the archaean of zimbabwe. *J. Petrol.*, 35(1): 43–94, 1 Feb. 1994.

A. M. Macgregor. An outline of the geological history of southern rhodesia. Technical report, Southern Rhodesia Geological Survey, Bulletin 38, 1947.

A. M. Macgregor. Some milestones in the precambrian of southern rhodesia. *Transactions of the Geological Society of South Africa*, 54:xxvii–lxxi, 1951.

V. Maneta and D. R. Baker. Exploring the effect of lithium on pegmatitic textures: An experimental study. *Am. Mineral.*, 99(7):1383–1403, 1 July 2014.

V. Maneta, D. R. Baker, and W. Minarik. Evidence for lithium-aluminosilicate supersaturation of pegmatite-forming melts. *Contrib. Mineral. Petrol.*, 170(1):4, 3 July 2015.

I. Mantäri. Mesoarchaean to lower jurassic U-pb and sm-nd ages from NW mozambique. *Geological Survey of Finland, Special Paper*, 48:81–119, 2008.

J. H. Marsh, T. R. Jorgensen, J. A. Petrus, M. A. Hamilton, and D. R. Mole. U-pb, trace element, and hafnium isotope composition of the maniitsoq zircon: A potential new archean zircon reference material. In *Goldschmidt Abstracts*, page 2161, 2019.

A. Martin, E. G. Nisbet, M. J. Bickle, and J. L. Orpen. Rock units and stratigraphy of the belingwe greenstone belt: The complexity of the tectonic setting. In *The Geology of the Belingwe Greenstone Belt, Zimbabwe*, pages 13–37. CRC Press, 1st edition edition, 26 Aug. 1993.

H. Martin. Chapter 6 the archean grey gneisses and the genesis of continental crust. *Developments in Precambrian Geology*, 11:205–259, 1994.

H. Martin. Adakitic magmas: modern analogues of archaean granitoids. *Lithos*, 46 (3):411–429, 1 Mar. 1999.

H. Martin and J.-F. Moyen. Secular changes in tonalite-trondhjemite-granodiorite composition as markers of the progressive cooling of earth. *Geology*, 30(4):319–322, 1 Apr. 2002.

H. Martin, R. H. Smithies, R. Rapp, J. F. Moyen, and D. Champion. An overview of adakite, tonalite-trondhjemiten-granodiorite (TTG), and sanukitoid: Relationships and some implications for crustal evolution. *Lithos*, 79(1-2 SPEC. ISS.):1–24, 1 Jan. 2005.

H. Martin, J.-F. Moyen, M. Guitreau, J. Blichert-Toft, and J.-L. Le Pennec. Why archaean TTG cannot be generated by MORB melting in subduction zones. *Lithos*, 198-199:1–13, 1 June 2014.

R. F. Martin and C. De Vito. The patterns of enrichment in felsic pegmatites ultimately depend on tectonic setting. *Can. Mineral.*, 43(6):2027–2048, 1 Dec. 2005.

S. Master, A. Bekker, and A. Hofmann. A review of the stratigraphy and geological setting of the palaeoproterozoic magondi supergroup, zimbabwe – type locality for the lomagundi carbon isotope excursion. *Precambrian Res.*, 182(4):254–273, Oct. 2010.

A. Mazoz, G. O. Gonçalves, C. Lana, I. S. Buick, F. Corfu, S. L. Kamo, H. Wang, Y.-H. Yang, R. Scholz, G. Queiroga, B. Fu, L. Martins, M. Schannor, A. T. de Abreu, M. Babinski, E. Peixoto, and R. Ventura Santos. Khan river and bear lake: Two

natural titanite reference materials for high-spatial resolution U-pb microanalysis. *Geostand. Geoanal. Res.*, 46(4):701–733, 1 Dec. 2022.

D. M. McCaffrey and S. M. Jowitt. The crystallization temperature of granitic pegmatites: The important relationship between undercooling and critical metal prospectivity. *Earth-Sci. Rev.*, 244:104541, 1 Sept. 2023.

W. F. McDonough and T. R. Ireland. Intraplate origin of komatiites inferred from trace elements in glass inclusions. *Nature*, 365(6445):432–434, Sept. 1993.

W. F. McDonough and S. s. Sun. The composition of the earth. *Chem. Geol.*, 120 (3-4):223–253, 1 Mar. 1995.

F. W. McDowell, W. C. McIntosh, and K. A. Farley. A precise 40Ar–39Ar reference age for the durango apatite (U–th)/he and fission-track dating standard. *Chem. Geol.*, 214(3-4):249–263, 25 Jan. 2005.

B. A. McNulty and S. M. Jowitt. Barriers to and uncertainties in understanding and quantifying global critical mineral and element supply. *iScience*, 24(7):102809, 23 July 2021.

A. Miyashiro. Paired and unpaired metamorphic belts. *Tectonophysics*, 17(3):241–254, 1 Apr. 1973.

S. Mkweli, B. Kamber, and M. Berger. Westward continuation of the craton-limpopo belt tectonic break in zimbabwe and new age constaints on the timing of the thrusting. *Journal - Geological Society (London)*, 152(1):77–83, 1995.

S. Moorbath, J. F. Wilson, and P. Cotterill. Early archaean age for the sebakwian group at selukwe, rhodesia. *Nature*, 264(5586):536–538, 1 Dec. 1976.

G. B. Morgan and D. London. Alteration of amphibolitic wallrocks around the tanco rare-element pegmatite, bernic lake, manitoba. *Am. Mineral.*, 72(11-12):1097–1121, 1987.

C. L. Morissette, E. Cecchi, and J.-F. Blais. Mineralogical variability of the whabouchi pegmatite and its effect on the li concentrations. *Can. Mineral.*, 60(5):759–774, 1 Sept. 2022.

J.-F. Moyen. The composite archaean grey gneisses: Petrological significance, and evidence for a non-unique tectonic setting for archaean crustal growth. *Lithos*, 123 (1-4):21–36, 1 Apr. 2011.

J. F. Moyen and H. Martin. Forty years of TTG research, 1 Sept. 2012.

J.-F. Moyen and G. Stevens. Experimental constraints on TTG petrogenesis: Implications for archean geodynamics. In *Archean Geodynamics and Environments*, Geophysical monograph, pages 149–175. American Geophysical Union, Washington, D. C., 2006.

J. F. Moyen, G. Stevens, and A. Kisters. Record of mid-archaean subduction from metamorphism in the barberton terrain, south africa. *Nature*, 442(7102):559–562, 3 Aug. 2006.

S. R. Mulcahy, S. M. Roeske, W. C. Mcclelland, J. R. Ellis, F. Jourdan, P. R. Renne, J. D. Vervoort, G. I. Vujovich, S. R. Mulcahy, S. M. Roeske, W. C. Mcclelland, J. R. Ellis, F. Jourdan, P. R. Renne, J. D. Vervoort, and G. I. Vujovich. Multiple migmatite events and cooling from granulite facies metamorphism within the famatina arc margin of northwest argentina. *Tectonics*, 33(1):1–25, 1 Jan. 2014.

A. Müller, R. L. Romer, and R. B. Pedersen. The sveconorwegian pegmatite province -thousands of pegmatites without parental granites. *Can. Mineral.*, 55(2):283–315, 11 Mar. 2017.

A. Müller, M. Brönner, J. Menuge, B. Williamson, C. Haase, G. Tassis, C. Pohl, K. Brauch, K. Saalmann, A. Teodoro, E. Roda-Robles, J. Cardoso-Fernandes, K. Smith, F. Wall, A. Lima, D. Santos, M. Hopfner, I. Garate-Olave, J. Errandonea-Martin, J. Harrop, L. Carter, W. Keyser, H. Zhou, T. Nazari-Dehkordi, E. Geiger, T. Unterweissacher, R. Steiner, W. Reimer, and C. Pueyo Lloret. The GREENPEG project toolset to explore for buried pegmatites hosting lithium, high-purity quartz, and other critical raw materials. *Econ. Geol.*, 21 Mar. 2025.

L. A. Munk, S. A. Hynek, D. C. Bradley, D. Boutt, K. Labay, and H. Jochens. Lithium brines: A global perspective. In *Rare Earth and Critical Elements in Ore Deposits*, volume 18, pages 339–365. Society of Economic Geologists, 2016.

M. E. Murphy, J. E. Macdonald, S. Fischer, N. J. Gardiner, R. W. White, and P. S. Savage. Silicon isotopes in an archaean migmatite confirm seawater silicification of TTG sources. *Geochim. Cosmochim. Acta*, 368:34–49, 1 Mar. 2024.

P. I. Nabelek, A. G. Whittington, and M.-L. C. Sirbescu. The role of H2O in rapid emplacement and crystallization of granite pegmatites: resolving the paradox of

large crystals in highly undercooled melts. *Contrib. Mineral. Petrol.*, 160(3):313–325, 1 Sept. 2010.

T. F. Nägler, J. D. Kramers, B. S. Kamber, R. Frei, and M. D. A. Prendergast. Growth of subcontinental lithospheric mantle beneath zimbabwe started at or before 3.8 ga: Re-os study on chromites. *Geology*, 25(11):983–986, 1 Nov. 1997.

N. T. Nassar and S. M. Fortier. Methodology and technical input for the 2021 review and revision of the U.S. critical minerals list, 2021.

S. M. N. Ncube. Geological map of zimbabwe, 1994.

O. Nebel. Rb–sr dating. In *Encyclopedia of Scientific Dating Methods*, pages 1–19. Springer Netherlands, Dordrecht, 2014.

O. Nebel, F. A. Capitanio, J. F. Moyen, R. F. Weinberg, F. Clos, Y. J. Nebel-Jacobsen, and P. A. Cawood. When crust comes of age: on the chemical evolution of archaean, felsic continental crust by crustal drip tectonics. *Philosophical Transactions of the Royal Society A: Mathematical, Physical and Engineering Sciences*, 376(2132), 13 Nov. 2018.

P. Niggli. *The volatile components in the magma*. Preisschriften der Furstlich Jablonowskischen Gesellscahft, Leipzig, 1920.

E. G. Nisbet, M. J. Bickle, and A. Martin. The mafic and ultramafic lavas of the belingwe greenstone belt, rhodesia. *J. Petrol.*, 18(4):521–566, 1 Nov. 1977.

E. G. Nisbet, M. J. Bickle, A. Martin, and J. L. Orpen. Sedimentology of the brooklands formation, zimbabwe: Development of an archaean greenstone belt in a rifted graben. In *The Geology of the Belingwe Greenstone Belt, Zimbabwe*, pages 87–120. CRC Press, 1st edition edition, 26 Aug. 1993.

K. G. Nymoen, D. R. Mole, P. C. Thurston, D. K. Tinkham, J. H. Marsh, and R. A. Stern. Crustal evolution and architecture of the wawa subprovince, superior province: Insights from zircon U-pb-hf-O isotopes and geochemistry. *Precambrian Res.*, 418(107705):107705, 1 Mar. 2025.

T. Oberthür, D. W. Davis, T. G. Blenkinsop, and A. Höhndorf. Precise U–pb mineral ages, rb–sr and sm–nd systematics for the great dyke, zimbabwe–constraints on late archean events in the zimbabwe craton and limpopo belt. *Precambrian Res.*, 113 (3-4):293–305, 31 Jan. 2002.

O. Okina, S. Lyapunov, M. Avdosyeva, B. Ermolaev, V. Golubchikov, A. Gorbunov, and V. Sheshukov. An investigation of the reliability of HF acid mixtures in the bomb digestion of silicate rocks for the determination of trace elements by ICP-MS. *Geostand. Geoanal. Res.*, 40(4):583–597, Dec. 2016.

R. M. Palin and R. W. White. Emergence of blueschists on earth linked to secular changes in oceanic crust composition. *Nat. Geosci.*, 9(1):60–64, Jan. 2016.

R. M. Palin, R. W. White, and E. C. R. Green. Partial melting of metabasic rocks and the generation of tonalitic–trondhjemitic–granodioritic (TTG) crust in the archaean: Constraints from phase equilibrium modelling. *Precambrian Res.*, 287: 73–90, 1 Dec. 2016a.

R. M. Palin, R. W. White, E. C. R. Green, J. F. A. Diener, R. Powell, and T. J. B. Holland. High-grade metamorphism and partial melting of basic and intermediate rocks. *J. Metamorph. Geol.*, 34(9):871–892, 1 Dec. 2016b.

R. M. Palin, M. Santosh, W. Cao, S. S. Li, D. Hernández-Uribe, and A. Parsons. Secular change and the onset of plate tectonics on earth. *Earth-Sci. Rev.*, 207: 103172, 1 Aug. 2020.

S. Papeschi, F. Mazzarini, G. Musumeci, and A. R. Cruden. Emplacement of a felsic dyke swarm during progressive heterogeneous deformation, eastern elba dyke complex (island of elba, italy). *Journal of Structural Geology*, 159:104600, 1 June 2022.

G. A. Partington. *The geochronology, tectonic environment and structural controls on intrusion of the giant rare-metal pegmatite at Greenbushes, Western Australia.* PhD thesis, University of Western Australia, 1988.

G. A. Partington, N. J. McNaughton, D. A. Kepert, W. Compston, and I. S. Williams. Geochronology of the balingup metamorphic belt: constraints on the temporal evolution of the greenbushes pegmatite district. Technical report, Australian bureau of Mineral Resources, 1 Jan. 1986.

G. A. Partington, N. J. McNaughton, and I. S. Williams. A review of the geology, mineralization, and geochronology of the greenbushes pegmatite, western australia. *Econ. Geol.*, 90(3):616–635, 1 May 1995.

C. Paton, J. D. Woodhead, J. C. Hellstrom, J. M. Hergt, A. Greig, and R. Maas. Improved laser ablation U-pb zircon geochronology through robust downhole fractionation correction. *Geochem. Geophys. Geosyst.*, 11(3), Mar. 2010.

C. Paton, J. Hellstrom, B. Paul, J. Woodhead, and J. Hergt. Iolite: Freeware for the visualisation and processing of mass spectrometric data. *J. Anal. At. Spectrom.*, 26(12):2508, 2011.

J. A. Pearce. Geochemical fingerprinting of oceanic basalts with applications to ophiolite classification and the search for archean oceanic crust. *Lithos*, 100(1-4): 14–48, 1 Jan. 2008.

J. A. Percival and K. D. Card. Archean crust as revealed in the kapuskasing uplift, superior province, canada. *Geology*, 11(6):323–326, 1 June 1983.

J. A. Percival and G. F. West. The kapuskasing uplift: a geological and geophysical synthesis. *Can. J. Earth Sci.*, 31(7):1256–1286, 1 July 1994.

J. A. Petrus and B. S. Kamber. VizualAge: A novel approach to laser ablation ICP-MS U-pb geochronology data reduction. *Geostand. Geoanal. Res.*, 36(3):247–270, Sept. 2012.

F. J. Pettijohn. Chemical composition of sandstones, excluding carbonate and volcanic sands. Technical report, USGS, 1963.

J. D. Pfister, D. J. Kontak, and L. A. Groat. Textural and mineralogical evolution of the little nahanni pegmatite group (NWT, canada) with implications for metasomatism, rare-metal mineralization, and pegmatite–wall rock interaction. *The Canadian Journal of Mineralogy and Petrology*, 61(3):467–505, 1 May 2023.

A. E. Phaup. The granitic rocks of the rhodesian craton. *Spec. Pub. Geol. Soc. S. Afr.*, 3:59–67, 1973.

A. Piccolo, R. M. Palin, B. J. P. Kaus, and R. W. White. Generation of earth's early continents from a relatively cool archean mantle. *Geochem. Geophys. Geosyst.*, 20 (4):1679–1697, 1 Apr. 2019.

A. Plunder, L. Le Pourhiet, L. Räss, E. Gloaguen, M. Pichavant, and C. Gumiaux. Pegmatites as geological expressions of spontaneous crustal flow localisation. *Lithos*, 416-417:106652, 1 May 2022.

A. Polat. Growth of archean continental crust in oceanic island arcs. *Geology*, 40(4): 383–384, 1 Apr. 2012.

A. Pourteau, L. S. Doucet, E. R. Blereau, S. Volante, T. E. Johnson, W. J. Collins, Z.-X. Li, and D. C. Champion. TTG generation by fluid-fluxed crustal melting: Direct evidence from the proterozoic georgetown inlier, NE australia. *Earth Planet. Sci. Lett.*, 550(116548):116548, 15 Nov. 2020.

Premier African Minerals Limited. Zulu assay results. Technical report, Premier African Minerals Limited, 27 Feb. 2023.

Premier African Minerals Limited. New mineral resource statement zulu. Technical report, Premier African Minerals Limited, 9 Feb. 2024.

Prendergast and M. T. D. Wingate. Zircon geochronology of late archean komatiitic sills and their felsic country rocks, south-central zimbabwe: A revised age for the reliance komatiitic event and its implications. *Precambrian Res.*, 229:105–124, 1 May 2013.

M. D. Prendergast. The bulawayan supergroup: a late archaean passive margin-related large igneous province in the zimbabwe craton. *J. Geol. Soc. London*, 161 (3):431–445, May 2004a.

M. D. Prendergast. Contact relations between the koodoovale- and manjeri-type lithostratigraphic units of the late archaean bulawayan supergroup at hunters road, central zimbabwe. *South Afr. J. Geol.*, 107(3):325–332, 1 Sept. 2004b.

M. D. Prendergast and M. T. D. Wingate. Zircon geochronology and partial structural re-interpretation of the late archaean mashaba igneous complex, south-central zimbabwe. *South Afr. J. Geol.*, 110(4):585–596, 1 Dec. 2007.

F. Putzolu, R. N. Armstrong, T. R. Benson, D. F. Boutt, K. L. Butler, A. Dolgopolova, R. J. Herrington, D. E. Ibarra, and L. A. Munk. Volcano-sedimentary deposits: Overview of an emerging type of lithium resource. *Econ. Geol.*, 14 Mar. 2025.

Q. Qian and J. Hermann. Partial melting of lower crust at 10–15 kbar: constraints on adakite and TTG formation. *Contrib. Mineral. Petrol.*, 165(6):1195–1224, 3 June 2013.

R. P. Rapp, E. B. Watson, and C. F. Miller. Partial melting of amphibolite/eclogite and the origin of archean trondhjemites and tonalites. *Precambrian Res.*, 51(1-4): 1–25, 1 June 1991.

R. P. Rapp, N. Shimizu, and M. D. Norman. Growth of early continental crust by partial melting of eclogite. *Nature*, 425(6958):605–609, 9 Oct. 2003.

S. P. Reidel, V. E. Camp, T. L. Tolan, and B. S. Martin. The columbia river flood basalt province: Stratigraphy, areal extent, volume, and physical volcanology. In *The Columbia River Flood Basalt Province*, Geological Society of America Special Papers, pages 1–43. Geological Society of America, Aug. 2013.

J. R. Reimink and A. J. Smye. Subaerial weathering drove stabilization of continents. *Nature*, 629(8012):609–615, 8 May 2024.

N. Riel, B. J. P. Kaus, E. C. R. Green, and N. Berlie. MAGEMin, an efficient gibbs energy minimizer: Application to igneous systems. *Geochem. Geophys. Geosyst.*, 23(7):e2022GC010427, 1 July 2022.

S. Rino, T. Komiya, B. F. Windley, I. Katayama, A. Motoki, and T. Hirata. Major episodic increases of continental crustal growth determined from zircon ages of river sands; implications for mantle overturns in the early precambrian. *Phys. Earth Planet. Inter.*, 146(1-2):369–394, Aug. 2004.

N. M. W. Roberts. Chicken or egg? recipes for creating earth's continental crust. *The Innovation Geoscience*, 2(3):100091, 14 Aug. 2024.

E. Roda Robles, A. Pesquera Perez, F. Velasco Roldan, and F. Fontan. The granitic pegmatites of the fregeneda area (salamanca, spain): characteristics and petrogenesis. *Mineral. Mag.*, 63(4):535–558, Aug. 1999.

E. Roda-Robles, C. Villaseca, A. Pesquera, P. P. Gil-Crespo, R. Vieira, A. Lima, and I. Garate-Olave. Petrogenetic relationships between variscan granitoids and li-(F-P)-rich aplite-pegmatites in the central iberian zone: Geological and geochemical constraints and implications for other regions from the european variscides. *Ore Geology Reviews*, 95:408–430, 1 Apr. 2018.

E. Roda-Robles, R. Vieira, A. Lima, J. Errandonea-Martin, A. Pesquera, J. Cardoso-Fernandes, and I. Garate-Olave. Li-rich pegmatites and related peraluminous granites of the fregeneda-almendra field (spain-portugal): A case study of magmatic signature for li enrichment. *Lithos*, 452-453:107195, 1 Sept. 2023.

H. Rollinson. The growth of the zimbabwe craton during the neoarchaean. *Contrib. Mineral. Petrol.*, 178(1):1, 25 Dec. 2022.

H. Rollinson and T. Blenkinsop. The magmatic, metamorphic and tectonic evolution of the northern marginal zone of the limpopo belt in zimbabwe. *J. Geol. Soc. London*, 152(1):65–75, Feb. 1995.

H. Rollinson, G. Chagondah, and A. Hofmann. The late archaean granite paradox: A case study from the zimbabwe craton. *Precambrian Res.*, 410(107491):107491, 15 Aug. 2024.

H. R. Rollinson. Garnet–orthopyroxene thermobarometry of granulites from the north marginal zone of the limpopo belt, zimbabwe. *Geol. Soc. Spec. Publ.*, 43(1):331–335, Jan. 1989.

H. R. Rollinson and M. Whitehouse. The growth of the zimbabwe craton during the late archaean: An ion microprobe U-pb zircon study. *J. Geol. Soc. London*, 168 (4):941–952, 2011.

D. Rösel and T. Zack. LA-ICP-MS/MS single-spot rb-sr dating. *Geostand. Geoanal. Res.*, 46(2):143–168, 1 June 2022.

C. L. Rosenberg and M. R. Handy. Experimental deformation of partially melted granite revisited: implications for the continental crust. *J. Metamorph. Geol.*, 23 (1):19–28, Jan. 2005.

A. Roza Llera, M. Fuertes-Fuente, A. Cepedal, and A. Martin-Izard. Barren and li–sn–ta mineralized pegmatites from NW spain (central galicia): A comparative study of their mineralogy, geochemistry, and wallrock metasomatism. *Minerals*, 9 (12):739, 29 Nov. 2019.

A. M. Rubin. Getting granite dikes out of the source region. *J. Geophys. Res. Solid Earth*, 100(B4):5911–5929, Apr. 1995.

R. L. Rudnick. Making continental crust. *Nature*, 378(6557):571–578, Dec. 1995.

J. Rumble. *CRC handbook of chemistry and physics*. CRC Press, London, England, 106 edition, 16 June 2025.

J. K. Rybakowski. Lithium - past, present, future. *Int. J. Psychiatry Clin. Pract.*, 24 (4):330–340, Nov. 2020.

V. J. M. Salters and A. Stracke. Composition of the depleted mantle: DEPLETED MANTLE. *Geochem. Geophys. Geosyst.*, 5(5), 1 May 2004.

E. W. Sawyer, B. Cesare, and M. Brown. When the continental crust melts. *Elements*, 7(4):229–234, Aug. 2011.

J. B. Selway. A review of rare-element (li-cs-ta) pegmatite exploration techniques for the superior province, canada, and large worldwide tantalum deposits. *Explor. Min. Geol.*, 14(1-4):1–30, 1 Jan. 2005.

D. M. Shaw. Geochemistry of pelitic rocks. part III: Major elements and general geochemistry. *Bulletin of the Geological Society of America*, 67(7):919–934, 1956.

D. M. Shaw. Trace element fractionation during anatexis. *Geochim. Cosmochim. Acta*, 34(2):237–243, 1 Feb. 1970.

R. A. Shaw, K. M. Goodenough, N. M. W. Roberts, M. S. A. Horstwood, S. R. Chenery, and A. G. Gunn. Petrogenesis of rare-metal pegmatites in high-grade metamorphic terranes: A case study from the lewisian gneiss complex of north-west scotland. *Precambrian Res.*, 281:338–362, 1 Aug. 2016.

R. A. Shaw, K. M. Goodenough, E. Deady, P. Nex, B. Ruzvidzo, J. C. Rushton, and I. Mounteney. The magmatic–hydrothermal transition in lithium pegmatites: Petrographic and geochemical characteristics of pegmatites from the kamativi area, zimbabwe. *Can. Mineral.*, 60(6):957–987, 1 Nov. 2022.

K. Shimizu, E. Nakamura, and S. Maruyama. The geochemistry of ultramafic to mafic volcanics from the belingwe greenstone belt, zimbabwe: Magmatism in an archean continental large igneous province. *J. Petrol.*, 46(11):2367–2394, 1 Nov. 2005.

R. H. Sibson, J. M. M. Moore, and A. H. Rankin. Seismic pumping–a hydrothermal fluid transport mechanism. *J. Geol. Soc. London*, 131(6):653–659, 1 Dec. 1975.

W. Siebel. Inferences about magma mixing and thermal events from isotopic variations in redwitzites near the KTB site. Technical report, Bundesrepublik Deutschland im Niedersächsischen Landesamt für Bodenforschung, 1994.

D. Silva, L. Groat, T. Martins, and R. Linnen. Structural controls on the origin and emplacement of lithium-bearing pegmatites. *The Canadian Journal of Mineralogy and Petrology*, 61(6):1053–1062, 1 Nov. 2023.

W. B. Simmons, E. E. Foord, A. U. Falster, and V. T. King. Evidence for an anatectic origin of granitic pegmatites, western maine, USA. In *Geological Society of America Annual Meeting, New Orleans Abstracts*, A411, page 27, 1995.

W. B. s. Simmons and K. L. Webber. Pegmatite genesis: state of the art. *Eur. J. Mineral.*, 20(4):421–438, 1 July 2008.

B. Simons, J. C. O. Andersen, R. K. Shail, and F. E. Jenner. Fractionation of li, be, ga, nb, ta, in, sn, sb, W and bi in the peraluminous early permian variscan granites of the cornubian batholith: Precursor processes to magmatic-hydrothermal mineralisation. *Lithos*, 278-281:491–512, 1 May 2017.

M.-L. C. Sirbescu, C. Schmidt, I. V. Veksler, A. G. Whittington, and M. Wilke. Experimental crystallization of undercooled felsic liquids: Generation of pegmatitic texture. *J. Petrol.*, 58(3):539–568, 1 Mar. 2017.

J. Sláma, J. Košler, D. J. Condon, J. L. Crowley, A. Gerdes, J. M. Hanchar, M. S. A. Horstwood, G. A. Morris, L. Nasdala, N. Norberg, U. Schaltegger, B. Schoene, M. N. Tubrett, and M. J. Whitehouse. Plešovice zircon – a new natural reference material for U–pb and hf isotopic microanalysis. *Chem. Geol.*, 249(1-2):1–35, 30 Mar. 2008.

R. H. Smithies. The archaean tonalite–trondhjemite–granodiorite (TTG) series is not an analogue of cenozoic adakite. *Earth Planet. Sci. Lett.*, 182(1):115–125, 15 Oct. 2000.

R. H. Smithies, Y. Lu, K. Gessner, W. M. T. D., and D. C. Champion. *Geochemistry of Archean granitic rocks in the South West Terrane of the Yilgarn Craton*. Geological Survey of Western Australia, 2018.

C. Spandler, J. Hammerli, P. Sha, H. Hilbert-Wolf, Y. Hu, E. Roberts, and M. Schmitz. MKED1: A new titanite standard for in situ analysis of sm–nd isotopes and U–pb geochronology. *Chem. Geol.*, 425:110–126, 1 May 2016.

J. G. Stagman. An outline of the geological history of rhodesia. Technical report, Rhodesia Geological Survey Bulletin, 80, 1978.

M. Stein and A. W. Hofmann. Mantle plumes and episodic crustal growth. *Nature*, 372(6501):63–68, Nov. 1994.

R. A. Stern, S. Bodorkos, S. L. Kamo, A. H. Hickman, and F. Corfu. Measurement of SIMS instrumental mass fractionation of pb isotopes during zircon dating. *Geostand. Geoanal. Res.*, 33(2):145–168, 1 June 2009.

R. J. Stern. Evidence from ophiolites, blueschists, and ultrahigh-pressure metamorphic terranes that the modern episode of subduction tectonics began in neoproterozoic time. *Geology*, 33(7):557–560, 1 July 2005.

D. B. Stewart. Petrogenesis of lithium-rich pegmatites. *Am. Mineral.*, 63(9-10): 970–980, 1 Oct. 1978.

A. Stilling, P. Cerny, and P. J. Vanstone. THE TANCO PEGMATITE AT BERNIC LAKE, MANITOBA. XVI. ZONAL AND BULK COMPOSITIONS AND THEIR PETROGENETIC SIGNIFICANCE. *Can. Mineral.*, 44(3):599–623, 1 June 2006.

C. W. Stowe. The geology of the country south and west of selukwe. Technical Report 59, Zimbabwe Geological Survey, 1968.

C. W. Stowe. A sequence of plutons in the central portion of the rhodesdale granitic terrane, rhodesia. *Transactions of the Geological Society of South Africa*, 82:277–285, 1979.

C. W. Stowe. Wrench tectonics in the archaean rhodesian craton. *Transactions of the Geological Society of South Africa*, 83:193–205, 1980.

S. E. Swanson. MINERALOGY OF SPODUMENE PEGMATITES AND RELATED ROCKS IN THE TIN–SPODUMENE BELT OF NORTH CAROLINA AND SOUTH CAROLINA, USA. *Can. Mineral.*, 50(6):1589–1608, 1 Dec. 2012.

M. T. Sweetapple. *Characteristics of Sn-Ta-Be-Li-Industrial MIneral Deposits*. Australian Geological Survey Organization, June 2000.

M. T. Sweetapple and P. L. F. Collins. Genetic framework for the classification and distribution of archean rare metal pegmatites in the north pilbara craton, western australia. *Econ. Geol.*, 97(4):873–895, 1 July 2002.

M. T. Sweetapple, M. W. Grigson, P. Tornatora, and S. Urgine. The archean mt. cattlin spodumene pegmatite group and 3D geochemical mapping of large "unzoned" pegmatites of economic significance. *Can. Mineral.*, 57(5):803–805, 30 Sept. 2019.

M. T. Sweetapple, P. J. Vanstone, G. R. Lumpkin, and P. L. F. Collins. A review of lithogeochemical dispersion haloes of LCT pegmatites, and their application to rare metal exploration, with special reference to lithium in an australian context. *Aust. J. Earth Sci.*, pages 1–35, 9 Sept. 2024.

K. Szilas, J. E. Hoffmann, T. Schulz, C. Hansmeier, A. Polat, S. Viehmann, H. U. Kasper, and C. Münker. Combined bulk-rock hf- and nd-isotope compositions of mesoarchaean metavolcanic rocks from the ivisaartoq supracrustal belt, SW greenland: Deviations from the mantle array caused by crustal recycling. *Chem. Erde*, 76(4):543–554, 1 Dec. 2016.

R. Tamblyn, J. Hermann, D. Hasterok, P. Sossi, T. Pettke, and S. Chatterjee. Hydrated komatiites as a source of water for TTG formation in the archean. *Earth Planet. Sci. Lett.*, 603(117982):117982, 1 Feb. 2023.

P. N. Taylor, J. D. Kramersb, S. Moorbatha, J. F. Wilson, J. L. Orpen, and A. Martin. Pb/pb, SmNd and RbSr geochronology in the archean craton of zimbabwe. *Chemical Geology: Isotope Geoscience Section*, 87(3-4):175–196, 1991.

S. R. Taylor and S. M. McLennan. The geochemical evolution of the continental crust. *Reviews of Geophysics*, 33(2):241–265, 1 May 1995.

S. R. Taylor and S. M. McLennan. Chemical composition and element distribution in the earth's crust. In R. A. Meyers, editor, *Encyclopedia of Physical Science and Technology (Third Edition)*, pages 697–719. Academic Press, New York, 1 Jan. 2003.

F. Z. Teng, W. Y. Li, R. L. Rudnick, and L. R. Gardner. Contrasting lithium and magnesium isotope fractionation during continental weathering. *Earth Planet. Sci. Lett.*, 300(1-2):63–71, 15 Nov. 2010.

S. N. Thomson, G. E. Gehrels, J. Ruiz, and R. Buchwaldt. Routine low-damage apatite U-pb dating using laser ablation–multicollector–ICPMS. *Geochem. Geophys. Geosyst.*, 13(2), Feb. 2012.

E. L. Tomlinson and T. J. B. Holland. A thermodynamic model for the subsolidus evolution and melting of peridotite. *J. Petrol.*, 62(1), 24 Mar. 2021.

Z. Tóth, B. Lafrance, A. Haataja, B. Mark, K. R. Strongman, H. L. Gibson, D. K. Tinkham, M. A. Hamilton, and J. H. Marsh. Coeval development of dome-and-keel

and linear accretionary architectures in the eastern wabigoon superterrane, canada: geology and geochronology. *Can. J. Earth Sci.*, 27 May 2025.

U.S. Geological Survey. Mineral commodity summaries 2023. Technical report, U.S. Geological Survey, 2023.

US Geological Survey. Mineral commodity summaries 2025. Technical report, US Geological Survey, 2025.

J. van Hunen and J.-F. Moyen. Archean subduction: Fact or fiction? *Annu. Rev. Earth Planet. Sci.*, 40(1):195–219, 30 May 2012.

M. J. Van Kranendonk. Two types of archean continental crust: Plume and plate tectonics on early earth. *Am. J. Sci.*, 310(10):1187–1209, 1 Dec. 2010.

O. Vanderhaeghe. Pervasive melt migration from migmatites to leucogranite in the shuswap metamorphic core complex, canada: control of regional deformation. *Tectonophysics*, 312(1):35–55, 30 Oct. 1999.

P. Černý. The tanco pegmatite at bernic lake, southeastern manitoba. In *Mineralogical Association of Canada Short Course Handbook 8*, pages 527–543. Mineralogical Association of Canada, 1982.

P. Černý. Characteristics of pegmatite deposits of tantalum. In *Lanthanides, Tantalum and Niobium*, pages 195–239. Springer Berlin Heidelberg, Berlin, Heidelberg, 1989.

P. Černý. Rare-element granitic pegmatites. part I: Anatomy and internal evolution of pegmatitic deposits. *GSA Today*, 6 June 1991a.

P. Černý. Rare-element granitic pegmatites. part II: Regional to global environments and petrogenesis. *Geosci. Can.*, 18:68–81, 6 June 1991b.

P. Černý, D. London, and M. Novák. Granitic pegmatites as reflections of their sources. *Elements*, 8(4):289–294, 1 Aug. 2012.

P. Vermeesch. IsoplotR: A free and open toolbox for geochronology. *Geosci. Front.*, 9(5):1479–1493, Sept. 2018.

P. Vermeesch. On the treatment of discordant detrital zircon U–pb data. *Geochronology*, 3(1):247–257, 29 Apr. 2021.

J. L. Vigneresse and B. Tikoff. Strain partitioning during partial melting and crystallizing felsic magmas. *Tectonophysics*, 312(2):117–132, 5 Nov. 1999.

J. L. Vigneresse, P. Barbey, and M. Cuney. Rheological transitions during partial melting and crystallization with application to felsic magma segregation and transfer. *J. Petrol.*, 37(6):1579–1600, 1996.

M. L. Vinyu, R. E. Hanson, M. W. Martin, S. A. Bowring, H. A. Jelsma, and P. H. G. M. Dirks. U-pb zircon ages from a craton-margin archaean orogenic belt in northern zimbabwe. *J. Afr. Earth Sci.*, 32(1):103–114, Jan. 2001.

N. J. Vlaar, P. E. van Keken, and A. P. van den Berg. Cooling of the earth in the archaean: Consequences of pressure-release melting in a hotter mantle. *Earth Planet. Sci. Lett.*, 121(1-2):1–18, Jan. 1994.

R. F. Weinberg and Y. Y. Podladchikov. The rise of solid-state diapirs. *J. Struct. Geol.*, 17(8):1183–1195, 1 Aug. 1995.

O. M. Weller, T. J. B. Holland, C. R. Soderman, E. C. R. Green, R. Powell, C. D. Beard, and N. Riel. New thermodynamic models for anhydrous alkaline-silicate magmatic systems. *J. Petrol.*, 65(10):egae098, 1 Oct. 2024.

C. J. Wheller and R. Powell. A new thermodynamic model for sapphirine: calculated phase equilibria in K2 O-FeO-MgO-Al2 O3 -SiO2 -H2 O-TiO2 -Fe2 O3. *J. Metamorph. Geol.*, 32(3):287–299, Apr. 2014.

White, Powell, Holland, and Worley. The effect of TiO2 and Fe2 O3 on metapelitic assemblages at greenschist and amphibolite facies conditions: mineral equilibria calculations in the system K2 O-FeO-MgO-Al2 O3 -SiO2 -H2 O-TiO2 -Fe2 O3. *J. Metamorph. Geol.*, 18(5):497–511, Sept. 2000.

R. W. White, R. Powell, T. J. B. Holland, T. E. Johnson, and E. C. R. Green. New mineral activity-composition relations for thermodynamic calculations in metapelitic systems. *J. Metamorph. Geol.*, 32(3):261–286, Apr. 2014a.

R. W. White, R. Powell, T. J. B. Holland, T. E. Johnson, and E. C. R. Green. New mineral activity-composition relations for thermodynamic calculations in metapelitic systems. *J. Metamorph. Geol.*, 32(3):261–286, Apr. 2014b.

R. W. White, R. Powell, and T. E. Johnson. The effect of mn on mineral stability in metapelites revisited: new a -x relations for manganese-bearing minerals. *J. Metamorph. Geol.*, 32(8):809–828, Oct. 2014c.

M. Wiedenbeck, P. Allé, F. Corfu, W. L. Griffin, M. Meier, F. Oberli, A. V. O. N. Quadt, J. C. Roddick, and W. Spiegel. Three natural zircon standards for u-th-pb, lu-hf, trace element and ree analyses. *Geostand. Newsl.*, 19(1):1–23, Apr. 1995.

A. Wilde, A. Otto, and S. McCracken. Geology of the goulamina spodumene pegmatite field, mali. *Ore Geol. Rev.*, 134:104162, 1 July 2021.

A. H. Wilson. The great dyke of zimbabwe. *Developments in Petrology*, 15(C):365–402, 1 Jan. 1996.

J. F. Wilson. A preliminary reappraisal of the rhodesian basement complex. *Geological Society of South Africa Special Publication*, 5:1–23, 1979.

J. F. Wilson. A craton and its cracks: some of the behaviour of the zimbabwe block from the late archaean to the mesozoic in response to horizontal movements, and the significance of some of its mafic dyke fracture patterns. *J. Afr. Earth Sci. (Middle East)*, 10(3):483–501, 1 Jan. 1990.

J. F. Wilson, R. W. Nesbitt, and C. M. Fanning. Zircon geochronology of archaean felsic sequences in the zimbabwe craton: A revision of greenstone stratigraphy and a model for crustal growth. *Geol. Soc. Spec. Publ.*, 95(95):109–126, 1995.

M. T. D. Wingate. Ion microprobe U–pb zircon and baddeleyite ages for the great dyke and its satellite dykes, zimbabwe. *South Afr. J. Geol.*, 103(1):74–80, 1 Mar. 2000.

M. Wise. Characterization and classification of NYF-type pegmatites. *The Candian Mineralogist*, 37:802–803, 1999.

M. Wise, W. B. Simmons, K. L. Webber, A. U. Falster, E. Roda-Robles, S. L. Hanson, M. L. Márquez-Zavaha, and M. A. Galliski. The discrimination of LCT and NYF granitic pegmatites using mineral chemistry: A pilot study. In W. B. Simmons, K. L. Webber, A. U. Falster, E. Roda-Robles, S. L. Hanson, M. L. Márquez-Zavaha, and M. A. Galliski, editors, *6th International Symposium on Granitic Pegmatite*, pages 156–157. Rubellite Press, New Orleans, 2013.

M. A. Wise, R. S. Harmon, A. Curry, M. Jennings, Z. Grimac, and D. Khashchevskaya. Handheld LIBS for li exploration: An example from the carolina tin-spodumene belt, USA. *Minerals*, 12(1):77, 9 Jan. 2022a.

M. A. Wise, A. Müller, and W. B. Simmons. A proposed new mineralogical classification system for granitic pegmatites. *Can. Mineral.*, 60(2):229–248, 1 Mar. 2022b.

M. B. Wolf and P. J. Wyllie. Dehydration-melting of amphibolite at 10 kbar: the effects of temperature and time. *Contrib. Mineral. Petrol.*, 115(4):369–383, Feb. 1994.

J. D. Woodhead and J. M. Hergt. Strontium, neodymium and lead isotope analyses of NIST glass certified reference materials: SRM 610, 612, 614. *Geostandards Newsletter*, 25(2-3):261–266, 1 Dec. 2001.

B. G. Worst. The great dyke of southern rhodesia. Technical report, Southern Rhodesia Geological Survey Bulletin 47, 1960.

L. A. I. Wyborn, C. A. Heinrich, and A. L. Jaques. Australian proterozoic mineral systems: Essential ingredients and mappable criteria. In *1994 AuslMM Annual Conference*, pages 109–115, Aug. 1994.

D. A. Wyman. A critical assessment of neoarchean "plume only" geodynamics: Evidence from the superior province. *Precambrian Res.*, 229:3–19, 1 May 2013.

J. Xie and Y.-C. Lu. A retrospective on lithium-ion batteries. *Nat. Commun.*, 11(1): 2499, 19 May 2020.

X. Xiong, H. Keppler, A. Audetat, G. Gudfinnsson, W. Sun, M. Song, W. Xiao, and L. Yuan. Experimental constraints on rutile saturation during partial melting of metabasalt at the amphibolite to eclogite transition, with applications to TTG genesis. *Am. Mineral.*, 94(8-9):1175–1186, 1 Aug. 2009.

S. Yao. Lithium supply race heats up. Technical report, S&P Global Market Intelligence, 11 Feb. 2022.

V. Ye. Zagorsky, V. M. Makagon, and B. M. Shmakin. SYSTEMATICS OF GRANITIC PEGMATITES. *Russ. Geol. Geophys.*, 44(5):422–435, 1 May 2003.

X. Zhang, H. Zhang, Z.-L. Ma, Y. Tang, Z.-H. Lv, J.-Y. Zhao, and Y.-L. Liu. A new model for the granite–pegmatite genetic relationships in the kaluan–azubai–qiongkuer pegmatite-related ore fields, the chinese altay. *J. Asian Earth Sci.*, 124: 139–155, 1 July 2016.

P. Zhao, X. Chu, A. E. Williams-Jones, J. Mao, and S. Yuan. The role of phyllosilicate partial melting in segregating tungsten and tin deposits in W-sn metallogenic provinces. *Geology*, 50(1):121–125, 1 Jan. 2022.